



**HAL**  
open science

# Carbon dioxide as reagent for the carbonation of epoxidized polymers and copolymers: from batch process to reactive extrusion

Bruno Guerdener

► **To cite this version:**

Bruno Guerdener. Carbon dioxide as reagent for the carbonation of epoxidized polymers and copolymers: from batch process to reactive extrusion. *Polymers*. Université Jean Monnet - Saint-Etienne, 2023. English. NNT: 2023STET0055 . tel-04579319

**HAL Id: tel-04579319**

**<https://theses.hal.science/tel-04579319v1>**

Submitted on 17 May 2024

**HAL** is a multi-disciplinary open access archive for the deposit and dissemination of scientific research documents, whether they are published or not. The documents may come from teaching and research institutions in France or abroad, or from public or private research centers.

L'archive ouverte pluridisciplinaire **HAL**, est destinée au dépôt et à la diffusion de documents scientifiques de niveau recherche, publiés ou non, émanant des établissements d'enseignement et de recherche français ou étrangers, des laboratoires publics ou privés.



N°d'ordre NNT : 2023STET055

**THÈSE de DOCTORAT  
DE L'UNIVERSITÉ JEAN MONNET SAINT-ÉTIENNE**

**Membre de l'Université de LYON**

**École Doctorale N° 488  
Science Ingénierie Santé**

**Spécialité de doctorat** : Chimie et science des matériaux

Soutenue publiquement le 12/12/2023, par :  
**Bruno Guerdener**

---

**Le dioxyde de carbone comme réactif dans la  
carbonatation de polymères et copolymères  
époxydés : du procédé en batch à l'extrusion réactive**

---

Devant le jury composé de :

Burel Fabrice  
Raquez Jean-Marie  
Rozes Laurence  
Grau Etienne

Professeur, INSA Rouen Normandie  
Professeur, Université de Mons (Belgique)  
Professeure, Sorbonne Université  
Maître de conférences, Université de Bordeaux

Rapporteur  
Rapporteur  
Examinatrice  
Examineur

Chalamet Yvan  
Dufaud Véronique  
Raynaud Jean

Professeur, Université Jean Monnet  
Directrice de recherche, CNRS  
Chargé de recherche, CNRS

Directeur de thèse  
Co-directrice de thèse  
Co-directeur de thèse

Bounor-Legaré Véronique  
Monteil Vincent

Directrice de recherche, CNRS  
Directeur de recherche, CNRS

Invitée  
Invité



## Remerciements

C'est avec un grand plaisir que je remercie toutes les personnes que j'ai côtoyées durant ces trois années de thèse, et qui m'ont aidé de près ou de loin à la réalisation de ce projet professionnel et personnel que l'on ne vit qu'une seule fois dans sa vie.

Tout d'abord, je tiens à remercier l'ensemble du jury d'avoir accepté d'évaluer mes travaux de thèse, en particulier Fabrice Burel et Jean-Marie Raquez pour avoir accepté leur rôle de rapporteur, et Laurence Rozes et Etienne Grau pour leur présence en qualité d'examineur.

Cette thèse a été réalisée au sein des laboratoires IMP (Ingénierie des Matériaux Polymères) et CP2M (Catalyse, Polymérisation, Procédés et Matériaux). Je remercie la directrice de l'IMP, Jannick Duchet-Rumeau, et le directeur du CP2M, Timothy McKenna, pour m'avoir accueilli au sein de leurs laboratoires.

De manière générale, Je tiens à remercier mes encadrants pour la confiance qu'ils m'ont accordée, pour avoir toujours été reconnaissants envers mon travail, et pour leurs contributions très complémentaires qui ont permis la réalisation de cette thèse. Bien qu'étant cinq, ce qui peut paraître beaucoup pour un encadrement de thèse, il a toujours été très agréable de travailler avec eux, notamment pour leur côté humain.

Plus précisément, je remercie mon directeur de thèse, Yvan Chalamet, pour sa bienveillance, les connaissances qu'il m'a apportées sur un domaine que je connaissais peu qui est l'extrusion. Il m'a permis également d'exercer le rôle d'encadrant de TP, ce qui fut une expérience riche et intense. J'aimerais également remercier Véronique Bounor-Legaré, pour m'avoir accompagné et poussé toujours avec enthousiasme, notamment sur certaines parties de ce projet, ce qui a permis de l'enrichir.

Je remercie également Véronique Dufaud pour son sens du détail et son soutien tout le long de cette thèse, notamment lors de la rédaction et de la préparation de la soutenance. Je tiens à remercier Jean Raynaud, qui a su me transmettre sa passion, son optimisme et sa motivation. Il a toujours su me guider et m'aider à prendre la bonne direction, et j'ai toujours apprécié nos discussions scientifiques riches sur la chimie. Enfin je tiens à remercier Vincent Monteil, s'il ne m'avait jamais envoyé de mail pendant que j'étais étudiant à CPE Lyon pour une offre de stage, je ne serais probablement pas ici aujourd'hui, je le remercie de m'avoir fait confiance si tôt. Son avis critique et sa vue d'ensemble du projet a été très bénéfique.

Ces travaux de thèse n'auraient également jamais vu le jour sans les nombreuses collaborations scientifiques. En effet, j'ai travaillé pendant la 1<sup>ère</sup> année avec Virgile Ayzac sur

ce projet, post doctorant au CP2M. Son efficacité et sa productivité a permis de démarrer cette thèse dans les meilleures conditions.

L'extrusion en CO<sub>2</sub> n'aurait jamais été possible sans Paul Besognet, ingénieur extrusion de l'IMP, avec qui j'ai partagé de nombreux jours de manips, étant même parfois obligé d'ouvrir l'extrudeuse et d'utiliser le chalumeau pour démonter le profil de vis... Travailler avec lui a toujours été très agréable. Je remercie aussi Karim Delage, ingénieur procédé de l'IMP, avec qui j'ai pu réaliser la compatibilisation, les échantillons pour les tests mécaniques, et l'époxydation en extrudeuse. Il m'a également conduit une fois de Lyon à Saint Etienne en voiture pour transporter 100 kg de polymères, vive le procédé !

Un grand merci à Pierre Alcouffe et Marius Otto pour toutes la préparation des échantillons et des images en MEB, à Sébastien Norsic, le magicien du CP2M qui fait fonctionner les réacteurs et trouve les fuites de CO<sub>2</sub>, à Nesrine Oueslati, Carlos Fernandez de Alba et Patrick Goetinck pour leur aide dans la caractérisation des polymères par RMN, à Olivier Boyron, Manel Taam et Marion Colella pour m'avoir formé et aidé en SEC, DSC et ATG. Un grand merci également à Noëllie Ylla pour m'avoir formé en rhéologie, mélangeur HAAKE et sur l'utilisation de la presse, à Edgar Espinosa pour ses conseils techniques au laboratoire, à Damien Montarnal pour avoir pris le temps de m'expliquer la rhéologie et la DMA à la toute fin de ma thèse, et à Pierre-Yves Dugas pour avoir géré les problèmes informatiques. Je souhaiterai aussi remercier Mélinda Desse, professeure à l'université de Jean Monnet, pour m'avoir aidé dans ma recherche d'emploi. Merci également à Marie-Emilie Annez de Taboada, que j'ai encadrée pendant son stage de 1 mois, et qui a fourni un travail remarquable et à montrer de très bonnes capacités scientifiques.

Bien qu'étant un projet personnel, la thèse se vit en groupe, et j'ai eu l'occasion de rencontrer de nombreuses personnes avec qui j'ai passé d'excellents moments et j'en garde de très bons souvenirs, au labo comme en dehors.

Je tiens à remercier Marie, Thibaut, Camille, Magalie, Laura et Stan, vous êtes le sang et même la moelle ! Tant de bon moments partagés au labo, aux bars, aux restau, en voyage ! Merci d'avoir été là et d'avoir organisé toutes ses sorties et événements, c'était l'occasion pour moi de relâcher Dark Bruno durant les soirées traquenards de Marie...

Je suis obligé de remercier Tiffaine, pour les cours de musculation et pour les idées de brunchs où on mange comme des gros. Merci à Julie, toujours souriante et disant bonjour de bonne

humeur, même un lundi matin ! Vous avez officiellement toutes les deux le titre de gazelles de Marrakech (on peut écrire ça ?).

J'ai passé de très bons moments également avec Johan, voisin de bureau du CP2M et petit ange parti trop tôt en post doc en Allemagne. C'est fou d'avoir autant de points communs, même si on préférera oublier notre tentative de brassage de bière (Sérieux pourquoi elle était si amère cette bière ?), par contre on se boit une quadruple IPA à l'occasion.

Je garde aussi de très bons souvenirs avec Marion, également ancienne voisine de bureau du CP2M. Tous ces moments à parler et à se tacler (gentiment) resteront de très bons souvenirs.

Toujours concernant mes voisins de bureau, j'ai beaucoup aimé l'ambiance de travail au côté de Nam, Rahman, Tommaso (le maître du café), Florian, Ibrahim et Sofiane. D'ailleurs, Sofiane si tu me lis, arrête de travailler et repose-toi. J'ai quand même apprécié nos petits repas le soir à CPE en période de rédaction, c'est vrai que c'est pas mal Pépé Chicken, par contre Tasty Pizza...

Même si j'ai passé peu de moment à mon bureau à l'IMP, j'ai été très content de l'accueil qui m'a été fait à chaque fois, et je remercie mes collègues de bureau Hussein, Gabriella, Alexane et Fanny pour leur gentillesse.

J'ai également passé de très bon moment à échanger avec Léa ; Nedjma, Samy, Léo, Felipe, et Adamu.

En plus de toutes ses personnes, je ne serai probablement pas arrivé jusqu'ici sans le soutien de mes amis et de ma famille.

Merci Flora pour tous tes encouragements ! Ravi d'avoir comme amie quelqu'un qui fait des blagues aussi nulles que moi ! Ce serait bien se refaire à l'occasion des parties de Smash bros ou de Bowling (toi qui try hard tant) et me montrer ton nouveau niveau.

Merci au GANA gang Stéphane, Yoann et Antoine, à quand nos lives sur Twitch où on se fait démonter sur Rocket League ? On a passé de très bons moments (amicalement parlant), à jouer mais aussi au bowling, et à toutes les soirées avec les Kékés.

Bien sur je remercie ma famille, mon frere, ma sœur, mes nièces Emma, Marlene, Elsa, mon neveu Leon, mes grands-parents et le reste de ma famille pour tous ses bons moments et votre soutien. Je tiens à remercier particulièrement mes parents pour tous les sacrifices et l'aide qu'ils m'ont apporté tout le long de ma scolarité. Je sais où je vais mais je me rappelle aussi

d'où je viens. Je pense que la différence culturelle qui vient de ma famille reste un atout qui me permet de voir les choses différemment, je sais que j'ai de la chance d'être là et que tous n'ont pas eu cette opportunité.

Enfin, Je tiens à remercier Laura. Maintenant 8 ans qu'on se connaît. Je suis très heureux de pouvoir te rendre fière et du chemin qu'on a accompli depuis nos débuts à CPE. Tu m'as toujours poussé à faire de mon mieux et à ne pas me satisfaire du strict minimum. Merci d'avoir été là et d'avoir gardé cette simplicité et joie de vivre. Je suis heureux de savoir que la prochaine étape sera avec toi et je ne vois que du positif pour la suite.

*Pour Mémé Manon*



## Résumé

### **Titre : Le dioxyde de carbone comme réactif dans la carbonatation de polymères et copolymères époxydés : du procédé en batch à l'extrusion réactive**

La fonctionnalisation de polymères en utilisant le dioxyde de carbone comme réactif est une approche innovante et éco-conçue pour moduler la réactivité et les propriétés physico-chimiques des polymères. La méthodologie de fonctionnalisation développée dans cette thèse permet l'introduction de groupements carbonates cycliques sur des polymères amorphes et semi-cristallins comportant des fonctions époxydes ou des insaturations. Des polymères semi-cristallins et relativement apolaires à base de [éthylène - méthacrylate de glycidyle] contenant des groupements époxydes pendants ont d'abord été fonctionnalisés avec succès en utilisant le CO<sub>2</sub> en réacteur batch grâce à des sels d'ammonium commerciaux comme organocatalyseurs, et la fonctionnalisation a été transposée pour la première fois à un procédé d'extrusion réactive continu et sans solvant, produisant des polymères fonctionnalisés prêts à l'emploi à l'échelle du kilogramme.

Cette fonctionnalisation au CO<sub>2</sub> a été étendue aux polymères contenant des insaturations, tels que des polybutadiènes, polyisoprènes et copolymères contenant des monomères diéniques. Une fonctionnalisation en deux étapes a été étudiée. La première étape (réaction d'époxydation) a été réalisée avec succès avec des peracides (y compris des peracides « verts » formés par le mélange H<sub>2</sub>O<sub>2</sub>/acide carboxylique) pour tous les différents polymères utilisés. Ensuite, la deuxième étape (réaction de carbonatation) a été optimisée et réalisée sur les différents polymères époxydés, et des polybutadiènes, polyisoprènes et copolymères [styrène-bloc-butadiène-bloc-styrène] carbonatés ont été obtenus avec succès.

Ensuite, les polymères carbonatés ont été utilisés comme intermédiaires pour la synthèse de polyhydroxyuréthanes à l'aide d'amines. Plus précisément, la réactivité orthogonale des fonctions carbonates cycliques et époxydes résiduelles avec les amines a été démontrée avec succès, les carbonates cycliques étant nettement plus réactifs que les époxydes vis-à-vis de l'attaque nucléophile d'amines. L'utilisation des polymères carbonatés à base de [éthylène - méthacrylate de glycidyle] en tant que nouveaux compatibilisants réactifs efficaces pour un mélange HDPE/PC (80/20) (p/p) a également été mise en évidence, avec une réduction significative de la taille de la phase dispersée et une amélioration de l'allongement à la rupture et de la résistance à l'impact Charpy du mélange. Ainsi, les polymères carbonatés pourraient être utilisés comme précurseurs pour la production de matériaux hybrides réticulés avec

différents nœuds de réticulation, et comme un nouveau type de compatibilisants réactifs pour le mélange de polyoléfines avec des polycarbonates, polyamides, polyesters et polyacides.

**Mots clés :** carbonatation, dioxyde de carbone, carbonate cyclique, époxyde, extrusion réactive, fonctionnalisation, polymère

## Abstract

### **Title: Carbon dioxide as reagent for the carbonatation of epoxidized polymers and copolymers: from batch process to reactive extrusion**

The functionalization of polymers using carbon dioxide as reagent is an innovative and eco-designed approach to modulate the polymers' reactivity and physico-chemical properties. The functionalization methodology developed in this thesis allows the introduction of cyclic carbonate moieties on amorphous and semi-crystalline polymers. Semi-crystalline and relatively apolar [ethylene – glycidyl methacrylate] based polymers containing pendant epoxides moieties were first successfully functionalized by CO<sub>2</sub> in batch using commercial ammonium salts as organocatalysts, and the functionalization was transposed for the first time to a solvent-free and continuous reactive extrusion process, producing ready-to-use functionalized polymers at kilogram scale.

This functionalization with CO<sub>2</sub> was extended to polymers containing unsaturations, such as polybutadienes, polyisoprenes, and copolymers containing diene monomers. A two-steps functionalization was investigated. The first step (epoxidation reaction) was successfully achieved with peracids (including “green ones” from H<sub>2</sub>O<sub>2</sub>/carboxylic acid mixture) for all the different polymers used. Then, the second step (carbonatation reaction) was optimized and performed on the different epoxidized polymers, and carbonated polybutadienes, polyisoprene and [styrene-*block*-butadiene-*block*-styrene] copolymer were successfully obtained.

Afterwards, the carbonated polymers were used as intermediates for the synthesis of polyhydroxyurethanes using amines. More specifically, the orthogonal reactivity of the cyclic carbonates and residual epoxides moieties with amines was successfully demonstrated, the cyclic carbonates being significantly more susceptible to amine nucleophilic attack than the epoxides. The use of the carbonated [ethylene – glycidyl methacrylate] based polymers as new and efficient reactive compatibilizers for a HDPE/PC (80/20) (w/w) blend was also highlighted, with a significant reduction of the dispersed phase size, and improvement of the elongation at break and notched Charpy impact strength of the blend. Thus, the carbonated polymers could be used as precursors for the production of hybrid cross-linked materials with different cross-linking knots, and as a new type of reactive compatibilizers for blending of polyolefins with polycarbonates, polyamides, polyesters and polyacids.

**Keywords:** carbonatation, carbon dioxide, cyclic carbonate, epoxide, reactive extrusion, functionalization, polymer

## Outline

<b>General introduction</b> .....	<b>3</b>
<b>Experimental section</b> .....	<b>9</b>
<b>I. Materials and methods</b> .....	<b>13</b>
<b>II. General procedures</b> .....	<b>18</b>
<b>Chapter 1: Literature review on the carbonatation reaction, from molecular synthesis to polymers functionalization</b>	
<b>I. Introduction</b> .....	<b>27</b>
<b>II. Carbonatation of molecular compounds</b> .....	<b>30</b>
II.1. Onium salts as nucleophilic catalysts for the carbonatation of epoxides .....	30
II.1.a. Catalytic cycle mechanism.....	30
II.1.b. Reactivity with terminal epoxides.....	31
II.1.c. Reactivity with disubstituted epoxides .....	40
II.1.d. Reactivity of trisubstituted and tetrasubstituted epoxides.....	43
II.2. Carbonatation of epoxides with hindered nucleophilic catalysts .....	47
II.2.a. Catalytic cycle mechanism.....	47
II.2.b. Influence of the base structure .....	48
II.3. Acidic co-catalysts .....	51
II.3.a. Lewis acids.....	51
II.3.b. Brønsted acids .....	57
II.4. Oxydative carbonatation of alkenes in one-pot.....	59
<b>III. Carbonatation of polymers</b> .....	<b>65</b>
III.1. Carbonatation of glycidyl methacrylate based copolymers.....	65
III.1.a. Effect of the reaction conditions.....	66
III.1.b. Effect of the polymer structure.....	70
III.1.c. Polymerisation and carbonatation of GMA in one-pot.....	72

III.1.d. Self-catalyzed carbonatation of GMA based copolymers containing ammonium salts moieties .....	74
III.1.e. Use of the carbonated GMA based polymers in polymer blends.....	75
III.1.f. Influence of DOMMA content on the thermal properties.....	75
III.2. Carbonatation of epoxidized polydienes.....	76
III.2.a. Two-steps oxidative carbonatation of polybutadienes.....	76
III.2.b. Carbonatation of epoxidized natural rubbers .....	79
<b>IV. Conclusions of the review and objectives of this thesis .....</b>	<b>80</b>
<b>V. References.....</b>	<b>82</b>

## **Chapter 2: Carbonatation of [ethylene – glycidyl methacrylate] based copolymers with carbon dioxide as a reagent: from batch to solvent-free reactive extrusion**

<b>I. Résumé .....</b>	<b>94</b>
<b>II. Abstract .....</b>	<b>95</b>
<b>III. Introduction.....</b>	<b>96</b>
<b>IV. Results and discussion .....</b>	<b>99</b>
IV.1. Optimisation of the conditions in batch.....	99
IV.1.a. Screening of the catalysts.....	99
IV.1.b. Influence of the halides .....	102
IV.1.c. Influence of the alkyl chains.....	104
IV.1.d. Influence of the reaction parameters .....	106
IV.1.e. Influence of the acrylate comonomer .....	108
IV.2. Methodology transposition to reactive extrusion .....	109
IV.2.a. Effect of the extrusion parameters on the mean residence time .....	110
IV.2.b. Optimisation of the reactive extrusion process .....	115
IV.2.c. Comparison of the reaction kinetics of the batch and reactive extrusion processes.....	118

<b>V. Conclusion</b> .....	<b>121</b>
<b>VI. References</b> .....	<b>123</b>

### **Chapter 3: Two-steps functionalization of polydienes with peracids and carbon dioxide as reagent**

<b>I. Résumé</b> .....	<b>135</b>
<b>II. Abstract</b> .....	<b>136</b>
<b>III. Introduction</b> .....	<b>137</b>
<b>IV. Results and discussion</b> .....	<b>139</b>
IV.1. Epoxidation of polydienes .....	139
IV.1.a. Study of the epoxidation on polybutadiene .....	139
IV.1.b. Scope of the epoxidation on unsaturated polymers .....	144
IV.1.c. Epoxidation transposed to reactive extrusion .....	148
IV.2. Carbonatation of epoxidized polydienes .....	150
IV.2.a. Study of the reaction on epoxidized polybutadiene .....	150
IV.2.b. Scope of the carbonatation reaction .....	154
IV.2.c. Evolution of the thermal properties .....	158
<b>V. Conclusions</b> .....	<b>165</b>
<b>VI. References</b> .....	<b>167</b>

### **Chapter 4: Synthesis of polyhydroxyurethanes from carbonated polymers**

<b>I. Abstract</b> .....	<b>180</b>
<b>II. Introduction</b> .....	<b>181</b>
<b>III. Results and discussion</b> .....	<b>185</b>
III.1. Synthesis of hydroxyurethane functions on carbonated [ethylene – glycidylmethacrylate-methyl acrylate] polymer .....	185
III.2. Synthesis of hydroxyurethane functions on partially carbonated [ethylene – glycidylmethacrylate-methyl acrylate] polymer .....	188

III.3. Synthesis of hydroxyurethane functions on partially carbonated polydiene with a monoamine.....	192
III.4. Synthesis of cross-linked PHUs from carbonated polydienes with hexamethylene diamine .....	195
<b>IV. Conclusions .....</b>	<b>200</b>
<b>V. References.....</b>	<b>201</b>

**Chapter 5: Carbonated [ethylene - glycidyl methacrylate] based polymers as compatibilizers for polyethylene/polycarbonate blends by reactive extrusion**

<b>I. Abstract .....</b>	<b>209</b>
<b>II. Introduction.....</b>	<b>211</b>
<b>III. Results and discussion.....</b>	<b>214</b>
III.1. Compatibilization of HDPE/PC (80/20) blend.....	214
III.1.a. Morphologies of the blends.....	214
III.1.b. Spectroscopic characterizations .....	218
III.1.c. Mechanical properties.....	222
III.1.d. Thermal properties.....	225
III.2. Compatibilization of PC/HDPE (80/20) blend.....	228
III.2.a. Morphologies of the blends.....	228
III.2.b. Spectroscopic characterizations .....	230
III.2.c. Mechanical properties.....	233
III.2.d. Thermal properties.....	235
<b>IV. Conclusions .....</b>	<b>236</b>
<b>V. References.....</b>	<b>237</b>
<b>General conclusion.....</b>	<b>239</b>
<b>Appendices.....</b>	<b>247</b>





## Abbreviations

<b>CH<sub>3</sub>COOH</b>	Acetic acid
<b><i>E<sub>a</sub></i></b>	Activation energy
<b>PPNCl</b>	Bis(triphenylphosphoranylidene)ammonium chloride
<b>C<sub>1</sub>C<sub>4</sub>ImOAc</b>	1-Butyl-3-methylimidazolium acetate
<b>C<sub>1</sub>C<sub>4</sub>ImBr</b>	1-Butyl-3-methylimidazolium bromide
<b>PPh<sub>3</sub>BuBr</b>	Butyltriphenylphosphonium bromide
<b>CO<sub>2</sub></b>	Carbon dioxide
<b>CTAB</b>	Cetyltrimethylammonium bromide
<b><i>G(X)</i></b>	Conversion distribution
<b>CP/MAS NMR</b>	Cross polarization/magic angle spinning nuclear magnetic resonance
<b>C<sub>6</sub>D<sub>6</sub></b>	Deuterated benzene
<b>CDCl<sub>3</sub></b>	Deuterated chloroform
<b>DBU</b>	1,8-Diazabicyclo(5.4.0)undec-7-ene
<b>DDAB</b>	didodecyldimethylammonium bromide
<b>DSC</b>	Differential scanning calorimetry
<b>DODAB</b>	dioctadecyldimethylammonium bromide
<b>DTAB</b>	Dodecyltrimethylammonium bromide
<b>E-GMA</b>	[Ethylene-glycidyl methacrylate] copolymer
<b>E-GMA-BA</b>	[Ethylene-glycidyl methacrylate-butyl acrylate] terpolymer
<b>E-GMA-MA</b>	[Ethylene-glycidyl methacrylate-methyl acrylate] terpolymer
<b>EPDM-DCPD</b>	[Ethylene-propylene-dicyclopentadiene] terpolymer
<b>EPDM-ENB</b>	[Ethylene-propylene-ethylidene norbornene] terpolymer
<b>HCOOH</b>	Formic acid
<b><i>T<sub>g</sub></i></b>	Glass transition temperature
<b>GMA</b>	Glycidyl methacrylate
<b>HMDA</b>	Hexamethylene diamine
<b>HA</b>	Hexylamine
<b>HDPE</b>	High-density polyethylene
<b>H<sub>2</sub>O<sub>2</sub></b>	Hydrogen peroxide
<b>IR-ATR</b>	Infrared-attenuated total reflectance
<b>LDPE</b>	Low-density polyethylene
<b>LLDPE</b>	Linear low-density polyethylene
<b><math>\bar{X}</math></b>	Mean conversion

$\bar{t}_m$	Mean residence time
$T_m$	Melting temperature
<b>mCPBA</b>	<i>Meta</i> -perchlorobenzoic acid
<b>C<sub>1</sub>C<sub>4</sub>ImBF<sub>4</sub></b>	1-Methyl-3-octylimidazolium tetrafluoroborate
<b>MEK</b>	Methyl ethyl ketone
<b>NR</b>	Natural rubber
<b>NIPU</b>	Non-isocyanate polyurethane
<b>NMR</b>	Nuclear magnetic resonance
<b>PBU</b>	Polybutadiene
<b>PC</b>	Polycarbonate
<b>PE</b>	Polyethylene
<b>PHU</b>	Polyhydroxyurethane
<b>PU</b>	Polyurethane
<b><i>E(t)</i></b>	Residence time distribution
<b>SEM</b>	Scanning electron microscopy
<b>SEC</b>	Size exclusion chromatography
<b>SBS</b>	[Styrene- <i>block</i> -butadiene- <i>block</i> -styrene] copolymer
<b>SIS</b>	[Styrene- <i>block</i> -isoprene- <i>block</i> -styrene] copolymer
<b>TBAB</b>	Tetrabutylammonium bromide
<b>TBAC</b>	Tetrabutylammonium chloride
<b>TBAF</b>	Tetrabutylammonium fluoride
<b>TBAI</b>	Tetrabutylammonium iodide
<b>TCE</b>	Tetrachloroethylene
<b>TEAB</b>	Tetraethylammonium bromide
<b>THAB</b>	Tetrahexylammonium bromide
<b>TOAB</b>	Tetraoctylammonium bromide
<b>TGA</b>	Thermal gravimetric analysis
<b>TBD</b>	1,5,7-Triazabicyclo[4.4.0]dec-5-ene

---

# **General Introduction**

---



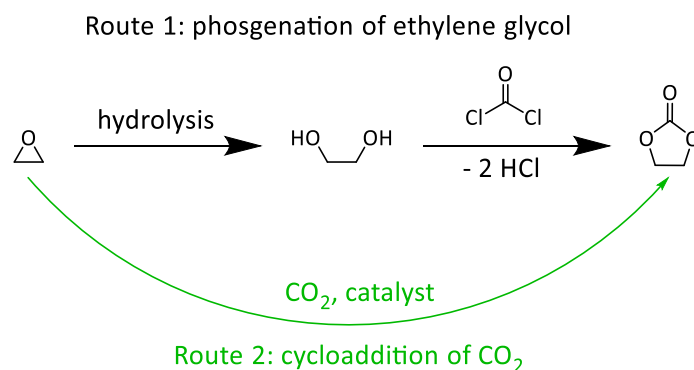
Nowadays, human activities strongly affect the environment through various aspects. Climate change, loss of biodiversity, chemical pollution, ocean acidification, life cycle deregulation of water, nitrogen and phosphorus among others, with a considerable intensification of all these phenomena since the Industrial Revolution.<sup>[1,2]</sup>

In this context, the design of new industrial processes, products or services with low environmental impact, called eco-design, is necessary but represents a major challenge. In eco-design, each step must be considered to determine the impact of a process, from the extraction of the raw materials used to the disposal of the final products.

In chemistry, the reduction of chemical waste production (atom economy, solvent-free processes), CO<sub>2</sub> emissions and energy consumption as well as the use of renewable feedstock are one of the fundamental principles of green chemistry and a pillar in the logic of eco-design. Catalysis is a key tool for the development of synthetic routes with high atom economy and energy efficiency. Catalysis, by lowering the energy barrier, makes possible chemicals transformations from reagents that have a high activation energy. These routes could provide sustainable alternatives for the production of compounds or materials that are usually produced from highly reactive and toxic reagents and under harsh conditions.

The synthesis of ethylene carbonate at an industrial scale from ethylene oxide is a perfect example that illustrates the advantages of catalysis. Two main routes have been developed for this synthesis (*Scheme 1*).<sup>[3,4]</sup> Route 1 is a multi-step pathway that uses the highly toxic phosgene and produces hydrochloric acid as by-product. Conversely, Route 2 is a single step route using CO<sub>2</sub> as green reagent and a non-toxic organocatalyst supported on an anion exchange resin,<sup>[4]</sup> with a theoretical atom economy of 100 %.

On the other hand, in the polymer industry, reactive extrusion has emerged as an innovative process for the solvent-free continuous production of specialty polymers ready for use *via* controlled chemical modifications. Twin-screw extrusion can homogenize viscous melted substrates (polymers for post-functionalization, or monomers in the case of polymerization) with reactive additives under solvent-free conditions. The functionalization of polymer by reactive extrusion becomes even more interesting in a logic of eco-design when no chemical waste is produced (neither solvent nor by-product), and if it is used for the valorization of polymer waste.



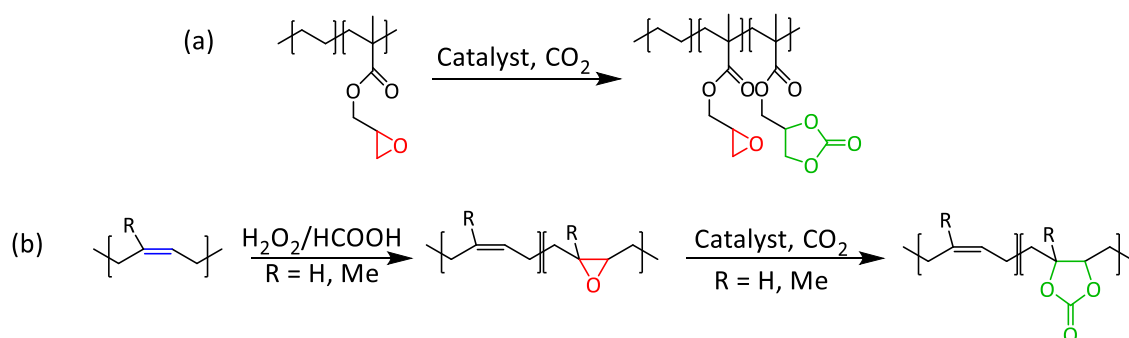
*Scheme 1. Synthesis of ethylene carbonate from ethylene oxide.*

In this thesis work, the use of CO<sub>2</sub>, a greenhouse gas, to functionalize polymers harnessing batch and reactive extrusion processes is described. This thesis takes place in the frame of the DICARBOREX project, founded by Institut Carnot Ingénierie@Lyon, and is a collaboration between IMP and CP2M laboratories. The aim of this project is to develop polymer materials using reactive extrusion with modular functionalities by implementing a sustainable chemistry based on the use of carbon dioxide as a carbon source. The core of the study is to introduce cyclic carbonate functions from CO<sub>2</sub>, *via* carbonatation reactions, on industrial relevant polymers to modify their physicochemical characteristics such as their polarity, crystallinity, and reactivity without limiting their recyclability. The great challenge of the project is to apply such chemical modifications on polyolefins in a one-step reactive extrusion by processing the reactive system under high pressure of carbon dioxide.

This thesis is divided in five chapters. **Chapter 1** is a literature study of the reactivity of epoxides and alkenes with CO<sub>2</sub> to synthesize cyclic carbonates. An overview of the common catalytic systems used for the carbonatation of molecular epoxides and the oxidative carbonatation of molecular alkenes will be presented, as well as the main strategies for the synthesis of carbonated polymers (*i.e.* polymers containing cyclic carbonate moieties).

**Chapter 2** focuses on the carbonatation of industrial non-polar semi-crystalline polymers containing epoxide pendant groups to obtain modified polymers with both epoxide and cyclic carbonate functions (*Scheme 2 (a)*). The reaction will be first studied in batch for a better understanding of the influence of the different reaction parameters, and then transposed to a solvent-free reactive extrusion process to develop an original continuous process for the modification of epoxidized polymers with CO<sub>2</sub>. This chapter is based on our first article published in 2023 in *Green Chemistry*,<sup>[5]</sup> with additional results and discussions.

In **Chapter 3**, the functionalization with CO<sub>2</sub> will be extended to polydienes and polymers containing unsaturations (*Scheme 2 (b)*). A two-step synthesis (epoxidation and carbonatation) will be presented using peracids and organocatalysts to form cyclic carbonate functions on unsaturated polymers. The epoxidation step will first be studied in a batch process, then transposed to a reactive extrusion process. The carbonatation step will be optimized in a batch process using ammonium salts as organocatalysts.



*Scheme 2. Carbonatation of polymers with CO<sub>2</sub>.*

Finally, two different applications will be explored for the synthesized carbonated polymers. In **Chapter 4**, the generation of hydroxyurethane functions on carbonated polymers using amines will be investigated. Here, controlling the regioselective and stereoselective aminolysis of cyclic carbonates relative to residual epoxides will be essential to develop further orthogonal functionalizations exploiting both epoxide and cyclic carbonate moieties on polymers in order to produce hybrid-cross-linked polymers with different crosslinking knots.

In **Chapter 5**, the carbonated [ethylene – glycidyl methacrylate] based copolymers will be studied as compatibilizers for polyethylene/polycarbonate blends. The compatibilization of incompatible polymers is necessary for the mechanical recycling of plastic wastes, as well as for the production of low cost engineering polymers. The effect of the compatibilizer structure on the morphologies, the mechanical and thermal properties of the blends will be studied.



## References

- [1] Rockström, J.; Steffen, W.; Noone, K.; Persson, Å.; Chapin, F.S.; Lambin, E.F.; Lenton, T.M.; Scheffer, M.; Folke, C.; Schellnhuber, H.J.; Nykvist, B.; Wit, C.A. de; Hughes, T.; Leeuw, S. van der; Rodhe, H.; Sörlin, S.; Snyder, P.K.; Costanza, R.; Svedin, U.; Falkenmark, M.; Karlberg, L.; Corell, R.W.; Fabry, V.J.; Hansen, J.; Walker, B.; Liverman, D.; Richardson, K.; Crutzen, P.; Foley, J.A. A safe operating space for humanity. *Nature* **2009**, *461*(7263), 472–475.
- [2] Wang-Erlandsson, L.; Tobian, A.; Ent, R.J. van der; Fetzer, I.; Wierik, S. te; Porkka, M.; Staal, A.; Jaramillo, F.; Dahlmann, H.; Singh, C.; Greve, P.; Gerten, D.; Keys, P.W.; Gleeson, T.; Cornell, S.E.; Steffen, W.; Bai, X.; Rockström, J. A planetary boundary for green water. *Nat Rev Earth Environ* **2022**, *3*(6), 380–392.
- [3] Cokoja, M.; Wilhelm, M.E.; Anthofer, M.H.; Herrmann, W.A.; Kühn, F.E. Synthesis of Cyclic Carbonates from Epoxides and Carbon Dioxide by Using Organocatalysts. *ChemSusChem* **2015**, *8*(15), 2436–2454.
- [4] Raines, D.A.; Ainsworth, O.C.; Peppel, W.J. ETHYLENE CARBONATE PROCESS. 1980.
- [5] Guerdener, B.; Ayzac, V.; Norsic, S.; Besognet, P.; Bounor-Legaré, V.; Monteil, V.; Dufaud, V.; Raynaud, J.; Chalamet, Y. Carbonatation of [ethylene-glycidyl methacrylate]-based copolymers with carbon dioxide as a reagent: from batch to solvent-free reactive extrusion. *Green Chem.* **2023**, *25*(16), 6355–6364.

---

# **Experimental Section**

---



## Table of Contents

<b>I. Materials and methods .....</b>	<b>13</b>
I.1. Commercial polymers.....	13
I.2. Commercial reagents and catalysts.....	13
I.3. Equipment.....	14
I.4. Analytical methods .....	16
<b>II. General procedures.....</b>	<b>18</b>
II.1. Chapter 2.....	18
II.1.a. Carbonatation of [ethylene – glycidyl methacrylate] based copolymers in batch .....	18
II.1.b. Carbonatation of [ethylene – glycidyl methacrylate] based copolymers in extruder .....	19
II.2. Chapter 3.....	19
II.2.a. Epoxidation of polydienes in batch.....	19
II.2.b. Epoxidation of polybutadiene in reactive extrusion.....	19
II.2.c. Carbonatation of epoxidized polydienes in batch.....	20
II.3. Chapter 4.....	20
II.3.a. Aminolysis of carbonated ethylene-glycidyl methacrylate-methyl acrylate terpolymer .....	20
II.3.b. Kinetic study of aminolysis reaction monitored by <sup>1</sup> H NMR .....	20
II.3.c. Cross-linking of carbonated polybutadiene with hexamethylene diamine .....	21
II.4. Chapter 5.....	21
II.4.a. Preparation of HDPE/PC/compatibilizer (72/18/10) (w/w/w) blends by twin-screw extrusion .....	21
II.4.b. Extraction of the PC phase from the HDPE/PC/compatibilizer blends.....	21



## I. Materials and methods

### I.1. Commercial polymers

In **Chapter 2** and **Chapter 5**, the ethylene glycidyl methacrylate based polymers used are Lotader® AX8900 ([ethylene-glycidyl methacrylate-methyl acrylate] terpolymer) AX8700 ([ethylene-glycidyl methacrylate-butyl acrylate] terpolymer) and AX8840 ([ethylene-glycidyl methacrylate] copolymer) and were purchased from Arkema.

In **Chapter 3**, the polybutadienes used in batch reactions (PBU-1, PBU-2, PBU-3), the natural rubber (NR-1) and the [styrene-*block*-butadiene-*block*-styrene] copolymer (SBS) were purchased from Sigma Aldrich. The 1,2-polybutadiene B-1000 (PBU-4) used in reactive extrusion and the epoxidized polybutadiene JP-100 (36 mol% of epoxide) (E-PBU-3) were furnished by Nippon Soda. The [styrene-*block*-isoprene-*block*-styrene] copolymer used is KRATON® D1161PT (SIS). The [ethylene-propylene-dicyclopentadiene] terpolymer used is Trilene® 65 (EPDM-DCPD) and was purchased from Lion Elastomers. The [ethylene-propylene-ethylidene norbornene] terpolymer used is MITSUI® EPT 3092PM (EPDM-ENB) and was purchased from Mitsui Chemicals. Finally, the epoxidized natural rubber used is DYNATHAI® Epoxyrene 50 (E-NR-1) and was purchased from Muang Mai Guthrie Company Limited.

In **Chapter 5**, The polyethylene used is a high density polyethylene (HDPE) produced by TotalEnergies and commercialized under the name Lumicene® Supertough 22ST05 and 32ST05, the polycarbonate (PC) used is produced by Shenzhen Plastic Trading Co. (China) and commercialized under the name Makrolon® 2405.

### I.2. Commercial reagents and catalysts.

In **Chapter 2** and **Chapter 3**, CO<sub>2</sub> was purchased from Air Liquide and the purity was 99.995 %, For the batch study, 1-butyl-3-methylimidazolium acetate (C<sub>1</sub>C<sub>4</sub>ImOAc) was purchased from Strem Chemicals. Toluene and all the other catalysts were supplied by Sigma Aldrich.

In **Chapter 2**, for the reactive extrusion optimization, tetrabutylammonium bromide (TBAB) and tetrabutylammonium iodide (TBAI) were purchased from TCI Chemicals and

tetrahexylammonium bromide (THAB) was purchased from Sigma Aldrich. All the chemicals were used without further purification.

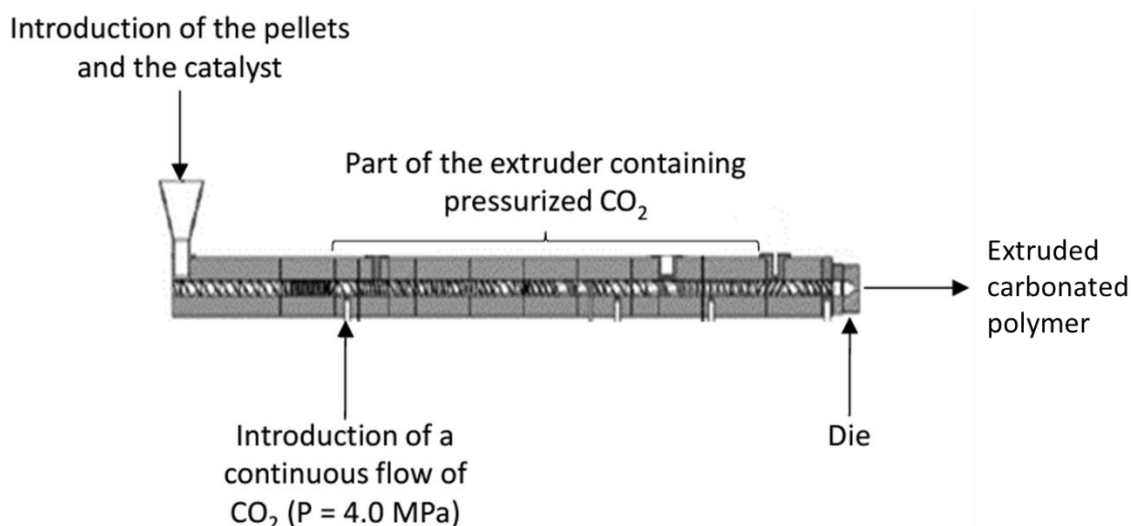
In **Chapter 3**, peroxide hydrogen in water (30 wt%), formic acid, acetic acid and *meta*-chloroperoxybenzoic acid (mCPBA) were purchased from Sigma Aldrich.

In **Chapter 4**, hexylamine, hexamethylene diamine (HMDA) and 1,5,7-triazabicyclo[4.4.0]dec-5-ene (TBD) were purchased from Sigma Aldrich.

### I.3. Equipment

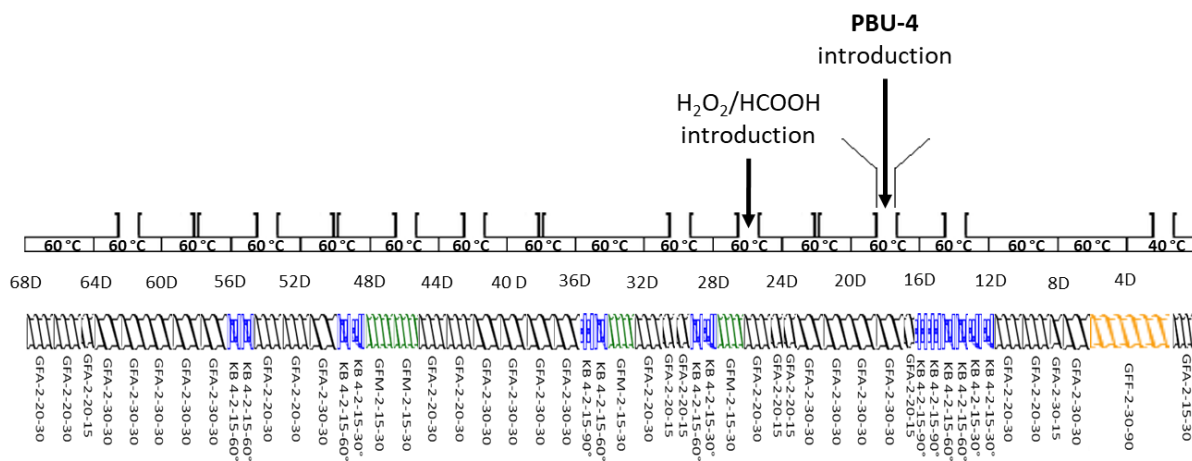
In **Chapter 2** and **Chapter 3**, all batch reactions with CO<sub>2</sub> were performed in a 0.16 L stainless steel reactor from "PARR INSTRUMENT COMPANY", connected to a ballast used for condensation of CO<sub>2</sub> to get high pressures up to 340 bar; the temperature varies in the ballast *via* oil circulation, using an oil bath functioning from -60 °C to 80 °C. The reactor temperature was also regulated *via* oil circulation, using an oil bath functioning from 30 °C to 200 °C.

In **Chapter 2**, The reactive extrusion experiments were conducted in a twin-screw extruder, a BC 21 (L/D = 36, screw diameter = 25 mm) from Clextral, using a co-rotative configuration. The extruder had 9 barrels, numbered consecutively from 1 to 9 from the feed port to the die. The die had a diameter of 3 mm and a length of 10 mm. The extruder had 9 heating zones. The process is presented in [Figure 1](#). The screw profile is not disclosed due to IP issues.



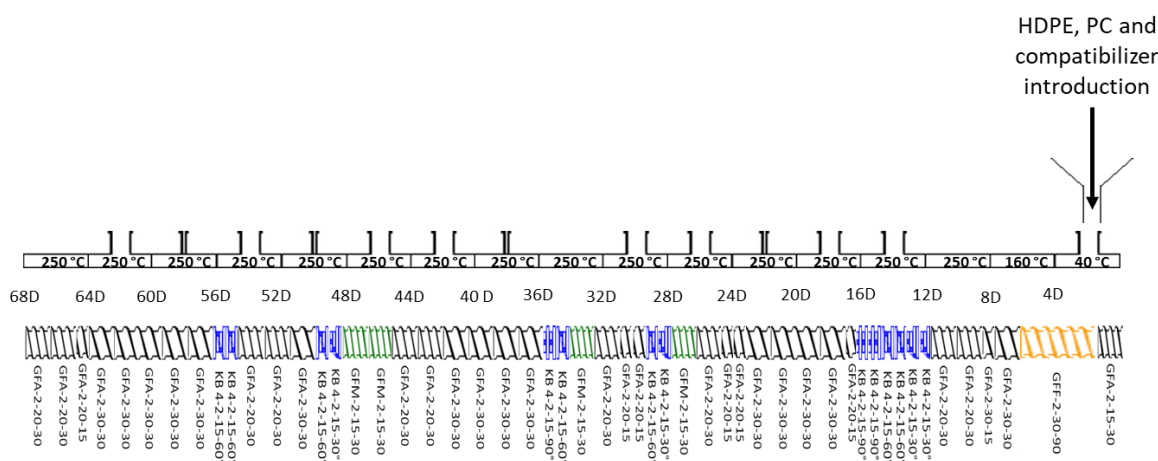
*Figure 1. Flowchart of the reactive extrusion process with CO<sub>2</sub>.*

In **Chapter 3** (for the epoxidation by reactive extrusion) the experiments were performed in a co-rotating twin-screw extruder Leistritz ZSE18HPE-60D model (diameter 18 mm, L/D = 60) at 50 -70 °C, with a total mass flow of 350 g/h of polymer, a flow a oxidant of 7.5-15 mL/min and a screw speed of 100 rpm. The screw and temperature profiles are described in *Figure 2*.



*Figure 2. Screw and temperature profiles of the extruder used for epoxidation.*

In **Chapter 5**, The blend experiments were also performed in the co-rotating twin-screw extruder Leistritz ZSE18HPE-60D model (diameter 18 mm, L/D = 60) at 250 °C, a total mass flow of 3.0 kg/h of polymer blend and screw speed of 400 rpm. The screw and temperature profiles are described in *Figure 3*.



*Figure 3. Screw and temperature profiles of the extruder used for HPDE/PC/compatibilizer blending.*



#### I.4. Analytical methods

**Infrared Attenuated Total Reflectance (IR-ATR)** were performed at room temperature on Nicolet i550 FT-IR apparatus from ThermoFischer with 32 scans and a resolution of 4.

In **Chapter 2, Chapter 4 and Chapter 5**, **<sup>1</sup>H Nuclear Magnetic Resonance (NMR) analyses** were recorded using a Bruker 400 Avance III operating at 400 MHz. The probe was a 5 mm BBFO+ with a z-gradient coil. **<sup>13</sup>C NMR spectra** were recorded using a Bruker Avance II operating at 100 MHz with a 10 mm SEX probe, **<sup>13</sup>C selective** with a z-gradient coil. The pulse sequence includes a decoupling proton with NOE effects, and a 70° spin excitation. The method is "semi-quantitative". A tetrachloroethylene/benzene-d<sub>6</sub> (2/1) (v/v) mixture or CDCl<sub>3</sub> were used as deuterated solvents. NMR analyses were performed at 363 K or 298 K. Chemical shifts are given in parts per million (ppm) and were measured relative to residual <sup>1</sup>H or <sup>13</sup>C resonance of the deuterated solvent.

In **Chapter 3**, **<sup>1</sup>H and <sup>13</sup>C NMR analyses** were performed on a Bruker Avance 300 spectrometer operating at 300 MHz for <sup>1</sup>H and 75 MHz for <sup>13</sup>C using a 5 mm BBO probe with a z-gradient coil, in CDCl<sub>3</sub> at room temperature, or in tetrachloroethylene/benzene-d<sub>6</sub> (2/1) (v/v) mixture at 363 K. A "zg30" pulse sequence was used. Chemical shifts are given in parts per million (ppm) and were measured relative to residual <sup>1</sup>H or <sup>13</sup>C resonance of the deuterated solvent.

**Cross Polarization/Magic Angle Spinning (CP/MAS) NMR (<sup>13</sup>C, <sup>15</sup>N)** analyses were performed on a Bruker Avance II 500 MHz spectrometer at 125 MHz for <sup>13</sup>C and 50 MHz for <sup>15</sup>N. The sample was packed into a 4-mm ZrO<sub>2</sub> rotor and rotated at magic angle spinning (MAS) rates of 10 kHz, using a conventional 4 mm HX probe. The sample was grinded into smaller pieces in order to achieve stable spinning of the NMR rotor. For CP MAS spectrum, transverse magnetization was obtained from <sup>1</sup>H using contact pulse duration of 2 ms, recycle delay of 5 s. SPINAL 64 <sup>1</sup>H decoupling was applied during acquisition. The chemical shifts were referenced to the TMS using adamantane as an external standard. All results shown have been recorded at room temperature at 10 kHz MAS spinning frequency.

**Differential Scanning Calorimetry (DSC)** experiments were conducted with a Mettler Toledo DSC 3+, calibrated with Indium and Zinc standards for temperature, heat flow and tau-lag. For all the experiments, aluminum capsules with a volume of 40  $\mu\text{L}$  and a sample weight of 5-10 mg were used. Measurements were carried out by two successive heating cycles (10  $^{\circ}\text{C}/\text{min}$ ). Melting and glass transition temperatures were recorded on the second cycle.

**Thermogravimetric analyses (TGA)** were performed on a Mettler Toledo TGA 2 between 20 and 700  $^{\circ}\text{C}$  under a stream of nitrogen at a constant heating rate of 10  $^{\circ}\text{C}/\text{min}$ . Samples of about 1–7 mg were weighed into 70  $\mu\text{L}$  alumina crucibles.

**Size-Exclusion Chromatography (SEC) analyses in THF** were performed using a Viscotek system (Malvern Instruments) including a four-capillary differential viscometer, a differential refractive index (RI) detector and a UV detector. THF was used as the mobile phase at a flow rate of 1  $\text{mL min}^{-1}$  at 35  $^{\circ}\text{C}$ . All samples were injected at a concentration of 3  $\text{mg}/\text{mL}$  after filtration through a 0.45  $\mu\text{m}$  PTFE membrane. The separation was carried out on three Polymer Standard Service columns (SDVB, 5  $\mu\text{m}$ , 300  $\times$  7.5 mm) and a guard column. The average molar masses (number-average molar mass,  $M_n$ , and weight-average molar mass,  $M_w$ ) and the dispersity,  $\mathcal{D} = M_w/M_n$ , were calculated from the RI signal with a calibration curve based on polystyrene standards (Polymer Standards Service).

**SEC analyses in 1,2,4-trichlorobenzene (1,2,4-TCB)** were performed using a Viscotek High-Temperature Triple Detection SEC (HT-SEC) system (Malvern Instruments). 1,2,4-Trichlorobenzene (TCB) was used as the mobile phase at a flow rate of 1  $\text{mL}/\text{min}$ . TCB was stabilized with 2,6-di(tert-butyl)-4-methylphenol. The separation was carried out on three mixed bed columns (PLgel Olexis 300  $\times$  7.8 mm from Malvern Instrument) and a guard column (75  $\times$  7.5 mm). Columns and detectors were maintained at 150  $^{\circ}\text{C}$ . Sample volumes of 200  $\mu\text{L}$  were analyzed at concentrations of 1  $\text{mg}/\text{mL}$ . The Omnisec software was used for data acquisition and data analysis. The molar mass distributions were calculated by means of a conventional calibration curve on the basis of linear polyethylene standards from 300 to 130 000  $\text{g mol}^{-1}$  (Polymer Standards Service).

**Tensile tests** were performed on a Shimadzu Autograph AGS at 23 °C using dumbbell specimens (section size: 5.4x2.0 mm). Crosshead speed was 10 mm/min. All the reported results for tensile determination are the average of five measurements at least.

**Charpy impact tests** were performed at 23 °C on a CEAST Resil Impactor Junior using notched specimens (75x10x4 mm, notch depth of 2 mm). All the reported results for Charpy impact strength determination are the average of five measurements at least.

**Scanning Electron Microscopy (SEM)** were performed with a FEI Quanta 250 electron microscope, the phase morphology was observed under high vacuum, the acceleration voltage was 10 kV. A flat surface of specimens was obtained with an ultramicrotome UC7 Leica at room temperature using an ultra-sonic diamond knife (Diatome). In order to contrast the two phases, the samples were soaked for 48 hours in a 50:50 water:sodium hypochlorite solution with 2 wt% of ruthenium tetroxide. The radius of the dispersed phase and its distribution was analyzed by the ImageJ software.

## II. General procedures

### II.1. [Chapter 2](#)

II.1.a. Carbonatation of [ethylene – glycidyl methacrylate] based copolymers in batch  
2.0 g of a [ethylene-glycidyl methacrylate] based polymer (1.1 mmol of glycidyl methacrylate), 18 mg of TBAB (0.056 mmol, 5 mol%) and 2.0 mL of toluene were added in a 0.16 L stainless steel reactor. The reactor was sealed, and then the mixture was stirred at 300 rpm and heated up to 110 °C. When the desired temperature was reached, 4.0 MPa of CO<sub>2</sub> was introduced. The mixture was stirred at 300 rpm and 110 °C for 5 hours. Finally, CO<sub>2</sub> was degassed, the medium was dried under vacuum and the resultant polymer was recovered without further purification. A cyclic carbonate moiety was obtained with a yield of 99 % according to <sup>1</sup>H NMR analysis (**Chapter 2**, [Table 1](#), entry 1).

### II.1.b. Carbonatation of [ethylene – glycidyl methacrylate] based copolymers in extruder

The [ethylene-glycidyl methacrylate] based polymer and the catalyst were fed at a throughput of 2 kg/h (1.1 mol/h of glycidyl methacrylate) and 0.083 mol/h (7.5 mol%) respectively in the first barrel. Under optimal conditions, the temperatures were 60, 120, 150, 150, 150, 150, 150, 150 and 150 °C, respectively. The die was also heated to 150 °C. The screw speed was 150 rpm. When the flow of the extruded polymer was stabilized, CO<sub>2</sub> was continuously injected into the third barrel using a Linde pump (DSD 500). The pressure and the throughput were regulated by the pump. The resulting modified polymer had a stable composition after a time equal to twice the residence time, and thus it was collected from this moment, cooled with compressed air and pelletized by a pelletizer.

## II.2. Chapter 3

### II.2.a. Epoxidation of polydienes in batch

In a typical procedure for the epoxidation of polybutadiene **PBU-1**, 5.0 g of **PBU-1** and 5.0 mL of toluene were heated to 50 °C and stirred at 600 rpm in a round bottom flask. When the temperature reached 50°C and the reaction medium was homogenous, formic acid (10 mol% according to butadiene units) and hydrogen peroxide 30 % (10 mol% according to butadiene units) were added. The reaction medium was stirred at 50 °C for 6 hours and the polymer was dried at 50 °C under vacuum overnight. The epoxide content was determined by <sup>1</sup>H NMR analysis.

In the case of epoxidation of high molar mass polybutadiene or copolymers containing dienes units, similar conditions were used, but the polymer concentration was reduced to decrease the solution viscosity, and the amount of oxidant was adapted to the diene contents. At the end of the reaction, acetone was added to make precipitated the polymer, and it was filtered, washed with acetone and dried under vacuum at 50°C overnight.

### II.2.b. Epoxidation of polybutadiene in reactive extrusion

Polybutadiene E-PBU-4 was fed at a throughput of 350 g/h in the 5<sup>th</sup> barrel. The temperature was 60 °C and the screw speed was 100 rpm. When the flow of the extruded polymer was stabilized, A stoichiometric mixture of peroxide hydrogen 30 %/ formic acid was injected into the 7<sup>th</sup> barrel using a pump at a flow of 1.5 mL/min (10 mol% according to butadiene units).

After 10 min, the polymer was recovered and analyzed by  $^1\text{H}$  NMR to determine epoxide content.

### II.2.c. Carbonatation of epoxidized polydienes in batch

In a typical procedure, 1.0 g of epoxidized polydiene, tetraoctylammonium bromide (TOAB, 5 mol% according to epoxide content) and 1.0-5.0 mL of toluene were added in a 0.16 L stainless steel reactor. The reactor was sealed, and then the mixture was stirred at 300 rpm and heated up to 110 °C. When the desired temperature was reached, 4.0 MPa of  $\text{CO}_2$  was introduced. The mixture was stirred at 300 rpm and 110 °C for 6 hours. Finally,  $\text{CO}_2$  was degassed, the medium was dried under vacuum and the resultant polymer was recovered without further purification. The cyclic carbonate moiety yield was determined by  $^1\text{H}$  NMR analysis.

## II.3. Chapter 4

### II.3.a. Aminolysis of carbonated ethylene-glycidyl methacrylate-methyl acrylate terpolymer

In a typical procedure, 5.0 g of carbonated [ethylene-glycidyl methacrylate-methyl acrylate terpolymer], 30 mL of toluene and TBD (5 mol% according to cyclic carbonate units) were stirred and heated to 90 °C in a round bottom flask. Then, 5 equivalents (according to cyclic carbonate units) of hexylamine were added. Samples were taken every hour, the samples were precipitated with acetone, filtered, washed with acetone and dried under ambient conditions, and the decreased of the cyclic carbonate contents was followed by IR-ATR. The reaction was stopped after complete disappearance of the cyclic carbonate band ( $1821\text{ cm}^{-1}$ ) on the IR-ATR spectra. At the end of the reaction, the polymer was precipitated with acetone, filtered, washed with acetone and dried under vacuum at 50 °C overnight.

### II.3.b. Kinetic study of aminolysis reaction monitored by $^1\text{H}$ NMR

In a 5 mm NMR tube, 58.8 mg of carbonated polybutadiene (3 mol% of cyclic carbonate, 7 mol% of epoxide) 0.5 mL of tetrachloroethylene/benzene- $\text{d}_6$  (2/1) (v/v) mixture, 7.0  $\mu\text{L}$  of mesitylene, and 1.4 mg of TBD (30 mol% according to cyclic carbonate content) were added. Then, 20  $\mu\text{L}$  of hexylamine (5 equiv. according to cyclic carbonate units) were added. The NMR tube was introduced into the NMR spectrometer and heated to 90 °C. When the temperature was stabilized,  $^1\text{H}$  NMR spectra were recorded (16 scans) every 30 min for 16 hours.

### II.3.c. Cross-linking of carbonated polybutadiene with hexamethylene diamine

500 mg of carbonated polybutadiene (24 mol% of cyclic carbonate, 12 mol% of epoxide) and 105 mg of hexamethylene diamine (1 equiv of amine function according to cyclic carbonate and epoxide units) were mixed at room temperature in chloroform. The solvent was evaporated at room temperature and the mixture was cured at 90 °C for 16 hours.

## II.4. Chapter 5

### II.4.a. Preparation of HDPE/PC/compatibilizer (72/18/10) (w/w/w) blends by twin-screw extrusion

The PC resin was dried prior blending with a polymer dryer at 80 °C overnight. The different blends were formulated by melt-blending in a co-rotating twin-screw extruder (Leistritz ZSE18HPE-60D model, diameter 18 mm, L/D = 60). The HDPE, PC and compatibilizer were feed at a total throughput of 3.0 kg/h in a weight proportion of 72/18/10 or 18/72/10 in the first barrel. The blends were extruded at 250 °C with a screw speed of 400 rpm. The extruded blends were cooled down in a water bath at room temperature, pelletized and dried under vacuum at 80 °C overnight.

### II.4.b. Extraction of the PC phase from the HDPE/PC/compatibilizer blends

The PC phases were extracted from the pellet blends with dichloromethane using a Soxhlet extractor for 24 hours at reflux temperature. The solvent was evaporated with a rotary evaporator, and the polymer obtained was dried under vacuum for at least 6 hours.



---

# Chapter 1:

## Literature review on the carbonatation reaction, from molecular synthesis to polymers functionalization

---

**Chapter 1** is a literature review on the reactivity of epoxides and alkenes with CO<sub>2</sub> to synthesize cyclic carbonates. An overview of the common catalytic systems used for the carbonatation of molecular epoxides and the oxidative carbonatation of molecular alkenes will be presented, as well as the main strategies for the synthesis of carbonated polymers (*i.e.* polymers containing cyclic carbonate moieties).





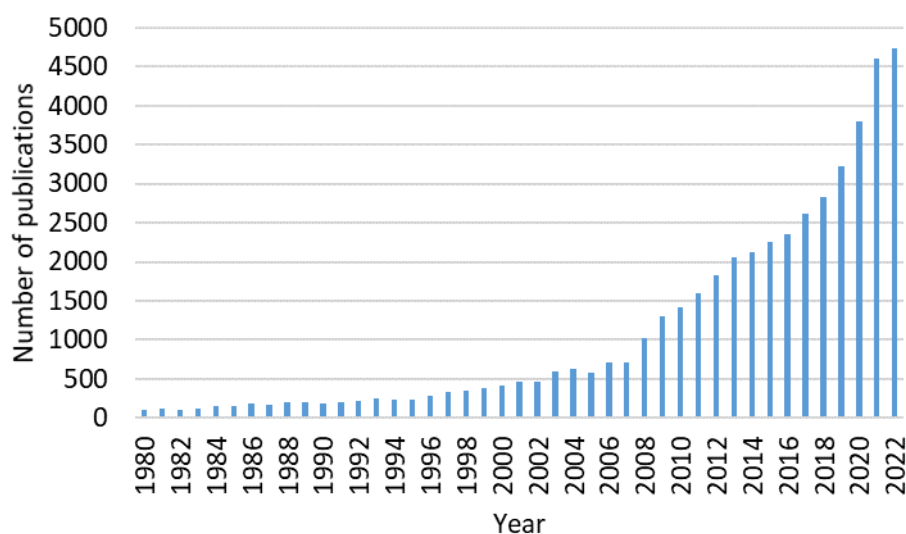
## Table of Contents

<b>I. Introduction.....</b>	<b>27</b>
<b>II. Carbonation of molecular compounds .....</b>	<b>30</b>
II.1. Onium salts as nucleophilic catalysts for the carbonation of epoxides .....	30
II.1.a. Catalytic cycle mechanism.....	30
II.1.b. Reactivity with terminal epoxides.....	31
II.1.c. Reactivity with disubstituted epoxides .....	40
II.1.d. Reactivity of trisubstituted and tetrasubstituted epoxides.....	43
II.2. Carbonation of epoxides with hindered nucleophilic catalysts .....	47
II.2.a. Catalytic cycle mechanism.....	47
II.2.b. Influence of the base structure .....	48
II.3. Acidic co-catalysts.....	51
II.3.a. Lewis acids.....	51
II.3.b. Brønsted acids .....	57
II.4. Oxydative carbonation of alkenes in one-pot.....	59
<b>III. Carbonation of polymers.....</b>	<b>65</b>
III.1. Carbonation of glycidyl methacrylate based copolymers.....	65
III.1.a. Effect of the reaction conditions.....	66
III.1.b. Effect of the polymer structure.....	70
III.1.c. Polymerisation and carbonation of GMA in one-pot.....	72
III.1.d. Self-catalyzed carbonation of GMA based copolymers containing ammonium salts moieties .....	74
III.1.e. Use of the carbonated GMA based polymers in polymer blends.....	75
III.1.f. Influence of DOMMA content on the thermal properties.....	75
III.2. Carbonation of epoxidized polydienes.....	76
III.2.a. Two-steps oxidative carbonation of polybutadienes.....	76
III.2.b. Carbonation of epoxidized natural rubbers .....	79

<b>IV. Conclusions of the review and objectives of this thesis .....</b>	<b>80</b>
<b>V. References .....</b>	<b>82</b>

## I. Introduction

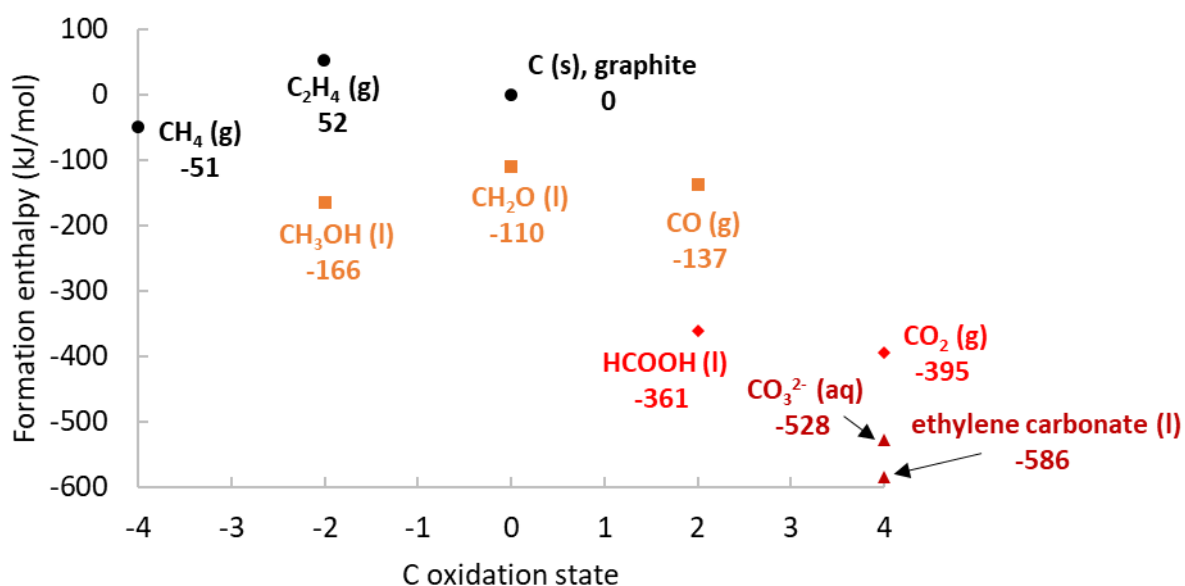
The anthropogenic carbon dioxide emissions are following an exponential growth since the First Industrial Revolution starting at the end of the XVIII<sup>th</sup> century, which has a significant impact on climate change.<sup>[1]</sup> In 2019, the production of energy was the sector that emitted the most of CO<sub>2</sub> (15.83 GtCO<sub>2</sub>), followed by the transport (8.43 GtCO<sub>2</sub>), manufacturing & construction (6.30 GtCO<sub>2</sub>) and agriculture sectors (5.79 GtCO<sub>2</sub>).<sup>[2]</sup> The industry sector emitted 3.06 GtCO<sub>2</sub>,<sup>[2]</sup> mainly from the production of mineral (e.g. cement, lime, glass), chemical (e.g. ammonia, nitric acid, adipic acid) and metal products.<sup>[3]</sup> In this context, the valorization of CO<sub>2</sub> into molecules and materials platforms has been a subject of great interest over the last decades. Since 1980, the number of publications for the chemical conversion of CO<sub>2</sub> has increased exponentially (*Figure 1*). Indeed, CO<sub>2</sub> is recognized as environmentally benign, inexpensive, and an abundant renewable C1 building block, which could be beneficially utilized in the development of organic synthetic transformations to produce value-added molecules.



*Figure 1. Number of publications obtained with the keywords “conversion” and “carbon dioxide” on SciFinder<sup>m</sup>.*

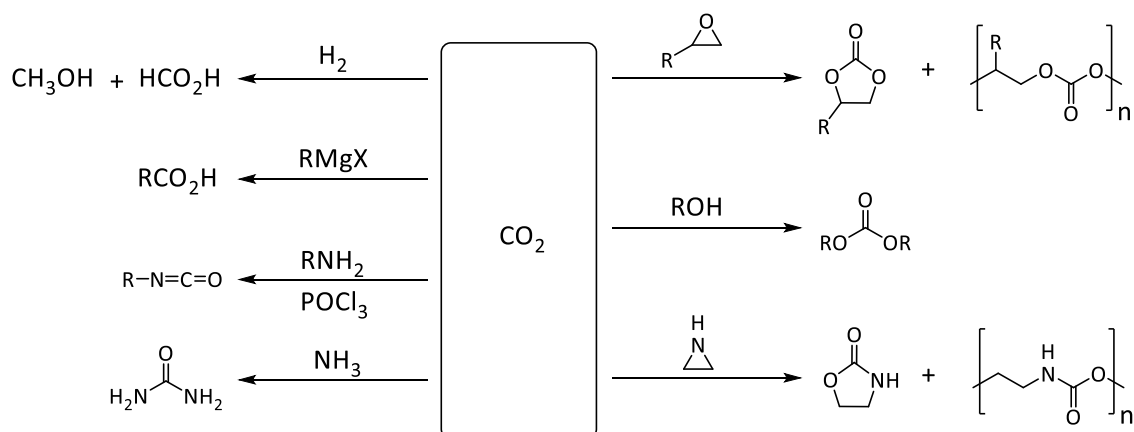
However, carbon dioxide is the carbon source with one of the lowest formation enthalpy (- 395 kJ/mol) and the highest oxidation state, thus it has a high thermodynamic stability.<sup>[4]</sup> Therefore, four main strategies have been developed to activate the CO<sub>2</sub> molecule for use as reagent<sup>[5]</sup>:

- Using high-energy co-reactants such as epoxides, H<sub>2</sub>, NH<sub>3</sub>, unsaturated molecules, organometallic complexes or small cyclic compounds.
- The synthesis of oxidized compounds with low formation energy could be targeted (e.g. organic and inorganic carbonates). As shown in *Figure 2*, at a constant carbon oxidation state, the addition of an oxygen atom significantly reduces the enthalpy of formation, thus carbonate compounds have lower formation enthalpy than CO<sub>2</sub>.<sup>[4,6]</sup>
- Shifting the equilibrium with the release of a by-product.
- Supplying physical energy such as electricity or light to overcome the energy barrier.



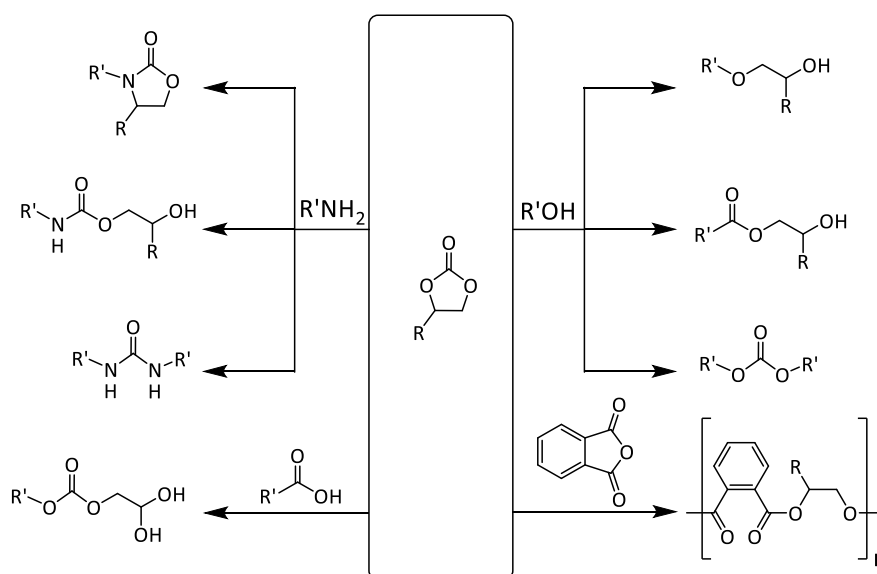
*Figure 2. Formation enthalpy depending on the carbon oxidation state and the number of oxygen atoms in the molecules.*<sup>[4,6]</sup>

By using these strategies, different valorizable molecules and materials can be synthesized from CO<sub>2</sub> (*Scheme 1*). Currently, urea, methanol, ethylene carbonate and polycarbonate are produced industrially from CO<sub>2</sub>,<sup>[5]</sup> but other compounds of interest such as carboxylic acids, isocyanates, linear carbonates, cyclic carbamates and polyurethanes could also be obtained.



*Scheme 1. Main reactions involving CO<sub>2</sub> as reagent.<sup>[5]</sup>*

Particularly, cyclic carbonates are subject of a great interest due to their reactivity and physico-chemical properties. Cyclic carbonates are precursors for a wide range of compounds: hydroxyurethanes, cyclic carbamates, ureas, linear carbonates, ethers and esters derivatives (*Scheme 2*).<sup>[7]</sup> Thanks to their polarity, they are also used as solvent<sup>[8]</sup> and electrolytes for batteries.<sup>[9]</sup>



*Scheme 2. Main reactions using cyclic carbonates as reagents.<sup>[7]</sup>*

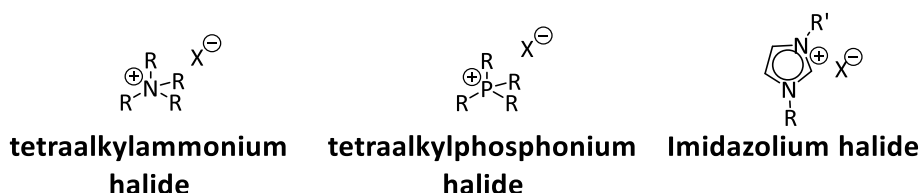
In this chapter, we will focus on the synthesis of cyclic carbonates, in a first part on molecular compounds (from epoxides and alkenes), in order to understand the influence of the substrate and catalyst structural features, as well as on the different reaction parameters at play in this type of transformation. Then the carbonation of polymers will be discussed, in order to understand how the chemical use of CO<sub>2</sub> as a C1 block could be transposed to the modification of macromolecules.

## II. Carbonatation of molecular compounds

The synthesis of cyclic carbonates *via* the cycloaddition of CO<sub>2</sub> with epoxides requires the use of a nucleophilic catalyst, which either opens the epoxide ring (unhindered nucleophiles, typically halide anions I<sup>-</sup>, Br<sup>-</sup> and Cl<sup>-</sup>), or activates the CO<sub>2</sub> molecule to form a carboxylate (hindered nucleophiles with a delocalized negative charge: 1,5,7-triazabicyclo[4.4.0]dec-5-ene (TBD), 1,8-Diazabicyclo[5.4.0]undec-7-ene (DBU), BF<sub>4</sub><sup>-</sup>, PF<sub>6</sub><sup>-</sup>). The reactivity of epoxides is usually enhanced by the introduction of a Lewis acid (metal complexes such as metal halide, metal – salen and metal - porphyrin complexes) or a Brønsted acid (polyphenols, fluorinated alcohols, guanidines, carboxylic acids).

### II.1. Onium salts as nucleophilic catalysts for the carbonatation of epoxides

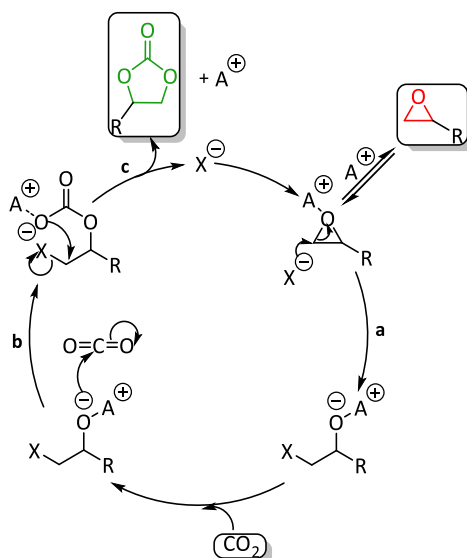
The use of onium salts such as ammonium salts (R<sub>4</sub>N<sup>+</sup>X<sup>-</sup>, X = Cl, Br or I), phosphonium (R<sub>4</sub>PX) and imidazolium (C<sub>x</sub>C<sub>y</sub>ImX) is widely reported in the literature as catalyst allowing the opening of the oxirane ring (*Scheme 3*).<sup>[7,10,11]</sup> The hindrance of the R<sub>4</sub>N<sup>+</sup>, R<sub>4</sub>P<sup>+</sup> and C<sub>x</sub>C<sub>y</sub>Im<sup>+</sup> cations makes it possible to decrease the electrostatic interactions with the X<sup>-</sup> anion and thus increase its nucleophilicity. The X<sup>-</sup> anion must also be a good leaving group to promote the formation of the cyclic carbonate.



*Scheme 3. Structure of onium salts.*

#### II.1.a. Catalytic cycle mechanism

In this route, the nucleophile attacks the less hindered carbon atom of the epoxide, to form the alkoxide anion (*Scheme 4*, step **a**), which subsequently activates the CO<sub>2</sub> molecule to form the corresponding linear carbonate (*Scheme 4*, step **b**). Finally, the cyclic carbonate is formed by an intramolecular ring-closure, leading to the regeneration of the halide based catalyst (*Scheme 4*, step **c**).<sup>[12]</sup>

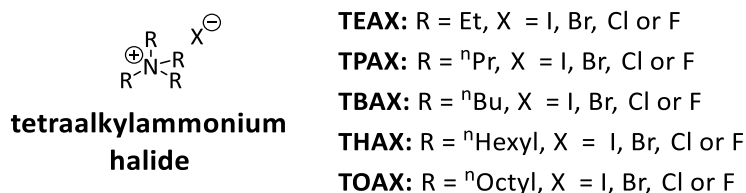


*Scheme 4. Catalytic cycle for the carbonatation of epoxides with halides.<sup>[13]</sup>*

As mentioned before, a selected Lewis acid (designed metal-based complexes),<sup>[14–26]</sup> Brønsted acid (hydrogen bond organic donor)<sup>[27–31]</sup> or bifunctional activator  $A^+$  could be used in conjunction with the nucleophilic catalyst to synergistically activate the epoxide and stabilize the different intermediates.

### II.1.b. Reactivity with terminal epoxides

Ammonium halide salts are among the first catalysts used for the production of cyclic carbonates from  $CO_2$  and epoxides (*Scheme 5*). In 1956, Lichtenwalter and Cooper showed that tetrabutylammonium bromide (TBAB) and tetraethylammonium bromide (TEAB) could catalyze the carbonatation of ethylene oxide,<sup>[32]</sup> and were more active than the catalyst previously used (sodium hydroxide on activated charcoal), and were commercially available.<sup>[33]</sup> The influence of the structure of these salts (nature of the anion and alkyl chain, steric hindrance, and addition of acidic functions) have since been widely studied in the literature.



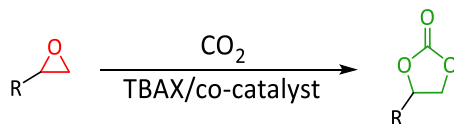
*Scheme 5. Structure of tetraalkylammonium halides.*



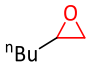
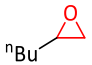
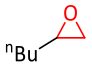
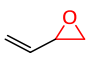
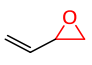
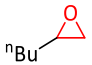
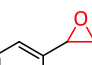
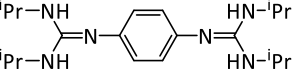
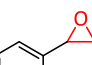
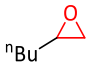
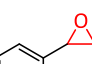
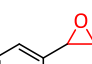
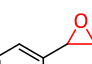
The halide with the best catalytic activity for the formation of cyclic carbonates depends on the nature of the epoxide. The following order of catalytic activity has been commonly observed:  $\text{I}^- > \text{Br}^- > \text{Cl}^- > \text{F}^-$  when the reaction is carried out on terminal, low sterically hindered epoxides under neat conditions (*Table 1*). This order of activity is not altered by the addition of an electron donor or withdrawing substituent and by the change of the reaction conditions, *i.e.* change of pressure, temperature or nature of the co-catalyst. This order coincides with the order of nucleophilicity and size of the halides. In this case,  $\text{I}^-$  is the most nucleophilic anion and the best leaving group, thus it is the most active halide.<sup>[12,16,22,30,31,34-36]</sup>

However, the electronic effect of the substituent impacts the reactivity of the epoxide. Electron withdrawing groups activate the epoxide *via* inductive effect, whereas electron donor groups decrease the electrophilicity of the epoxide. In *Table 1*, the reaction conditions tend to be harsher with epoxides containing electron donor substituents. Under the same conditions (*Table 1*, entries 4, 5, 12, 13, 17, 18), a decrease of the cyclic carbonate yield was observed by increasing the electron donor ability of the substituent.

Table 1. Effect of the halide on the carbonatation of terminal epoxides under neat conditions.



Entry	Epoxide	Catalyst (mol%)	Lewis acid / Brønsted acid (mol%)	T (°C)	P (MPa)	t (h)	Selectivity (%)	Yield (%)	Ref.
1		TBAI (5)						92	
2		TBAB (5)	2-pyridinemethanol (5)	25	0.1	24	Not reported	67	[34]
3		TBAC (5)						52	
4		TBAI (5)	[Fe(TPhOA)] <sub>2</sub> (0.5)	25	0.2	18	> 99	83	[36]
5		TBAB (5)					> 99	76	
6		TBAI (5)					98	76	
7		TBAB (5)	3-BTFP (5)	35	0.5	24	99	61	[31]
8		TBAC (5)					99	47	
9		TBAI (2)					> 99	83	
10		TBAB (2)	Zn <sub>4</sub> (OCOCF <sub>3</sub> ) <sub>6</sub> O (1.0)	25	0.1	6	99	73	[22]
11		TBAC (2)					90	27	
12		TBAI (5)	[Fe(TPhOA)] <sub>2</sub> (0.5)	25	0.2	18	> 99	74	[36]
13		TBAB (5)					> 99	65	

Entry	Epoxide	Catalyst (mol%)	Lewis acid / Brønsted acid (mol%)	T (°C)	P (MPa)	t (h)	Selectivity (%)	Yield (%)	Ref.
14		TBAI (5)						95	
15		TBAB (5)	3-hydroxypyridine (5.0)	40	0.1	24	Not reported	82	[35]
16		TBAC (5)						36	
17		TBAI (5)					> 99	70	
18		TBAB (5)	[Fe(TPhOA)] <sub>2</sub> (0.5)	25	0.2	18	> 99	62	[36]
19		TBAI (2)					> 99	92	
20		TBAB (2)		70	0.1	24	> 99	69	[30]
21		TBAC (2)					> 99	40	
22		TBAF (2)					> 99	3	
23		TBAI (0.3)					> 99	54	
24		TBAB (0.3)	ZnBr <sub>2</sub> (0.3)	80	8	0.5	> 99	34	[16]
25		TBAC (0.3)					> 99	26	

However, under certain conditions, the physico-chemical properties of the catalyst can play an essential role. For example, in the case of the carbonation of styrene oxide with tetrabutylammonium halides (TBAX), the homogeneity of the system will depend on the solubility of the catalyst, which itself depends on the nature of the anion. In this case, Shim *et al.* observed the following order of activity:  $\text{Br}^- > \text{Cl}^- > \text{I}^-$  because TBAB exhibited a greater solubility than TBAC and TBAI under the reaction conditions (2 mol% of catalyst, 120 °C, 3.9 MPa, neat, 2 h).<sup>[37]</sup>

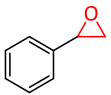
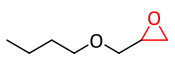
The stability of the ammonium salt obviously plays a role on its catalytic activity and varies according to the nature of the anion. For example, J.-Q. Wang *et al.* obtained the following order of activity:  $\text{Br}^- > \text{I}^- \approx \text{Cl}^- > \text{F}^-$  for the carbonation of propylene oxide with TBAX. This partly respects the order of nucleophilicity and size of the halides, except for  $\text{I}^-$ , which showed a lower activity than  $\text{Br}^-$  because of its lower stability under the reaction conditions according to the authors (150 °C, 8 MPa, 10 h).<sup>[38]</sup>

In the case where the epoxide is more sterically hindered, the halide must have a limited steric hindrance to access the electrophilic site. In this case, the effect of steric hindrance predominates over the nucleophilicity of the anion, which explains why  $\text{Br}^-$  or  $\text{Cl}^-$  are more active catalysts than  $\text{I}^-$  for the carbonation of 3,3-dimethyl-1,2-epoxybutane (terminal epoxide with a *ter*-butyl group) and butyl glycidyl ether.<sup>[36,39]</sup> In all cases,  $\text{F}^-$  was found the least active due to its poor leaving group ability.<sup>[38,40-42]</sup>

The length of the alkyl chains of the ammonium salt also has an influence on its catalytic performance (*Table 2*). Sun *et al.* have shown that increasing the length of the alkyl chains makes the ammonium cation bulkier, and thus decreases the interaction strength between the cation and the halide anion rendering the halide more nucleophilic. This explains the following order of activity : THAB > TBAB > TEAB obtained for the carbonation of styrene oxide with  $\text{ZnBr}_2$  as co-catalyst (*Table 2*, entries 1-3).<sup>[16]</sup>

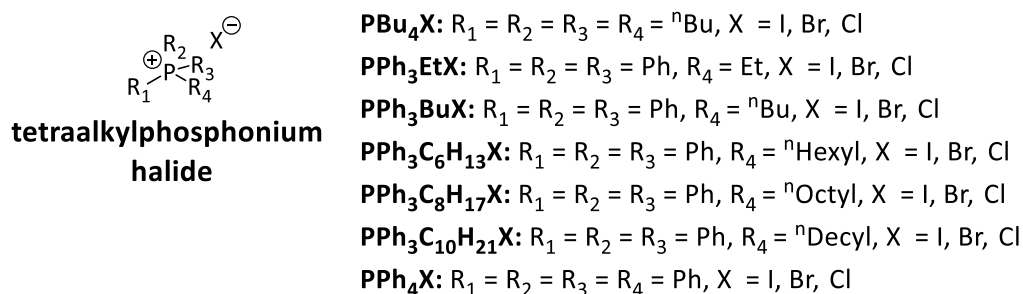
The same THAC > TBAC > TPAC trend was obtained for the carboxylation of glycidyl butyl ether (*Table 2*, entries 4-6). On the other hand, TOAC showed a slightly lower catalytic activity because of the instability of the intermediate formed after the opening of the epoxide ring by  $\text{Cl}^-$  (*Table 2*, entry 7). Indeed, the steric hindrance of the  $\text{TOA}^+$  cation is too important for the formation/stabilization of this intermediate.<sup>[39]</sup>

Table 2. Effect of the ammonium alkyl chains on the carbonatation of terminal epoxides.<sup>a</sup>

Entry	Epoxide	Catalyst	Lewis acid	T (°C)	P (MPa)	t (h)	Selectivity (%)	Conv. (%)	Ref.
1		TEAB					> 99	0.4	
2		TBAB	ZnBr <sub>2</sub>	80	0.8	0.5	> 99	37	[16]
3		THAB					> 99	41	
4		TPAC						78.5	
5		TBAC					Not reported	79.6	
6		THAC	-	100	0.9 <sup>a</sup>	6	Not reported	81.4	[39]
7		TOAC						77.9	

<sup>a</sup>CO<sub>2</sub> pressure at 25 °C, neat. E = ethyl, P = propyl, B = butyl, H = hexyl and O = octyl.

Phosphonium salts (*Scheme 6*) are analogue to ammonium salts. The main advantage of their use is their very good thermal stability, better than that of ammonium salts.<sup>[43]</sup>



*Scheme 6. Structure of tetra(alkyl/phenyl)phosphonium halides.*

As seen previously with ammonium salts, the order of activity of the phosphonium salt halide is as follows for weakly hindered terminal epoxides: I<sup>-</sup> ≥ Br<sup>-</sup> > Cl<sup>-</sup>.<sup>[44,45]</sup> For the carbonatation of propylene oxide using PPh<sub>3</sub>BuX/ZnCl<sub>2</sub> catalytic system, yields of 95.1 %, 95.0 % and 67 % were achieved with I<sup>-</sup>, Br<sup>-</sup> and Cl<sup>-</sup> as counter-anions, respectively (*Table 3*, entries 1-3). With the PPh<sub>4</sub>X/ZnBr<sub>2</sub> system, a similar trend was observed with yield of 89.6 %, 82.4 % and 48.4 % respectively for I<sup>-</sup>, Br<sup>-</sup> and Cl<sup>-</sup> anions (*Table 3*, entries 8-10). A drop in yield was

observed with  $\text{Cl}^-$  with both catalyst systems due to the lower dissociation of  $\text{Cl}^-$  with the cation according to the authors.

As seen previously, the increase in the bulkiness of the cation makes it possible to reduce the electrostatic interactions between the cation and the halide and, in turn, to improve the nucleophilicity of the halide.<sup>[44,45]</sup> This can be done either by increasing the length of the alkyl chains,<sup>[44]</sup> or by replacing the alkyl chains with bulkier groups such as the phenyl group.<sup>[45]</sup>

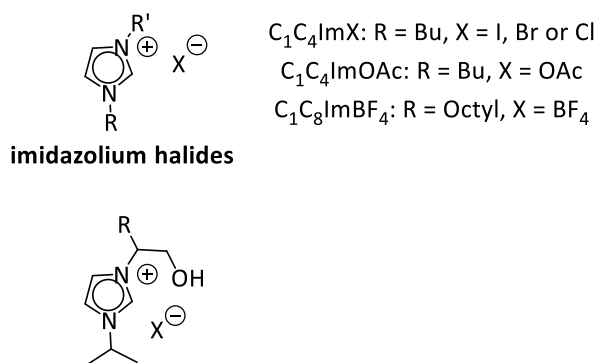
For the  $\text{PPh}_3\text{RX}/\text{ZnCl}_2$  catalytic system, the yield increased when the alkyl chain length increased, and reached 98.5 % with decyl chains (*Table 3*, entries 1, 4-7). Finally, with  $\text{PPh}_4\text{-yR}_y\text{X}/\text{ZnBr}_2$  system, the presence of phenyl groups increased the activity of the catalyst, and the highest yield (82.4 %) was obtained with  $\text{PPh}_4\text{Br}$ , (*Table 3*, entries 9, 11, 12).

Table 3. Carbonatation of propylene oxide using phosphonium halides under neat conditions.

Entry	Catalyst	Lewis acid (mol%)	T (°C)	P (MPa)	t (h)	Selectivity (%)	Yield (%)	Ref.
1 <sup>a</sup>	PPh <sub>3</sub> BuI					> 99	95.1	
2 <sup>a</sup>	PPh <sub>3</sub> BuBr					> 99	95.0	
3 <sup>a</sup>	PPh <sub>3</sub> BuCl					> 99	67.0	
4 <sup>a</sup>	PPh <sub>3</sub> EtBr	ZnCl <sub>2</sub> (0.02)	120	1.5	1	> 99	93.0	[44]
5 <sup>a</sup>	PPh <sub>3</sub> C <sub>6</sub> H <sub>13</sub> Br					> 99	96.0	
6 <sup>a</sup>	PPh <sub>3</sub> C <sub>8</sub> H <sub>17</sub> Br					> 99	97.1	
7 <sup>a</sup>	PPh <sub>3</sub> C <sub>10</sub> H <sub>21</sub> Br					> 99	98.5	
8 <sup>b</sup>	PPh <sub>4</sub> I					> 99	89.6	
9 <sup>b</sup>	PPh <sub>4</sub> Br					> 99	82.4	
10 <sup>b</sup>	PPh <sub>4</sub> Cl	ZnBr <sub>2</sub> (0.09)	120	2.5	1	> 99	48.4	[45]
11 <sup>b</sup>	<sup>n</sup> Bu <sub>4</sub> PBr					> 99	56.6	
12 <sup>b</sup>	PPh <sub>3</sub> C <sub>6</sub> H <sub>13</sub> Br					> 99	77.4	

<sup>a</sup>0.1 mol% of catalyst. <sup>b</sup>0.01 mol% of catalyst.

Ionic liquids such as imidazolium halides were also investigated as organocatalysts for the carbonation of epoxides (*Scheme 7*).



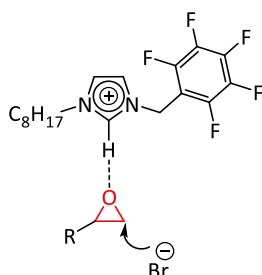
*Scheme 7. Structure of common imidazolium salts used as catalysts.*

These ionic liquids are known to be good solvent for  $CO_2$  and therefore appeared as a good medium for epoxide carbonation. In most of the studies, imidazolium salts are functionalized, supported or used with metal halide co-catalysts, to enhance their reactivity.<sup>[10,46]</sup> As seen before, the catalytic activity depends on the nature of the halide and of the cation. For terminal epoxides, the catalytic activity is still following the nucleophilicity and the leaving group ability of the halide under neat conditions:  $I^- \geq Br^- > Cl^-$ .<sup>[47-50]</sup> Girard *et al.*<sup>[48]</sup> showed that  $C_1C_4ImI$  and  $C_1C_4ImBr$  were the best imidazolium catalysts for the conversion of styrene oxide, a 99 % yield was obtained with both catalysts under the following conditions : 5 bar of  $CO_2$ , 10 mol% of catalyst at 150 °C under neat conditions for 4 hours. The use of  $C_1C_4ImCl$  led to a lower selectivity of 46 % due to the poor leaving group ability of the chloride anion.

The alkyl chains R and R' length also has a strong influence on reactivity. As seen before, an optimum has to be determined for the length of the alkyl chains. Denizaltı<sup>[49]</sup> studied the influence of alkyl groups on imidazolium bromide bearing hydroxyl group. The catalytic activity increased in the following order: ethyl < hexyl  $\approx$  octyl  $\approx$  decyl < butyl for the conversion of propylene oxide with 2 mol% of catalyst at 60 °C under 1.0 MPa of  $CO_2$  and neat conditions after 3 hours. From ethyl to butyl, the yield increased from 46 to 70 %, but then decreased from butyl to hexyl to 60 %. Similar yield was obtained with hexyl, octyl and decyl alkyl groups. The introduction of hydrogen bond donor groups such as hydroxyl and carboxyl improved significantly the reactivity, compared to non-functionalized imidazolium halides<sup>[47,51]</sup>. For example, Sun *et al.*<sup>[51]</sup> showed for the carbonation of propylene oxide (1.6 mol% of catalyst, 125 °C, 2.0 MPa, 1 h, neat) that the addition of hydroxyl group on  $C_1C_2ImBr$  increased the yield from 83 to 99 %.



Imidazolium cations are also hydrogen bond donors, the introduction of electron-withdrawing substituents such as pentafluorobenzyl groups increases the protons acidity and thus improves the hydrogen bond donor ability of the imidazolium cation (*Scheme 8*).<sup>[52,11]</sup> For the carbonatation of propylene oxide, the yield increased from 73 to 91 % when the benzyl group was replaced by the fluorinated derivative (Conditions: 10 mol% of catalyst, 4 bar, 70 °C, 22 h, neat).<sup>[52]</sup>



*Scheme 8. Activation of the epoxide with imidazolium bromide bearing pentafluorobenzyl group.*

### II.1.c. Reactivity with disubstituted epoxides

The carbonatation of internal disubstituted epoxides requires the use of harsher conditions, or more active co-catalysts, because of their lower reactivity. Days-long reaction time, high temperature (more than 120 °C), elevated CO<sub>2</sub> pressure or large catalyst content are needed to obtain satisfying yields.<sup>[48,53-55]</sup> The common systems used are onium salts in combination with an acidic co-catalyst (metal halides, metallic complexes, polyoxometalates). More specific systems such as the multicomponent CaI<sub>2</sub>/crown ether/Ph<sub>3</sub>P catalytic system that provides stereochemical selectivity under mild conditions (45 °C, 0.5 MPa) can be used. In the following paragraphs, a focus will be done on ammonium halides catalysts for their good reactivity and solubility in both polar and poorly polar media, and on the carbonatation of epoxidized oils, as they are convenient molecular model for further carbonatation of epoxidized polymers.

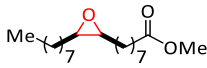
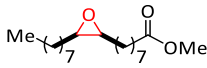
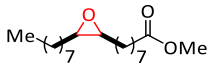
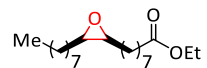
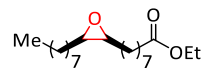
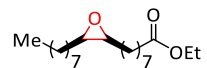



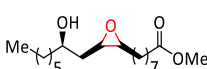
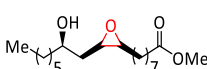
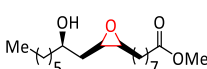



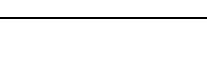
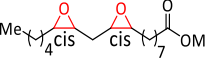
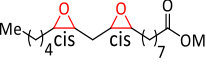
Unlike the carbonatation of terminal epoxides that is optimal with TBAI in most of the cases under neat conditions, disubstituted epoxides are usually carbonated with TBAB.<sup>[55-61]</sup> when no co-catalyst is used. TBAC and PPnCl also showed good activity when used with acid co-catalysts such as ascorbic acid<sup>[62]</sup> or aluminium complexes.<sup>[24]</sup>

Fei Chen *et al.*<sup>[58]</sup> compared the influence of the halide for the carbonatation of different epoxidized oils with TBAX/iron complex catalytic systems. TBAB was the best nucleophilic

## Chapter 1: Literature review on the carbonation reaction

catalyst (*Table 4*), with a yield range of 66-92 %, except for the carbonation of methyl linoleate (*Table 4*, entries 17-19), where TBAI and TBAC showed a better activity.

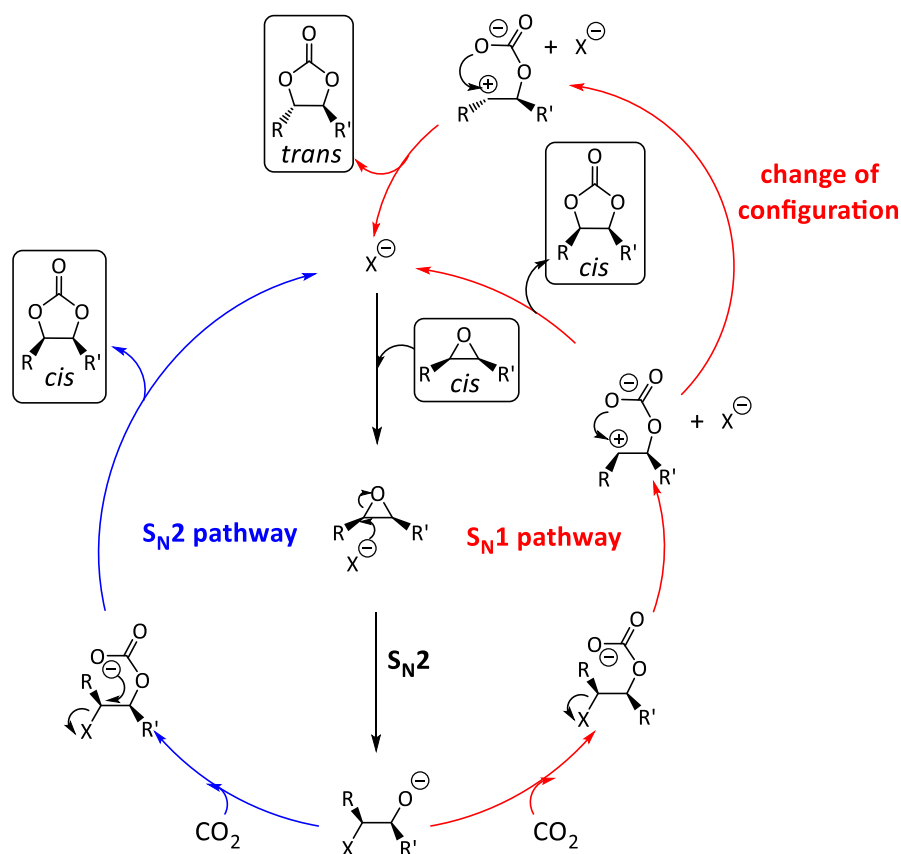
*Table 4. Effect of the halides on the carbonation of epoxidized oils.<sup>a</sup> [58]*

Entry	Epoxidized oils	Catalyst	Yield (%)	<i>Cis:trans</i> ratio
1 <sup>b</sup>		TBAI	75	< 1:99
2 <sup>b</sup>		TBAB	85	15:85
3 <sup>b</sup>		TBAC	72	76:24
5 <sup>c</sup>		TBAI	83	< 1:99
6 <sup>c</sup>		TBAB	92	< 1:99
7 <sup>c</sup>		TBAC	85	96:4
8 <sup>c</sup>		TBAI	73	15:85
9 <sup>c</sup>		TBAB	88	< 1:99
10 <sup>c</sup>		TBAC	87	> 99:1
11 <sup>c</sup>		TBAI	43	<1:99
12 <sup>c</sup>		TBAB	66	<1:99
13 <sup>c</sup>		TBAC	60	> 99:1
14 <sup>c</sup>		TBAI	78	17:83
15 <sup>c</sup>		TBAB	81	11:89
16 <sup>c</sup>		TBAC	79	7:93
17 <sup>c</sup>		TBAI	84	16:84
18 <sup>c</sup>		TBAB	70	25:75
19 <sup>c</sup>		TBAC	77	85:15

<sup>a</sup>100 °C, 0.5 MPa, 24 h, neat. <sup>b</sup>6 mol% of catalyst and 0.6 mol% of co-catalyst. <sup>c</sup>10 mol% of catalyst and 1 mol% of co-catalyst.

Moreover, the nature of the halide has an influence on the *cis/trans* ratio of the cyclic product. With large halides (I<sup>-</sup> and Br<sup>-</sup>), the formation of the *trans* cyclic carbonate was favored, whereas with the small halide Cl<sup>-</sup>, the product kept the initial configuration of the epoxide.

This difference of stereoselectivity could be explained by considering the mechanism of the intramolecular nucleophilic substitution during the formation of the cyclic carbonate (*Scheme 9*). With Br<sup>-</sup> and I<sup>-</sup>, a S<sub>N</sub><sup>1</sup> pathway occurs during the intramolecular attack. During this step, a change of the configuration is possible, and the *trans* formation product is favoured because of its higher thermodynamic stability. Conversely, a S<sub>N</sub><sup>2</sup> pathway occurs with Cl<sup>-</sup>, no change of the configuration is possible, thus *cis* epoxides are mainly converted to *cis* cyclic carbonates, and *trans* epoxides are mainly converted to *trans* cyclic carbonates.

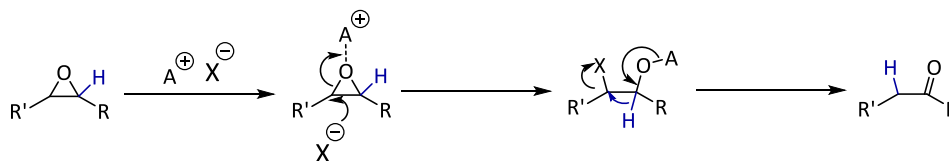


*Scheme 9. Catalytic cycle for the carbonation of epoxidized oils.*

For the carbonation of *cis*-epoxidized methyl oleate with PE-supported imidazolium bromide, It was also observed that an increase in temperature promoted the formation of the *trans* carbonates up to 70 %.<sup>[63]</sup>

Finally, in addition to the cyclic products, the undesirable formation of ketone functions *via* Meinwald rearrangement was reported several time in the literature, especially for the carbonation of epoxidized oils.<sup>[62–65]</sup> This reaction is catalyzed by a Brønsted or Lewis acid A<sup>+</sup>. The selectivity for cyclic carbonate vs the ketone by-product follows the trend: Cl<sup>-</sup> > Br<sup>-</sup> > I<sup>-</sup>. This shows that the formation of the ketone depends on the leaving group ability of the

halide, which is coherent with the Meinwald rearrangement mechanism, where the ketone is formed *via* intramolecular nucleophilic substitution of the halide by the hydride (*Scheme 10*).



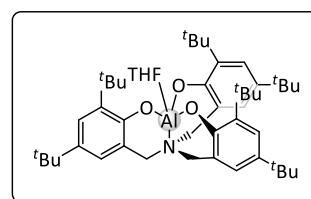
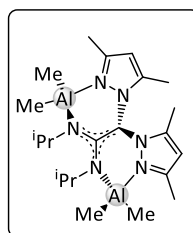
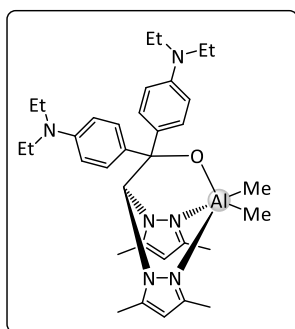
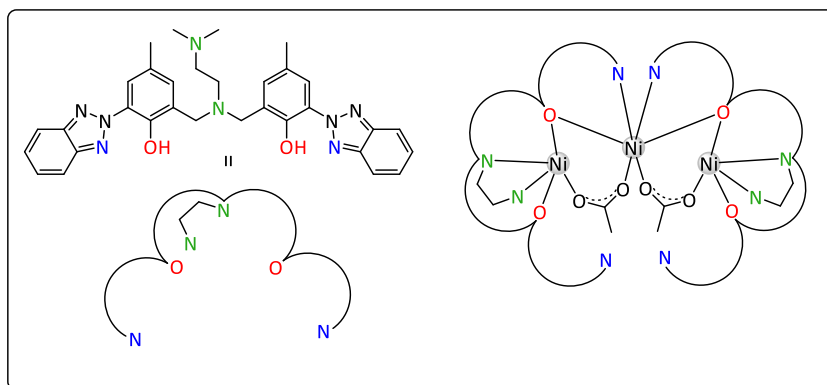
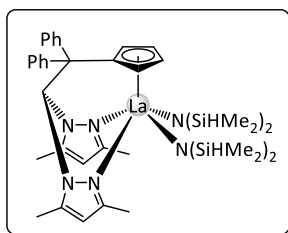
*Scheme 10. Mechanism of Meinwald rearrangement.*

#### II.1.d. Reactivity of trisubstituted and tetrasubstituted epoxides

Bio-based trisubstituted epoxides such as limonene oxide are interesting substrates for the synthesis of bio-based platform molecules and polymers. However, they are much more stable than terminal and disubstituted epoxides. The use of single component catalytic system is not efficient enough to obtain satisfactory yields. Moreover, ammonium chloride showed better activity compared to bromide and iodide derivatives. TBAC, in combination with a co-catalyst (*Scheme 11*), was used for the carbonation of limonene oxide, and moderate yields were obtained (*Table 5*, entries 1-3).<sup>[66-68]</sup>

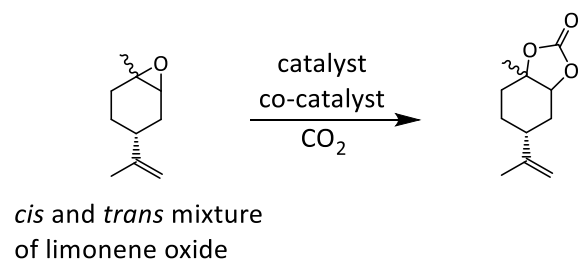
Bis(triphenylphosphoranylidene)ammonium chloride (PPNCl) also showed interesting activity. Navarro *et al.*<sup>[69]</sup> used PPNCl with an organoaluminum complex co-catalyst for the carbonation of *cis* and *trans* mixture of limonene oxide in methyl ethyl ketone (MEK) with a yield up to 52 %. Interestingly, when the catalytic system was used on pure *trans* limonene oxide, the yield increased to 76 % (*Table 5*, entries 4, 5).

Similar results were shown by Fiorani *et al.*,<sup>[70]</sup> higher yields were obtained with pure *trans* limonene oxide than with *cis* and *trans* mixtures, whereas a very poor yield of 4 % was obtained with pure *cis* limonene oxide (*Table 5*, entries 6-8).



Scheme 11. Catalysts used for the carbonation of limonene oxide.

Table 5. Carbonatation of limonene oxide using chloride as catalyst and metallic complexes as co-catalysts.



Entry	Epoxide <i>cis:trans</i> ratio	Catalyst (mol%)	Lewis acid co-catalyst (mol%)	T (°C)	P <sub>CO<sub>2</sub></sub> (MPa)	t (h)	Yield (%)	Cyclic carbonate <i>cis:trans</i> ratio	Ref.
1 <sup>a</sup>	40:60	TBAC (4)	Lanthanum heteroscorpionate (1)	100	1	16	43	8:92	[66]
2 <sup>a</sup>	Not reported	TBAC (5)	trimetallic cobalt complexe (0.1)	80	2	24	33	Not reported	[67]
3 <sup>a</sup>	Not reported	TBAC (3)	Al complexe (1)	80	1	66	48	Not reported	[68]
4 <sup>b</sup>	43:57	PPNCl (3)	Organoaluminium complexe (1)	70	1	66	52	1:99	[69]
5 <sup>b,c</sup>	0:100			76	0:100				

Entry	Epoxide <i>cis:trans</i> ratio	Catalyst (mol%)	Lewis acid co-catalyst (mol%)	T (°C)	P <sub>CO2</sub> (MPa)	t (h)	Yield (%)	Cyclic carbonate <i>cis:trans</i> ratio	Ref.
6 <sup>b</sup>	40:60						43	1:99	
7 <sup>b,c</sup>	0:100	PPNCl (3)	Al complexe (1)	85	1	66	57	99:1	[70]
8 <sup>b,d</sup>	100:0						4	4:96	

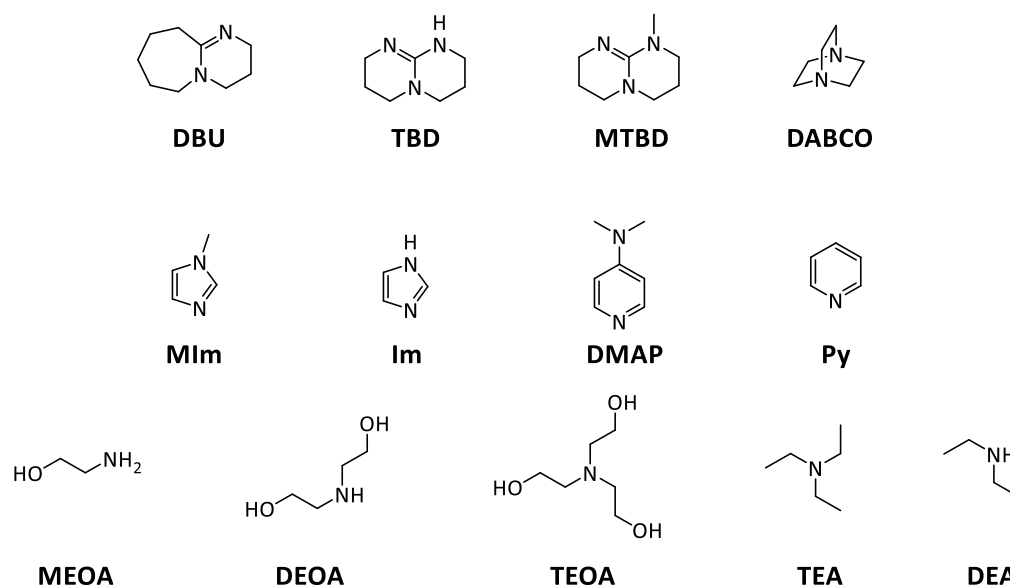
<sup>a</sup>Neat. <sup>b</sup>MEK as solvent. <sup>c</sup>Pure *trans* limonene oxide. <sup>d</sup>Pure *cis* limonene oxide.

Concerning the carbonatation of tetrasubstituted epoxides, no catalytic systems have been developed for now with a good activity. Maeda *et al.*<sup>[71]</sup> tested a bifunctional catalyst composed of ammonium bromide and a zinc porphyrin complex, on a range of different epoxides, and no reaction was observed with a tetrasubstituted epoxide after 96 h. Moreover, the following trend for the reactivity of epoxides with CO<sub>2</sub> was observed: **terminal > disubstituted >> trisubstitued >> tetrasubstituted**.

## II.2. Carbonatation of epoxides with hindered nucleophilic catalysts

### II.2.a. Catalytic cycle mechanism

The second route for the carbonatation of epoxides involves the use of hindered bases or anions with a delocalized negative charge as catalyst. A variety of organic bases were used such as 1,8-diazabicyclo[5.4.0]-undec-7-ene (DBU), 1,5,7-triazabicyclo[4.4.0]dec-5-ene (TBD), 7-methyl-1,5,7-triazabicyclo[4.4.0]dec-5-ene (MTBD), 1,4-diazabicyclo[2.2.2]octane (DABCO), N-methylimidazole (MIm), imidazole (Im), N,Ndimethylaminopyridine (DMAP), pyridine (Py), monoethanolamine (MEOA), diethanolamine (DEOA), triethanolamine (TEOA), trimethylamine (TEA), and diethylamine (DEA) (*Scheme 12*).<sup>[72]</sup> The most hindered anions used are tetrafluoroborate (BF<sub>4</sub><sup>-</sup>) and hexafluorophosphate (PF<sub>6</sub><sup>-</sup>).<sup>[73]</sup>

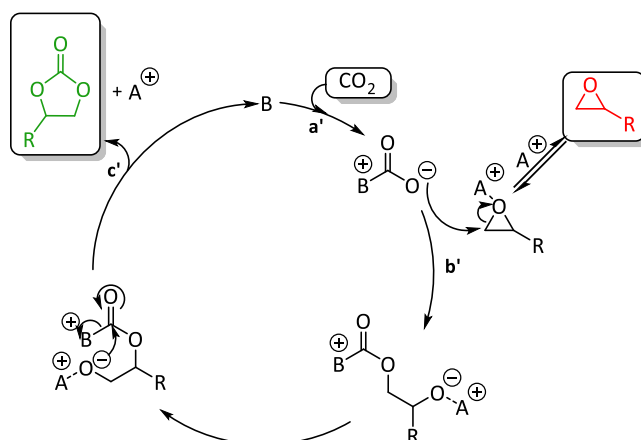


*Scheme 12. Structure of organic nitrogen bases used as catalysts.*

In this route, CO<sub>2</sub> is first activated by the catalyst, leading to the formation of the carboxylate intermediate (*Scheme 13*, step a'). The less hindered carbon atom of the epoxide is then



attacked by the carboxylate (*Scheme 13*, step **b'**) and an intramolecular ring-closure forms the cyclic carbonate and regenerates the catalyst (*Scheme 13*, step **c'**).<sup>[74,73,75]</sup> The carboxylate intermediate formed with TBD was isolated and characterized.<sup>[76]</sup>



*Scheme 13. Catalytic mechanism for the carbonatation of epoxides using hindered nucleophilic catalyst.*<sup>[13]</sup>

## II.2.b. Influence of the base structure

Sun *et al.* compared several organic bases as catalysts, in combination with cellulose as co-catalyst, for the carbonatation of propylene oxide (PO) under the following conditions: PO (1 mL), base (225 mg), cellulose (15 mg), 120 °C, 2.0MPa, 2h (*Table 6*).<sup>[72]</sup> The catalytic activity did not exactly followed the basicity of the base. The steric hindrance and the presence of alcohol groups also had a strong impact on the epoxide conversion. The best catalyst was DBU with a conversion of 93 % (, entry 1). TBD and MTBD showed much lower activity (*Table 6*, entries 2 and 3), owing to their too high steric hindrance. The presence of alcohol group enhanced the activity *via* the epoxide activation with hydrogen bonding, as much higher conversions were obtained with TEOA and DEOA compared to TEA and DEA (*Table 6*, entries 10-13). Good conversions were also obtained with DABCO, MIm and DMAP (*Table 6*, entries 4, 5 and 7).

Table 6. Carbonation of propylene oxide with organic bases.<sup>a</sup> [72]

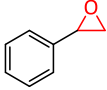
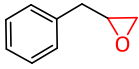
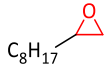
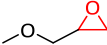
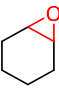
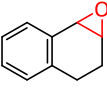
Entry	Base	pKa <sup>b</sup>	Conversion <sup>c</sup> (%)	Selectivity <sup>c</sup> (%)
1	DBU	24.3	93	99
2	TBD	26.0	8	96
3	MTBD	25.5	15	99
4	DABCO	(8.7)	80	98
5	MIm	(7.1)	74	99
6	Im	(7.0)	10	93
7	DMAP	18.0	87	99
8	Py	12.5	30	92
9	MEOA	(9.5)	64	88
10	DEOA	(8.9)	74	94
11	TEOA	(7.8)	81	93
12	TEA	18.8	41	95
13	DEA	(11.0)	34	95

<sup>a</sup>Reaction conditions: PO (1 mL), base (225 mg), cellulose (15 mg), 120 °C, 2.0 MPa, 2 h. <sup>b</sup>pK<sub>a</sub> value of the conjugated acid in acetonitrile or water (brackets). <sup>c</sup>Determined by GC/GC-MS, main by-product is 1,2-propylene glycol.

MTBD and TBD supported on silica were used as catalysts for the conversion of various terminal and internal epoxides into cyclic carbonates under the following conditions: 4 mol% of catalyst, 140 °C, 5 MPa of CO<sub>2</sub> and acetonitrile as solvent.<sup>[77]</sup> The homogeneous catalyst MTBD showed a better activity than the heterogeneous derivatives due to mass transfer limitation. High yields (from 82 to 98 %) were obtained for the carbonation of terminal epoxides such as styrene oxide (2,3-epoxypropyl)benzene, 1,2-epoxydecane and glycidyl

methyl ether after 20 hours with MTBD. In the case of heterogeneous catalysts, a longer time (70 h) was needed to achieve similar yields (from 77 to 95 %). Good and moderate yields were obtained with internal epoxides such as cyclohexene oxide and 1,2-epoxy-1,2,3,4-tetrahydronaphthalene with MTBD after 20 hours (70 % and 60 % respectively) and with the heterogeneous catalyst after 70 hours (67 % and 55 % respectively) (*Table 7*).

*Table 7. Carbonatation of epoxides using MTBD and supported TBD as catalysts.<sup>a, [77]</sup>*

Entry	Substrate	Yield [selectivity] (%)	
		MTBD, 20 h	Supported TBD, 70 h
1		95 [97]	90 [92] <sup>a</sup>
2		98 [99]	95 [97]
3		82 [95]	77 [90]
4		88 [90]	79 [90]
5		88 [90]	79 [90]
6		70 [97]	67 [94]

<sup>a</sup>4 mol% of catalyst, 140 °C, 5 MPa of CO<sub>2</sub>, acetonitrile. The by-products recovered were carbonyl compounds, mainly ketone.

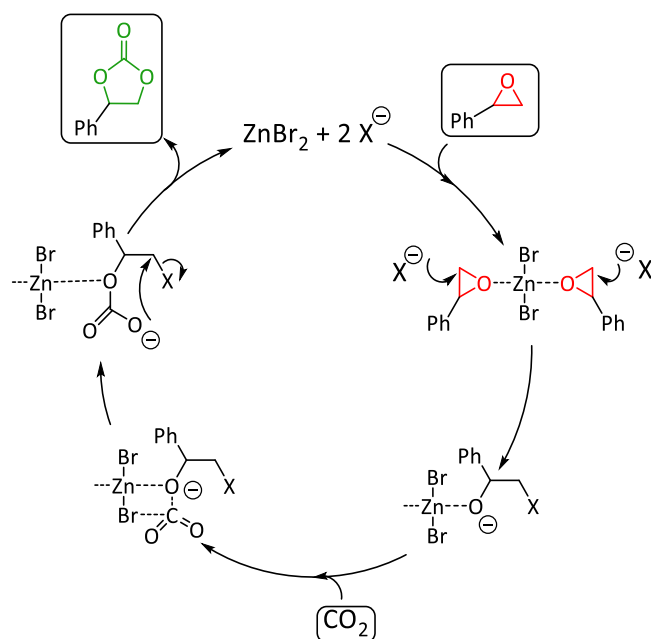
### II.3. Acidic co-catalysts

#### II.3.a. Lewis acids

Acidic co-catalysts have been widely used in order to perform the carbonation reaction under milder conditions (ambient temperature and atmospheric pressure of CO<sub>2</sub>). In the following paragraphs, several metallic salts and complexes (metal halides, metal – porphyrin and metal – salen complexes) will be studied to understand the influence of the metallic center and the ligands on the catalytic activity.

M<sup>n+</sup>Y<sup>-</sup><sub>n</sub> type salts (where M<sup>n+</sup> is a metal center and Y<sup>-</sup> a halide), especially ZnY<sub>2</sub>, in combination with ammonium, phosphonium, or imidazolium salts were found to be particularly effective to promote the carbonation of epoxides. Sun *et al.* investigated the influence of the metal center and obtained the following order of activity for the carbonation of styrene oxide with TBAI (0.3 mol% of catalyst, 0.3 mol% of Lewis acid, 80 °C, 8 MPa, 30 min) and C<sub>1</sub>C<sub>4</sub>ImCl (2 mol% of catalyst, 1 mol% of Lewis acid, 80 °C, 14 MPa, 1 h) as catalysts: Zn<sup>2+</sup> > Fe<sup>3+</sup> > Fe<sup>2+</sup> > Mg<sup>2+</sup> > Li<sup>+</sup> > Na<sup>+</sup>, in agreement with the order of Lewis acidity of the metal centers. [16,78]

The nature of the anion Y also plays an important role, the order of activity being ZnBr<sub>2</sub> > ZnI<sub>2</sub> > ZnCl<sub>2</sub> with an optimal molar ratio of 2 for both ZnBr<sub>2</sub>/TBAI and ZnBr<sub>2</sub>/C<sub>1</sub>C<sub>4</sub>ImCl catalytic systems. To account for these results, the authors proposed the *in situ* formation of a zinc complex bearing two epoxides coordinated to the zinc atom (*Scheme 14*). The better activity of ZnBr<sub>2</sub> compared to ZnCl<sub>2</sub> and ZnI<sub>2</sub> could be explained by the fact that the Y<sup>-</sup> anion also coordinates to the CO<sub>2</sub> carbon, and this interaction would be favored by good nucleophilicity but also a low steric hindrance of Br<sup>-</sup>. [16,78]

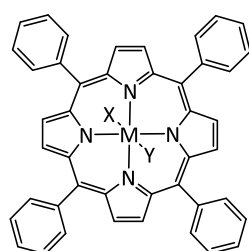


*Scheme 14. Catalytic cycle for the carbonation of styrene oxide with halide as catalyst and  $ZnBr_2$  as co-catalyst.*<sup>[16,78]</sup>

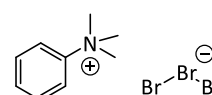
Kim *et al.* have shown that  $(1\text{-butyl-3-methylimidazolium})_2ZnX_2Y_2$  ( $X = Cl$  or  $Br$ ,  $Y = Cl$  or  $Br$ ) complexes were formed *in situ* during the carbonation of ethylene oxide and propylene oxide with the initial catalytic system  $1\text{-butyl-3-methylimidazolium}X/ZnY_2$ .  $(1\text{-butyl-3-methylimidazolium})_2ZnX_2Y_2$  complexes were isolated and had the same activity than the  $1\text{-butyl-3-methylimidazolium}X/ZnY_2$  catalytic system. The following order of activity was obtained for the anion :  $[ZnBr_4]^{2-} > [ZnBr_2Cl_2]^{2-} > [ZnCl_4]^{2-}$  in accordance with the results of Sun *et al.*<sup>[14]</sup>

Finally, Wu *et al.* showed that  $ZnBr_2$  can be used with the phosphonium  $Ph_4PI$  for the carbonation of propylene oxide (0.9 mol% of catalyst, 0.01 mol% of Lewis acid, 2.5 MPa as initial pressure, 120 °C, 1h), and the activity of the zinc salts followed the order:  $ZnBr_2 > ZnI_2 > ZnCl_2 > ZnSO_4 >> ZnO$ .<sup>[45]</sup>

Metal-porphyrin complexes (M(porphyrin)) present a great interest due to their robustness and the highly Lewis acidity of the metallic center. Transitions metal - tetraphenylporphyrin complexes (M(TPP)Y<sub>2</sub>) containing Cr<sup>III</sup>,<sup>[79]</sup> Mn<sup>III</sup>,<sup>[80]</sup> Fe<sup>III</sup>,<sup>[80]</sup> Co<sup>III</sup>,<sup>[53,80]</sup> Cu<sup>II</sup>,<sup>[81]</sup> and Ru<sup>III</sup><sup>[80]</sup> showed catalytic activity when used in combination with phenyltrimethylammonium tribromide (TPAT) or DMAP (*Scheme 15*), but it is also possible to use non transition metal centers such as Sn<sup>II</sup>, Sn<sup>IV</sup>, Mg<sup>II</sup> and Al<sup>III</sup>.<sup>[40]</sup>



M = Cr, Mn, Fe, Co, Cu, Sn, Mg or Al  
X = Cl or none  
Y = Cl or none



Metal - tetraphenylporphyrin complex (M(TPP)XY)

Phenyltrimethylammonium tribromide (TPAT)

*Scheme 15. Structure of metal – tetraphenylporphyrin complexes and TPAT.*

Lili Jin *et al.*<sup>[80]</sup> compared the influence of the transition metal center of M<sup>III</sup>(TPP)Cl complexes activity with PTAT for the carbonation of propylene oxide at 25 °C, under 0.7 MPa and neat conditions. After 3 hours of reactions, the following order of activity was observed: Co<sup>III</sup> > Mn<sup>III</sup> > Ru<sup>III</sup> > Fe<sup>III</sup> (*Table 8*).

*Table 8. Carbonation of propylene oxide with metal – porphyrin complexes as co-catalyst.*<sup>[80]</sup>

Entry	M(TPP)Cl	Yield (%)	TON	TOF (h <sup>-1</sup> )
1	Co <sup>III</sup> (TPP)Cl	88	880	293
2	Mn <sup>III</sup> (TPP)Cl	27	270	90
3	Fe <sup>III</sup> (TPP)Cl	10	98	33
4	Ru <sup>III</sup> (TPP)(PPh <sub>3</sub> )Cl	14	140	46

Reaction conditions: M(TPP)Cl (0.1 mol%), PTAT (0.2 mol%), 0.7 MPa of CO<sub>2</sub>, 25 °C, 3 h.

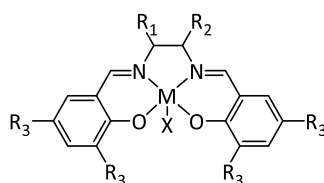
Metal – tetraphenylporphyrin complexes showed also high activity with non-transition metals such as Sn<sup>II</sup>, Sn<sup>IV</sup>, Mg<sup>II</sup> and Al<sup>III</sup> for the carbonation of propylene oxide using different nucleophilic catalysts such as DMAP, TBAI or phenyltrimethylammonium tribromide (TPAT).<sup>[40]</sup> According to *Table 9*, the following order of activity was observed: Al<sup>III</sup> > Mg<sup>II</sup> > Sn<sup>IV</sup> > Sn<sup>II</sup>, which follows the order of Lewis acidity. With DMAP as catalyst, at 150 °C under

1.4 MPa of CO<sub>2</sub> and neat conditions, a yield of 51 % was obtained with Sn<sup>II</sup>(TPP) after 10 hours, whereas Sn<sup>IV</sup>(TPP)Cl<sub>2</sub> afforded an almost quantitative yield (99 %) after only 5 hours (*Table 9*, entries 1-2), which demonstrates the better catalytic efficiency of Sn<sup>IV</sup> metallic center. By using Mg<sup>II</sup>(TPP) with TBAI, a quantitative yield was reached at ambient temperature (25 °C) but with a longer reaction time (24 h) (*Table 9*, entry 3). Finally, with Al<sup>III</sup>(TPP)Cl in combination with TPAP, a quantitative yield was obtained at ambient temperature, lower pressure (1.0 MPa) and shorter reaction time (5 h) (*Table 9*, entry 4).

*Table 9. Carbonatation of propylene oxide using non-transition metal – tetraphenylporphyrin complexes under neat conditions.<sup>31</sup>*

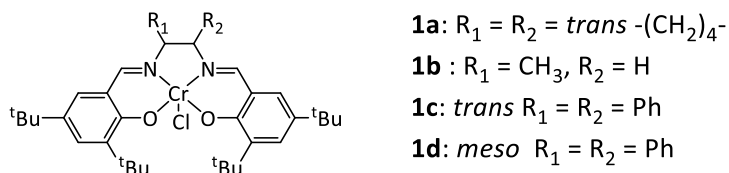
Entry	Catalyst (mol%)	M(porphyrin) (mol%)	Temperature (°C)	Pressure (MPa)	Reaction time (h)	Yield (%)
1	DMAP (0.125)	Sn <sup>II</sup> (TPP) (0.025)	150	1.4	10	51
2	DMAP (0.125)	Sn <sup>IV</sup> (TPP)Cl <sub>2</sub> (0.025)	150	1.4	5	99
3	TBAI (0.1)	Mg <sup>II</sup> (TPP) (0.05)	25	1.4	24	99
4	PTAT (0.2)	Al <sup>III</sup> (TPP)Cl (0.1)	25	1.0	5	99

The coordination complexes with N,N'-bis(salicylidene)ethylenediamine derivative ligands, also called salen complexes (*Scheme 16*), have been extensively studied as co-catalysts for the cycloaddition of CO<sub>2</sub> onto epoxides. Their synthesis is easier than with the porphyrin complexes, which makes them more suitable for industrial applications. The salen ligands can be coordinated to a wide variety of metal cations, and their structure could also be easily modified with bulky, electro-donor or electro-withdrawing groups, in order to control the approach of the substrates and to tune the acidity of the metal center.



Scheme 16. Structure of metal - salen complexes.

Different Chromium III - salen complexes (Scheme 17) were tested as co-catalysts for the carbonation of propylene oxide with DMAP as nucleophilic catalyst in dichloromethane (DCM).<sup>[82,83]</sup> The complex **1d** was the most active catalyst because of its more accessible metal center (Table 10). Moreover, an increase in temperature from 75 °C to 100 °C significantly improved the turnover frequency (TOF) from 254 to 916 h<sup>-1</sup>.



Scheme 17. Structure of Cr(salen) complexes used as co-catalysts with DMAP for the carbonation of propylene oxide.

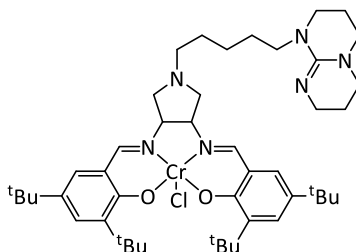
Table 10. Carbonation of propylene oxide with DMAP/ Cr(salen) complexes system.<sup>[82]</sup>

Entry	Cr(salen)	Temperature (°C)	Reaction time (h)	TON	TOF (h <sup>-1</sup> )
1	1a	75	2	323	162
2	1b	75	2	338	169
3	1c	75	2	253	127
4	1d	75	2	507	254
5	1d	100	1	916	916

Reaction conditions: PO (4 mL, 3.32 g, 5.72×10<sup>-2</sup> mol), CH<sub>2</sub>Cl<sub>2</sub> (0.5 mL), Cr(salen) (0.075 mol %), DMAP (0.075 mol%), 0.8 MPa of CO<sub>2</sub>. TON = turnover number, TOF = turnover frequency.

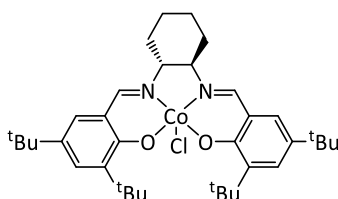


Bifunctional catalysts based on Cr(salen) complexes and 7-methyl-1,5,7-triazabicyclo[4.4.0]dec-5-ene (MTBD) (*Scheme 18*) have been tested in order to improve the catalytic activity. The bifunctional catalyst showed a higher activity than the binary systems Cr(salen)/MTBD and Cr(salen)/DMAP, with a TOF up to 2120 h<sup>-1</sup> under 2 MPa at 80 °C under neat conditions.



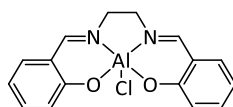
*Scheme 18. Structure of bifunctional Cr(salen)/MTBD co-catalyst.*

Cobalt III salen complexes (*Scheme 19*) also showed catalytic activity for the carbonation of propylene oxide. A TOF of 1200 h<sup>-1</sup> was obtained with the system Co(salen) (0.066 mol%)/DMAP (0.132 mol%) (100 °C, 2.2 MPa of CO<sub>2</sub>, DCM), which was higher than with the Cr(salen)/DMAP system.<sup>[84]</sup>



*Scheme 19. Structure of Co(salen) co-catalysts.*

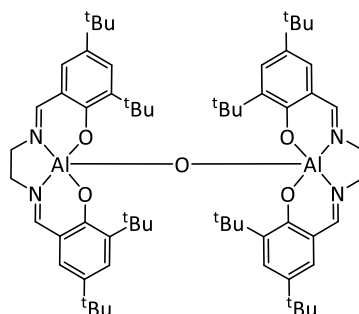
Aluminium salen complexes (*Scheme 20*), in combination with nucleophilic catalyst such as TBAB, were used for the carbonation of ethylene oxide under supercritical conditions. A TOF of 3070 h<sup>-1</sup> was obtained under the following conditions: Al(salen) (0.02 mol%), TBAB (0.02 mol%), 120 °C, 1 h, 15–16 MPa of CO<sub>2</sub>. The high activity was attributed to the high miscibility of ethylene oxide with supercritical CO<sub>2</sub>.<sup>[85]</sup>



*Scheme 20. Structure of Al(salen) co-catalyst.*

Bimetallic Al(salen) complexes (*Scheme 21*), in combination with TBAB, was one of the first systems to show a high activity under mild conditions (2.5 mol% of catalyst, 25 °C, 1 atm of

CO<sub>2</sub>) for the conversion of styrene oxide, a conversion up to 62 % was obtained after 3 hours.<sup>[86]</sup>



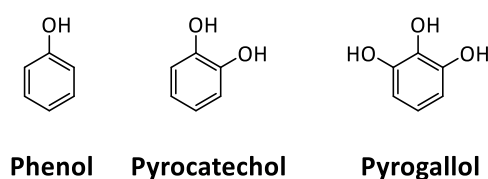
*Scheme 21. Structure of bimetallic Al(salen) complex.*

Finally, zinc and copper salen complexes were used as co-catalysts and compared to cobalt counterparts. Under similar conditions (100 °C, DCM, M(salen) (0.1 mol%), DMAP (0.2 mol%), 3.4 MPa of CO<sub>2</sub>), the following order of activity was observed: Co<sup>II</sup> > Zn<sup>II</sup> > Cu<sup>II</sup>, according to the TOF obtained : 800, 702 and 397 h<sup>-1</sup>, respectively.<sup>[87]</sup>

### II.3.b. Brønsted acids

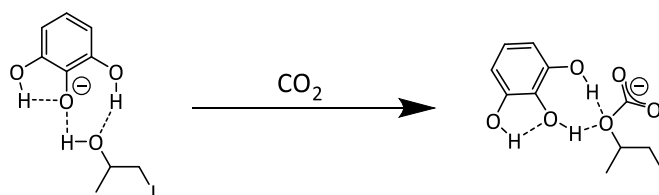
The use of hydrogen-bond donor compounds to activate the epoxide by improving its electrophilicity, in a similar way that metallic complexes do has also been investigated. The main advantages of using commercial organic co-catalysts instead of metallic complexes are the reduction of the costs, their high availability, the simplification of the process as there is no need to synthesize the co-catalyst, and the reduction of the co-catalyst toxicity. However, their catalytic efficiency was found to be much lower than that of metallic complexes, requiring higher concentration of co-catalysts and harsher conditions. Different classes of hydrogen bond donors have shown catalytic activity for the cycloaddition of CO<sub>2</sub> with epoxides.

Various functionalized phenolic compounds (*Scheme 22*) were used as co-catalysts with TBAI for the carbonation of 1,2-epoxyhexane under mild conditions (45 °C, 1 MPa of CO<sub>2</sub>, TBAI (5 mol%), co-catalyst (5 mol%), MEK, 18 h).<sup>[88]</sup>



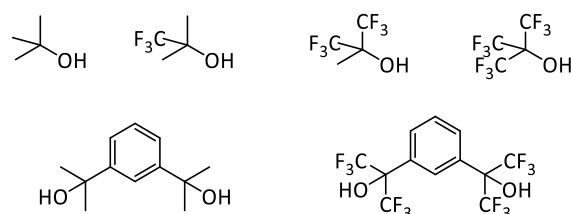
*Scheme 22. Structure of phenolic compounds used as co-catalysts.*

The presence of adjacent alcohol groups appeared to be crucial to obtain high yields. With phenol, a 15 % yield was obtained. When it was replaced with pyrocatechol, the yield reached 75 %. Finally, by using pyrogallol, the yield was quantitative. The use of isomeric derivatives 1,2,4-trihydroxybenzene and 1,3,5-trihydroxybenzene led to a decrease of the yield to 74 % and 30 % respectively, which highlights the importance and the synergic effect of the adjacent hydroxy groups. A mechanism was proposed where the polyphenol synergistically stabilized the alkoxide and carboxylate intermediates (*Scheme 23*).



*Scheme 23. Structure of the intermediates stabilized by pyrogallol during carbonatation of propylene oxide.<sup>[88]</sup>*

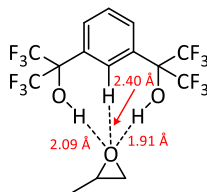
Fluorinated alcohols are also another class of hydrogen bond donor compounds that show interesting activity. A variety of aliphatic and aromatic fluorinated and non-fluorinated alcohols (*Scheme 24*) were compared by Sandro Gennen *et al.*<sup>[28]</sup> as co-catalysts for the carbonatation of 1,2-epoxydodecane under the following conditions: 80 °C, 8 MPa of CO<sub>2</sub>, TBAI (2.5 mol%), co-catalyst (2.5 mol%).



*Scheme 24. Structure of ter-butanol,  $\alpha,\alpha'$ -dihydroxy-1,3-diisopropylbenzene and their fluorinated derivatives used as co-catalysts.*

The reactions were followed by Raman spectroscopy to determine the reaction time necessary for quantitative yield. The presence of CF<sub>3</sub> groups improved the activity of the co-catalyst. When 1, 2 and 3 methyl groups of terbutanol were substituted by CF<sub>3</sub> groups, the reaction rate constant increased from 0.0014 min<sup>-1</sup> to 0.0034, 0.0290 and 0.0826 min<sup>-1</sup> respectively. The hydrogen bonding interactions between 1,3-bis(2-hydroxyhexafluoroisopropyl)benzene and propylene oxide were investigated by DFT calculations, showing the occurrence of hydrogen bonding between the epoxide and the two

alcohol groups, but also with the aromatic hydrogen in ortho position of the two fluorinated substituents (*Scheme 25*).



*Scheme 25. Structure of the 1,3-bis(2-hydroxyhexafluoroisopropyl)benzene-propylene oxide adduct.*<sup>[28]</sup>

A similar trend was observed when  $\alpha,\alpha'$ -dihydroxy-1,3-diisopropylbenzene and its fluorinated derivative 1,3-bis(2-hydroxyhexafluoroisopropyl)benzene were used. Reaction rate constants of 0.0020 and 0.1200  $\text{min}^{-1}$  were obtained respectively, showing the significant effect of the  $\text{CF}_3$  electron-withdrawing groups.

1,3-bis(2-hydroxyhexafluoroisopropyl)benzene was also compared to 1,2,3-trihydroxybenzene under the following conditions: 60 °C, 2 MPa of  $\text{CO}_2$ , TBAB (3 mol%), co-catalyst (3 mol%). The fluorinated compound was more active than the phenolic co-catalyst, with reaction rate constants of 0,027 and 0.0162  $\text{min}^{-1}$  respectively. This higher activity was attributed to the higher proton acidity due to the presence of the electron-withdrawing group.

#### II.4. Oxydative carbonatation of alkenes in one-pot

The synthesis of cyclic carbonates from olefins appeared to be a good synthesis strategy to avoid the use of toxic and relatively expensive epoxide and to eliminate possibly a reaction step in the case of a one-pot reaction, or at least to eliminate the isolation step of the epoxide in the case of a two-step reaction. The two-step synthesis involves first an epoxidation of the double bond followed by a carbonatation step, whereas the one-pot synthesis converts directly the alkenes into the cyclic carbonate derivatives without isolation of the epoxide generated *in situ*. The following parts will focus on the one-pot synthesis of cyclic carbonates.

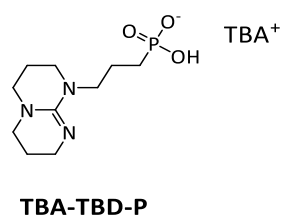
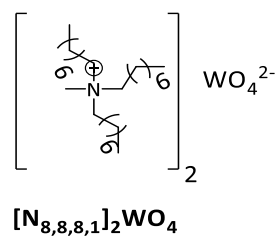
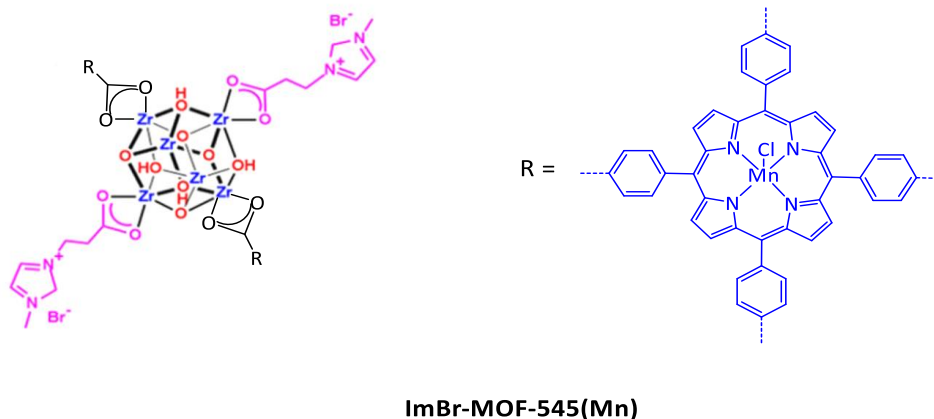
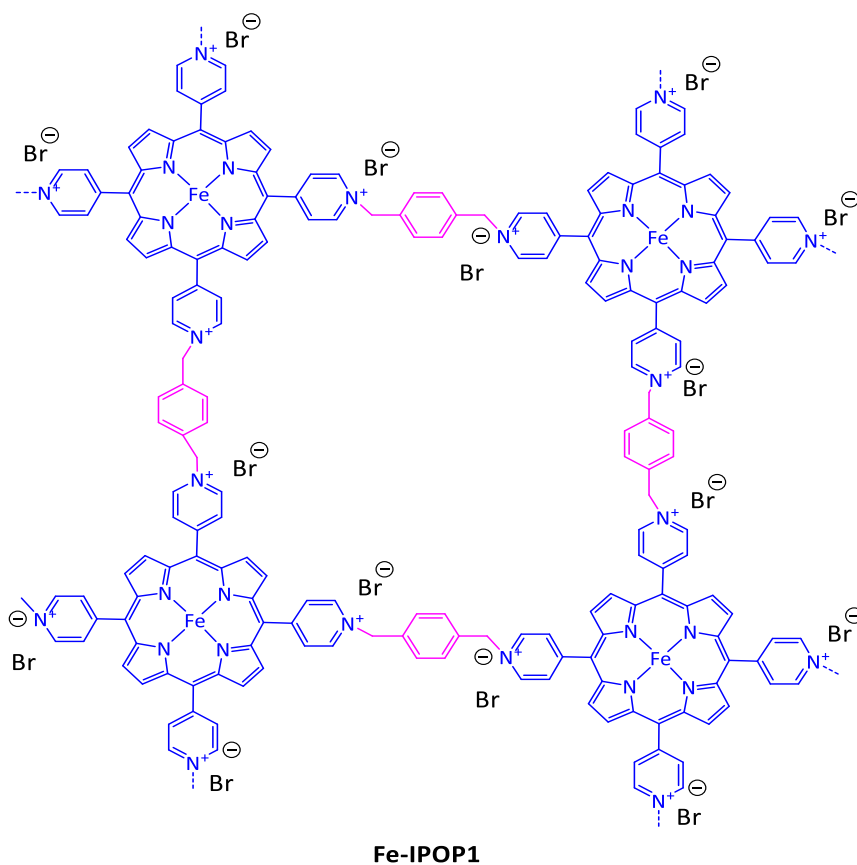
There are two pathways for the one-pot synthesis of cyclic carbonates from olefins, using metal organic frameworks (MOF) and functionalized ammonium salts as catalysts (*Scheme 26*). The first one is the two-step synthesis with the epoxidation directly followed by the carbonatation, without isolation and purification of the epoxide (*Scheme 27*).<sup>[89,90]</sup> This strategy is used when the catalytic system for carbonatation is not compatible with the

epoxidation conditions, thus the catalyst for carbonatation is added in the reaction medium after completion of the epoxidation step.

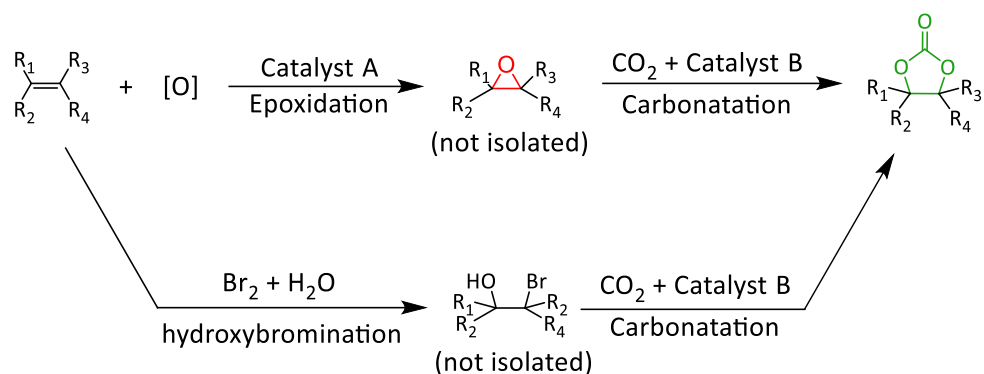
For example, the oxidative carbonatation of 1-octene in one-pot using TPHP/ MoO<sub>2</sub>(acac)<sub>2</sub> as oxidant system and TBAB as catalyst for carbonatation was only possible with a two-step synthesis and a yield up to 83 % of cyclic carbonate was obtained (*Table 11*, entry 1).<sup>[89]</sup>

For the oxidative carbonatation of methyl oleate, the tungstate salt [N<sub>8,8,8,1</sub>]<sub>2</sub>WO<sub>4</sub> appeared as a good catalyst for the epoxidation step with H<sub>2</sub>O<sub>2</sub> under acid-free conditions. The WO<sub>4</sub><sup>2-</sup> anion also exhibited catalytic activity for the carbonatation of the epoxidized methyl oleate, the cyclic carbonate was obtained *via* the formation of the WO<sub>4</sub><sup>2-</sup>/CO<sub>2</sub> adduct, but with a low conversion (28 %) and selectivity (64 %). Thus, a halide salt QX (Q<sup>+</sup> = TBA<sup>+</sup>, Na<sup>+</sup>, K<sup>+</sup> and X<sup>-</sup> = I<sup>-</sup>, Br<sup>-</sup> or Cl<sup>-</sup>) was used as co-catalyst for the carbonatation step and was added in the medium directly after completion of the epoxidation. A counter-anion exchange *in situ* led to the formation of [N<sub>8,8,8,1</sub>]X which was the active catalyst for the carbonatation. A quantitative yield in the cyclic product was obtained with QX = KBr (*Table 11*, entry 2).

Xie *et al.* also developed a different route where olefins were converted to hydroxybromo derivatives instead of epoxides, using a hydroxybromination system (K<sub>2</sub>S<sub>2</sub>O<sub>8</sub> + NaBr + H<sub>2</sub>O), followed by the carbonatation using K<sub>2</sub>CO<sub>3</sub>/PEG<sub>1000</sub> as catalyst. A yield up to 79 % was obtained for the oxidative carbonatation of styrene (*Table 11*, entry 3).<sup>[91]</sup>

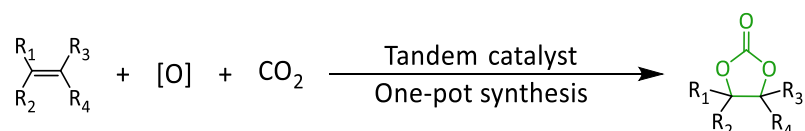


Scheme 26. Structure of catalysts for the one-pot synthesis of cyclic carbonates from olefins.



*Scheme 27. One-pot synthesis of cyclic carbonates from olefins in two steps.*

The second pathway for the one-pot synthesis is the combination of the epoxidation and carbonatation reactions using a tandem catalyst for both epoxidation and carbonatation reactions (*Scheme 28*).<sup>[92-95]</sup>

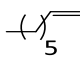
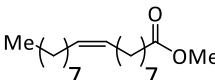
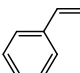


*Scheme 28. One-pot synthesis of cyclic carbonates from olefins with a tandem catalyst.*

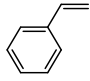
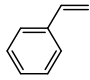
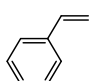
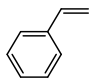
The use of a tandem catalyst could improve the feasibility of the one-pot synthesis, by excluding the chemical interactions between two different catalytic systems, and reducing the cost and side reactions.

Different oxidant/catalyst systems were used for the oxidative carbonatation of styrene. With the PhIO/ Fe(III)-porphyrin frameworks and O<sub>2</sub>/ImBr-MOF-545(Mn) (with addition of isobutyraldehyde as dihydrogen acceptor) systems, very high yields were obtained (96 % and 94 % respectively) (*Table 11*, entries 4 and 5). The TBHP/[C<sub>1</sub>C<sub>4</sub>Im][HCO<sub>3</sub>] and TBHP/TBA-TBD-P/ZnBr<sub>2</sub> systems were less active and selective (*Table 11*, entries 6 and 7).

Table 11. One-pot synthesis of cyclic carbonates from olefins.

Entry	substrate	oxidant	Two-step or tandem	Catalytic system		P <sub>CO2</sub> (MPa)	T (°C)	t (h)	Yield (%)	Selectivity (%)	Ref.
				Epoxidation	Carbonation						
1		TBHP (1.1 equiv.)	Two-step	MoO <sub>2</sub> (acac) <sub>2</sub> (0.1 mol%)	TBAB (5 mol%)	3	100/140	1/1	83	-	[[89]
2		H <sub>2</sub> O <sub>2</sub> (2 equiv.)	Two-step	[N <sub>8,8,8,1</sub> ] <sub>2</sub> WO <sub>4</sub> (5 mol%)	[N <sub>8,8,8,1</sub> ] <sub>2</sub> WO <sub>4</sub> (5 mol%) KBr (5 mol%)	5.0	100	4/16	>99	>99	[90]
3		K <sub>2</sub> S <sub>2</sub> O <sub>8</sub> (1.2 equiv.) + H <sub>2</sub> O (28 equiv.) + NaBr (1.2 equiv.)	Two-step	None	K <sub>2</sub> CO <sub>3</sub> (1 equiv.) + PEG <sub>1000</sub> (0.5 equiv.)	3	60	5/5	79	85	[91]

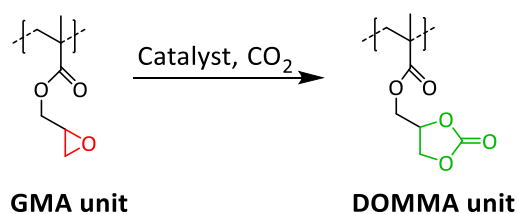


4		PhIO (1.5 equiv.)	tandem	Fe(III)-porphyrin frameworks (10 mg/mmol of olefins)	0.1	80	24	96	96	[92]
5		O <sub>2</sub> (0.5 MPa)	tandem	ImBr-MOF-545(Mn) (10 mg/mmol of olefins) + isobutyraldehyde (2 equiv.)	0.5	60	10	94	95	[93]
6		TBHP (2 equiv.)	tandem	[C <sub>1</sub> C <sub>4</sub> Im][HCO <sub>3</sub> ]	2.0	65	30	75	82	[94]
7		TBHP (1 equiv.)	tandem	TBA-TBD-P (3.3 mol%) + ZnBr <sub>2</sub> (1.6 mol%)	0.1	80	10	70	70	[95]

### III. Carbonatation of polymers

#### III.1. Carbonatation of glycidyl methacrylate based copolymers

The transposition of the carbonatation reaction from molecular compounds to macromolecules containing epoxy groups required several adaptations. Polymers are more difficult to solubilize, the epoxide functions are less accessible and the solution viscosity could limit the mass transfer ( $\text{CO}_2$  diffusion into the liquid phase and approach of the catalyst to the active site). Moreover, the reaction selectivity is crucial, as potential polyethers formation as by-product could lead to insoluble polymers.<sup>[96-101]</sup> The functionalization of polymers with  $\text{CO}_2$  has been mainly performed on polar glycidyl methacrylate (GMA) based copolymers to obtain (2-oxo-1,3-dioxolane-4-yl methyl methacrylate (DOMMA) units (*Scheme 29*).



*Scheme 29. Carbonatation of polymers containing GMA monomer.*

GMA can easily polymerize to form homo or copolymers, and the epoxide is activated by the presence of the withdrawing-electron ester group. Thus, simple catalytic system can be used, such inorganic or ammonium salts. This route to obtain carbonated poly(glycidyl methacrylate) (PGMA) was more preferred than the route where GMA is carbonated to obtain DOMMA before homopolymerisation, due to instability of the carbonated monomer. Indeed, DOMMA could not be purified by distillation, due to its spontaneous polymerization during the purification, and the purified monomer by chromatography column was not stable even at room temperature and also undergone radical polymerization.<sup>[102-105]</sup> Non-purified DOMMA (94 % of purity) was stable until 100 °C.<sup>[103]</sup>

In the following paragraphs, the influence of the catalyst, temperature and co-monomer on the cyclic carbonate yield and on the selectivity will be discussed for the carbonatation of GMA based copolymers.

### III.1.a. Effect of the reaction conditions

In 1992, PGMA have been carbonated for the first time with a quantitative yield with NaI + PPh<sub>3</sub> (1.5 mol%) as catalyst in DMF at 100 °C under atmospheric pressure of CO<sub>2</sub> after 24 hours (*Table 12*, entry 1).<sup>[106]</sup> Good solubility of the catalyst in the reaction medium is essential to obtain satisfying yields. Similar yields were obtained with dimethylacetamide (DMAc), and 2-methylpyrrolidinone (NMP) as solvents (*Table 12*, entries 2-4), where poor yield was obtained with dimethyl sulfoxide (DMSO) due to oxidation of the catalyst and with chlorobenzene due to insolubility of the catalyst (*Table 12*, entries 5, 6). Crosslinking reaction of the polymer was observed when the temperature was increased to 120 °C.

*Table 12. Influence of the solvent for the carbonatation of p(GMA) with NaI/Ph<sub>3</sub>.<sup>a, [106]</sup>*

Entry	solvent	Yield (%)
1 <sup>b</sup>	DMF	99
2	DMF	89
3	DMAc	84
4	NMP	84
5	DMSO	59
6	chlorobenzene	34

<sup>a</sup>Reaction conditions: concentration of GMA unit of 1 mol/L, NaI (1.5 mol%), PPh<sub>3</sub> (1.5 mol%), 1 atm of CO<sub>2</sub>, 100 °C, 24 h. <sup>b</sup>Concentration of GMA unit of 2 mol/L.

Other salts were also studied as catalysts: LiX, NaX, KX and PhCH<sub>2</sub>NMe<sub>3</sub>X (X = I, Br, Cl or F) (*Table 13*). Quantitative yields were obtained with LiCl, LiBr and PhCH<sub>2</sub>NMe<sub>3</sub>Cl after 2 hours of reaction at 100 °C (*Table 13*, entries 2, 3 and 14). The lithium salts globally showed the best activity due to the good Lewis acidity of Li<sup>+</sup>, and the bromide and chloride anions were the most active due to their good nucleophilicity in polar solvent, leaving group ability and relatively small size.<sup>[104]</sup>

## Chapter 1: Literature review on the carbonation reaction

*Table 13. Effect of the anion and cation on the carbonation of PGMA in NMP.<sup>a</sup>, [104]*

Entry	Anion	Cation	Yield <sup>b</sup> (%)
1 <sup>c</sup>		F <sup>-</sup>	0
2	Li <sup>+</sup>	Cl <sup>-</sup>	99
3		Br <sup>-</sup>	98
4		I <sup>-</sup>	8
5 <sup>c</sup>		F <sup>-</sup>	0
6 <sup>c</sup>	Na <sup>+</sup>	Cl <sup>-</sup>	74
7		Br <sup>-</sup>	74
8		I <sup>-</sup>	8
9		F <sup>-</sup>	4
10	K <sup>+</sup>	Cl <sup>-</sup>	47
11		Br <sup>-</sup>	55
12		I <sup>-</sup>	14
13		F <sup>-</sup>	63
14	PhCH <sub>2</sub> NMe <sub>3</sub> <sup>+</sup>	Cl <sup>-</sup>	100
15		Br <sup>-</sup>	41
16		I <sup>-</sup>	10

<sup>a</sup>Reaction conditions: NMP (GMA unit concentration of 0.2 mol/L), 10 mol% of catalyst, atmospheric pressure of CO<sub>2</sub>, 100 °C, 2 h. <sup>b</sup>Estimated by <sup>1</sup>H NMR. <sup>c</sup>Heterogenous system.

Park *et al.*<sup>[107]</sup> reported the use of ammonium salts as catalysts for the functionalization of poly(glycidyl methacrylate-co-ethyl acrylate) (p(GMA-co-EA)) in DMSO at 100 °C. For the cation effect, they observed the following activity trend: TOAC > THAC > TBAC. As explained

in the previous parts on the carbonatation of molecular epoxides, the pair ions dissociation was favored when the alkyl chains length of the ammonium cation increased, thus enhancing anion nucleophilicity. An optimal length was generally observed, *i.e.* too long alkyl chains disfavored the stabilization of the alkoxide intermediate, but it depends on the reaction conditions and on the substrate structure. Moreover, the effect of the anion was studied, and the following activity order was observed  $\text{Cl}^- > \text{Br}^- > \text{I}^-$ , which follows the nucleophilicity order in polar solvent.

Ochiai *et al.*<sup>[96]</sup> reported the carbonatation of poly(glycidyl methacrylate-co-methyl acrylate) (poly(GMA-co-MA)) using ammonium salts in solid-gas phases reactions. The reactions were performed under solvent-free conditions in TGA instrument, where polymeric films containing the catalyst (6 mol%) were functionalized under an atmospheric pressure and continuous flow of  $\text{CO}_2$  (200 mL/min) and isothermal conditions (110 °C or 120 °C) for 500 minutes. The increase of the sample mass during the reaction was directly related to the  $\text{CO}_2$  incorporation, and thus to the GMA conversion to DOMMA.  $\text{BnBu}_3\text{NCl}$  exhibited both high activity and high selectivity, compared to other ammonium salts. More specifically, the effect of the cation was studied in detail for the carbonatation of poly(GMA-co-MMA). It was observed, at 110 °C, the following trend with  $\text{Cl}^-$ :  $(\text{C}_7\text{H}_{15})_4\text{N}^+ > (\text{C}_6\text{H}_{13})_4\text{N}^+ > \text{TBA}^+ > (\text{C}_5\text{H}_{11})_4\text{N}^+ > \text{BnBu}_3\text{N}^+ > \text{BnEt}_3\text{N}^+ > \text{BnMe}_3\text{N}^+ > \text{TEA}^+$  (Table 14, entries 1, 3, 5, 7, 9, 11, 13, 15). Longer alkyl chains tend to improve the catalytic activity. However, at 120 °C, crosslinking reaction of the polymer was observed with tetraalkylammonium chloride salts (Table 14, entries 10, 12, 14 and 16), the copolymerization of the cyclic carbonate *via* decarboxylation reaction has been proposed to account for the decrease in cyclic carbonate yield. They also reported that  $\text{BnMe}_3\text{NCl}$  was more active than  $\text{BnMe}_3\text{NBr}$  for reactions at 100-130 °C under similar conditions. The stronger interactions between  $\text{Br}^-$  and the polar p(GMA-co-MMA) copolymers compared to  $\text{Cl}^-$  could decrease the activity of the bromide anion, as it occurs in polar solvent.<sup>[97]</sup>

In another study, Ochai *et al.* showed that DBU-BnCl catalyst could prevent crosslinking side reaction for the carbonatation of poly(GMA-co-BMA) under similar conditions at 120 °C, and quantitative yield was reached.<sup>[98]</sup>

## Chapter 1: Literature review on the carbonation reaction

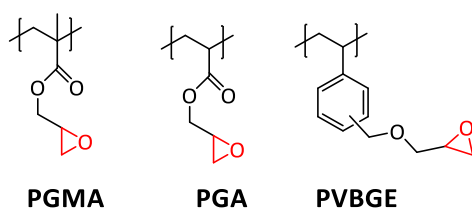
*Table 14. Carbonation of poly(GMA-co-MMA) polymer films using ammonium chlorides as catalysts.<sup>[96]</sup>*

Entry	Catalyst	Temperature (°C)	Yield <sup>c</sup> (%) <sup>b</sup>
1	BnMe <sub>3</sub> NCl	110	62
2		120	71
3	BnEt <sub>3</sub> NCl	110	66
4		120	72
5	BnBu <sub>3</sub> NCl	110	76
6		120	79
7	TEAC	110	53
8		120	63
9	TBAC	110	77
10		120	66
11	(C <sub>5</sub> H <sub>11</sub> ) <sub>4</sub> NCl	110	73
12		120	63
13	(C <sub>6</sub> H <sub>13</sub> ) <sub>4</sub> NCl	110	78
14		120	63
15	(C <sub>7</sub> H <sub>15</sub> ) <sub>4</sub> NCl	110	80
16		120	63

<sup>a</sup>Reaction conditions: catalyst (6 mol%), CO<sub>2</sub> flow rate 200 mL/min, 500 min. <sup>b</sup>Estimated by weight increase measured by TGA.

### III.1.b. Effect of the polymer structure

The effect of the monomer structure on the carbonatation of homopolymers was investigated. Macromolecular epoxides such as PGMA, poly(glycidyl acrylate) (PGA) and poly(vinylbenzyl glycidyl ether) (PVBGE) (*Scheme 30*) were carbonated with LiBr (10 mol%) under the following conditions: 100 °C, 1 atm of CO<sub>2</sub>, NMP (*Table 15*).<sup>[104]</sup> Whereas quantitative yield of cyclic carbonate was obtained for the functionalization of PGMA and PGA after 2 hours, a 95 % yield was obtained for the functionalization of PVBGE after 3 hours under similar conditions. The replacement of the ester groups by aryl ether groups into the polymer structure slightly reduce the reactivity of the epoxide monomer, which could be explained by the better affinity of CO<sub>2</sub> with esters than with aryl ether groups.



*Scheme 30. Structure of PGMA, PGA and PVBGE.*

*Table 15. influence of the homopolymer structure on the carbonatation reaction.*<sup>a, [104]</sup>

Entry	polymer	$M_n$ (g/mol)	$\bar{D}$	Reaction time (h)	Yield <sup>b</sup> (%)
1	PGMA	29 000	2.23	2	98
2	PGA	260 000	1.36	2	99
3	PVBGE	5 400	2.35	3	95

<sup>a</sup>Reaction conditions: NMP (epoxide monomer concentration of 0.2 mol/L), 10 mol% of LiBr, atmospheric pressure of CO<sub>2</sub>, 100 °C. <sup>b</sup>Estimated by <sup>1</sup>H NMR.

Moreover, the introduction of co-monomers into PGMA modifies its polarity, solubility and steric hindrance, and thus has an impact on the GMA units reactivity. When methyl methacrylate (MMA) co-monomer was introduced into PGMA, the catalytic activity of LiBr did not change no matter the composition of the polymer for the carbonatation reaction at 100 °C in NMP (*Table 16*, entries 1-3), whereas introduction of acrylonitrile (ACN) or styrene co-monomers tended to decrease the activity of the catalyst (*Table 16*, entries 4-9). The proton acidity of ACN may inhibit the catalyst, and the steric hindrance induced by the interaction of

the styrene monomers may decrease the epoxide activity.<sup>[104]</sup> The ester groups of MMA may also interact with CO<sub>2</sub> and favor the reaction.

Table 16. Influence of the comonomer on the carbonation of GMA copolymers.<sup>[104]</sup>

Entry	comonomer	Mol% of GMA	Mol% of comonomer	Yield (%)
1		26	74	75
2	MMA	49	51	72
3		74	26	75
4		24	76	37
5	ACN	45	55	74
6		70	30	70
7		27	73	46
8	Styrene	50	50	54
9		74	26	62

Reaction conditions: NMP (0.2 mol/L of GMA unit), 100 °C, 30 min, LiBr (10 mol%), 1 atm of CO<sub>2</sub>.

Ochiai *et al.* also investigated the influence of the co-monomer structure for the solid-gas phase reaction of GMA based copolymers monitored by TGA.<sup>[96]</sup> Films of GMA copolymers containing ethyl methacrylate (EMA), butyl methacrylate (BMA), hexyl methacrylate (HMA) and diethylene glycol methyl ether methacrylate (DGMMA) were carbonated with BnBu<sub>3</sub>NCl (6 mol%) at 100 and 110°C for 500 minutes. At 100 °C, the incorporation of CO<sub>2</sub> increased when the alkyl chains of the methacrylate monomers increased from ethyl to butyl but decreased with hexyl group (Table 17, entries 1-4). The yield depends on the polymer *T<sub>g</sub>* and alkyl chains hindrance. Lower the *T<sub>g</sub>* and better the catalyst and CO<sub>2</sub> mobility in the polymer matrix, but too high hindrance also decreased the epoxide reactivity. Low yield was also obtained with DGMMA due to its high polarity that decreased the affinity of CO<sub>2</sub> with the polymer, according to the authors (Table 17, entry 5). At 110 °C, the cross-linking reaction



was favored, leading to a decrease in the solubility of the polymers a and consumption of cyclic carbonate, and therefore a reduction in the carbonate yield in the case of the carbonatation of poly(BMA-co-GMA) and poly(HMA-co-GMA).

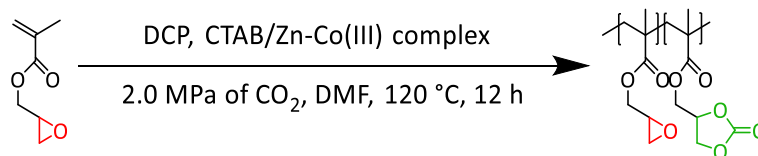
*Table 17. Influence of the comonomer for the carbonatation of GMA copolymers films using BnBu<sub>3</sub>Cl as catalyst.<sup>[96]</sup>*

<b>Entry</b>	<b>copolymer</b>	<b>T<sub>g</sub> (°C)</b>	<b>Yield<sup>b</sup> (%) after reaction at 100/110°C</b>	<b>Solubility in DMF after reaction at 100/110 °C</b>
1	Poly(MMA-co-GMA)	105	51/76	Insoluble/insoluble
2	Poly(EMA-co-GMA)	74	71/73	Soluble/partially soluble
3	Poly(BMA-co-GMA)	48	82/77	Soluble/partially soluble
4	Poly(HMA-co-GMA)	25	54/50	Soluble/soluble
5 <sup>c</sup>	Poly(DGMMA-co-GMA)	-23	59	Insoluble

<sup>a</sup>Reaction conditions: BnBu<sub>3</sub>Cl (6 mol%), CO<sub>2</sub> flow rate 200 mL/min, 500 min. <sup>b</sup>Estimated by weight increase measured by TGA. <sup>c</sup>Reaction at 100 °C.

### III.1.c. Polymerisation and carbonatation of GMA in one-pot

Free radical polymerization and carbonatation reactions of GMA have also been carried out in one-pot to convert directly GMA to polymers containing both cyclic carbonate and epoxide moieties.<sup>[99,100,108]</sup>



*Scheme 31. Homopolymerization of GMA and carbonatation reaction in one-pot.*

Ochiai *et al.*<sup>[100]</sup> produced poly(GMA-co-DOMMA) polymer particles using AIBN as radical initiator and ammonium salts as carbonatation catalyst, by precipitation polymerization of GMA with concomitant carbonatation reaction under atmospheric pressure of CO<sub>2</sub> at 80 °C in dioxane. Whereas LiBr and BnMe<sub>3</sub>NBr showed no activity because of their insolubility in dioxane (*Table 18*, entries 2 and 3), cyclic carbonate moieties were formed during the polymerization of GMA with TBAB and TBAC. TBAC showed higher activity than TBAB after 5 hours of reaction (*Table 18*, entries 1 and 4), but an insoluble polymer was obtained with TBAC because of cross-linking reaction after 24 hours, while GMA units were converted to DOMMA units at 93 % with TBAB, and a soluble polymer was obtained.

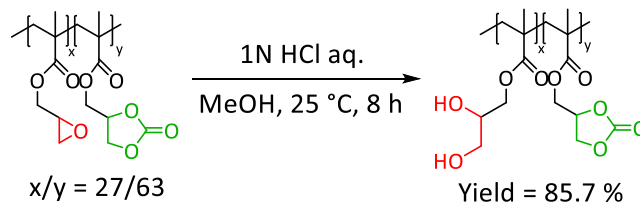
In another study,<sup>[99]</sup> the GMA units of the polymer particles stabilized by cellulose acetate were selectively hydrolysis by HCl (1N) *via* an heterogeneous reaction at room temperature in methanol without any hydrolysis of the DOMMA units.

*Table 18. Precipitation polymerization of GMA with concomitant carbonatation reaction.*<sup>[100]</sup>

Entry	Catalyst	Reaction time (h)	Co-polymer composition (x/y) <sup>b,c</sup>	<i>M<sub>n</sub></i> (g/mol) ( <i>D</i> ) <sup>d</sup>
1	LiBr	5	0/100	14 600 (2.05)
2	BnMe <sub>3</sub> NBr	5	0/100	15 600 (5.46)
3	TBAB	5	40/60	14 800 (2.34)
4	TBAC	5	66/34	34 000 (3.36)
5	TBAB	24	93/7	16 800 (2.75)
6	TBAC	24	-	insoluble

<sup>a</sup>Reactions conditions: GMA (1.00 mmol), CO<sub>2</sub> (1 atm), AIBN and catalyst: 3 mol%, dioxane (0.50 mL), 80 °C. <sup>b</sup>Determined by <sup>1</sup>H NMR. <sup>c</sup>x and y indicate the composition of the carbonate

and oxirane units, respectively. <sup>d</sup>Estimated by SEC (DMF containing 10 mM LiBr, polystyrene standard).



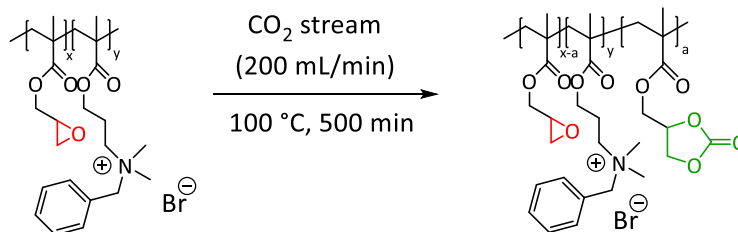
*Scheme 32. Selective hydrolysis of GMA units in particles of poly(GMA-co-DOMMA) with HCl.<sup>[99]</sup>*

Bin Lu *et al.*<sup>[108]</sup> used a cetrimonium bromide (CTAB)/zinc-cobalt complex as catalytic system for the carbonatation reaction, and polymerization of the double bond was achieved with and without radical initiator (AIBN or dicumyl peroxide (DCP)). Full conversion of epoxide and alkene moieties was observed under the following conditions: 7.5 mol/L of GMA, DCP as initiator (1.5 mol%), CTAB (0.65 mol%)/Zn-Co(III) complex (0.3 mol%), 2.0 MPa of CO<sub>2</sub>, DMF, 120° C, 12 h.

#### III.1.d. Self-catalyzed carbonatation of GMA based copolymers containing ammonium salts moieties

Another route for the carbonatation of GMA based polymers was to introduce ammonium bromide monomers into the polymer structure followed by the functionalization with CO<sub>2</sub> (*Scheme 33*).<sup>[109,101]</sup>

Kihara *et al.*<sup>[109]</sup> synthesized GMA based copolymers containing 6 mol% of N-benzyl-N-[2-(methacryloyloxy)ethyl]-N,N-dimethylammonium bromide units and showed that this system was more active for the carbonatation reaction than the usual BnMe<sub>3</sub>NBr catalyst (6 mol%) in the case of a solid state reaction under atmospheric pressure of CO<sub>2</sub> at 140 °C, contrary to the reaction in solution (0.48 mol/L of GMA units, 1 atm of CO<sub>2</sub>, NMP, 100 °C, 24 h). However cross-linking reaction was still observed and was favored by the increase of temperature. Ochiai *et al.* made similar observations for the self-catalyzed reaction of poly(GMA-CO-MA) containing ammonium bromide units.<sup>[101]</sup>



Scheme 33. Self-catalyzed carbonatation reaction.<sup>[109,101]</sup>

### III.1.e. Use of the carbonated GMA based polymers in polymer blends

Park *et al.* synthesized different DOMMA based copolymers and investigated their behaviour in polymer blends.<sup>[105,107,110]</sup> It was found that poly(DOMMA-co-EA) was miscible with poly(vinyl chloride) (PVC) and poly(methyl methacrylate) (PMMA) in the whole composition ranges, according to DSC, as the blends exhibit unique  $T_g$ . Hydrogen bonding between the carbonyl groups and the hydrogen on the polymers backbone, according to FT-IR, could account for the greater miscibility of the polymers.<sup>[107]</sup>

Similar studies were carried out for the miscibility of PDOMMA/poly(MMA-EA), poly(DOMMA-co-acrylonitrile)/poly(MMA-EA) and poly(DOMMA-co-acrylonitrile)/poly(styrene-co-acrylonitrile) and it was also found that the polymers blends exhibit a single  $T_g$  and were miscible in the whole composition ranges, contrary to PGMA based polymers blends that showed two different  $T_g$  by DSC analyses.<sup>[105,110]</sup>

### III.1.f. Influence of DOMMA content on the thermal properties

Various poly(DOMMA-MMA), poly(DOMMA-BA) and poly(DOMMA-styrene) with different contents of DOMMA (from 30 to 83 mol%) were synthesized with the concomitant polymerization and carbonatation reactions of GMA, and their thermal properties were analyzed by DMA and TGA (*Table 19*).<sup>[111]</sup> The increase of the DOMMA content led to an increase of the polymer polarity and inter-chains Van der Waals interactions, which decreased the chains mobility and thus increased the polymers'  $T_g$ . The effect of the DOMMA content on the thermal stability was also investigated. For poly(DOMMA-MMA) and poly(DOMMA-styrene), a two-steps degradation was observed with high content of DOMMA (higher than 75 mol%) in TGA. The first step is the degradation of the DOMMA units with the elimination of CO<sub>2</sub> from the cyclic carbonate moieties, starting at 213 and 220 °C for poly(DOMMA-MMA) and poly(DOMMA-styrene) (*Table 19*, entries 1 and 7) respectively, and

the second step is the degradation of the polymer backbones, starting at 240 and 280 °C, respectively.

*Table 19. Influence of the DOMMA content on the polymers' thermal properties.<sup>[111]</sup>*

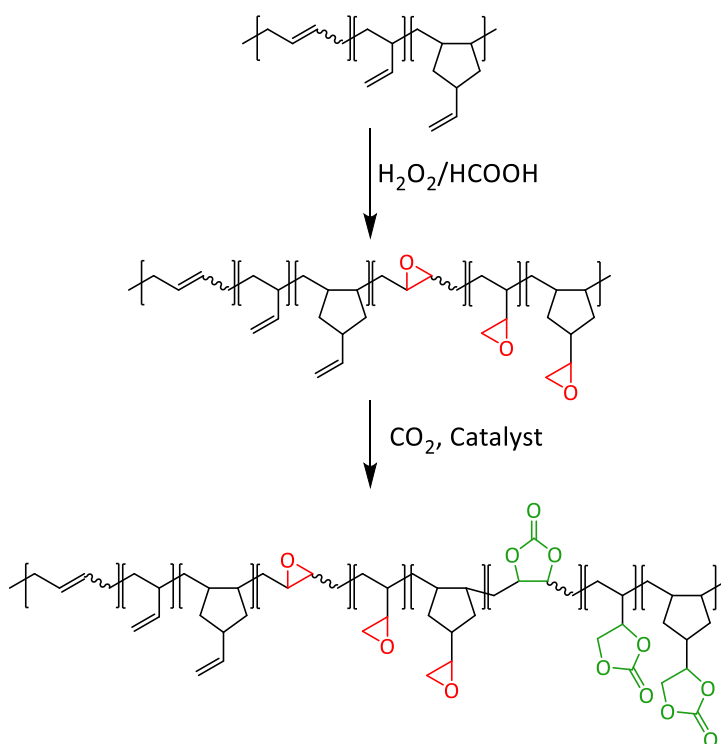
Entry	Polymer	Composition (mol%)	$T_g^a$ (°C)	$T_i^b$ (°C)	$T_f^b$ (°C)
1		83	156	213	460
2	DOMMA-GMA-MMA	55	153	231	444
3		30	148	242	439
4		77	127	225	522
5	DOMMA-GMA-MMA	50	97	246	450
6		30	1	252	460
7		73	149	220	460
8	DOMMA-GMA-MMA	50	136	251	448
9		32	127	283	448

<sup>a</sup>Determined by DMA. <sup>b</sup>Determined by TGA.

## III.2. Carbonatation of epoxidized polydienes

### III.2.a. Two-steps oxidative carbonatation of polybutadienes

The synthesis of carbonated polybutadienes (*i.e.* polybutadienes containing cyclic carbonates functions) was first reported by Dechent *et al.*<sup>[112]</sup> on four different PBU in two successive steps (epoxidation and carbonatation) (*Scheme 34*). The epoxidation step was performed with 0.64 wt% of H<sub>2</sub>O<sub>2</sub>/HCOOH at 60 °C in toluene for 3.5 hours, and epoxide contents between 10-14 mol% were obtained depending on the PBU.



*Scheme 34. Oxidative carbonatation of polybutadiene in two successive steps.<sup>[112]</sup>*

For the carbonatation step, Bis(triphenylphosphoranylidene)ammonium halides (PPNX) and TBAX (X = I, Br or Cl) were used as catalysts. The solvent showed to have a high influence on the yield. Much higher conversion were obtained in MEK than in toluene, due to the better solubility of CO<sub>2</sub> in MEK. Cl<sup>-</sup> and Br<sup>-</sup> proved to be better catalysts than I<sup>-</sup> as it has been already reported for hindered epoxides. TBAB and PPnCl were the most efficient catalysts under the the following conditions: 10 mol% of catalyst, 110 °C, 2.0 MPa of CO<sub>2</sub> at room temperature, 110 °C, MEK, 24 hours, depending on the molar mass of the polybutadienes. PPnCl was the most active catalyst with low masses epoxidized polybutadienes (*Table 20*, entries 1-4). The increase in *M<sub>n</sub>* negatively impacted the reactivity of PPnCl and higher conversion were obtained with TBAB (*Table 20*, entries 5-8).

The carbonated polybutadienes were then used as intermediates for the synthesis of cross linked polyhydroxyurethanes with diamines. The cross-linking reaction with 1,8-octane diamine (2 equiv.) with the carbonated polybutadiene at 70 °C for 16 hours led to the complete conversion of the cyclic carbonate, with no ring-opening of the residual epoxides.

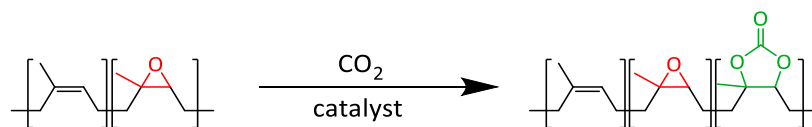
Table 20. Carbonatation of epoxidized polybutadienes with TBAB and PPNCI in MEK.<sup>[112]</sup>

Entry	$M_n$ (kg/mol)	Double bond units (mol%)		Epoxide units (mol%)		catalyst	Cyclic carbonate yield (%)
		1,4 <i>cis/trans</i>	Vinyl/cyclic	1,4 <i>cis/trans</i>	Vinyl/cyclic		
1	1.25	28.4	59.7	5.95/6.50	1.47	TBAB	58
2						PPNCI	60
3	3.00	72.1	19.6	4.02/3.85	0.39	TBAB	32
4						PPNCI	80
5	13.2	74.41	13.8	5.95/5.74	0.07	TBAB	60
6						PPNCI	49
7	45.8	79.3	10.2	5.32/5.13	0.20	TBAB	50
8						PPNCI	31

Reaction conditions: 10 mol% of catalyst, 110 °C, 2.0 MPa of CO<sub>2</sub> at room temperature, MEK, 24 h.

### III.2.b. Carbonation of epoxidized natural rubbers

Very few studies present the carbonation of epoxidized natural rubbers (ENR) (i.e. epoxidized *cis* polyisoprene) (*Scheme 35*).



*Scheme 35. Carbonation of ENR using halide catalyst.*

Kawahara and Saito<sup>[113]</sup> reported for the first time the carbonation of ENR containing 33.5 mol% of epoxide (prepared with peracetic acid) with LiBr (10 mol%) as catalyst. A film of the ENR with LiBr was prepared and carbonated in a high-pressure reactor. A maximum cyclic carbonate content of 7.2 % was obtained under harsh conditions: 20 MPa of CO<sub>2</sub>, 130 °C, 6 h.

More recently, Jiang *et al.* synthesized partially carbonated ENR using TBAI (10 mol%) as catalyst in toluene and obtained a maximum epoxide conversion of 51 % under the following conditions: 0.3 g/mL of ENR, 1 MPa of CO<sub>2</sub>, 130 °C, 30 h.<sup>[114]</sup> The carbonated ENR was then used as intermediate for the synthesis of a cross-linked materials containing disulfide and boronic ester dynamic bonds.



## IV. Conclusions of the review and objectives of this thesis

The reactivity of CO<sub>2</sub> could be enhanced using several strategies. In particular, the carbonatation of molecular epoxides and alkenes with CO<sub>2</sub> could be achieved using metallic and organocatalysts. The catalyst structure has to be designed in accordance to the epoxide structure. While terminal epoxides exhibit relatively high reactivity, and thus simple catalyst systems such ammonium salts are sufficient for their conversion to cyclic carbonates (addition of co-catalysts is possible to reduce the reaction temperature and CO<sub>2</sub> pressure), internal epoxides are more stable and therefore more difficult to convert to carbonates. The use of harsher conditions and highly active catalyst/co-catalyst systems are essential to obtain satisfactory yields in a relatively short reaction time.

Moreover, the functionalization of polymers with CO<sub>2</sub>, which was mostly studied in the literature on poly(glycidyl methacrylate), adds more limitation due to the high viscosity of the medium and the high steric hindrance of the macromolecules. The presence of polar comonomers in the glycidyl methacrylate copolymers may interact and inhibit the reaction, and cross-linking could occur with the formation of ether linkages.

Very few studies report on the functionalization of polymers with CO<sub>2</sub> under solvent free conditions, which have been carried out only with low quantity of polymers using a TGA apparatus for hours-long reaction time. The large-scale production of carbonated polymers has so far never been reported, as well as the carbonatation of more apolar semi-crystalline epoxidized polymers containing e.g. a high amount of ethylene as comonomer (instead or in addition to polar comonomer), and represent a true challenge.

In this thesis, the carbonatation of more apolar semi-crystalline epoxidized polymers, and the transposition to a solvent free-reactive extrusion process will be investigated (**Chapter 2**). The effect of the catalyst and reaction conditions on the carbonatation reaction needed to be fully understood, in order to obtain high selectivity and high catalytic activity. The extend of the carbonatation reaction starting from polymers containing unsaturation will also be explored, as very few studies report these functionalization on polydienes (**Chapter 3**).

Moreover, the potential applications of polymers containing cyclic carbonate moieties will be investigated. As polymer containing both epoxide and cyclic carbonate functions will be obtained in the case of no quantitative carbonatation, the reactivity of these two functions has to be studied, in order to potentially target orthogonal functionalization. Especially, the

reaction of these functions with amines will be studied, in order to selectively convert the cyclic carbonates to hydroxyurethanes (**Chapter 4**).

Finally, partially carbonated ethylene copolymers present an interesting polarity, with an apolar carbon backbone and polar pendant groups, that could act as compatibilizers for polar/apolar polymers blends such as high density polyethylene/polycarbonate blends. The new reactivity brought by the cyclic carbonate functions could also be beneficial for targeting reactive compatibilisation, thus the compatibility and mechanical properties of high density polyethylene/polycarbonate blends compatibilized by carbonated polymers will be explored (**Chapter 5**).

## V. References

- [1] IPCC, 2023: Summary for Policymakers. In: Climate Change 2023: Synthesis Report. Contribution of Working Groups I, II and III to the Sixth Assessment Report of the Intergovernmental Panel on Climate Change [Core Writing Team, H. Lee and J. Romero (eds.)]. IPCC, Geneva, Switzerland, pp. 1-34, doi: 10.59327/IPCC/AR6-9789291691647.001
- [1] Hannah Ritchie, Pablo Rosado and Max Roser (2020) - "Emissions by sector". Published online at OurWorldInData.org. Retrieved from: '<https://ourworldindata.org/emissions-by-sector>' [Online Resource]
- [3] Liu, Z. National carbon emissions from the industry process: Production of glass, soda ash, ammonia, calcium carbide and alumina. *Applied Energy* **2016**, *166*, 239–244.
- [4] Aresta, M.; Dibenedetto, A.; Angelini, A. Catalysis for the Valorization of Exhaust Carbon: from CO<sub>2</sub> to Chemicals, Materials, and Fuels. Technological Use of CO<sub>2</sub>. *Chem. Rev.* **2014**, *114*(3), 1709–1742.
- [5] Sakakura, T.; Choi, J.-C.; Yasuda, H. Transformation of Carbon Dioxide. *Chem. Rev.* **2007**, *107*(6), 2365–2387.
- [6] Calhoun, W.L. Enthalpies of combustion and formation of ethylene carbonate. *J. Chem. Eng. Data* **1983**, *28*(2), 146–148.
- [7] Sun, J.; Fujita, S.; Arai, M. Development in the green synthesis of cyclic carbonate from carbon dioxide using ionic liquids. *Journal of Organometallic Chemistry* **2005**, *690*(15), 3490–3497.
- [8] Schäffner, B.; Schäffner, F.; Verevkin, S.P.; Börner, A. Organic Carbonates as Solvents in Synthesis and Catalysis. *Chem. Rev.* **2010**, *110*(8), 4554–4581.
- [9] Su, C.-C.; He, M.; Amine, R.; Chen, Z.; Sahore, R.; Dietz Rago, N.; Amine, K. Cyclic carbonate for highly stable cycling of high voltage lithium metal batteries. *Energy Storage Materials* **2019**, *17*, 284–292.
- [10] He, Q.; O'Brien, J.W.; Kitselman, K.A.; Tompkins, L.E.; Curtis, G.C.T.; Kerton, F.M. Synthesis of cyclic carbonates from CO<sub>2</sub> and epoxides using ionic liquids and related catalysts including choline chloride–metal halide mixtures. *Catal. Sci. Technol.* **2014**, *4*(6), 1513–1528.
- [11] Cokoja, M.; Wilhelm, M.E.; Anthofer, M.H.; Herrmann, W.A.; Kühn, F.E. Synthesis of Cyclic Carbonates from Epoxides and Carbon Dioxide by Using Organocatalysts. *ChemSusChem* **2015**, *8*(15), 2436–2454.
- [12] Caló, V.; Nacci, A.; Monopoli, A.; Fanizzi, A. Cyclic Carbonate Formation from Carbon Dioxide and Oxiranes in Tetrabutylammonium Halides as Solvents and Catalysts. *Org. Lett.* **2002**, *4*(15), 2561–2563.
- [13] Guo, L.; Lamb, K.J.; North, M. Recent developments in organocatalysed transformations of epoxides and carbon dioxide into cyclic carbonates. *Green Chem.* **2021**, *23*(1), 77–118.

- [14] Kim, H. Imidazolium zinc tetrahalide-catalyzed coupling reaction of CO<sub>2</sub> and ethylene oxide or propylene oxide. *Journal of Catalysis* **2003**, *220*(1), 44–46.
- [15] Darensbourg, D.J.; Lewis, S.J.; Rodgers, J.L.; Yarbrough, J.C. Carbon Dioxide/Epoxyde Coupling Reactions Utilizing Lewis Base Adducts of Zinc Halides as Catalysts. Cyclic Carbonate versus Polycarbonate Production. *Inorg. Chem.* **2003**, *42*(2), 581–589.
- [16] Sun, J.; Fujita, S.-I.; Zhao, F.; Arai, M. A highly efficient catalyst system of ZnBr<sub>2</sub>/*n*-Bu<sub>4</sub>NI for the synthesis of styrene carbonate from styrene oxide and supercritical carbon dioxide. *Applied Catalysis A: General* **2005**, *287*(2), 221–226.
- [17] Sugimoto, H.; Kuroda, K. The Cobalt Porphyrin–Lewis Base System: A Highly Selective Catalyst for Alternating Copolymerization of CO<sub>2</sub> and Epoxyde under Mild Conditions. *Macromolecules* **2008**, *41*(2), 312–317.
- [18] Sibaouih, A.; Ryan, P.; Leskelä, M.; Rieger, B.; Repo, T. Facile synthesis of cyclic carbonates from CO<sub>2</sub> and epoxides with cobalt(II)/onium salt based catalysts. *Applied Catalysis A: General* **2009**, *365*(2), 194–198.
- [19] Darensbourg, D.J.; Moncada, A.I. Tuning the Selectivity of the Oxetane and CO<sub>2</sub> Coupling Process Catalyzed by (Salen)CrCl/ *n*-Bu<sub>4</sub> NX: Cyclic Carbonate Formation vs Aliphatic Polycarbonate Production. *Macromolecules* **2010**, *43*(14), 5996–6003.
- [20] Lu, X.-B.; Darensbourg, D.J. Cobalt catalysts for the coupling of CO<sub>2</sub> and epoxides to provide polycarbonates and cyclic carbonates. *Chem. Soc. Rev.* **2012**, *41*(4), 1462–1484.
- [21] Tian, D.; Liu, B.; Gan, Q.; Li, H.; Darensbourg, Donald.J. Formation of Cyclic Carbonates from Carbon Dioxide and Epoxides Coupling Reactions Efficiently Catalyzed by Robust, Recyclable One-Component Aluminum-Salen Complexes. *ACS Catal.* **2012**, *2*(9), 2029–2035.
- [22] Yang, Y.; Hayashi, Y.; Fujii, Y.; Nagano, T.; Kita, Y.; Ohshima, T.; Okuda, J.; Mashima, K. Efficient cyclic carbonate synthesis catalyzed by zinc cluster systems under mild conditions. *Catal. Sci. Technol.* **2012**, *2*(3), 509–513.
- [23] Whiteoak, C.J.; Kielland, N.; Laserna, V.; Castro-Gómez, F.; Martin, E.; Escudero-Adán, E.C.; Bo, C.; Kleij, A.W. Highly Active Aluminium Catalysts for the Formation of Organic Carbonates from CO<sub>2</sub> and Oxiranes. *Chem. Eur. J.* **2014**, *20*(8), 2264–2275.
- [24] Rintjema, J.; Kleij, A.W. Aluminum-Mediated Formation of Cyclic Carbonates: Benchmarking Catalytic Performance Metrics. *ChemSusChem* **2017**, *10*(6), 1274–1282.
- [25] Meléndez, D.O.; Lara-Sánchez, A.; Martínez, J.; Wu, X.; Otero, A.; Castro-Osma, J.A.; North, M.; Rojas, R.S. Amidinate Aluminium Complexes as Catalysts for Carbon Dioxide Fixation into Cyclic Carbonates. *ChemCatChem* **2018**, *10*(10), 2271–2277.
- [26] Yao, Q.; Shi, Y.; Wang, Y.; Zhu, X.; Yuan, D.; Yao, Y. Bifunctional Rare-Earth Metal Catalysts for Conversion of CO<sub>2</sub> and Epoxides into Cyclic Carbonates. *Asian Journal of Organic Chemistry* **2022**, *11*(8), e202200106.
- [27] Chatelet, B.; Joucla, L.; Dutasta, J.-P.; Martinez, A.; Szeto, K.C.; Dufaud, V. Azaphosphatranes as Structurally Tunable Organocatalysts for Carbonate Synthesis from CO<sub>2</sub> and Epoxides. *J. Am. Chem. Soc.* **2013**, *135*(14), 5348–5351.

- [28] Gennen, S.; Alves, M.; Méreau, R.; Tassaing, T.; Gilbert, B.; Detrembleur, C.; Jerome, C.; Grignard, B. Fluorinated Alcohols as Activators for the Solvent-Free Chemical Fixation of Carbon Dioxide into Epoxides. *ChemSusChem* **2015**, *8*(11), 1845–1849.
- [29] Arayachukiat, S.; Kongtes, C.; Barthel, A.; Vummaleti, S.V.C.; Poater, A.; Wannakao, S.; Cavallo, L.; D’Elia, V. Ascorbic Acid as a Bifunctional Hydrogen Bond Donor for the Synthesis of Cyclic Carbonates from CO<sub>2</sub> under Ambient Conditions. *ACS Sustainable Chem. Eng.* **2017**, *5*(8), 6392–6397.
- [30] Mesías-Salazar, Á.; Martínez, J.; Rojas, R.S.; Carrillo-Hermosilla, F.; Ramos, A.; Fernández-Galán, R.; Antiñolo, A. Aromatic guanidines as highly active binary catalytic systems for the fixation of CO<sub>2</sub> into cyclic carbonates under mild conditions. *Catal. Sci. Technol.* **2019**, *9*(15), 3879–3886.
- [31] Ma, H.; Zeng, J.; Tu, D.; Mao, W.; Zhao, B.; Wang, K.; Liu, Z.; Lu, J. 3-Bromo-1,1,1-trifluoro-2-propanol assisted chemical fixation of CO<sub>2</sub> and epoxides. *Tetrahedron Letters* **2020**, *61*(11), 151593.
- [32] Lichtenwalter, M.; Cooper, J.F. CATALYTIC PROCESS FOR PRODUCING ALKYLENE CARBONATES. 5. 1956.
- [33] Peppel, W.J. Preparation and Properties of the Alkylene Carbonates. *Ind. Eng. Chem.* **1958**, *50*(5), 767–770.
- [34] Wang, L.; Zhang, G.; Kodama, K.; Hirose, T. An efficient metal- and solvent-free organocatalytic system for chemical fixation of CO<sub>2</sub> into cyclic carbonates under mild conditions. *Green Chem.* **2016**, *18*(5), 1229–1233.
- [35] Wang, X.; Wang, L.; Zhao, Y.; Kodama, K.; Hirose, T. Efficient and practical organocatalytic system for the synthesis of cyclic carbonates from carbon dioxide and epoxides: 3-hydroxypyridine/tetra-n-butylammonium iodide. *Tetrahedron* **2017**, *73*(8), 1190–1195.
- [36] Whiteoak, C.J.; Martin, E.; Belmonte, M.M.; Benet-Buchholz, J.; Kleij, A.W. An Efficient Iron Catalyst for the Synthesis of Five- and Six-Membered Organic Carbonates under Mild Conditions. *Adv. Synth. Catal.* **2012**, *354*(2–3), 469–476.
- [37] Shim, J.-J.; Kim, D.; Ra, C.S. Carboxylation of Styrene Oxide Catalyzed by Quaternary Onium Salts under Solvent-free Conditions. *Bull. Korean Chem. Soc.* **2006**, *27*(5), 744–746.
- [38] Wang, J.-Q.; Kong, D.-L.; Chen, J.-Y.; Cai, F.; He, L.-N. Synthesis of cyclic carbonates from epoxides and carbon dioxide over silica-supported quaternary ammonium salts under supercritical conditions. *Journal of Molecular Catalysis A: Chemical* **2006**, *249*(1–2), 143–148.
- [39] Ju, H.-Y.; Manju, M.-D.; Kim, K.-H.; Park, S.-W.; Park, D.-W. Catalytic performance of quaternary ammonium salts in the reaction of butyl glycidyl ether and carbon dioxide. *Journal of Industrial and Engineering Chemistry* **2008**, *14*(2), 157–160.
- [40] Bai, D.; Duan, S.; Hai, L.; Jing, H. Carbon Dioxide Fixation by Cycloaddition with Epoxides, Catalyzed by Biomimetic Metalloporphyrins. *ChemCatChem* **2012**, *4*(11), 1752–1758.

- [41] Kihara, N.; Hara, N.; Endo, T. Catalytic activity of various salts in the reaction of 2,3-epoxypropyl phenyl ether and carbon dioxide under atmospheric pressure. *J. Org. Chem.* **1993**, *58*(23), 6198–6202.
- [42] Clegg, W.; Harrington, R.W.; North, M.; Pasquale, R. Cyclic Carbonate Synthesis Catalysed by Bimetallic Aluminium-Salen Complexes. *Chem. Eur. J.* **2010**, *16*(23), 6828–6843.
- [43] Del Sesto, R.E.; Corley, C.; Robertson, A.; Wilkes, J.S. Tetraalkylphosphonium-based ionic liquids. *Journal of Organometallic Chemistry* **2005**, *690*(10), 2536–2542.
- [44] Sun, J.; Wang, L.; Zhang, S.; Li, Z.; Zhang, X.; Dai, W.; Mori, R. ZnCl<sub>2</sub>/phosphonium halide: An efficient Lewis acid/base catalyst for the synthesis of cyclic carbonate. *Journal of Molecular Catalysis A: Chemical* **2006**, *256*(1–2), 295–300.
- [45] Wu, S.-S.; Zhang, X.-W.; Dai, W.-L.; Yin, S.-F.; Li, W.-S.; Ren, Y.-Q.; Au, C.-T. ZnBr<sub>2</sub>–Ph<sub>4</sub>PI as highly efficient catalyst for cyclic carbonates synthesis from terminal epoxides and carbon dioxide. *Applied Catalysis A: General* **2008**, *341*(1–2), 106–111.
- [46] Bobbink, F.D.; Dyson, P.J. Synthesis of carbonates and related compounds incorporating CO<sub>2</sub> using ionic liquid-type catalysts: State-of-the-art and beyond. *Journal of Catalysis* **2016**, *343*, 52–61.
- [47] Sun, J.; Cheng, W.; Fan, W.; Wang, Y.; Meng, Z.; Zhang, S. Reusable and efficient polymer-supported task-specific ionic liquid catalyst for cycloaddition of epoxide with CO<sub>2</sub>. *Catalysis Today* **2009**, *148*(3–4), 361–367.
- [48] Girard, A.-L.; Simon, N.; Zanatta, M.; Marmitt, S.; Gonçalves, P.; Dupont, J. Insights on recyclable catalytic system composed of task-specific ionic liquids for the chemical fixation of carbon dioxide. *Green Chem.* **2014**, *16*(5), 2815–2825.
- [49] Denizaltı, S. Imidazolium based ionic liquids bearing a hydroxyl group as highly efficient catalysts for the addition of CO<sub>2</sub> to epoxides. *RSC Adv.* **2015**, *5*(56), 45454–45458.
- [50] Castro-Osma, J.A.; Martínez, J.; Cruz-Martínez, F. de la; Caballero, M.P.; Fernández-Baeza, J.; Rodríguez-López, J.; Otero, A.; Lara-Sánchez, A.; Tejada, J. Development of hydroxy-containing imidazole organocatalysts for CO<sub>2</sub> fixation into cyclic carbonates. *Catal. Sci. Technol.* **2018**, *8*(7), 1981–1987.
- [51] Sun, J.; Zhang, S.; Cheng, W.; Ren, J. Hydroxyl-functionalized ionic liquid: a novel efficient catalyst for chemical fixation of CO<sub>2</sub> to cyclic carbonate. *Tetrahedron Letters* **2008**, *49*(22), 3588–3591.
- [52] Anthofer, M.H.; Wilhelm, M.E.; Cokoja, M.; Markovits, I.I.E.; Pöthig, A.; Mink, J.; Herrmann, W.A.; Kühn, F.E. Cycloaddition of CO<sub>2</sub> and epoxides catalyzed by imidazolium bromides under mild conditions: influence of the cation on catalyst activity. *Catal. Sci. Technol.* **2014**, *4*(6), 1749.
- [53] Paddock, R.L.; Hiyama, Y.; McKay, J.M.; Nguyen, S.T. Co(III) porphyrin/DMAP: an efficient catalyst system for the synthesis of cyclic carbonates from CO<sub>2</sub> and epoxides. *Tetrahedron Letters* **2004**, *45*(9), 2023–2026.

- [54] Beattie, C.; North, M.; Villuendas, P.; Young, C. Influence of Temperature and Pressure on Cyclic Carbonate Synthesis Catalyzed by Bimetallic Aluminum Complexes and Application to Overall *syn*-Bis-hydroxylation of Alkenes. *J. Org. Chem.* **2013**, *78*(2), 419–426.
- [55] Martínez-Rodríguez, L.; Ojalora Garmilla, J.; Kleij, A.W. Cavitand-Based Polyphenols as Highly Reactive Organocatalysts for the Coupling of Carbon Dioxide and Oxiranes. *ChemSusChem* **2016**, *9*(7), 749–755.
- [56] Doll, K.M.; Erhan, S.Z. The improved synthesis of carbonated soybean oil using supercritical carbon dioxide at a reduced reaction time. *Green Chem.* **2005**, *7*(12), 849–854.
- [57] Mann, N.; Mendon, S.K.; Rawlins, J.W.; Thames, S.F. Synthesis of Carbonated Vernonia Oil. *J Am Oil Chem Soc* **2008**, *85*(8), 791–796.
- [58] Chen, F.; Zhang, Q.-C.; Wei, D.; Bu, Q.; Dai, B.; Liu, N. Highly Stereo-Controlled Synthesis of Fatty Acid-Derived Cyclic Carbonates by Using Iron(II) Complex and Nucleophilic Halide. *J. Org. Chem.* **2019**, *84*(18), 11407–11416.
- [59] Zhang, L.; Luo, Y.; Hou, Z.; He, Z.; Eli, W. Synthesis of Carbonated Cotton Seed Oil and Its Application as Lubricating Base Oil. *Journal of the American Oil Chemists' Society* **2014**, *91*(1), 143–150.
- [60] Li, Z.; Zhao, Y.; Yan, S.; Wang, X.; Kang, M.; Wang, J.; Xiang, H. Catalytic Synthesis of Carbonated Soybean Oil. *Catal Lett* **2008**, *123*(3), 246–251.
- [61] Guzmán, A.F.; Echeverri, D.A.; Rios, L.A. Carbonation of epoxidized castor oil: a new bio-based building block for the chemical industry. *Journal of Chemical Technology & Biotechnology* **2017**, *92*(5), 1104–1110.
- [62] Natongchai, W.; Pornpraprom, S.; D'Elia, V. Synthesis of Bio-Based Cyclic Carbonates Using a Bio-Based Hydrogen Bond Donor: Application of Ascorbic Acid to the Cycloaddition of CO<sub>2</sub> to Oleochemicals. *Asian Journal of Organic Chemistry* **2020**, *9*(5), 801–810.
- [63] Akhdar, A.; Onida, K.; Vu, N.D.; Grollier, K.; Norsic, S.; Boisson, C.; D'Agosto, F.; Duguet, N. Thermomorphic Polyethylene-Supported Organocatalysts for the Valorization of Vegetable Oils and CO<sub>2</sub>. *Adv. Sustainable Syst.* **2021**, *5*(2), 2000218.
- [64] Langanke, J.; Greiner, L.; Leitner, W. Substrate dependent synergetic and antagonistic interaction of ammonium halide and polyoxometalate catalysts in the synthesis of cyclic carbonates from oleochemical epoxides and CO<sub>2</sub>. *Green Chem.* **2013**, *15*(5), 1173–1182.
- [65] Longwitz, L.; Steinbauer, J.; Spannenberg, A.; Werner, T. Calcium-Based Catalytic System for the Synthesis of Bio-Derived Cyclic Carbonates under Mild Conditions. *ACS Catal.* **2018**, *8*(1), 665–672.
- [66] Martínez, J.; Fernández-Baeza, J.; Sánchez-Barba, L.F.; Castro-Osma, J.A.; Lara-Sánchez, A.; Otero, A. An Efficient and Versatile Lanthanum Heteroscorpionate Catalyst for Carbon Dioxide Fixation into Cyclic Carbonates. *ChemSusChem* **2017**, *10*(14), 2886–2890.
- [67] Li, C.-Y.; Su, Y.-C.; Lin, C.-H.; Huang, H.-Y.; Tsai, C.-Y.; Lee, T.-Y.; Ko, B.-T. Synthesis and characterization of trimetallic cobalt, zinc and nickel complexes containing amine-

bis(benzotriazole phenolate) ligands: efficient catalysts for coupling of carbon dioxide with epoxides. *Dalton Trans.* **2017**, 46(44), 15399–15406.

[68] Cruz-Martínez, F. de la; Martínez de Sarasa Buchaca, M.; Martínez, J.; Fernández-Baeza, J.; Sánchez-Barba, L.F.; Rodríguez-Diéguez, A.; Castro-Osma, J.A.; Lara-Sánchez, A. Synthesis of Bio-Derived Cyclic Carbonates from Renewable Resources. *ACS Sustainable Chem. Eng.* **2019**, 7(24), 20126–20138.

[69] Navarro, M.; Sánchez-Barba, L.F.; Garcés, A.; Fernández-Baeza, J.; Fernández, I.; Lara-Sánchez, A.; Rodríguez, A.M. Bimetallic scorpionate-based helical organoaluminum complexes for efficient carbon dioxide fixation into a variety of cyclic carbonates. *Catal. Sci. Technol.* **2020**, 10(10), 3265–3278.

[70] Fiorani, G.; Stuck, M.; Martín, C.; Belmonte, M.M.; Martín, E.; Escudero-Adán, E.C.; Kleij, A.W. Catalytic Coupling of Carbon Dioxide with Terpene Scaffolds: Access to Challenging Bio-Based Organic Carbonates. *ChemSusChem* **2016**, 9(11), 1304–1311.

[71] Maeda, C.; Shimonishi, J.; Miyazaki, R.; Hasegawa, J.; Ema, T. Highly Active and Robust Metalloporphyrin Catalysts for the Synthesis of Cyclic Carbonates from a Broad Range of Epoxides and Carbon Dioxide. *Chemistry – A European Journal* **2016**, 22(19), 6556–6563.

[72] Sun, J.; Cheng, W.; Yang, Z.; Wang, J.; Xu, T.; Xin, J.; Zhang, S. Superbase/cellulose: an environmentally benign catalyst for chemical fixation of carbon dioxide into cyclic carbonates. *Green Chem.* **2014**, 16(6), 3071–3078.

[73] Seki, T.; Grunwaldt, J.-D.; Baiker, A. In Situ Attenuated Total Reflection Infrared Spectroscopy of Imidazolium-Based Room-Temperature Ionic Liquids under “Supercritical” CO<sub>2</sub>. *J. Phys. Chem. B* **2009**, 113(1), 114–122.

[74] Peng, J.; Deng, Y. Cycloaddition of carbon dioxide to propylene oxide catalyzed by ionic liquids. *New J. Chem.* **2001**, 25(4), 639–641.

[75] Natongchai, W.; Luque-Urrutia, J.A.; Phungpanya, C.; Solà, M.; D’Elia, V.; Poater, A.; Zipse, H. Cycloaddition of CO<sub>2</sub> to epoxides by highly nucleophilic 4-aminopyridines: establishing a relationship between carbon basicity and catalytic performance by experimental and DFT investigations. *Org. Chem. Front.* **2021**, 8(3), 613–627.

[76] Villiers, C.; Dognon, J.-P.; Pollet, R.; Thuéry, P.; Ephritikhine, M. An Isolated CO<sub>2</sub> Adduct of a Nitrogen Base: Crystal and Electronic Structures. *Angewandte Chemie International Edition* **2010**, 49(20), 3465–3468.

[77] Barbarini, A.; Maggi, R.; Mazzacani, A.; Mori, G.; Sartori, G.; Sartorio, R. Cycloaddition of CO<sub>2</sub> to epoxides over both homogeneous and silica-supported guanidine catalysts. *Tetrahedron Letters* **2003**, 44(14), 2931–2934.

[78] Sun, J.; Fujita, S.; Zhao, F.; Arai, M. Synthesis of styrene carbonate from styrene oxide and carbon dioxide in the presence of zinc bromide and ionic liquid under mild conditions. *Green Chem.* **2004**, 6(12), 613.

[79] Kruper, W.J.; Dellar, D.D. Catalytic Formation of Cyclic Carbonates from Epoxides and CO<sub>2</sub> with Chromium Metalloporphyrinates. *J. Org. Chem.* **1995**, 60, 725–727.



- [80] Jin, L.; Jing, H.; Chang, T.; Bu, X.; Wang, L.; Liu, Z. Metal porphyrin/phenyltrimethylammonium tribromide: High efficient catalysts for coupling reaction of CO<sub>2</sub> and epoxides. *Journal of Molecular Catalysis A: Chemical* **2007**, *261*(2), 262–266.
- [81] Srivastava, R.; Bennur, T.H.; Srinivas, D. Factors affecting activation and utilization of carbon dioxide in cyclic carbonates synthesis over Cu and Mn peraza macrocyclic complexes. *Journal of Molecular Catalysis A: Chemical* **2005**, *226*(2), 199–205.
- [82] Paddock, R.L.; Nguyen, S.T. Chemical CO<sub>2</sub> Fixation: Cr(III) Salen Complexes as Highly Efficient Catalysts for the Coupling of CO<sub>2</sub> and Epoxides. *J. Am. Chem. Soc.* **2001**, *123*(46), 11498–11499.
- [83] Decortes, A.; Castilla, A.M.; Kleij, A.W. Salen-Complex-Mediated Formation of Cyclic Carbonates by Cycloaddition of CO<sub>2</sub> to Epoxides. *Angewandte Chemie International Edition* **2010**, *49*(51), 9822–9837.
- [84] Paddock, R.L.; Nguyen, S.T. Chiral (salen)Co(III) catalyst for the synthesis of cyclic carbonates. *Chem. Commun.* **2004**, (14), 1622–1623.
- [85] Lu, X.-B.; He, R.; Bai, C.-X. Synthesis of ethylene carbonate from supercritical carbon dioxide/ethylene oxide mixture in the presence of bifunctional catalyst. *Journal of Molecular Catalysis A: Chemical* **2002**, *186*(1), 1–11.
- [86] Clegg, W.; Harrington, R.W.; North, M.; Pasquale, R. Cyclic Carbonate Synthesis Catalysed by Bimetallic Aluminium–Salen Complexes. *Chemistry – A European Journal* **2010**, *16*(23), 6828–6843.
- [87] Shen, Y.-M.; Duan, W.-L.; Shi, M. Chemical Fixation of Carbon Dioxide Catalyzed by Binaphthyldiamino Zn, Cu, and Co Salen-Type Complexes. *J. Org. Chem.* **2003**, *68*(4), 1559–1562.
- [88] Whiteoak, C.J.; Nova, A.; Maseras, F.; Kleij, A.W. Merging Sustainability with Organocatalysis in the Formation of Organic Carbonates by Using CO<sub>2</sub> as a Feedstock. *ChemSusChem* **2012**, *5*(10), 2032–2038.
- [89] Chen, F.; Dong, T.; Xu, T.; Li, X.; Hu, C. Direct synthesis of cyclic carbonates from olefins and CO<sub>2</sub> catalyzed by a MoO<sub>2</sub>(acac)<sub>2</sub>-quaternary ammonium salt system. *Green Chem.* **2011**, *13*(9), 2518.
- [90] Calmanti, R.; Sargentoni, N.; Selva, M.; Perosa, A. One-Pot Tandem Catalytic Epoxidation—CO<sub>2</sub> Insertion of Monounsaturated Methyl Oleate to the Corresponding Cyclic Organic Carbonate. *Catalysts* **2021**, *11*(12), 1477.
- [91] Xie, J.-N.; Diao, Z.-F.; Qiao, C.; Ma, R.; He, L.-N. One-pot stepwise synthesis of cyclic carbonates directly from olefins with CO<sub>2</sub> promoted by K<sub>2</sub>S<sub>2</sub>O<sub>8</sub>/NaBr. *Journal of CO<sub>2</sub> Utilization* **2016**, *16*, 313–317.
- [92] Das, R.; Kamra, S.; Nagaraja, C.M. Ionic Fe(III)-porphyrin frameworks for the one-pot synthesis of cyclic carbonates from olefins and CO<sub>2</sub>. *Inorg. Chem. Front.* **2023**, *10*(7), 2088–2099.

- [93] Yu, K.; Puthiaraj, P.; Ahn, W.-S. One-pot catalytic transformation of olefins into cyclic carbonates over an imidazolium bromide-functionalized Mn(III)-porphyrin metal–organic framework. *Applied Catalysis B: Environmental* **2020**, *273*, 119059.
- [94] Liu, J.; Yang, G.; Liu, Y.; Wu, D.; Hu, X.; Zhang, Z. Metal-free imidazolium hydrogen carbonate ionic liquids as bifunctional catalysts for the one-pot synthesis of cyclic carbonates from olefins and CO<sub>2</sub>. *Green Chem.* **2019**, *21*(14), 3834–3838.
- [95] Fang, J.; Li, K.; Wang, Z.; Li, D.; Ma, Y.; Gong, X.; Hou, Z. Direct oxidative carboxylation of olefins into cyclic carbonates at ambient pressure. *Journal of CO<sub>2</sub> Utilization* **2020**, *40*, 101204.
- [96] Ochiai, B.; Iwamoto, T.; Miyazaki, K.; Endo, T. Efficient Gas–Solid Phase Reaction of Atmospheric Carbon Dioxide into Copolymers with Pendent Oxirane Groups: Effect of Comonomer Component and Catalyst on Incorporation Behavior. *Macromolecules* **2005**, *38*(24), 9939–9943.
- [97] Ochiai, B.; Iwamoto, T.; Miyagawa, T.; Nagai, D.; Endo, T. Solid-phase incorporation of gaseous carbon dioxide into oxirane-containing copolymers. *Journal of Polymer Science Part A: Polymer Chemistry* **2004**, *42*(15), 3812–3817.
- [98] Ochiai, B.; Iwamoto, T.; Endo, T. Selective gas–solid phase fixation of carbon dioxide into oxirane-containing polymers: synthesis of polymer bearing cyclic carbonate group. *Green Chem.* **2006**, *8*(2), 138.
- [99] Ochiai, B.; Nakayama, T. Dispersion polymerization accompanied by CO<sub>2</sub> fixation: Synthesis of particles of polymers bearing cyclic carbonate and epoxide moieties. *Journal of Polymer Science Part A: Polymer Chemistry* **2010**, *48*(23), 5382–5390.
- [100] Ochiai, B.; Hatano, Y.; Endo, T. Facile synthesis of polymers bearing cyclic carbonate structure through radical solution and precipitation polymerizations accompanied by concurrent carbon dioxide fixation. *Journal of Polymer Science Part A: Polymer Chemistry* **2009**, *47*(12), 3170–3176.
- [101] Ochiai, B.; Iwamoto, T.; Miyagawa, T.; Nagai, D.; Endo, T. Direct incorporation of gaseous carbon dioxide into solid-state copolymer containing oxirane and quaternary ammonium halide structure as self-catalytic function. *Journal of Polymer Science Part A: Polymer Chemistry* **2004**, *42*(19), 4941–4947.
- [102] Katz, H.E. Preparation of soluble poly(carbonyldioxyglyceryl methacrylate). *Macromolecules* **1987**, *20*(8), 2026–2027.
- [103] Kihara, N.; Endo, T. Synthesis and reaction of polymethacrylate bearing cyclic carbonate moieties in the side chain. *Makromol. Chem.* **1992**, *193*(6), 1481–1492.
- [104] Sakai, T.; Kihara, N.; Endo, T. Polymer Reaction of Epoxide and Carbon Dioxide. Incorporation of Carbon Dioxide into Epoxide Polymers. *Macromolecules* **1995**, *28*(13), 4701–4706.
- [105] Park, S.-Y.; Lee, H.-S.; Ha, C.-S.; Park, D.-W. Synthesis of poly(2-oxo-1,3-dioxolane-4-yl) methyl methacrylate by polymer reaction of carbon dioxide and miscibility of its blends

with copolymers of methyl methacrylate and ethyl acrylate. *Journal of Applied Polymer Science* **2001**, *81*(9), 2161–2169.

[106] Kihara, N.; Endo, T. Incorporation of carbon dioxide into poly(glycidyl methacrylate). *Macromolecules* **1992**, *25*(18), 4824–4825.

[107] Park, S.-Y.; Park, H.-Y.; Lee, H.-S.; Park, S.-W.; Ha, C.-S.; Park, D.-W. Synthesis of poly[(2-oxo-1,3-dioxolane-4-yl) methyl methacrylate-co-ethyl acrylate] by incorporation of carbon dioxide into epoxide polymer and the miscibility behavior of its blends with poly(methyl methacrylate) or poly(vinyl chloride). *Journal of Polymer Science Part A: Polymer Chemistry* **2001**, *39*(9), 1472–1480.

[108] Liu, B.; Zhang, Y.-Y.; Zhang, X.-H.; Du, B.-Y.; Fan, Z.-Q. Fixation of carbon dioxide concurrently or in tandem with free radical polymerization for highly transparent polyacrylates with specific UV absorption. *Polymer Chemistry* **2016**, *9*.

[109] Kihara, N.; Endo, T. Self-Catalyzed Carbon Dioxide Incorporation System. The Reaction of Copolymers Bearing an Epoxide and a Quaternary Ammonium Group with Carbon Dioxide. *Macromolecules* **1994**, *27*(22), 6239–6244.

[110] Park, S.Y.; Park, H.Y.; Park, D.W.; Ha, C.S. DIRECT INCORPORATION OF CARBON DIOXIDE INTO POLY(GLYCIDYL METHACRYLATE-CO-ACRYLONITRILE) USING QUATERNARY AMMONIUM SALT CATALYST AND ITS APPLICATION TO POLYMER BLENDS. *Journal of Macromolecular Science, Part A* **2002**, *39*(6), 573–589.

[111] Yadollahi, M.; Bouhendi, H.; Zohuriaan-Mehr, M.J.; Farhadnejad, H.; Kabiri, K. Investigation of viscoelastic and thermal properties of cyclic carbonate bearing copolymers. *Polym. Sci. Ser. B* **2013**, *55*(5–6), 327–335.

[112] Dechent, S.-E.; Kleij, A.W.; Luinstra, G.A. Fully bio-derived CO<sub>2</sub> polymers for non-isocyanate based polyurethane synthesis. *Green Chem.* **2020**, *22*(3), 969–978.

[113] Kawahara, S.; Saito, T. Preparation of carbonated natural rubber. *Journal of Polymer Science Part A: Polymer Chemistry* **2006**, *44*(4), 1561–1567.

[114] Jiang, Q.; Gao, Y.; Liao, L.; Yu, R.; Liao, J. Biodegradable Natural Rubber Based on Novel Double Dynamic Covalent Cross-Linking. *Polymers* **2022**, *14*(7), 1380.

---

# Chapter 2:

## Carbonatation of [ethylene-glycidyl methacrylate]-based copolymers with carbon dioxide as a reagent: from batch to solvent-free reactive extrusion

---

**Chapter 2** focus on the carbonatation of industrial non-polar semi-crystalline polymers containing epoxide pendant groups to obtained modified polymers with both epoxides and cyclic carbonate functions. The reaction will be first studied in batch for a better understanding of the influence of the different reaction parameters, and then transposed to a solvent-free reactive extrusion process to develop an original continuous process for the modification of epoxidized polymers with CO<sub>2</sub>. This chapter is based on an article published in Green Chemistry (Guerdener *et al.*, **Green Chem.**, 2023,25, 6355-6364), with additional results and discussion. All the characterizations (<sup>1</sup>H, <sup>13</sup>C NMR, IR-ATR, DSC, SEC and TGA) are reported in Appendices.



## **Table of Contents**

<b>I. Résumé .....</b>	<b>94</b>
<b>II. Abstract .....</b>	<b>95</b>
<b>III. Introduction.....</b>	<b>96</b>
<b>IV. Results and discussion .....</b>	<b>99</b>
IV.1. Optimisation of the conditions in batch.....	99
IV.1.a. Screening of the catalysts.....	99
IV.1.b. Influence of the halides .....	102
IV.1.c. Influence of the alkyl chains.....	104
IV.1.d. Influence of the reaction parameters .....	106
IV.1.e. Influence of the acrylate comonomer .....	108
IV.2. Methodology transposition to reactive extrusion .....	109
IV.2.a. Effect of the extrusion parameters on the mean residence time .....	110
IV.2.b. Optimisation of the reactive extrusion process .....	115
IV.2.c. Comparison of the reaction kinetics of the batch and reactive extrusion processes.....	118
<b>V. Conclusion .....</b>	<b>121</b>
<b>VI. References.....</b>	<b>123</b>

## I. Résumé

La carbonatation de polymères semi-cristallins à base de monomères [éthylène-méthacrylate de glycidyle] a été réalisée en utilisant le dioxyde de carbone comme réactif et des sels d'ammonium quaternaires comme organocatalyseurs pour convertir les groupes pendants époxyde des polymères en groupements carbonate cyclique. Un réacteur batch nous a permis d'évaluer la cinétique, l'effet de la structure du catalyseur et le potentiel global de cette réaction. L'influence de la composition du sel d'ammonium (anion/cation) a été étudiée dans le toluène à 110 °C pour contourner les températures de fusion élevées de ces copolymères riches en unités éthylène et obtenir un milieu homogène. La quantité de catalyseur, la pression de CO<sub>2</sub> et la température ont également été optimisées (TBAB, 5 mol% par rapport à la teneur en époxy, 4,0 MPa, 110 °C) pour permettre une conversion quantitative des époxydes en carbonates cycliques.

Par la suite, la réaction a été transposée, pour la première fois, vers un procédé d'extrusion réactive sous CO<sub>2</sub> à l'aide d'une extrudeuse bi-vis co-rotative dédiée pour permettre le confinement du CO<sub>2</sub> dans le polymère fondu. Ce procédé réactif sans solvant est parfaitement adapté aux polymères semi-cristallins et/ou à haute  $T_g$ . Après optimisation, un rendement allant jusqu'à 78 % de carbonate cyclique, en plus de l'époxyde résiduel, a pu être obtenu avec THAB (7.5 mol% par rapport au taux en époxyde, ~30 g/h de catalyseur) à 150 °C avec un débit de polymère de 2 kg/h.

Les réactivités respectives des polymères [éthylène-méthacrylate de glycidyle-acrylate de méthyle] (E-GMA-MA), [éthylène-méthacrylate de glycidyle-acrylate de butyle] (E-GMA-BA) et [éthylène-méthacrylate de glycidyle] (E-GMA) ont été comparées en batch et en extrudeuse, révélant cette tendance à la carbonatation : E-GMA < E-GMA-BA < E-GMA-MA. La durabilité et la productivité accrue de la méthodologie de carbonatation développée ici reposent sur l'utilisation du CO<sub>2</sub> comme réactif pour la fonctionnalisation des polymères époxydés en exploitant un procédé d'extrusion réactif continu et propre permettant, en une seule opération et en quelques minutes, la production de polymères fonctionnels à l'échelle du kilogramme dans des conditions sans solvant.

## **II. Abstract**

The carbonatation of semi-crystalline [ethylene-glycidyl methacrylate]-based polymers was achieved using carbon dioxide as a reagent and quaternary ammonium salts as organocatalysts to transform the polymers' epoxide pendant groups into cyclic carbonate moieties. A batch reactor allowed us to assess the kinetics, dependence on a catalyst and overall potential of this carbonatation. The influence of the ammonium salt composition (anion/cation) was studied in toluene at 110 °C to circumvent the high melting temperatures of these ethylene unit-rich copolymers and obtain a homogeneous medium. The amount of catalyst, CO<sub>2</sub> pressure and temperature were also optimized (TBAB, 5 mol% vs. epoxy content, 4.0 MPa, 110 °C) to allow for quantitative conversion of epoxides into cyclic carbonates.

Subsequently, the reaction was transposed, for the 1<sup>st</sup> time, to reactive extrusion under CO<sub>2</sub> using a dedicated co-rotating twin-screw extruder to allow for CO<sub>2</sub> containment within the polymer melt. This solvent-free reactive process is perfectly adapted to semi-crystalline and/or high-*T<sub>g</sub>* polymers. After optimization, a yield of up to 78 % of cyclic carbonate, in addition to orthogonal epoxide, could be obtained with THAB (7.5 mol% vs. epoxy content, ~30 g/h of cat.) at 150 °C with an industry-compliant polymer flow rate of 2 kg/h.

The respective reactivities of [ethylene-glycidyl methacrylate-methyl acrylate]-(E-GMA-MA), [ethylene-glycidyl methacrylate-butyl acrylate]-(E-GMA-BA) and [ethylene-glycidyl methacrylate]-(E-GMA) polymers were compared in batch and in an extruder, unveiling this trend towards carbonatation: E-GMA < E-GMA-BA < E-GMA-MA. Sustainability and enhanced productivity of the carbonatation methodology developed herein relies on the use of CO<sub>2</sub> as a C1 reagent for the functionalization of epoxide-bearing polymers harnessing a continuous and clean reactive extrusion process allowing, in a single operation and a few minutes, the production of functional polymers at the kilogram scale under solvent-free conditions.



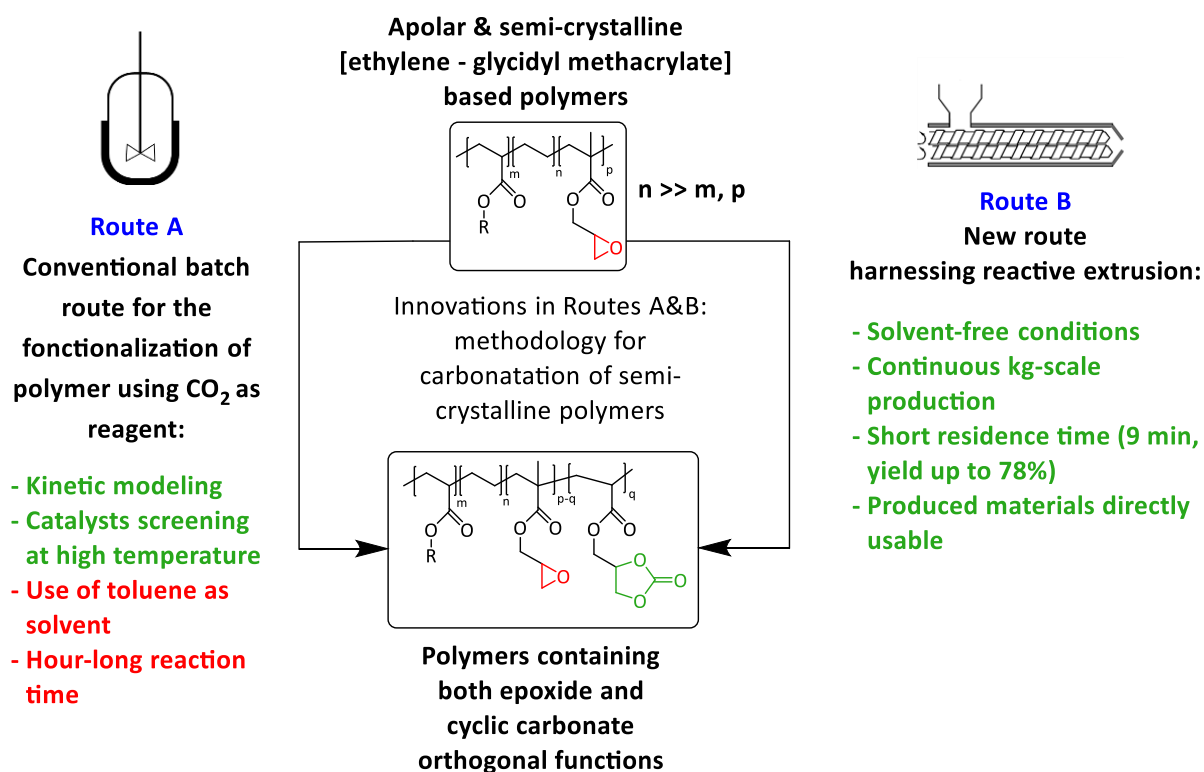
### III. Introduction

The chemical valorization of CO<sub>2</sub> into valuable products has been extensively studied in recent years.<sup>[1-5]</sup> More specifically, the synthesis of organic carbonates *via* the coupling reaction between inert CO<sub>2</sub> and energy-rich epoxides has been the subject of great interest, due to the multiple industrial applications of cyclic carbonates<sup>[6-8]</sup> and the high atom efficiency of this transformation.<sup>[9]</sup> By focusing on CO<sub>2</sub> upgrading for the advantageous derivatization of epoxides into cyclic carbonates (cycloaddition) or carbonate linkages (*e.g.* polymerization), one can indeed manufacture useful industrial platform molecules or benefit from the direct incorporation of CO<sub>2</sub> as a C1 building block in high-tonnage materials.<sup>[9-21]</sup> When post-modification of substrates more complex than simple epoxides is considered, *i.e.*, biosourced fatty acids,<sup>[22-27]</sup> bio-based epoxides<sup>[22,28-31]</sup> or synthetic polymers featuring epoxide moieties,<sup>[32-39]</sup> this transformation may be relevant to improve the usability prospects of (macro)molecules while utilizing abundant CO<sub>2</sub>. There are two possible routes for the cycloaddition of CO<sub>2</sub> to epoxides depending on the nature of the catalyst used. As catalysis is well reported and exemplified in the literature,<sup>[40-66]</sup> it is very easy to select and tune the solubility/reactivity/selectivity of the catalyst system to the needs for specific carbonation (physical steric and electronic properties of the substrates in particular). Very interestingly, when CO<sub>2</sub> is used in post-polymerization as a derivatization agent, novel polymers bearing cyclic carbonate functional groups can be created. They have found applications in different sectors. They can be used as solid electrolytes thanks to their good lithium ion conductivity,<sup>[67]</sup> they can also be mixed with other polymers to create homogeneous films,<sup>[34]</sup> or can play the role of reactive compatibilizers.<sup>[68]</sup>

Moreover, cyclic carbonates and epoxides may show orthogonal reactivity: cyclic carbonates are more prone to react with amines than epoxides to produce, for example, hydroxyurethane functions,<sup>[10,13,14,19,67]</sup> and epoxides are more susceptible to hydrolysis than cyclic carbonates.<sup>[38]</sup>

However, in most cases, functionalization with CO<sub>2</sub> is carried out on polar polymers, highly soluble in polar solvents, in a batch reactor.<sup>[32-39]</sup> The chemical fixation of CO<sub>2</sub> to an apolar and semi-crystalline polymer bearing epoxide moieties is much more challenging (*Scheme 1*) because of the difficulties in obtaining an intimate and homogeneous mixture of the polymer, the CO<sub>2</sub> reactant and the catalyst.

## Chapter 2: Carbonatation of [ethylene-glycidyl methacrylate]-based copolymers with carbon dioxide as a reagent



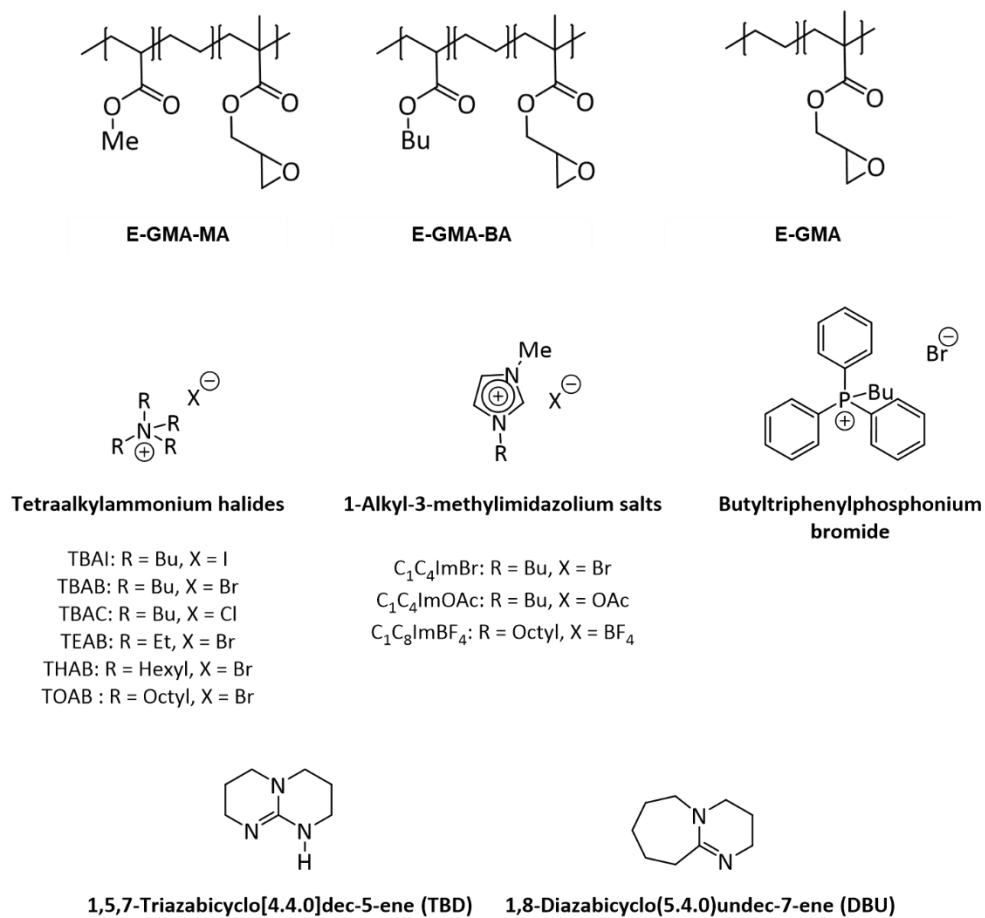
*Scheme 1.* Transposition of carbonatation from batch to reactive extrusion.

In this work, we report on the development and optimization of the conditions for converting the epoxide groups of three different ethylene-containing copolymers, thus mostly apolar copolymers – [ethylene-glycidyl methacrylate-methyl acrylate] terpolymer (E-GMA-MA), [ethylene-glycidyl methacrylate-butyl acrylate] terpolymer (E-GMA-BA) and [ethylene-glycidyl methacrylate] copolymer (E-GMA) (structure in *Scheme 2*) – into the corresponding cyclic carbonates *via* the organocatalyzed cycloaddition of CO<sub>2</sub> in batch and by reactive extrusion processes. The reaction conditions were first investigated in batch for a better understanding of the influence of the different reaction parameters, and then transposed to a solvent-free reactive extrusion process in order to develop an original sustainable continuous process for the modification of epoxidized polymers with CO<sub>2</sub>.

This strategy allows for the introduction of a cyclic carbonate moiety in addition to and orthogonal to the remaining epoxides, which could prove valuable for a wide variety of material applications.<sup>[19,69,70]</sup>

We chose to pursue metal-free mediated CO<sub>2</sub> fixation methodologies for sustainability and material compatibility considerations and to avoid problematic metallic residues in the final polymer products. Among the organocatalysts developed so far to enable the efficient

transformation of molecular epoxides, one can cite onium salts with ammonium or phosphonium halides, ionic liquids and organic bases. Their catalytic behavior towards glycidyl-methacrylate based polymers will be explored in the present work (*Scheme 2*).



*Scheme 2. Polymers and catalysts studied in this work.*

## IV. Results and discussion

### IV.1. Optimisation of the conditions in batch

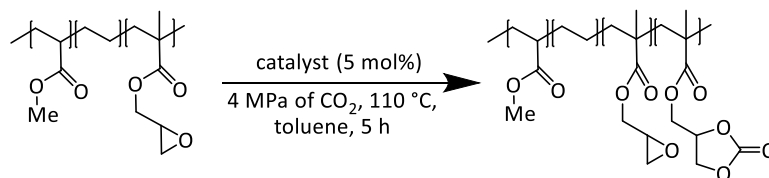
#### IV.1.a. Screening of the catalysts

First, commercially available organic salts such as tetrabutylammonium bromide (TBAB), butyltriphenylphosphonium bromide (PPh<sub>3</sub>BuBr), 1-butyl-3-methylimidazolium bromide (C<sub>1</sub>C<sub>4</sub>ImBr), 1-butyl-3-methylimidazolium acetate (C<sub>1</sub>C<sub>4</sub>ImOAc) and 1-methyl-3-octylimidazolium tetrafluoroborate (C<sub>1</sub>C<sub>8</sub>ImBF<sub>4</sub>), and organic bases such as 1,5,7-triazabicyclo[4.4.0]dec-5-ene (TBD) and 1,8-diazabicyclo[5.4.0]undec-7-ene (DBU) were tested as catalysts for the cycloaddition of CO<sub>2</sub> to E-GMA-MA under the following conditions: 110 °C, 5 h, 4.0 MPa of CO<sub>2</sub> and 5 mol% of catalyst. Toluene was used to solubilize the E-GMA-MA. We did attempt to realize the transformation under “solvent-free” conditions in our batch reaction; however, very heterogeneous reaction media were obtained, even after 5 hours of reaction, and inconsistent and low conversions in carbonates were achieved. Toluene is a good solvent for [ethylene-glycidyl methacrylate] based polymers and is easily accessible to most research teams. As shown in [Table 1](#), epoxide activation with halide anions proved to be the best route to achieve satisfactory conversion ([Table 1](#), entries 1–3), whereas only traces of cyclic carbonates were observed when using sterically hindered nucleophiles and bases ([Table 1](#), entries 4–7). TBAB showed the best performance for the carbonatation of E-GMA-MA with a quantitative yield of cyclic carbonate ([Table 1](#), entry 1). It should be noted that the imidazolium and phosphonium salts were only partially soluble in toluene at 110 °C unlike TBAB (completely soluble, even at room temperature), which may explain their low reactivity. The formation of the cyclic carbonate product was confirmed by IR-ATR ([Figure 1](#)) and <sup>1</sup>H NMR ([Figure 2](#)). After 5 hours of reaction of E-GMA-MA with CO<sub>2</sub> catalyzed by TBAB, the characteristic band of epoxide at 911 cm<sup>-1</sup> disappeared with the concomitant appearance of the band at 1820 cm<sup>-1</sup> typical of the C=O stretching vibration of cyclic carbonates<sup>[71]</sup> ([Figure 1](#)). On the other hand, the <sup>1</sup>H NMR signals g, h and i related to the glycidyl methacrylate monomers almost disappeared and new signals h', g' and i' corresponding to the carbonate product appeared.

Since tetrabutylammonium bromide proved to be the best performing catalyst, other key parameters such as the structural catalyst features and reaction conditions were assessed in

the following studies using tetraalkylammonium halide salts with different substituents and counteranions.

*Table 1. Screening of catalysts.<sup>a</sup>*



Entry	catalyst	Yield <sup>b</sup> (%)
<b>1</b>	<b>TBAB</b>	<b>99<sup>c</sup></b>
2	PPh <sub>3</sub> BuBr	6
3	C <sub>1</sub> C <sub>4</sub> ImBr	24
4	C <sub>1</sub> C <sub>8</sub> ImBF <sub>4</sub>	0
5	C <sub>1</sub> C <sub>4</sub> ImOAc	2
6	TBD	1
7	DBU	10

<sup>a</sup>Conditions: 2.0 g of E-GMA-MA (1.1 mmol of glycidyl methacrylate), 0.057 mmol of catalyst (5 mol%), 2.0 mL of toluene, 110 °C, 4.0 MPa of CO<sub>2</sub>, 5 h. <sup>b</sup>Yield determined by IR-ATR using a calibration curve (see [Figure S12](#) in appendices). <sup>c</sup>Yield determined by <sup>1</sup>H NMR (see [Figure S15](#) in appendices).

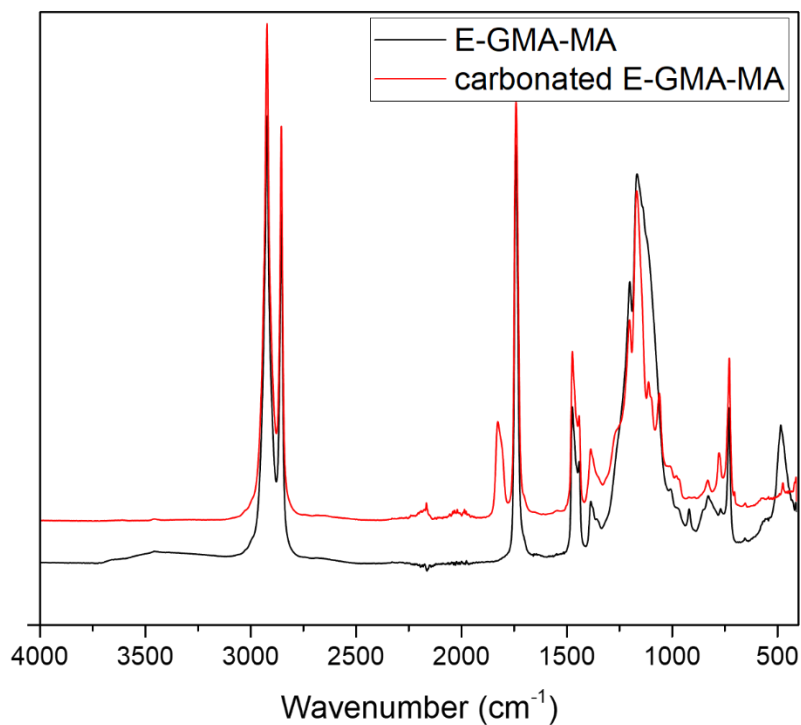


Figure 1. IR-ATR spectra of E-GMA-MA and modified E-GMA-MA with  $\text{CO}_2$  (Table 1, entry 1).

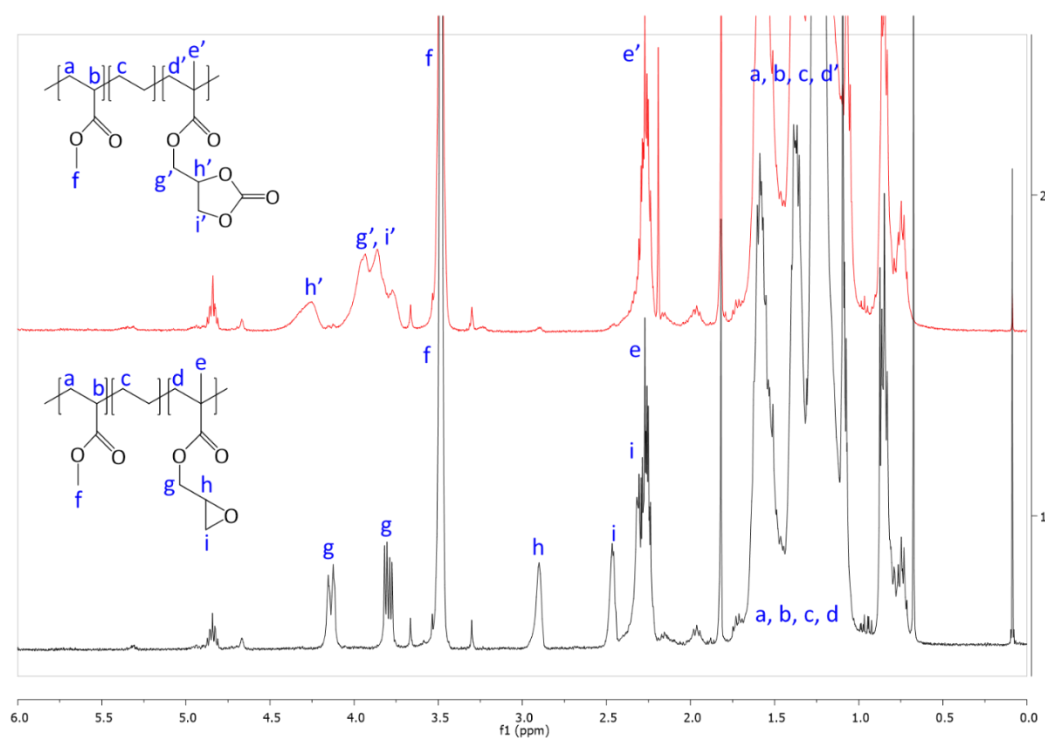


Figure 2.  $^1\text{H}$  NMR ( $\text{TCE}/\text{C}_6\text{D}_6$ , 400MHz) spectra of E-GMA-MA and modified E-GMA-MA with  $\text{CO}_2$  (Table 1, entry 1) (see also Figure S3 and Figure S15 in appendices).

#### IV.1.b. Influence of the halides

The influence of the halide anion on the reaction kinetics is a crucial parameter to take into account as it is involved in epoxide ring-opening, the first step of the catalytic cycle. The pseudo-first order kinetics of the reaction was assessed with tetrabutylammonium iodide (TBAI) and TBAB (*Figure 3*). Assuming that the concentrations of CO<sub>2</sub> and catalyst are constant in the liquid phase over time, the reaction rate could be written as:

$$-\frac{dC_{epoxide}}{dt} = k_{obs} \cdot C_{epoxide}^a \quad (1)$$

$$\text{where } k_{obs} = k \cdot C_{CO_2}^b \cdot C_{catalyst}^c$$

If the reaction follows a pseudo-first order kinetic, the differential equations can be integrated, and  $k_{obs}$  can be estimated:

$$\ln\left(\frac{C_{epoxide,o}}{C_{epoxide}}\right) = k_{obs} \cdot t \quad (2)$$

As no side-reaction was observed with TBAI and TBAB, the yield of the cyclic carbonate product is equal to the conversion of the epoxide moiety and can be expressed as follows:

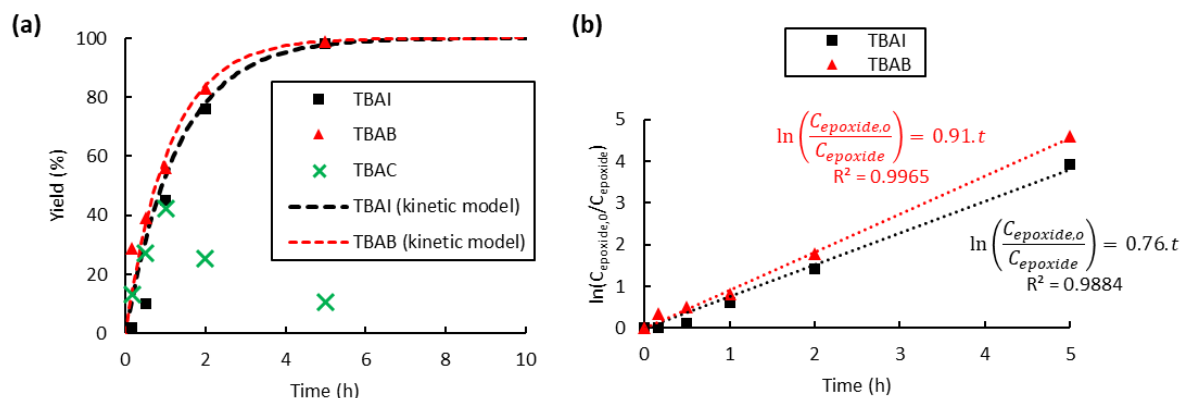
$$Yield = 1 - e^{-k_{obs} \cdot t} \quad (3)$$

*Figure 3* shows the plots of equation (2) and (3). From these data the rate constant  $k_{obs}$  was estimated to be 0.76 h<sup>-1</sup> and 0.91 h<sup>-1</sup> for the reaction catalyzed with respectively TBAI and TBAB, suggesting that Br<sup>-</sup> has a higher catalytic activity than I<sup>-</sup>. In the case of the carbonatation of terminal molecular epoxides under neat conditions or in apolar solvents such as toluene, the order of activity follows the order of halide nucleophilicity and leaving group ability: I<sup>-</sup> > Br<sup>-</sup> > Cl<sup>-</sup> > F<sup>-</sup> [40,44,52,63,64,72-74] But in the case of the carbonatation of sterically hindered terminal epoxides, a good balance between the halide size and its leaving group ability is required. [71,74] A too voluminous and polarizable halide would not favor the attack of the halide on the epoxide, which could explain why I<sup>-</sup> is less active than Br<sup>-</sup>.

In the case of tetrabutylammonium chloride (TBAC), the consumption of the formed cyclic carbonates was observed after 1 hour of reaction at 110 °C (*Figure 3 (a)*), which could be due to a secondary reaction, leading to a polymer less or even non-soluble in toluene, likely due to crosslinking, compared to the modified polymers obtained with TBAI and TBAB. Ochiai *et al.* observed a similar behaviour with CO<sub>2</sub> fixation to poly(glycidyl methacrylate-co-methyl methacrylate) catalyzed by tetrabutylammonium fluoride (TBAF) and suggested that polymerization of the sole epoxide to polyethers was favored due to the weak leaving group

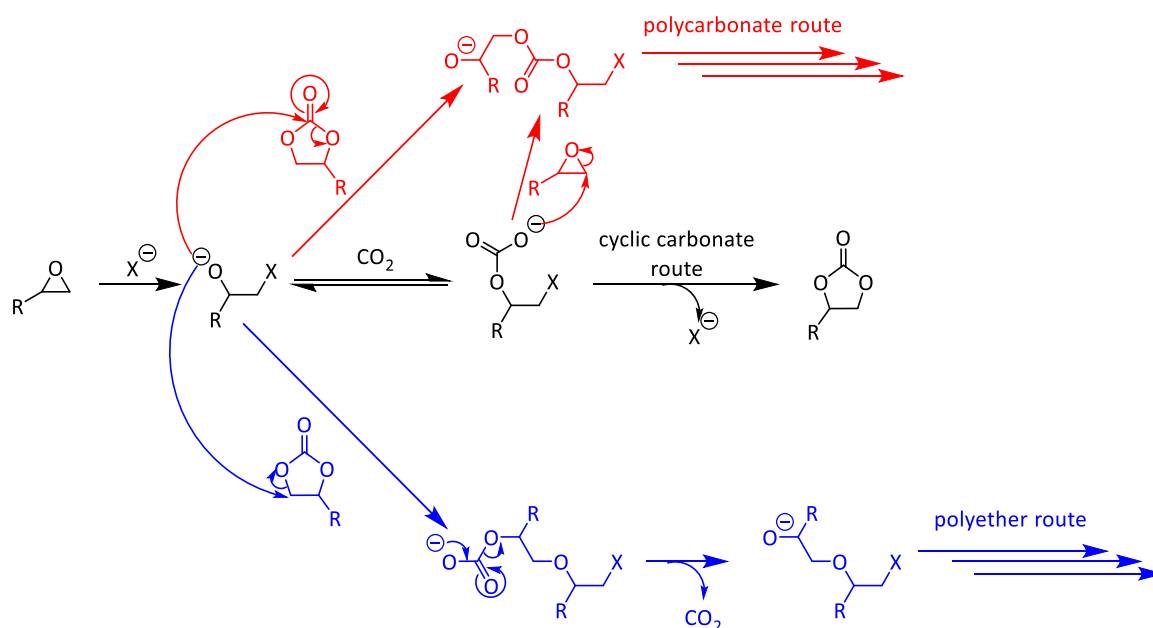
## Chapter 2: Carbonatation of [ethylene-glycidyl methacrylate]-based copolymers with carbon dioxide as a reagent

ability of the fluoride anion.<sup>[35]</sup> Once enough cyclic carbonate species are generated, a direct nucleophilic attack of the alkoxide on the carbonate ring with subsequent decarboxylation could yield several polyether repeating units leading to some insoluble material, which was also observed in our case (see *Scheme 3* and the CPMAS-NMR spectrum in *Figure S19* in appendices).



*Figure 3. Influence of the halide anion on the reaction kinetics in the cycloaddition of CO<sub>2</sub> to E-GMA-MA: (a) plot of equation (3) and (b) plot of equation (2). Conditions: 2.0 g of E-GMA-MA (1.1mmol of glycidyl methacrylate), 0.057 mmol of catalyst (5 mol%), 2.0 mL of toluene, 110 °C, 4.0 MPa of CO<sub>2</sub>. Yield was determined by IR-ATR using a calibration curve (see *Figure S12* in appendices).*





*Scheme 3. Potential side-reaction of epoxide with CO<sub>2</sub>. (see also ref [35]).*

#### IV.1.c. Influence of the alkyl chains

Ammonium bromide salts such as tetraethylammonium bromide (TEAB), TBAB, tetrahexylammonium bromide (THAB) and tetraoctylammonium bromide (TOAB) were chosen to study the influence of the alkyl chains' length. As shown in *Figure 4*, one can observe that the length does influence the catalytic activity. After 1 hour of reaction at 110 °C, the following catalytic reactivity order was obtained: TEAB  $\ll$  TOAB  $\approx$  TBAB < THAB. These results showed that increasing the length of the alkyl chains, while improving solubility in the apolar medium, makes the ammonium cation bulkier and thus decreases the electrostatic interactions between the ion pairs. This results in greater nucleophilicity of the anion and hence enhanced reactivity.<sup>[44]</sup> While the larger ammonium cation showed satisfactory activity at a short reaction time (more than 50 % yield after 1 hour), TEAB was completely inactive due to its insolubility in toluene. It has also been shown that a too bulky cation should disfavor the formation of the alkoxide intermediate,<sup>[71]</sup> explaining why TOAB was less active than THAB.

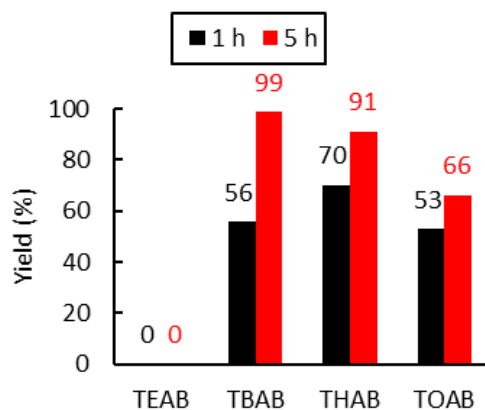
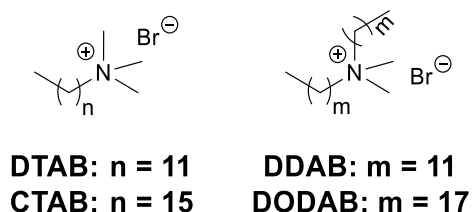


Figure 4. Influence of the alkyl chains on the tetraalkylammonium bromide activity. Conditions: 2.0 g of E-GMA-MA (1.1 mmol of glycidyl methacrylate), 0.057 mmol of catalyst (5 mol%), 2.0 mL of toluene, 110 °C, 4.0 MPa of CO<sub>2</sub>. Yield determined by IR-ATR using a calibration curve (see Figure S12 in appendices).

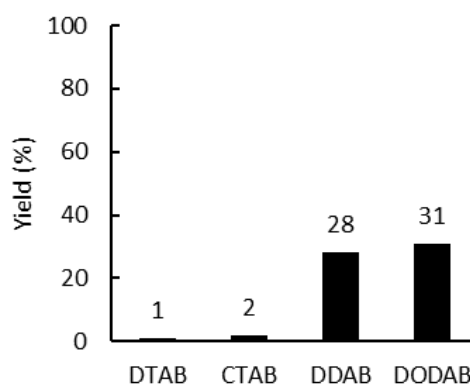
However, after 5 hour at 110 °C, the catalytic reactivity order changed as follows: TEAB  $\ll$  TOAB < THAB < TBAB. This could be explained by the fact that the bulkier the ammonium, the less stabilized the alkoxide intermediate, because of the decrease of the electrostatic interactions between the ion pairs. It would favor parallel side reactions between the alkoxides and the cyclic carbonates to produce polyether units *via* decarboxylation reactions, as reported before (see *Scheme 3*).<sup>[35]</sup> The overall enhanced solubility of the cation and ion pair dissociation could thus be a determining factor for improved kinetics at early stages, but a trade-off in terms of cation size would be ideal when it comes to selectivity over longer reaction times (see *Figure 4*).

Ammonium salts used as surfactants such as dodecyltrimethylammonium bromide (DTAB), cetyltrimethylammonium bromide (CTAB), didodecyltrimethylammonium bromide (DDAB) and dioctadecyltrimethylammonium bromide (DODAB) (*Scheme 4*) were also tested as catalysts under the following conditions: 5 mol% of catalyst, 110 °C, 4 MPa of CO<sub>2</sub>, toluene, 1 h. Very low yields were obtained with DTAB and CTAB (1 % and 2 % respectively), whereas higher yields were obtained with DDAB and DODAB (28 % and 31 % respectively) (*Figure 5*). These results showed that alkyltrimethylammonium bromide based catalysts (DTAB and CTAB) were very poor catalysts, likely due to weak ion pair dissociation. Indeed, the ammonium cation is not enough hindered because of the presence of only one long alkyl chain. Conversely, dialkyldimethylammonium catalysts showed better activity because of the better ion pair dissociation, caused by the presence of a second long alkyl chains that brought more

hindrance on the ammonium cation. The presence of long alkyl chains may also increase the affinity with the relative non-polar polymer. However, TBAB remains a better catalyst than DDAB and DODAB (yield of 56 % after 1 h) due to the presence of the four butyl chains, which dissociate the ammonium and the bromide halide more efficiently.



*Scheme 4. Structure of the surfactants used as catalysts.*



*Figure 5. Influence of the surfactant structure on the catalytic activity. Conditions: 2.0 g of E-GMA-MA (1.1 mmol of glycidyl methacrylate), 0.057 mmol of catalyst (5 mol%), 2.0 mL of toluene, 110 °C, 4.0 MPa of CO<sub>2</sub>, 1 h. Yield determined by IR-ATR using a calibration curve (see Figure S12 in appendices).*

#### IV.1.d. Influence of the reaction parameters

The dependence of the cyclic carbonate yield on the CO<sub>2</sub> pressure was investigated at 110 °C for a period of 1 hour using TBAI as a catalyst. As shown in *Figure 6 (a)*, increasing the pressure from 2 to 4 MPa led to an increase of the yield from 15 % to 45 %. This could be due to a higher concentration of CO<sub>2</sub> in the liquid phase, which may both increase the kinetic rate and reduce the viscosity of the reaction mixture *via* plasticization of the polymer, as already

reported for other polymers.<sup>[75,76]</sup> Beyond 4 MPa, the yield reaches a plateau and starts to slightly decrease from 10 MPa. This decrease in the yield with an increase of CO<sub>2</sub> pressure has previously been observed in the case of molecular epoxides,<sup>[42,44]</sup> with the supercritical state of CO<sub>2</sub> affecting the solubility of each component in the continuous phase through dilution or even forcing precipitation in our case. Some experiments were conducted using a sapphire-windowed reactor and for pressures slightly above 10 MPa (~12 MPa), the entire mixture of toluene and CO<sub>2</sub> became supercritical, which triggered the precipitation of the E-GMA copolymers. This could explain the best compromise of 40-80 bar to achieve both good solubility and enhanced availability of CO<sub>2</sub> in the liquid toluene phase.<sup>[77]</sup> Thus, a pressure of 4 MPa seems ideal for TBAI to operate efficiently. The influence of the amount of TBAI on catalytic performance was also studied (4.0 MPa of CO<sub>2</sub>, 110 °C, 1 h). The results in [Figure 6 \(b\)](#) show that increasing the concentration of TBAI from 1 to 5 mol% led to a marked improvement of the yield from 13 to 45 %. A further increase of the quantity of TBAI up to 15 mol% did not lead to further activity improvement. Thus, the TBAI catalyst concentration was set at 5 mol%.

Finally, the influence of the temperature on the carbonatation reaction of E-GMA-MA was studied (4.0 MPa of CO<sub>2</sub>, 5 mol% TBAI) as it could greatly impact both the reaction rate and the solubility/viscosity of the reaction medium particularly when polymers are at stake. The results shown in [Figure 6 \(c\)](#) reveal that the reaction temperature strongly affects catalyst reactivity as very low yields were obtained after 1 hour of reaction below 100 °C. Increasing the temperature further from 100 to 120 °C led to a significant improvement in the yield of the cyclic carbonate product from 5 to 65 %. A further increase of the temperature up to 130 °C did not lead to significant activity improvement. As stated above, the temperature may influence the kinetic rate and improve the gas-liquid transfer but partial or total degradation of the catalyst may also occur with the temperature increase. However, after 5 hours, an increase of the temperature from 110 °C to 130 °C led to a decrease of the yield from 99 % to 45 %. It could be explained by the formation of polyether repeating units and thus the consumption of the cyclic carbonate moiety *via* decarboxylation, as reported previously.<sup>[35]</sup> Therefore, the influence of the acrylate comonomer in the polymer structure on the reaction efficiency was assessed under the following optimal conditions: TBAB (5 mol%), 4 MPa of CO<sub>2</sub>, 110 °C, 5 h.

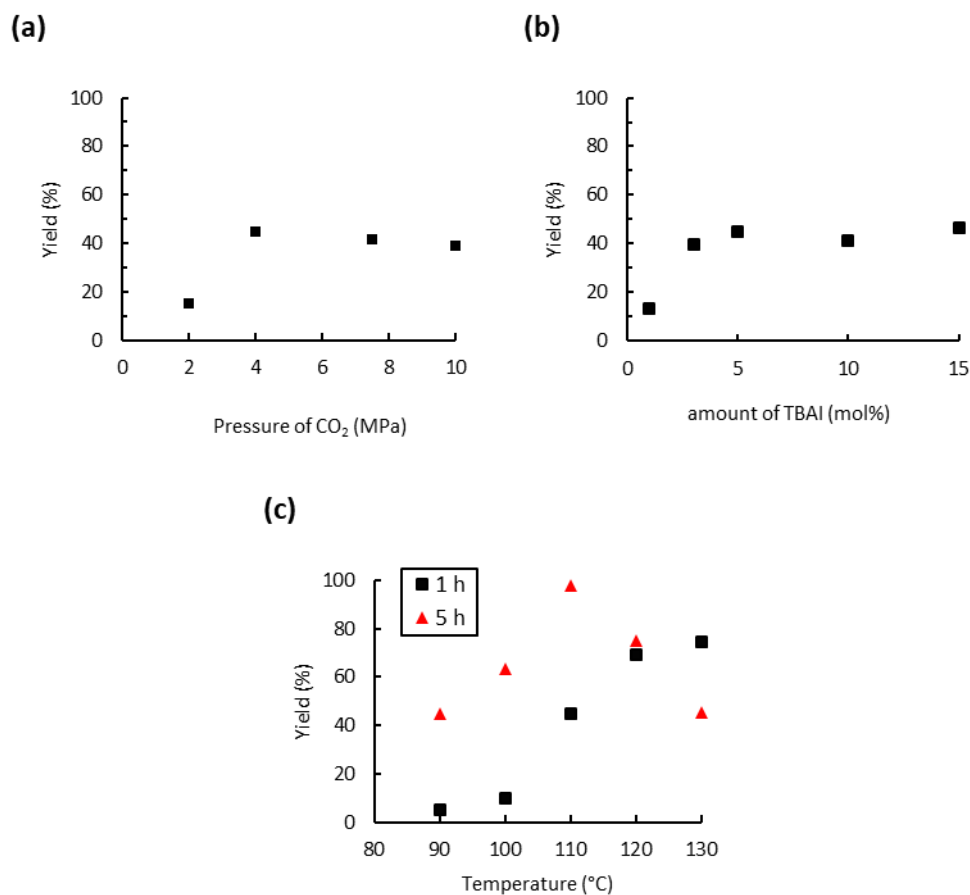


Figure 6. Influence of the CO<sub>2</sub> pressure (a), amount of TBAI (b) and temperature (c) on catalytic performance. Unless otherwise mentioned, reaction conditions: 2.0 g of E-GMA-MA (1.1 mmol of glycidyl methacrylate), 0.057 mmol of TBAI (5 mol%), 4.0 MPa of CO<sub>2</sub>, 2.0 mL of toluene, 110 °C, 1 h. Yield determined by IR-ATR using a calibration curve. (see Figure S12 in appendices)

#### IV.1.e. Influence of the acrylate comonomer

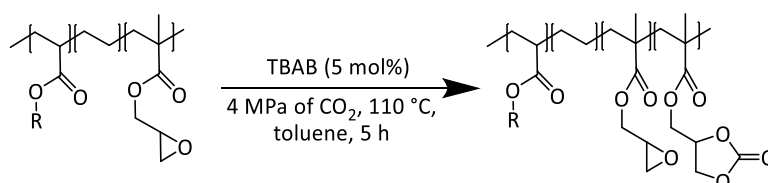
E-GMA-MA, E-GMA-BA and E-GMA were functionalized with CO<sub>2</sub> under optimal conditions to study the influence of the acrylate comonomer (type or presence) on the reaction efficiency. It is notable that the three polymers are soluble in toluene at 110 °C at a concentration of 1 g of polymer per mL of toluene.

Under these conditions, the factors that could influence the reaction outcome are the polarity of the polymer, the molar mass of the polymer, the CO<sub>2</sub> solubility in the liquid phase and the viscosity of the liquid phase. The results presented in [Table 2](#) show that the reactivity of the polymer increases in the following order: E-GMA < E-GMA-BA < E-GMA-MA, which also mirrors the polarity order. E-GMA-BA is more apolar than E-GMA-MA because of the presence

## Chapter 2: Carbonatation of [ethylene-glycidyl methacrylate]-based copolymers with carbon dioxide as a reagent

of butyl groups instead of methyl groups, and E-GMA is even more apolar because of the absence of the acrylate comonomer. This change of polarity may affect the CO<sub>2</sub> solubility in the liquid phase. It is well known that CO<sub>2</sub> is more soluble in relative polar media, due to its significant quadrupole moment.<sup>[78]</sup> The ester groups of the acrylate comonomer may interact with CO<sub>2</sub> and favor its solubility, thus favoring the reaction with the epoxide moieties.

Table 2. Influence of the alkyl acrylate monomer.



Entry	R	Polymer	Yield (%)
1	Me	E-GMA-MA	99
2	Bu	E-GMA-BA	82
3	-	E-GMA	62

Reaction conditions: 2.0 g of polymer (1.1 mmol of glycidyl methacrylate), 18 mg of TBAB (0.057 mmol, 5 mol%), 4.0 MPa of CO<sub>2</sub>, 2.0 mL of toluene, 110 °C, 5 h. Yield determined by <sup>1</sup>H NMR (see [Figure S15](#), [Figure S16](#), [Figure S17](#) in appendices).

### IV.2. Methodology transposition to reactive extrusion

The aforementioned autoclave results showed that ammonium halides were the most active catalysts for the carbonatation of [ethylene-glycidyl methacrylate] based polymers in toluene solution. Specifically, the use of TBAB, THAB and TBAI as catalysts provided the highest yields of cyclic carbonates, up to 99 % after 5 hours of reaction at 110 °C in the case of TBAB. These catalysts were therefore chosen for the carbonatation of [ethylene-glycidyl methacrylate] based polymers by reactive extrusion. Due to its flexibility in screw design and easily adjustable temperature profiles, the extrusion process provides remarkable mixing and homogenization capabilities for viscous systems in the molten state. Thus, the use of an extruder as a continuous reactor makes it possible to avoid resorting to hazardous solvents,

which are always difficult to extract industrially (costly devolatilization step). The reactive extrusion process is thus often considered as a promising green process, allowing for the continuous production of large quantities of modified polymers.

The use of CO<sub>2</sub><sup>[79]</sup> as a reagent for the carbonatation of polymers by a reactive extrusion process<sup>[80,81]</sup> has never been reported before. In contrast to radical processes, catalytic processes within reactive extruders are also extremely rare to the best of our knowledge, in particular in the realm of polymer functionalization.<sup>[82,83]</sup>

This constitutes a significant step forward since it both offers a solvent-free alternative and a scalable process amenable to industrial eco-design requirements. The transposition of the batch process to reactive extrusion was possible thanks to the adjustments of the batch reaction conditions. A co-rotating twin-screw extruder fed with the polymer, the catalyst and CO<sub>2</sub> was used to perform the experiments, at a flow rate of 2 kg/h and a rotational speed of 150 rpm. The overall design of this process is depicted in the **Experimental Section**, it provides containment of CO<sub>2</sub> pressure within the polymer melt for carbonatation to proceed.

The minimal temperature for the extrusion of the different ethylene-glycidyl methacrylate] based polymers was determined experimentally to be 120 °C (over the melting points of the E-GMA-MA, E-GMA-BA and E-GMA, which are respectively 65 °C, 72 °C and 104 °C).

In the next paragraphs, the effect of the extrusion parameters on the average residence time is described, as the residence time has to enter into consideration for further results interpretation. Moreover, optimization of the different twin-screw extruder parameters to obtain good yields in these very short residence times is described.

#### IV.2.a. Effect of the extrusion parameters on the mean residence time

The mean residence time ( $\overline{t_m}$ ) was precisely determined by colorimetric measurements through the time of the extruded E-GMA-MA using a magenta pigment as a tracer. A colorimeter measured the red, green and blue light intensities radiated from the extruded polymer. The green light intensity was the most sensible, compared to the blue and red intensities, thus it was correlated to the tracer concentration and used for the determination of the mean residence time.

For the determination of  $\overline{t_m}$ , the residence time distribution function  $E(t)$  was first determined as follows:

$$E(t) = \frac{C_i}{\sum_{t=1}^n C_i \Delta t} \quad (3)$$

Where  $C_i$  is the concentration of the tracer in the extruded polymer at the time  $t$ , and  $\Delta t$  is the time between each measurement, which was equal to 1 second in our case. Then, the mean residence time  $\bar{t}_m$  was calculated as follows:

$$\bar{t}_m = \sum_{t=1}^n t E(t) \Delta t \quad (4)$$

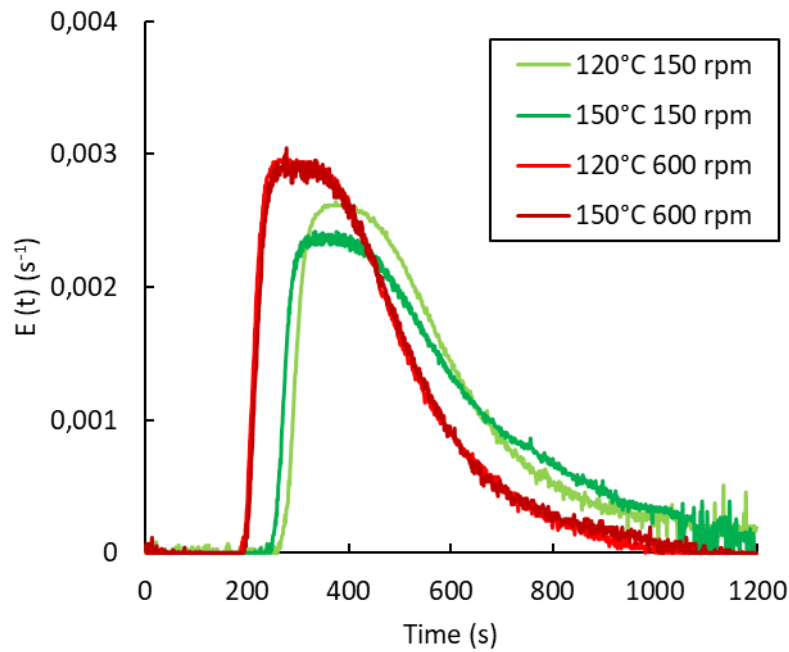
The standard deviation  $\sigma_t$  of the residence time can also be determined with the following equation:

$$\sigma_t^2 = \int_0^\infty (t - \bar{t}_m)^2 \cdot E(t) \cdot dt \cong \sum_{t=0}^\infty (t - \bar{t}_m)^2 \cdot E(t) \cdot \Delta t \quad (5)$$

$E(t)$  was plotted and  $\bar{t}_m$  was calculated for different screw rotational speeds, mass flows of polymer and temperatures.

First of all, the influence of the temperature was investigated for two different screw rotational speeds (150 and 600 rpm) with a mass flow rate of 2.0 kg/h ([Figure 7](#)). For each rotational speed, similar mean residence times were determined at 120 and 150 °C. This observation verified that viscosity did not affect the residence time during the extrusion process.

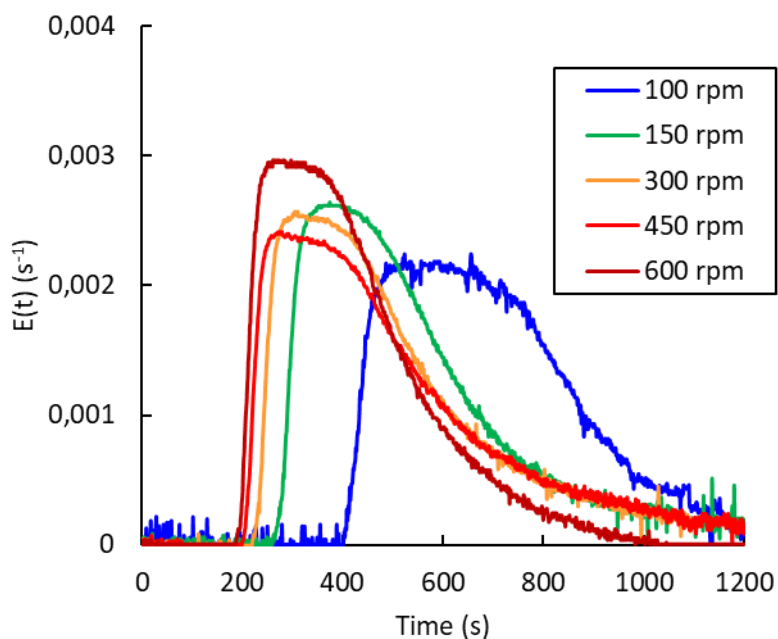




Entry	Rotational speed (rpm)	Temperature (°C)	Delay time (s)	$\bar{t}_m$ (s)	$\sigma_t$ (s)
1	150	120	259	539	200
2		150	235	538	202
3	600	120	197	417	153
4		150	192	429	164

Figure 7. Residence time distribution  $E(t)$ , delay time and mean residence time at different temperatures and screw speeds. Mass flow: 2.0 kg/h of E-GMA-MA.

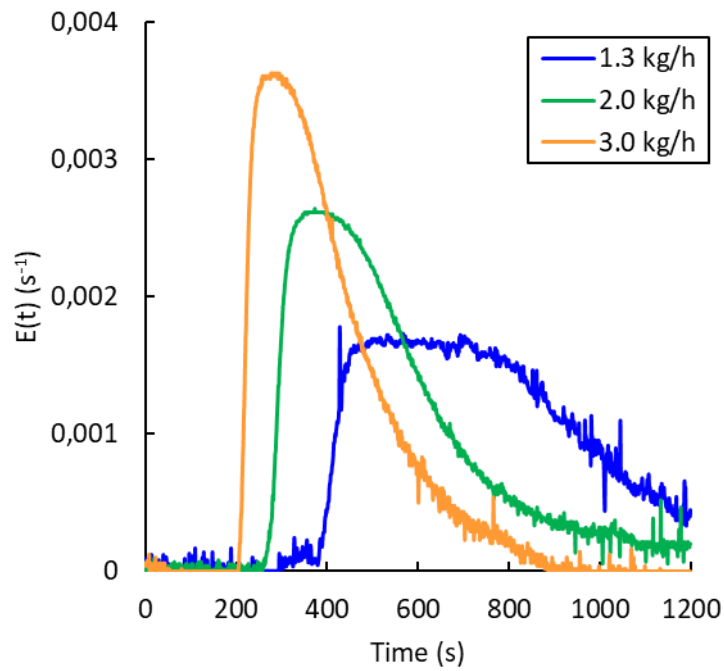
Afterwards, the influence of the screw rotational speed at 120 °C with a mass flow rate of 2.0 kg/h was investigated (Figure 8). A decrease of the delay time and of the mean residence time was observed when the rotational speed was increased, but they might tend to a limit, as their decrease were less and less important. Between 100 and 150 rpm, a difference of 143 seconds was observed for the mean residence time, whereas there was only a difference of 20 seconds between 450 and 600 rpm.



Entry	Rotational speed (rpm)	Delay time (s)	$\bar{t}_m$ (s)	$\sigma_t$ (s)
1	100	401	682	178
2	150	259	539	200
3	300	219	508	213
4	450	199	497	219
5	600	197	417	153

*Figure 8. Residence time distribution  $E(t)$ , delay time and average residence time at different screw speeds. Conditions: 2.0 kg/h of E-GMA-MA, 120 °C.*

Finally, the effect of the polymer mass flow was studied at 120 °C with a screw speed of 150 rpm (Figure 9). The decrease of the mass flow led to longer delay time and average residence time and broader residence time distribution.



Entry	Mass flow rate of E-GMA-MA (kg/h)	Delay time (s)	$\bar{t}_m$ (s)	$\sigma_t$ (s)
1	1.3	391	726	207
2	2.0	259	539	200
3	3.0	206	399	140

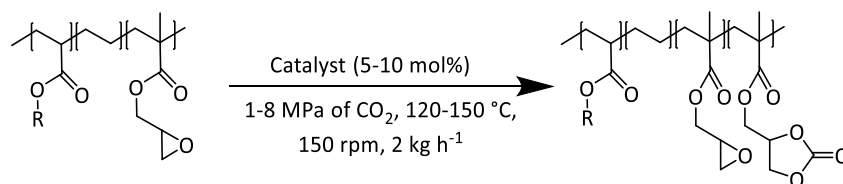
Figure 9. Residence time distribution  $E(t)$ , delay time and average residence time at different mass flow rates. Conditions: 1.3-2.9 kg/h of E-GMA-MA, 120 °C, 150 rpm.

In summary, this study showed that the mass flow rate and the screw speed had a significant influence on the residence time distribution  $E(t)$ , delay time and average residence time. An increase of these parameters led to a decrease of the delay time and average residence time, while the temperature variation in the study resulted in little modifications. Concerning the effect of the CO<sub>2</sub> pressure, it has been qualitatively observed that an increase of the pressure led to a decrease of the residence time, but it was not possible to quantitatively determine the average residence time due to foaming of the extruded polymer.

### IV.2.b. Optimisation of the reactive extrusion process

First, the influence of extrusion temperature and CO<sub>2</sub> pressure was studied on the carbonatation of E-GMA-MA (Scheme 5). As shown in Figure 10 (a), an increase in temperature led to an increase in carbonate yield. The optimum pressure was 4.0 MPa, which is probably a good compromise between maximal CO<sub>2</sub> solubilization/availability for reaction and the avoidance of phase separation in the melt. At this pressure, an increase of 10 °C led to an average yield increase of 15 %. As seen previously, the reaction temperature studied in this work had no effect on the residence time, thus the increase of yield is only related to an improvement of the catalytic activity. The temperature was not increased above 150 °C to avoid catalyst degradation that starts from 160 °C according to TGA analyses (see appendices).

Moreover, the amount of catalyst was optimized (Figure 10 (b)) with 4.0 MPa of CO<sub>2</sub>. An increase from 5.0 to 7.5 mol% led to a significant increase in yield from 53 % to 72 %. A further increase to 10 mol% did not lead to a significant improvement in the yield.



Scheme 5. Carbonatation of E-GMA-MA in extruder.

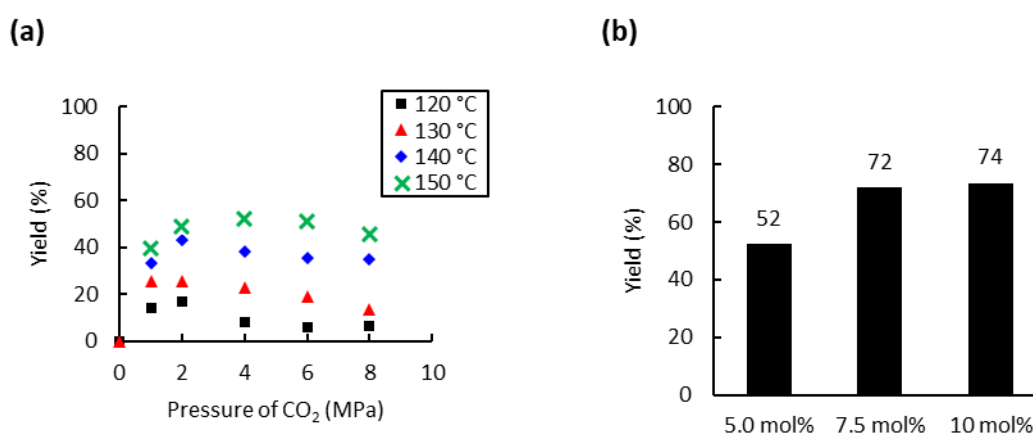
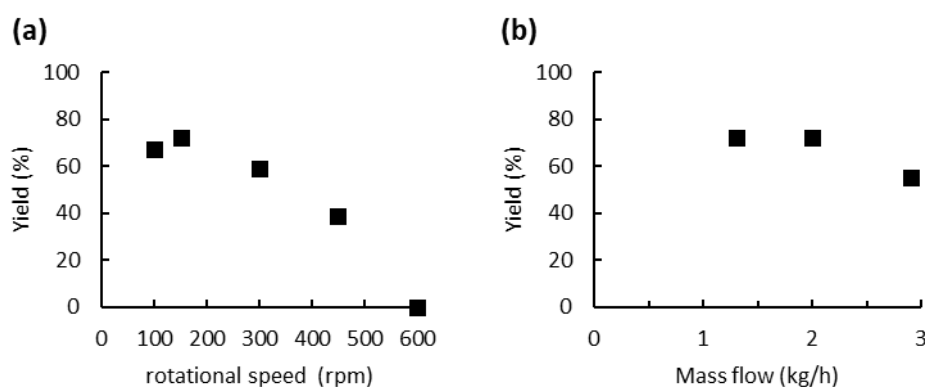


Figure 10. Influence of temperature and amount of catalyst. Unless otherwise mentioned, reaction conditions: 2 kg/h of E-GMA-MA, 18 g/h of TBAB (5 mol%), 150 °C, 150 rpm. Yield determined by IR-ATR using a calibration curve (see Figure S12 in appendices).

Furthermore, the rotational speed of the twin-screw and the polymer mass flow were investigated under the following conditions: TBAB (7.5 mol%), 4.0 MPa, 150 °C. According to [Figure 11 \(a\)](#), the optimal rotational speed is 150 rpm (yield of 72 %). A lower yield of 67 % was obtained at 100 rpm, possibly because of a slower mass transfer between components. However, above 150 rpm, a decrease in the carbonate yield was also observed when the speed increased. As seen before, the increase of the speed tends to decrease the average residence time, but it could also lead to a higher self-heating of the polymer matrix, observed by increase of temperature from 150 to more than 160 °C when the speed was change from A50 rpm to 600 rpm, depending on the extruder zone. This could result in catalyst degradation, and therefore in a decrease of the carbonate yield. At 600 rpm, a total degradation of the catalyst (starting at 160 °C according to TGA) may explain that no cyclic carbonate was formed.

Although the polymer mass flow has a strong influence on the residence time, it did not affect the cyclic carbonate yield when it was decreased from 2.0 to 1.3 kg/h. However, when it was increased to 2.9 kg/h, a marked decrease in yield from 72 to 55 % was observed. This may be due to the decrease of the mean residence time ([Figure 11 \(b\)](#)).



*Figure 11. Influence of (a) the rotational speed and (b) the polymer mass flow. Unless otherwise mentioned, reaction conditions: 2.0 kg/h of E-GMA-MA, 0.086 mol/h of TBAB (7.5 mol%), 150 °C, 4 MPa of CO<sub>2</sub>, 150 rpm. Yield determined by IR-ATR using a calibration curve (see [Figure S12 in appendices](#)).*

Subsequently, the influence of the nature of the catalyst was investigated under optimal conditions (7.5 mol% catalyst, 150 °C, 150 rpm, 2 kg/h) ([Figure 12](#)). With TBAI, a low yield of 33 % was obtained. This could be explained by the fact that the melting temperature of TBAI is 155 °C, thus it is in solid form during extrusion. The catalyst would therefore be less homogeneously dispersed within the polymer matrix, which would reduce the cyclic carbonate yield. Regarding TBAB and THAB, a similar activity to that in the batch reactor was

## Chapter 2: Carbonatation of [ethylene-glycidyl methacrylate]-based copolymers with carbon dioxide as a reagent

obtained, with a yield of 72 % and 78 % respectively. With their melting point being at about 100 °C, their liquid state under the reaction conditions may improve their dispersion in the medium and not affect their activity. Finally, E-GMA-BA and E-GMA were also modified with CO<sub>2</sub> in reactive extrusion under the optimal conditions (TBAB (7.5 mol%), 150 °C, 150 rpm, 2 kg/h) (Figure 13). The same reactivity order than that obtained in batch was observed: E-GMA << E-GMA-BA < E-GMA.

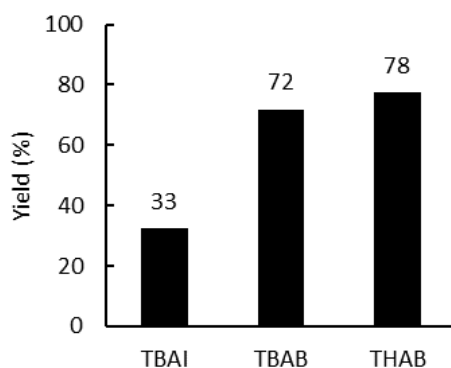


Figure 12. Influence of the nature of the catalyst. Unless otherwise mentioned, reaction conditions: 2 kg/h of E-GMA-MA, 0.086 mol/h of catalyst (7.5 mol%), 150 °C, 4 MPa of CO<sub>2</sub>, 150 rpm. Yield determined by IR-ATR using a calibration curve (see Figure S12 in appendices).

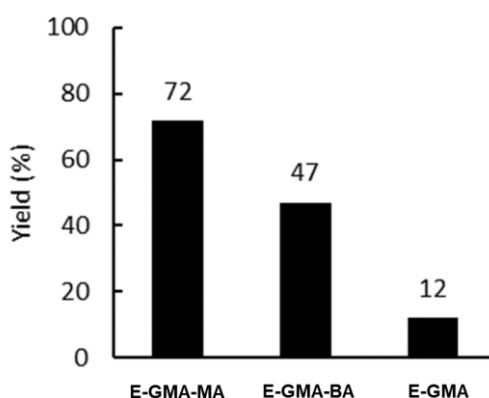


Figure 13. Influence of the acrylate monomer. Reaction conditions: 2 kg/h of polymer, 0.086 mol/h of TBAB (7.5 mol%), 150 °C, 4 MPa of CO<sub>2</sub>, 150 rpm. Yield determined by <sup>1</sup>H NMR (see Figure S27, Figure S28, Figure S29 in the appendices).

#### IV.2.c. Comparison of the reaction kinetics of the batch and reactive extrusion processes

The activation energy for the carbonation reaction of E-GMA-MA with TBAB as catalyst by reactive extrusion and in batch process was determined with the kinetic model used previously. For different temperatures, the observed kinetic constant  $k_{obs}$  can be calculated thanks to the equation:

$$k_{obs}(T) = -\frac{\ln(1-\text{Yield})}{t_m} \quad (6)$$

Then, the activation energy  $E_a$  can be determined with the Arrhenius law:

$$k_{obs}(T) = Ae^{-\frac{E_a}{RT}} \quad (7)$$

$$\Leftrightarrow \ln(k_{obs}(T)) = \ln(A) - \frac{E_a}{RT} \quad (8)$$

This model was applied for the carbonation of E-GMA-MA with TBAB (5 mol%) under 4.0 MPa of CO<sub>2</sub> by reactive extrusion ( $\overline{t_m} = 9$  min, at 120, 130, 140 and 150 °C), and for the batch reaction in toluene with the same catalyst, and similar amount of catalyst and pressure (t = 60 min, at 100, 110, 120 and 130 °C).

The plot of equation (8) for the reactive extrusion and batch process allows determining the activation energy  $E_a$  in both cases (*Figure 14*).

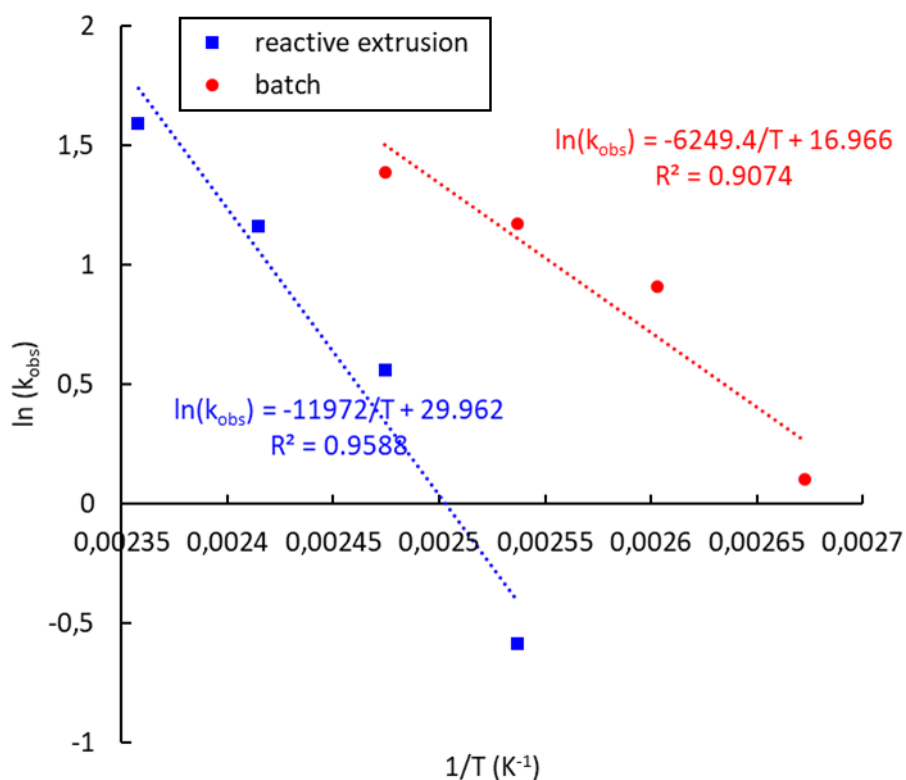


Figure 14. Plot of  $\ln(k_{obs})$  in function of  $1/T$ . Conditions for the reactive extrusion 2.0 kg/h of E-GMA-MA, TBAB (5 mol%), 4.0 MPa of  $CO_2$ , 150 rpm. Conditions in batch: 2.0 g of E-GMA-MA, 2 mL of toluene, TBAB (5 mol%), 4.0 MPa of  $CO_2$ , 1 h.

The activation energy was estimated equal to **100 kJ/mol** and **52 kJ/mol** for the extrusion and batch process respectively. These results show that 92 % more energy is required to activate the epoxide by reactive extrusion. A possible explanation is that the presence of toluene improved the interactions between the epoxides, the catalyst and the  $CO_2$ , and thus reduce the activation energy. During the reactive extrusion process, although the co-rotative twin screw provided excellent mixing of the reaction medium, the medium may not be completely homogenous on a molecular scale, thus there were less interactions between the reagents and the catalyst, and a higher activation energy was required. The activation energy for the batch process is in accordance with the literature,<sup>[84]</sup> which reported that the carbonatation of styrene oxide with TBAB has an activation energy of 55 kJ/mol.

The batch and the extrusion process could also be compared by the determination of the conversion distribution  $G(X)$  during the reactive extrusion process, by using the kinetics constants of the reaction during extrusion at 150 °C (TBAB (5 or 7.5 mol%), 4 MPa of  $CO_2$ ), and the extrapolated batch kinetic constant at 150°C (TBAB (5 mol%), 4 MPa of  $CO_2$ , toluene).



The conversion distribution  $G(X)$  (fraction of macromolecules with an epoxide conversion between  $X$  and  $X+\Delta X$ ) is the combination of the reaction kinetic ( $X = 1 - e^{(k_{\text{obs}}t)}$ ) and the distribution time  $E(t)$ .

By using equation (7) (with  $E_a = 52$  kJ/mol and  $A = 2.33 \cdot 10^7$ ) a  $k_{\text{obs}}$  of  $9.11 \text{ h}^{-1}$  was calculated for the batch process at  $150 \text{ }^\circ\text{C}$ . The conversion distribution  $G(X)$  can be determined with the following equation:

$$G(X) = \frac{C_i}{\sum_{i=1}^n C_i \Delta X} \quad (9)$$

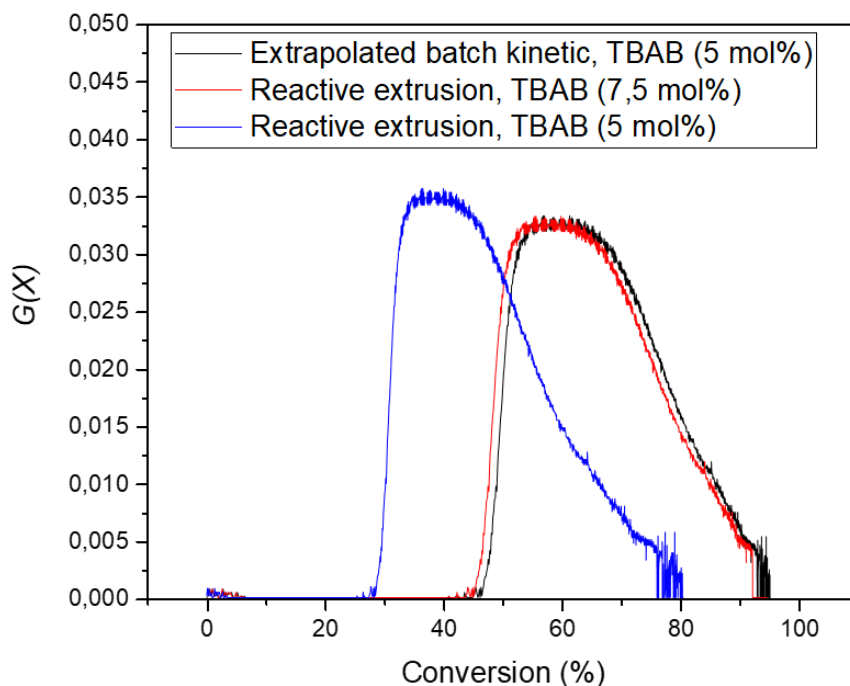
Where  $X$  is the conversion at the time  $t$ , and  $C_i$  the concentration of macromolecules with an epoxide conversion  $X$ .

Then, the mean conversion  $\bar{X}$  was determined with the following equation:

$$\bar{X} = \sum_{i=0}^{\infty} X G(X) \cdot \Delta X \quad (10)$$

*Figure 15* plots the conversion distributions  $G(X)$ , determined with the reactive extrusion kinetic constants for 5 and 7.5 mol% of TBAB at  $150 \text{ }^\circ\text{C}$  ( $4.89$  and  $8.76 \text{ h}^{-1}$ , respectively), and with the extrapolated batch process kinetic constant ( $9.11 \text{ h}^{-1}$ ) at  $150 \text{ }^\circ\text{C}$ .

The mean conversion  $\bar{X}$  calculated with the extrapolation of the batch process kinetic was 66 % (*Figure 15*, entry 2), which is higher than the mean conversion obtained with the reactive extrusion process using 5 mol% of TBAB (47 %), but similar to the mean conversion during reactive extrusion with 7.5 mol% of catalyst (65 %).



Entry	Process	Catalyst (mol%)	$k_{obs}(150\text{ }^{\circ}\text{C})\text{ (h}^{-1}\text{)}$	$\bar{X}\text{ (}\%\text{)}$
1	Reactive extrusion	TBAB (5)	4.89	47
2		TBAB (7.5)	8.76	65
3	Batch	TBAB (5)	9.11 (extrapolated)	66

*Figure 15. Conversion distribution of the epoxide function during the reactive extrusion process, using the reaction kinetic constants at 150 °C (TBAB 5 mol%, 4.0 MPa of CO<sub>2</sub>) of the extrusion process and batch process (by extrapolation).*

In conclusion, although the extrusion process provides excellent mixing of the solvent free medium and satisfying yields during a short period (up to 78 % with THAB (7.5 mol%) at 150 °C), it required higher catalyst amount, compared to the batch process, to reach similar reaction kinetic.

## V. Conclusion

Ethylene-glycidyl methacrylate based copolymers were successfully functionalized with carbon dioxide using commercial and non-toxic tetraalkylammonium halide catalysts, leading to the formation of cyclic carbonate pendant groups on the polymer chain, in a batch reactor

and an extruder. The influences of the catalyst structure and the reaction parameters were evaluated in batch and it was found that TBAI, THAB and TBAB were the most active catalysts, with TBAB achieving up to 99 % yield of cyclic carbonate.

The difference in reactivity between E-GMA-MA, E-GMA-BA and E-GMA suggested that the presence of polar groups, such as esters derived from acrylate comonomers, in the polymer structure may increase the CO<sub>2</sub> solubility and facilitate its approach to the epoxide moieties.

The procedure developed in an autoclave has been successfully transposed to a solvent-free reactive extrusion process, with a yield of cyclic carbonate up to 78 % using THAB as the catalyst on the E-GMA-MA, allowing access to cyclic carbonates in addition to the remaining epoxides. Modifications of E-GMA-BA and E-GMA were also successful.

Moreover, the effect of the extrusion parameters on the residence time distribution during extrusion was investigated. The mass flow rate and the screw speed were shown to have a significant influence on the residence time while temperature had no effect. Higher flow rate and higher screw speed led to shorter residence time.

Finally, the activation energies, calculated for the reaction in batch and extrusion process under similar conditions, showed that the epoxides functions required higher energy to be activated during the extrusion process, and thus the kinetic reaction was lower than during batch reaction, although extrusion provides excellent mixing of the polymer with CO<sub>2</sub> and the catalyst under solvent free-conditions.

These modified [cyclic carbonate + epoxide]-featuring polymers may have several direct applications *e.g.* as intermediates for the synthesis of polyhydroxyurethanes, as reactive compatibilizers for blends of polyolefins with polyamides, polyesters, polyacids and polycarbonates, and could also display good permeability properties for membranes. The enhanced sustainability of our reactive extrusion process (kg-scale production of functionalized polymers in a continuous fashion under solvent-free conditions using CO<sub>2</sub> as a direct C1 source) could pave the way for other industrially-relevant (co)polymers.

## VI. References

- [1] Sakakura, T.; Choi, J.-C.; Yasuda, H. Transformation of Carbon Dioxide. *Chem. Rev.* **2007**, *107*(6), 2365–2387.
- [2] Aresta, M.; Dibenedetto, A.; Angelini, A. Catalysis for the Valorization of Exhaust Carbon: from CO<sub>2</sub> to Chemicals, Materials, and Fuels. Technological Use of CO<sub>2</sub>. *Chem. Rev.* **2014**, *114*(3), 1709–1742.
- [3] Liu, Q.; Wu, L.; Jackstell, R.; Beller, M. Using carbon dioxide as a building block in organic synthesis. *Nat Commun* **2015**, *6*(1), 5933.
- [4] Lim, X. How to make the most of carbon dioxide. *Nature* **2015**, *526*, 628–630.
- [5] Hepburn, C.; Adlen, E.; Beddington, J.; Carter, E.A.; Fuss, S.; Mac Dowell, N.; Minx, J.C.; Smith, P.; Williams, C.K. The technological and economic prospects for CO<sub>2</sub> utilization and removal. *Nature* **2019**, *575*(7781), 87–97.
- [6] Shaikh, A.-A.G.; Sivaram, S. Organic Carbonates. *Chem. Rev.* **1996**, *96*(3), 951–976.
- [7] Clements, J.H. Reactive Applications of Cyclic Alkylene Carbonates. *Ind. Eng. Chem. Res.* **2003**, *42*(4), 663–674.
- [8] Schäffner, B.; Schäffner, F.; Verevkin, S.P.; Börner, A. Organic Carbonates as Solvents in Synthesis and Catalysis. *Chem. Rev.* **2010**, *110*(8), 4554–4581.
- [9] Darensbourg, D.J. Making Plastics from Carbon Dioxide: Salen Metal Complexes as Catalysts for the Production of Polycarbonates from Epoxides and CO<sub>2</sub>. *Chem. Rev.* **2007**, *107*(6), 2388–2410.
- [10] Boyer, A.; Cloutet, E.; Tassaing, T.; Gadenne, B.; Alfos, C.; Cramail, H. Solubility in CO<sub>2</sub> and carbonation studies of epoxidized fatty acid diesters: towards novel precursors for polyurethane synthesis. *Green Chem.* **2010**, *12*(12), 2205.
- [11] Kember, M.R.; Buchard, A.; Williams, C.K. Catalysts for CO<sub>2</sub> /epoxide copolymerisation. *Chem. Commun.* **2011**, *47*(1), 141–163.
- [12] Romain, C.; Williams, C.K. Chemoselective Polymerization Control: From Mixed-Monomer Feedstock to Copolymers. *Angewandte Chemie International Edition* **2014**, *53*(6), 1607–1610.
- [13] Maisonneuve, L.; Wirotius, A.-L.; Alfos, C.; Grau, E.; Cramail, H. Fatty acid-based (bis) 6-membered cyclic carbonates as efficient isocyanate free poly(hydroxyurethane) precursors. *Polym. Chem.* **2014**, *5*(21), 6142–6147.
- [14] Maisonneuve, L.; Lamarzelle, O.; Rix, E.; Grau, E.; Cramail, H. Isocyanate-Free Routes to Polyurethanes and Poly(hydroxy Urethane)s. *Chem. Rev.* **2015**, *115*(22), 12407–12439.
- [15] Zhu, Y.; Romain, C.; Williams, C.K. Sustainable polymers from renewable resources. *Nature* **2016**, *540*(7633), 354–362.

- [16] Kindermann, N.; Cristòfol, À.; Kleij, A.W. Access to Biorenewable Polycarbonates with Unusual Glass-Transition Temperature ( $T_g$ ) Modulation. *ACS Catal.* **2017**, *7*(6), 3860–3863.
- [17] Grignard, B.; Gennen, S.; Jérôme, C.; Kleij, A.W.; Detrembleur, C. Advances in the use of CO<sub>2</sub> as a renewable feedstock for the synthesis of polymers. *Chem. Soc. Rev.* **2019**, *48*(16), 4466–4514.
- [18] Deacy, A.C.; Moreby, E.; Phanopoulos, A.; Williams, C.K. Co(III)/Alkali-Metal(I) Heterodinuclear Catalysts for the Ring-Opening Copolymerization of CO<sub>2</sub> and Propylene Oxide. *J. Am. Chem. Soc.* **2020**, *142*(45), 19150–19160.
- [19] Dechent, S.-E.; Kleij, A.W.; Luinstra, G.A. Fully bio-derived CO<sub>2</sub> polymers for non-isocyanate based polyurethane synthesis. *Green Chem.* **2020**, *22*(3), 969–978.
- [20] Deacy, A.C.; Gregory, G.L.; Sulley, G.S.; Chen, T.T.D.; Williams, C.K. Sequence Control from Mixtures: Switchable Polymerization Catalysis and Future Materials Applications. *J. Am. Chem. Soc.* **2021**, *143*(27), 10021–10040.
- [21] Liu, X.; Yang, X.; Wang, S.; Wang, S.; Wang, Z.; Liu, S.; Xu, X.; Liu, H.; Song, Z. Fully Bio-Based Polyhydroxyurethanes with a Dynamic Network from a Terpene Derivative and Cyclic Carbonate Functional Soybean Oil. *ACS Sustainable Chem. Eng.* **2021**, *9*(11), 4175–4184.
- [22] Longwitz, L.; Steinbauer, J.; Spannenberg, A.; Werner, T. Calcium-Based Catalytic System for the Synthesis of Bio-Derived Cyclic Carbonates under Mild Conditions. *ACS Catal.* **2018**, *8*(1), 665–672.
- [23] Tenhumberg, N.; Büttner, H.; Schäffner, B.; Kruse, D.; Blumenstein, M.; Werner, T. Cooperative catalyst system for the synthesis of oleochemical cyclic carbonates from CO<sub>2</sub> and renewables. *Green Chem.* **2016**, *18*(13), 3775–3788.
- [24] Chen, F.; Zhang, Q.-C.; Wei, D.; Bu, Q.; Dai, B.; Liu, N. Highly Stereo-Controlled Synthesis of Fatty Acid-Derived Cyclic Carbonates by Using Iron(II) Complex and Nucleophilic Halide. *J. Org. Chem.* **2019**, *84*(18), 11407–11416.
- [25] Liu, W.; Lu, G.; Xiao, B.; Xie, C. Potassium iodide–polyethylene glycol catalyzed cycloaddition reaction of epoxidized soybean oil fatty acid methyl esters with CO<sub>2</sub>. *RSC Adv.* **2018**, *8*(54), 30860–30867.
- [26] Akhdar, A.; Onida, K.; Vu, N.D.; Grollier, K.; Norsic, S.; Boisson, C.; D’Agosto, F.; Duguet, N. Thermomorphic Polyethylene-Supported Organocatalysts for the Valorization of Vegetable Oils and CO<sub>2</sub>. *Adv. Sustainable Syst.* **2021**, *5*(2), 2000218.
- [27] Catalá, J.; Caballero, M.P.; Cruz-Martínez, F. de la; Tejeda, J.; Castro-Osma, J.A.; Lara-Sánchez, A.; García-Vargas, J.M.; García, M.T.; Ramos, M.J.; Gracia, I.; Rodríguez, J.F. Carbonation of epoxidized soybean oil in supercritical CO<sub>2</sub> assisted by imidazole-based organocatalysts. *Journal of CO<sub>2</sub> Utilization* **2022**, *61*, 102060.
- [28] Morikawa, H.; Minamoto, M.; Gorou, Y.; Yamaguchi, J.; Morinaga, H.; Motokucho, S. Two Diastereomers of *d*-Limonene-Derived Cyclic Carbonates from *d*-Limonene Oxide and Carbon Dioxide with a Tetrabutylammonium Chloride Catalyst. *BCSJ* **2018**, *91*(1), 92–94.

- [29] Rehman, A.; López Fernández, A.M.; Gunam Resul, M.F.M.; Harvey, A. Highly selective, sustainable synthesis of limonene cyclic carbonate from bio-based limonene oxide and CO<sub>2</sub>: A kinetic study. *Journal of CO<sub>2</sub> Utilization* **2019**, *29*, 126–133.
- [30] Cruz-Martínez, F. de la; Martínez de Sarasa Buchaca, M.; Martínez, J.; Fernández-Baeza, J.; Sánchez-Barba, L.F.; Rodríguez-Diéguez, A.; Castro-Osma, J.A.; Lara-Sánchez, A. Synthesis of Bio-Derived Cyclic Carbonates from Renewable Resources. *ACS Sustainable Chem. Eng.* **2019**, *7*(24), 20126–20138.
- [31] Navarro, M.; Sánchez-Barba, L.F.; Garcés, A.; Fernández-Baeza, J.; Fernández, I.; Lara-Sánchez, A.; Rodríguez, A.M. Bimetallic scorpionate-based helical organoaluminum complexes for efficient carbon dioxide fixation into a variety of cyclic carbonates. *Catal. Sci. Technol.* **2020**, *10*(10), 3265–3278.
- [32] Kihara, N.; Endo, T. Incorporation of carbon dioxide into poly(glycidyl methacrylate). *Macromolecules* **1992**, *25*(18), 4824–4825.
- [33] Moon, J.-Y.; Jang, H.-J.; Kim, K.-H.; Na, S.-E.; Park, D.-W.; Lee, J.-K. Chemical fixation of carbon dioxide to copolymers bearing cyclic carbonate group. *Korean J. Chem. Eng.* **1999**, *16*(6), 721–724.
- [34] Park, S.Y.; Park, H.Y.; Park, D.W.; Ha, C.S. DIRECT INCORPORATION OF CARBON DIOXIDE INTO POLY(GLYCIDYL METHACRYLATE-CO-ACRYLONITRILE) USING QUATERNARY AMMONIUM SALT CATALYST AND ITS APPLICATION TO POLYMER BLENDS. *Journal of Macromolecular Science, Part A* **2002**, *39*(6), 573–589.
- [35] Ochiai, B.; Iwamoto, T.; Miyazaki, K.; Endo, T. Efficient Gas–Solid Phase Reaction of Atmospheric Carbon Dioxide into Copolymers with Pendent Oxirane Groups: Effect of Comonomer Component and Catalyst on Incorporation Behavior. *Macromolecules* **2005**, *38*(24), 9939–9943.
- [36] Park, S.; Choi, B.; Lee, B.; Park, D.; Kim, S. Chemical Absorption of Carbon Dioxide into Glycidyl Methacrylate Solution with Tetrabutylammonium Bromide. *Separation Science and Technology* **2006**, *41*(5), 829–839.
- [37] Ochiai, B.; Hatano, Y.; Endo, T. Facile synthesis of polymers bearing cyclic carbonate structure through radical solution and precipitation polymerizations accompanied by concurrent carbon dioxide fixation. *Journal of Polymer Science Part A: Polymer Chemistry* **2009**, *47*(12), 3170–3176.
- [38] Ochiai, B.; Nakayama, T. Dispersion polymerization accompanied by CO<sub>2</sub> fixation: Synthesis of particles of polymers bearing cyclic carbonate and epoxide moieties. *Journal of Polymer Science Part A: Polymer Chemistry* **2010**, *48*(23), 5382–5390.
- [39] Liu, B.; Zhang, Y.-Y.; Zhang, X.-H.; Du, B.-Y.; Fan, Z.-Q. Fixation of carbon dioxide concurrently or in tandem with free radical polymerization for highly transparent polyacrylates with specific UV absorption. *Polymer Chemistry* **2016**, *9*.
- [40] Caló, V.; Nacci, A.; Monopoli, A.; Fanizzi, A. Cyclic Carbonate Formation from Carbon Dioxide and Oxiranes in Tetrabutylammonium Halides as Solvents and Catalysts. *Org. Lett.* **2002**, *4*(15), 2561–2563.

- [41] Kim, H. Imidazolium zinc tetrahalide-catalyzed coupling reaction of CO<sub>2</sub> and ethylene oxide or propylene oxide. *Journal of Catalysis* **2003**, *220*(1), 44–46.
- [42] Kawanami, H.; Sasaki, A.; Matsui, K.; Ikushima, Y. A rapid and effective synthesis of propylene carbonate using a supercritical CO<sub>2</sub>-ionic liquid system. *Chem. Commun.* **2003**, (7), 896–897.
- [43] Darensbourg, D.J.; Lewis, S.J.; Rodgers, J.L.; Yarbrough, J.C. Carbon Dioxide/Epoxyde Coupling Reactions Utilizing Lewis Base Adducts of Zinc Halides as Catalysts. Cyclic Carbonate versus Polycarbonate Production. *Inorg. Chem.* **2003**, *42*(2), 581–589.
- [44] Sun, J.; Fujita, S.-I.; Zhao, F.; Arai, M. A highly efficient catalyst system of ZnBr<sub>2</sub>/n-Bu<sub>4</sub>NI for the synthesis of styrene carbonate from styrene oxide and supercritical carbon dioxide. *Applied Catalysis A: General* **2005**, *287*(2), 221–226.
- [45] Sugimoto, H.; Kuroda, K. The Cobalt Porphyrin–Lewis Base System: A Highly Selective Catalyst for Alternating Copolymerization of CO<sub>2</sub> and Epoxyde under Mild Conditions. *Macromolecules* **2008**, *41*(2), 312–317.
- [46] Sibaoui, A.; Ryan, P.; Leskelä, M.; Rieger, B.; Repo, T. Facile synthesis of cyclic carbonates from CO<sub>2</sub> and epoxides with cobalt(II)/onium salt based catalysts. *Applied Catalysis A: General* **2009**, *365*(2), 194–198.
- [47] Seki, T.; Grunwaldt, J.-D.; Baiker, A. In Situ Attenuated Total Reflection Infrared Spectroscopy of Imidazolium-Based Room-Temperature Ionic Liquids under “Supercritical” CO<sub>2</sub>. *J. Phys. Chem. B* **2009**, *113*(1), 114–122.
- [48] Chang, T.; Jin, L.; Jing, H. Bifunctional Chiral Catalyst for the Synthesis of Chiral Cyclic Carbonates from Carbon Dioxide and Epoxides. *ChemCatChem* **2009**, *1*(3), 379–383.
- [49] Darensbourg, D.J.; Moncada, A.I. Tuning the Selectivity of the Oxetane and CO<sub>2</sub> Coupling Process Catalyzed by (Salen)CrCl/ n -Bu<sub>4</sub> NX: Cyclic Carbonate Formation vs Aliphatic Polycarbonate Production. *Macromolecules* **2010**, *43*(14), 5996–6003.
- [50] Lu, X.-B.; Darensbourg, D.J. Cobalt catalysts for the coupling of CO<sub>2</sub> and epoxides to provide polycarbonates and cyclic carbonates. *Chem. Soc. Rev.* **2012**, *41*(4), 1462–1484.
- [51] Tian, D.; Liu, B.; Gan, Q.; Li, H.; Darensbourg, Donald.J. Formation of Cyclic Carbonates from Carbon Dioxide and Epoxides Coupling Reactions Efficiently Catalyzed by Robust, Recyclable One-Component Aluminum-Salen Complexes. *ACS Catal.* **2012**, *2*(9), 2029–2035.
- [52] Yang, Y.; Hayashi, Y.; Fujii, Y.; Nagano, T.; Kita, Y.; Ohshima, T.; Okuda, J.; Mashima, K. Efficient cyclic carbonate synthesis catalyzed by zinc cluster systems under mild conditions. *Catal. Sci. Technol.* **2012**, *2*(3), 509–513.
- [53] Ema, T.; Miyazaki, Y.; Koyama, S.; Yano, Y.; Sakai, T. A bifunctional catalyst for carbon dioxide fixation: cooperative double activation of epoxides for the synthesis of cyclic carbonates. *Chem. Commun.* **2012**, *48*(37), 4489.
- [54] Chatelet, B.; Joucla, L.; Dutasta, J.-P.; Martinez, A.; Szeto, K.C.; Dufaud, V. Azaphosphatranes as Structurally Tunable Organocatalysts for Carbonate Synthesis from CO<sub>2</sub> and Epoxides. *J. Am. Chem. Soc.* **2013**, *135*(14), 5348–5351.

- [55] Fuchs, M.A.; Zevaco, T.A.; Ember, E.; Walter, O.; Held, I.; Dinjus, E.; Döring, M. Synthesis of cyclic carbonates from epoxides and carbon dioxide catalyzed by an easy-to-handle ionic iron(iii) complex. *Dalton Trans.* **2013**, 42(15), 5322.
- [56] Whiteoak, C.J.; Kielland, N.; Laserna, V.; Castro-Gómez, F.; Martin, E.; Escudero-Adán, E.C.; Bo, C.; Kleij, A.W. Highly Active Aluminium Catalysts for the Formation of Organic Carbonates from CO<sub>2</sub> and Oxiranes. *Chem. Eur. J.* **2014**, 20(8), 2264–2275.
- [57] Werner, T.; Büttner, H. Phosphorus-based Bifunctional Organocatalysts for the Addition of Carbon Dioxide and Epoxides. *ChemSusChem* **2014**, 7(12), 3268–3271.
- [58] Gennen, S.; Alves, M.; Méreau, R.; Tassaing, T.; Gilbert, B.; Detrembleur, C.; Jerome, C.; Grignard, B. Fluorinated Alcohols as Activators for the Solvent-Free Chemical Fixation of Carbon Dioxide into Epoxides. *ChemSusChem* **2015**, 8(11), 1845–1849.
- [59] Rintjema, J.; Kleij, A.W. Aluminum-Mediated Formation of Cyclic Carbonates: Benchmarking Catalytic Performance Metrics. *ChemSusChem* **2017**, 10(6), 1274–1282.
- [60] Arayachukiat, S.; Kongtes, C.; Barthel, A.; Vummaleti, S.V.C.; Poater, A.; Wannakao, S.; Cavallo, L.; D’Elia, V. Ascorbic Acid as a Bifunctional Hydrogen Bond Donor for the Synthesis of Cyclic Carbonates from CO<sub>2</sub> under Ambient Conditions. *ACS Sustainable Chem. Eng.* **2017**, 5(8), 6392–6397.
- [61] Meléndez, D.O.; Lara-Sánchez, A.; Martínez, J.; Wu, X.; Otero, A.; Castro-Osma, J.A.; North, M.; Rojas, R.S. Amidinate Aluminium Complexes as Catalysts for Carbon Dioxide Fixation into Cyclic Carbonates. *ChemCatChem* **2018**, 10(10), 2271–2277.
- [62] Hong, M.; Kim, Y.; Kim, H.; Cho, H.J.; Baik, M.-H.; Kim, Y. Scorpionate Catalysts for Coupling CO<sub>2</sub> and Epoxides to Cyclic Carbonates: A Rational Design Approach for Organocatalysts. *J. Org. Chem.* **2018**, 83(16), 9370–9380.
- [63] Mesías-Salazar, Á.; Martínez, J.; Rojas, R.S.; Carrillo-Hermosilla, F.; Ramos, A.; Fernández-Galán, R.; Antiñolo, A. Aromatic guanidines as highly active binary catalytic systems for the fixation of CO<sub>2</sub> into cyclic carbonates under mild conditions. *Catal. Sci. Technol.* **2019**, 9(15), 3879–3886.
- [64] Ma, H.; Zeng, J.; Tu, D.; Mao, W.; Zhao, B.; Wang, K.; Liu, Z.; Lu, J. 3-Bromo-1,1,1-trifluoro-2-propanol assisted chemical fixation of CO<sub>2</sub> and epoxides. *Tetrahedron Letters* **2020**, 61(11), 151593.
- [65] Natongchai, W.; Luque-Urrutia, J.A.; Phungpanya, C.; Solà, M.; D’Elia, V.; Poater, A.; Zipse, H. Cycloaddition of CO<sub>2</sub> to epoxides by highly nucleophilic 4-aminopyridines: establishing a relationship between carbon basicity and catalytic performance by experimental and DFT investigations. *Org. Chem. Front.* **2021**, 8(3), 613–627.
- [66] Yao, Q.; Shi, Y.; Wang, Y.; Zhu, X.; Yuan, D.; Yao, Y. Bifunctional Rare-Earth Metal Catalysts for Conversion of CO<sub>2</sub> and Epoxides into Cyclic Carbonates. *Asian Journal of Organic Chemistry* **2022**, 11(8), e202200106.



- [67] Jana, S.; Yu, H.; Parthiban, A.; Chai, C.L.L. Controlled synthesis and functionalization of PEGylated methacrylates bearing cyclic carbonate pendant groups. *Journal of Polymer Science Part A: Polymer Chemistry* **2010**, *48*(7), 1622–1632.
- [68] Hwang, S.W.; Park, D.H.; Kang, D.H.; Lee, S.B.; Shim, J.K. Reactive compatibilization of poly(L-lactic acid)/poly(propylene carbonate) blends: Thermal, thermomechanical, and morphological properties. *J. Appl. Polym. Sci.* **2016**, *133*(18), n/a-n/a.
- [69] Sun, J.; Fujita, S.; Arai, M. Development in the green synthesis of cyclic carbonate from carbon dioxide using ionic liquids. *Journal of Organometallic Chemistry* **2005**, *690*(15), 3490–3497.
- [70] Blain, M.; Jean-Gérard, L.; Auvergne, R.; Benazet, D.; Caillol, S.; Andrioletti, B. Rational investigations in the ring opening of cyclic carbonates by amines. *Green Chem.* **2014**, *16*(9), 4286–4291.
- [71] Ju, H.-Y.; Manju, M.-D.; Kim, K.-H.; Park, S.-W.; Park, D.-W. Catalytic performance of quaternary ammonium salts in the reaction of butyl glycidyl ether and carbon dioxide. *Journal of Industrial and Engineering Chemistry* **2008**, *14*(2), 157–160.
- [72] Wang, L.; Zhang, G.; Kodama, K.; Hirose, T. An efficient metal- and solvent-free organocatalytic system for chemical fixation of CO<sub>2</sub> into cyclic carbonates under mild conditions. *Green Chem.* **2016**, *18*(5), 1229–1233.
- [73] Wang, X.; Wang, L.; Zhao, Y.; Kodama, K.; Hirose, T. Efficient and practical organocatalytic system for the synthesis of cyclic carbonates from carbon dioxide and epoxides: 3-hydroxypyridine/tetra-n-butylammonium iodide. *Tetrahedron* **2017**, *73*(8), 1190–1195.
- [74] Whiteoak, C.J.; Martin, E.; Belmonte, M.M.; Benet-Buchholz, J.; Kleij, A.W. An Efficient Iron Catalyst for the Synthesis of Five- and Six-Membered Organic Carbonates under Mild Conditions. *Adv. Synth. Catal.* **2012**, *354*(2–3), 469–476.
- [75] Gourgouillon, D.; Avelino, H.M.N.T.; Fareleira, J.M.N.A.; Nunes da Ponte, M. Simultaneous viscosity and density measurement of supercritical CO<sub>2</sub>-saturated PEG 400. *The Journal of Supercritical Fluids* **1998**, *13*(1–3), 177–185.
- [76] Kwag, C.; Manke, C.W.; Gulari, E. Rheology of molten polystyrene with dissolved supercritical and near-critical gases. *Journal of Polymer Science Part B: Polymer Physics* **1999**, *37*(19), 2771–2781.
- [77] Zhang, H.; Liu, Z.; Han, B. Critical points and phase behavior of toluene-CO<sub>2</sub> and toluene-H<sub>2</sub>-CO<sub>2</sub> mixture in CO<sub>2</sub>-rich region. *The Journal of Supercritical Fluids* **2000**, *18*(3), 185–192.
- [78] Raveendran, P.; Ikushima, Y.; Wallen, S.L. Polar Attributes of Supercritical Carbon Dioxide. *Acc. Chem. Res.* **2005**, *38*(6), 478–485.
- [79] Rainglet, B.; Besognet, P.; Benoit, C.; Delage, K.; Bounor-Legaré, V.; Forest, C.; Cassagnau, P.; Chalamet, Y. TPV Foaming by CO<sub>2</sub> Extrusion: Processing and Modelling. *Polymers* **2022**, *14*(21), 4513.
- [80] Verny, L.; Ylla, N.; Cruz-Boisson, F.D.; Espuche, E.; Mercier, R.; Sudre, G.; Bounor-Legaré, V. Solvent-Free Reactive Extrusion As an Innovative and Efficient Process for the Synthesis of Polyimides. *Ind. Eng. Chem. Res.* **2020**, *59*(37), 16191–16204.

## Chapter 2: Carbonatation of [ethylene-glycidyl methacrylate]-based copolymers with carbon dioxide as a reagent

---

- [81] Dubois, C.; Marestin, C.; Cassagnau, P.; Delage, K.; Alcouffe, P.; Garois, N.; Bounor-Legaré, V. Innovative polypropylene based blends by in situ polymerization of a polyimide dispersed phase by reactive extrusion. *Polymer* **2022**, *254*, 125022.
- [82] Bolt, R.R.A.; Leitch, J.A.; Jones, A.C.; Nicholson, W.I.; Browne, D.L. Continuous flow mechanochemistry: reactive extrusion as an enabling technology in organic synthesis. *Chem. Soc. Rev.* **2022**, *51*(11), 4243–4260.
- [83] Martey, S.; Addison, B.; Wilson, N.; Tan, B.; Yu, J.; Dorgan, J.R.; Sobkowicz, M.J. Hybrid Chemomechanical Plastics Recycling: Solvent-free, High-Speed Reactive Extrusion of Low-Density Polyethylene. *ChemSusChem* **2021**, *14*(19), 4280–4290.
- [84] Rehman, A.; López Fernández, A.M.; Resul, M.F.M.G.; Harvey, A. Kinetic investigations of styrene carbonate synthesis from styrene oxide and CO<sub>2</sub> using a continuous flow tube-in-tube gas-liquid reactor. *Journal of CO<sub>2</sub> Utilization* **2018**, *24*, 341–349.
- [85] Hatada, K.; Kitayama, T.; Ute, K.; Terawaki, Y.; Yanagida, T. End-Group Analysis of Poly(methyl methacrylate) Prepared with Benzoyl Peroxide by 750 MHz High-Resolution <sup>1</sup>H NMR Spectroscopy. *Macromolecules* **1997**, *30*(22), 6754–6759.
- [86] Zentel, K.M.; Bungu, P.S.E.; Pasch, H.; Busch, M. Linking molecular structure to plant conditions: advanced analysis of a systematic set of mini-plant scale low density polyethylenes. *Polym. Chem.* **2021**, *12*(20), 3026–3041.



---

# Chapter 3:

## Two-steps functionalization of polydienes with peracids and carbon dioxide as reagent

---

In **Chapter 3**, the functionalization with CO<sub>2</sub> will be extended to polydienes and polymers containing unsaturations. A two-step synthesis (epoxidation and carbonatation) will be presented using peracids and organocatalysts to form cyclic carbonate functions on unsaturated polymers. The epoxidation step will first be studied in a batch process, then transposed to a reactive extrusion process. The carbonatation step will be optimized in a batch process using ammonium salts as organocatalysts. Full characterization of the polymers (<sup>1</sup>H NMR, IR-ATR, SEC and DSC) are reported in Appendices.



## Table of Contents

<b>I. Résumé .....</b>	<b>135</b>
<b>II. Abstract .....</b>	<b>136</b>
<b>III. Introduction.....</b>	<b>137</b>
<b>IV. Results and discussion .....</b>	<b>139</b>
IV.1. Epoxidation of polydienes.....	139
IV.1.a. Study of the epoxidation on polybutadiene.....	139
IV.1.b. Scope of the epoxidation on unsaturated polymers.....	144
IV.1.c. Epoxidation transposed to reactive extrusion .....	148
IV.2. Carbonatation of epoxidized polydienes.....	150
IV.2.a. Study of the reaction on epoxidized polybutadiene.....	150
IV.2.b. Scope of the carbonatation reaction.....	154
IV.2.c. Evolution of the thermal properties .....	158
<b>V. Conclusions .....</b>	<b>165</b>
<b>VI. References.....</b>	<b>167</b>



## I. Résumé

La fonctionnalisation en deux étapes de polydiènes en utilisant les systèmes 1)  $H_2O_2$ /acide carboxylique et 2) dioxyde de carbone/catalyseur organique a été réalisée sur des polymères contenant des alcènes disubstitués (par exemple les polybutadiènes) et trisubstitués (par exemple les polyisoprènes tels que le caoutchouc naturel). La première étape, c'est-à-dire l'époxydation, a été optimisée et réalisée avec le système oxydant  $H_2O_2/HCOOH$  sur plusieurs polybutadiènes, copolymères contenant du butadiène, polyisoprènes et grades d'EPDM. La réactivité de chaque polymère a été influencée par sa microstructure. Pour le polybutadiène, la réactivité des unités répétitives augmente dans l'ordre suivant : unités 1,2  $\ll$  unités 1,4 *trans* < unités 1,4 *cis*. Une tendance similaire a été observée pour les polyisoprènes : unités 3,4  $\ll$  unités 1,4. Dans le cas de l'EPDM, les unités dicyclopentadiène (DCPD) étaient moins réactives que les unités éthylidène norbornène (ENB). Il est intéressant de noter que la réaction d'époxydation a pu, être transposée à un procédé d'extrusion réactive avec la production de jusqu'à 1,3 mol% d'époxyde à partir d'un polybutadiène de faible masse molaire. L'étape de carbonatation a également été optimisée et la méthyléthylcétone (MEK) s'est avérée être un meilleur solvant que le toluène pour la réaction. En ce qui concerne le système catalytique, le bromure de tétraoctylammonium (TOAB) s'est révélé le plus performant pour la carbonatation des polybutadiènes contenant des époxydes principalement *cis*, tandis que le chlorure de bis(triphénylphosphine)iminium (PPNCl) s'est révélé meilleur pour la carbonatation des polybutadiènes contenant des époxydes *trans* et pour les polyisoprènes époxydés. Cependant, les EPDM époxydés n'ont montré aucune réactivité. La réaction d'époxydation n'a pas modifié de manière significative la  $T_g$  et la distribution de masses molaires des polymères (excepté pour **SIS** dont les masses molaires ont été fortement diminuées), alors que la formation de carbonates cycliques sur les chaînes des polymères a fortement augmenté la  $T_g$ . Des réactions de réticulation peuvent avoir eu lieu durant la carbonatation de polybutadiènes contenant principalement des époxydes *cis* (**C-PBU-1** et **C-PBU-2**), rendant ces polymères insolubles, tandis que ceux contenant principalement des époxydes *trans* (ou faible taux d'époxydes *cis*) n'ont pas eu de changement de masses molaires. Concernant la carbonatation de caoutchouc naturel époxydés (E-NR-1), une dégradation partielle des unités isoprènes par clivage oxydant et des réactions de réticulations ont pu être observées comme réactions secondaires.



## II. Abstract

The two-step functionalization of polydienes using 1) H<sub>2</sub>O<sub>2</sub>/carboxylic acid and 2) carbon dioxide/organic catalyst was achieved on disubstituted- (*e.g.* polybutadienes) and trisubstituted-alkene-containing polymers (*e.g.* polyisoprenes such as natural rubber). The first step, *i.e.* the epoxidation step, was optimized and performed with the H<sub>2</sub>O<sub>2</sub>/HCOOH oxidant system on several polybutadienes, butadiene-containing copolymers, polyisoprenes and EPDM grades. The reactivity of each polymer was influenced by its microstructure. For polybutadiene, the repeating unit reactivity increases in the following order: 1,2 units << 1,4 *trans* units < 1,4 *cis* units. A similar trend was observed with polyisoprenes: 3,4 units << 1,4 units. With EPDM, the dicyclopentadiene (DCPD) units were less reactive than the ethylidene norbornene (ENB) units. Interestingly, the epoxidation reaction could, for the first time, be transposed to a reactive extrusion process with the production of up to 1.3 mol% of epoxide from a low molar mass polybutadiene was. Then, the carbonation step was also optimized and methyl ethyl ketone (MEK) was found to be a better solvent than toluene for the reaction. Regarding the catalyst system, tetraoctylammonium bromide (TOAB) showed the best performance for the carbonation of polybutadienes containing mainly *cis* epoxides, whereas bis(triphenylphosphine)iminium chloride (PPNCl) was better for the carbonation of polybutadiene containing *trans* epoxides and for epoxidized polyisoprenes. However, epoxidized EPDM did not show any reactivity. The epoxidation reaction did not significantly alter the  $T_g$  and molar mass distribution of the polymers (except for **SIS**, whose molar masses were greatly reduced), while the formation of cyclic carbonates on the polymer chains greatly increased the  $T_g$ . Cross-linking reactions may have occurred during carbonation of polybutadienes containing mainly *cis* epoxides (**C-PBU-1** and **C-PBU-2**), making these polymers insoluble, while polybutadienes containing mainly *trans* epoxides (or with low content of *cis* epoxides) showed no change in molar mass (**C-PBU-3** and **C-SBS**). During the carbonation of epoxidized natural rubber (**E-NR-1**), partial degradation of isoprene units by oxidative cleavage and cross-linking reactions were observed as side reactions.

### III. Introduction

The post-functionalization of polymers offers new possibilities in term of material production, and is an innovative approach to potentially target polymer recycling or even better upcycling.<sup>[1]</sup> Carbon dioxide represents an interesting carbon feedstock when considering its high availability, non-toxicity and sustainability (with appropriate capture and sequestration).<sup>[2,3]</sup> The synthesis of poly(cyclic carbonates) from the cycloaddition of CO<sub>2</sub> on epoxide is a low-carbon footprint route, for the production of functionalized polymers that could find applications as intermediates for the synthesis of non-isocyanate polyurethanes (NIPUs),<sup>[4-9]</sup> reactive compatibilizers or solid electrolytes for batteries.<sup>[10-12]</sup>

Cyclic carbonate synthesis from epoxide has been widely studied on molecular compounds such as ethylene oxide<sup>[13]</sup>, propylene oxide<sup>[13-15]</sup>, styrene oxide,<sup>[16-18]</sup> or more complex molecules such as limonene oxide<sup>[19,20]</sup> and epoxidized vegetable oils.<sup>[21-27]</sup> Many catalytic systems have been used such as ammonium<sup>[19,28-30]</sup>, phosphonium<sup>[31-36]</sup> and imidazolium salts,<sup>[13,37-39]</sup> strong hindered bases,<sup>[40]</sup> metallic complexes,<sup>[41-48]</sup> and bifunctional catalysts.<sup>[36,39,45,49-53]</sup> The synthesis of cyclic carbonate functions on polymers containing epoxide pendant groups has also been studied but mainly on polar polymers containing high content of glycidyl methacrylate monomer.<sup>[54-56]</sup> We recently reported for the first time the carbonatation of semi-crystalline [ethylene – glycidyl methacrylate] copolymers in both batch and solvent-free reactive extrusion processes, using ammonium salts as catalysts.<sup>[57]</sup> It offers a methodology for the carbonatation of relatively apolar semi-crystalline polymers containing epoxide pendant groups with a solvent-free continuous process.

However, this polymer functionalization with CO<sub>2</sub> only targets terminal epoxides. A chemical strategy for carbonating any polymers bearing unsaturations would hold much potential for industrial CO<sub>2</sub> incorporation into ubiquitous polymers. As a model and excellent example, carbonated polymers from the epoxidation of polydienes such as polybutadiene, polyisoprene or copolymers containing dienes monomers could foster the development and production of high values materials such as elastomers containing exchangeable knots and thus a dynamic network, but the carbonatation of internal and tri-substituted epoxides is much more challenging because of their higher stability.

Before the carbonatation step, the formation of epoxide functions on the polymers backbone (or side chains) is required. The epoxidation of polymers containing dienes monomers have

already been reported for several type of polymers: polybutadienes,<sup>[58-65]</sup> natural rubbers (*cis*-1,4-polyisoprene),<sup>[66-68]</sup> *trans*-1,4-polyisoprene,<sup>[69]</sup> and ethylene-propylene-diene monomer terpolymers (EPDM).<sup>[70,71]</sup> Simple oxidant systems such as H<sub>2</sub>O<sub>2</sub>/RCOOH (R = H or alkyl chain),<sup>[58,63,65-69]</sup> *meta*-perchlorobenzoic acid (mCPBA),<sup>[59,64]</sup> and monoperoxy phthalic acid<sup>[61]</sup> were reported, as well as more complex systems such as H<sub>2</sub>O<sub>2</sub>/Methyltrioxorhenium,<sup>[60]</sup> dimethyldioxirane prepared *in situ*,<sup>[62,70]</sup> and H<sub>2</sub>O<sub>2</sub>/Mn(ClO<sub>4</sub>)<sub>2</sub> /sodium picolinate/sodium acetate/2,3-butanedione<sup>[71]</sup>. Regarding the use of peracids, Abdullin *et al.*<sup>[63]</sup> studied the effect of the alkyl chains on the peracid reactivity for the epoxidation of syndiotactic 1,2-polybutadiene composed of 84 mol% of 1,2 units, and observed the following reactivity order: m-CPBA > performic acid > peracetic acid > lactic peradic > propionic peracid under the following conditions: 50 mol% of peracid, 50 °C, toluene. m-CPBA was much more reactive than the other peracids, as all the 1,4 units were epoxidized, but also a part of the 1,2 units with a final epoxide content of 33.8 mol% after 2.7 hours. With the other peracids, the epoxide content did not exceed 15.7 mol%, as no 1,2 units were epoxidized. Thus the 1,4 units are much more reactive than the 1,2 units.

Few studies were reported for the carbonatation of epoxidized polydienes.<sup>[8,72,73]</sup> Especially, Dechent *et al.* reported the synthesis of carbonated polybutadienes (*i.e.* polybutadienes containing cyclic carbonate functions) using bis(triphenylphosphoranylidene)ammonium chloride (PPNCl) and tetrabutyl ammonium bromide (TBAB) organocatalysts in methyl ethyl ketone (MEK).<sup>[8]</sup>

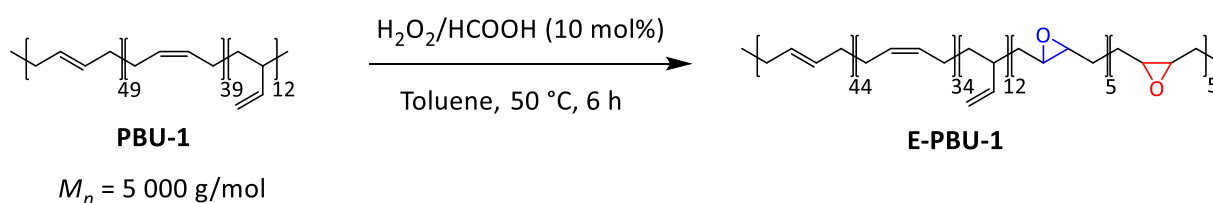
In this work, we present the oxidative carbonatation in two steps of several polydienes (polybutadienes and polyisoprenes) and polyolefins containing dienes comonomers. For each step (1) epoxidation & (2) carbonatation, the optimal conditions will be investigated and the influence of the polymer microstructure will be discussed.

## IV. Results and discussion

### IV.1. Epoxidation of polydienes

#### IV.1.a. Study of the epoxidation on polybutadiene

Polybutadiene **PBU-1** with a  $M_n$  of 5 000 g/mol and containing 49 mol% of *trans*-1,4 unit, 39 mol% of *cis*-1,4 unit and 12 mol% of vinyl unit was first chosen to study the epoxidation step. The epoxidation was carried out first with the oxidant system  $H_2O_2/HCOOH$  at 50 °C in toluene for 6 h. 10 mol% of oxidant was added (compared to butadiene units) to partially epoxidize the polymer, hence advantageously preserving its valuable mechanical properties (*Scheme 1*). The obtained polymer denoted **E-PBU-1** was characterized by  $^1H$ ,  $^{13}C$ , and DEPT NMR to identify and quantify each repeating unit.



*Scheme 1. Epoxidation of PBU-1 with peracetic acid formed in situ.*

On the  $^1H$  NMR spectrum of the polymer after reaction, the signals b' and d' corresponding to the 1,4-*trans* and 1,4-*cis* epoxides were clearly identified at 2.68 and 2.93 ppm respectively (*Figure 1*). The 1,4-*trans* and 1,4-*cis* epoxide units each represents 5 mol% of the total units, thus the total content of epoxides was 10 mol% (calculation detailed in appendices), which indicated that the oxidant was quantitatively converted. However, the vinyl units did not react at all, as the vinyl content did not vary and no pendant epoxide was observed, which highlights the much lower reactivity of the 1,2 units compared to the 1,4 units (the more substituted the alkene, the more electron-rich it is, which probably overcomes the steric obstacle in that instance). This observation is consistent with the literature.<sup>[63]</sup>

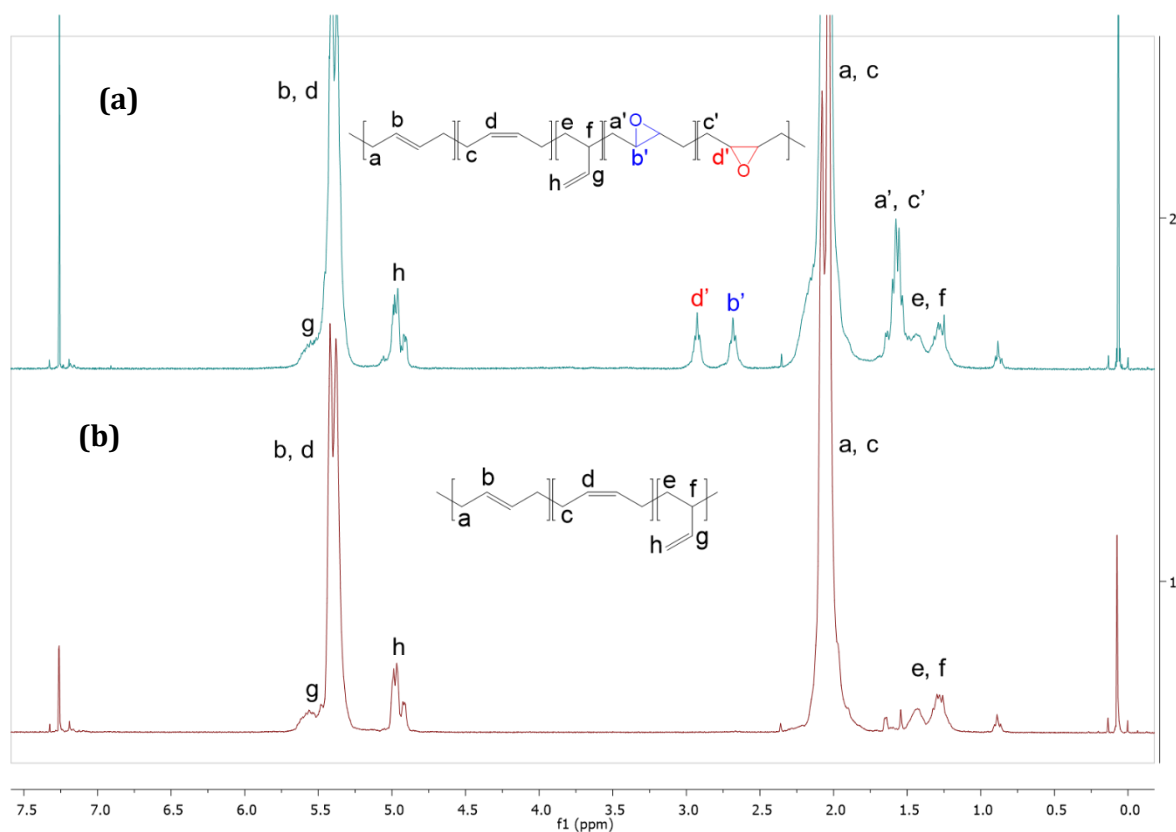


Figure 1.  $^1\text{H}$  NMR ( $\text{CDCl}_3$ , 300 MHz) spectra of (a) *E*-PBU-1 and (b) PBU-1.

The formation of epoxide *s* was also confirmed by  $^{13}\text{C}$  NMR and DEPT 135, in particular the *cis* and *trans* epoxide signals corresponding to the CH groups could be observed at 56.76 and 58.47 ppm respectively, (Figure 2). It is interesting to notice that the *cis:trans* epoxide ratio obtained (50: 50) did not exactly correspond to the initial *cis:trans* butadiene units ratio (45:55) estimated by  $^{13}\text{C}$  NMR, which demonstrates that *cis* units are slightly more reactive than *trans* units. According to these observation, the following order of reactivity was observed: **1,4-*cis* unit > 1,4-*trans* unit >> 1,2 unit.**

### Chapter 3: Two-steps functionalization of polydienes with peracids and carbon dioxide as reagent

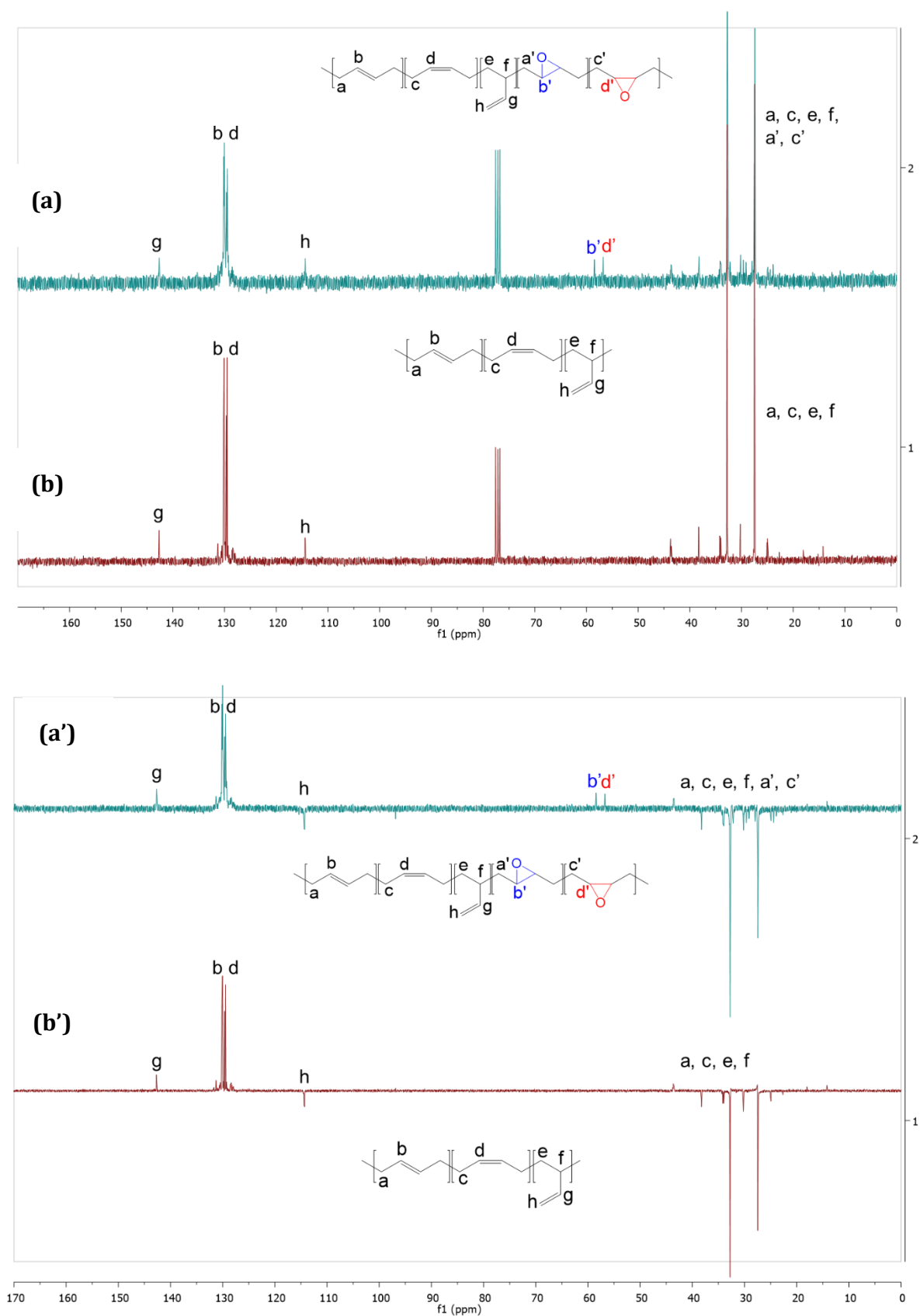


Figure 2.  $^{13}\text{C}$  NMR ( $\text{CDCl}_3$ , 75 MHz) spectra of (a) **E-PBU-1** and (b) **PBU-1**, DEPT 135 spectra of (a') **E-PBU-1** and (b') **PBU-1**.

The temperature has a great influence on the epoxidation reaction. Performic acid decomposes spontaneously to  $\text{CO}_2$  and  $\text{H}_2\text{O}$ ,<sup>[74]</sup> even at room temperature, and its degradation is favored with increasing temperature. This is why the *in situ* formation of the peracid is preferable, to prevent any degradation before reaction. Secondary reactions could also occur such as the opening of epoxides by hydrolysis catalyzed by the presence of acid, and the oxidative cleavage of epoxide functions into aldehydes caused by the presence of  $\text{H}_2\text{O}_2$  and high temperature.<sup>[75]</sup>

To study the influence of the temperature, the formation of epoxide was followed by  $^1\text{H}$  NMR using mesitylene as internal standard, for different temperatures with the  $\text{H}_2\text{O}_2/\text{HCOOH}$  oxidant system (Figure 3). According to Figure 3, the optimal temperature was 50 °C, where the epoxide yield was quantitative after 3 hours of reaction. As the temperature increases, a decrease in epoxide yield was observed. After 3 hours, yields of 64, 61 and 54 % were obtained at 70, 90 and 110 °C, respectively. Concerning the configuration of the epoxides formed, both *cis* and *trans* epoxides are obtained with a *cis:trans* ratio of 50: 50, and no epoxides were formed on the pendant vinyl units for each temperature.

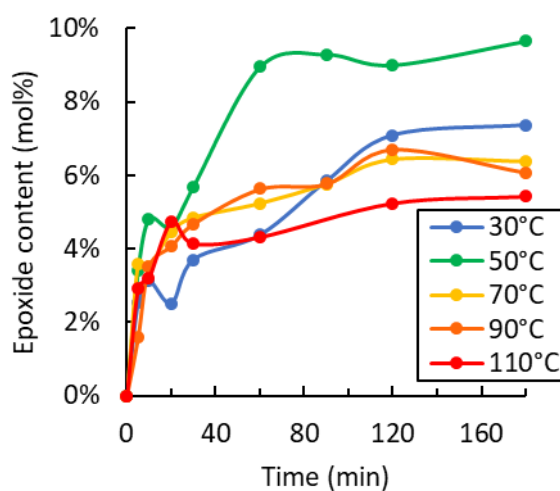


Figure 3. Influence of the temperature on the epoxide content for the epoxidation of **PBU-1**. Epoxide content determined by  $^1\text{H}$  NMR ( $\text{CDCl}_3$ , 300 MHz) using mesitylene as internal standard.

In Figure 4, the  $^1\text{H}$  NMR spectra of the reaction mixture at 50 °C for different reaction times are presented. The *cis* and *trans* epoxide signals increased over time. The signals of mesitylene

(6.81, 2.29 ppm), HCOOH (7.98 ppm), HCO<sub>3</sub>H (8.25 ppm) and H<sub>2</sub>O<sub>2</sub> (6.5-5.5 ppm) were also observed.

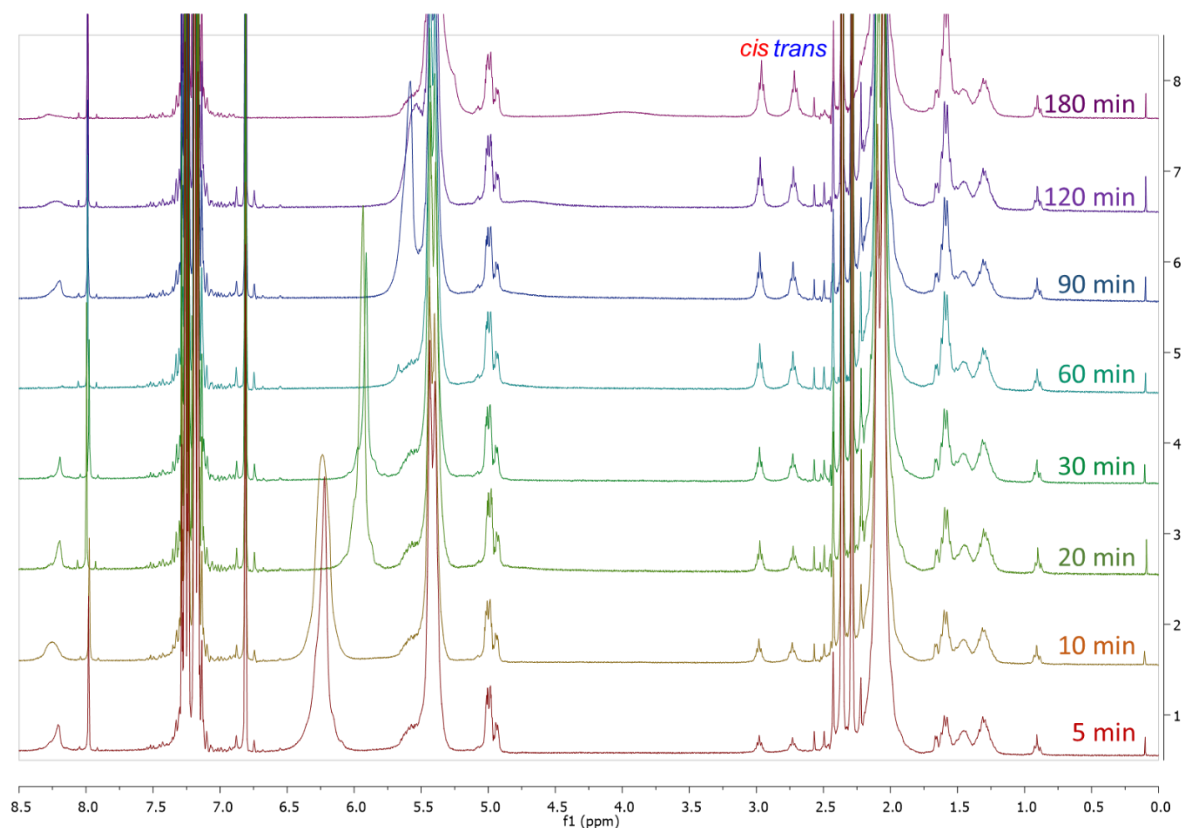


Figure 4. Evolution overtime of the <sup>1</sup>H NMR (CDCl<sub>3</sub>, 300 MHz) spectra of the crude reaction mixture for the epoxidation of **PBU-1** with 10 mol% of H<sub>2</sub>O<sub>2</sub>/HCOOH at 50 °C in toluene.

For the epoxidation of polybutadiene, H<sub>2</sub>O<sub>2</sub>/HCOOH, H<sub>2</sub>O<sub>2</sub>/AcOH and m-CPBA are the most common oxidant and widely used at industrial scale. These oxidants were tested at 110 °C to determine the most stable system at the optimal temperature for the carbonation step (Figure 5). By replacing formic acid with acetic acid, epoxides formation is slower. In contrast, using mCPBA as an oxidant allows epoxides to form more quickly during the first 5 minutes. However, after 5 minutes of reaction, a decrease in the epoxide rate is observed. In <sup>1</sup>H NMR spectrum of the crude reaction mixture after 180 min, broad signals at 3.3-4.3 ppm corresponding to the proton in alpha position to the alcohol groups were observed, which confirmed the partial hydrolysis of the epoxide moieties (see Figure S71 in the appendices). As H<sub>2</sub>O<sub>2</sub>/HCOOH showed a good compromise between reactivity and selectivity, it was chosen to study the scope of the reaction.



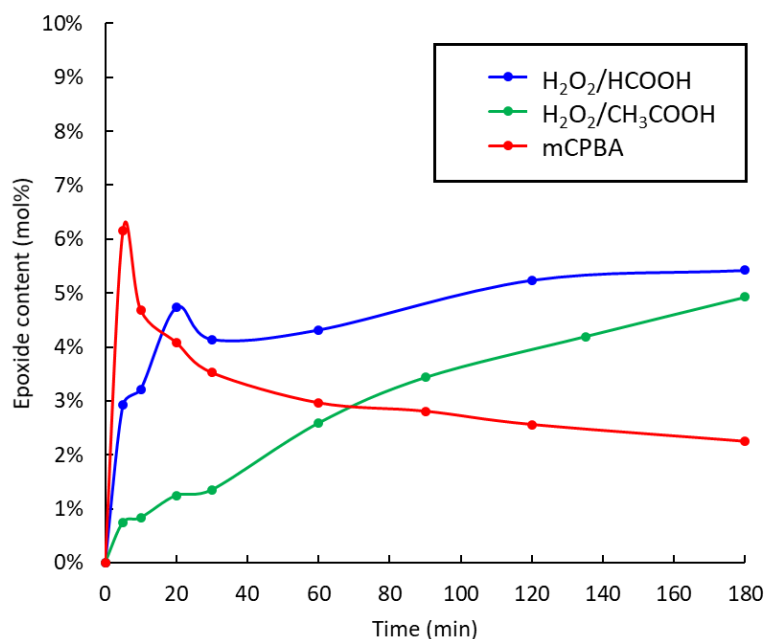


Figure 5. Evolution of the epoxide content on **PBU-1** at 110 °C with different oxidative systems.

#### IV.1.b. Scope of the epoxidation on unsaturated polymers

Several polybutadienes, polyisoprenes and copolymers containing diene units (molar composition and main characteristics are described in *Scheme 2*) were epoxidized with H<sub>2</sub>O<sub>2</sub>/HCOOH at 50 °C in toluene. The molar composition of the epoxidized polymers was determined by <sup>1</sup>H NMR (see detailed calculation in appendices). The yield of epoxide was determined with the following equation:

$$Yield = \frac{\text{mol\% (epoxide)}}{\text{maximum mol\% (epoxide)}} = \frac{\text{mol\% (epoxide)}}{\text{mol\% (oxidant)}} \quad (1)$$

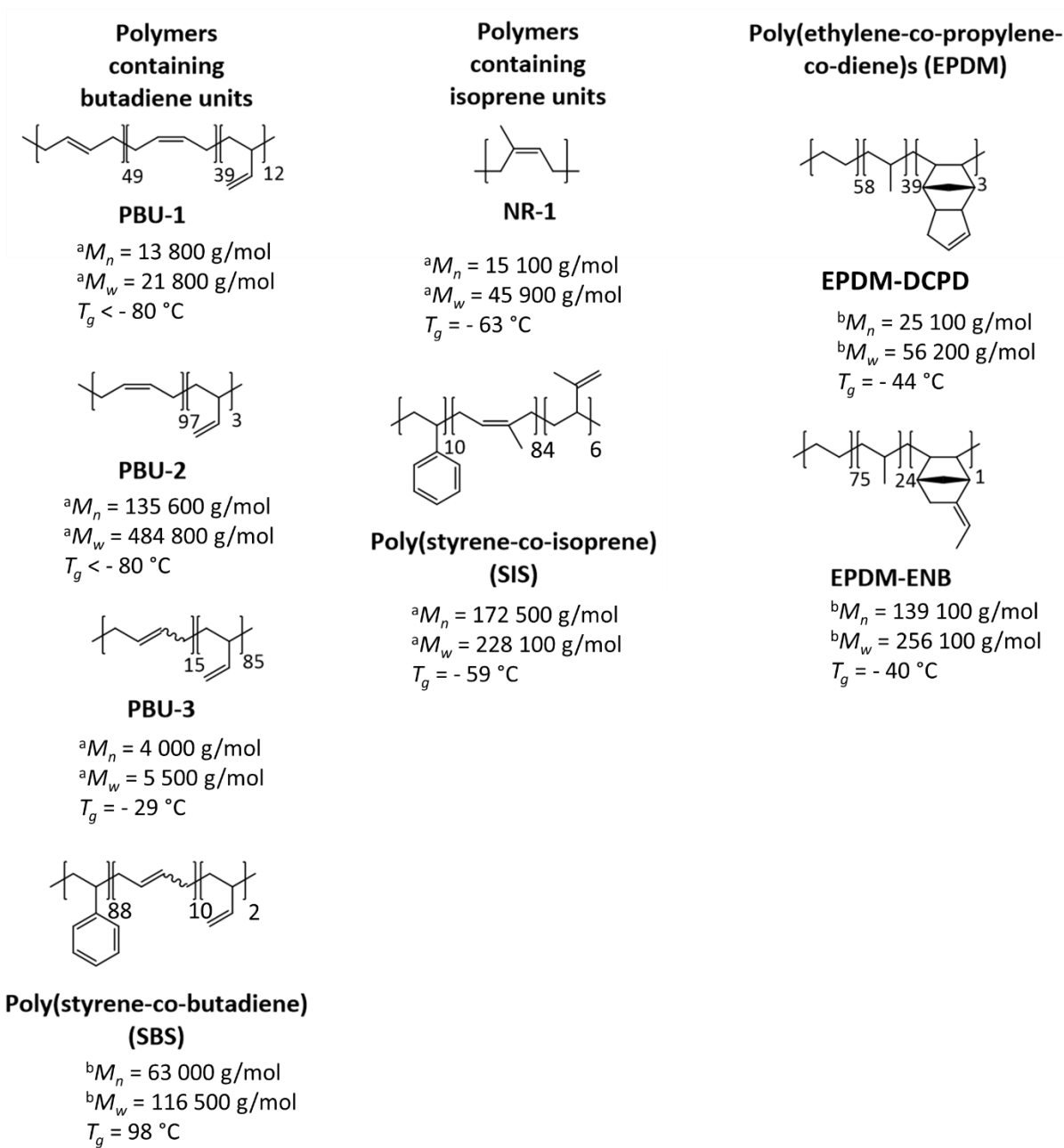
As there was no excess of oxidant, the maximum amount of epoxide that could be obtained correspond to the amount of H<sub>2</sub>O<sub>2</sub>/HCOOH added at the beginning of the reaction. For all epoxidation reaction, no by-product formation was observed.

First, polybutadienes and [styrene-block-butadiene-block-styrene] copolymer (**SBS**) were epoxidized (*Table 1*, entries 1-4). The polymer concentration was adapted to the polymer viscosity. **PBU-1** and **PBU-3** had a relatively low viscosity, which made possible the reaction at a high concentration (1 g of polymer per mL of toluene), whereas epoxidation of **PBU-2** and **SBS** was performed at 0.1 g/mL due to their higher viscosity in toluene. The amount of oxidant and the reaction time were also adapted for each polymer grade in order to obtain an epoxide content between approximately 5 and 15 mol% after reaction. The highest yield of epoxide

was obtained with **PBU-1** and **PBU-2** (99 % and 85 % respectively), which mainly contain 1,4 units, whereas lower yield was obtained with **PBU-3** and **SBS** (20 % and 37 % respectively). The epoxidation of **PBU-2** confirmed that no change of the configuration occurred after epoxidation, as only *cis* epoxide was obtained from 1,4-*cis* butadiene units (*Table 1*, entry 2). Moreover, as previously observed with **PBU-1**, the low reactivity of the vinyl groups was confirmed with the epoxidation of **PBU-3**. Indeed, a *cis:trans:vinyl* epoxide ratio of 15:75:10 was obtained, showing that 1,4 units were more converted to epoxide even when their content was almost 6 times lower than the vinyl content (*Table 1*, entry 3). **SBS** with low content of 1,4 (10 mol%) and 1,2 units (2 mol%) was epoxidized with 1 equiv. of oxidant relative to 1,4 units. A *cis:trans:vinyl* ratio of 43:56:0 and a yield of 30 % was obtained after 16 hours (*Table 1*, entry 4), due to the low concentration of 1,4-butadiene units in the medium at the beginning of the reaction (0.10 mol/L).

Thereafter, polymers containing isoprene units were epoxidized (*Table 1*, entries 5 and 6). A natural rubber containing essentially 1,4-*cis* units (**NR-1**) was epoxidized with 10 mol% of H<sub>2</sub>O<sub>2</sub>/HCOOH for 16 hours at a concentration of 1 g/mL, and an epoxide content of 9 mol% was obtained (90 % of yield). Thus, the epoxidation was not entirely complete, showing that 1,4-isoprene units are less reactive than 1,4 butadiene units (steric constraints could play a stronger role here). A **SIS** copolymer containing high content of isoprene (84 mol% of 1,4-*cis* and 6 mol% of 3,4 units) was epoxidized with 10 mol% of oxidant at a concentration of 0.1 g/mL. Only *cis* epoxide was obtained with an epoxide content of 5 mol% (50 % of yield). The 3,4 units (vinylidene groups) were completely unreactive, which is in accordance with the epoxidation of model molecules such as limonene. Indeed, limonene could be epoxidized to limonene oxide by the selective epoxidation of the trisubstituted double bond and without epoxidation of the vinylidene group.<sup>[76–78]</sup>

Finally, two different [ethylene-propylene-diene monomer] terpolymer (EPDM) (**EPDM-DCPD** and **EPDM-ENB** containing 3 and 1 mol% of diene respectively) were epoxidized with 1 equiv. of oxidant (according to diene unit) for 16 hours at a concentration of 0.1 and 0.063 g/mL respectively (*Table 1*, entries 7 and 8). A yield of 50 % and 70 % was obtained, respectively. The trisubstituted double bond of ENB may be more easily converted to epoxide compared to the double bonds contained in the cyclic structure of DCPD. In a similar case, during the epoxidation of terpinolene (containing a trisubstituted cyclic double bond and a tetra-substituted double bond), the tetrasubstituted epoxide was selectively obtained.<sup>[79,80]</sup>



*Scheme 2. Composition of the polydienes used in this study and their main properties. Composition calculation from <sup>1</sup>H NMR analyses detailed in appendices. <sup>a</sup>Determined by SEC in THF. <sup>b</sup>Determined by SEC in 1,2,4-TCB. T<sub>g</sub> determined by DSC.*

### Chapter 3: Two-steps functionalization of polydienes with peracids and carbon dioxide as reagent

Table 1. Epoxidation of polydienes.<sup>a</sup>

Entry	Polymer	Diene content (mol%) [ <i>cis:trans</i> :pendant ratio]	Polymer concentration (g/mL)	Amount of H <sub>2</sub> O <sub>2</sub> /HCOOH (mol%)	Reaction time (h)	Epoxide content (mol%)	Yield (%)	<i>Cis:trans</i> :pendant ratio
1	PBU-1	100 [39:49:12]	1	10	6	10	99	50:50:0
2	PBU-2	100 [97:0:3]	0.1	20	6	17	85	100:0:0
3	PBU-3	100 [15 mol% of 1,4, 85 mol% of 1,2]	1	20	16	4	20	15:75:10
4	SBS	12 [10 mol% of 1,4, 2 mol% of 1,2]	0.1	10	16	3	30	43:56:0
5	NR-1	100 [100:0:0]	1	10	16	9	90	100:0:0
6	SIS	90 [92:0:8]	0.1	10	16	5	50	100:0:0
7	DCPD- EPDM	3	0.1	3	16	1.5	50	/
8	ENB- EPDM	1	0.0625	1	16	0.7	70	/

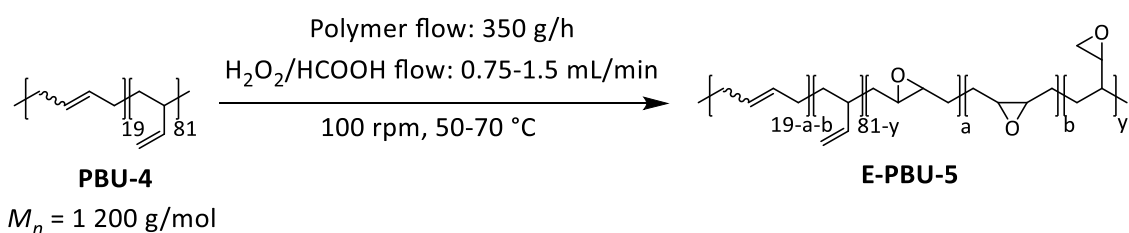
<sup>a</sup>Reaction conditions: 5 g of polymer, H<sub>2</sub>O<sub>2</sub>/HCOOH, 50 °C, toluene.

#### IV.1.c. Epoxidation transposed to reactive extrusion

During the last decades, reactive extrusion has demonstrated to be a remarkable process for the chemical transformation of highly viscous substrates under solvent-free conditions.<sup>[81,82]</sup> It is most of the time implemented using a co-rotating twin-screw extruder and could offers the possibility to produce high volume of functionalized polymers (from 10 kg/h to several tonnes/h). Its modularity in terms of temperature, screw speed and throughput makes it easy to adapt and control the production and chemical modification of high-value materials. However, the residence times are generally very short, from 1 to 10 minutes, which requires a thorough optimization of the reaction conditions to observe reactivity within these short times.

The epoxidation by reactive extrusion was performed with a low molar mass (1200 g/mol) polybutadiene **PBU-4** composed of 81 mol% of 1,2 units and 19 mol% of 1,4 units mainly in *trans* configuration using the H<sub>2</sub>O<sub>2</sub>/HCOOH system (*Scheme 3* and *Table 2*, entry 1). The lower viscosity of **PBU-4**, compared to the other liquid polymers (**PBU-1**, **PBU-2**, **PBU-3**, **NR-1** and **EPDM-DCPD**) made possible its introduction into the extruder using a gear pump at a flow rate of 350 g/h and a screw speed set at 100 rpm. The use of the polymers under pellets form (**SBS**, **SIS** and **EPDM-ENB**) was also not possible due too their too high extrusion temperature that are not suitable for the epoxidation reaction. First, the effect of the amount of oxidant was investigated at 50 °C. 5 mol% and 10 mol% have been tested, and in both cases, a very similar epoxide content was obtained (0.4 and 0.5 mol%, *Table 2*, entries 2 and 3). The *trans* epoxide was mostly obtained, and only few vinyl units were epoxidized. By increasing the temperature to 60 °C with 10 mol% of oxidant, the epoxide content increased to 1.3 mol% (*Table 2*, entry 4). However, a low gas emission was observed, and could be related to the degradation of the performic acid to carbon dioxide and water. When the temperature was further increased to 70 °C, the gas emission was even stronger, and the epoxide content decreased drastically to 0.1 mol% (*Table 2*, entry 5). According to these results, the epoxidation in reactive extrusion has to be performed in a temperature range of 50-60 °C to obtain satisfactory reactivity and to avoid degradation of the performic acid, as already observed when conducting the reaction in batch . This low temperature required to achieve efficient epoxidation does not allow us to consider the epoxidation of polymers having high  $T_g$  and/or a high molar mass by reactive extrusion. One possibility would be the use of less active but more stable peracids such as peracetic acid to perform extrusion at higher temperature.

### Chapter 3: Two-steps functionalization of polydienes with peracids and carbon dioxide as reagent



*Scheme 3. Epoxidation of PBU-4 by reactive extrusion.*

*Table 2. Screening of conditions for the epoxidation of PBU-4 by reactive extrusion.*

Entry	Temperature (°C)	H <sub>2</sub> O <sub>2</sub> /HCOOH (mol%)	Epoxide content (mol%)	Cis:trans:vinyl epoxide ratio
1	50	5	0,4	23:70:7
2	50	10	0,5	22:65:13
3	60	10	1,3	6:91:3
4	70	10	0,1	18:55:27

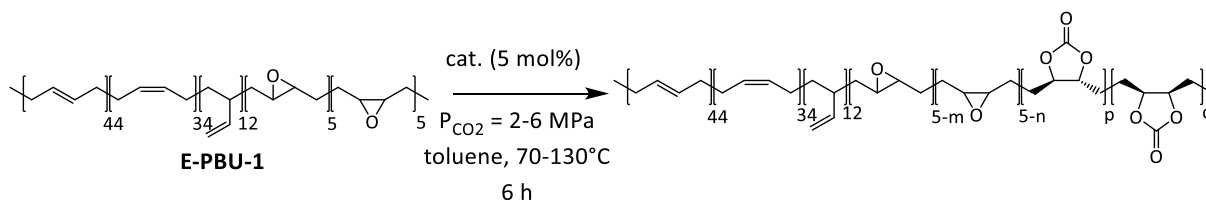
Reaction conditions: 350 g/h of **PBU-4** (81 mol% of 1,2 unit, 19 mol% of 1,4 units, mainly *trans*), 100 rpm. Epoxide content determined by <sup>1</sup>H NMR of the crude mixture directly after extrusion. See <sup>1</sup>H NMR spectra in appendices ([Figure S89](#)).

In the next paragraph, the carbonatation reaction will be studied and the optimal conditions will be applied to the carbonatation of the synthesized epoxidized polymers, as well as commercial polymers with high epoxide content.

## IV.2. Carbonatation of epoxidized polydienes

### IV.2.a. Study of the reaction on epoxidized polybutadiene

First of all, the carbonatation reaction was carried out on epoxidized polybutadiene **E-PBU-1** containing 10 mol% of epoxide (50:50 *cis:trans* ratio) using ammonium halides in an autoclave (*Scheme 4*).



*Scheme 4. Carbonatation reaction on epoxidized polybutadiene E-PBU-1.*

The conversion of epoxide and the yield of carbonate was calculated from the polymers  $^1\text{H}$  NMR analyses using the butadiene units as internal standard:

$$\text{Conversion} = 1 - \frac{S_{\text{epoxide}}}{S_{\text{epoxide,initial}}} \quad (2)$$

$$\text{Yield} = \frac{S_{\text{carbonate}}}{S_{\text{epoxide}} + S_{\text{carbonate}}} \quad (3)$$

The influence of the nature of the halide was first investigated using TBAC, TBAB and TBAI as catalysts, under 4.0 MPa of  $\text{CO}_2$ , in toluene at 110 °C for 6 hours (*Table 3*, entries 1-3). The following order of activity was observed: TBAI < TBAC < TBAB according to the yield of cyclic carbonate obtained: 9, 19 and 22 % respectively. The bromide is a good compromise between a good nucleophile and a good leaving group. Moreover, the nature of the halide has an influence on the *cis:trans* cyclic carbonate ratio. With TBAC, a 55:45 ratio was obtained. The *trans* cyclic carbonate formation was favoured under the reaction conditions, as the theoretical *cis:trans* ratio should be 74:26 and if we assume that no change of the configuration occurred (according to *cis* and *trans* epoxide conversion ratio of 74:26 calculated from *Table 3*, entry 1). With TBAB and TBAI, ratios of 32:68 and 18:81 were obtained, respectively. The use of a larger anion favoured the formation of *trans* cyclic carbonate. These observations are in accordance with the literature data,<sup>[21,83,84]</sup> and this change in the *cis:trans* ratio could be explained by the mechanism of the cyclic carbonate formation (*Scheme 5*). After the ring-opening of the epoxide and the formation of the carboxylate intermediate, two mechanisms are possible for the ring-closure of the carbonate: a monomolecular substitution ( $\text{S}_{\text{N}}1$ ), with the formation of a carbocation intermediate that

leads to a possible change of configuration, or a bimolecular substitution ( $S_N2$ ) that does not change the configuration. During the epoxide ring opening by the halide *via*  $S_N2$  mechanism, the configuration is changed by the Walden inversion. When the carboxylate attacks to form the cyclic carbonate *via*  $S_N2$  mechanism, a second Walden inversion occurs to go back to the initial configuration. With the  $S_N1$  mechanism, the formation of a carbocation can form both *cis* and *trans* cyclic carbonate. A mix of these two mechanisms could occur during the reaction, but the  $S_N1$  pathway could be even more favoured by using a large nucleophilic catalyst like I<sup>-</sup> or Br<sup>-</sup>. Concerning the reactivity of the epoxides, the *cis* epoxide appeared to be much more reactive than the *trans* epoxide in every case, which is again consistent with the literature.<sup>[8]</sup>

Since bromide was identified as the most active halide, different ammonium bromides were tested to understand the influence of alkyl chains on yield and selectivity (*Table 3*). It was observed that the presence of hexyl chains instead of butyl chains leads to an increase in yield to 36 %. The yield slightly increased with tetraoctylammonium bromide (TOAB) to 38 %. The increase in alkyl chain length allows for a better dissociation of the ammonium/bromide ion pair, which increases the nucleophilicity of the bromide, and it also increases the solubility of the ammonium salt in the reaction medium. Regarding the secondary reactions, the Meinwald rearrangement, where the epoxide is converted to a ketone, was observed, evidenced by the appearance of a small carbonyl band at 1719 cm<sup>-1</sup> in IR-ATR and a <sup>1</sup>H NMR signal in CDCl<sub>3</sub> at 2.39 ppm that is characteristic of an  $\alpha$ -proton of a ketone, and confirms what has been previously observed in the literature in the case of the carbonatation of epoxidized vegetable oils.<sup>[21,85]</sup> A decrease of the pressure from 4.0 to 2.0 led to a decrease of the yield from 38 to 30 %, whereas an increase of the pressure to 6.0 MPa slightly improved the cyclic carbonate yield to 43 %.

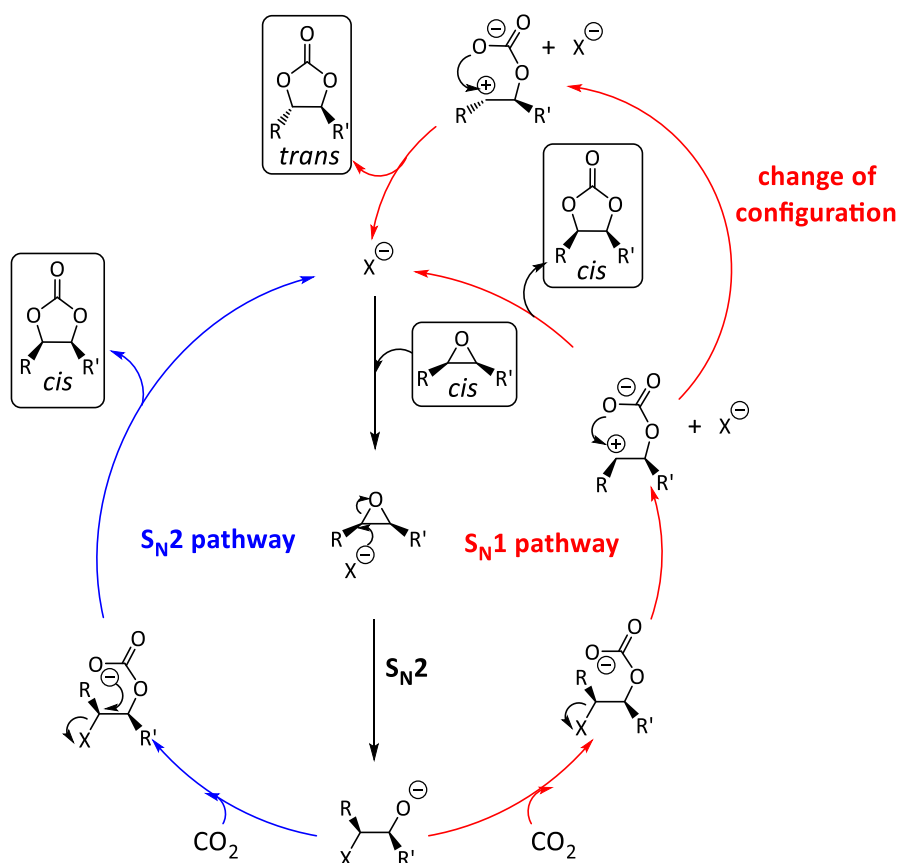
Finally, Bis(triphenylphosphoranylidene)ammonium chloride (PPNCl) has been reported as a good catalyst for the carbonatation of hindered epoxides<sup>[45,86]</sup> and epoxidized polybutadiene in methyl ethyl ketone (MEK) as solvent.<sup>[8]</sup> The effect of MEK and PPNCl was therefore studied. When MEK was used instead of toluene with TOAB as catalyst, a significant improvement of the yield was observed, with an increase of the yield from 38 % to 60 %. However, when PPNCl was used instead of TOAB in MEK, some insoluble materials were formed after reaction, and the yield reached only 47 % according to the <sup>1</sup>H NMR of the soluble part. A 47: 53 *cis:trans* ratio was obtained, which is similar to the ratio obtained with TBAC.



Table 3. Screening of the catalysts and reactions conditions for the carbonatation reaction.<sup>a</sup>

Entry	catalyst	solvent	Conversion (%)			Yield (%)	Selectivity (%)	<i>Cis:trans</i> ratio
			<i>cis</i>	<i>trans</i>	total			
1	TBAC	Toluene	28	10	19	19	99	55:45
2	TBAI	Toluene	16	1	9	9	99	18:81
3	TBAB	Toluene	36	7	22	22	99	32:68
4	THAB	Toluene	57	22	40	36	90	28:72
5	TOAB	Toluene	63	25	44	38	86	24:76
6 <sup>b</sup>	TOAB	Toluene	63	15	38	30	79	21:79
7 <sup>c</sup>	TOAB	Toluene	73	26	49	43	88	23:77
8	TOAB	MEK	88	40	64	60	94	24:76
9 <sup>d</sup>	PPNCl	MEK	69	42	56	47	84	47:53

<sup>a</sup>Reaction conditions: 1.0 g of **E-PBU-1** (78 mol% of 1,4 units, 12 mol% of 1,2 units, 10 mol% of epoxide, 50:50 *cis:trans* ratio,  $M_n = 16\ 000$  g/mol,  $M_w = 25\ 800$  g/mol), 1.0 mL of toluene, 5 mol% of catalyst, 4.0 MPa of CO<sub>2</sub>, 110 °C, 6 h, <sup>b</sup>2.0 MPa of CO<sub>2</sub>, <sup>c</sup>6.0 MPa of CO<sub>2</sub>. <sup>d</sup>Insoluble residue.



Scheme 5. Mechanism for the carbonatation of *cis* epoxide catalyzed by halides. By starting from *trans* epoxide,  $S_N2$  pathway gives *trans* carbonate.

Figure 6. shows the effect of the temperature on the conversion of *cis* and *trans* epoxides, the overall yield of cyclic carbonate and the *cis:trans* ratio of the cyclic carbonate product. An optimum was observed for the yield (38 %) at 110 °C. Concerning the conversions, it is highlighted that the *cis* epoxide is much more reactive than the *trans* epoxide. After 6 hours at 110 °C with TOAB, the *cis* epoxide was converted at 63 % whereas the *trans* epoxide was converted at 25 %. Interestingly, the increase in temperature favoured the formation of the *trans* cyclic carbonate (Figure 6b), suggesting that the  $S_N1$  mechanism, which leads to a change of configuration, is favoured at higher temperature.<sup>[21]</sup> The control of the carbonate configuration is essential for further functionalization requiring short reaction time. As reported in Chapter 4, the *trans* carbonate is less reactive than *cis* carbonate for the nucleophilic attack by amines to produce hydroxyurethane moieties, thus a too high proportion of *trans* carbonate could be a limitation.

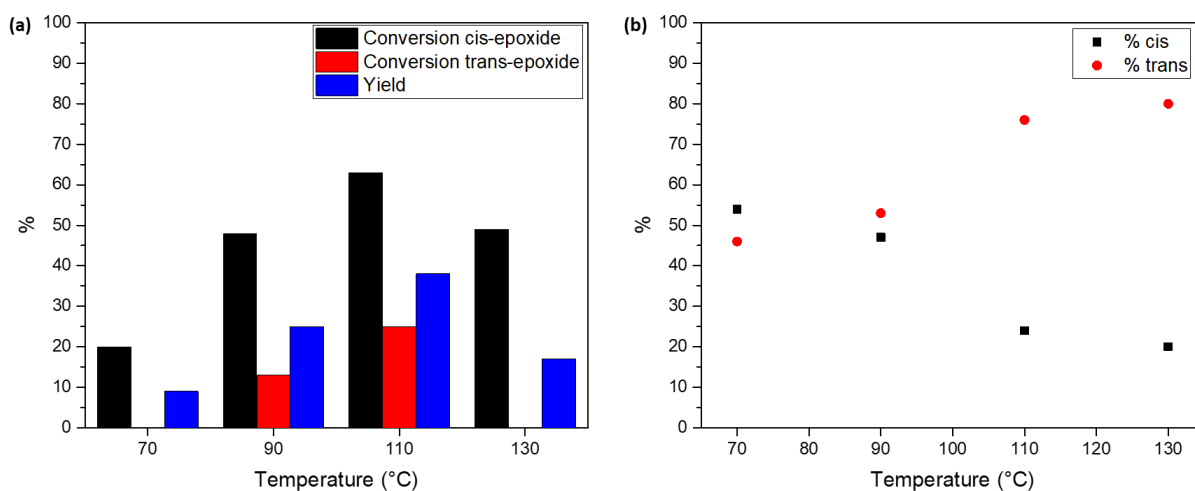


Figure 6. Effect of the temperature on (a) epoxide conversion and yield and (b) cis: trans cyclic carbonate ratio. Conditions, unless otherwise mentioned: 1 g of **E-PBU-1**, TOAB (5 mol%), 4.0 MPa of CO<sub>2</sub>, 110 °C, 1 mL of toluene, 6 h. The conversion, yield and cis:trans ratio were determined by <sup>1</sup>H NMR.

#### IV.2.b. Scope of the carbonatation reaction

The carbonatation reaction was performed on epoxidized polymers obtained from the study of the epoxidation step and on commercial polymers (**E-PBU-3** and **E-NR-1**) with high content of epoxide (Scheme 6). For each polymer, the catalyst, solvent and concentration were adapted as a function of the polymer microstructure, solubility and viscosity. Low molar masses polymers were used in a concentration of 1 g/mL (**E-PBU-1**, **E-PBU-3**, **E-PBU-4**, **E-NR-2**, **E-EPDM-DCPD**), whereas polymers with higher molar masses were used at 0.2 g/mL. For the carbonation of **E-PBU-2** (Table 4, entries 2 and 3), TOAB and PPnCl had a similar activity in MEK (yield of 45 % and 46 %, respectively) but a partially insoluble product was obtained with PPnCl, as observed before with the carbonatation of **E-PBU-1**, which might suggest some undesired crosslinking.<sup>[57,87]</sup> A cis:trans ratio of 93:7 was obtained with PPnCl, which confirmed that the chloride anion favoured S<sub>N</sub>2 mechanism.

For the carbonation of **E-PBU-3** (Table 4, entries 4-6), which contained mainly 1,4 *trans* epoxide, PPnCl was more active than TOAB in MEK with a conversion of epoxide up to 94 %. The yield of cyclic carbonate was not possible to determine by <sup>1</sup>H NMR because of the overlapping of the 1,4 and 1,2 cyclic carbonate signals. However, no significant ketone

absorption band was observable by ATR-IR analyses (*Figure S94* in appendices), which indicated that the Meinwald rearrangement might be insignificant. These results showed that TOAB catalyst is preferable for PBU containing mainly *cis* epoxide, while PPNCl is more efficient for *trans* epoxide.

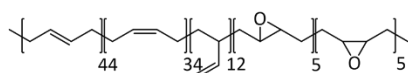
With **E-PBU-4**, that contains only 4 mol% of epoxides (mainly *trans* configuration), only traces of cyclic carbonates were observed by ATR-IR analysis (*Figure S95* in appendices) after reaction with PPNCl, which confirmed the low reactivity of *trans* epoxide.

With **E-SBS** (containing 1.8 mol% of *trans* and 1.4 mol% of *cis* epoxide), a good yield of 78 % was obtained with PPNCl in MEK, and the *cis* epoxide were more converted than the *trans* (conversion of 91% and 70 %; respectively).

For the carbonatation of **E-NR-1** (epoxidized NR containing 50 mol% of *cis* isoprene units and 50 mol% of epoxide), TOAB, TBAC and PPNCl were tested in toluene and MEK. In toluene, only traces of carbonate were obtained with the three catalysts according to ATR-IR analyses. The low activity of PPNCl may be due to its poor solubility in toluene. However in MEK, an increase in the yield was observed with the three catalysts. The order of activity was as follows: PPNCl >> TBAC > TOAB with yield of 23 %, 6 % and 3 % respectively. These results confirm the higher catalytic activity of PPNCl compared to other ammonium salts for the carbonatation of trisubstituted epoxides.<sup>[45,86]</sup> With **E-NR-2** and **E-SIS**, which contain 10 mol% and 5 mol% of epoxides respectively, only traces of carbonate were observed by ATR-IR after reaction with PPNCl (*Figure S98* in appendices), probably due to the lower concentration of epoxides.

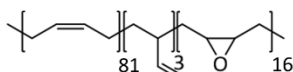
Finally, no reactivity was observed with **E-DCPD-EPDM** and **E-ENB-EPDM** with TBAC in toluene. The reaction was not performed with PPNCl and in MEK due to insolubility issues. As seen before, the TBAC/toluene system is less active than the PPNCl/MEK one, which could explain why no reactivity was observed.

**Polymers containing epoxy-butadiene units**



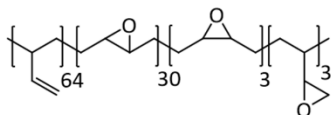
**E-PBU-1**

$^aM_n = 16\ 000\ \text{g/mol}$   
 $^aM_w = 25\ 800\ \text{g/mol}$   
 $T_g < -80\ ^\circ\text{C}$



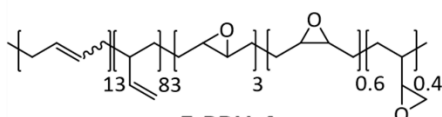
**E-PBU-2**

$^aM_n = 127\ 200\ \text{g/mol}$   
 $^aM_w = 507\ 600\ \text{g/mol}$   
 $T_g < -80\ ^\circ\text{C}$



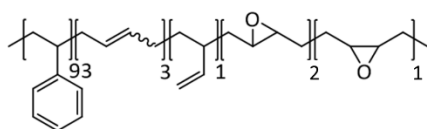
**E-PBU-3**

$^aM_n = 2\ 800\ \text{g/mol}$   
 $^aM_w = 4\ 400\ \text{g/mol}$   
 $T_g = -17\ ^\circ\text{C}$



**E-PBU-4**

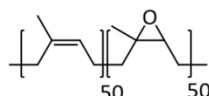
$^aM_n = 4\ 000\ \text{g/mol}$   
 $^aM_w = 5\ 500\ \text{g/mol}$   
 $T_g = -27\ ^\circ\text{C}$



**E-SBS**

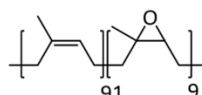
$^bM_n = 64\ 700\ \text{g/mol}$   
 $^bM_w = 112\ 500\ \text{g/mol}$   
 $T_g = -93\ ^\circ\text{C}$

**Polymers containing epoxy-isoprene units**



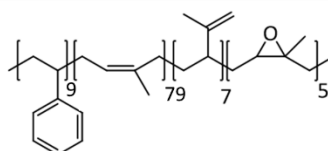
**E-NR-1**

$^aM_n = 141\ 000\ \text{g/mol}$   
 $^aM_w = 655\ 800\ \text{g/mol}$   
 $T_g = -20\ ^\circ\text{C}$



**E-NR-2**

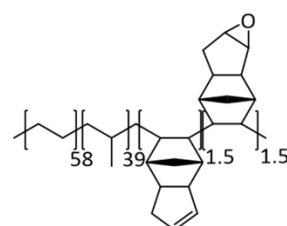
$^aM_n = 15\ 400\ \text{g/mol}$   
 $^aM_w = 55\ 800\ \text{g/mol}$   
 $T_g = -56\ ^\circ\text{C}$



**E-SIS**

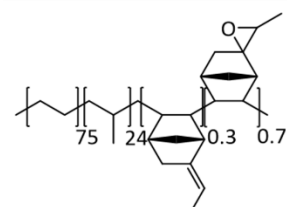
$^aM_n = 67\ 200\ \text{g/mol}$   
 $^aM_w = 164\ 500\ \text{g/mol}$   
 $T_g = -57\ ^\circ\text{C}$

**Epoxidized poly(ethylene-co-propylene-co-diene) (E-EPDM)**



**E-EPDM-DICPD**

$^bM_n = 23\ 200\ \text{g/mol}$   
 $^bM_w = 41\ 400\ \text{g/mol}$   
 $T_g = -45\ ^\circ\text{C}$



**E-EPDM-ENB**

$^bM_n = 122\ 400\ \text{g/mol}$   
 $^bM_w = 224\ 800\ \text{g/mol}$   
 $T_g = -45\ ^\circ\text{C}$

*Scheme 6. Structure of the epoxidized polydienes and their main properties. Composition calculation from  $^1\text{H}$  NMR analyses detailed in appendices.  $^a$ Determined by SEC in THF.  $^b$ Determined by SEC in 1,2,4-TCB.  $T_g$  determined by DSC.*

### Chapter 3: Two-steps functionalization of polydienes with peracids and carbon dioxide as reagent

Table 4. Carbonatation of epoxidized polydienes.

Entry	Polymer	Epoxide content (mol%)	<i>Cis:trans:</i> pendant epoxide ratio	Catalyst	Solvent	Epoxide conversion (%)				Yield (%)	<i>Cis:trans:</i> pendant carbonate ratio
						<i>Cis</i>	<i>Trans</i>	Pendant	Total		
1 <sup>a</sup>	<b>E-PBU-1</b>	10	50:50:0	TOAB	MEK	88	40	/	64	60	24:76:0
2 <sup>b</sup>	<b>E-PBU 2</b>	16	100:0:0	TOAB	MEK	50	/	/	50	45	27:73:0
3 <sup>b,c</sup>				PPNCl	MEK	52	/	/	52	46	93:7:0
4 <sup>a</sup>	<b>E-PBU 3</b>	36	8:84:8	TOAB	Toluene	58	67	53	66	/	/
5 <sup>a</sup>				TOAB	MEK	72	74	73	73	/	/
6 <sup>a</sup>				PPNCl	MEK	99	93	99	94	/	/
7 <sup>a</sup>	<b>E-PBU 4</b>	4	15:75:10	PPNCl	MEK	43	24	55	30	/	/
8 <sup>b</sup>	<b>E-SBS</b>	3	43:56	PPNCl	MEK	91	70	/	79	78	38:62:0
9 <sup>b</sup>	<b>E-NR-1</b>	50	100:0:0	TOAB	Toluene	/	/	/	/	Traces	/
10 <sup>b</sup>				TOAB	MEK	3	/	/	/	3	/
11 <sup>b</sup>				TBAC	Toluene	/	/	/	/	Traces	/
12 <sup>b</sup>				TBAC	MEK	6	/	/	6	6	/
13				PPNCl	Toluene	/	/	/	/	Traces	/
14				PPNCl	MEK	23	/	/	23	23	/
15 <sup>a</sup>	<b>E-NR-2</b>	9	100:0:0	PPNCl	MEK	/	/	/	Traces	/	
16 <sup>b</sup>	<b>E-SIS</b>	5	100:0:0	PPNCl	MEK	/	/	/	Traces	/	
17	<b>E-EPDM-DCPD</b>	1.5	/	TOAB	Toluene	/	/	/	/	0	/
18				TBAC	Toluene	/	/	/	/	0	/
19 <sup>b</sup>	<b>E-EPDM-ENB</b>	0.7	/	TBAC	Toluene	/	/	/	/	0	/

<sup>a</sup>Polymer concentration of 1 g/mL, <sup>b</sup>Polymer concentration of 0.2 g/mL, <sup>c</sup>Insoluble materials obtained.

#### IV.2.c. Evolution of the molar masses and thermal properties

The molar masses of the epoxidized and carbonated polymers obtained under the optimal conditions (see *Scheme 7* for the carbonated polymers composition and their main properties) was determined by SEC in THF (calibrated with polystyrene standards) and SEC in 1,2,4-trichlorobenzene (1,2,4-TCB) (calibrated with polyethylene standards) in order to investigate the evolution of the molar mass distributions after each step (epoxidation and carbonatation).

After epoxidation, the molar mass distribution of the polymers containing butadiene units (*Figure 7 (a), (b), (c), (d)*) and the EPDM terpolymers (*Figure 8 (b), (c)*) exhibits low modification. The  $M_n$  and dispersity of **PBU-1**, **PBU-3**, **PBU-4** and **SBS** were not modified (*Table 5*, entries 1, 2, 7, 8, 11-14), and the  $M_n$  of **PBU-2** only slightly decreased (from 135 600 to 127 200 g/mol) (*Table 5*, entries 4, 5). For **EPDM-DCPD** and **EPDM-ENB**, their  $M_n$  decreased of 8 and 12 % respectively (*Table 5*, entries 22-25). However, for the polymers containing isoprene units, more significant change of the molar mass distribution was observed (*Figure 7 (f), (h)*). Especially for **SIS**, a high decrease of the  $M_n$  was observed (from 172 500 to 67 200 g/mol) (*Table 5*, entries 20-21). A part of the epoxidized isoprene units could degraded during epoxidation *via* chains cleavage and aldehyde formation as chain-end groups,<sup>[88]</sup> which is also in accordance with the ATR-IR spectra of **E-SIS** showing a small bands at 1718  $\text{cm}^{-1}$  (C=O stretching) (see *Figure S67* in appendices). The change of the polymer polarity may also modify the hydrodynamic volume of the macromolecules in THF, and the interactions between the macromolecules and the stationary phase during SEC measurement, and thus modify the retention time. This possibility has to be kept in mind for the SEC analyses interpretation.

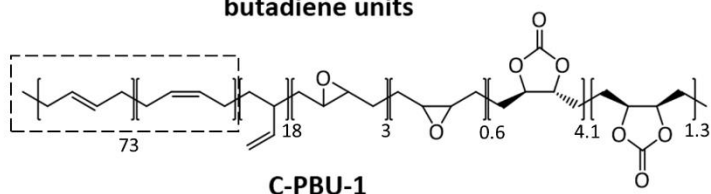
After carbonatation of epoxidized polybutadienes **E-PBU-1** and **E-PBU-2**, carbonated polybutadienes **C-PBU-1** and **C-PBU-2** were obtained but could not be analyzed by SEC due to insolubility issues in THF and 1,2,4-TCB. Their solubility evolved after their synthesis, as they were viscous liquid fully soluble in toluene at room temperature directly after their synthesis, they became insoluble and swelled in toluene at room temperature few months later. This may indicate that cross-linking occurred during the storage by the formation of ether and/or linear carbonates linkages catalyzed by the residual catalyst.

Carbonated **C-PBU-3**, **C-SBS** and **C-NR-1** were fully soluble in their corresponding SEC solvents. According to the molar masses distributions of **E-NR-1** and **C-NR-1** (*Figure 7 (g)*), a multimodal distribution was obtained after carbonation. Three populations could be distinguished for **C-NR-1**: two at lower molar masses compared to **E-NR-1**, and one at higher molar masses. The  $M_n$  decreased from 141 000 to 23 500 g/mol (*Table 5*, entries 18-19). Two phenomena explain this change of the molar masses distribution. A part of the epoxidized isoprene units could be degraded *via* chains cleavage and aldehyde formation as chain-end groups,<sup>[88]</sup> and some cross-linking may also have occurred, as explained before. After the carbonation of **E-PBU-3** (containing mainly *trans* epoxide), there was no significant change in the molar mass distribution (*Figure 7 (e)* and *Table 5*, entries 9-10), and **C-PBU-3** was fully soluble in THF, thus no cross-linking was observed. Polymers containing mainly *trans* epoxide may be less subject to cross-linking due to the lower reactivity of the *trans* epoxide, compared to the *cis* epoxide.

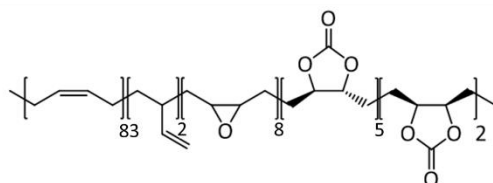
Finally, for the carbonation of **E-SBS**, no significant change in the molar mass distribution was observed (*Figure 8 (a)* and *Table 5*, entries 14-15).



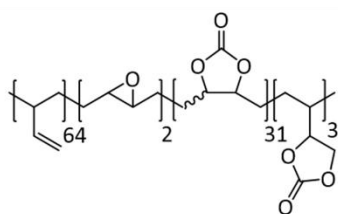
**Polymers containing  
cyclic carbonate-  
butadiene units**



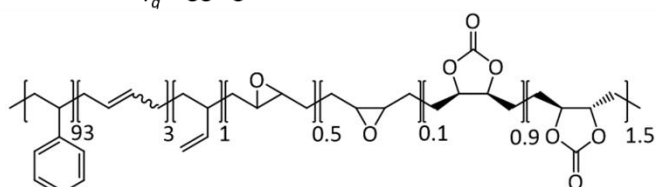
Insoluble in THF and 1,2,4-TCB  
 $T_g < -80\text{ }^\circ\text{C}$



Insoluble in THF and 1,2,4-TCB  
 $T_g < -80\text{ }^\circ\text{C}$

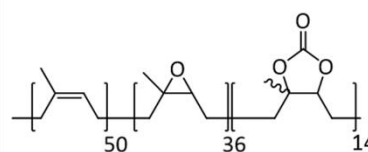


$^aM_n = 3\ 100\text{ g/mol}$   
 $^aM_w = 4\ 800\text{ g/mol}$   
 $T_g = 33\text{ }^\circ\text{C}$



$^aM_n = 59\ 500\text{ g/mol}$   
 $^aM_w = 104\ 600\text{ g/mol}$   
 $T_g = 92\text{ }^\circ\text{C}$

**Polymers containing  
cyclic carbonate-  
isoprene units**



$^aM_n = 23\ 500\text{ g/mol}$   
 $^aM_w = 410\ 900\text{ g/mol}$   
 $T_g = -3\text{ }^\circ\text{C}$

*Scheme 7. Carbonated polymers synthesized and their main properties. Composition calculation from  $^1\text{H}$  NMR analyses detailed in appendices. <sup>a</sup>Determined by SEC in THF. <sup>b</sup>Determined by SEC in 1,2,4-TCB.  $T_g$  determined by DSC.*

### Chapter 3: Two-steps functionalization of polydienes with peracids and carbon dioxide as reagent

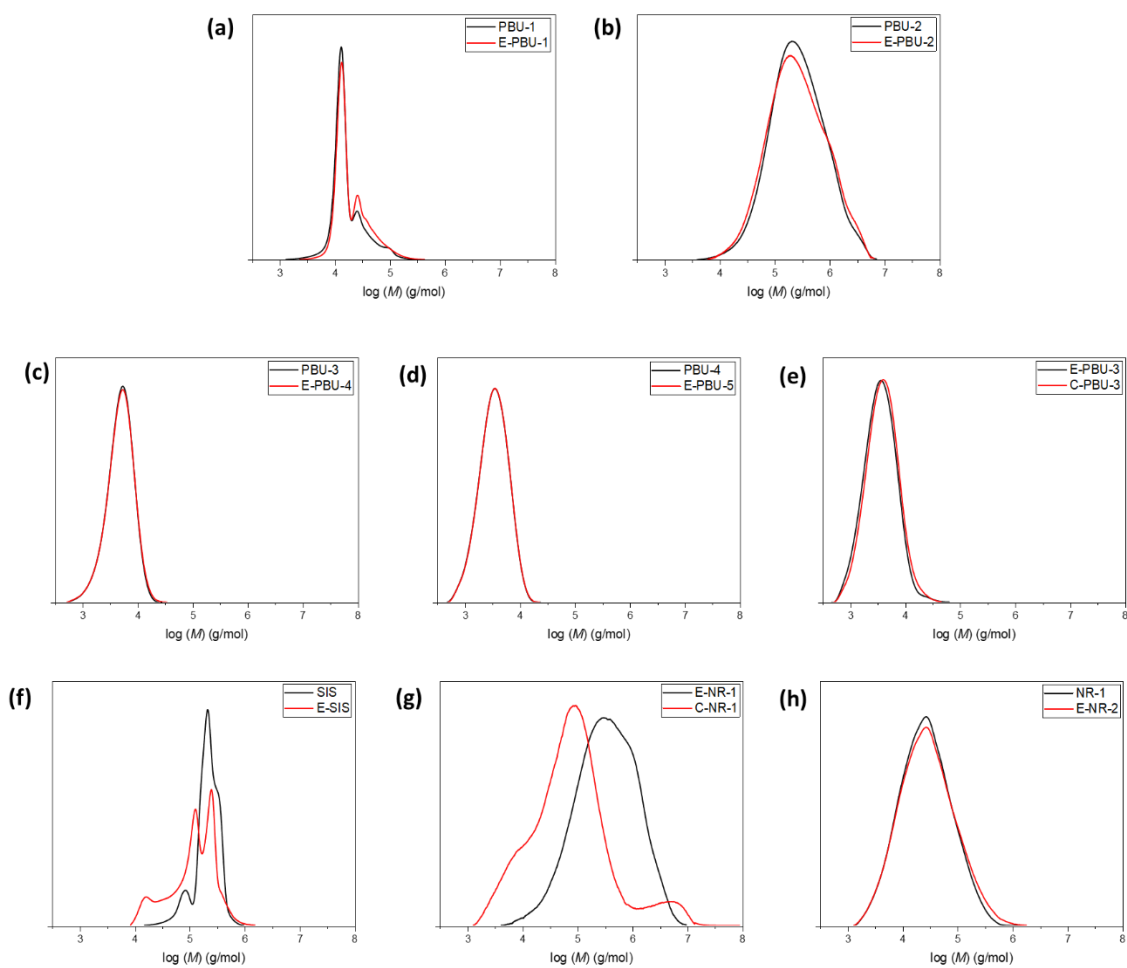


Figure 7. Molar mass distributions of polydienes measured by SEC in THF.

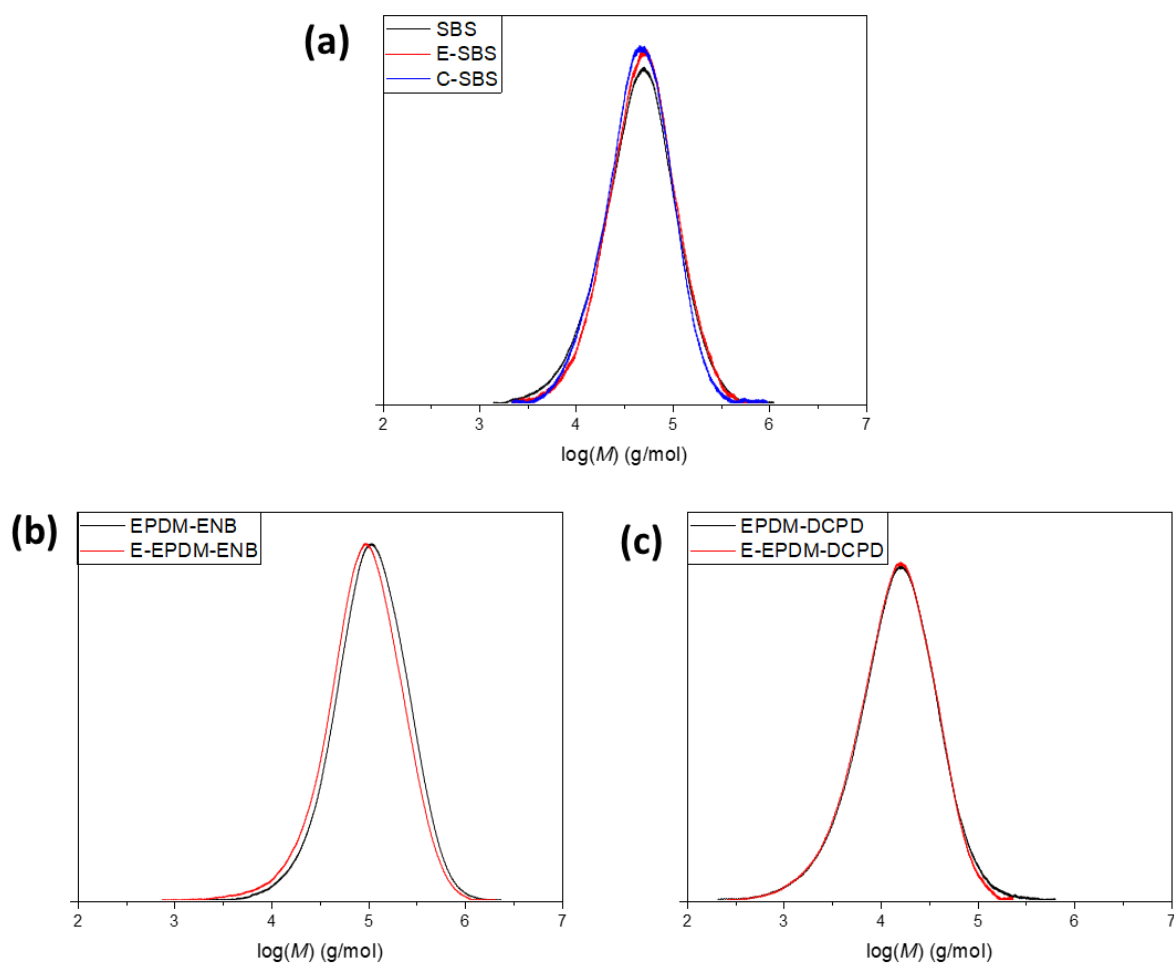


Figure 8. Molar masses distributions of SBS, EPDM-ENB and EPDM-DCPD and the epoxidized and carbonated derivatives measured by SEC in 1,2,4-TCB.

**Chapter 3: Two-steps functionalization of polydienes with peracids and carbon dioxide as reagent**

*Table 5. Main properties of the polydienes.*

Entry	Polymer	Epoxide content (mol%)	Cyclic carbonate content (mol%)	$M_n$ ( $\bar{M}$ ) (g/mol)	$T_g^a$ (°C)	$T_m^a$ (°C)
1	PBU-1	0	0	13 800 (1.6) <sup>b</sup>	< -80	/
2	E-PBU-1	10	0	16 000 (1.6) <sup>b</sup>	< -80	/
3	C-PBU-1	4	6	insoluble	< -80	/
4	PBU-2	0	0	135 600 (3.6) <sup>b</sup>	< -80	-3
5	E-PBU-2	16	0	127 200 (4.0) <sup>b</sup>	< -80	/
6	C-PBU-2	9	7	insoluble	< -80	/
7	PBU-3	0	0	4 000 (1.4) <sup>b</sup>	-29	/
8	E-PBU-4	4	0	4 000 (1.4) <sup>b</sup>	-27	/
9	E-PBU-3	36	0	2 800 (1.6) <sup>b</sup>	-17	/
10	C-PBU-3	3	33	3 100 (1.5) <sup>b</sup>	33	/
11	PBU-4	0	0	2 700 (1.4) <sup>b</sup>	-44	/
12	E-PBU-5	1.3	0	2 700 (1.4) <sup>b</sup>	-44	/
13	SBS	0	0	63 000 (1.8) <sup>c</sup>	98	/
14	E-SBS	3	0	64 700 (1.7) <sup>c</sup>	93	/
15	C-SBS	1	2	59 500 (1.8) <sup>c</sup>	92	/
16	NR-1	0	0	15 100 (3.0) <sup>b</sup>	-63	/
17	E-NR-2	9	0	15 400 (3.6) <sup>b</sup>	-56	/
18	E-NR-1	50	0	141 000 (4.7) <sup>b</sup>	-20	/
19	C-NR-1	36	14	23 500 (17.5) <sup>b</sup>	-3	/
20	SIS	0	0	172 500 (1.3) <sup>b</sup>	-59	/
21	E-SIS	5	0	67 200 (2.4) <sup>b</sup>	-57	/
22	EPDM-DCPD	0	0	25 100 (2.2) <sup>c</sup>	-44	/
23	E-EPDM-DCPD	1.5	0	23 200 (1.8) <sup>c</sup>	-45	/
24	EPDM- ENB	0	0	139 100 (1.8) <sup>c</sup>	-40	37
25	E-EPDM-ENB	0.7	0	122 400 (1.8) <sup>c</sup>	-45	36

<sup>a</sup>Measured by DSC. <sup>b</sup>Determined by SEC in THF. <sup>c</sup>Determined by SEC in 1,2,4-TCB.

The thermal properties of the native, epoxidized and carbonated polydienes were measured by DSC to observe the influence of the epoxide and cyclic carbonate functions on  $T_g$  and, for semi-crystalline polymers, on  $T_m$ . In the case of **PBU-1** and **PBU-2**, the  $T_g$  was lower than -80 °C and could not be measured by DSC, as well as the polymers obtained after epoxidation and carbonatation (*Table 5*, entries 1-6).

In general, after epoxidation within a range of 1-16 mol% of epoxide content, no significant change in the  $T_g$  was observed (*Table 5*, entries 7, 8, 11-14, 16, 17, 20- 25). In the case of epoxidation of semi-crystalline polymers, the epoxides could influence the crystallinity of the polymer depending on their concentration. For **PBU-2**, which has a  $T_m$  of -3 °C, no crystallinity was observed after epoxidation with an epoxide content of 17 % (*Table 5*, entries 5 and 6). For **ENB-EPDM**, the formation of 1.5 % of epoxide did not change the  $T_m$  of the polymer (*Table 5*, entries 24 and 25).

The cyclic carbonate content exhibits a strong impact on the  $T_g$ . When **E-NR-1** was carbonated with a final carbonate content of 14 %, the  $T_g$  increased from -20 to -3 °C (*Table 5*, entries 18, 19). After carbonatation of **E-PBU-3** with a carbonate content of 34 %, the increase of the  $T_g$  was even higher and changed from -17 to 33 °C (*Table 5*, entries 9 and 10).

## V. Conclusions

The functionalization of various polybutadienes was achieved *via* epoxidation and subsequent carbonatation reactions. The optimal epoxidation conditions were H<sub>2</sub>O<sub>2</sub>/HCOOH, 50 °C in toluene. Under these conditions, various polybutadienes, polyisoprenes and copolymers containing dienes monomers were successfully partially epoxidized, within a range of epoxide content of 4-17 mol%.

For the polybutadienes, the reactivity of the monomers units followed this trend: **1,4-*cis* unit > 1,4-*trans* unit >> 1,2 unit**. For the polyisoprenes, a similar trend was observed: **1,4 unit >> 3,4 unit**. Two different EPDM were also epoxidized and the reactivity of the ENB diene-derived unit was higher than the DCPD diene-derived unit. Moreover, the epoxidation of a PBU containing 81 mol% of 1,2 units with a low molar mass was performed in a tailored reactive extrusion process under solvent-free conditions. Under the optimal conditions (10 mol% of H<sub>2</sub>O<sub>2</sub>/HCOOH, 60 °C), an epoxide content of 1,3 mol% mostly composed of *trans* epoxide was obtained.

Furthermore, the carbonatation reaction was optimized. TOAB and PPnCl showed the best activity, depending on the polymer microstructure. TOAB was more convenient for polybutadienes containing predominantly *cis* epoxide, whereas PPnCl was more active for polybutadienes containing predominantly *trans* epoxide and epoxidized polyisoprenes. TBAC, which is more active than TOAB for the carbonatation of trisubstituted epoxide, was tested as catalyst for the carbonatation of epoxidized EPDM, but no reactivity was observed. Further conditions optimization have to be investigated, as for example the used of Brønsted acids as co-catalysts (polyphenols or fluorinated compounds).

After the epoxidation step, the molar masses distribution of the polymers did not significantly changed, excepted for **SIS**, where a decrease of the molar masses was observed by SEC, which could be due to oxidative cleavage of the isoprene units during epoxidation. After carbonatation, the solubility of **C-PBU-1** and **C-PBU-2** evolved and became insoluble. The carbonatation of **E-NR-1** led to a polymer with a significant lower  $M_n$  (related to the lower stability of isoprene), but a small proportion of macromolecules also exhibited higher molar masses. During carbonatation, formation of cross-linking *via* the formation of ether or linear carbonate linkages could decrease the polymers solubility and partially increased the macromolecules molar masses, in the case of polymers containing mainly *cis* epoxide.

Conversely, for polymers containing low content of *cis* epoxide (**E-PBU-3**, **E-SBS**), no cross-linking were observed and the molar masses were unchanged after carbonatation.

For the thermal properties, after epoxidation reaction, no significant change in the  $T_g$  was observed, but in the case of the epoxidation of the semi crystalline **PBU-2**, an amorphous polymer was obtained. After carbonatation reaction, a high increase of the  $T_g$  was observed with high carbonate content. The polymers obtained could be used as intermediates for the synthesis of crosslinked materials featuring a dynamic network using diamines, or as compatibilizers for reactive blends of polyolefins with polar polymers such as polyamides or polycarbonates.

## VI. References

- [1] Jehanno, C.; Alty, J.W.; Roosen, M.; De Meester, S.; Dove, A.P.; Chen, E.Y.-X.; Leibfarth, F.A.; Sardon, H. Critical advances and future opportunities in upcycling commodity polymers. *Nature* **2022**, *603*(7903), 803–814.
- [2] Sakakura, T.; Choi, J.-C.; Yasuda, H. Transformation of Carbon Dioxide. *Chem. Rev.* **2007**, *107*(6), 2365–2387.
- [3] Lim, X. How to make the most of carbon dioxide. *Nature* **2015**, *526*, 628–630.
- [4] Zhang, K.; Nelson, A.M.; Talley, S.J.; Chen, M.; Margareta, E.; Hudson, A.G.; Moore, R.B.; Long, T.E. Non-isocyanate poly(amide-hydroxyurethane)s from sustainable resources. *Green Chem.* **2016**, *18*(17), 4667–4681.
- [5] Carré, C.; Ecochard, Y.; Caillol, S.; Avérous, L. From the Synthesis of Biobased Cyclic Carbonate to Polyhydroxyurethanes: A Promising Route towards Renewable Non-Isocyanate Polyurethanes. *ChemSusChem* **2019**, *12*(15), 3410–3430.
- [6] Hu, S.; Chen, X.; Torkelson, J.M. Biobased Reprocessable Polyhydroxyurethane Networks: Full Recovery of Crosslink Density with Three Concurrent Dynamic Chemistries. *ACS Sustainable Chem. Eng.* **2019**, *7*(11), 10025–10034.
- [7] Gomez-Lopez, A.; Panchireddy, S.; Grignard, B.; Calvo, I.; Jerome, C.; Detrembleur, C.; Sardon, H. Poly(hydroxyurethane) Adhesives and Coatings: State-of-the-Art and Future Directions. *ACS Sustainable Chem. Eng.* **2021**, *9*(29), 9541–9562.
- [8] Dechent, S.-E.; Kleij, A.W.; Luinstra, G.A. Fully bio-derived CO<sub>2</sub> polymers for non-isocyanate based polyurethane synthesis. *Green Chem.* **2020**, *22*(3), 969–978.
- [9] Liu, X.; Yang, X.; Wang, S.; Wang, S.; Wang, Z.; Liu, S.; Xu, X.; Liu, H.; Song, Z. Fully Bio-Based Polyhydroxyurethanes with a Dynamic Network from a Terpene Derivative and Cyclic Carbonate Functional Soybean Oil. *ACS Sustainable Chem. Eng.* **2021**, *9*(11), 4175–4184.
- [10] Webster, D.C. Cyclic carbonate functional polymers and their applications. *Progress in Organic Coatings* **2003**, *47*(1), 77–86.
- [11] Michan, A.L.; Parimalam, Bharathy.S.; Leskes, M.; Kerber, R.N.; Yoon, T.; Grey, C.P.; Lucht, B.L. Fluoroethylene Carbonate and Vinylene Carbonate Reduction: Understanding Lithium-Ion Battery Electrolyte Additives and Solid Electrolyte Interphase Formation. *Chem. Mater.* **2016**, *28*(22), 8149–8159.
- [12] You, D.; Hu, W.; Song, L.; Wei, W.; Xiong, H. High-Energy Metallic Lithium Batteries Enabled by Polymer-in-Salt Electrolytes of Cyclic Carbonate Substituted Polyethers. *ACS Applied Polymer Materials* **2022**.
- [13] Kim, H. Imidazolium zinc tetrahalide-catalyzed coupling reaction of CO<sub>2</sub> and ethylene oxide or propylene oxide. *Journal of Catalysis* **2003**, *220*(1), 44–46.



- [14] Peng, J.; Deng, Y. Cycloaddition of carbon dioxide to propylene oxide catalyzed by ionic liquids. *New J. Chem.* **2001**, *25*(4), 639–641.
- [15] Du, Y.; Cai, F.; Kong, D.-L.; He, L.-N. Organic solvent-free process for the synthesis of propylene carbonate from supercritical carbon dioxide and propylene oxide catalyzed by insoluble ion exchange resins. *Green Chem.* **2005**, *7*(7), 518.
- [16] Sun, J.; Fujita, S.; Zhao, F.; Arai, M. Synthesis of styrene carbonate from styrene oxide and carbon dioxide in the presence of zinc bromide and ionic liquid under mild conditions. *Green Chem.* **2004**, *6*(12), 613.
- [17] Sun, J.; Fujita, S.-I.; Zhao, F.; Arai, M. A highly efficient catalyst system of ZnBr<sub>2</sub>/n-Bu<sub>4</sub>N<sup>+</sup>I<sup>-</sup> for the synthesis of styrene carbonate from styrene oxide and supercritical carbon dioxide. *Applied Catalysis A: General* **2005**, *287*(2), 221–226.
- [18] Shim, J.-J.; Kim, D.; Ra, C.S. Carboxylation of Styrene Oxide Catalyzed by Quaternary Onium Salts under Solvent-free Conditions. *Bull. Korean Chem. Soc.* **2006**, *27*(5), 744–746.
- [19] Morikawa, H.; Minamoto, M.; Gorou, Y.; Yamaguchi, J.; Morinaga, H.; Motokucho, S. Two Diastereomers of *d*-Limonene-Derived Cyclic Carbonates from *d*-Limonene Oxide and Carbon Dioxide with a Tetrabutylammonium Chloride Catalyst. *BCSJ* **2018**, *91*(1), 92–94.
- [20] Rehman, A.; López Fernández, A.M.; Gunam Resul, M.F.M.; Harvey, A. Highly selective, sustainable synthesis of limonene cyclic carbonate from bio-based limonene oxide and CO<sub>2</sub>: A kinetic study. *Journal of CO<sub>2</sub> Utilization* **2019**, *29*, 126–133.
- [21] Akhdar, A.; Onida, K.; Vu, N.D.; Grollier, K.; Norsic, S.; Boisson, C.; D'Agosto, F.; Duguet, N. Thermomorphic Polyethylene-Supported Organocatalysts for the Valorization of Vegetable Oils and CO<sub>2</sub>. *Adv. Sustainable Syst.* **2021**, *5*(2), 2000218.
- [22] Catalá, J.; Caballero, M.P.; Cruz-Martínez, F. de la; Tejeda, J.; Castro-Osma, J.A.; Lara-Sánchez, A.; García-Vargas, J.M.; García, M.T.; Ramos, M.J.; Gracia, I.; Rodríguez, J.F. Carbonation of epoxidized soybean oil in supercritical CO<sub>2</sub> assisted by imidazole-based organocatalysts. *Journal of CO<sub>2</sub> Utilization* **2022**, *61*, 102060.
- [23] Doll, K.M.; Erhan, S.Z. The improved synthesis of carbonated soybean oil using supercritical carbon dioxide at a reduced reaction time. *Green Chem.* **2005**, *7*(12), 849–854.
- [24] Guzmán, A.F.; Echeverri, D.A.; Rios, L.A. Carbonation of epoxidized castor oil: a new bio-based building block for the chemical industry. *Journal of Chemical Technology & Biotechnology* **2017**, *92*(5), 1104–1110.
- [25] Helbling, P.; Hermant, F.; Petit, M.; Tassaing, T.; Vidil, T.; Cramail, H. Unveiling the reactivity of epoxides in carbonated epoxidized soybean oil and application in the stepwise synthesis of hybrid poly(hydroxyurethane) thermosets. *Polym. Chem.* **2023**, *14*(4), 500–513.
- [26] Li, Z.; Zhao, Y.; Yan, S.; Wang, X.; Kang, M.; Wang, J.; Xiang, H. Catalytic Synthesis of Carbonated Soybean Oil. *Catal Lett* **2008**, *123*(3), 246–251.
- [27] Mann, N.; Mendon, S.K.; Rawlins, J.W.; Thames, S.F. Synthesis of Carbonated Vernonia Oil. *J Am Oil Chem Soc* **2008**, *85*(8), 791–796.

- [28] Caló, V.; Nacci, A.; Monopoli, A.; Fanizzi, A. Cyclic Carbonate Formation from Carbon Dioxide and Oxiranes in Tetrabutylammonium Halides as Solvents and Catalysts. *Org. Lett.* **2002**, *4*(15), 2561–2563.
- [29] Aoyagi, N.; Furusho, Y.; Endo, T. Convenient synthesis of cyclic carbonates from CO<sub>2</sub> and epoxides by simple secondary and primary ammonium iodides as metal-free catalysts under mild conditions and its application to synthesis of polymer bearing cyclic carbonate moiety. *Journal of Polymer Science Part A: Polymer Chemistry* **2013**, *51*(5), 1230–1242.
- [30] Ju, H.-Y.; Manju, M.-D.; Kim, K.-H.; Park, S.-W.; Park, D.-W. Catalytic performance of quaternary ammonium salts in the reaction of butyl glycidyl ether and carbon dioxide. *Journal of Industrial and Engineering Chemistry* **2008**, *14*(2), 157–160.
- [31] Sun, J.; Wang, L.; Zhang, S.; Li, Z.; Zhang, X.; Dai, W.; Mori, R. ZnCl<sub>2</sub>/phosphonium halide: An efficient Lewis acid/base catalyst for the synthesis of cyclic carbonate. *Journal of Molecular Catalysis A: Chemical* **2006**, *256*(1–2), 295–300.
- [32] Tian, J.-S.; Cai, F.; Wang, J.-Q.; Du, Y.; He, L.-N. Environmentally Benign Chemical Conversion of CO<sub>2</sub> into Organic Carbonates Catalyzed by Phosphonium Salts. *Phosphorus, Sulfur, and Silicon and the Related Elements* **2008**, *183*(2–3), 494–498.
- [33] Aoyagi, N.; Furusho, Y.; Endo, T. Effective synthesis of cyclic carbonates from carbon dioxide and epoxides by phosphonium iodides as catalysts in alcoholic solvents. *Tetrahedron Letters* **2013**, *54*(51), 7031–7034.
- [34] Wei-Li, D.; Bi, J.; Sheng-Lian, L.; Xu-Biao, L.; Xin-Man, T.; Chak-Tong, A. Functionalized phosphonium-based ionic liquids as efficient catalysts for the synthesis of cyclic carbonate from epoxides and carbon dioxide. *Applied Catalysis A: General* **2014**, *470*, 183–188.
- [35] Toda, Y.; Komiyama, Y.; Kikuchi, A.; Suga, H. Tetraarylphosphonium Salt-Catalyzed Carbon Dioxide Fixation at Atmospheric Pressure for the Synthesis of Cyclic Carbonates. *ACS Catal.* **2016**, *6*(10), 6906–6910.
- [36] Steinbauer, J.; Longwitz, L.; Frank, M.; Epping, J.; Kragl, U.; Werner, T. Immobilized bifunctional phosphonium salts as recyclable organocatalysts in the cycloaddition of CO<sub>2</sub> and epoxides. *Green Chem.* **2017**, *19*(18), 4435–4445.
- [37] Anthofer, M.H.; Wilhelm, M.E.; Cokoja, M.; Markovits, I.I.E.; Pöthig, A.; Mink, J.; Herrmann, W.A.; Kühn, F.E. Cycloaddition of CO<sub>2</sub> and epoxides catalyzed by imidazolium bromides under mild conditions: influence of the cation on catalyst activity. *Catal. Sci. Technol.* **2014**, *4*(6), 1749.
- [38] Denizalti, S. Imidazolium based ionic liquids bearing a hydroxyl group as highly efficient catalysts for the addition of CO<sub>2</sub> to epoxides. *RSC Adv.* **2015**, *5*(56), 45454–45458.
- [39] Liu, J.; Yang, G.; Liu, Y.; Wu, D.; Hu, X.; Zhang, Z. Metal-free imidazolium hydrogen carbonate ionic liquids as bifunctional catalysts for the one-pot synthesis of cyclic carbonates from olefins and CO<sub>2</sub>. *Green Chem.* **2019**, *21*(14), 3834–3838.

- [40] Wang, L.; Kodama, K.; Hirose, T. DBU/benzyl bromide: an efficient catalytic system for the chemical fixation of CO<sub>2</sub> into cyclic carbonates under metal- and solvent-free conditions. *Catal. Sci. Technol.* **2016**, *6*(11), 3872–3877.
- [41] Meléndez, J.; North, M.; Pasquale, R. Synthesis of Cyclic Carbonates from Atmospheric Pressure Carbon Dioxide Using Exceptionally Active Aluminium(salen) Complexes as Catalysts. *Eur. J. Inorg. Chem.* **2007**, *2007*(21), 3323–3326.
- [42] Clegg, W.; Harrington, R.W.; North, M.; Pasquale, R. Cyclic Carbonate Synthesis Catalysed by Bimetallic Aluminium-Salen Complexes. *Chem. Eur. J.* **2010**, *16*(23), 6828–6843.
- [43] Li, C.-Y.; Su, Y.-C.; Lin, C.-H.; Huang, H.-Y.; Tsai, C.-Y.; Lee, T.-Y.; Ko, B.-T. Synthesis and characterization of trimetallic cobalt, zinc and nickel complexes containing amine-bis(benzotriazole phenolate) ligands: efficient catalysts for coupling of carbon dioxide with epoxides. *Dalton Trans.* **2017**, *46*(44), 15399–15406.
- [44] Meléndez, D.O.; Lara-Sánchez, A.; Martínez, J.; Wu, X.; Otero, A.; Castro-Osma, J.A.; North, M.; Rojas, R.S. Amidinate Aluminium Complexes as Catalysts for Carbon Dioxide Fixation into Cyclic Carbonates. *ChemCatChem* **2018**, *10*(10), 2271–2277.
- [45] Navarro, M.; F. Sánchez-Barba, L.; Garcés, A.; Fernández-Baeza, J.; Fernández, I.; Lara-Sánchez, A.; M. Rodríguez, A. Bimetallic scorpionate-based helical organoaluminum complexes for efficient carbon dioxide fixation into a variety of cyclic carbonates. *Catalysis Science & Technology* **2020**, *10*(10), 3265–3278.
- [46] Butera, V.; Detz, H. Cyclic Carbonate Formation from Epoxides and CO<sub>2</sub> Catalyzed by Sustainable Alkali Halide–Glycol Complexes: A DFT Study to Elucidate Reaction Mechanism and Catalytic Activity. *ACS Omega* **2020**, *5*(29), 18064–18072.
- [47] Aomchad, V.; Del Gobbo, S.; Yingcharoen, P.; Poater, A.; D’Elia, V. Exploring the potential of group III salen complexes for the conversion of CO<sub>2</sub> under ambient conditions. *Catalysis Today* **2021**, *375*, 324–334.
- [48] Laiwattanapaisarn, N.; Virachotikul, A.; Phomphrai, K. Cycloaddition of carbon dioxide to epoxides by highly active constrained aluminum chloride complexes. *Dalton Trans.* **2021**, *50*(32), 11039–11048.
- [49] Büttner, H.; Steinbauer, J.; Werner, T. Synthesis of Cyclic Carbonates from Epoxides and Carbon Dioxide by Using Bifunctional One-Component Phosphorus-Based Organocatalysts. *ChemSusChem* **2015**, *8*(16), 2655–2669.
- [50] Büttner, H.; Lau, K.; Spannenberg, A.; Werner, T. Bifunctional One-Component Catalysts for the Addition of Carbon Dioxide to Epoxides. *ChemCatChem* **2015**, *7*(3), 459–467.
- [51] Chang, T.; Jin, L.; Jing, H. Bifunctional Chiral Catalyst for the Synthesis of Chiral Cyclic Carbonates from Carbon Dioxide and Epoxides. *ChemCatChem* **2009**, *1*(3), 379–383.
- [52] Ema, T.; Miyazaki, Y.; Koyama, S.; Yano, Y.; Sakai, T. A bifunctional catalyst for carbon dioxide fixation: cooperative double activation of epoxides for the synthesis of cyclic carbonates. *Chem. Commun.* **2012**, *48*(37), 4489.
- [53] Werner, T.; Büttner, H. Phosphorus-based Bifunctional Organocatalysts for the Addition of Carbon Dioxide and Epoxides. *ChemSusChem* **2014**, *7*(12), 3268–3271.

### Chapter 3: Two-steps functionalization of polydienes with peracids and carbon dioxide as reagent

---

- [54] Kihara, N.; Endo, T. Incorporation of carbon dioxide into poly(glycidyl methacrylate). *Macromolecules* **1992**, *25*(18), 4824–4825.
- [55] Park, S.Y.; Park, H.Y.; Park, D.W.; Ha, C.S. DIRECT INCORPORATION OF CARBON DIOXIDE INTO POLY(GLYCIDYL METHACRYLATE-CO-ACRYLONITRILE) USING QUATERNARY AMMONIUM SALT CATALYST AND ITS APPLICATION TO POLYMER BLENDS. *Journal of Macromolecular Science, Part A* **2002**, *39*(6), 573–589.
- [56] Yamamoto, S.-I.; Kawabata, K.; Moriya, O.; Endo, T. Effective fixation of carbon dioxide into poly(glycidyl methacrylate) in the presence of pyrrolidone polymers. *Journal of Polymer Science Part A: Polymer Chemistry* **2005**, *43*(19), 4578–4585.
- [57] Guerdener, B.; Ayzac, V.; Norsic, S.; Besognet, P.; Bounor-Legaré, V.; Monteil, V.; Dufaud, V.; Raynaud, J.; Chalamet, Y. Carbonatation of [ethylene-glycidyl methacrylate]-based copolymers with carbon dioxide as a reagent: from batch to solvent-free reactive extrusion. *Green Chem.* **2023**, *25*(16), 6355–6364.
- [58] Kurusu, Y.; Masuyama, Y.; Miyamoto, M. Reactivity and Microstructure in the Epoxidation of Polybutadiene. *Polym J* **1994**, *26*(10), 1163–1169.
- [59] Aguiar, M.; Menezes, S.C. de; Akcelrud, L. Configurational double bond selectivity in the epoxidation of hydroxy-terminated polybutadiene with m-chloroperbenzoic acid. *Macromol. Chem. Phys.* **1994**, *195*(12), 3937–3948.
- [60] Gregório, J.; Gerbase, A.; Martinelli, M.; Jacobi, M.; Freitas, L.; Holleben, M.; Marcico, P. Very efficient epoxidation of 1,4-polybutadiene with the biphasic system methyltrioxorhenium (MTO)CH<sub>2</sub>Cl<sub>2</sub>/H<sub>2</sub>O<sub>2</sub>. *Macromolecular Rapid Communications - MACROMOL RAPID COMMUN* **2000**, *21*, 401–403.
- [61] Zhang, Y.; Chen, X.-Z.; Zhang, Y.; Zhang, Y.-X. Preparation of epoxidized rubber using a reactive processing technique. I. Synthesis and characterization of epoxidized polybutadiene rubber. *Journal of Applied Polymer Science* **2001**, *81*(12), 2987–2992.
- [62] Nikje, M.M.A.; Rafiee, A.; Haghshenas, M. Epoxidation of polybutadiene using in situ generated dimethyl dioxirane (DMD) in the presence of tetra-n-butyl ammonium bromide. *Designed Monomers and Polymers* **2006**, *9*(3), 293–303.
- [63] Abdullin, M.I.; Basyrov, A.A.; Kukovinets, O.S.; Glazyrin, A.B.; Khamidullina, G.I. Epoxidation of syndiotactic 1,2-polybutadiene with peracids. *Polym. Sci. Ser. B* **2013**, *55*(5–6), 349–354.
- [64] Srivastava, V.K.; Basak, G.C.; Maiti, M.; Jasra, R.V. Synthesis and utilization of epoxidized polybutadiene rubber as an alternate compatibilizer in green-tire composites. *Int J Ind Chem* **2017**, *8*(4), 411–424.
- [65] Siegmeier, R.; Grund, A.; Prescher, G.; Brandt, U. Process for the preparation of epoxidized polybutadienes. 1989.
- [66] Heping, Y.; Sidong, L.; Zheng, P. Preparation and Study of Epoxidized Natural Rubber. *Journal of Thermal Analysis and Calorimetry* **1999**, *58*(2), 293–299.

- [67] Ruksakulpiwat, C.; Nuasaen, S.; Poonsawat, C.; Khansawai, P. Synthesis and Modification of Epoxidized Natural Rubber from Natural Rubber Latex. *Advanced Materials Research* **2008**, *47–50*, 734–737.
- [68] Ngudsuntear, K.; Limtrakul, S.; Arayapranee, W. Synthesis of Hydrogenated Natural Rubber Having Epoxide Groups Using Diimide. *ACS Omega* **2022**, *7*(25), 21483–21491.
- [69] Zhao, Y.; Huang, B.; Yao, W.; Cong, H.; Shao, H.; Du, A. Epoxidation of high trans-1,4-polyisoprene and its properties. *Journal of Applied Polymer Science* **2008**, *107*(5), 2986–2993.
- [70] Nikje, M.M.A.; Motahari, S.; Haghshenas, M.; Sanami, R.K. Epoxidation of Ethylene Propylene Diene Monomer (EPDM) Rubber by Using *In-Situ* Generated Dimethyldioxirane (DMD) and MoO<sub>3</sub>. *Journal of Macromolecular Science, Part A* **2006**, *43*(8), 1205–1214.
- [71] Roo, C.M. de; Kasper, J.B.; Duin, M. van; Mecozzi, F.; Browne, W. Off-line analysis in the manganese catalysed epoxidation of ethylene-propylene-diene rubber (EPDM) with hydrogen peroxide. *RSC Adv.* **2021**, *11*(51), 32505–32512.
- [72] Kawahara, S.; Saito, T. Preparation of carbonated natural rubber. *Journal of Polymer Science Part A: Polymer Chemistry* **2006**, *44*(4), 1561–1567.
- [73] Jiang, Q.; Gao, Y.; Liao, L.; Yu, R.; Liao, J. Biodegradable Natural Rubber Based on Novel Double Dynamic Covalent Cross-Linking. *Polymers* **2022**, *14*(7), 1380.
- [74] Santacesaria, E.; Russo, V.; Tesser, R.; Turco, R.; Di Serio, M. Kinetics of Performic Acid Synthesis and Decomposition. *Ind. Eng. Chem. Res.* **2017**, *56*(45), 12940–12952.
- [75] De Dios Miguel, T.; Duc Vu, N.; Lemaire, M.; Duguet, N. Biobased Aldehydes from Fatty Epoxides through Thermal Cleavage of  $\beta$ -Hydroxy Hydroperoxides\*\*. *ChemSusChem* **2021**, *14*(1), 379–386.
- [76] Villa de P, A.L.; Taborda A, F.; Montes de Correa, C. Kinetics of limonene epoxidation by hydrogen peroxide on PW-Amberlite. *Journal of Molecular Catalysis A: Chemical* **2002**, *185*(1), 269–277.
- [77] Grigoropoulou, G.; H. Clark, J.; A. Elings, J. Recent developments on the epoxidation of alkenes using hydrogen peroxide as an oxidant. *Green Chemistry* **2003**, *5*(1), 1–7.
- [78] Grigoropoulou, G.; Clark, J.H. A catalytic, environmentally benign method for the epoxidation of unsaturated terpenes with hydrogen peroxide. *Tetrahedron Letters* **2006**, *47*(26), 4461–4463.
- [79] Wolf, B.; Rack, M.; BENSON, S.; Kraus, H.; Götz, R.; Narayanan, S.; GALAM, C.R. A process for the preparation of terpinolene epoxide. 2020.
- [80] Liu, J.; Cui, J.; Chen, L.; Chen, J.; Zheng, H.; Ted Oyama, S. Advantages of tandem versus simultaneous operation: The case of isomerization/hydrogenation of terpinolene epoxide to Terpinen-4-ol using a Ni/TiO<sub>2</sub>-SiO<sub>2</sub> bifunctional catalyst. *Chemical Engineering Science* **2022**, *259*, 117828.
- [81] Tzoganakis, C. Reactive extrusion of polymers: A review. *Advances in Polymer Technology* **1989**, *9*(4), 321–330.

- [82] Smit, K.D.; Wieme, T.; Marien, Y.W.; Steenberge, P.H.M.V.; D'hooge, D.R.; Edeleva, M. Multi-scale reactive extrusion modelling approaches to design polymer synthesis, modification and mechanical recycling. *React. Chem. Eng.* **2022**, *7*(2), 245–263.
- [83] Carrodegua, L.P.; Cristòfol, À.; Fraile, J.M.; Mayoral, J.A.; Dorado, V.; Herrerías, C.I.; Kleij, A.W. Fatty acid based biocarbonates: Al-mediated stereoselective preparation of mono-, di- and tricarbonates under mild and solvent-less conditions. *Green Chem.* **2017**, *19*(15), 3535–3541.
- [84] Chen, F.; Zhang, Q.-C.; Wei, D.; Bu, Q.; Dai, B.; Liu, N. Highly Stereo-Controlled Synthesis of Fatty Acid-Derived Cyclic Carbonates by Using Iron(II) Complex and Nucleophilic Halide. *J. Org. Chem.* **2019**, *84*(18), 11407–11416.
- [85] Langanke, J.; Greiner, L.; Leitner, W. Substrate dependent synergetic and antagonistic interaction of ammonium halide and polyoxometalate catalysts in the synthesis of cyclic carbonates from oleochemical epoxides and CO<sub>2</sub>. *Green Chem.* **2013**, *15*(5), 1173–1182.
- [86] Fiorani, G.; Stuck, M.; Martín, C.; Belmonte, M.M.; Martin, E.; Escudero-Adán, E.C.; Kleij, A.W. Catalytic Coupling of Carbon Dioxide with Terpene Scaffolds: Access to Challenging Bio-Based Organic Carbonates. *ChemSusChem* **2016**, *9*(11), 1304–1311.
- [87] Ochiai, B.; Iwamoto, T.; Miyazaki, K.; Endo, T. Efficient Gas–Solid Phase Reaction of Atmospheric Carbon Dioxide into Copolymers with Pendent Oxirane Groups: Effect of Comonomer Component and Catalyst on Incorporation Behavior. *Macromolecules* **2005**, *38*(24), 9939–9943.
- [88] Berto, P.; Grelier, S.; Peruch, F. Controlled degradation of polyisoprene and polybutadiene: A comparative study of two methods. *Polymer Degradation and Stability* **2018**, *154*, 295–303.



---

# **Chapter 4:**

## **Synthesis of polyhydroxyurethanes from carbonated polymers**

---

In **Chapter 4**, the generation of hydroxyurethane functions on carbonated polymers using amines will be investigated. Here, controlling the regioselective and stereoselective aminolysis of cyclic carbonates relative to residual epoxides will be essential to develop further orthogonal functionalizations exploiting both epoxide and cyclic carbonate moieties on polymers in order to produce hybrid-cross-linked polymers with different crosslinking knots.





## Table of Contents

<b>I. Abstract .....</b>	<b>180</b>
<b>II. Introduction.....</b>	<b>181</b>
<b>III. Results and discussion .....</b>	<b>185</b>
III.1. Synthesis of hydroxyurethane functions on carbonated [ethylene – glycidylmethacrylate-methyl acrylate] polymer.....	185
III.2. Synthesis of hydroxyurethane functions on partially carbonated [ethylene – glycidylmethacrylate-methyl acrylate] polymer.....	188
III.3. Synthesis of hydroxyurethane functions on partially carbonated polydiene with a monoamine.....	192
III.4. Synthesis of cross-linked PHUs from carbonated polydienes with hexamethylene diamine	195
<b>IV. Conclusions .....</b>	<b>200</b>
<b>V. References.....</b>	<b>201</b>



### I. Résumé

Au cours des dernières décennies, la synthèse de polyhydroxyuréthanes (PHU) à partir de poly(carbonates cycliques) et de polyamines a été largement étudiée. Ces matériaux sont des alternatives potentielles aux polyuréthanes (PU), évitant l'utilisation de phosgène et d'isocyanates hautement toxiques, tout en conservant des propriétés adaptées aux applications industrielles. Cependant, les interactions chimiques et physiques qui se produisent lors de la synthèse des PHU ne sont pas encore totalement comprises et constituent la principale limite à leur utilisation industrielle.

Dans ce travail, des polyhydroxyuréthanes à base de polyoléfines (PHUs basés sur un squelette PE semi-cristallin) ont été synthétisés avec succès à partir de polymères époxydés partiellement carbonatés et d'amines. L'aminolyse du terpolymère [éthylène -méthacrylate de glycidyle-acrylate de méthyle] partiellement carbonaté avec l'hexylamine et le 1,5,7-triazabicyclo[4.4.0]dec-5-ene (TBD) comme catalyseur a d'abord été réalisée pour étudier la différence de réactivité entre les carbonates cycliques et les époxydes présents dans le polymère. Le carbonate cyclique terminal a été complètement converti en hydroxyuréthanes, alors que les époxydes n'ont réagi que partiellement à 90 °C, d'après les analyses <sup>1</sup>H NMR.

La réactivité des carbonates cycliques internes et des époxydes a également été comparée lors de l'aminolyse d'un polybutadiène partiellement carbonaté et époxydé avec l'hexylamine et le TBD comme catalyseur. Une étude cinétique de la réaction a montré l'ordre de réactivité suivant : **carbonate cyclique *cis* > carbonate cyclique *trans* >> époxyde**, car aucune conversion d'époxyde n'a été observée après 17,5 heures de réaction à 90 °C dans le TCE/C<sub>6</sub>D<sub>6</sub>, d'après les analyses RMN <sup>1</sup>H.

Enfin, un polybutadiène époxydé partiellement carbonaté a été réticulé avec de l'hexaméthylène diamine sans catalyseur. Les groupements carbonates cycliques ont été entièrement convertis en hydroxyuréthanes et un matériau ductile insoluble a été obtenu. Dans des conditions similaires, un polybutadiène époxydé a montré une réactivité nettement moindre, seules des traces du produit de la réaction d'ouverture de cycle ont été observées après la réaction.

## II. Abstract

In the last decades, the synthesis of polyhydroxyurethanes (PHUs) from poly(cyclic carbonate)s and polyamines have been widely studied. These materials are potential alternatives to polyurethanes (PUs), avoiding the use of the highly toxic phosgene and isocyanates, while keeping suitable properties for industrial applications. However, the chemical and physical interactions that occur during the synthesis of PHUs are not fully understood yet and are the main limitation for their industrial use.

In this work, polyolefins-based polyhydroxyurethanes (PHUs based on a semi-crystalline PO backbone) were successfully synthesized from partially carbonated epoxidized polymers and amines. The aminolysis of partially carbonated [ethylene rich-glycidyl methacrylate-methyl acrylate] terpolymer with hexylamine and 1,5,7-triazabicyclo[4.4.0]dec-5-ene (TBD) as catalyst was first carried out to study the difference of reactivity between the cyclic carbonates and epoxide moieties present in the polymer. The terminal cyclic carbonate was completely converted to hydroxyurethanes, whereas the epoxides only partially reacted at 90 °C, according to <sup>1</sup>H NMR analyses.

The reactivity of internal cyclic carbonates and epoxides was also compared during the aminolysis of partially carbonated epoxidized polybutadiene with hexylamine and TBD. A kinetic study of the reaction showed the following order of reactivity: *cis* cyclic carbonate > *trans* cyclic carbonate >> epoxide, as no conversion of epoxide was observed after 17.5 hours of reaction at 90 °C in TCE/C<sub>6</sub>D<sub>6</sub>, based on <sup>1</sup>H NMR analyses.

Finally, a partially carbonated epoxidized polybutadiene was cross-linked with hexamethylene diamine without catalyst. The cyclic carbonate moieties were fully converted to hydroxyurethanes and an insoluble ductile material was obtained. Under similar conditions, an epoxidized polybutadiene showed significantly less reactivity, only traces of the ring-opening reaction product was observed after reaction.

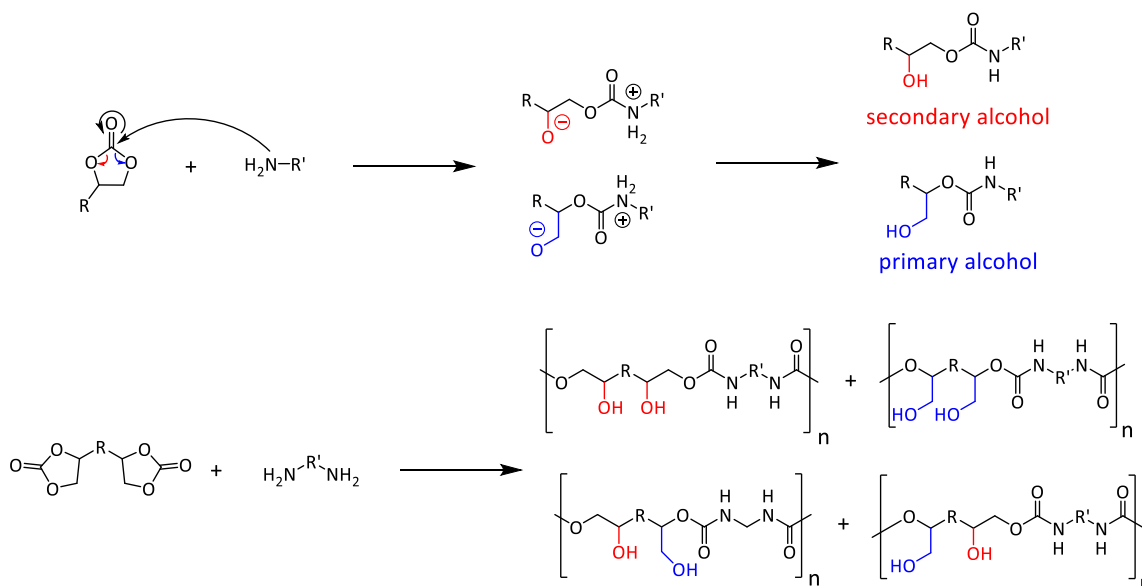
### III. Introduction

Polyurethanes (PUs) are an important class of polymers used in a multitude of applications such as building and construction, transportation, furniture and textiles under different forms (foams, composites, coatings).<sup>[1,2]</sup> PUs are generally obtained *via* the polyaddition of polyol prepolymers on diisocyanates.<sup>[1]</sup> However, the use of isocyanates, obtained from phosgene and amines, is a major drawback due to the high toxicity of isocyanates and phosgene.<sup>[2]</sup>

During the last decades, non-isocyanate polyurethanes (NIPUs) have emerged and now spark a growing interest as an alternative method to produce PUs.<sup>[2-5]</sup> Especially polyhydroxyurethanes (PHUs), obtained from cyclic carbonates and diamines, are widely studied, in order to use non-toxic and potentially bio-based and CO<sub>2</sub>-based polymer precursors (comonomers and prepolymers) such as carbonated fatty esters or terpene derivatives.<sup>[5]</sup> The presence of hydroxyl groups favors the intra- and intermolecular interactions *via* hydrogen bonding, which procures interesting properties to the materials, such as a better chemical resistance, especially to hydrolysis compared to PUs with similar structures. PHUs have also excellent adhesion properties due to the hydroxyl groups, which make them suitable for coating applications.<sup>[6-8]</sup>

Moreover, the synthesis of cross-linked materials with dynamic hydroxyurethane networks to produce vitrimer materials from carbonated vegetable oils has been the subject of several studies.<sup>[9-13]</sup> Reversible transcarbamoylation (or urethane/hydroxyl exchange) and transesterification reactions participate to the break and the formation of new covalent bonds within the network structure above a specific temperature. Whereas conventional cross-linked materials are not recyclable, these cross-linked PHUs could be recycled and reprocessed without significant loss of their mechanical properties.

However, the synthesis of PHUs has still some limitations. Low molar masses (less than 30 000 g/mol) are generally obtained.<sup>[14]</sup> Whereas PUs can be produced at ambient temperature, the synthesis of PHUs requires higher temperatures (from room temperature to more than 100 °C, depending on the carbonate and amine reactivity) which favors secondary reactions such as urea and cyclic carbamate formation. Herein, hydroxyurethane compounds were synthesized from model compounds in order to fully understand the effect of the cyclic carbonate structure and reaction parameters to achieve ring opening under mild conditions.<sup>[15-18]</sup> The substituents of the cyclic carbonate strongly affect its reactivity and the selectivity toward the formation of primary and secondary alcohols (*Scheme 1*).



*Scheme 1. Synthesis of hydroxyurethanes with monoamines, and polyhydroxyurethanes with diamines, and formation of the primary and secondary alcohols.*

Tomita *et al.*<sup>[15]</sup> observed that the presence of strong electron-withdrawing groups (CF<sub>3</sub>, ester groups) increases significantly the reactivity of the cyclic carbonate, whereas lower reactivity was observed with electron-donor groups (hydrogen, alkyl groups). Moreover, the secondary alcohol product was selectively obtained with the strong electron-withdrawing group CF<sub>3</sub>, due to the stabilization of the secondary alkoxide intermediate formed after the nucleophilic attack of the hexylamine, *via* the acceptor inductive effect of the CF<sub>3</sub> group. Conversely, the primary/secondary alcohol ratio increased with the increase of the electron-donor ability of the substituents. Blain *et al.*<sup>[16]</sup> also evaluated the influence of several parameters such as the nature of the amine, the use of catalysts and the temperature on the synthesis efficiency. Weakly hindered and nucleophilic alkylamines such as butylamine and cyclohexylmethylamine showed the best reactivity with propylene carbonate at 25 °C without any catalyst, with an almost complete conversion after 10 h. Under the same conditions, aniline was not reactive and cyclohexylamine had a moderate reactivity; The latter was thus chosen to evaluate different Lewis acid and organocatalysts, such as thiourea derivatives, that could activate the carbonyl group of the carbonate, and organic superbases such as 1,5,7-triazabicyclo[4.4.0]dec-5-ene (TBD) and 1,8-Diazabicyclo[5.4.0]undec-7-ene (DBU) that could facilitate the residual proton transfer after the ring-opening addition of the amine. TBD and a thiourea derivatives were the most active commercial organocatalysts, but the thiourea showed a better selectivity at 100 °C and a better activity at low catalyst loading (under 1 mol%) and for hour-long reactions (10 h). Sopena *et al.*<sup>[17]</sup> showed that the use of TBD as

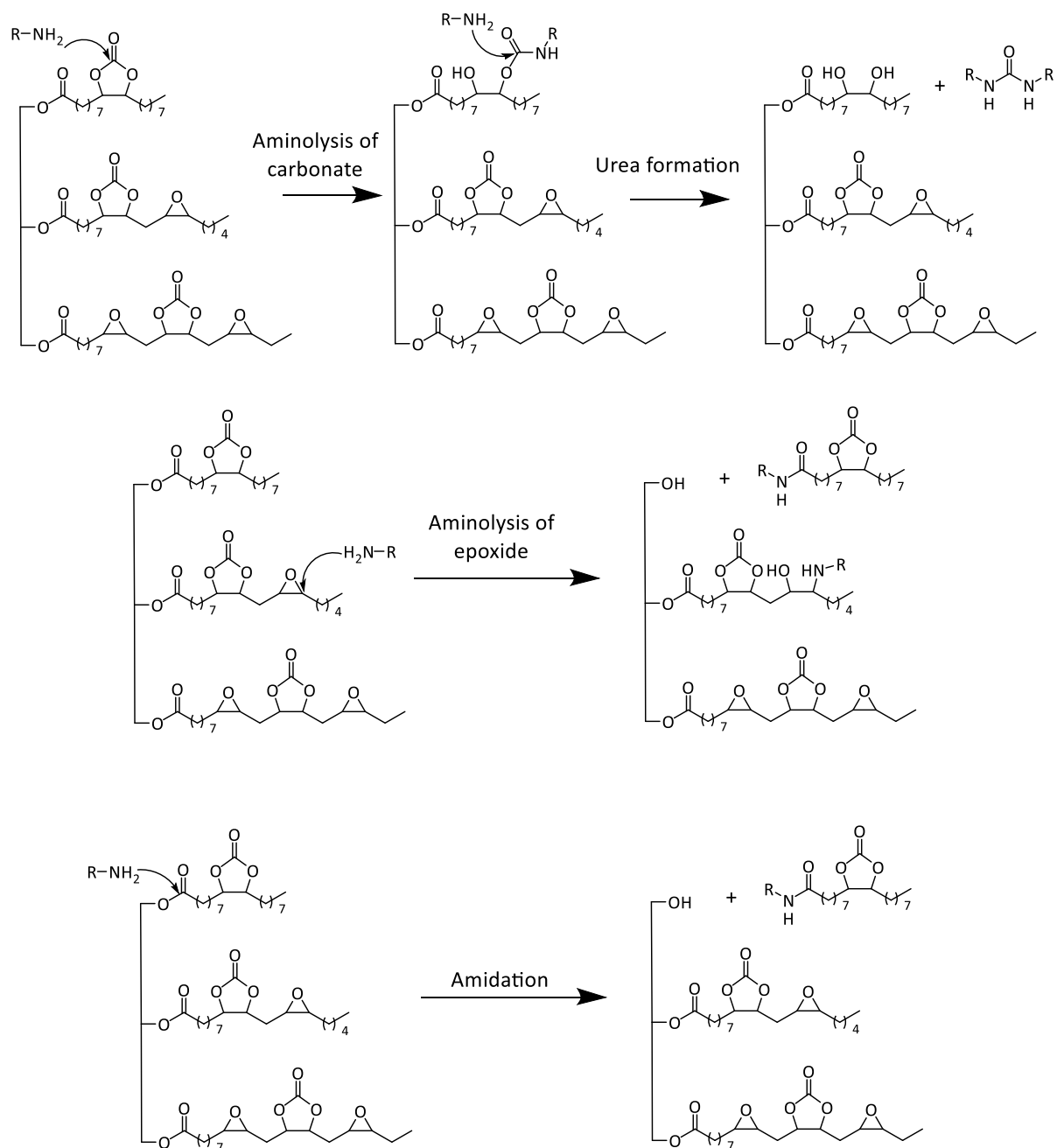
catalyst led to selective formation of the secondary alcohol with three different amines (morpholine, piperidine and pyrrolidine) and various cyclic carbonates (*gem*-disubstituted, trisubstituted and tetrasubstituted cyclic carbonates) *via* the formation of a “ternary complex” between TBD, the amine and the cyclic carbonate.

Moreover, when epoxide functions are also present in the system (in the case of partially carbonated epoxidized oils or polymers), the ring-opening reaction of the oxiranes with amine could be in competition with the PHUs formation. However, some studies showed that cyclic carbonates could be completely converted to hydroxyurethane functions whereas the epoxides were not or poorly converted below 100 °C. For example, Dechent *et al.*<sup>[19]</sup> showed that during aminolysis of polybutadienes containing cyclic carbonate and epoxide functions with a diamine at 90 °C, only the carbonates were converted to hydroxyurethane after 16 h, with no reaction of the epoxides. Helbling *et al.*<sup>[20]</sup> also showed the higher reactivity of cyclic carbonate compared to epoxide for the aminolysis of partially carbonated epoxidized soybean oils with diamines (*Scheme 2*), the epoxide conversion did not reach 20 % for reaction temperature below 80 °C after 4 hours, whereas the cyclic carbonate was converted to more than 70 %. The epoxide aminolysis was favored by the increase of the curing temperature to 120 °C and by the presence of cyclic carbonate. The presence of cyclic carbonate was essential for the cross-linking reaction of the carbonated oil. Without cyclic carbonates, there is a competition between the ring-opening of the epoxide, and the amidation of the ester groups at 120 °C, which degrades the triglyceride skeleton and thus inhibits cross-linking. In presence of cyclic carbonate, the amidation reaction rate was significantly decreased, which prevents the degradation of the triglyceride skeleton and produced hybrid poly(hydroxyurethane) thermoset materials.

In our previous studies, we described the carbonatation reactions of various epoxidized polymers with CO<sub>2</sub> using organocatalysts. [Ethylene – glycidylmethacrylate] based copolymers<sup>[21]</sup> and epoxidized polydienes were partially carbonated, and the epoxide reactivity towards carbonatation followed the order: terminal > *cis* > *trans*.

In this work, the aminolysis of these partially carbonated epoxidized polymers is described, in order to understand the effect of the cyclic carbonate structure (terminal, *cis* or *trans*) on its reactivity with amines, and the reactivity of cyclic carbonate and epoxide moieties is compared.



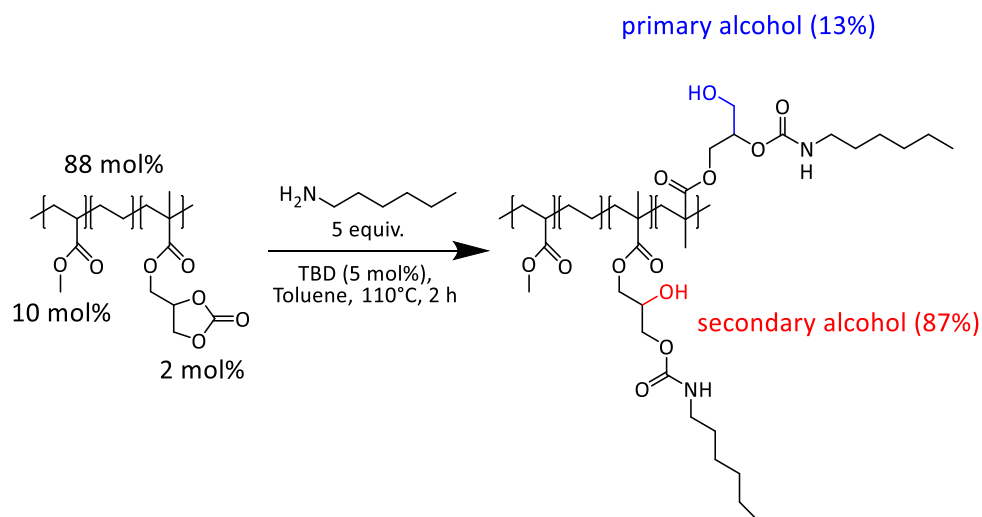


*Scheme 2. Possible reactions during aminolysis of partially carbonated epoxidized soybean oil.*

## IV. Results and discussion

### IV.1. Synthesis of hydroxyurethane functions on carbonated [ethylene – glycidyl methacrylate-methyl acrylate] polymer

First, the synthesis of hydroxyurethane pendant groups on the fully carbonated [ethylene – glycidyl methacrylate – methylacrylate] ter-polymer (E-GMA-MA) was carried out using an excess of hexylamine (5 equiv. relative to cyclic carbonate units) and TBD as catalyst (5 mol% relative to cyclic carbonate units), in toluene at 110 °C (*Scheme 3*) (Marie-Emilie Annez de Taboada participated to this work during her one-month internship in CP2M lab). After 2 hours, the cyclic carbonates moieties were fully converted and both primary and secondary alcohols functions were obtained.



*Scheme 3. Synthesis of hydroxyurethane functions on carbonated E-GMA-MA.*

The IR-ATR analyses showed the complete disappearance of the cyclic carbonate vibration ( $1821\text{ cm}^{-1}$ , C=O stretching) after 2 hours of reaction, and the appearance of the characteristic hydroxyurethane band ( $1528\text{ cm}^{-1}$ , N-H bending) (*Figure 1*). The appearance of a large band at  $3100\text{--}3700\text{ cm}^{-1}$  (O-H and N-H stretching) also indicated the formation of alcohol and amide groups on the polymer. The C=O band of the hydroxyurethane overlapped with the C=O band of the ester group ( $1735\text{ cm}^{-1}$ , C=O stretching). These observations are in accordance with the literature.<sup>[22]</sup>

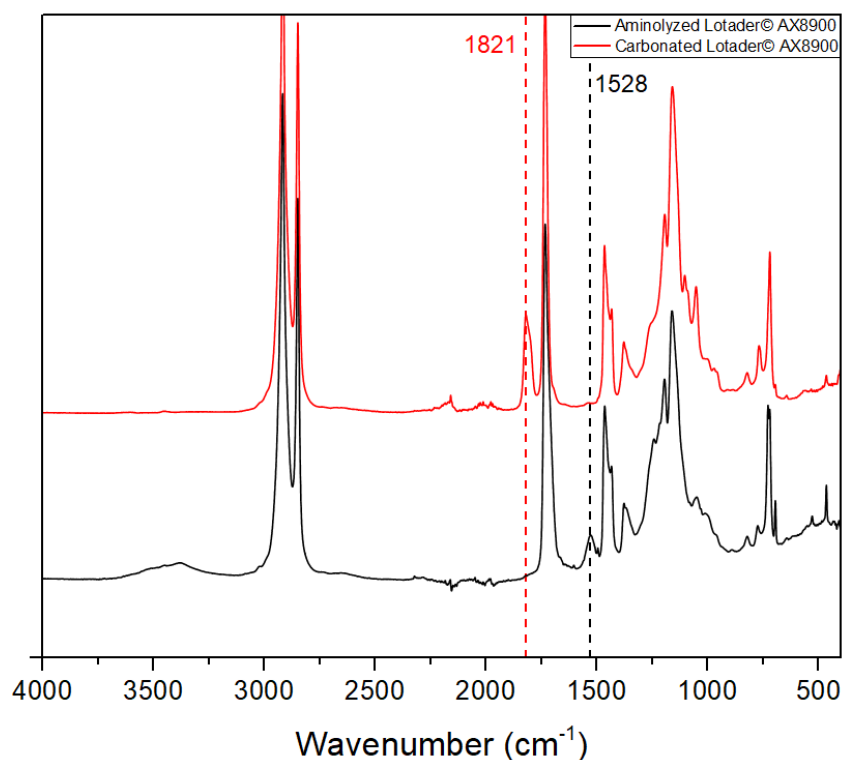


Figure 1. ATR-IR spectra of carbonated E-GMA-MA (red) and E-GMA-MA containing hydroxyurethane functions (black).

The formation of hydroxyurethane functions was also confirmed by  $^1\text{H}$  NMR, with the disappearance of the cyclic carbonate signals g, f and h, and the presence of new signals corresponding to the hydroxyurethane groups at 3.5-5.0 ppm (Figure 2). The formation of the secondary alcohol hydroxyurethane product was confirmed with the new signals f', g', h' and i', observed in the spectral region 2.7-5.5 ppm. Primary alcohol was also formed but to a lesser extent as evidenced by the new signals f'', g'', h'' and i'', in accordance with the literature.<sup>[16]</sup> The presence of the ester acceptor group favoured the formation of the secondary alcohol, where the alkoxide intermediate is more stabilized. Thus, a primary: secondary alcohols ratio of 13:87 was obtained according to the  $^1\text{H}$  NMR analysis.

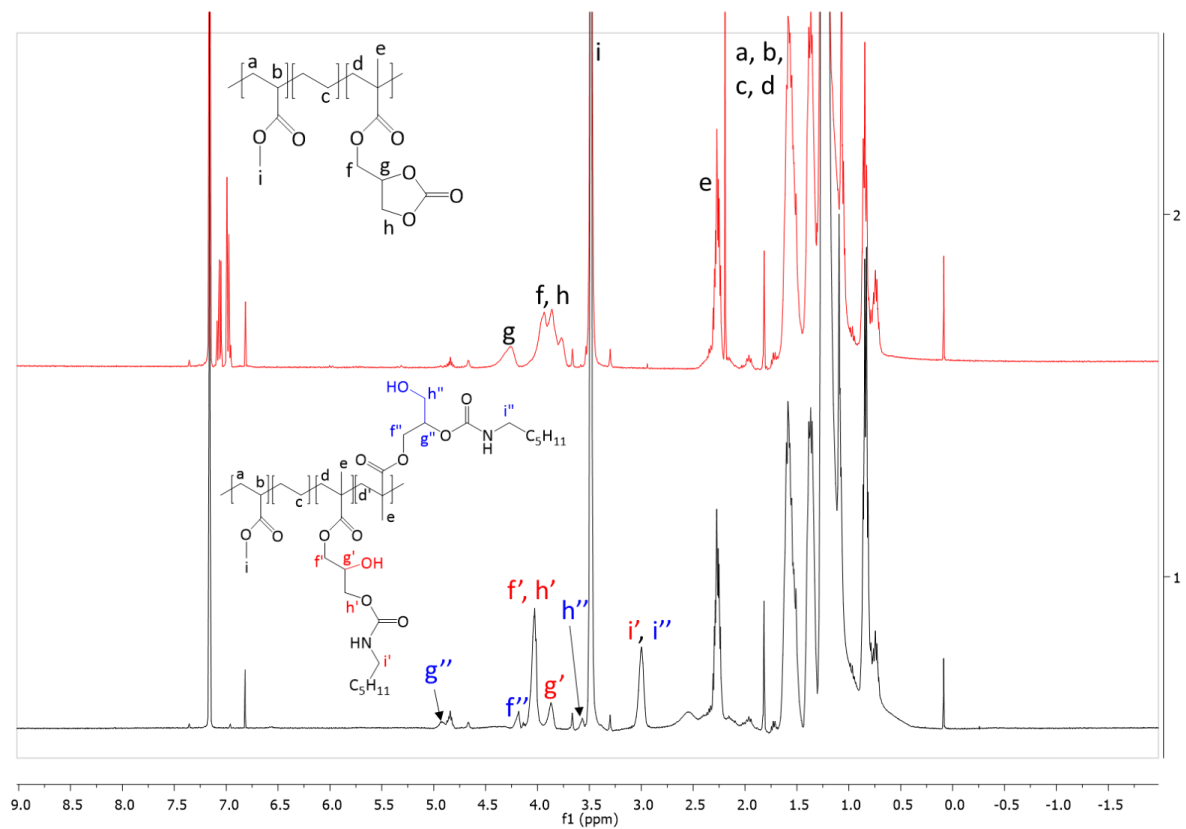
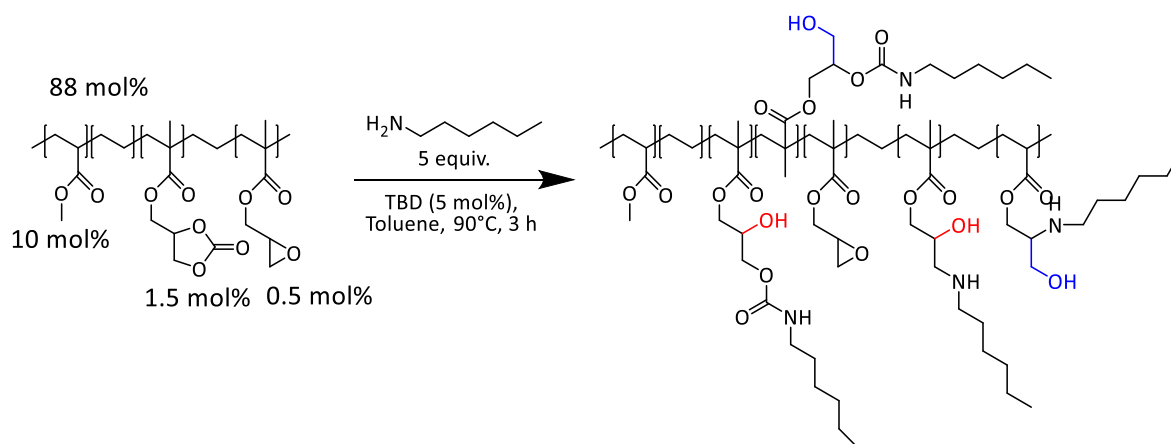


Figure 2.  $^1\text{H}$  NMR (TCE/ $\text{C}_6\text{D}_6$ , 400 MHz) spectra of carbonated E-GMA-MA (red) and E-GMA-MA containing hydroxyurethane functions (black).

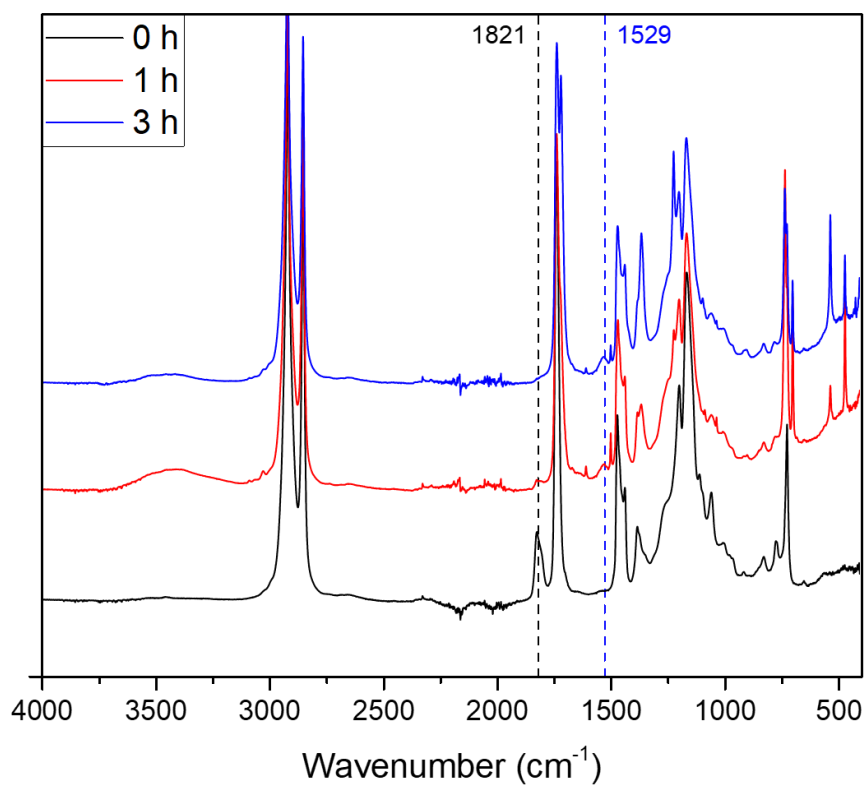
## IV.2. Synthesis of hydroxyurethane functions on partially carbonated [ethylene – glycidyl methacrylate-methyl acrylate] polymer

Moreover, the orthogonality of the cyclic carbonate and epoxide reactivity was investigated by following the reaction between partially carbonated E-GMA-MA (ratio carbonate: epoxide of 73: 27) and hexylamine (5 equiv. relative to carbonate units) with TBD (5 mol% relative to carbonate units) in toluene at 90 °C (*Scheme 4*).



*Scheme 4. Aminolysis of partially carbonated E-GMA-MA.*

According to IR-ATR analyses, the cyclic carbonate band at 1821 cm<sup>-1</sup> (C=O stretching) completely disappeared after reaction, and a new band at 1529 cm<sup>-1</sup> (N-H bending) corresponding to urethane was observed by IR-ATR (*Figure 3*). Moreover, after 3 hours of reaction, remaining epoxide functions were observed by <sup>1</sup>H NMR (*Figure 4*). The conversions of the carbonate and the epoxide functions were determined with the integration of the characteristic <sup>1</sup>H NMR signals of the carbonate at 4.28 ppm (named C on *Figure 4*) and of the epoxide at 2.90 ppm (named E on *Figure 4*) using the signal at 1.96 ppm as internal standard (corresponding to the protons on the polymer backbone, named IS on *Figure 4*). After 3 hours, the cyclic carbonate was completely converted whereas the epoxide was converted at 47 %. The formation of the hydroxyurethane was confirmed with the appearance of the characteristic signals at 4.03 and 3.00 ppm (named HU on *Figure 4*). The signals of the hydroxyamine formed *via* the addition of the amine on the epoxide was not observed because they appeared at 4.0 and 2.3 ppm as large signals according to the literature,<sup>[23]</sup> and thus overlapped with other signals. These results showed the higher reactivity of cyclic carbonate moieties compared to the epoxide moieties with alkyl amines.



*Figure 3. ATR-IR spectra of the polymer obtained after reaction at 90 °C between partially carbonated E-GMA-MA and hexylamine.*

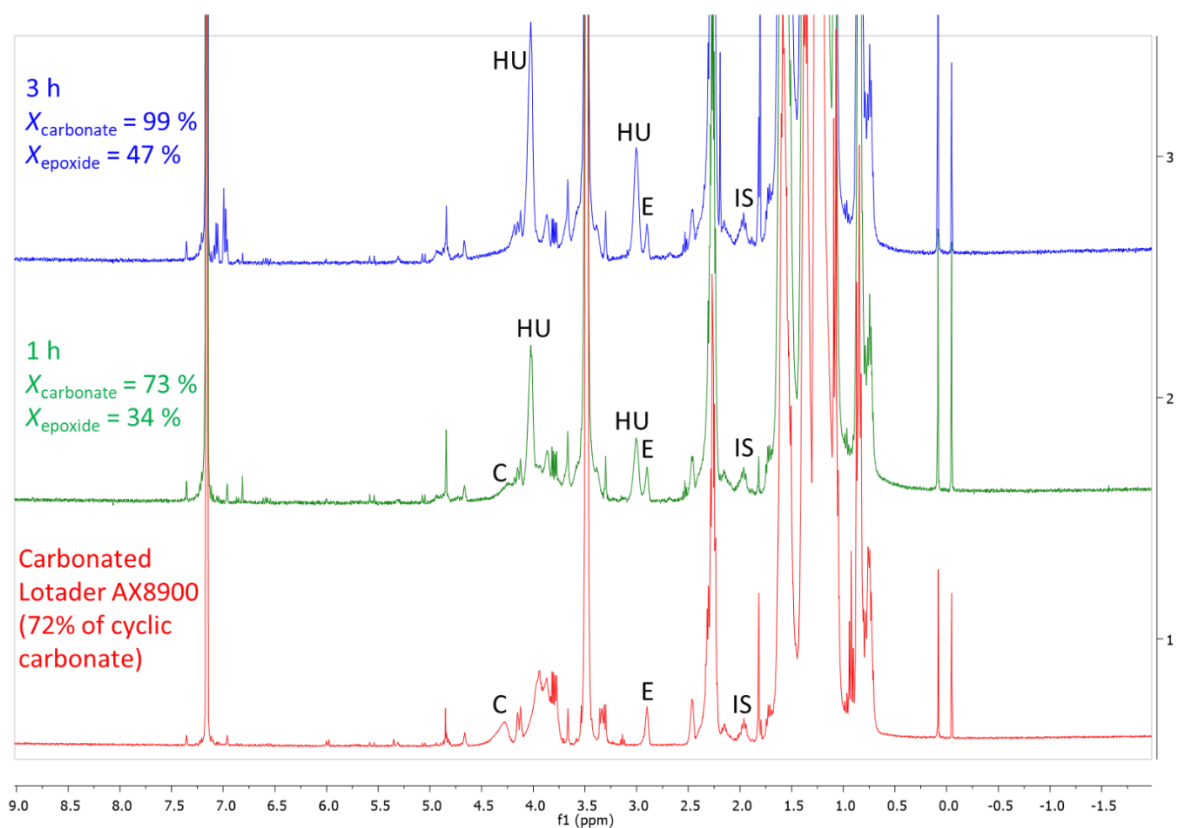
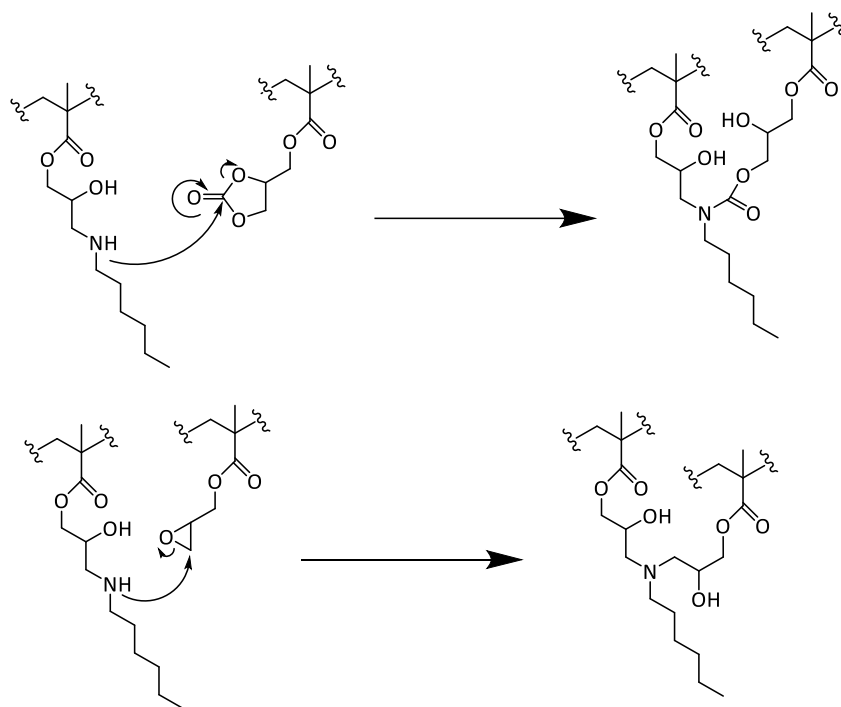


Figure 4.  $^1\text{H}$  NMR spectra of the polymer obtained after reaction between partially carbonated E-GMA-MA and hexylamine.

After 4 hours, it was not possible to continue the reaction due to a too high viscosity of the reaction medium. After the ring – opening of the epoxide with hexylamine, the secondary amine could react with another epoxide, or cyclic carbonate, and initiate the cross-linking of the polymer. The hydroxyl group formed after the aminolysis of the cyclic carbonate and epoxide may as well undergo nucleophilic attacks on cyclic carbonate, catalyzed by TBD, and formed linear carbonates linkages (*Scheme 5*).

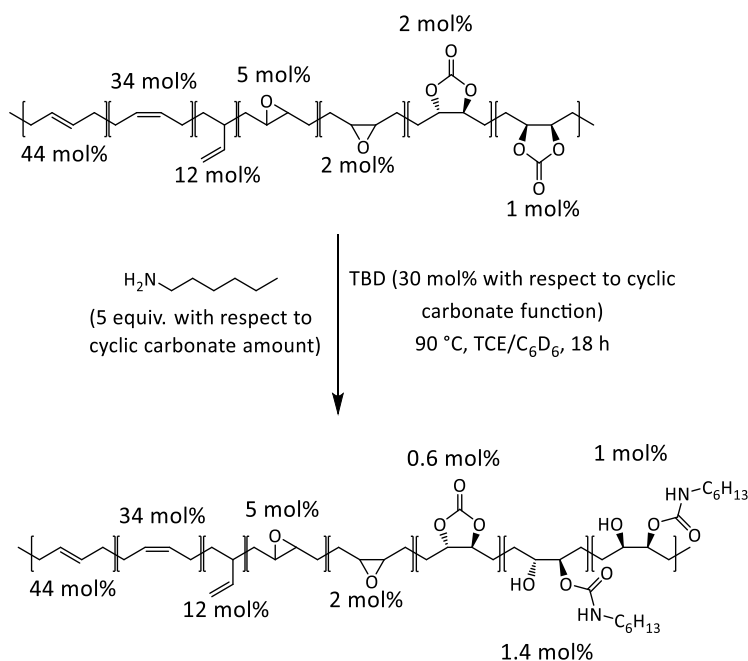


*Scheme 5. Cross-linking reaction from secondary amines and GMA units. OH groups formed after aminolysis of cyclic carbonate and epoxide may also attack residual carbonates and epoxides.*



### IV.3. Synthesis of hydroxyurethane functions on partially carbonated polydiene with a monoamine

The aminolysis of internal cyclic carbonate contained in carbonated polybutadienes was also investigated. The reaction of hexylamine (5 equiv.) with a polybutadiene containing both epoxide (7 mol%) and cyclic carbonate (3 mol%) functions (prepared from E-PBU-1) was monitored by  $^1\text{H}$  NMR using mesitylene as internal standard. The reaction was conducted in a 5 mm NMR tube, using TBD (30 mol%) as catalyst and TCE/ $\text{C}_6\text{D}_6$  (2/1) as solvent, at 90 °C (*Scheme 6*). A high mol% of TBD was used because of the high dilution of the system (polymer concentration of 118 mg/mL, and cyclic carbonate concentration of 0.06 mol/L) and in order to observe reactivity during the kinetic monitoring.



*Scheme 6. Synthesis of hydroxyurethane functions on partially carbonated polybutadiene with hexylamine.*

According to the  $^1\text{H}$  NMR analyses (*Figure 5*), the consumption of the *trans* and *cis* cyclic carbonate was clearly demonstrated by the decrease of the g and h intensities at 3.93 and 4.24 ppm, respectively, whereas no change was observed for the epoxide signals e and f at 2.45 and 2.69 ppm. Moreover, the TBD signal 1 shifted over time, from 2.89 (after 2.5 hours of reaction) to 2.95 ppm (after 18 hours of reaction). It is well known that TBD forms a ternary complex with cyclic carbonates and amines,<sup>[17]</sup> thus a similar complex could be obtained by

hydrogen bonding between TBD and the hydroxyurethane function, which could explain this chemical shift (Scheme 7).

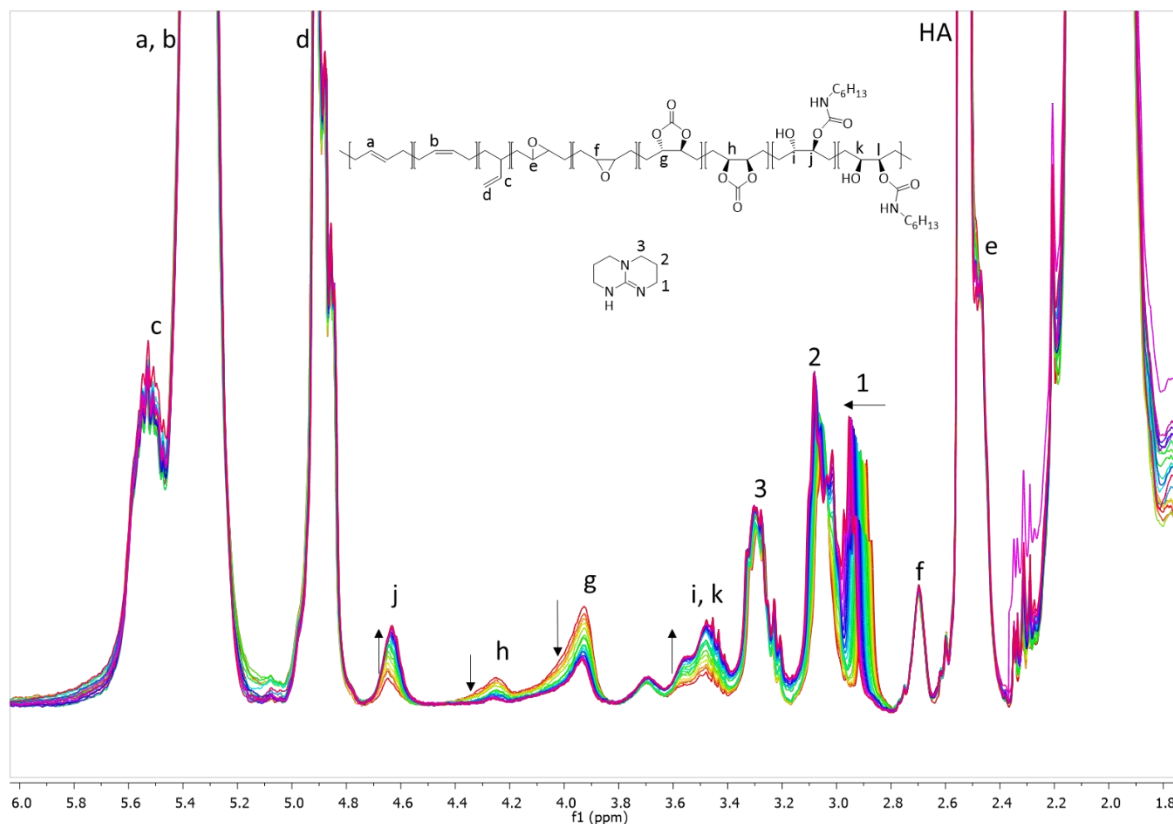
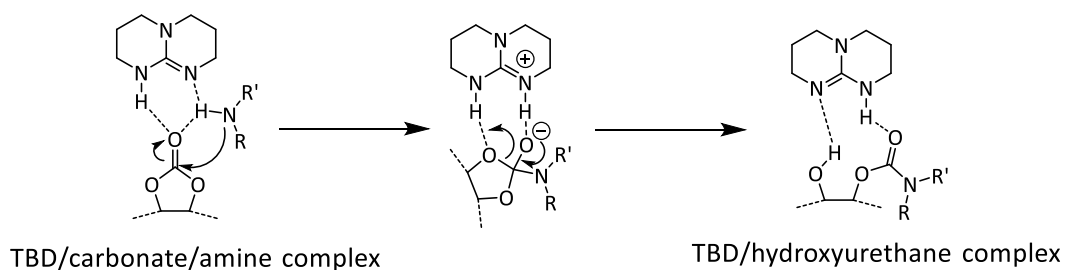


Figure 5.  $^1\text{H}$  NMR (300 MHz,  $\text{CDCl}_3$ ) spectra of the reaction mixture over time for the synthesis of hydroxyurethane function on carbonated polybutadiene with hexylamine (HA). The first spectrum (red) and the last spectrum (pink) were recorded 2.5 and 17.5 hours respectively after the addition of the hexylamine.



Scheme 7. Mechanism of aminolysis with TBD as catalyst.

The epoxide and cyclic carbonate conversion was determined over time by  $^1\text{H}$  NMR to assess the kinetics of the cyclic carbonate aminolysis reaction. The *cis* cyclic carbonate showed a higher reactivity than the *trans* derivative. After 18 hours of reaction, the *cis* and *trans* cyclic carbonates were converted at 96 % and 69 % respectively. A pseudo first order kinetic model

was applied on the conversion of *cis* and *trans* carbonates, and the observed kinetic constants  $k_{obs}$  were determined with the plot of the following equation:

$$\ln\left(\frac{C_{carbonate}}{C_{carbonate,0}}\right) = -k_{obs} \cdot t \quad (1)$$

the  $k_{obs}$  was equal to 0.21 and 0.08 h<sup>-1</sup> for the *cis* and *trans* cyclic carbonates, respectively, which confirmed the higher reactivity of the *cis* carbonate (Figure 6).

No significant reactivity of *cis* epoxide was observed, as the conversion was between 0 and 6 % during all the reaction, although a high amount of catalyst was used. The conversion of the *trans* epoxide could not be estimated due to the overlap of its signal with the signal from the proton in alpha position to the NH<sub>2</sub> group of hexylamine. However, the *trans* epoxide is much less reactive than the *cis* epoxide, thus it was possible to conclude that *trans* epoxide did not react with hexylamine. These results demonstrate the orthogonal reactivity of the epoxide and cyclic carbonate moieties, *i.e.* the cyclic carbonate moieties could be selectively converted to hydroxyurethane function, with no reactivity of the epoxide moieties, in the case of the functionalization of partially carbonated epoxidized polybutadienes. This could be particularly useful to the development of new vitrimers featuring covalent-adaptive networks (CANs), or even enhanced adhesives or sealants.

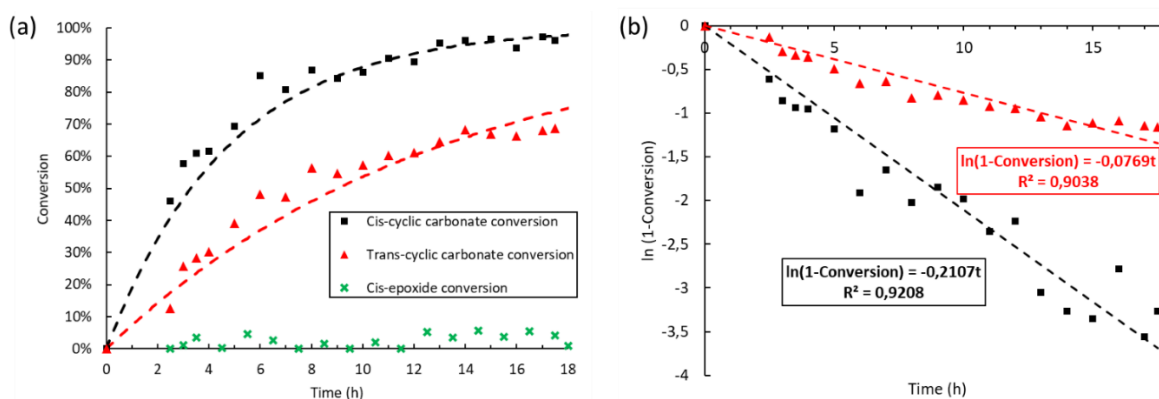
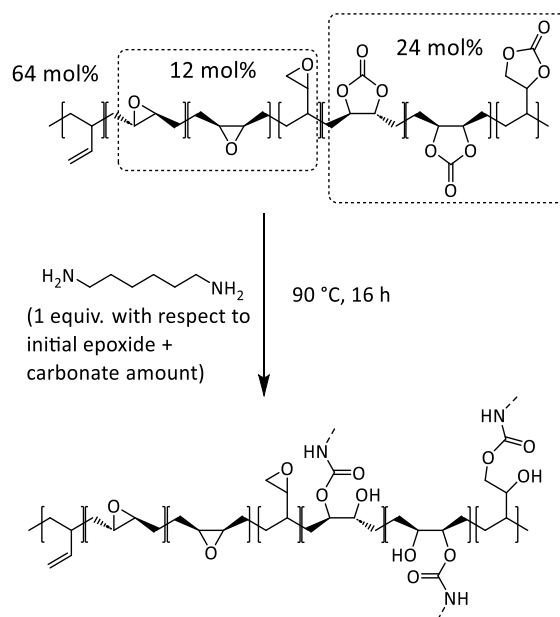


Figure 6. Kinetic study for the synthesis of hydroxyurethane functions on partially carbonated polybutadiene with hexylamine at 90 °C (initial cyclic carbonate and epoxide concentration: 0.06 mol/L and 0.2 mol/L, respectively): (a) conversion of the *cis* and *trans* carbonates and *cis* epoxide over time, (b) plot of equation (1). IR-ATR spectra before and after reaction in appendices (Figure S108).

IV.4. Synthesis of cross-linked PHUs from carbonated polydienes with hexamethylene diamine

In the previous paragraphs, the synthesis of hydroxyurethane functions on carbonated polymers with a monoamine was achieved in order to characterize the structure of the modified polymers and compare the reactivity of the cyclic carbonate and epoxide moieties. However, the main application of cyclic carbonates is the synthesis of crosslinked materials *via* the formation of PHU networks with a diamine. Thus, it was necessary to compare the reactivity of cyclic carbonate and epoxide functions to a diamine nucleophilic attack because of their higher reactivity compared to monoamines.

The synthesis of cross-linked polybutadiene *via* hydroxyurethane-based network formation was first attempted with a carbonated polybutadiene containing 64 mol% of vinyl unit, 24 mol% of cyclic carbonate and 12 mol% of epoxide and hexamethylene diamine (HMDA). The polymer and the amine was mixed in chloroform at room temperature, and a film was formed *via* evaporation of the solvent at room temperature. Then, the mixture was cured at 90 °C for 16 hours and a ductile material was obtained.



*Scheme 8. Crosslinking of carbonated polybutadiene via hydroxyurethane network formation with HDA.*

IR-ATR and solid state NMR (liquid state NMR impossible due to insolubility of the material) analyses showed that the cyclic carbonate functions were ~ completely converted to hydroxyurethane functions (*Figure 7 and 8*). The characteristic band of cyclic carbonate at

1793  $\text{cm}^{-1}$  almost disappeared after reaction and new bands at 3313 (N-H, O-H stretching), 1692 (C=O stretching) and 1534  $\text{cm}^{-1}$  (N-H bending), corresponding to hydroxyurethane, appeared. However, the epoxide characteristic band overlaps with the vinyl units bands (906  $\text{cm}^{-1}$ , C-H wagging), thus it was not possible to conclude on the epoxide reactivity.

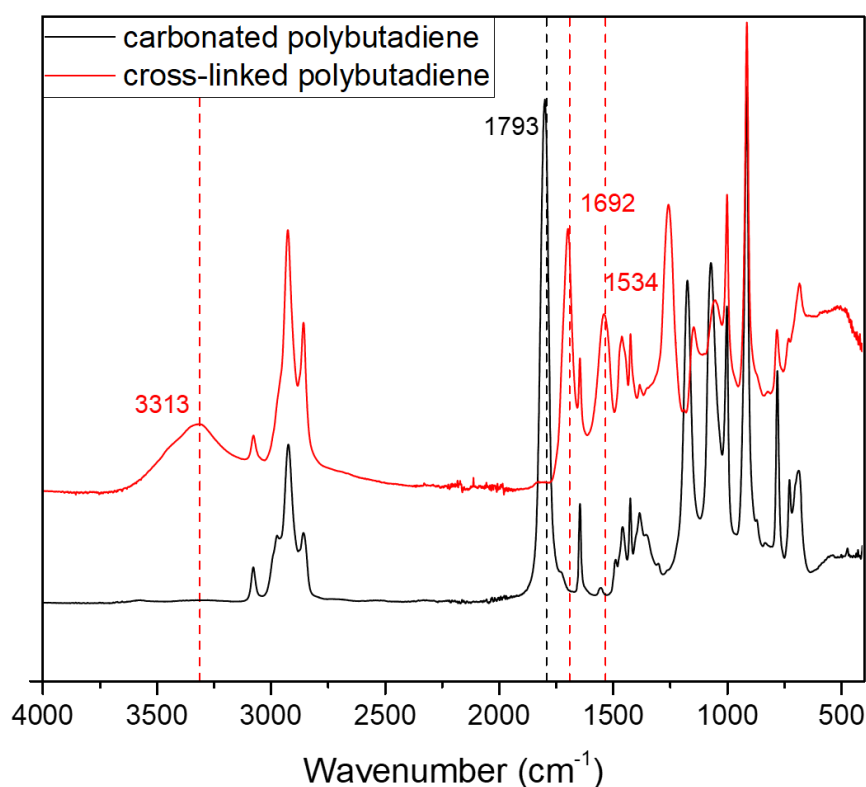


Figure 7. ATR-IR spectra of the carbonated polybutadiene (black) and cross-linked polybutadiene (red).

For insolubility issues, solid-state CP/MAS  $^{13}\text{C}$  and  $^{15}\text{N}$  NMR were performed to confirm the formation of the hydroxyurethane functions. As shown in Figure 8 and taking into account the width of the signals, we could not differentiate the carbonyl signal of the cyclic carbonate (expected at 156.1 ppm) from that of hydroxyurethane one (expected at 157.4 ppm). However, significant changes were observed in the 50-90 ppm spectral region. The signals g, h, i corresponding to the CH of the cyclic carbonates (chemical shift of *trans* and *cis* CH carbonate at 84 ppm and 76 ppm respectively, and terminal carbonate at 77-75 ppm (CH) and 69-71 ppm ( $\text{CH}_2$ ) according to the literature<sup>[24,25]</sup>) showed a decrease of intensity, but it was not possible to confirm their total disappearance. New signals g' and h' corresponding to the hydroxyurethanes (**CH-O-CO-NH**, **CH<sub>2</sub>-CO-NH** and **CH-OH** shift at 77-75 ppm, 67-65 ppm and

## Chapter 4: Synthesis of polyhydroxyurethanes from carbonated polymers

72-70 ppm, respectively, according to literature<sup>[26]</sup>) appeared and overlapped with the epoxide signals c, d, e, f.

The <sup>15</sup>N CP/MAS NMR spectrum of the cross-linked polymer showed a unique signal at 84 ppm, attributed to the hydroxyurethane functions. The signal of HDMA at 30-40 ppm was not observed,<sup>[27]</sup> due to its too low concentration in the final product.

However, based solely on <sup>13</sup>C CP/MAS NMR, it is not possible to state with certainty that no reaction took place with the epoxide. Thus, the reactivity of epoxidized polybutadiene with HMDA was also studied under the same conditions.

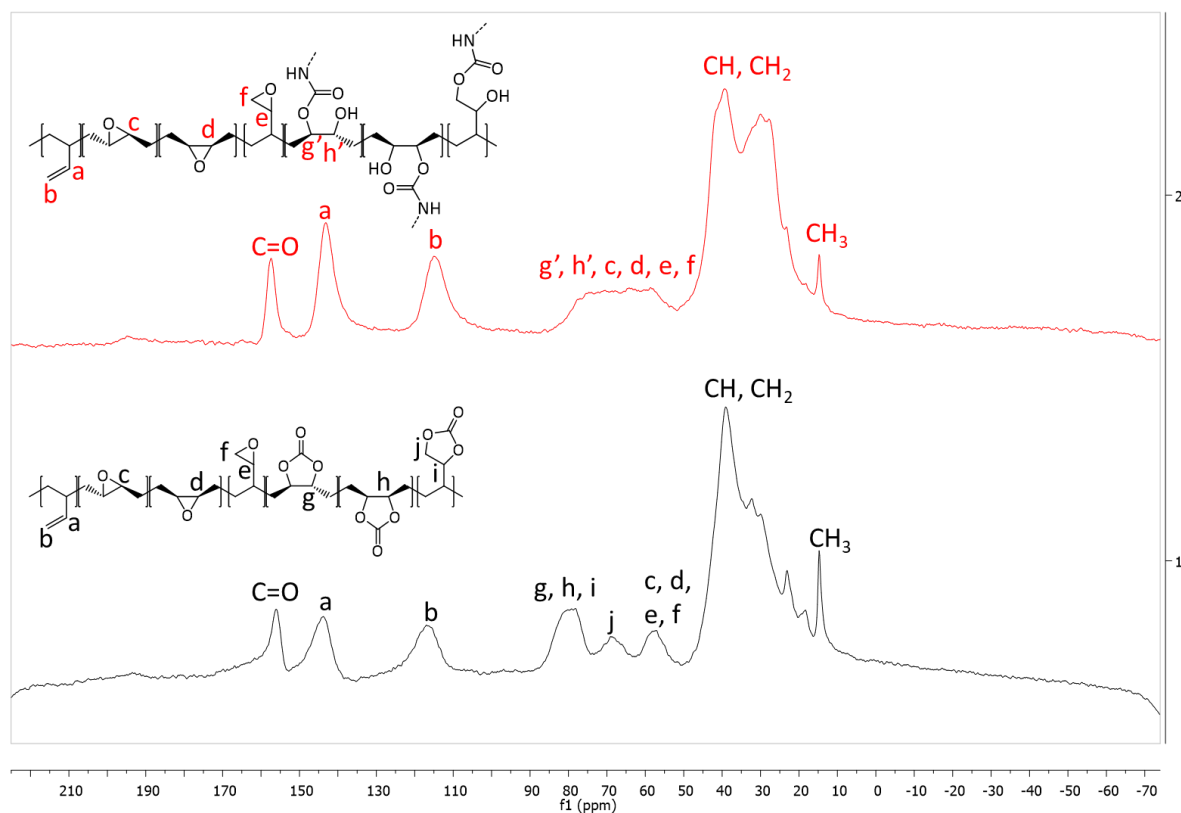


Figure 8. CP/MAS <sup>13</sup>C NMR of the carbonated polybutadiene (black) and cross-linked polybutadiene (red).

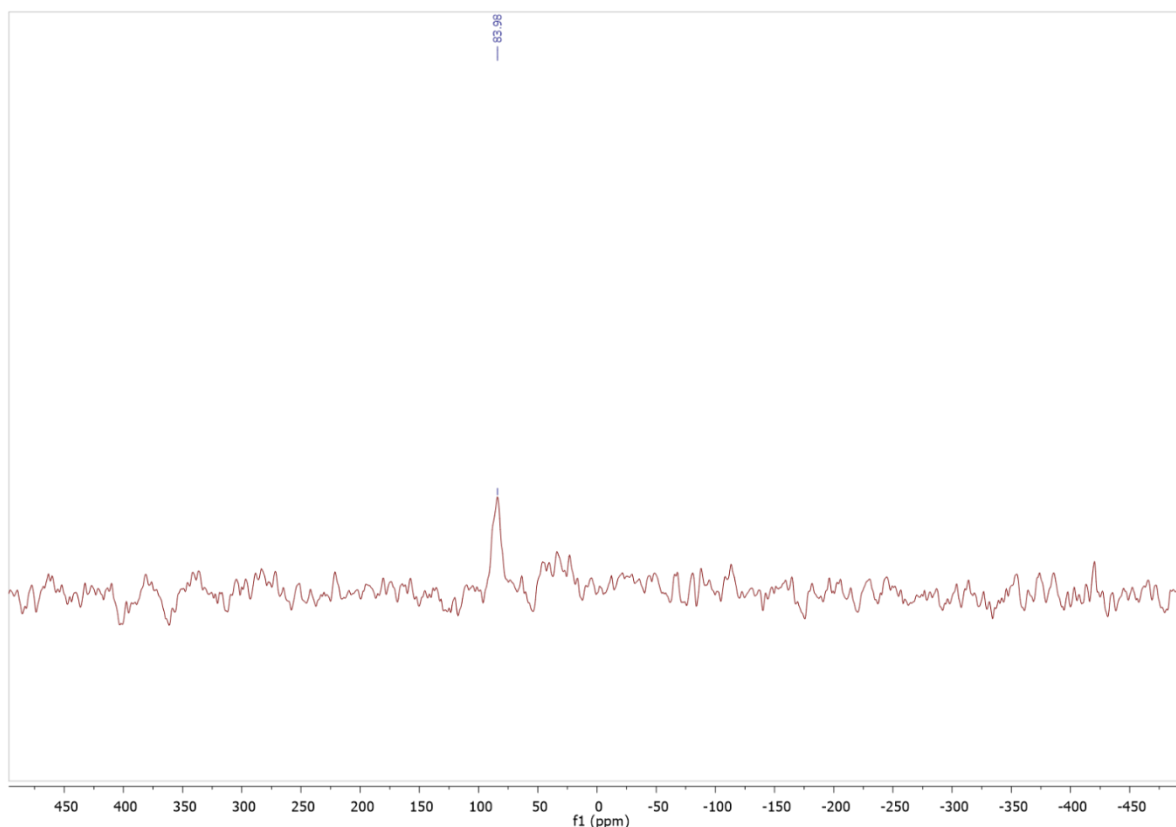
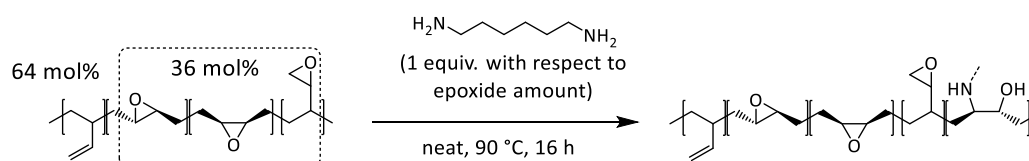


Figure 9. CP/MAS  $^{15}\text{N}$  NMR of the cross-linked polybutadiene.

Consequently, epoxidized polybutadiene E-PBU-3 (64 mol% of vinyl units, *cis:trans:vinyl* epoxide ratio: 8:92:8) was cured with HMDA at 90 °C for 16 hours (Scheme 9), to compare its reactivity with the carbonated polybutadiene. According to ATR-IR analyses, only a small decreased of the epoxide bands intensity at 828 and 863  $\text{cm}^{-1}$  was observed after 16 hours (Figure S109 in appendices). The polymer obtained was fully soluble and analysed by liquid state  $^1\text{H}$  NMR spectroscopy. Only traces of the hydroxyamine fragment could be observed, with the small signal d' at 3.5 ppm corresponding to the proton in  $\alpha$ -position to the alcohol. Approximately 5 % of epoxide were converted according to the  $^1\text{H}$  NMR analysis, these results highlight the much higher reactivity of the internal and terminal cyclic carbonates compared to the internal and terminal epoxides. The poor epoxide reactivity with HDMA is in accordance with the literature



Scheme 9. Reaction of hexamethylene diamine with epoxidized polybutadiene.

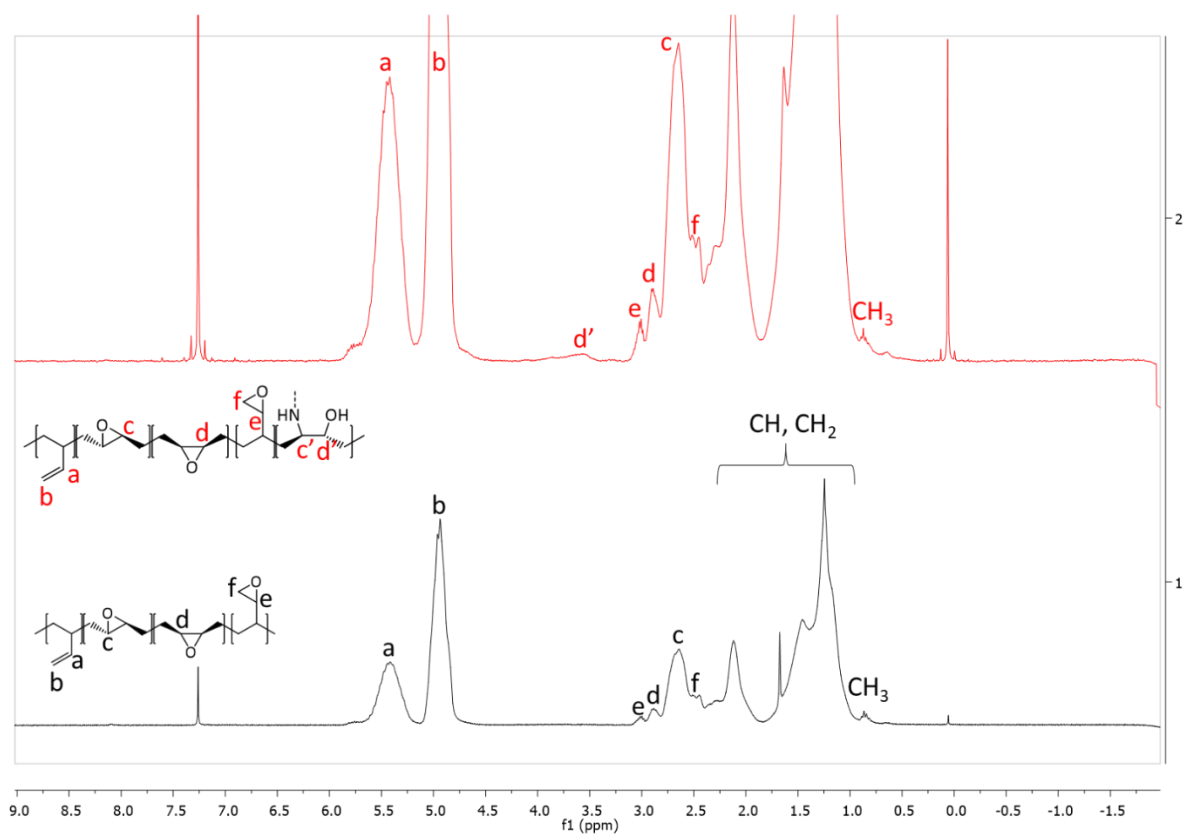


Figure 10.  $^1\text{H}$  NMR spectra of epoxidized polybutadiene before (black) and after reaction with HMDA (1 equiv.) for 16 h at 90 °C (red).



## V. Conclusions

The functionalization of polymers containing terminal, *cis* and/or *trans* cyclic carbonates moieties with amines to form “polyolefins backbone”-based hydroxyurethane materials was successfully achieved. A partially carbonated epoxidized semi-crystalline [ethylene rich-glycidyl methacrylate-methyl acrylate] polymer was effectively functionalized with hexylamine using TBD as catalyst. The terminal cyclic carbonate moiety showed greater reactivity compared to the corresponding epoxide moiety, with complete conversion of the carbonate after 3 hours at 90 °C, whereas the epoxide was converted at 47 %. The reaction should be conducted at a lower temperature to reduce the epoxide reactivity and increase the selectivity towards the hydroxyurethane product.

Moreover, the aminolysis of carbonated epoxidized polybutadienes showed that internal epoxides were not reactive in presence of TBD (30 mol%) with an excess of hexylamine at 90 °C after 17.5 hours, whereas *cis* and *trans* carbonates were readily converted at 96 and 69 % respectively. Thus the following order of carbonate reactivity was observed: *cis* carbonate > *trans* carbonate >> epoxide.

The same conclusions have been drawn with the reaction with hexamethylene diamine, where the carbonated polybutadiene was successfully cross-linked at 90 °C without catalyst, and the cyclic carbonates were completely converted, whereas only minute traces of the ring-opening product from an epoxidized polybutadiene and HDMA reaction was observed by NMR spectroscopy, which is not usually reported in the literature.

This chapter established the proof of concept of the orthogonal cyclic carbonate and epoxide reactivity. This work has to be completed with a study of the rheological, mechanical and thermal properties of the crossed-linked materials obtained from carbonated polymers and diamines, in order to understand the relationship between the hydroxyurethane network structure and the physico-chemical properties of the material. In particular, the exchange rates for CANs & vitrimers could be determined to access the potential of these novel materials both in the melt and under end usage. Their mechanical and chemical resistance and the adhesion properties should be compared with PUs having similar structures to demonstrate the possible industrial use of these materials.

## VI. References

- [1] Akindoyo, J.O.; Beg, M.D.H.; Ghazali, S.; Islam, M.R.; Jeyaratnam, N.; Yuvaraj, A.R. Polyurethane types, synthesis and applications – a review. *RSC Adv.* **2016**, *6*(115), 114453–114482.
- [2] Cornille, A.; Auvergne, R.; Figovsky, O.; Boutevin, B.; Caillol, S. A perspective approach to sustainable routes for non-isocyanate polyurethanes. *European Polymer Journal* **2017**, *87*, 535–552.
- [3] Maisonneuve, L.; Lamarzelle, O.; Rix, E.; Grau, E.; Cramail, H. Isocyanate-Free Routes to Polyurethanes and Poly(hydroxy Urethane)s. *Chem. Rev.* **2015**, *115*(22), 12407–12439.
- [4] Delebecq, E.; Pascault, J.-P.; Boutevin, B.; Ganachaud, F. On the Versatility of Urethane/Urea Bonds: Reversibility, Blocked Isocyanate, and Non-isocyanate Polyurethane. *Chem. Rev.* **2013**, *113*(1), 80–118.
- [5] Blattmann, H.; Fleischer, M.; Bähr, M.; Mülhaupt, R. Isocyanate- and Phosgene-Free Routes to Polyfunctional Cyclic Carbonates and Green Polyurethanes by Fixation of Carbon Dioxide. *Macromolecular Rapid Communications* **2014**, *35*(14), 1238–1254.
- [6] Rokicki, G.; Parzuchowski, P.G.; Mazurek, M. Non-isocyanate polyurethanes: synthesis, properties, and applications: Non-Isocyanate Polyurethanes: Synthesis, Properties, and Applications. *Polym. Adv. Technol.* **2015**, *26*(7), 707–761.
- [7] Gomez-Lopez, A.; Panchireddy, S.; Grignard, B.; Calvo, I.; Jerome, C.; Detrembleur, C.; Sardon, H. Poly(hydroxyurethane) Adhesives and Coatings: State-of-the-Art and Future Directions. *ACS Sustainable Chem. Eng.* **2021**, *9*(29), 9541–9562.
- [8] Pouladi, J.; Mirabedini, S.M.; Eivaz Mohammadloo, H.; Rad, N.G. Synthesis of novel plant oil-based isocyanate-free urethane coatings and study of their anti-corrosion properties. *European Polymer Journal* **2021**, *153*, 110502.
- [9] Liu, X.; Yang, X.; Wang, S.; Wang, S.; Wang, Z.; Liu, S.; Xu, X.; Liu, H.; Song, Z. Fully Bio-Based Polyhydroxyurethanes with a Dynamic Network from a Terpene Derivative and Cyclic Carbonate Functional Soybean Oil. *ACS Sustainable Chem. Eng.* **2021**, *9*(11), 4175–4184.
- [10] Hu, S.; Chen, X.; Torkelson, J.M. Biobased Reprocessable Polyhydroxyurethane Networks: Full Recovery of Crosslink Density with Three Concurrent Dynamic Chemistries. *ACS Sustainable Chem. Eng.* **2019**, *7*(11), 10025–10034.
- [11] Carré, C.; Ecochard, Y.; Caillol, S.; Avérous, L. From the Synthesis of Biobased Cyclic Carbonate to Polyhydroxyurethanes: A Promising Route towards Renewable Non-Isocyanate Polyurethanes. *ChemSusChem* **2019**, *12*(15), 3410–3430.
- [12] Mhd. Haniffa, Mhd.Abd.C.; Munawar, K.; Ching, Y.C.; Illias, H.A.; Chuah, C.H. Bio-based Poly(hydroxy urethane)s: Synthesis and Pre/Post-Functionalization. *Chemistry – An Asian Journal* **2021**, *16*(11), 1281–1297.
- [13] Zhang, B.; Yang, X.; Lin, X.; Shang, H.; Liu, Q.; Wang, H.; Liu, S.; Xu, X.; Dong, F. High-Strength, Self-Healing, Recyclable, and Catalyst-Free Bio-Based Non-Isocyanate Polyurethane. *ACS Sustainable Chem. Eng.* **2023**, *11*(15), 6100–6113.

- [14] Besse, V.; Camara, F.; Méchin, F.; Fleury, E.; Caillol, S.; Pascault, J.-P.; Boutevin, B. How to explain low molar masses in PolyHydroxyUrethanes (PHUs). *European Polymer Journal* **2015**, *71*, 1–11.
- [15] Tomita, H.; Sanda, F.; Endo, T. Model reaction for the synthesis of polyhydroxyurethanes from cyclic carbonates with amines: Substituent effect on the reactivity and selectivity of ring-opening direction in the reaction of five-membered cyclic carbonates with amine. *Journal of Polymer Science Part A: Polymer Chemistry* **2001**, *39*(21), 3678–3685.
- [16] Blain, M.; Jean-Gérard, L.; Auvergne, R.; Benazet, D.; Caillol, S.; Andrioletti, B. Rational investigations in the ring opening of cyclic carbonates by amines. *Green Chem.* **2014**, *16*(9), 4286–4291.
- [17] Sopena, S.; Laserna, V.; Guo, W.; Martin, E.; Escudero-Adán, E.C.; Kleij, A.W. Regioselective Organocatalytic Formation of Carbamates from Substituted Cyclic Carbonates. *Adv. Synth. Catal.* **2016**, *358*(13), 2172–2178.
- [18] Cornille, A.; Blain, M.; Auvergne, R.; Andrioletti, B.; Boutevin, B.; Caillol, S. A study of cyclic carbonate aminolysis at room temperature: effect of cyclic carbonate structures and solvents on polyhydroxyurethane synthesis. *Polym. Chem.* **2017**, *8*(3), 592–604.
- [19] Dechent, S.-E.; Kleij, A.W.; Luinstra, G.A. Fully bio-derived CO<sub>2</sub> polymers for non-isocyanate based polyurethane synthesis. *Green Chem.* **2020**, *22*(3), 969–978.
- [20] Helbling, P.; Hermant, F.; Petit, M.; Tassaing, T.; Vidil, T.; Cramail, H. Unveiling the reactivity of epoxides in carbonated epoxidized soybean oil and application in the stepwise synthesis of hybrid poly(hydroxyurethane) thermosets. *Polym. Chem.* **2023**, *14*(4), 500–513.
- [21] Guerdener, B.; Ayzac, V.; Norsic, S.; Besognet, P.; Bounor-Legaré, V.; Monteil, V.; Dufaud, V.; Raynaud, J.; Chalamet, Y. Carbonatation of [ethylene-glycidyl methacrylate]-based copolymers with carbon dioxide as a reagent: from batch to solvent-free reactive extrusion. *Green Chem.* **2023**, *25*(16), 6355–6364.
- [22] Yadollahi, M.; Bouhendi, H.; Zohuriaan-Mehr, M.J.; Farhadnejad, H.; Kabiri, K.; Mirabedini, S.M. Glycidyl Methacrylate Copolymers Modified with CO<sub>2</sub>. *Soft Materials* **2013**, *11*(4), 430–439.
- [23] Gao, H.; Elsabahy, M.; Giger, E.V.; Li, D.; Prud'homme, R.E.; Leroux, J.-C. Aminated Linear and Star-Shape Poly(glycerol methacrylate)s: Synthesis and Self-Assembling Properties. *Biomacromolecules* **2010**, *11*(4), 889–895.
- [24] Tezuka, K.; Komatsu, K.; Haba, O. The anionic ring-opening polymerization of five-membered cyclic carbonates fused to the cyclohexane ring. *Polym J* **2013**, *45*(12), 1183–1187.
- [25] Wang, L.; Lin, L.; Zhang, G.; Kodama, K.; Yasutake, M.; Hirose, T. Synthesis of cyclic carbonates from CO<sub>2</sub> and epoxides catalyzed by low loadings of benzyl bromide/DMF at ambient pressure. *Chem. Commun.* **2014**, *50*(94), 14813–14816.
- [26] Nohra, B.; Candy, L.; Blanco, J.-F.; Raoul, Y.; Mouloungui, Z. Aminolysis Reaction of Glycerol Carbonate in Organic and Hydroorganic Medium. *Journal of the American Oil Chemists' Society* **2012**, *89*(6), 1125–1133.

[27] Iacomino, M.; Paez, J.I.; Avolio, R.; Carpentieri, A.; Panzella, L.; Falco, G.; Pizzo, E.; Errico, M.E.; Napolitano, A.; Campo, A. del; Ischia, M. d'. Multifunctional Thin Films and Coatings from Caffeic Acid and a Cross-Linking Diamine. *Langmuir* **2017**, *33*(9), 2096–2102.



---

# **Chapter 5:**

## **Carbonated [ethylene – glycidyl methacrylate] based polymers as compatibilizers for polyethylene/polycarbonate blends by reactive extrusion**

---

In **Chapter 5**, the carbonated [ethylene – glycidyl methacrylate] based copolymers will be studied as compatibilizers for polyethylene/polycarbonate blends. The effect of the compatibilizer structure on the morphologies, the mechanical and thermal properties of the blends will be studied.



## Table of Contents

<b>I. Abstract .....</b>	<b>209</b>
<b>II. Introduction.....</b>	<b>211</b>
<b>III. Results and discussion .....</b>	<b>214</b>
III.1.    Compatibilization of HDPE/PC (80/20) blend.....	214
III.1.a.    Morphologies of the blends.....	214
III.1.b.    Spectroscopic characterizations .....	218
III.1.c.    Mechanical properties.....	222
III.1.d.    Thermal properties.....	225
III.2.    Compatibilization of PC/HDPE (80/20) blend.....	228
III.2.a.    Morphologies of the blends.....	228
III.2.b.    Spectroscopic characterizations .....	230
III.2.c.    Mechanical properties.....	233
III.2.d.    Thermal properties.....	235
<b>IV. Conclusions .....</b>	<b>236</b>
<b>V. References.....</b>	<b>237</b>





## I. Résumé

La compatibilisation *in situ* d'un mélange HDPE/PC (80/20) et PC/HDPE (80/20) (w/w) a été réalisée par extrusion réactive en comparant l'efficacité de trois terpolymères différents à base d'[éthylène - méthacrylate de glycidyle] (E-GMA) et de leurs dérivés carbonatés (groupe pendant époxyde du méthacrylate de glycidyle partiellement converti en son dérivé carbonate cyclique).

Dans le cas de la compatibilisation du mélange HDPE/PC (80/20), la dispersion de la phase PC a été améliorée avec les compatibilisants carbonatés, la distribution de taille et le rayon moyen de la phase PC dispersée ayant été réduits. Aucune réactivité de l'époxyde n'a été observée avec le PC, selon les analyses IR-ATR et <sup>1</sup>H NMR, mais les groupes pendants carbonates cycliques ont montré une réactivité partielle, qui pourrait être attribuée à la formation *in situ* du polymère PC-*graft*-CO<sub>2</sub>-E-GMA-MA.

L'allongement à la rupture et la résistance au choc Charpy des mélanges HDPE/PC/compatibilisant (72/18/10) ont été améliorés lorsque les compatibilisants carbonatés à base d'E-GMA ont été utilisés à la place de compatibilisants non carbonatés. La stabilité thermique de la phase PC a diminué lors de l'ajout d'un comptabilisant carbonaté, ce qui confirme le changement de la structure chimique du PC lorsque le groupe pendant carbonate cyclique est présent sur la chaîne polymère.

Dans le cas de la compatibilisation du mélange PC/HDPE (80/20), un comportement différent a été observé. Bien que l'allongement à la rupture ait été amélioré pour les mélanges ternaires avec les compatibilisants carbonatés, ils ont présenté un comportement ductile, et la résistance à l'impact Charpy à l'entaille était très inférieure à celle des mélanges ternaires avec les compatibilisants non carbonatés. Les mélanges compatibilisés ont montré une meilleure adhérence à l'interface. Alors qu'aucune réactivité ou dégradation de l'époxyde n'a été observée avec l'E-GMA-MA comme compatibilisant, les fonctions cycliques du carbonate et de l'époxyde n'ont pas été observées après compatibilisation avec le CO<sub>2</sub>-E-GMA-MA, ce qui pourrait être dû à une compatibilisation réactive et/ou à une dégradation.

## II. Abstract

The *in situ* compatibilization of a HDPE/PC (80/20) and PC/HDPE (80/20) (w/w) blend was performed through reactive extrusion by comparing the efficiency of three different [ethylene – glycidyl methacrylate] (E-GMA) based terpolymers and their carbonated derivatives (epoxide pendant group from glycidyl methacrylate partially converted to its cyclic carbonate derivative).

In the case of the compatibilization of the HDPE/PC (80/20) blend, the dispersion of the PC phase was enhanced with the carbonated compatibilizers as the size distribution and mean radius of the dispersed PC phase was reduced. No reactivity of the epoxide was observed with PC, according to IR-ATR and  $^1\text{H}$  NMR analyses, but cyclic carbonate pendant groups showed partial reactivity, that could be attributed to the *in situ* formation of PC-*graft*-CO<sub>2</sub>-E-GMA-MA polymer.

The elongation at break and the Charpy impact strength of the HDPE/PC/E-GMA based terpolymer (72/18/10) blends were improved when carbonated E-GMA based terpolymers were used instead of non-carbonated terpolymers. The thermal stability of the PC phase decreased with the addition of CO<sub>2</sub>-E-GMA-MA, which confirmed the change of the PC chemical structure when cyclic carbonate pendant group is present on the polymer chain.

In the case of the compatibilisation of the PC/HDPE (80/20) blend, a different behavior was observed. Although the elongation at break was improved for the ternary blends with the carbonated compatibilizers, they exhibited a ductile behavior, and the notch Charpy impact strength was really lower compared to the ternary blends with the non-carbonated compatibilizers. The compatibilized blends showed a better interface adhesion. Whereas no reactivity or degradation of the epoxide was observed with E-GMA-MA as compatibilizer, the cyclic carbonate and epoxide functions were not observed after compatibilization with CO<sub>2</sub>-E-GMA-MA, which might be due to reactive compatibilization and/or degradation.

### **III. Introduction**

Polyethylene (PE) is a semi-crystalline thermoplastic polymer widely used for its low cost production in the domain of packaging, but it also finds applications in biomedical and body protections for example. The macromolecular architecture of PE can be controlled to produce a range of different plastic materials.<sup>[1]</sup> High density PE (HDPE) is a linear polymer with a high degree of crystallinity, thus confer high rigidity and excellent chemical resistance. Some HDPE resins can be obtained by copolymerization of ethylene and low concentrations of  $\alpha$ -olefin (e.g. 1-butene, 1-hexene or 1-octene), in order to decrease the crystallinity. Conversely, low density PE (LDPE) is a branched polymer with a low degree of crystallinity. It is flexible, transparent but has weaker mechanical properties than others PE. Linear low density PE (LLDPE) is a copolymer of ethylene and an  $\alpha$ -olefin. Its higher degree of crystallinity gives better chemical resistance and mechanical properties than LDPE.

However, mechanical and thermal properties of the different PE are not suitable for high-performance applications. Their use is particularly limited by their mechanical and thermal resistance. This is why engineering polymers, such as polycarbonate, are produced and found applications where high mechanical and thermal resistance are required, in the domains of construction, aeronautics, electronics, optics.

Blending polyolefins with high performance polymers present a growing interest, with the objective to produce materials with better properties than pure polyolefins for a wide range of applications, while limiting the cost of production. However, blending of incompatible polymers such as polyethylene and polycarbonate without compatibilizing agent produce materials with poor physico-chemical properties. Structure and polarity differences lead to thermodynamically immiscible blends that present phase separation with weak interfacial adhesion.<sup>[2-4]</sup>

A practical way to improve properties of incompatible polymers blends are the use of compatibilizers which are partially miscible with the two phases to reduce interfacial tension between the different phases, thus improve the dispersion and the cohesion. Moreover, reactive blending are an interesting method to improve interfacial interaction *via* chemical (hydrogen, ionic or covalent) bonding between the different phases.<sup>[2]</sup>

For binary PE/PC blends, it has been commonly observed that the interfacial adhesion was weak when no compatibilizer was used. <sup>[5-9]</sup>. Several non-reactive and reactive

compatibilizers have been reported. LDPE-*graft*-DBAE (diallyl bisphenol A ether) copolymer containing 2.5 wt% of DBAE was used as a premade compatibilizer in PE/PC blends.<sup>[8]</sup> Compatibilized blends with 5 wt% of LDPE-*graft*-DBAE and different composition of PC (from 0 to 35 wt%) were compounded in a co-rotating twin screw extruder with the following profile temperature: 190, 250, 260, 250 °C. The compatibilized blends showed better mechanical properties than the binary blends. Especially, the notch impact strength increased from 19 to 55 kJ/m<sup>2</sup> with 15 wt% of PC when the compatibilizer was used.

Oxidized PE (OPE) (containing 0.125 mol of carboxylic function per gram of polymer) was found to be an effective compatibilizer for the blends of recycled LDPE containing 30 wt% of CaCO<sub>3</sub> with PC resin<sup>[10]</sup>. LDPE/PC (50/50) (w/w) blends without and with compatibilizer were prepared in an internal mixer at 220 °C, 90 rpm for 30 minutes. The addition of 5 wt% of OPE in the blend improved the tensile strength from 15 to 24 MPa, but the elongation at break stayed very low, and only increased from 1.8 to 4.5 %.<sup>[10]</sup>

Closer to our study, Yin *et al.* followed the change of PE/PC (80/20) (w/w) blend morphology without and with the addition of 10 wt% of [ethylene-methyl acrylate-glycidyl methacrylate] (E-GMA-MA) terpolymer (Lotader<sup>®</sup> E-GMA-MA) during extrusion at 250 °C.<sup>[11]</sup> The screw profile was composed of two kneading zones, and samples were taken before and after each kneading zone. The effect of the compatibilizer and of the screw speed was studied, and they found out that the addition of compatibilizer reduce the size of the dispersed phase. After the second kneading zone, at 125 rpm, the mean diameter was decreased from 0.90 to 0.72 μm by using the compatibilizer. A higher screw speed also improved the dispersion. By increasing the speed from 48 to 125 rpm, the mean diameter decreased from 1.14 to 0.72 μm after the second kneading zone with compatibilizer. The decrease of the dispersed phase size was also observed all along the screw at 48 and 125 rpm and for the binary and ternary blends. For example, at 48 rpm without compatibilizer, the mean diameter was 5.00 μm after the first kneading zone, and decreased to 1.16 μm after the second kneading zone.

Moreover, reactive compatibilization has also been reported, PC-*graft*-ethylene-co-acrylic acid (PC-*graft*-EAA) copolymer was employed to modify PE/PC (80/20) (w:w) blends with the *in situ* synthesis of the compatibilizer in a co-rotating twin screw extruder at 250 °C using the catalyst dibutyl tin oxide (DBTO). The formation of the compatibilizer was demonstrated by the increased of the torque during the mixing of PC with EAA (20/80) (w/w) in presence of DBTO (0.8 wt%) at 250 °C in a internal mixer, and the reduction of the crystallinity of the EAA backbone with addition of PC and DBTO, according to DSC analyses. The mean diameter

of the PC dispersed phase in the PE/PC/EAA/DBTO (80/20/5/1) blends decreased from 1.055 to 0.634  $\mu\text{m}$ .<sup>[12]</sup>

Finally, polyethylene glycol (PEG) 2000 was used to compatibilize PC/PE (80/20) blends using a co-rotative twin-screw extruder at 180-250 °C. PEG 2000 and the moisture present in the compatibilizer initiated *in situ* degradation and functionalization of PC, with formation of PEG-*graft*-PC copolymers and carboxylic functions, and partial depolymerization of the PC.<sup>[14]</sup> The addition of 2.5 wt% of PEG 2000 improved the tensile strength from 40 to 50.5 MPa, and change of the thermal properties were observed by DSC (lower crystallinity of the PE phase, and the  $T_g$ 's of the two phases became closer), that indicated the compatibilization of the blend occurred.

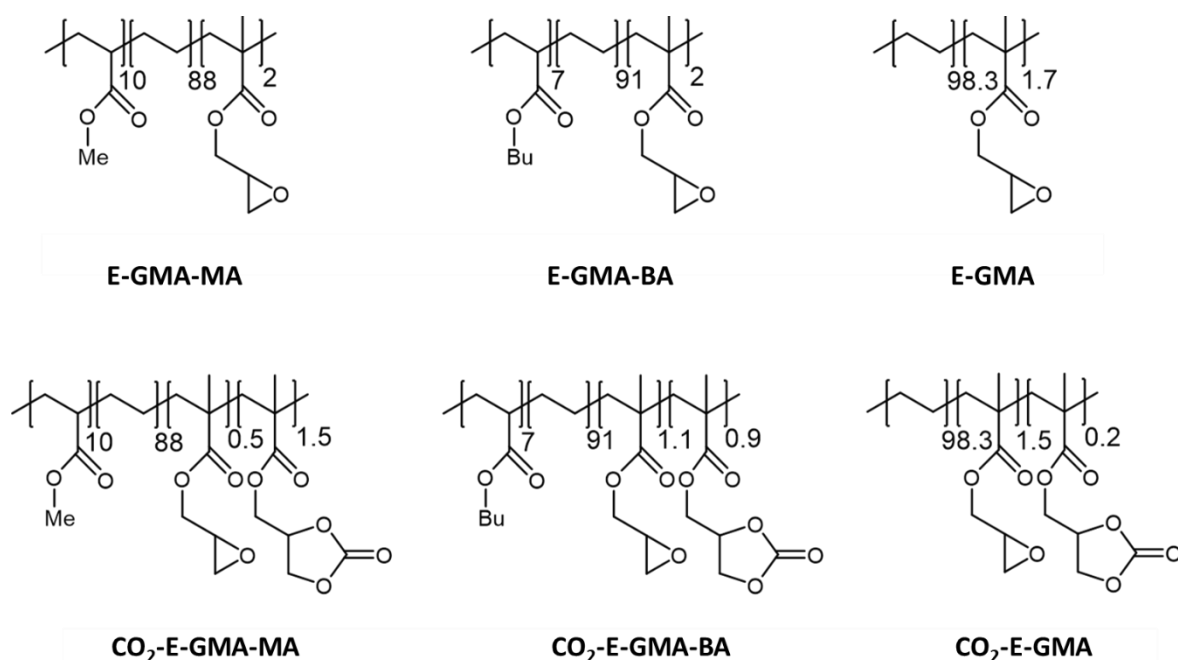
In our previous work, a new process for the carbonatation of apolar semi-crystalline [ethylene – glycidyl methacrylate] based polymers (E-GMA-MA, E-GMA-BA, E-GMA) using carbon dioxide as reagent by reactive extrusion has been described for the first time.<sup>[15]</sup> The glycidyl methacrylate units were partially converted to their cyclic carbonate derivatives, leading to polymers containing both epoxide and cyclic carbonate orthogonal functions.

In this work, the effect of the cyclic carbonate function on the compatibilization of HDPE/PC blends by twin-screw extrusion was investigated. Mechanical properties, morphologies and spectroscopic characterization of the HDPE/PC blends compatibilized with non-carbonated and carbonated compatibilizer was used to determine the influence of the compatibilizers structure and to identify the nature of the interaction at the interface of the HDPE and PC phases.

## IV. Results and discussion

### IV.1. Compatibilization of HDPE/PC (80/20) blend

The six different [ethylene – glycidyl methacrylate] based polymers (*Scheme 1*) have been evaluated as compatibilizers for HDPE/PC blends using twin-screw extruder. The blends were all processed at 250 °C and 400 rpm with throughput of 3.0 kg/h. The final composition of the HDPE/PC/compatibilizer ternary blends was (10/72/18) (w/w/w).



*Scheme 1. Polymers tested as compatibilizers.*

The mechanical and thermal properties of the blends are directly influenced by the strength of the interfacial adhesion that ensures stress transmission between the HDPE and PC phases. Thus the morphologies of the blends will be first be investigated, in order to evaluated the efficiency of the compatibilisation.

#### IV.1.a. Morphologies of the blends

Samples of HDPE/PC (80/20), and HDPE/PC/compatibilizer (72/18/10) blends (directly recovered at the die exit and cooled in a bath water at room temperature) were cryogenically fractured in liquid nitrogen and observed by MEB microscopy (*Figure 1*). The blends present nodular morphologies. Without compatibilizer, the poor adhesion between HDPE and PC phases was highlighted, and voids can be observed in the blends at places where the PC nodules have been pulled off during the cryo-fracture. The average radius in number  $R_n$  of the

dispersed PC phase was 0.71  $\mu\text{m}$ , and the average radius in volume  $R_v$  was 1.53  $\mu\text{m}$  (*Figure 2 (a)*).

The different size distribution of the PC phase in the different formulations showed the effect of the compatibilizers structure on the compatibilization (*Figure 2*). Non-carbonated compatibilizers did not reduce the size distribution of the dispersed PC phase (*Figure 2 (b), (c), (d)*). With E-GMA-MA, the  $R_n$  of the particles was similar (0.71 and 0.74  $\mu\text{m}$  without and with E-GMA-MA, respectively), but the average radius in volume  $R_v$  was smaller, compared to the binary blend (1.53 and 1.11  $\mu\text{m}$  without and with E-GMA-MA, respectively), which indicated a narrower size distribution. With E-GMA-BA, the  $R_n$  was higher (0.91  $\mu\text{m}$ ) and the size distribution was similar ( $R_v = 1.49 \mu\text{m}$ ). Finally, higher  $R_n$  and  $R_v$  were obtained with E-GMA (1.13 and 2.20  $\mu\text{m}$ , respectively). However, a better adhesion was observed at the interface of the two phases (*Figure 1*).

With the addition of a carbonated compatibilizer, the compatibilization of the blend was significantly improved (*Figure 2 (b'), (c'), (d')*).  $R_n$  and  $R_v$  of the dispersed phase decreased for the three grades of GMA copolymers derivatives, compared with native compatibilizers ( $R_n$  was 0.59 , 0.46 and 0.38  $\mu\text{m}$  for  $\text{CO}_2$ -E-GMA-MA,  $\text{CO}_2$ - E-GMA-BA and  $\text{CO}_2$ -E-GMA, respectively), which confirmed that presence of cyclic carbonate had a positive effect on the compatibilization of HDPE and PC. The adhesion between HDPE and PC phases was also improved compared to the binary HDPE/PC (80/20) blend.

It is more complex to establish the effect of the acrylate co-monomer structure on the PC phase dispersion. For the blends with non-carbonated compatibilizer, the mean radius of the PC phase increased and broader size distribution was obtained according to the following trends: E-GMA-MA < E-GMA-BA < E-GMA. It could be directly linked to the polymer polarity that follows the same order. However, the opposite trend was observed with the carbonated compatibilizer:  $\text{CO}_2$ -E-GMA <  $\text{CO}_2$ -E-GMA-BA <  $\text{CO}_2$ -E-GMA-MA for the mean size of the PC phase. Other properties such as blend viscosity, compatibilizer molar masses and cyclic carbonate contents have to be taken into account to fully understand the impact of acrylate structure.



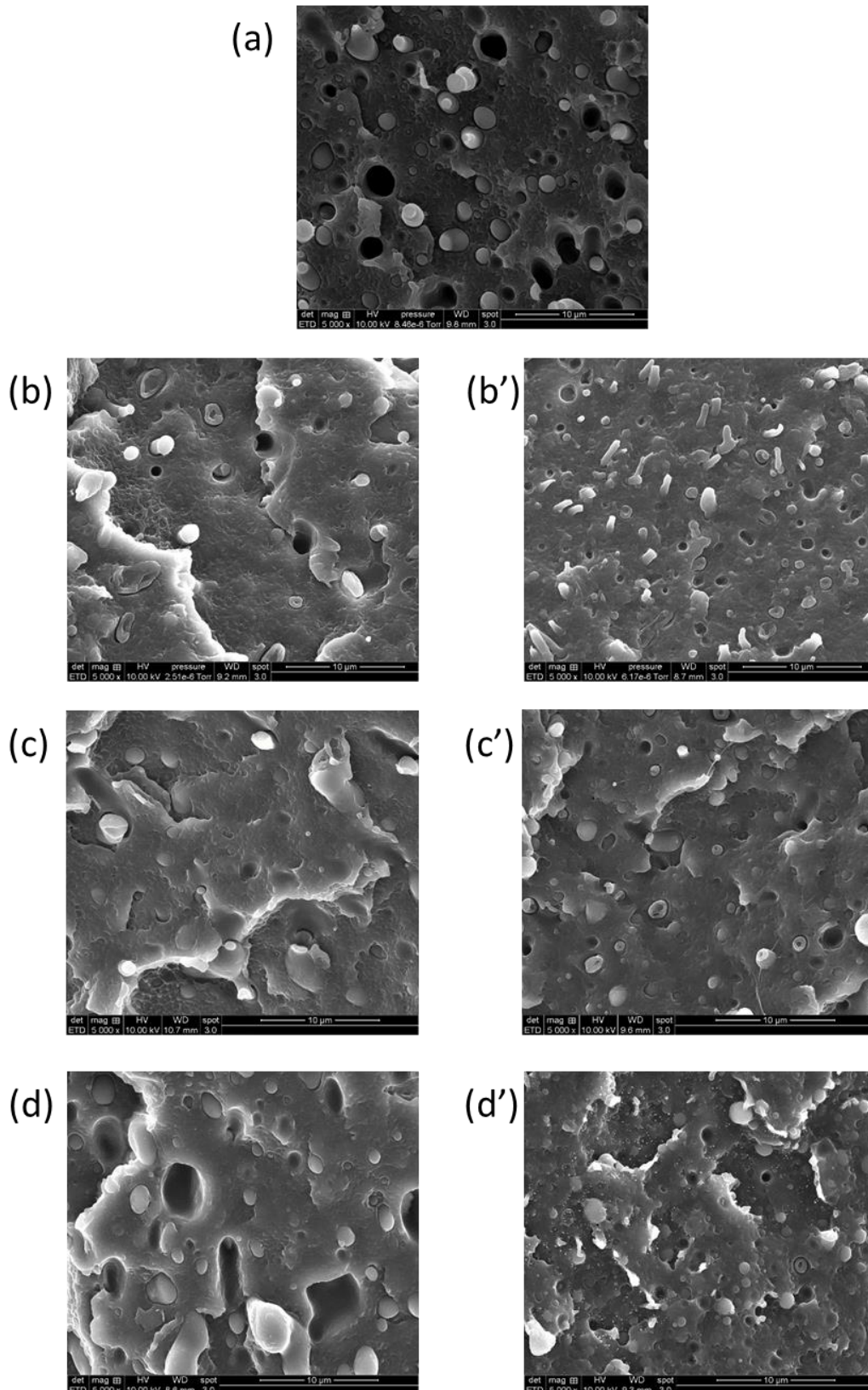


Figure 1. SEM images of (a) HDPE/PC (80/20) (w/w) blend and HDPE/PC/compatibilizer (72/18/10) (w/w/w) blends: (b) E-GMA-MA, (b') CO<sub>2</sub>-E-GMA-MA, (c) E-GMA-BA, (c') CO<sub>2</sub>-E-GMA-BA, (d) E-GMA and (d') CO<sub>2</sub>-E-GMA.

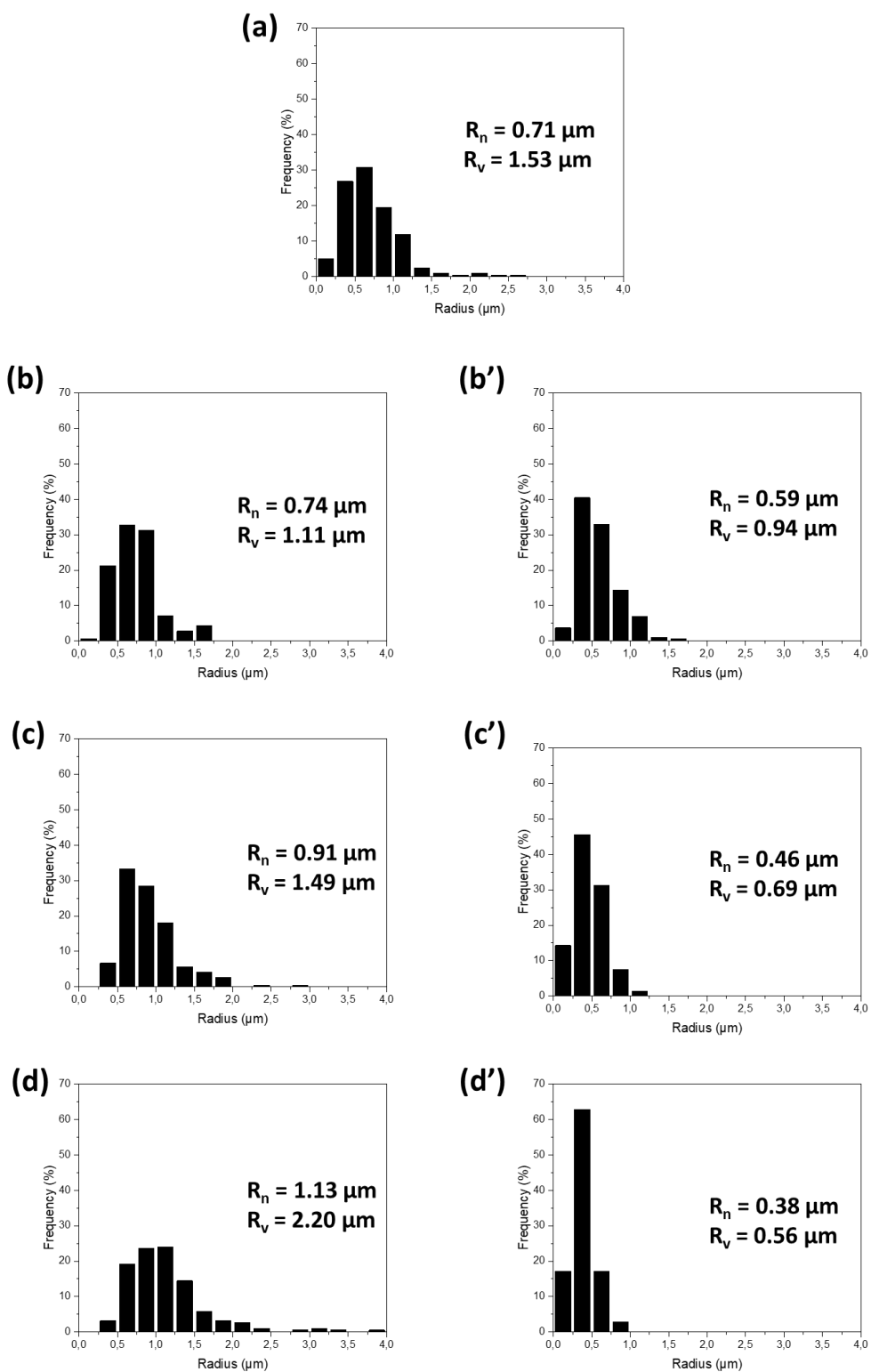


Figure 2. Size distribution of the dispersed PC phase in (a) HDPE/PC (80/20) (w/w) blend and HDPE/PC/compatibilizer (72/18/10) (w/w/w) blends: (b) E-GMA-MA, (b') CO<sub>2</sub>-E-GMA-MA, (c) E-GMA-BA, (c') CO<sub>2</sub>-E-GMA-BA, (d) E-GMA and (d') CO<sub>2</sub>-E-GMA.

#### IV.1.b. Spectroscopic characterizations

The PC phases of the HDPE/PC/E-GMA-MA and HDPE/PC/CO<sub>2</sub>-E-GMA-MA blends were extracted from the HDPE matrices using Soxhlet extractor and dichloromethane as solvent. 41 wt% of the total mass of PC and E-GMA-MA was extracted from the HDPE/PC/E-GMA-MA blend, and 52 wt% from the HDPE/PC/CO<sub>2</sub>-E-GMA-MA blend. Thus, a part of the compatibilizer and PC were still in PE phase. A higher extraction rate was obtained for the blend with the carbonated compatibilizer, which showed the better compatibility of the carbonated compatibilizer with PC, compared to the non-carbonated compatibilizer. Each phase was characterized by IR-ATR and <sup>1</sup>H NMR spectroscopies, to observe any reaction of the epoxide or cyclic carbonate functions.

IR-ATR spectra of HDPE and PC extracted phases of the HDPE/PC/E-GMA-MA (72/18/10) blend (*Figure 3 (a)*) showed that HDPE phase was still containing residue of PC and E-GMA-MA after extraction. The characteristic ester band of E-GMA-MA (1735 cm<sup>-1</sup>) and carbonate band of PC (1764 cm<sup>-1</sup>) were still present, but at a very low intensity. Conversely, the PC phase spectrum showed a higher intensity of the E-GMA-MA characteristic band, which demonstrates the good affinity of the E-GMA-MA with PC. The same observations were made with the HDPE/PC/CO<sub>2</sub>-E-GMA-MA (78/18/10) blend (*Figure 3 (b)*). Residues of carbonated compatibilizer and PC were still present in the HDPE phase, and the strong ester characteristic band of the carbonated CO<sub>2</sub>-E-GMA-MA was observed in the PC phase IR spectrum. The characteristic band of the cyclic carbonate (1820 cm<sup>-1</sup>) was also present. According to these IR analyses, cyclic carbonate functions are still present in the polymer blends.

According to the literature<sup>[16–18]</sup> and to the <sup>1</sup>H and <sup>13</sup>C NMR spectra of the pure PC (see *Figure S118* and *Figure S119* appendices), the polymer contains phenolic and tertbutoxy end groups, with the characteristic signals of the phenolic groups at 6.8 ppm in <sup>1</sup>H NMR and 114.9 ppm in <sup>13</sup>C NMR, and signals of tertbutyl-phenoxy group at 1.36 ppm in <sup>1</sup>H NMR, 31.53 and 34.66 ppm in <sup>13</sup>C NMR.

<sup>1</sup>H NMR analyses of the blends were in accordance with the IR spectra. For the HDPE/PC/E-GMA-MA (72/18/10) (*Figure 4 (a)*), <sup>1</sup>H NMR spectrum of the HDPE phase also showed residual signals of E-GMA-MA (methyl acrylate signal at 3.50 ppm) and PC (aromatic proton signals at 7.00-7.20 ppm) and the epoxide proton signals a, b and c were identified. In the PC phase, methyl acrylate and epoxide signals were also observed. The ratio between the integration of the signal a and methyl acrylate signal was calculated on the native E-GMA-MA and the PC phase <sup>1</sup>H NMR spectra; and was equal to 0.067 and 0.070, respectively. Therefore,

the epoxide signals intensity did not significantly change after blending, and thus no reactivity of epoxyde function was observed.

For the blends with CO<sub>2</sub>-E-GMA-MA (*Figure 4 (b)*), <sup>1</sup>H NMR of the HDPE phase showed the carbonated compatibilizer signals (methyl acrylate signal at 3.50 ppm, cyclic carbonate signals d, e and f at 3.75-4.5 ppm and epoxide signals). <sup>1</sup>H NMR spectrum of the PC phases also showed signals of CO<sub>2</sub>-E-GMA-MA. The epoxide and cyclic carbonate signals were still present. However, the ratio between signal a and methyl acrylate, and signal e and methyl acrylate were calculated on the native CO<sub>2</sub>-E-GMA-MA (0.019 and 0.034 respectively) and PC phase (0.016 and 0.024, respectively) from the <sup>1</sup>H NMR spectra. The intensity of the epoxide signal did not significantly decrease, but the carbonate signal decreased of 30 % in intensity. This decrease could be due to the partial reactivity of cyclic carbonate with PC and the *in situ* formation of PC-*graft*-CO<sub>2</sub>-E-GMA-MA. Moreover, a new signal at 6.5 ppm may indicate that the end groups of PC reacted with the compatibilizer.

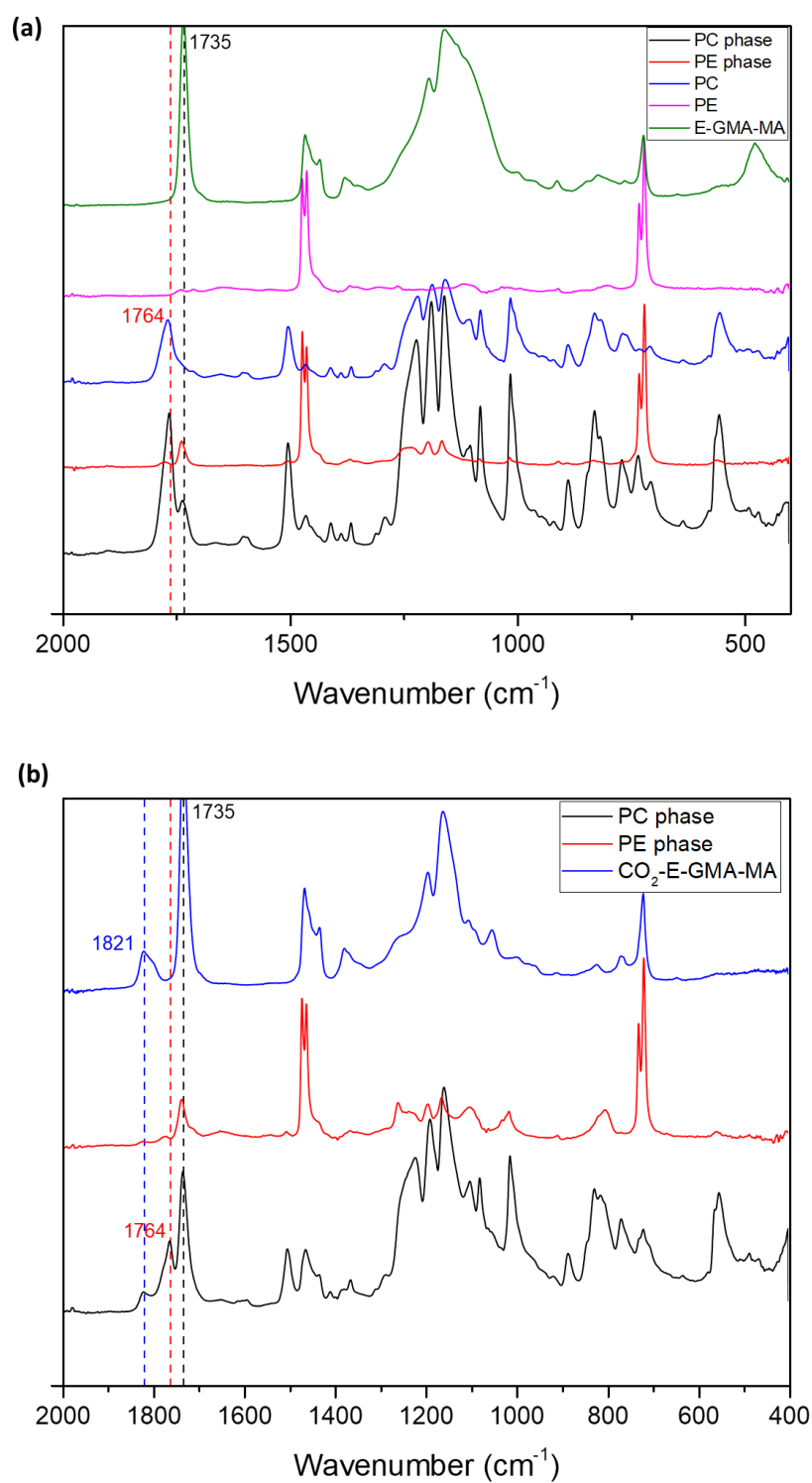


Figure 3. IR-ATR spectra of PC and HDPE phases of (a) HDPE/PC/E-GMA-MA (72/18/10) blend and (b) HDPE/PC/CO<sub>2</sub>-E-GMA-MA (72/18/10) blend.

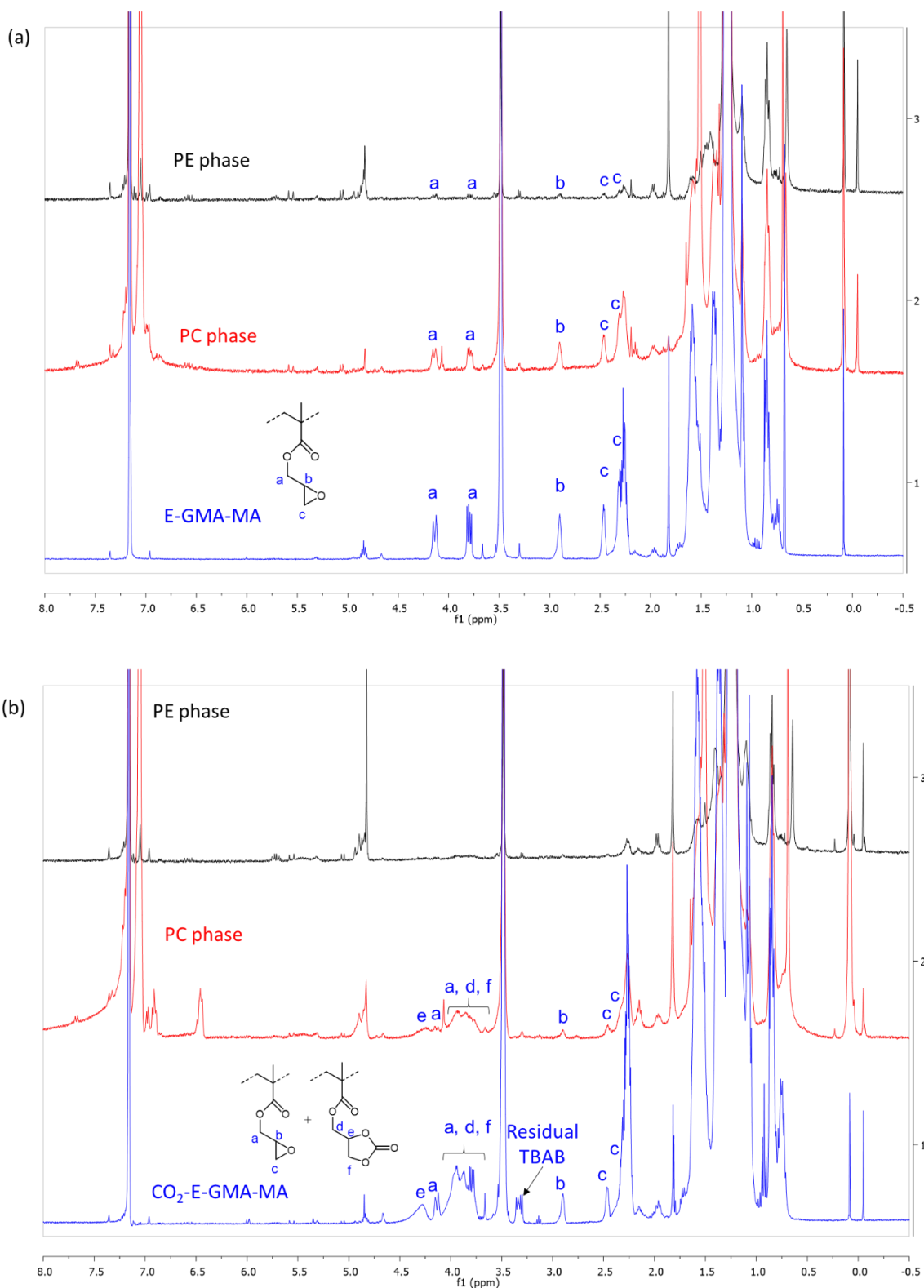


Figure 4. <sup>1</sup>H NMR (TCE/C<sub>6</sub>D<sub>6</sub>, 400 MHz) spectra of PC and HDPE phases of (a) HDPE/PC/E-GMA-MA (72/18/10) blend and (b) HDPE/PC/ CO<sub>2</sub>-E-GMA-MA (72/18/10) blend.

#### IV.1.c. Mechanical properties

Tensile tests (tensile curves of the blends in appendices) and Charpy impact tests were performed at 23 °C on the pure HDPE and PC, and on the HDPE/PC/compatibilizer blends to determine their Young's modulus, tensile strength, elongation at break and Charpy impact strength. Notched specimens (notch of 2 mm) were used for the Charpy impact tests.

*Table 1* compares the mechanical properties of pure HDPE and PC, and of the different HDPE/PC/compatibilizer blends. PC showed a higher Young's modulus and tensile strength. The two polymers had a similar elongation at break, and finally, HDPE exhibited a much higher Charpy impact strength, due to the lower  $T_g$  of HDPE. Without compatibilizer, HDPE/PC blend (80/20) showed a slight increase of the modulus and tensile strength compared with HDPE due to the addition of PC, but a bad compatibility of the two phases was confirmed, according to the low elongation at break and Charpy impact strength (*Table 1*, entry 1). Addition of compatibilizer, in every case, led to a slight decrease of the modulus and tensile strength because of the elastic properties of the compatibilizers but the elongation at break and Charpy impact strength were improved in every case, compared with the binary HDPE/PC blend. Interestingly, the benefic effect from the cyclic carbonate functions was observed with the significant improvement of the elongation at break and Charpy impact strength when carbonated E-GMA based copolymers was used as compatibilizer instead of non-carbonated E-GMA based polymers. When CO<sub>2</sub>-E-GMA-MA was added instead of E-GMA-MA, the elongation at break increased from 35 to 90 %, which is an improvement of 157%, and the impact strength increased from 24.8 to 39.8 kJ/m<sup>2</sup>, thus it was improved to 60 % (*Table 1*, entries 2 and 5). Similar trend was observed with CO<sub>2</sub>-E-GMA-BA and CO<sub>2</sub>-E-GMA, where the elongation at break and impact strength were improved compared with E-GMA-BA and E-GMA (*Table 1*, entries 3, 4, 6, 7).

Charpy Impact strength was also impacted by the acrylate comonomer structure. The following trend were observed E-GMA-MA > E-GMA-BA > E-GMA and it is in accordance with the decrease of the polymer's polarity (*Table 1*, entries 2-4). E-GMA is the most apolar as it contains 92 wt% of ethylene, and E-GMA-BA is less polar than E-GMA-MA as it contained butyl acrylate instead of methyl acrylate. The higher polarity of E-GMA-MA improved the affinity between the HDPE and PC phases. For the carbonated compatibilizer the same trend was observed: CO<sub>2</sub>-E-GMA-MA > CO<sub>2</sub>-E-GMA-BA > CO<sub>2</sub>-E-GMA (*Table 1*, entries 5-7), and could be also related to the cyclic carbonate content which also decreases in this order (73, 47, 12 %

of epoxide converted to cyclic carbonate for CO<sub>2</sub>-E-GMA-MA, CO<sub>2</sub>-E-GMA-BA, CO<sub>2</sub>-E-GMA, respectively).

Finally, mechanical properties of HDPE/PC/CO<sub>2</sub>-E-GMA-MA (*Table 1*, entry 5) were closed to initial HDPE properties. The two materials had a similar tensile strength and elongation at break and HDPE had a slightly higher modulus, but the impact strength was much higher for the compatibilized blend (39.8 kJ/m<sup>2</sup> instead of 25.0 kJ/m<sup>2</sup>).

The blends were also characterized by DSC and TGA to study the impact of the compatibilizer on the HDPE crystallinity and thermal stability of the blend.

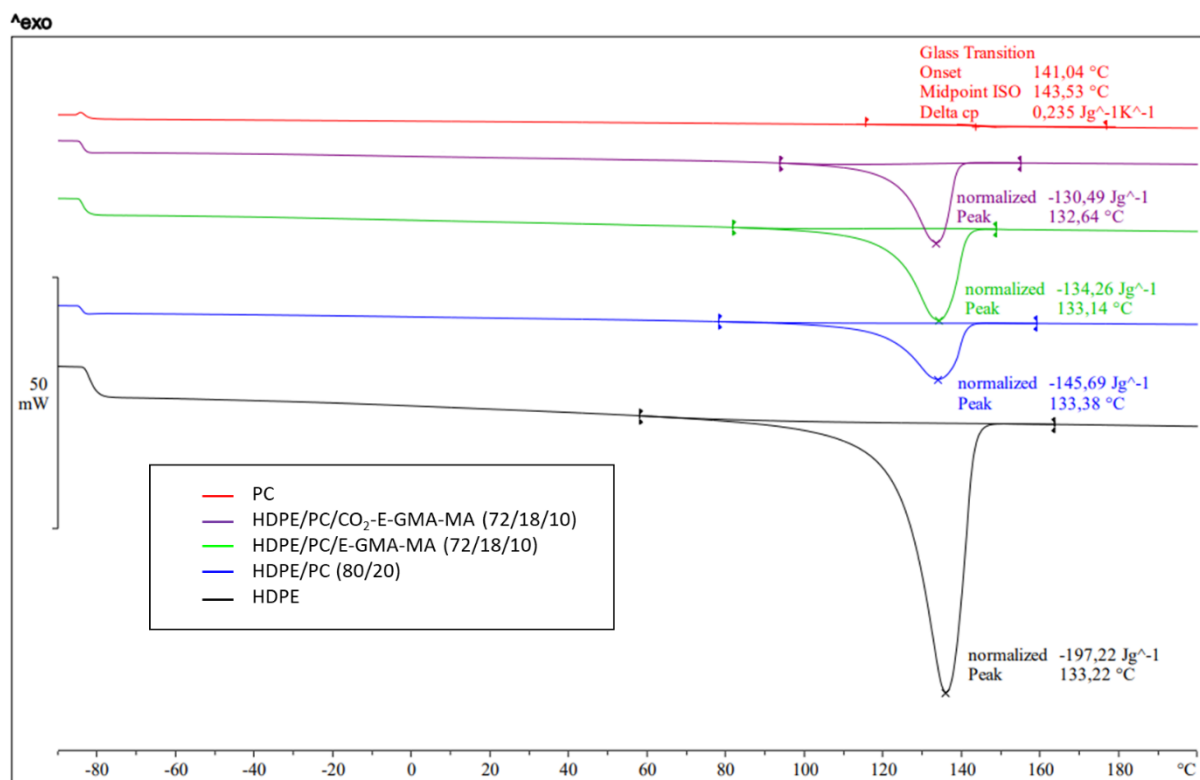


Table 1. Mechanical properties of the HDPE/PC/E-GMA based terpolymer (72/18/10) blends.

Entry	Compatibilizer	HDPE/PC/compatibilizer weight proportion	Young's Modulus (GPa)	Tensile Strength (MPa)	Elongation at break (%)	Impact strength (kJ/m <sup>2</sup> )
1	/	100/0/0	0.78 ± 0.08	29 ± 2	120 ± 40	25.0 ± 2.0
2	/	0/100/0	1.6 ± 0.1	73 ± 5	116 ± 15	9.3 ± 0.9
3	/	80/20/0	0.89 ± 0.02	35 ± 2	23 ± 4	4.4 ± 0.9
4	E-GMA-MA	72/18/10	0.66 ± 0.03	31 ± 2	35 ± 5	24.8 ± 2.0
5	E-GMA-NA		0.70 ± 0.04	29.1 ± 0.5	32 ± 9	9.9 ± 1.3
6	E-GMA		0.78 ± 0.02	30 ± 2	32 ± 3	5.0 ± 0.8
7	<b>CO<sub>2</sub>-E-GMA-MA</b>		<b>0.63 ± 0.04</b>	<b>27 ± 2</b>	<b>90 ± 20</b>	<b>39.8 ± 3.8</b>
8	CO <sub>2</sub> -E-GMA-NA		0.71 ± 0.03	27 ± 1	54 ± 5	14.6 ± 4.8
9	CO <sub>2</sub> -E-GMA		0.80 ± 0.03	29 ± 2	86 ± 12	6.7 ± 0.8

IV.1.d. Thermal properties

In *Figure 5*, the DSC curves of HDPE, PC and of the blends are presented. Compared to pure HDPE, the HDPE/PC binary blend exhibited a significant decrease of the melting enthalpy (absolute values decreased from 197.2 to 182.1 J/g of HDPE). With the ternary HDPE/PC/E-GMA-MA (72/18/10) and HDPE/PC/CO<sub>2</sub>-E-GMA-MA (72/18/10) blends, there was no significant change of the HDPE melting enthalpy (186.5 and 181.2 J/g). Concerning the  $T_g$  of the PC, it could not be observed in the different blends due to the too low concentration of PC.



*Figure 5. DSC of HDPE/PC/compatibilizer (72/18/10) blends.*

The thermal stability of the pure polymers and of the blends was investigated by TGA (*Figure 6*). According to temperature at 10 % of decomposition ( $T_{10\%}$ ) and the residual ash at 650 °C (*Table 2*), the thermal stability decreased as followed: PC > HDPE > HDPE/PC (80/20) > HDPE/PC/E-GMA-MA (72/18/10)  $\approx$  HDPE/PC/CO<sub>2</sub>-E-GMA-MA (72/18/10). The compatibilized blends exhibit a lower stability due to the degradation of GMA and MA units starting at lower temperature (10 % decomposition of E-GMA-MA and CO<sub>2</sub>-E-GMA-MA at 410 °C, see *Figure S10* and *Figure S23* appendices), compared to pure HDPE.

Moreover, on the first derivatives of the TGA curves (*Figure 6 (b)*), the peak decomposition of PC at 524.5 °C was observed for HDPE/PC and HDPE/PC/E-GMA-MA blends, but it was not

the case for the HDPE/PC/CO<sub>2</sub>-E-GMA-MA blend. The change of the thermal properties of the PC phase in this case indicated that a possible change of the chemical structure occurred during the blending process. This observation could be explained by the reactive compatibilization and formation of the PC-*graft*-CO<sub>2</sub>-E-GMA-MA copolymer.

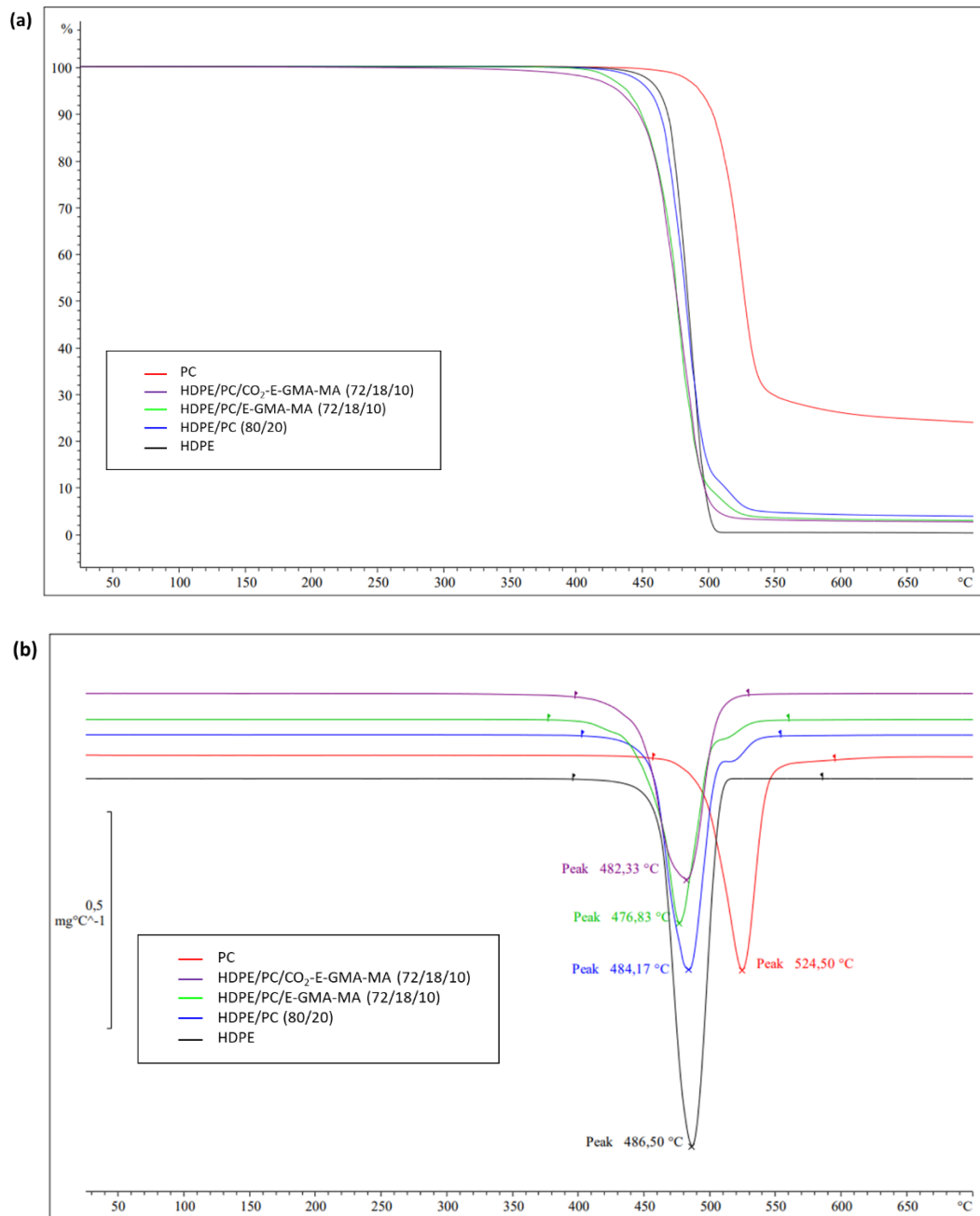


Figure 6. (a) TGA (10 °C/min, under N<sub>2</sub> ( mL/min) curves and (b) first derivatives of TGA curves of HDPE/PC/compatibilizer (72/18/10) blends.

**Chapter 5: Carbonated [ethylene - glycidyl methacrylate] based polymers as compatibilizers for polyethylene/polycarbonate blends by reactive extrusion**

---

*Table 2. Thermal degradation of HPDE/PC/compatibilizer (72/18/10) blends.*

---

<b>Entry</b>	<b>Compatibilizer</b>	<b>HPDE/PC/Compatibilizer composition (w/w/w)</b>	<b><math>T_{d,10\%}</math> (°C)</b>	<b><math>T_{max}</math> (°C)</b>	<b>Residual ash at 650 °C (%)</b>
1	/	100/0/0	470	486.5	0.2
2	/	0/100/0	504	524.5	24.1
3	/	80/20/0	465	484.2	4.0
4	E-GMA-MA	72/18/10	450	476.8	3.0
5	CO <sub>2</sub> -E-GMA-MA	72/18/10	446	482.3	2.8

---

## IV.2. Compatibilization of PC/HDPE (80/20) blend

Although PC exhibits very high mechanical resistance (high modulus and high impact strength), one of its main drawbacks is its notch sensitivity.<sup>[14,19-21]</sup> The addition of HDPE in PC could be an interesting method to improve the notch sensitivity by improving the softness of the material. Thus, the compatibilization of PC/HDPE (80/20) blend was investigated. The six different compatibilizers were used as compatibilizers and the effect of their structure on the mechanical properties and morphology of the blend was studied, as previously with the HDPE/PC (80/20) blend.

### IV.2.a. Morphologies of the blends

The morphologies of the binary blends PC/HDPE (80/20) and of the HDPE/PC/E-GMA-MA and HDPE/PC/CO<sub>2</sub>-E-GMA-MA (18/72/10) ternary blends were observed in MEB to study the influence of the compatibilizer structure on the interface adhesion and the dispersion of the HDPE phase.

According to the SEM images (*Figure 7*), the adhesion at the interface of the PC and HDPE phases was improved by using the non-carbonated and carbonated compatibilizers. The size of the dispersed PE phase was also reduced using the non-carbonated E-GMA-MA. The  $R_n$  and the  $R_v$  were respectively decreased from 0.74 to 0.59  $\mu\text{m}$  and from 1.11 to 0.94  $\mu\text{m}$  (*Figure 8*).

The morphology of the HDPE phase in the ternary blend with the CO<sub>2</sub>-E-GMA-MA was more complex, it was not possible to identify PE and PC phases and thus to determine the size distribution of the PC phase in this case.

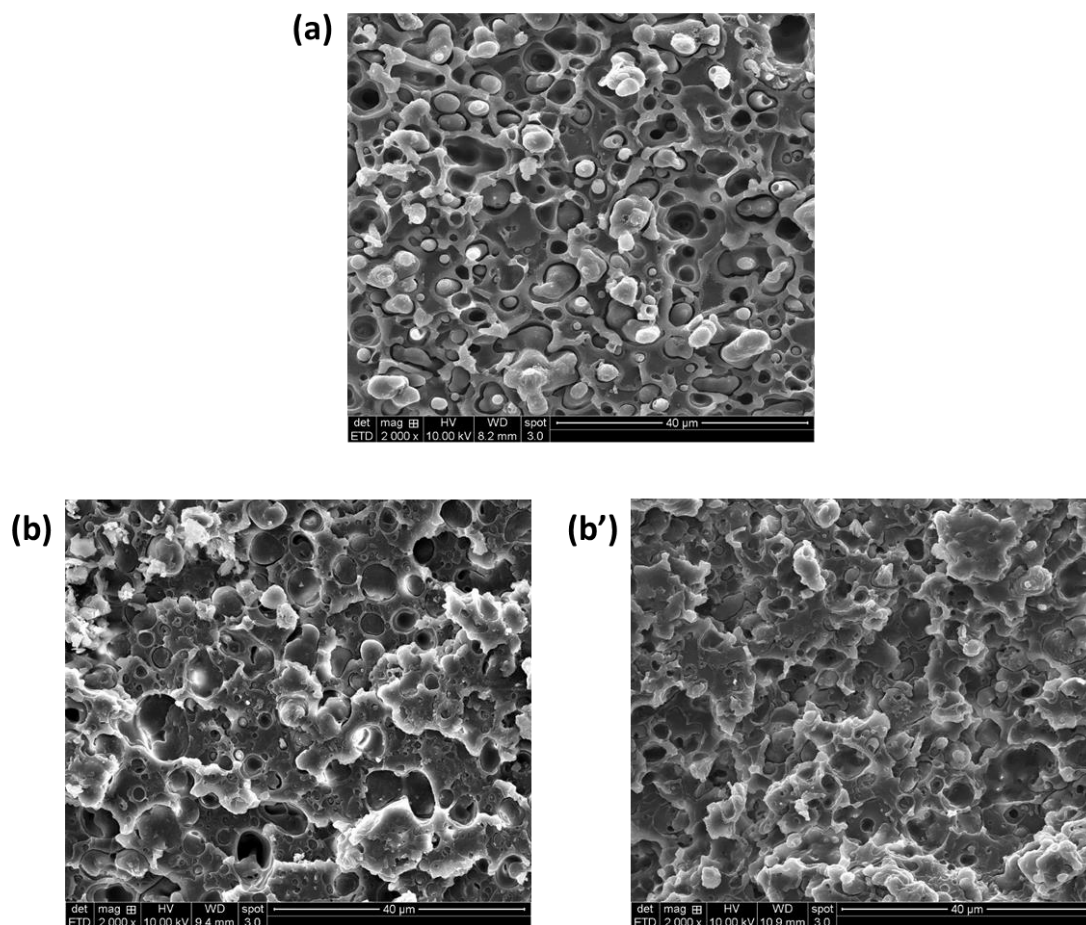


Figure 7. SEM images of (a) PC/HDPE (80/20) (w/w) blend and HDPE/PC/compatibilizer (18/72/10) (w/w/w) blends: (b) E-GMA-MA and (b') CO<sub>2</sub>-E-GMA-MA.

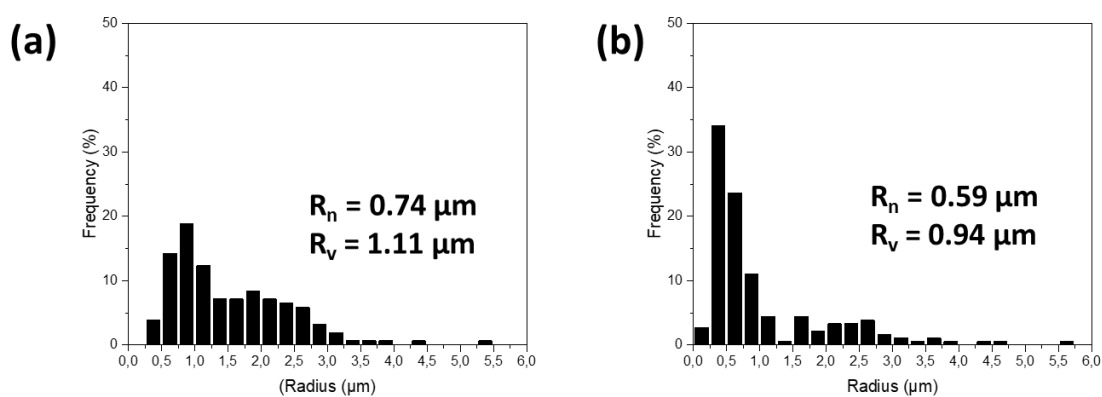


Figure 8. Size distribution of the dispersed PC phase in (a) PC/HDPE (80/20) (w/w) blend and (b) HDPE/PC/E-GMA-MA (72/18/10) (w/w/w) blend.

#### IV.2.b. Spectroscopic characterizations

The PC phases of the HDPE/PC/E-GMA-MA and HDPE/PC/CO<sub>2</sub>-E-GMA-MA (18/72/10) blends were extracted by Soxhlet extractor with dichloromethane. 93 wt% of the total mass of PC and E-GMA-MA was extracted from the HDPE/PC/E-GMA-MA blend, and 93 wt% from the HDPE/PC/CO<sub>2</sub>-E-GMA-MA blend. The PC and HDPE phases were analyzed by ATR-IR and <sup>1</sup>H NMR.

According to the ATR-IR analyses, the characteristic bands of PC (1764 cm<sup>-1</sup>) and E-GMA-MA (1735 cm<sup>-1</sup>) were still present in the PE phase of the HDPE/PC/E-GMA-MA blend, with a relatively high intensity. Thus, the PC phase was not completely extracted (*Figure 9 (a)*). In comparison, the IR spectra of the PC phase showed the characteristic band of E-GMA-MA, but at a low intensity. Thus the main part of E-GMA-MA remained in the PE phase. At too high concentration of the PC, E-GMA-MA may have a better compatibility with HDPE.

Conversely, for the HDPE/PC/CO<sub>2</sub>-E-GMA-MA blend, no PC was detected in the HDPE phase, and the ester characteristic band of CO<sub>2</sub>-E-GMA-MA was observed at low intensity (*Figure 9 (b)*). The cyclic carbonate band (1821 cm<sup>-1</sup>) was not observed in the HDPE and PC phases, which could be attributed to a possible reaction or degradation of the cyclic carbonate functions.

In <sup>1</sup>H NMR spectra, the epoxide function was observed in the HDPE and PC phases of the HDPE/PC/E-GMA-MA (18/72/10) blend. In PC phase <sup>1</sup>H NMR spectrum, the ratio between the integration of the signal b and methyl acrylate signal (3.50 ppm) was calculated, and was similar to the ratio calculated on the native E-GMA-MA <sup>1</sup>H spectrum. (0.068 and 0.067, respectively). Therefore, the epoxide signals intensity did not significantly change after blending, and thus no reactivity was observed. The same observation was made with the HDPE phase, the ratio between the two signals was 0.068 (*Figure 10 (a)*).

Conversely, the signals of the cyclic carbonate and epoxide were not observed in the <sup>1</sup>H NMR spectra of the HDPE and PC phases of the HDPE/PC/CO<sub>2</sub>-E-GMA-MA blends (*Figure 10 (b)*). Possible reactive compatibilization could explain the disappearance of these signals, but the degradation of the cyclic carbonate and epoxide could also occur. In presence of traces of water and residual tetrabutylammonium bromide from the carbonation step, the cyclic carbonate and epoxide could be hydrolyzed to form the corresponding diol.<sup>[22]</sup> Moreover, the new signal at 6.5 ppm observed in the PC phase <sup>1</sup>H NMR spectra (attributed to aromatic protons) may be due to possible degradation of the PC with residual water present in CO<sub>2</sub>-E-GMA-MA, which could form OH groups on the PC macromolecules, or due to the reaction of

OH end groups with the cyclic carbonate to produce PC-*graft*-E-GMA-MA polymers, as observed before.

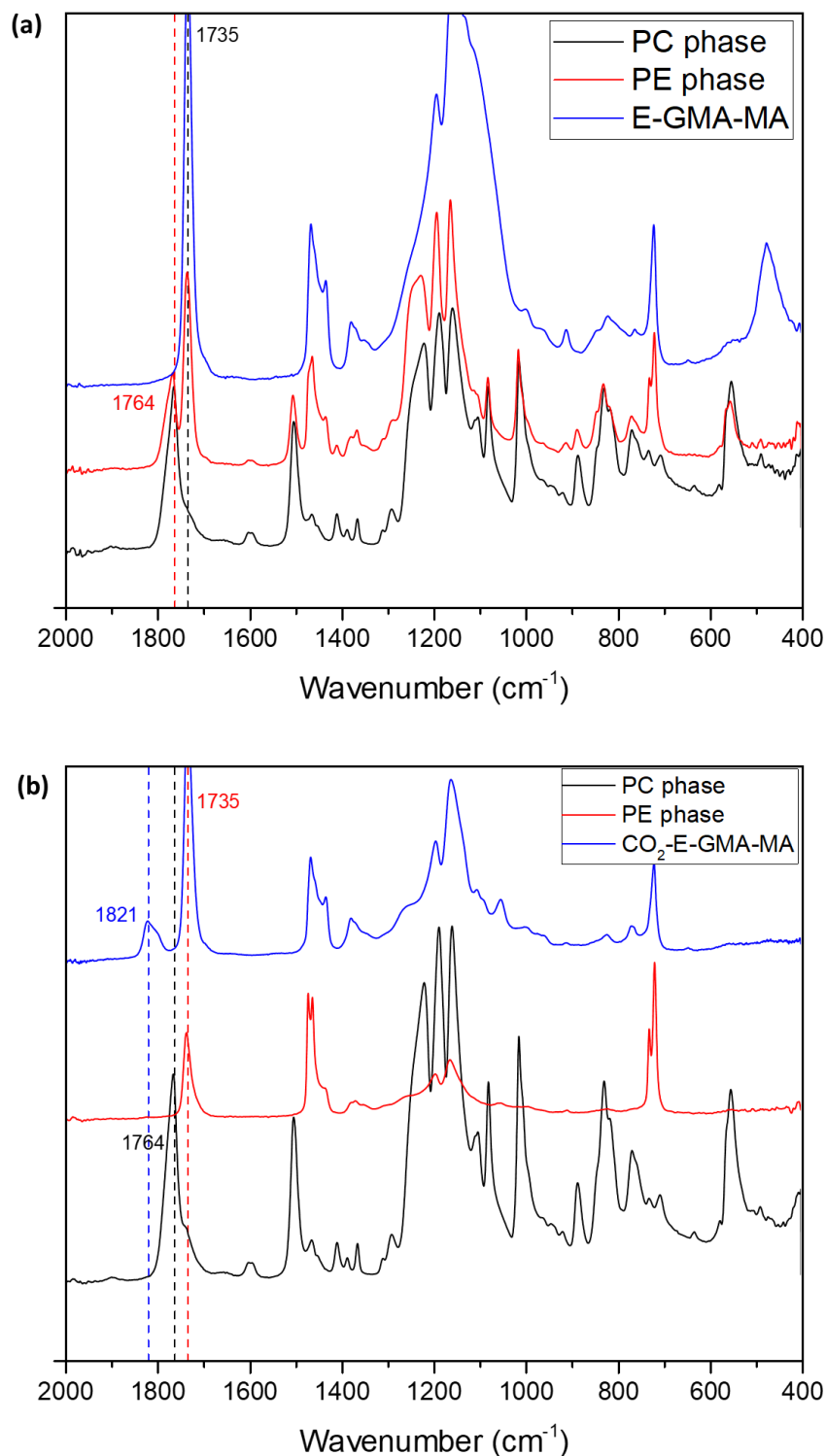


Figure 9. IR-ATR spectra of PC and HDPE phases of (a) HDPE/PC/E-GMA-MA (18/72/10) blend and (b) HDPE/PC/CO<sub>2</sub>-E-GMA-MA (18/72/10) blend.



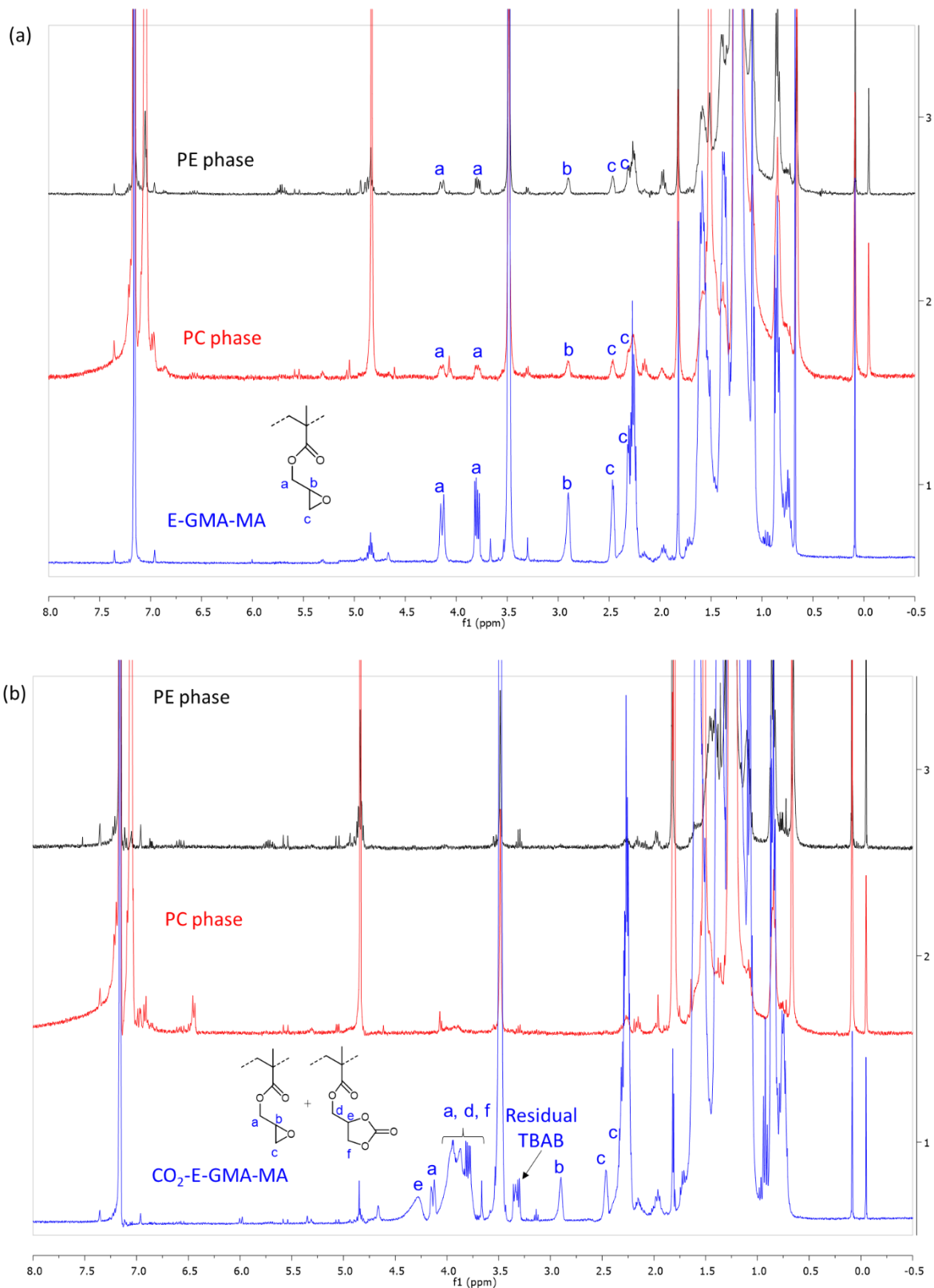


Figure 10.  $^1\text{H}$  NMR ( $\text{TCE}/\text{C}_6\text{D}_6$ ) spectra of PC and HDPE phases of (a) HDPE/PC/E-GMA-MA (18/72/10) blend and (b) HDPE/PC/ $\text{CO}_2$ -E-GMA-MA (18/72/10) blend.

#### IV.2.c. Mechanical properties

The mechanical properties of the different blends are presented in *Table 3* (tensile curves of the blends in appendices). Compared to pure PC (*Table 1*, entry 2), the PC/HDPE (80/20) blend exhibited slightly lower modulus and tensile strength due to the addition of HDPE, and a significant lower elongation at break, which decreased from 116 % to 42 %. However, the impact strength was improved and increased from 9.3 to 18.9 kJ/m<sup>2</sup>, because of the addition of HDPE that increased the softness of the material (*Table 3*, entry 1).

When the compatibilizers were added to the blend, the modulus and the tensile strength slightly decrease in all the cases compared to the binary blend because of the elastic properties of the compatibilizer.

The addition of non-carbonated compatibilizers did not improved the elongation at break. In the case of E-GMA-MA, the elongation was similar, and in the case of E-GMA-BA and E-GMA, it decreases from 42 to 22 and 27 %, respectively (*Table 3*, entries 2-4). With carbonated compatibilizer, improvement of the elongation at break was observed with CO<sub>2</sub>-E-GMA-BA and CO<sub>2</sub>-E-GMA, which increased from 42 % to 55 % and 80 %, respectively (*Table 3*, entries 5-7).

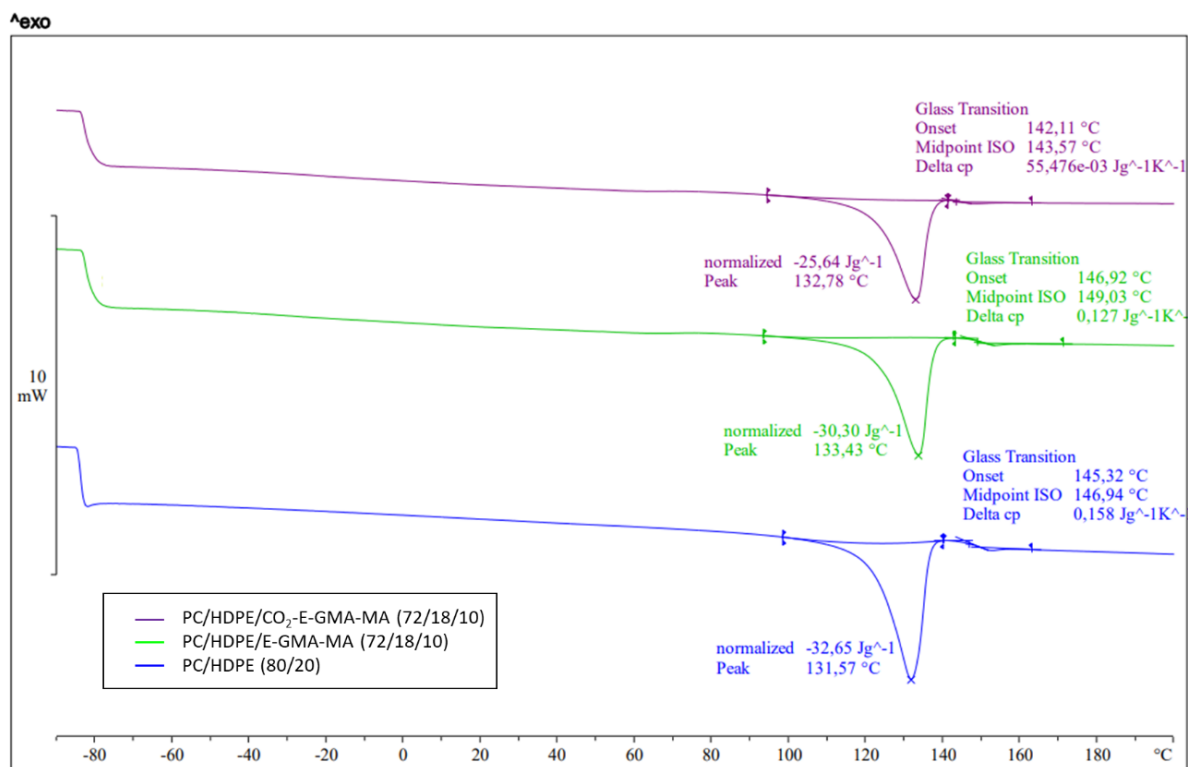
Surprisingly, for the impact strength, an opposite trend was observed. The use of the non-carbonated compatibilizer improved it in all the cases (*Table 3*, entries 2-4). A maximum of 30.9 kJ/m<sup>2</sup> was reached with E-GMA-BA as compatibilizer. When carbonated compatibilizers were used, the blends had a ductile behavior and a high notch sensitivity, the Charpy impact strength decreased from 18.9 to 9.6, 13.9 and 6.8 kJ/m<sup>2</sup> with CO<sub>2</sub>-E-GMA-MA, CO<sub>2</sub>-E-GMA-BA and CO<sub>2</sub>-E-GMA, respectively (*Table 3*, entries 5-7).

Table 3. Mechanical properties of the HDPE/PC/compatibilizer (18/72/10) blends.

Entry	Compatibilizer	HDPE/PC/compatibilizer weight proportion	Young's modulus (GPa)	Tensile Strength (MPa)	Elongation at break (%)	Impact strength (kJ/m <sup>2</sup> )
1	-	20/80/0	1.28 ± 0.06	46 ± 2	42 ± 3	18.9 ± 0.7
2	E-GMA-MA	18/72/10	1.09 ± 0.02	40.3 ± 0.8	43 ± 21	29.6 ± 1.3
3	<b>E-GMA-BA</b>		<b>1.02 ± 0.04</b>	<b>38.8 ± 0.5</b>	<b>22 ± 4</b>	<b>30.9 ± 1.4</b>
4	E-GMA		1.09 ± 0.08	41 ± 2	27 ± 5	21.4 ± 0.9
5	CO <sub>2</sub> -E-GMA-MA		1.1 ± 0.2	40 ± 8	42 ± 12	9.6 ± 1.2
6	CO <sub>2</sub> -E-GMA-BA		1.04 ± 0.06	39.0 ± 0.9	55 ± 5	13.9 ± 1.2
7	CO <sub>2</sub> -E-GMA		1.2 ± 0.1	41 ± 2	80 ± 4	6.8 ± 0.7

IV.2.d. Thermal properties

In *Figure 11*, the DSC curves of the blends are presented. The absolute values of the HDPE melting enthalpy for PC/HDPE (80/20) and PC/HDPE/E-GMA-MA (72/18/10) were similar (163.3 and 168.3 J/g of HDPE, respectively), whereas a decrease of the enthalpy was observed for the PC/HDPE /CO<sub>2</sub>-E-GMA-MA (72/18/10) blend (142.4 J/g of HDPE). The decrease of the melting enthalpy indicated a decrease of the HDPE phase crystallinity, and thus a better compatibilization of the blend, as it was reported in the literature. Concerning the  $T_g$  of the PC, no significant change was observed.



*Figure 11. DSC of HDPE/PC/compatibilizer (18/72/10) blends.*

## V. Conclusions

Carbonated [ethylene – glycidyl methacrylate] based polymers containing epoxide and cyclic carbonate pendant groups were used as new compatibilizers for a HDPE/PC (80/20) and PC/HDPE (80/20) (w/w) blends through twin-screw extrusion. A significant improvement of PC dispersion was obtained, when carbonated compatibilizers were used instead of non-carbonated compatibilizers (only epoxide pendant groups) for the HDPE/PC (80/20) blend, according to the decreased of the mean radius of the PC phases, and a better interfacial adhesion was observed.

Spectroscopic characterizations of the HDPE and PC phases of compatibilized blends with a non-carbonated and a carbonated compatibilizer showed that epoxide pendant groups do not react with the PC, but the cyclic carbonate partially reacted, according to  $^1\text{H}$  NMR analysis. The better compatibilization with the carbonated polymers may be explained by the partial reactivity of the cyclic carbonate with the alcohol end groups of PC and the *in situ* formation of the PC-*graft*-CO<sub>2</sub>-E-GMA-MA polymer.

Compared to the blend with E-GMA-MA, the elongation at break and the Charpy impact strength were also improved with the carbonated compatibilizer, the crystallinity of the HDPE phase was also reduced, and the thermal stability of the PC phase was modified, which indicates a better compatibilization and a chemical change of the PC phase.

With the PC/HDPE (80/20) blend, different results were obtained. Whereas elongation at break was better with the carbonated compatibilizers, especially CO<sub>2</sub>-E-GMA, the Charpy impact strength was improved with the non carbonated compatibilizers. According to the MEB images, the HDPE phase had a better adhesion with the PC phase when compatibilizers were used, and the dispersed phase size was reduced with the E-GMA-MA, whereas the measure of the size distribution with CO<sub>2</sub>-E-GMA-MA was not possible because of the more complex morphology of the blend. According to the spectroscopic analyses, the epoxide moieties of the E-GMA-MA were still present after blending with PC and HDPE, whereas the cyclic carbonates and epoxide of CO<sub>2</sub>-E-GMA-MA were not observed. It could be due to reactive compatibilization and/or hydrolysis of the functions.

These promising results suggested that other blends such as a polyethylene/polyamide (PA) blend could also be compatibilized by reactive blending, with the aminolysis of the cyclic carbonate pendant groups by the amine end groups of polyamide, and thus by the *in situ* formation of PA-*graft*-CO<sub>2</sub>-E-GMA based polymers.

## VI. References

- [1] Peacock, A. *Handbook of Polyethylene: Structures: Properties, and Applications*. CRC Press: 2000; 545 pp.
- [2] Utracki, L.A. Compatibilization of Polymer Blends. *Can. J. Chem. Eng.* **2002**, *80*(6), 1008–1016.
- [3] Higgins, J.S.; Lipson, J.E.G.; White, R.P. A simple approach to polymer mixture miscibility. *Philosophical Transactions of the Royal Society A: Mathematical, Physical and Engineering Sciences* **2010**, *368*(1914), 1009–1025.
- [4] Dorigato, A. Recycling of polymer blends. *Advanced Industrial and Engineering Polymer Research* **2021**, *4*(2), 53–69.
- [5] Kunori, T.; Geil, P.H. Morphology-property relationships in polycarbonate-based blends. I. Modulus. *Journal of Macromolecular Science, Part B* **1980**, *18*(1), 93–134.
- [6] Kunori, T.; Geil, P.H. Morphology-property relationships in polycarbonate-based blends. II. Tensile and impact strength. *Journal of Macromolecular Science, Part B: Physics* **1980**, *18*(1), 135–175.
- [7] Yang, M.; Li, Z.; Feng, J. Studies on high density polyethylene/polycarbonate blend system compatibilized with low density polyethylene grafted diallyl bisphenol A ether. *Polymer Engineering & Science* **1998**, *38*(6), 879–883.
- [8] Li, Z.M.; Yang, M.B.; Feng, J.M.; Huang, R. Fibre formation based toughening in polycarbonate/polyethylene alloy compatibilized with diallyl bisphenol A ether grafted polyethylene. *Journal of Materials Science* **2001**, *36*(8), 2013–2018.
- [9] Yin, B.; Zhao, Y.; Yu, R.-Z.; An, H.-N.; Yang, M.-B. Morphology development of PC/PE blends during compounding in a twin-screw extruder. *Polymer Engineering & Science* **2007**, *47*(1), 14–25.
- [10] Ghosh, A. Recycled polyethylene/polycarbonate blends compatibilized with oxidized polyethylene/CaCO<sub>3</sub>. *Journal of Applied Polymer Science* **2022**, *139*(15), 51919.
- [11] Yin, B.; Lan, J.; Li, L.-P.; Yang, M.-B. Morphology Evolution in PC/PE Blends with and without Compatibilization During Twin-Screw Extrusion. *Polymer-Plastics Technology and Engineering* **2010**, *49*(5), 503–509.
- [12] Yin, B.; Zhao, Y.; Pan, M.; Yang, M. Morphology and thermal properties of a PC/PE blend with reactive compatibilization. *Polym. Adv. Technol.* **2007**, *18*(6), 439–445.
- [13] Mascia, L.; Valenza, A. Reactive dual-component compatibilizers for polycarbonate/high-density polyethylene blends. *Advances in Polymer Technology* **1995**, *14*(4), 327–335.
- [14] Manjunatha Nanjegowda, L.; Bommulu, R.; Juikar, V.; Hatna, S. Investigation on the Influence of Different Compatibilizers on Polycarbonate and High Density Polyethylene

Blends: Mechanical Properties, Thermal Properties, Morphology, and Chemical Resistance. *Ind. Eng. Chem. Res.* **2013**, *52*(16), 5672–5682.

[15] Guerdener, B.; Ayzac, V.; Norsic, S.; Besognet, P.; Bounor-Legaré, V.; Monteil, V.; Dufaud, V.; Raynaud, J.; Chalamet, Y. Carbonatation of [ethylene-glycidyl methacrylate]-based copolymers with carbon dioxide as a reagent: from batch to solvent-free reactive extrusion. *Green Chem.* **2023**, *25*(16), 6355–6364.

[16] Ito, Y.; Ogasawara, H.; Ishida, Y.; Ohtani, H.; Tsuge, S. Characterization of End Groups in Polycarbonates by Reactive Pyrolysis-Gas Chromatography. *Polym J* **1996**, *28*(12), 1090–1095.

[17] Kim, J.; Gracz, H.S.; Roberts, G.W.; Kiserow, D.J. Spectroscopic analysis of poly(bisphenol A carbonate) using high resolution <sup>13</sup>C and <sup>1</sup>H NMR. *Polymer* **2008**, *49*(2), 394–404.

[18] Heuer, H.-W.; Wehrmann, R. (54) COPOLYCARBONATES HAVING IMPROVED FLOWABILITY..

[19] Kayano, Y.; Keskkula, H.; Paul, D.R. Effect of polycarbonate molecular weight and processing conditions on mechanical behaviour of blends with a core-shell impact modifier. *Polymer* **1996**, *37*(20), 4505–4518.

[20] Kayano, Y.; Keskkula, H.; Paul, D.R. Fracture behaviour of polycarbonate blends with a core-shell impact modifier. *Polymer* **1998**, *39*(4), 821–834.

[21] Li, C.; Zhang, Y.; Zhang, Y.; Zhang, C. Blends of polycarbonate and ethylene-1-octylene copolymer. *European Polymer Journal* **2003**, *39*(2), 305–311.

[22] Sun, J.; Yao, X.; Cheng, W.; Zhang, S. 1,3-Dimethylimidazolium-2-carboxylate: a zwitterionic salt for the efficient synthesis of vicinal diols from cyclic carbonates. *Green Chem.* **2014**, *16*(6), 3297–3304.

---

## **General Conclusion**

---

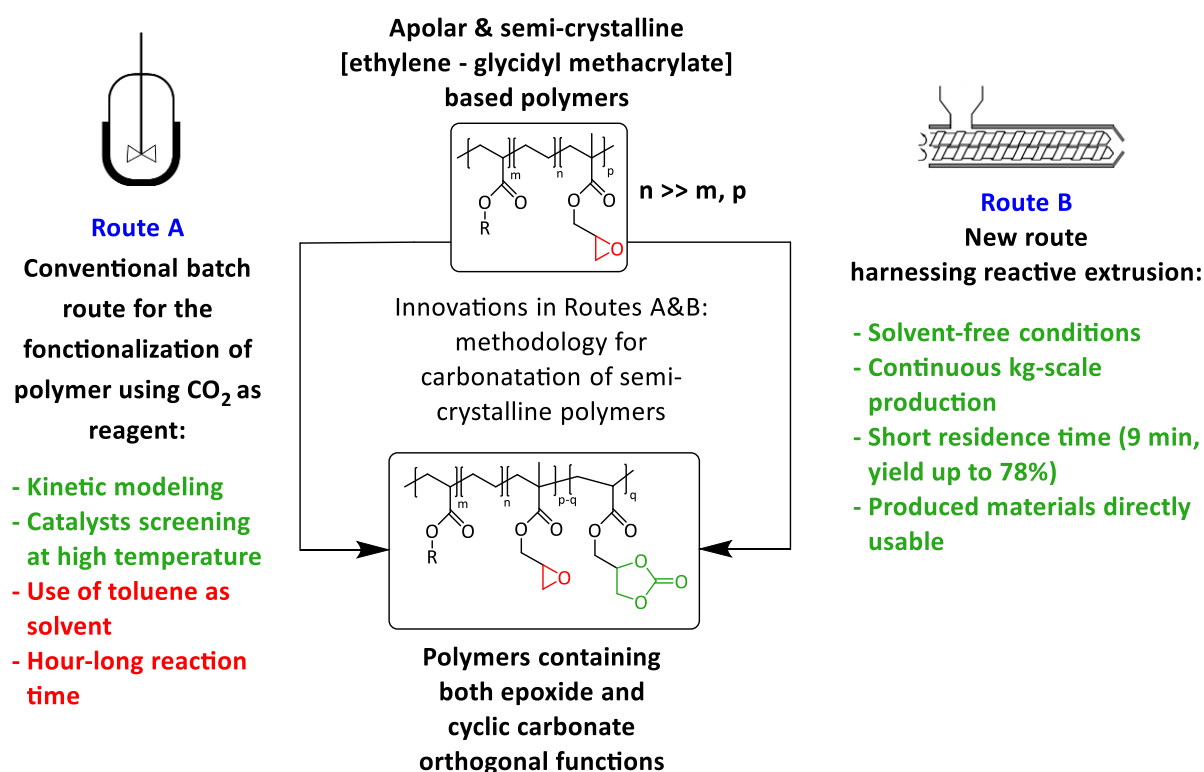




The development of more sustainable and eco-designed processes in the chemistry and polymer industry is nowadays one of the most important challenges to tackle in order to minimize the impact of human activities on the ecosystem. This objective can only be achieved if we intensify the use of renewables feedstock, and reduce our energy and resources consumption as well as our production of waste. During this thesis, the integration of these environmental considerations into our research work has always been a priority, from the synthesis of carbonated polymers, to their production and use in potential applications.

The literature review (**Chapter 1**), highlighted the possibility of using organocatalysts for the carbonation reaction of epoxides and alkenes. However, the substitution of the epoxide highly impacts its reactivity. Especially, trisubstituted epoxides are much less reactive than disubstituted and terminal epoxides, and tetrasubstituted epoxides are completely unreactive with the actual catalytic systems. It also showed the possibility of transposing this chemistry to the functionalization of polymers, although only carbonation of highly polar polymers was reported.

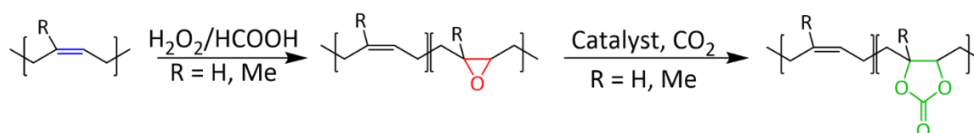
In **Chapter 2** the carbonation of semi- crystalline [ethylene – glycidyl methacrylate] based copolymers, using CO<sub>2</sub> as reagent and ammonium salts as organocatalysts, was reported for the first time and two methods were applied (*Scheme 1*).



*Scheme 1. Transposition of carbonation from batch to reactive extrusion.*

The first method implemented in batch reactor was developed in order to assess reaction kinetics and optimize the reaction conditions. The influence of the ammonium salt composition (anion/cation) was studied in toluene at 110 °C to circumvent the high melting temperatures of these ethylene unit-rich copolymers and obtain a homogeneous medium. The amount of catalyst, CO<sub>2</sub> pressure and temperature were also optimized (tetrabutylammonium bromide catalyst, 5 mol% vs. epoxy content, 4.0 MPa, 110 °C) to allow for quantitative conversion of epoxides into cyclic carbonates. Another innovation of our work is the successful transposition of this reaction to a solvent free, continuous extrusion process under high pressure of CO<sub>2</sub>, producing polymers containing both epoxide and cyclic carbonate moieties at kilogram scale. After optimization, a yield of up to 78 % of cyclic carbonate could be obtained with tetrahexylammonium bromide (7.5 mol% vs. epoxy content, ~30 g/h of catalyst) at 150 °C with an industry-compliant polymer flow rate of 2 kg/h. One of the main limitation is the catalyst recovery from the polymer matrix, which could be achieved by adding an extraction step at the end of the extrusion process by using supercritical carbon dioxide as extraction solvent.

Moreover, the carbonatation of polymers was extended to polydienes. Several polymers containing butadiene (polybutadiene with a mixture of 1,4 and 1,2 units, 1,4-*cis* polybutadiene, 1,2-polybutadiene and [styrene-*block*-butadiene-*block*-styrene] copolymer) and isoprene units (natural rubber and [styrene-*block*-isoprene-*block*-styrene] copolymer) were functionalized with CO<sub>2</sub> in two steps (**Chapter 3**) (*Scheme 2*).



*Scheme 2. Two-steps functionalization of polydienes using peracids and carbon dioxide as reagents.*

The first step (epoxidation step), was studied and readily achieved using performic acid formed *in situ*, and all the polymers were successfully epoxidized (epoxide content between 4 and 16 mol%) at 50 °C in toluene, the only by-products were water and formic acid. The starting polymer microstructure influenced their double bonds reactivity toward epoxidation, and thus affected their epoxide contents. For the polybutadienes, the reactivity of the monomers units followed this trend: **1,4-*cis* unit > 1,4-*trans* unit >> 1,2 unit**. For the polyisoprenes, a similar trend was observed: **1,4 unit >> 3,4 unit**. Two different EPDM were also epoxidized and the reactivity of the ENB diene-derived unit was higher than the DCPD

diene-derived unit. Moreover, the epoxidation of a PBU containing 81 mol% of 1,2 units with a low molar mass was performed in a tailored reactive extrusion process under solvent-free conditions. Under the optimal conditions (10 mol% of H<sub>2</sub>O<sub>2</sub>/HCOOH, 60 °C), an epoxide content of 1,3 mol% mostly composed of *trans* epoxide was obtained.

Then, the carbonatation step was also optimized using ammonium salts as organocatalysts, and the epoxidized polymers reactivity was directly related to the epoxide configuration (pendant, *cis* or *trans*). TOAB and PPNCl showed the best activity, depending on the polymer microstructure. TOAB was more convenient for polybutadienes containing predominantly *cis* epoxide (cyclic carbonate yield up to 60 %), whereas PPNCl was more active for polybutadienes containing predominantly *trans* epoxide (yield up to 94 %) and epoxidized polyisoprenes (yield up to 26 %). TBAC, which is more active than TOAB for the carbonatation of trisubstituted epoxide, was tested as catalyst for the carbonatation of epoxidized EPDM, but no reactivity was observed. Further conditions optimization have to be investigated, as for example the use of Brønsted acids as co-catalysts (polyphenols or fluorinated compounds).

The evolution of the main characteristic properties of the resulting polymers was followed after each step (molar mass distribution and thermal properties). After the epoxidation step, the molar masses distribution of the polymers did not significantly changed, except for **SIS**, where a decrease in the molar masses was observed by SEC, which could be due to oxidative cleavage of the isoprene units during epoxidation. After carbonatation of polybutadienes containing a high content of *cis* epoxide, the solubility of the carbonated polybutadienes evolved and became insoluble. The carbonatation of an epoxidized natural rubber led to a polymer with a significant lower Mn (related to the lower stability of isoprene), but a small proportion of macromolecules also exhibited higher molar masses. During carbonatation, formation of cross-linking *via* the formation of ether or linear carbonate linkages could decrease the polymers solubility and partially increased the macromolecules molar masses, in the case of polymers containing mainly *cis* epoxide. Conversely, for polymers containing low content of *cis* epoxide, no cross-linking was observed and the molar masses were unchanged after carbonatation. Regarding the thermal properties, after epoxidation reaction, no significant change in the  $T_g$  was observed, but in the case of the epoxidation of the semi crystalline 1,4-*cis* polybutadiene, an amorphous polymer was obtained. After carbonatation reaction, a high increase in the  $T_g$  was observed with high carbonate content.

Although the epoxidation step was successfully transposed to solvent-free reactive extrusion using a low molar mass polybutadiene and H<sub>2</sub>O<sub>2</sub>/HCOOH as oxidant, a focus on the use of thermally more stable oxidant has to be considered, in order to perform epoxidation by reactive extrusion above 100 °C. Moreover, the carbonatation step of epoxidized polydienes could not be explored, due to the physical form of the obtained epoxidized polydienes (liquid or rubbery polymers) which makes impossible the transposition to extrusion process under high pressure of CO<sub>2</sub>. The optimization of the epoxidation by reactive extrusion of polyolefins containing diene monomers, such as SBS, SIS or EPDM, would be essential, in order to produce larger amount of epoxidized polymers that could then be carbonated by reactive extrusion. The development of a one-pot reaction could be also another route to produce in one-step carbonated polymers from polymers containing unsaturation, but this proves much more challenging.

In this thesis, two different applications were investigated for the carbonated polymers: their use as intermediates for polyhydroxyurethanes synthesis (**Chapter 4**), and as compatibilizers for polyethylene/polycarbonate blends. In the case of the polyhydroxyurethanes synthesis, the orthogonality of the reaction was demonstrated, especially for the aminolysis of partially carbonated epoxidized polybutadiene with a monoamine, where only the carbonates reacted with the amine, and the epoxides were completely unreactive (*Figure 1*). The *cis* carbonate also showed a higher reactivity than the *trans* derivative. Thus, the control of the cyclic carbonate stereoselectivity during the carbonatation of polymers containing internal epoxides is essential, as a high reactivity is most of the time required for industrial applications.

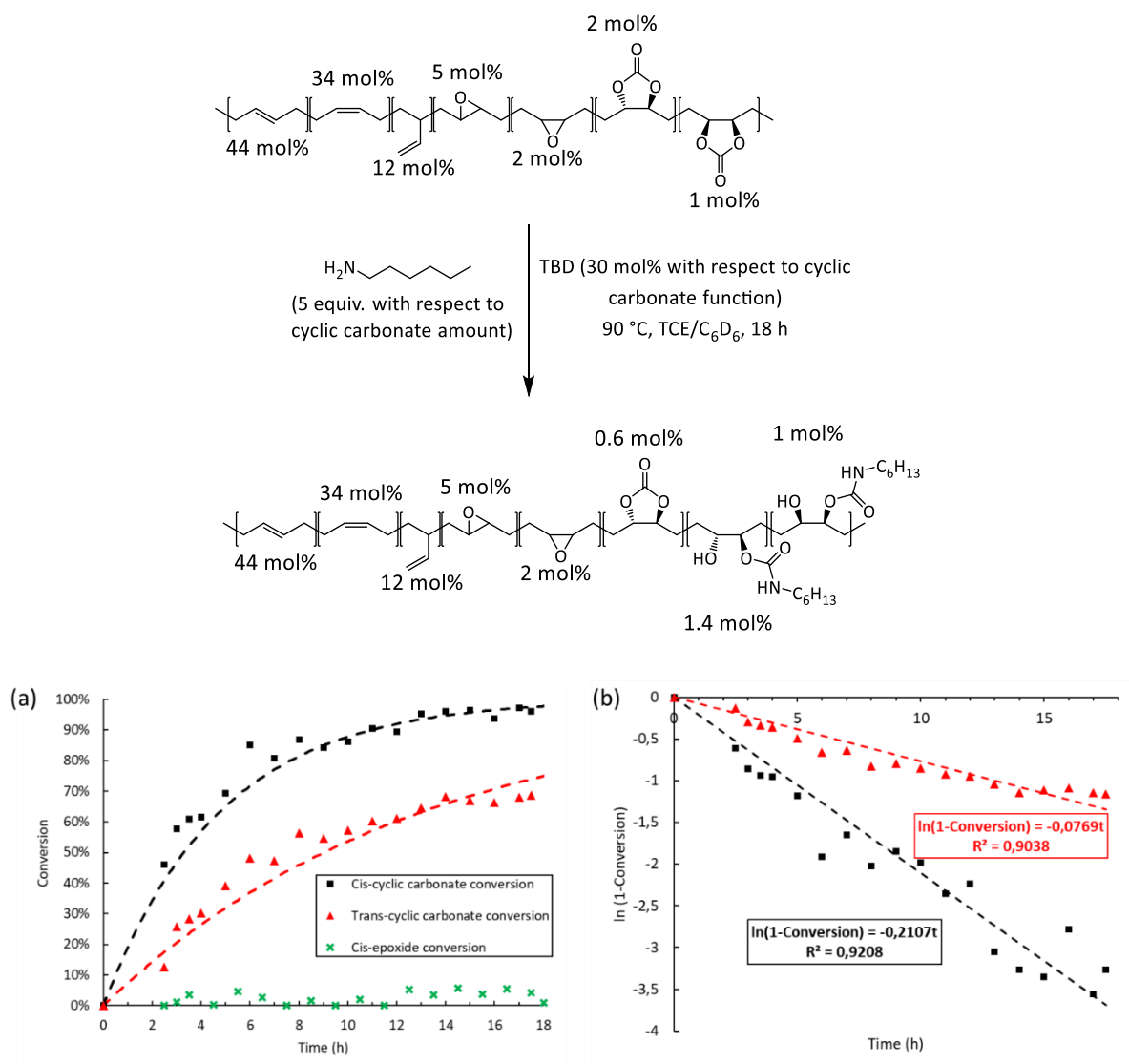


Figure 1. Kinetic study for the synthesis of hydroxyurethane functions on partially carbonated polybutadiene with hexylamine (5 equiv. according to cyclic carbonate content) at 90 °C with TBD (30 mol% according to cyclic carbonate content) (initial cyclic carbonate and epoxide concentration: 0.06 mol/L and 0.2 mol/L, respectively): (a) conversion of the cis and trans carbonates and cis epoxide over time, (b) plot of equation (1).

A cross-linked polybutadiene *via* the reaction of carbonated polybutadiene with a diamine was also successfully synthesized. Further investigation on the rheological properties have to be studied, in order to demonstrate the occurrence of a dynamic hydroxyurethane network. Polydienes containing appropriate carbonate content should also be designed for more specific applications in order to produce recyclable elastomers (high molar mass and low carbonate content), or resins for coating with excellent mechanical properties (low molar mass and high carbonate content).

Finally, HDPE/PC (80/20) and PC/HDPE (80/20) blends were compatibilized by extrusion with carbonated and non-carbonated [ethylene-glycidyl methacrylate] based polymers (**Chapter 5**). For the HDPE/PC (80/20) blend, the use of carbonated compatibilizers improved the dispersion of the minor phase and the mechanical properties (increase of elongation at break **from 23 to 90 %** and Charpy impact strength from **4.4 to 39.8 kJ/m<sup>2</sup>**). A decrease in the carbonate content after extrusion may indicate that reactive compatibilization occurred. In the case of the (PC/HDPE) (80/20), the notched Charpy impact strength was improved with non-carbonated compatibilizers (from **18.9 to 30.9 kJ/m<sup>2</sup>**) and the elongation at break was better with carbonated compatibilizers (increase from **42 to 80 %**). The carbonate functions were in this case completely converted after blending. This may be due to reaction with hydroxyl end groups of PC, and/or thermal degradation. Others blends compatibilization such as polyethylene/polyamide blend could be explored.

In conclusion, the carbonatation of polymers using carbon dioxide as reactant is linked to multiple disciplines. Organic chemistry, catalysis, polymer science, process engineering and material science have been involved for the different stages of this thesis. The functionalization of polymers with CO<sub>2</sub> required further optimization, but our work paves the way towards the conception of innovative and more sustainable materials such as recyclable elastomers and resins and new type of compatibilizers.

---

# **Appendices**

---





---

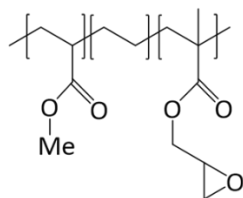
## Table of Contents

<b>I. Chapter 2</b> .....	<b>251</b>
I.1. Structure and main properties of the commercial polymers.....	251
I.2. Characterization of the commercial polymers and catalysts.....	251
I.2.a. IR-ATR spectra .....	251
I.2.b. <sup>1</sup> H NMR spectra .....	253
I.2.c. <sup>13</sup> C NMR spectra.....	256
I.2.d. DSC analyses.....	258
I.2.e. TGA.....	259
I.3. Carbonatation of [ethylene – glycidyl methacrylate] based copolymers in batch.	260
I.3.a. Calibration curve for the determination of cyclic carbonate yield for the carbonatation of E-GMA-MA terpolymer by IR-ATR.....	260
I.3.b. IR-ATR spectra .....	264
I.3.c. <sup>1</sup> H NMR spectra .....	265
I.3.d. <sup>13</sup> C NMR spectra.....	268
I.3.e. DSC analyses.....	272
I.3.f. TGA.....	273
I.5. Carbonatation of [ethylene – glycidyl methacrylate] based copolymers by reactive extrusion.....	274
I.5.a. IR-ATR spectra .....	274
I.5.b. <sup>1</sup> H NMR spectra .....	276
I.5.c. DSC analyses.....	279
<b>I.6.</b> TGA.....	<b>280</b>
I.6.a. High temperature SEC analyses in TCB.....	282
I.7. Summary table of SEC and DSC analyses .....	283
<b>II. Chapter 3</b> .....	<b>284</b>
II.1. Solubility of the polymers and catalysts .....	284

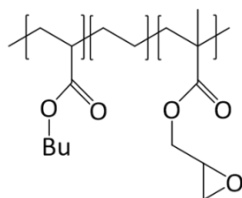
II.2.	Characterization of the commercial polymers .....	285
II.2.a.	IR-ATR spectra .....	285
II.2.b.	<sup>1</sup> H NMR spectra .....	289
II.2.c.	DSC analyses.....	297
II.3.	Epoxidation of polydienes in batch.....	301
II.3.a.	IR-ATR spectra .....	301
II.3.b.	<sup>1</sup> H NMR spectra .....	306
II.3.c.	DSC analyses.....	317
II.4.	Epoxidation of polybutadiene by reactive extrusion .....	321
II.4.a.	<sup>1</sup> H NMR spectra .....	321
II.4.b.	DSC analyses.....	322
II.5.	Carbonatation of partially epoxidized polydienes .....	323
II.5.a.	IR-ATR spectra .....	323
II.5.b.	<sup>1</sup> H NMR spectra .....	327
II.5.c.	DSC analyses.....	333
<b>III.</b>	<b>Chapter 4.....</b>	<b>335</b>
<b>IV.</b>	<b>Chapter 5.....</b>	<b>337</b>
IV.1.	Tensile curves.....	337
IV.2.	NMR spectra of PC .....	345

## I. Chapter 2

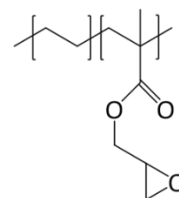
### I.1. Structure and main properties of the commercial polymers

**E-GMA-MA**

methyl acrylate: 24 wt%  
glycidyl methacrylate: 8 wt%  
 $T_f = 65\text{ }^\circ\text{C}$

**E-GMA-BA**

butyl acrylate: 25 wt%  
glycidyl methacrylate: 8 wt%  
 $T_f = 72\text{ }^\circ\text{C}$

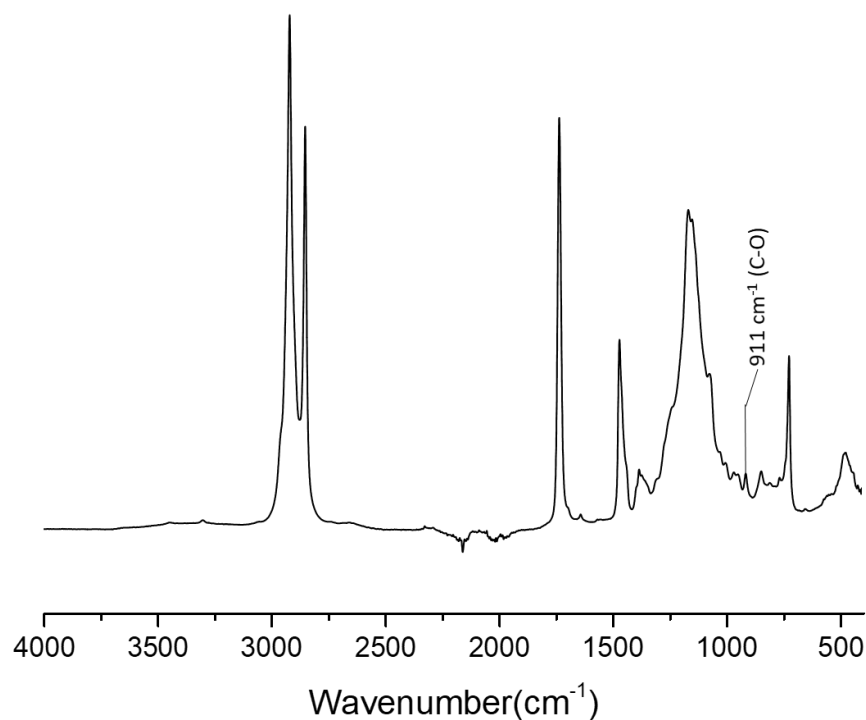
**E-GMA**

glycidyl methacrylate: 8 wt%  
 $T_f = 104\text{ }^\circ\text{C}$

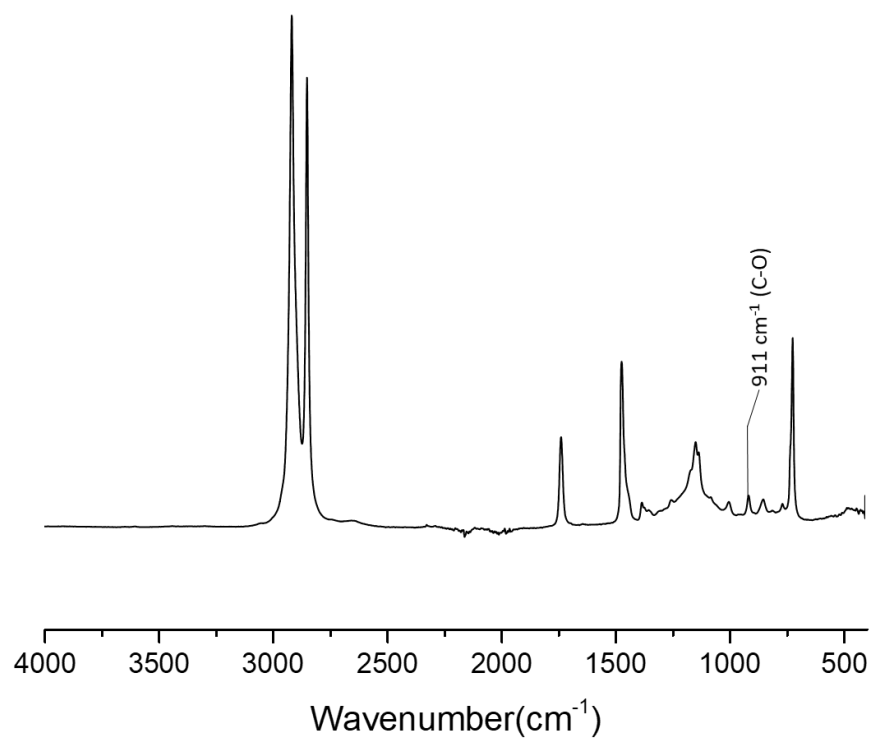
*Scheme S1. Structure and main properties of E-GMA-MA, E-GMA-BA and E-GMA.*

### I.2. Characterization of the commercial polymers and catalysts

#### I.2.a. IR-ATR spectra



*Figure S1. IR-ATR spectrum of E-GMA-BA.*



*Figure S2. IR-ATR spectrum of the E-GMA.*

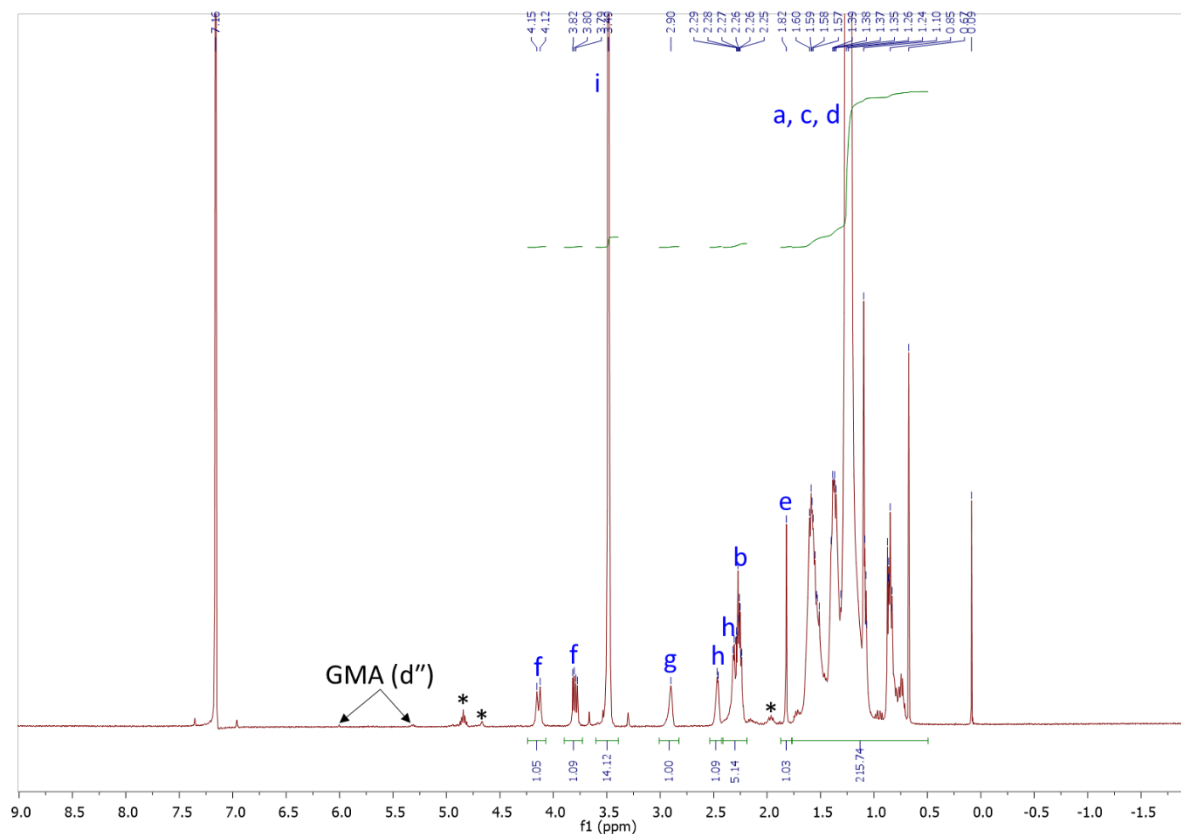
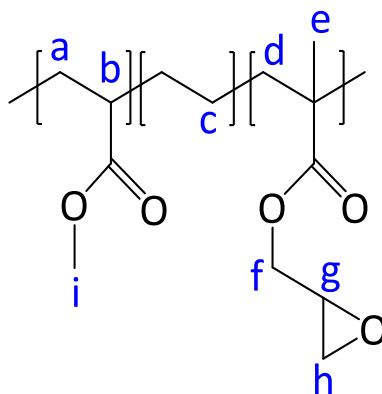
I.2.b.  $^1\text{H}$  NMR spectra

Figure S3.  $^1\text{H}$  NMR (TCE/ $\text{C}_6\text{D}_6$ , 400 MHz) spectrum of the E-GMA-MA.



$^1\text{H}$  NMR (400 MHz, TCE/ $\text{C}_6\text{D}_6$ )  $\delta$ : 4.14 (dd,  $J = 12.0, 3.7$  Hz, f), 3.80 (dd,  $J = 12.1, 5.6$  Hz, f), 3.49 (s, i), 2.90 (m, g), 2.46 (m, h), 2.41 – 2.19 (m, b, h), 1.82 – 0.49 (m, a, c, d, e).

\*: chain ends due to the radical copolymerization (termination by disproportionation) method used to synthesize these ethylene-rich copolymers<sup>[85]</sup> ; almost no residual GMA monomer is present.

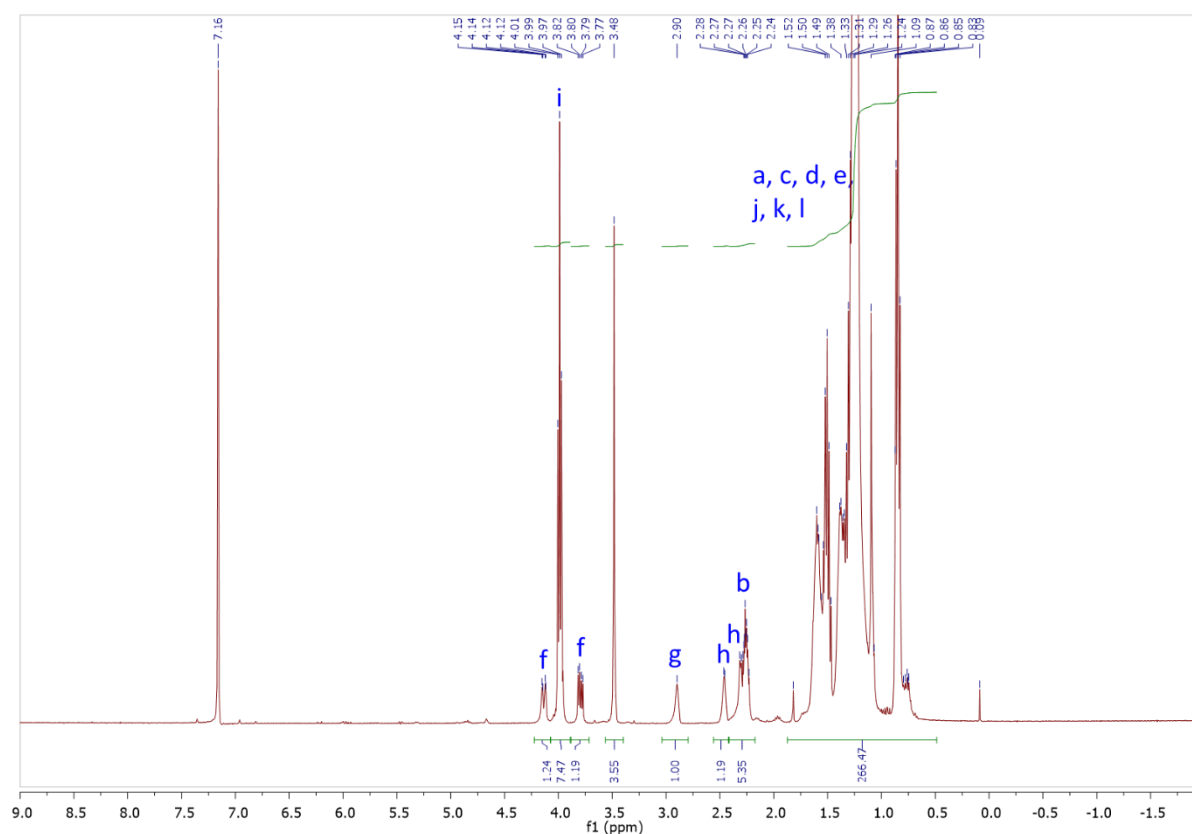
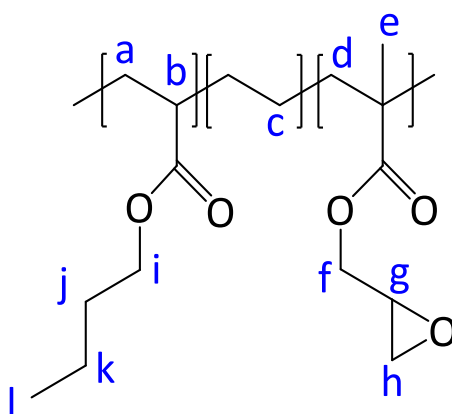


Figure S4.  $^1\text{H}$  NMR (TCE/ $\text{C}_6\text{D}_6$ , 400 MHz) spectrum of the E-GMA-BA.



$^1\text{H}$  NMR (400 MHz, TCE/ $\text{C}_6\text{D}_6$ )  $\delta$  : 4.13 (dd,  $J = 11.4, 2.9$  Hz, f), 3.99 (t,  $J = 6.6$  Hz, i), 3.79 (dd,  $J = 12.1, 5.6$  Hz, f), 3.48 (s, 3H, methyl acrylate), 2.90 (m, g), 2.46 (m, h), 2.41 – 2.18 (m, b, h), 1.87 – 0.54 (m, a, c, d, e, j, k, l).

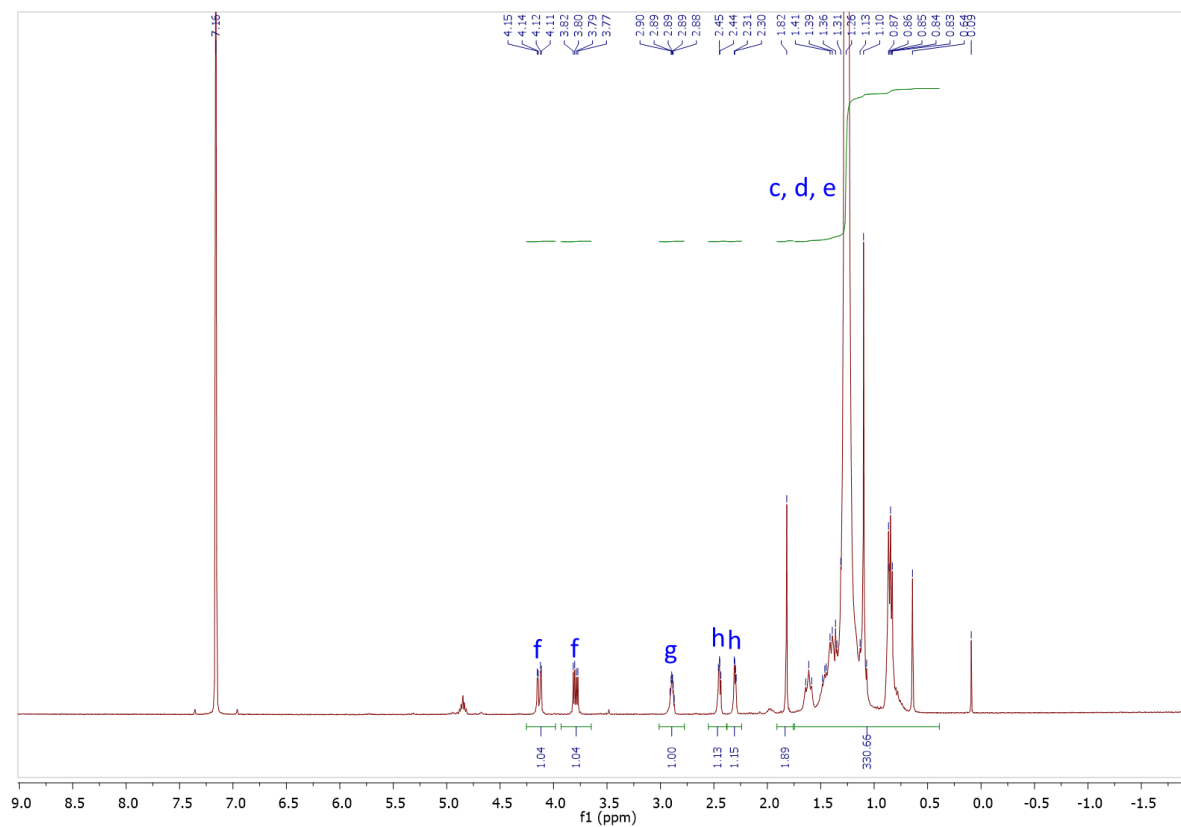
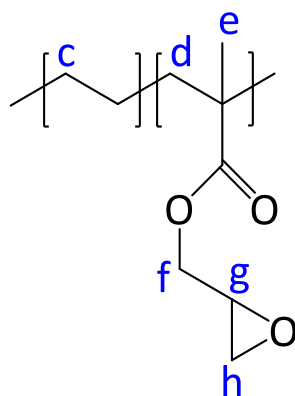


Figure S5.  $^1\text{H}$  NMR (TCE/ $\text{C}_6\text{D}_6$ , 400 MHz) spectrum of the E-GMA.



$^1\text{H}$  NMR (400 MHz, TCE/ $\text{C}_6\text{D}_6$ )  $\delta$  : 4.13 (dd,  $J = 12.1, 3.7$  Hz, **f**), 3.79 (dd,  $J = 12.1, 5.6$  Hz, **f**), 3.01 – 2.83 (m, **g**), 2.45 (dd,  $J = 5.1, 4.1$  Hz, **h**), 2.30 (dd,  $J = 5.3, 2.4$  Hz, **h**), 1.87 – 0.37 (m, **c, d, e**).



### I.2.c. $^{13}\text{C}$ NMR spectra

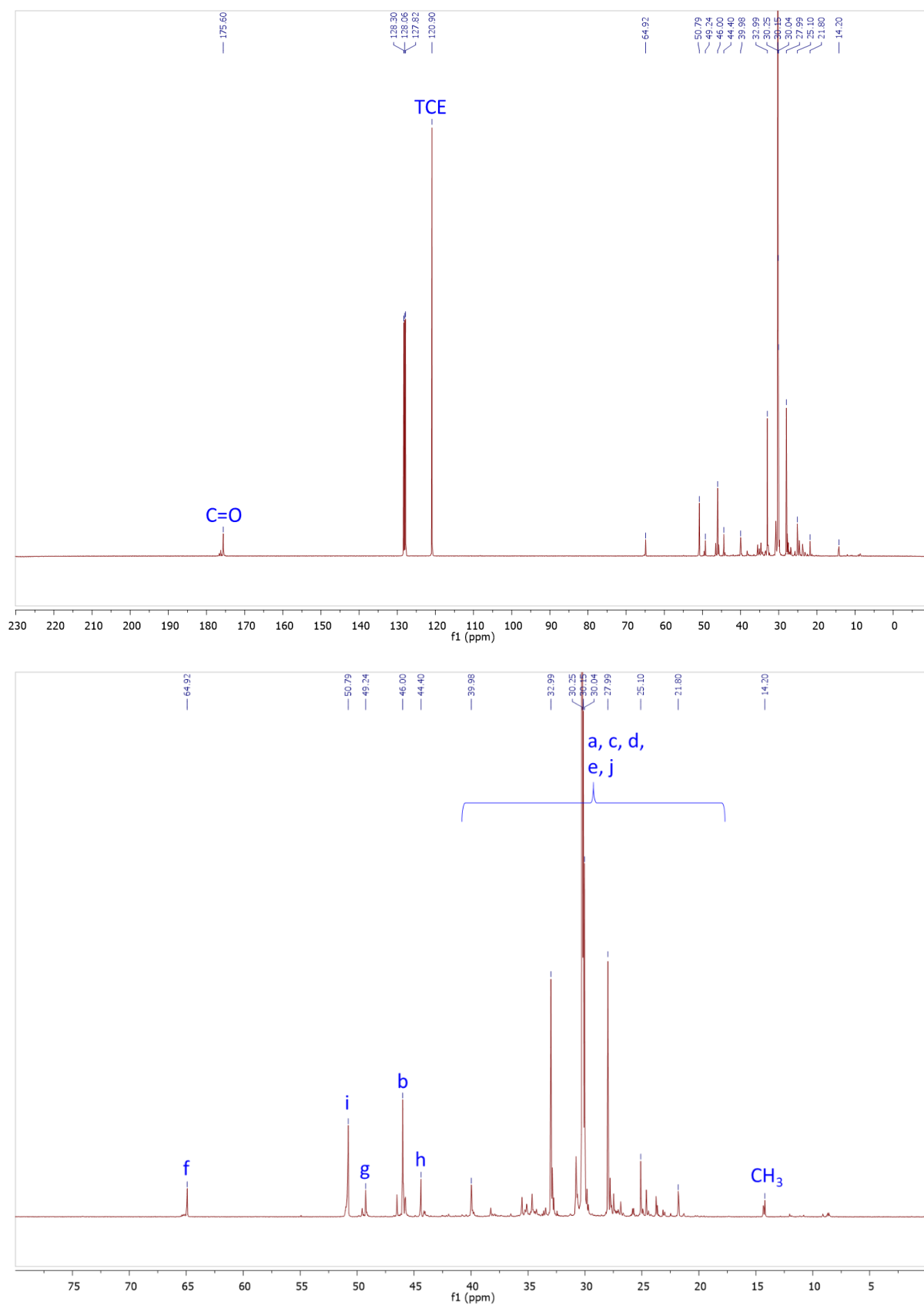
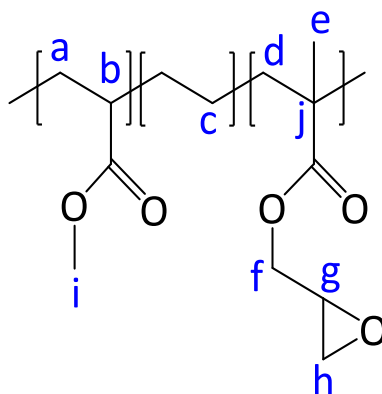


Figure S6.  $^{13}\text{C}$  NMR (101 MHz, TCE/ $\text{C}_6\text{D}_6$ ) spectrum of the E-GMA-MA.



$^{13}\text{C}$  NMR (101 MHz, TCE/ $\text{C}_6\text{D}_6$ )  $\delta$ : 175.60 (C=O), 64.92 (f), 50.79 (i), 49.24 (g), 46.00 (b), 44.40 (h), 41.27 – 18.04 (a, c, d, e, j), 14.20 ( $\text{CH}_3$ ).

### I.2.d. DSC analyses

On the following DSC curves, the glass transition and the melting endotherm of the polymers overlap. Thus, the baseline for the integration of the melting endothermic event is a tangential right line to take into account the change of baseline induced by the glass transition (common practice for DSC of polymers with overlapping thermal events).

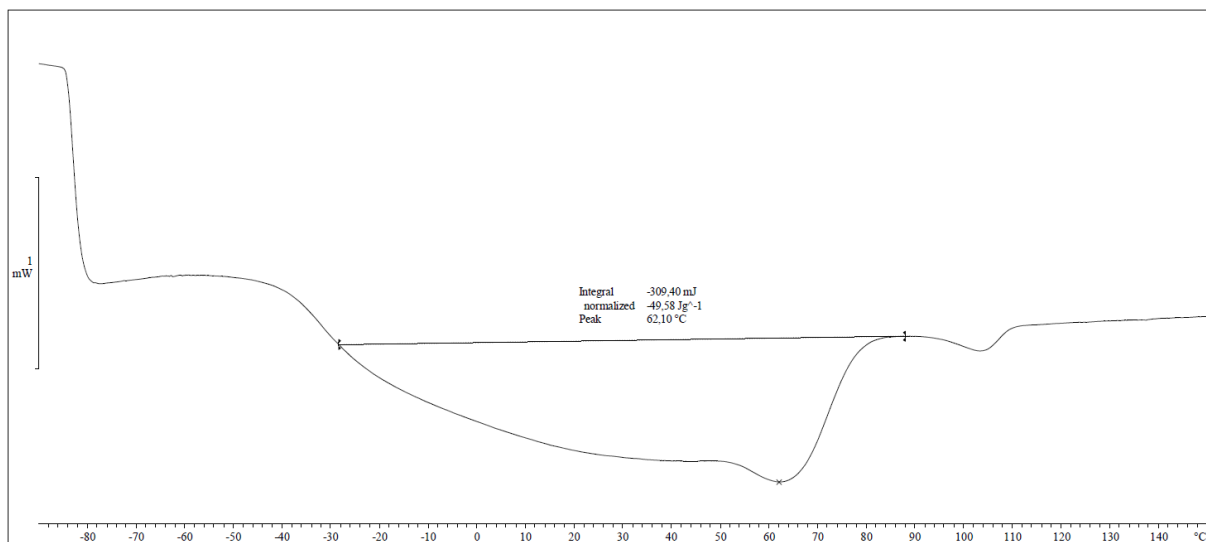


Figure S7. DSC analysis of the E-GMA-MA.

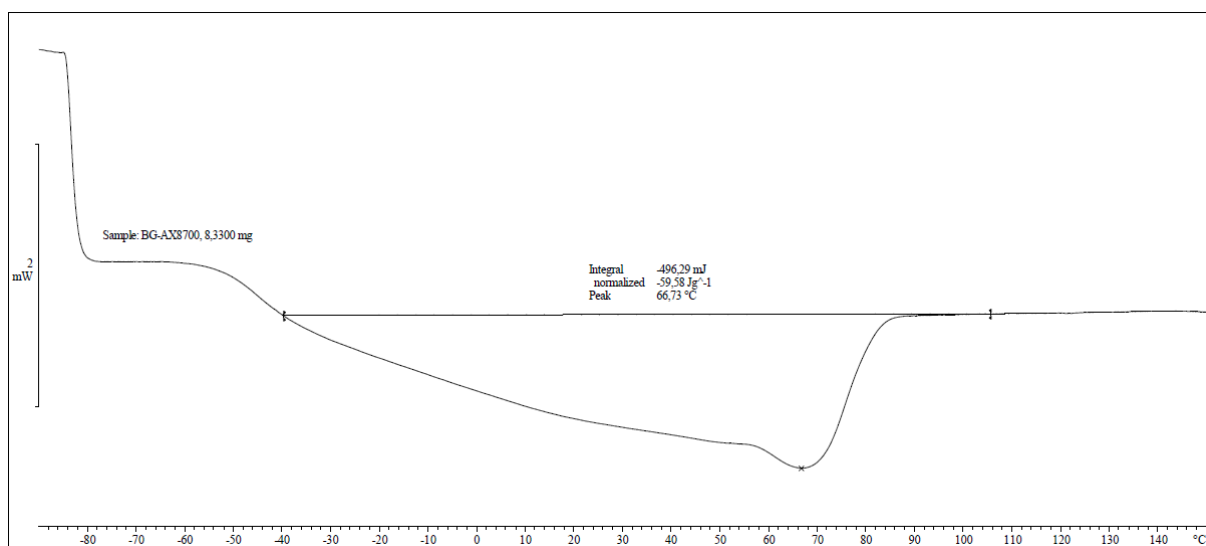


Figure S8. DSC analysis of the E-GMA-BA.

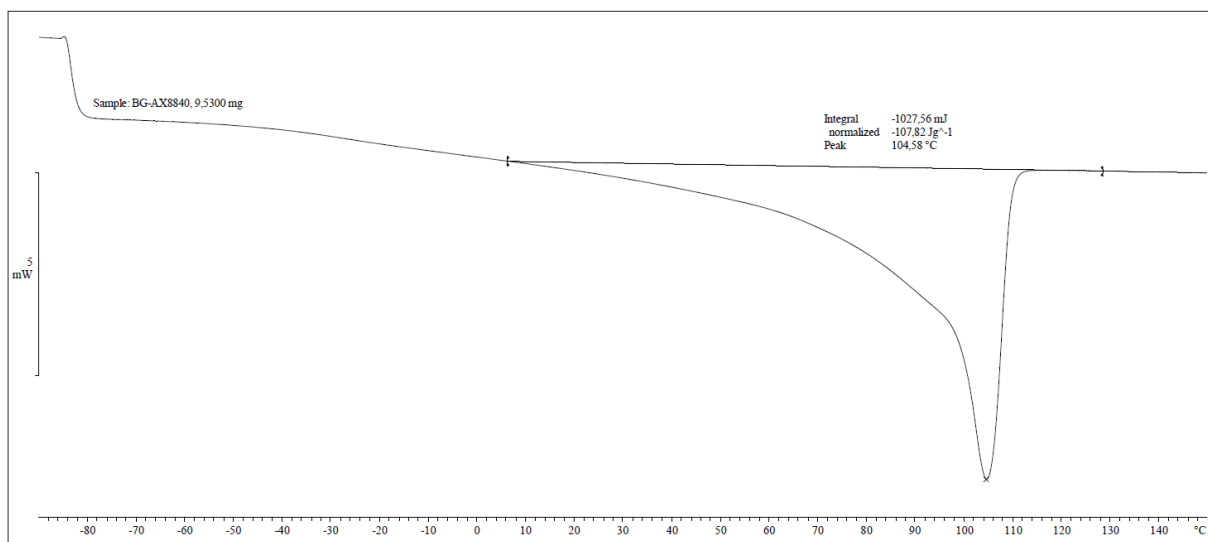


Figure S9. DSC analysis of the E-GMA.

I.2.e. TGA

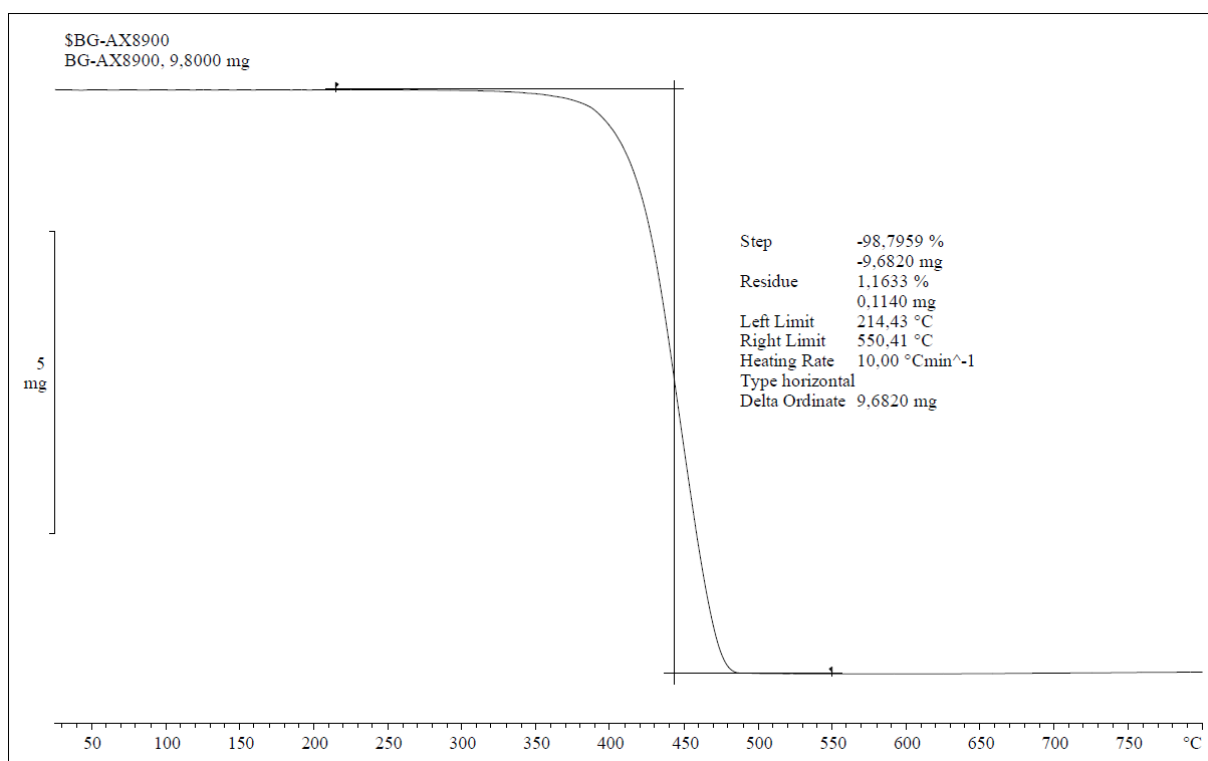


Figure S10. TGA analysis of the E-GMA-MA.

### I.3. Carbonatation of [ethylene – glycidyl methacrylate] based copolymers in batch

#### I.3.a. Calibration curve for the determination of cyclic carbonate yield for the carbonatation of E-GMA-MA terpolymer by IR-ATR

The reaction with TBAB using E-GMA-MA (5 mol% of catalyst, 4.0 MPa of CO<sub>2</sub>, 110 °C, toluene) was followed by <sup>1</sup>H NMR and IR-ATR. The cyclic carbonate yield determined by <sup>1</sup>H NMR was correlate to the ratio C=O cyclic carbonate band area (1820 cm<sup>-1</sup>) / C=O ester band area (1734 cm<sup>-1</sup>) calculated by IR-ATR. As shown in [Table S1](#), for each reaction time, three samples were analyzed by IR-ATR to confirm the homogeneity of the modified polymer, allowing the calculation of an average ratio based on these three different analyses. The linear correlation between the cyclic carbonate yield and the average ratio is shown on Figure S18. All the cyclic carbonate yields for the modification of E-GMA-MA were determined using this calibration curve.

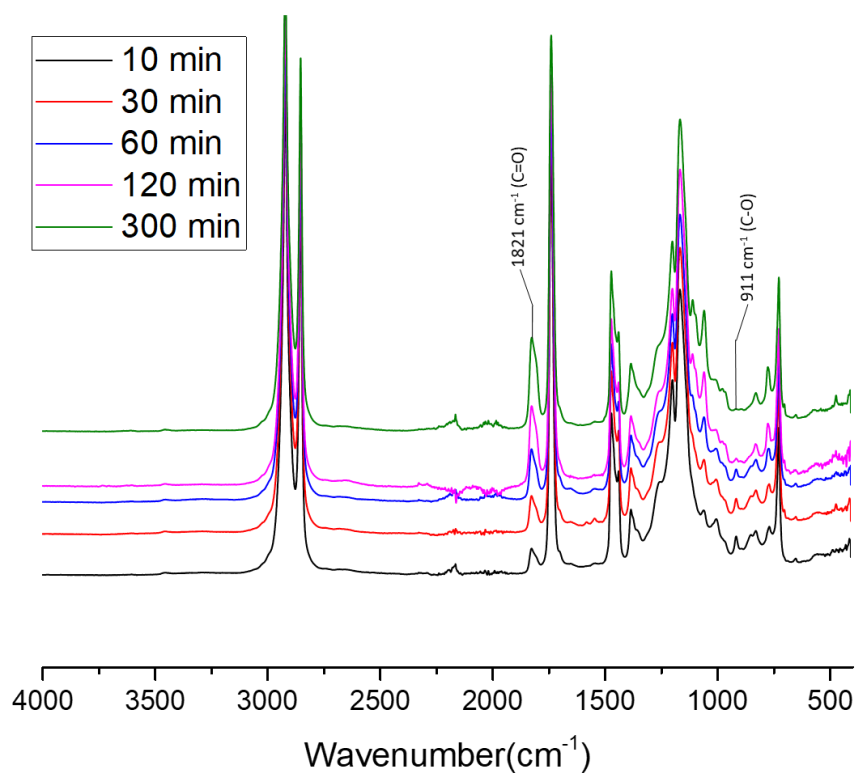
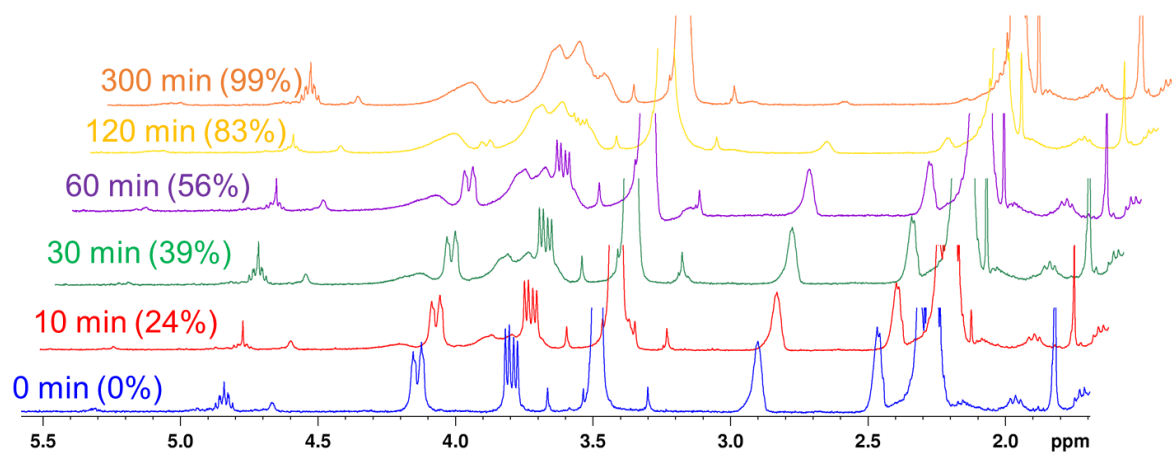


Figure S11. Reaction with TBAB in batch followed by  $^1\text{H}$  NMR (TCE/ $\text{C}_6\text{D}_6$ , 400MHz) and IR-ATR. Conditions: 2.0 g of E-GMA-MA (1.1 mmol of glycidyl methacrylate), 18 mg of TBAB (0.057 mmol, 5 mol%), 2.0 mL of toluene, 110  $^\circ\text{C}$ , 4.0 MPa of  $\text{CO}_2$ .

Table S1. Calculation of the ratio cyclic carbonate C=O band area (1820 cm<sup>-1</sup>) / ester C=O band area (1734 cm<sup>-1</sup>) for the reaction with E-GMA-MA using TBAB as catalyst.

Reaction time (min)	Cyclic carbonate C=O area	Ester C=O area	Ratio cyclic carbonate C=O area / ester C=O area	Ratio average	Yield (%)
10	0.433	6.200	0.0698	<b>0.0702</b>	<b>24</b>
	0.427	6.053	0.0705		
	0.428	6.084	0.0703		
30	0.680	6.138	0.1108	<b>0.1172</b>	<b>39</b>
	0.720	5.933	0.1213		
	0.733	6.140	0.1194		
60	0.999	5.991	0.1668	<b>0.1638</b>	<b>56</b>
	1.074	6.343	0.1693		
	0.908	5.848	0.1553		
120	1.727	6.423	0.2689	<b>0.2682</b>	<b>83</b>
	1.742	6.406	0.2719		
	1.647	6.241	0.2639		
300	2.059	6.174	0.3335	<b>0.3359</b>	<b>99</b>
	2.013	6.025	0.3341		
	2.089	6.145	0.3400		

Conditions: 2.0 g of E-GMA-MA (1.1 mmol of glycidyl methacrylate), 18 mg of TBAB (0.057 mmol, 5 mol%), 2.0 mL of toluene, 110 °C, 4.0 MPa of CO<sub>2</sub>.

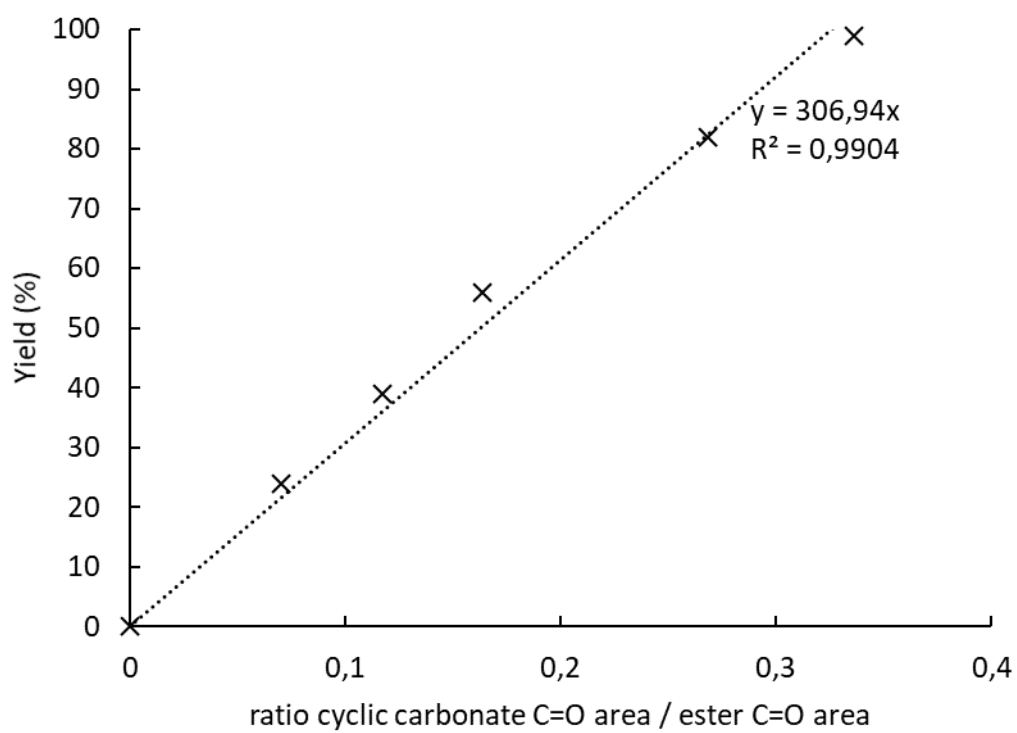


Figure S12. Calibration curve for the calculation of the cyclic carbonate yield with E-GMA-MA established from Table S1.



I.3.b. IR-ATR spectra

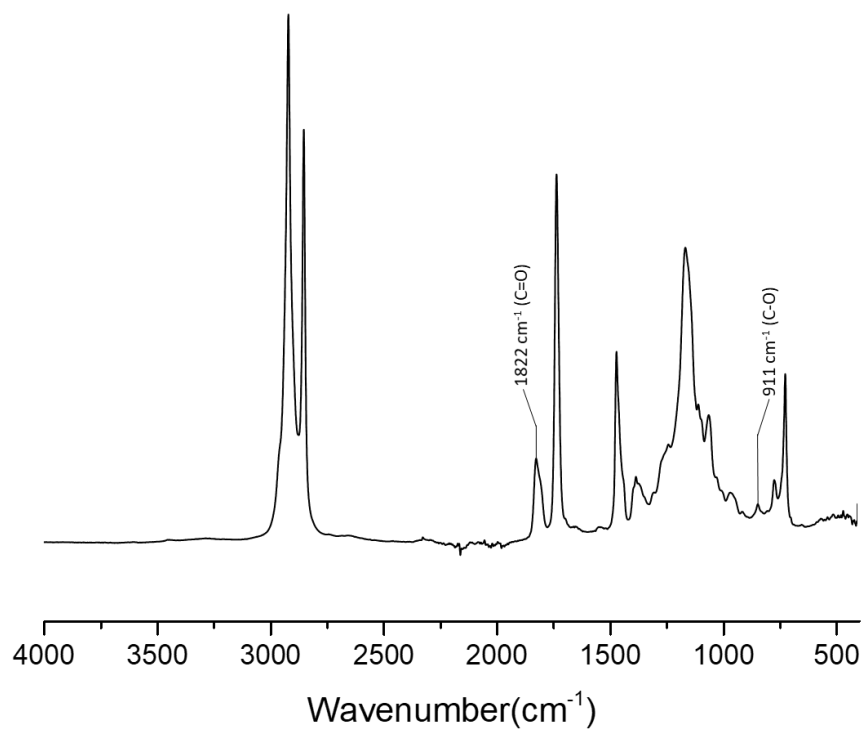


Figure S13. IR-ATR spectrum of E-GMA-BA modified with CO<sub>2</sub> in batch.

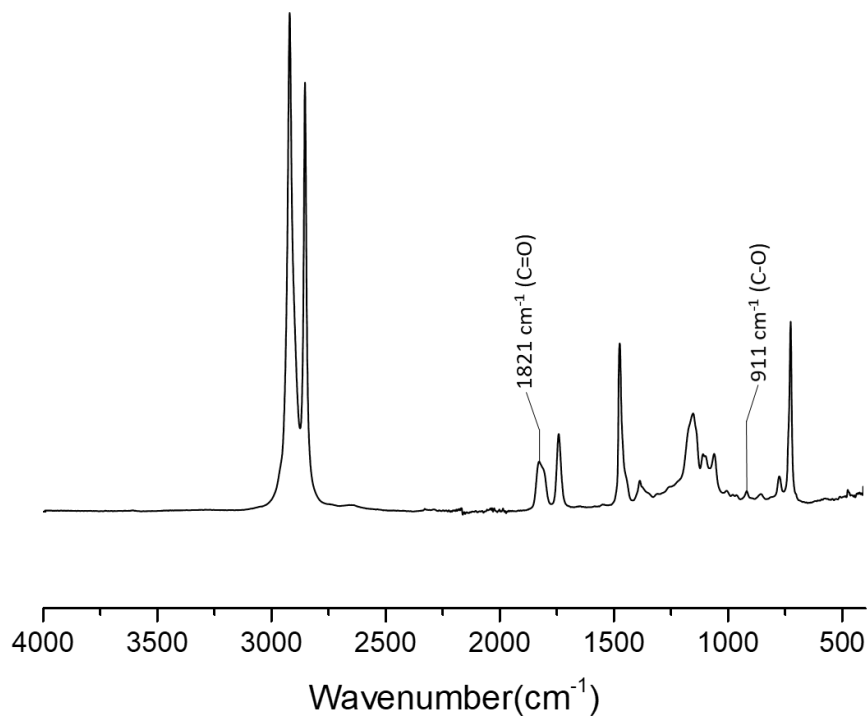


Figure S14. IR-ATR spectrum of E-GMA modified with CO<sub>2</sub> in batch.

I.3.c.  $^1\text{H}$  NMR spectra

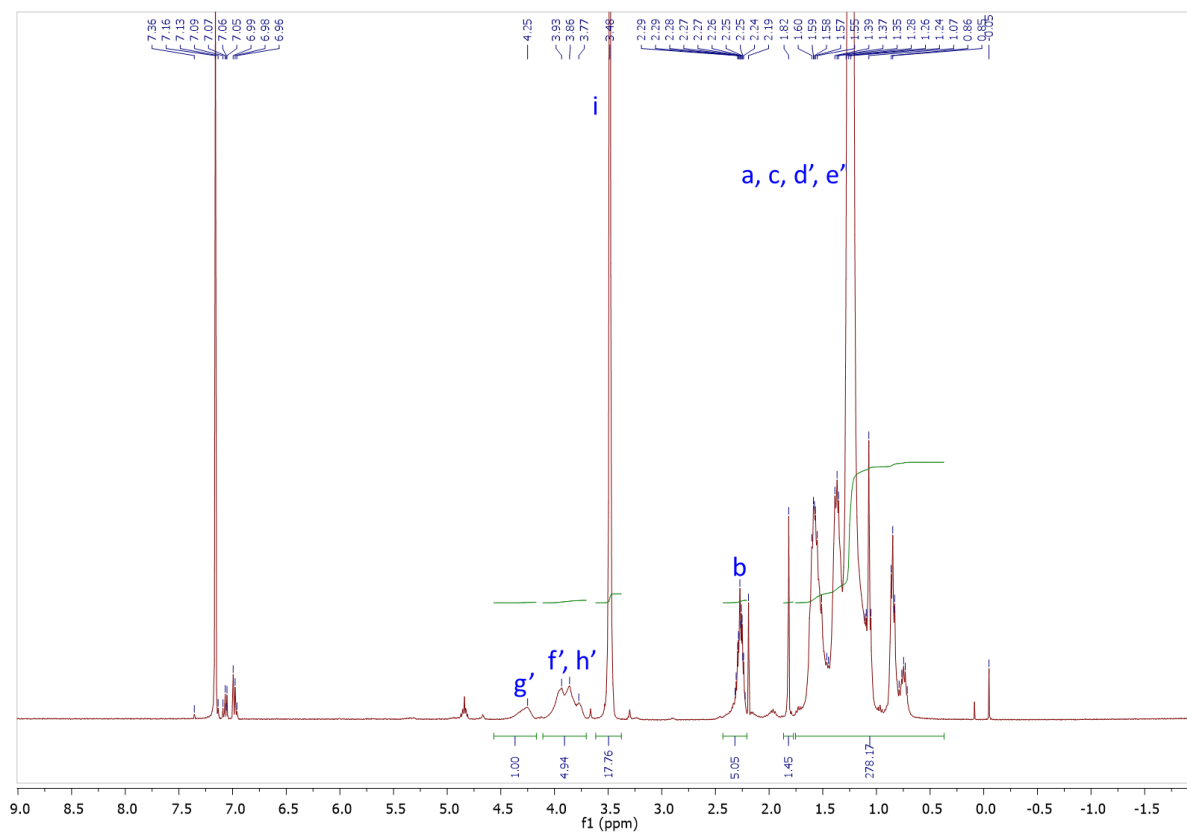
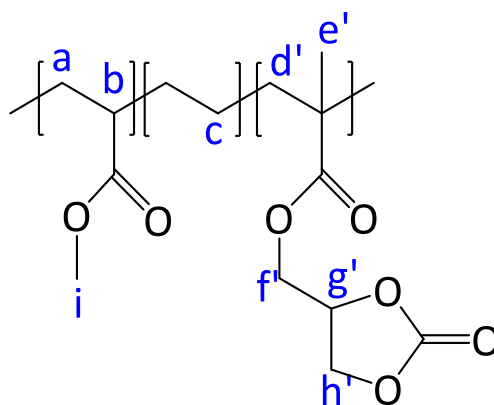


Figure S15.  $^1\text{H}$  NMR (TCE/ $\text{C}_6\text{D}_6$ , 400 MHz) spectrum of the modified E-GMA-MA with  $\text{CO}_2$  in batch.



$^1\text{H}$  NMR (400 MHz, TCE/ $\text{C}_6\text{D}_6$ )  $\delta$ : 4.25 (m,  $g'$ ), 4.07 – 3.70 (m,  $f'$ ,  $h'$ ), 3.48 (s,  $i$ ), 2.38 – 2.21 (m,  $b$ ), 1.84 – 0.33 (m,  $a$ ,  $c'$ ,  $d'$ ,  $e'$ ).

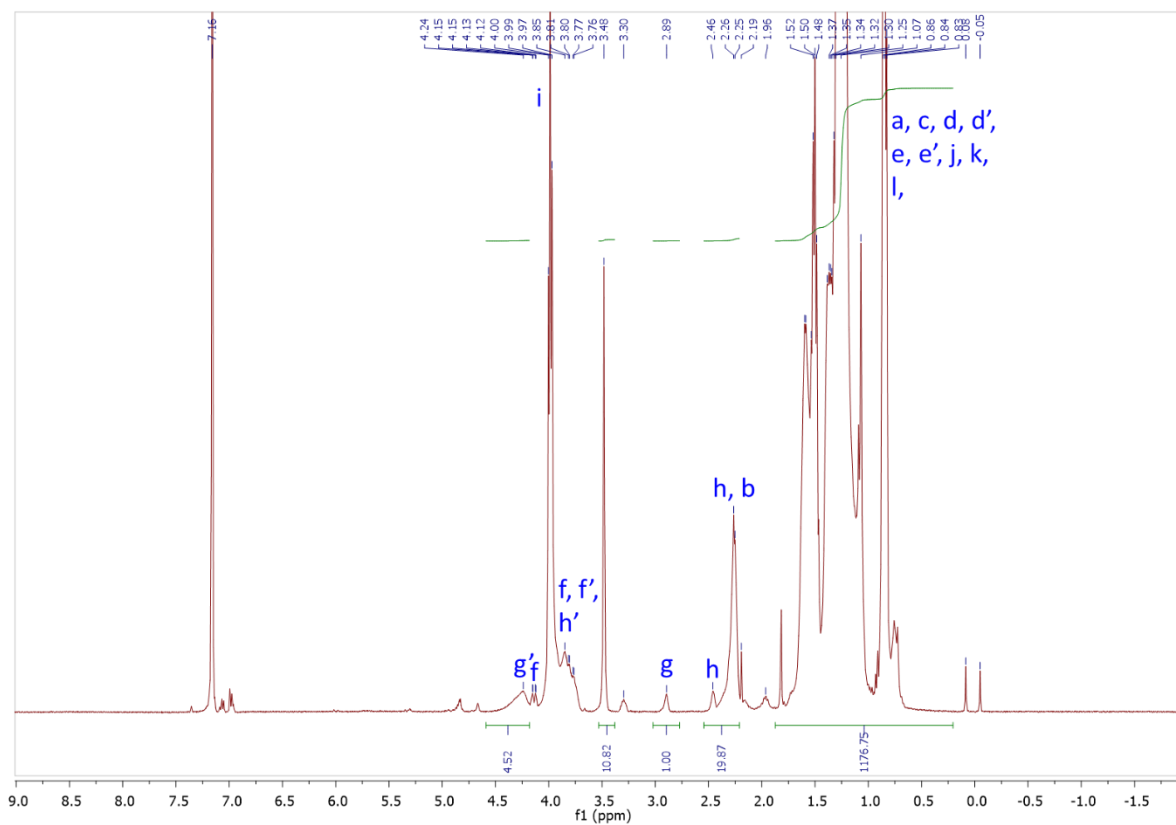
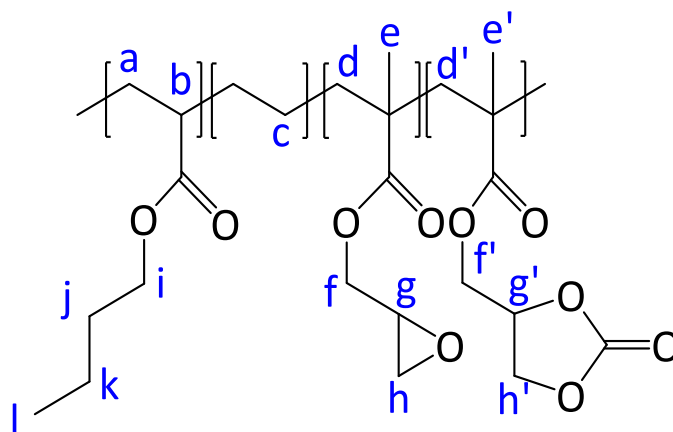


Figure S16.  $^1\text{H}$  NMR (TCE/ $\text{C}_6\text{D}_6$ , 400 MHz) spectrum of the modified E-GMA-BA with  $\text{CO}_2$  in batch.



$^1\text{H}$  NMR (400 MHz, TCE/ $\text{C}_6\text{D}_6$ )  $\delta$ : 4.24 (m,  $g'$ ), 4.14 (dd,  $J = 11.4, 2.9$  Hz,  $f$ ), 4.09 – 3.69 (m,  $f, f', h', i$ ), 3.48 (methyl acrylate), 2.89 (m,  $g$ ), 2.53 – 2.21 (m,  $h, b$ ), 1.88 – 0.37 (m,  $a, c, d, d', e, e', j, k, l$ ).

$$\text{Yield of cyclic carbonate} = \frac{S_{g'}}{S_g + S_{g'}} = \frac{4.52}{4.52 + 1.00} = 82\%$$

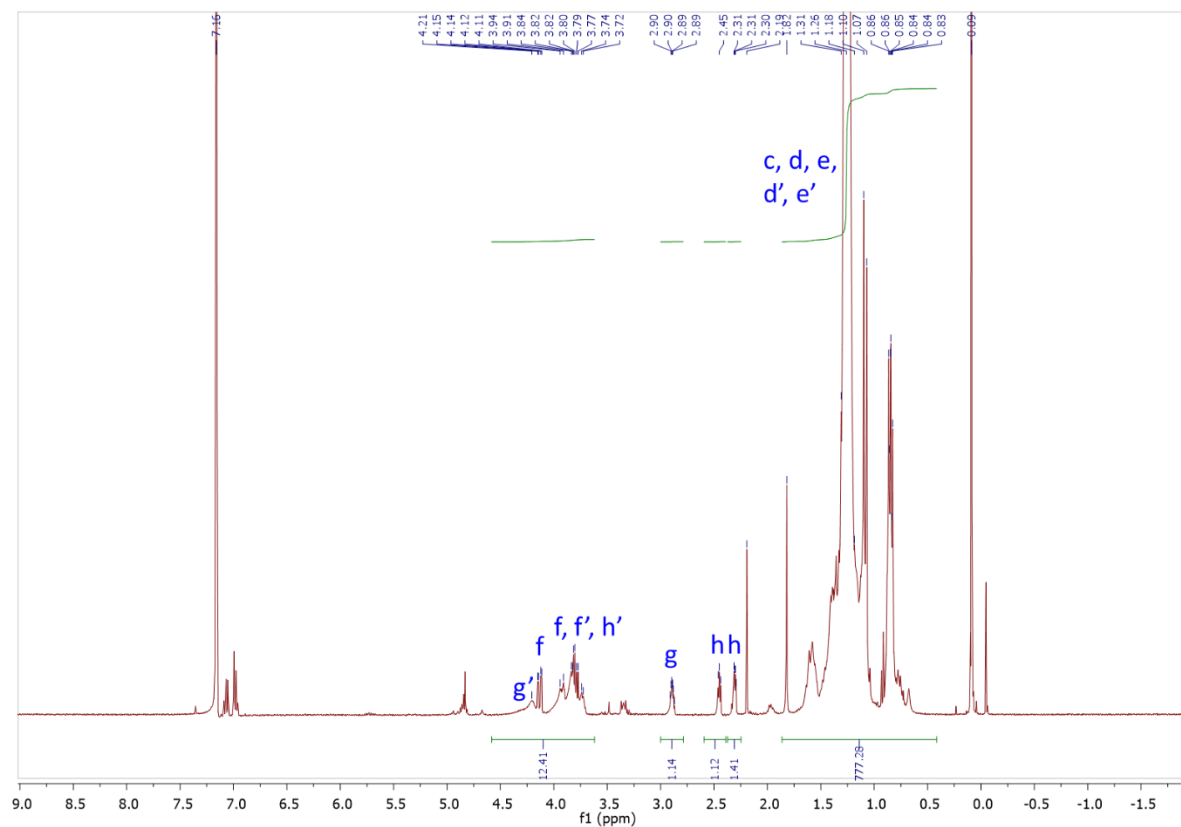
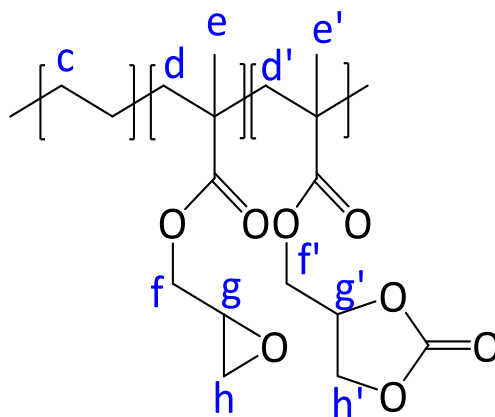


Figure S17.  $^1\text{H}$  NMR (TCE/ $\text{C}_6\text{D}_6$ , 400 MHz) spectrum of E-GMA modified with  $\text{CO}_2$  in batch.



$^1\text{H}$  NMR (400 MHz, TCE/ $\text{C}_6\text{D}_6$ )  $\delta$  : 4.51 – 3.66 (m,  $g'$ ,  $f$ ,  $f'$ ,  $h'$ ), 2.90 (m,  $g$ ), 2.45 (dd,  $J = 5.1, 4.1$  Hz,  $h$ ), 2.30 (dd,  $J = 5.3, 2.4$  Hz,  $h$ ), 1.87 – 0.45 (m,  $c, d, d', e, e'$ ).

$$\text{Yield of cyclic carbonate} = \frac{S_{f'} + S_{g'} + S_{h'}}{S_f + S_g + S_h + S_{f'} + S_{g'} + S_{h'}} = \frac{11.95 - 1.17 \times 2}{1.00 + 1.10 + 1.40 + 11.95} = 62\%$$

I.3.d.  $^{13}\text{C}$  NMR spectra

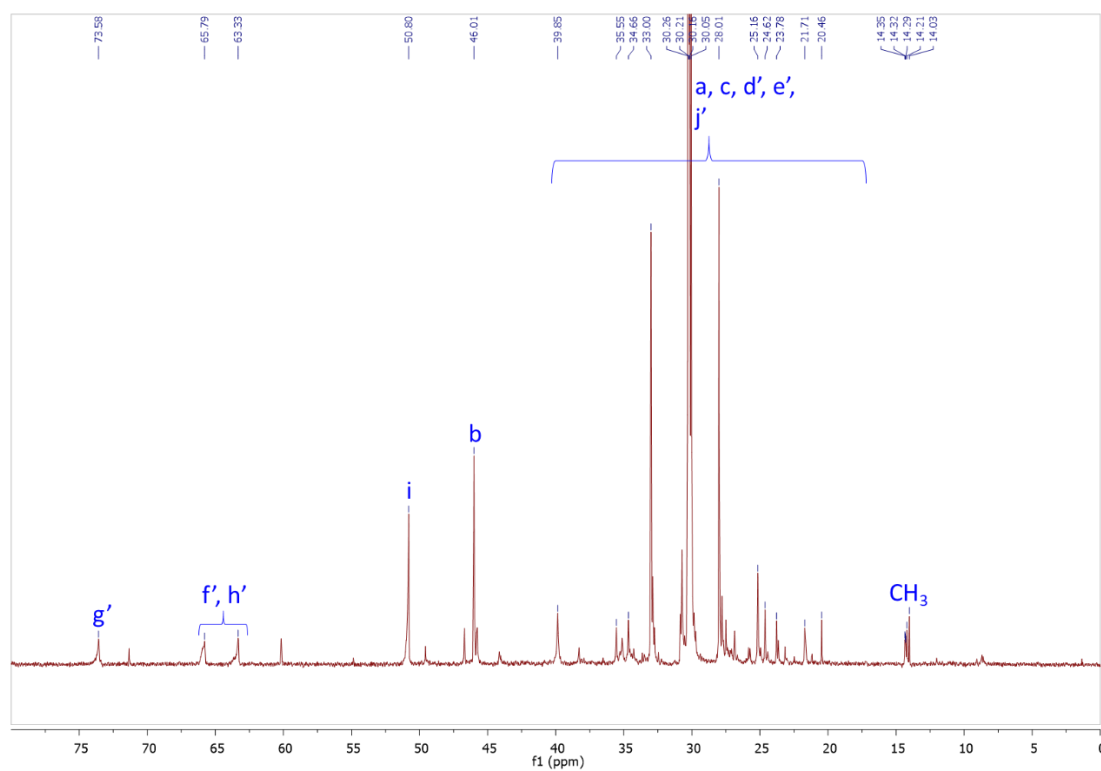
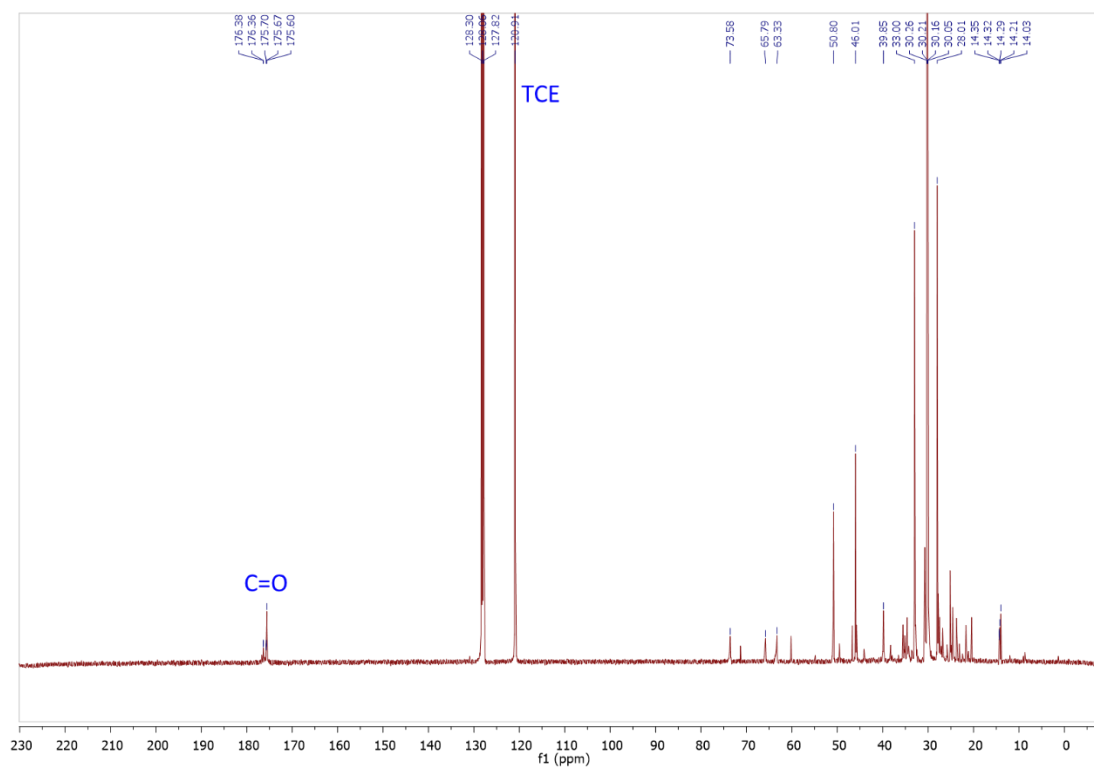
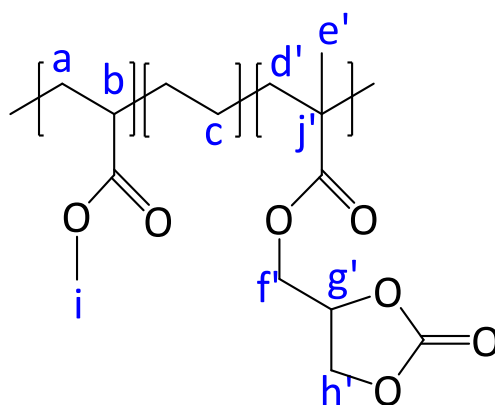


Figure S18.  $^{13}\text{C}$  NMR (101 MHz, TCE/ $\text{C}_6\text{D}_6$ ) spectrum of E-GMA-MA modified with  $\text{CO}_2$  in batch.



$^{13}\text{C}$  NMR (101 MHz, TCE/ $\text{C}_6\text{D}_6$ )  $\delta$ : 175.60 (C=O), 120.91 (TCE), 73.58 (g'), 65.79 – 63.33 (f', h'), 50.80 (i), 46.01 (b), 39.85 – 20.46 (a, c, d', e', j'), 14.35-14.03 ( $\text{CH}_3$ ).

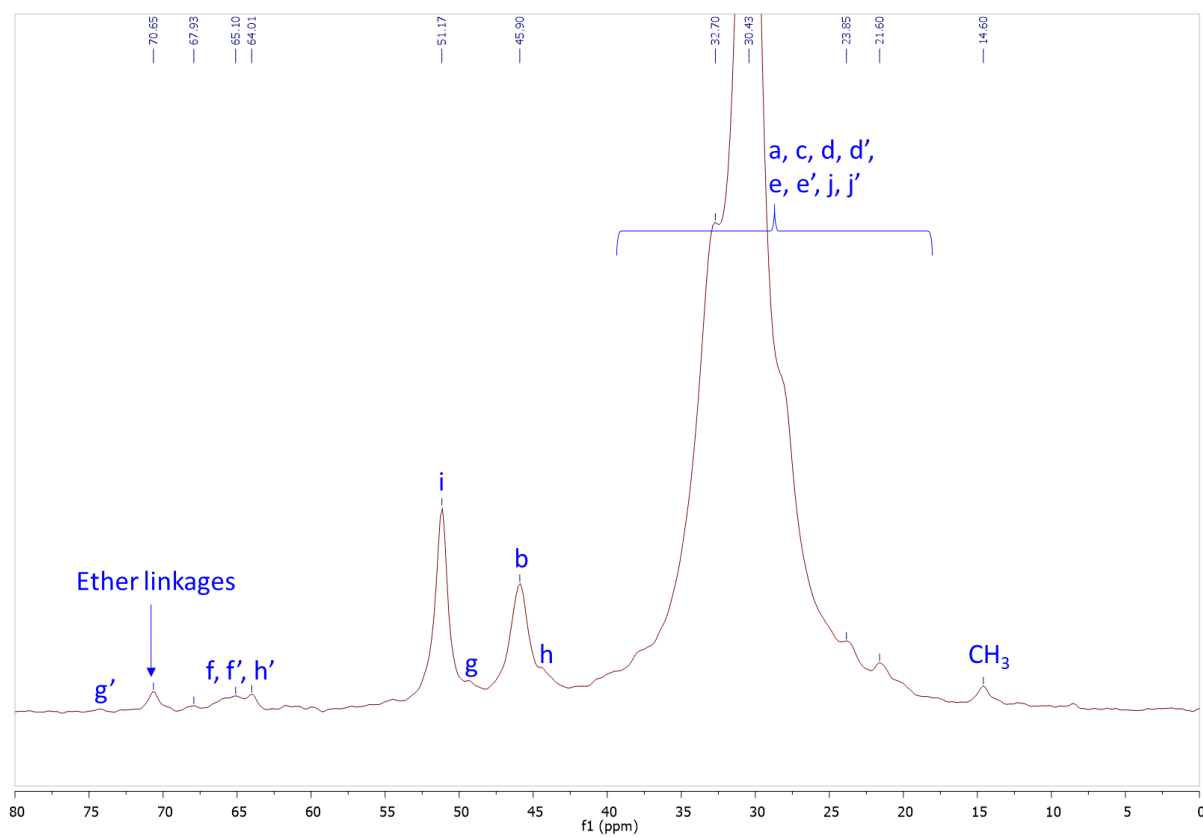
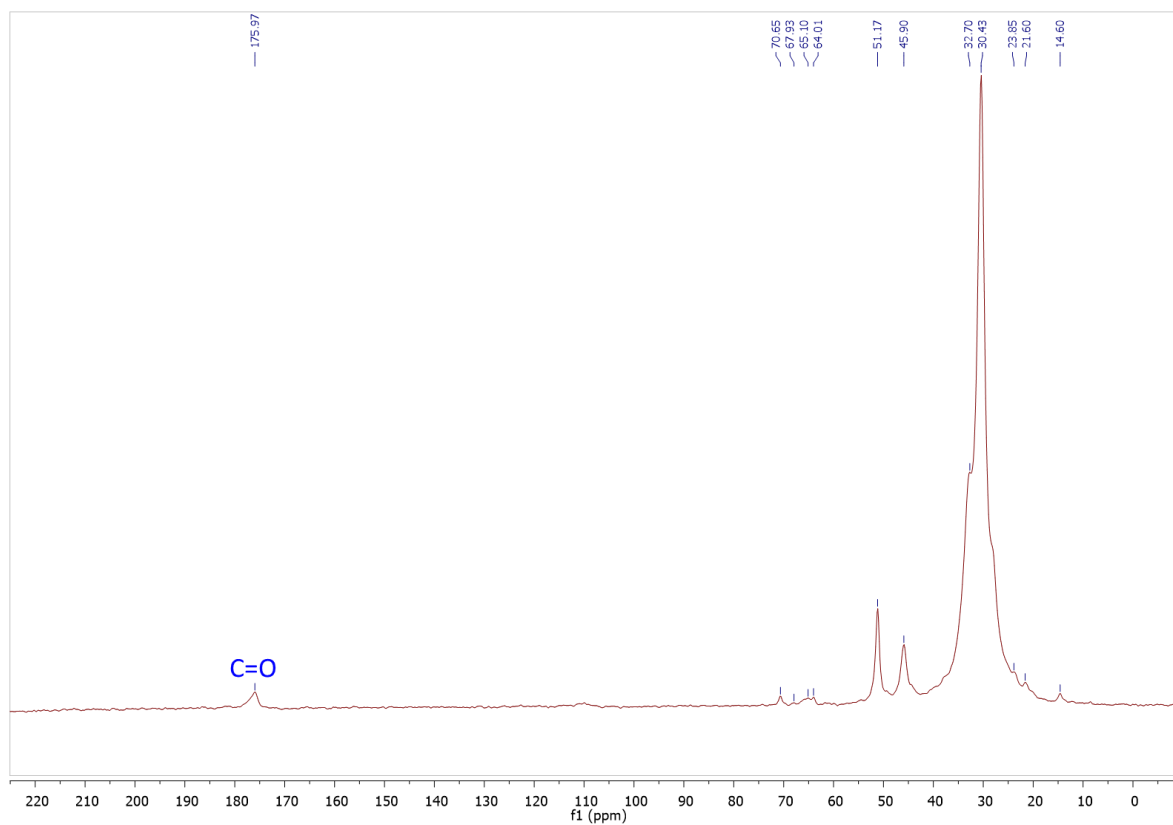
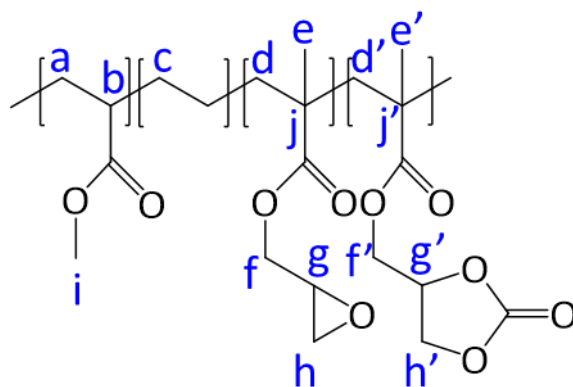


Figure S19. CP/MAS  $^{13}\text{C}$  NMR (126 MHz) spectrum of E-GMA-MA modified with  $\text{CO}_2$  and catalyzed by TBAC in batch.



CP/MAS  $^{13}\text{C}$  NMR (126 MHz)  $\delta$  175.97 (C=O), 74.25 ( $g'$ ), 70.65 (ether linkages), 69.19 – 62.61 ( $f, f', h'$ ), 51.17 ( $i$ ), 49.38 ( $g$ ), 45.90 ( $b$ ), 41.59 – 18.59 ( $a, c, d, d', e, e', j, j'$ ), 14.60 ( $\text{CH}_3$ ).



### I.3.e. DSC analyses

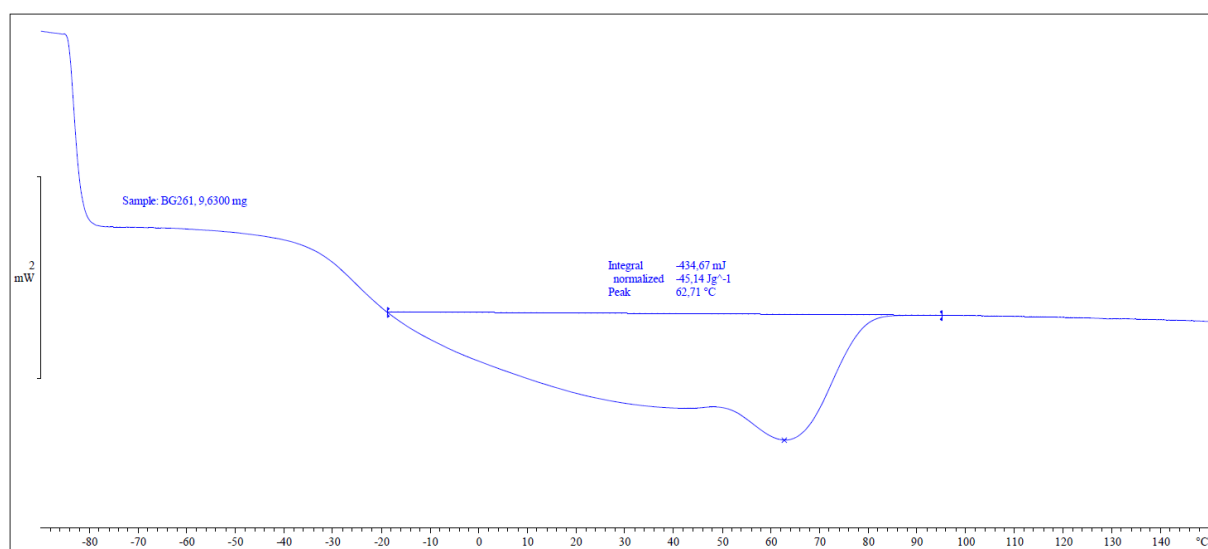


Figure S20. DSC analysis of E-GMA-MA modified with CO<sub>2</sub> in batch.

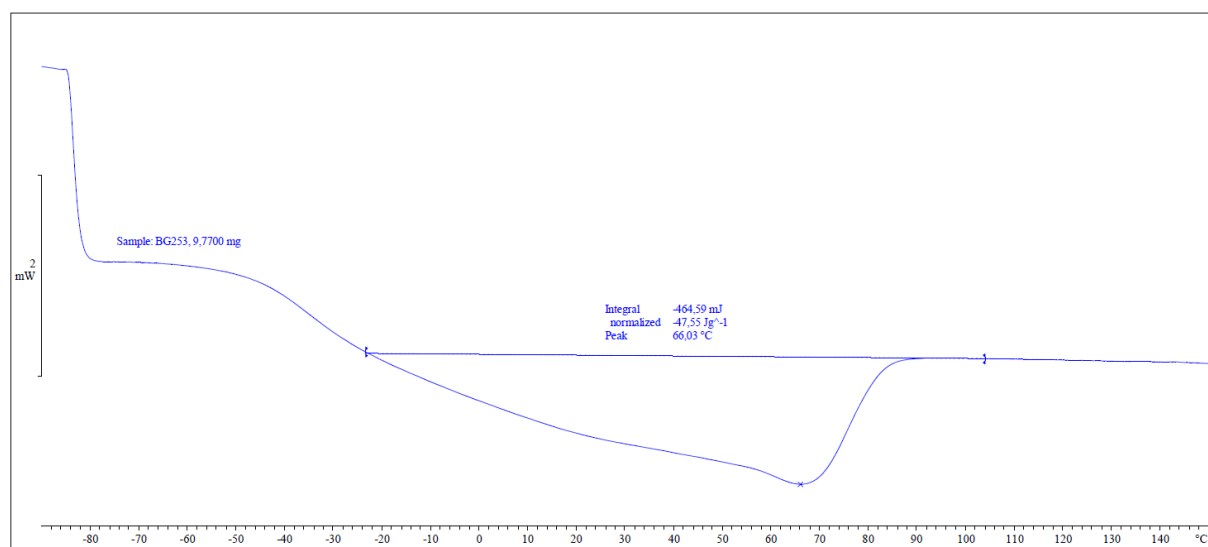


Figure S21. DSC analysis of E-GMA-BA modified with CO<sub>2</sub> in batch.

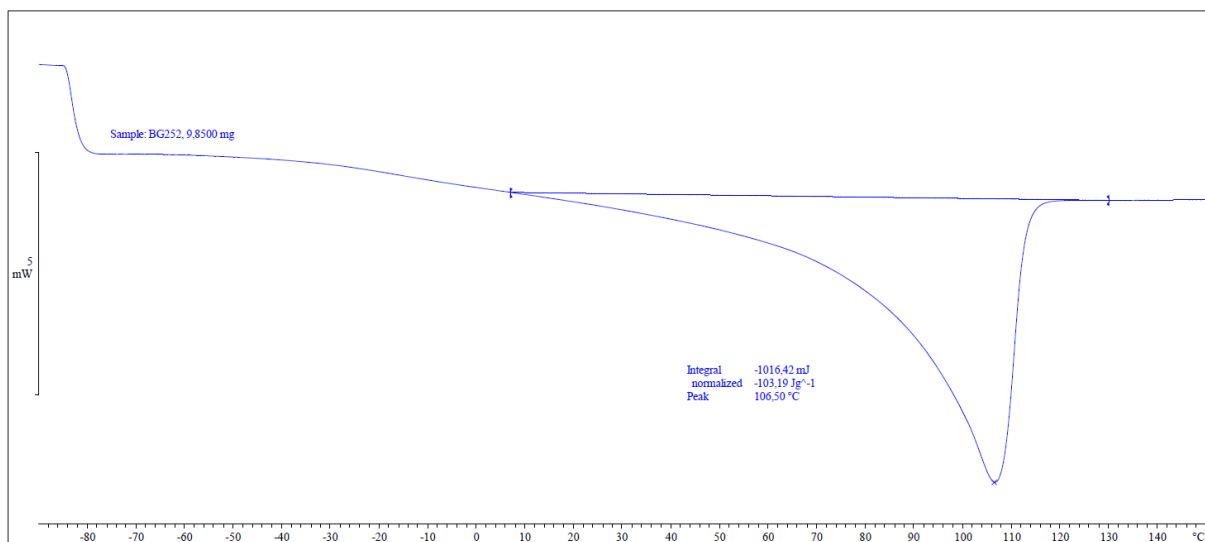


Figure S22. DSC analysis of E-GMA modified with CO<sub>2</sub> in batch.

I.3.f. TGA

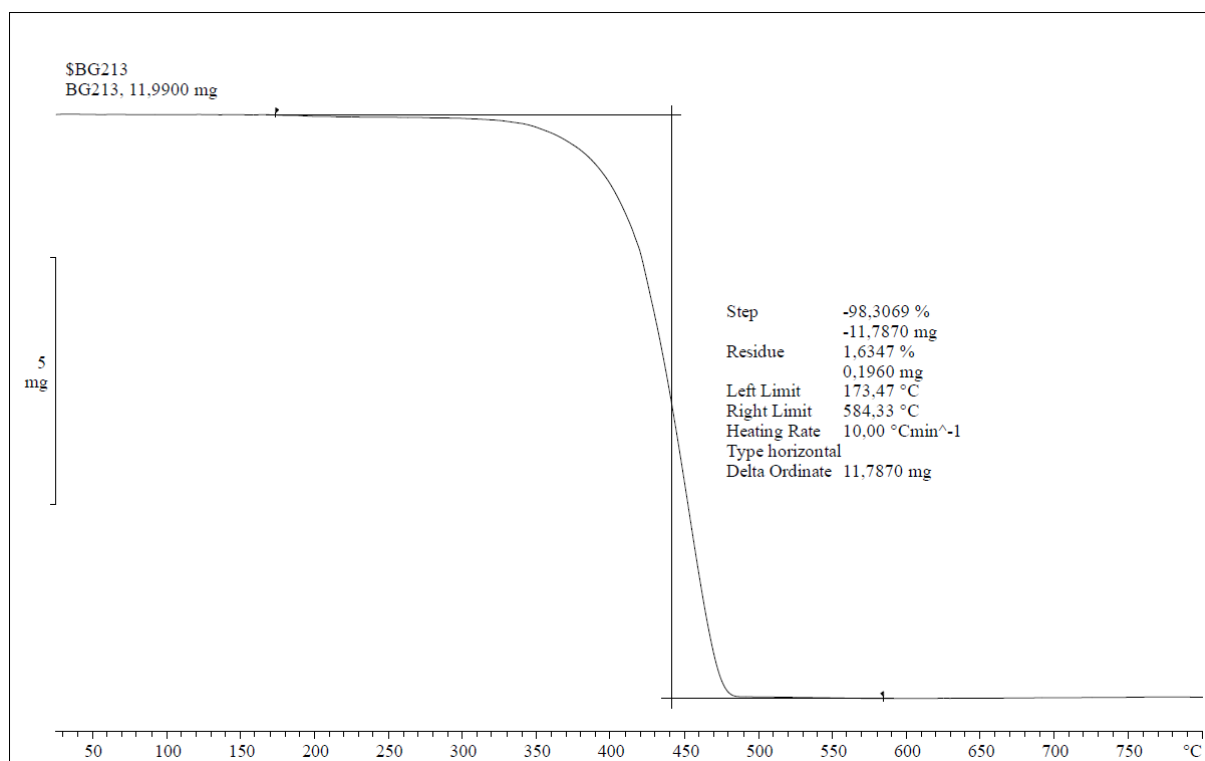


Figure S23. TGA analysis of E-GMA-MA modified with CO<sub>2</sub> in batch.

#### I.4. Carbonatation of [ethylene – glycidyl methacrylate] based copolymers by reactive extrusion

##### I.4.a. IR-ATR spectra

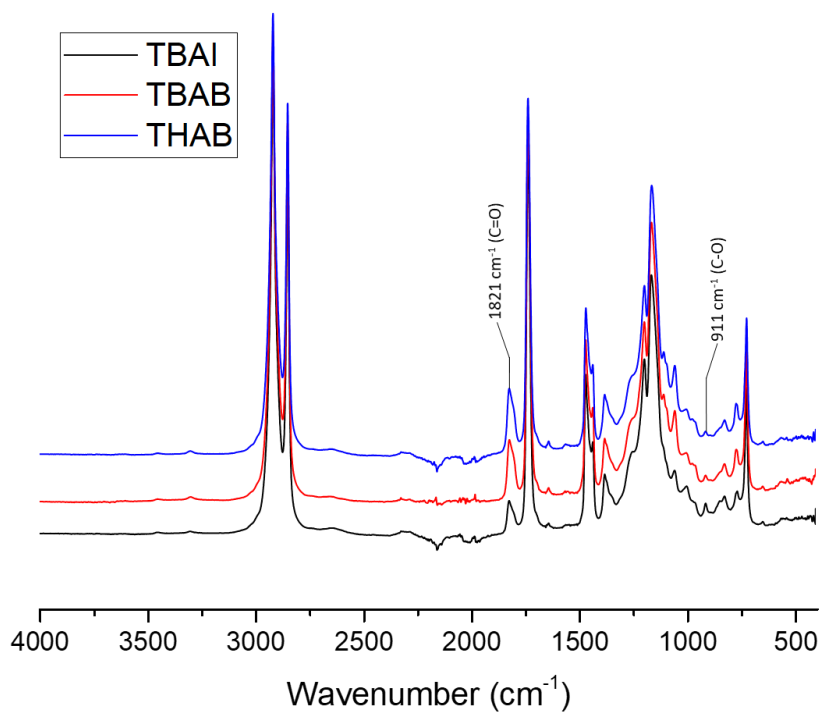


Figure S24. IR-ATR spectra of E-GMA-MA modified with CO<sub>2</sub> (catalyst (7.5 mol%), 150 °C, 4 MPa of CO<sub>2</sub>, 150 rpm, 2.0 kg/h) with different catalysts.

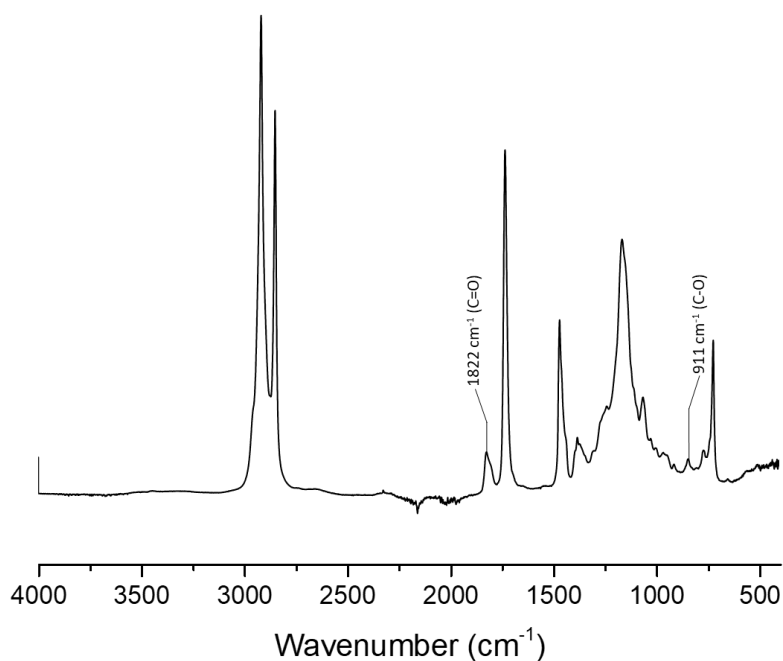


Figure S25. IR-ATR spectrum of E-GMA-BA modified with CO<sub>2</sub> in extruder.

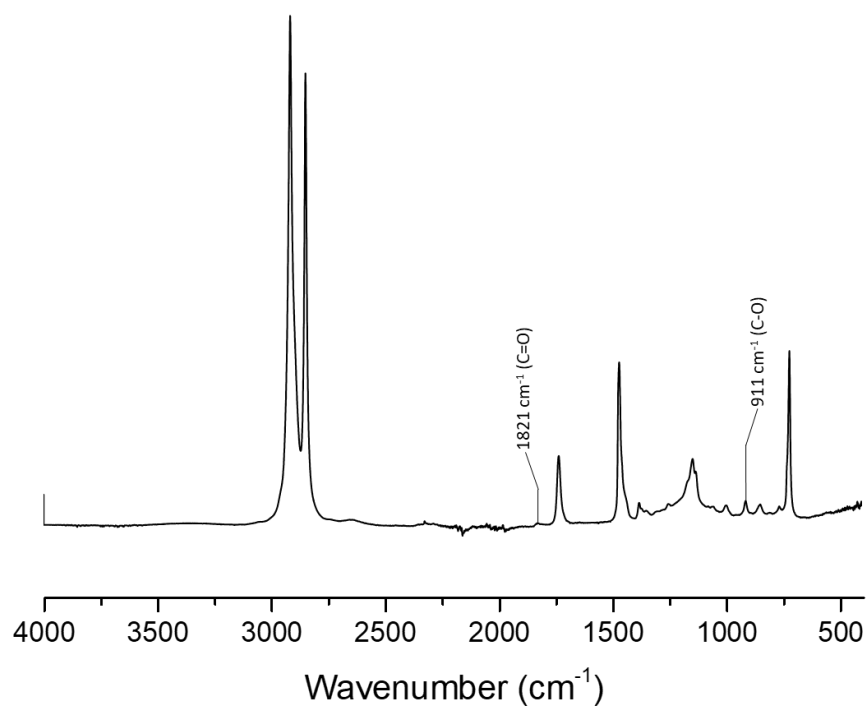


Figure S26. IR-ATR spectrum of E-GMA modified with  $\text{CO}_2$  in extruder.

### I.4.b. <sup>1</sup>H NMR spectra

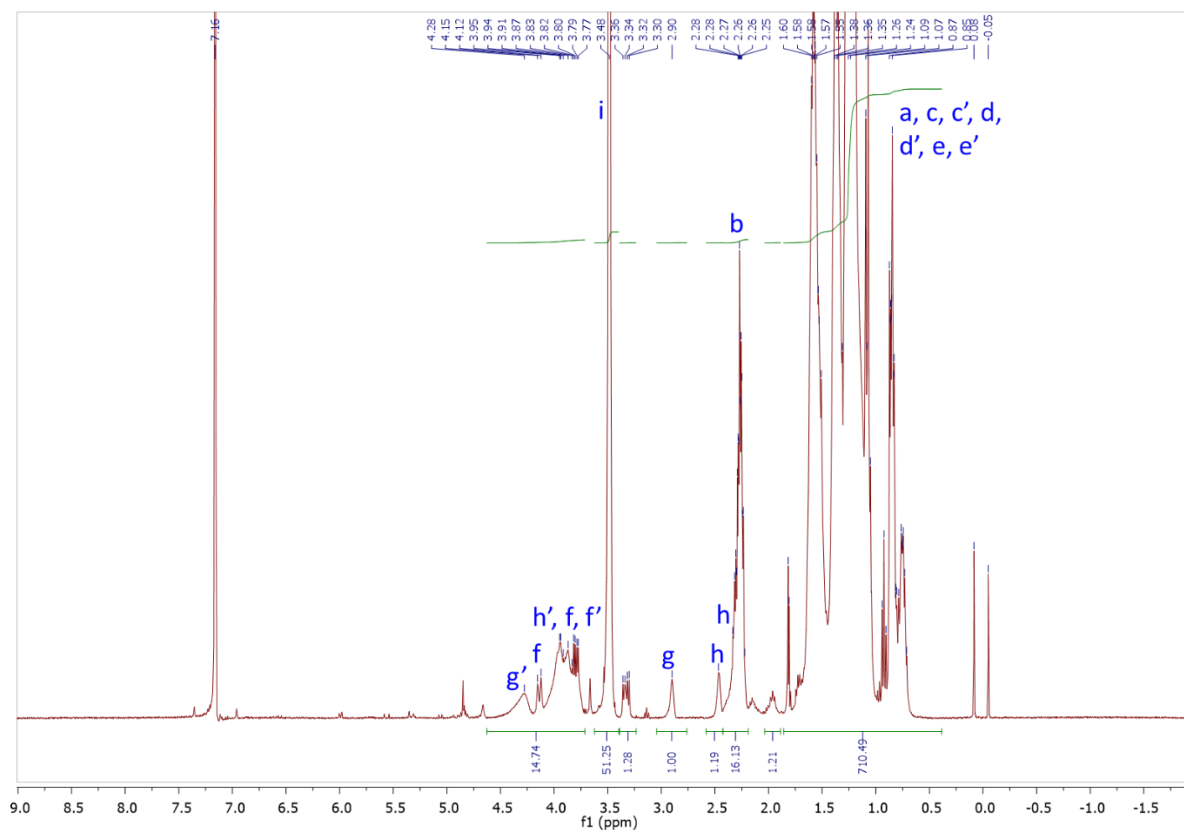
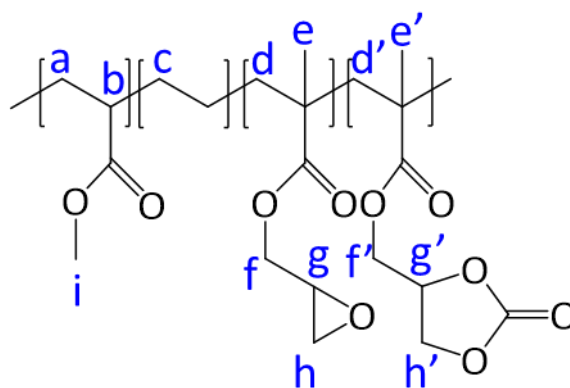


Figure S27. <sup>1</sup>H NMR (TCE/C<sub>6</sub>D<sub>6</sub>, 400 MHz) spectrum of the modified E-GMA-MA with CO<sub>2</sub> in extruder.



<sup>1</sup>H NMR (400 MHz, TCE/C<sub>6</sub>D<sub>6</sub>)  $\delta$ : 4.28 (m, g'), 4.14 (dd, J = 11.4, 2.9 Hz, f), 4.09 – 3.72 (m, f, f', h'), 3.48 (s, i) 2.90 (m, g), 2.53 – 2.21 (m, h, b), 1.88 – 0.42 (m, a, c, d, d', e, e', j, k, l).

$$\text{Yield of cyclic carbonate} = \frac{(S_{f''} + S_{g'} + S_{h'})/5}{S_g + (S_{f''} + S_{g'} + S_{h'})/5} = \frac{(14.74 - 2.00)/5}{(14.74 - 2)/5 + 1.00} = 72\%$$

Repeated experiment : 74 %

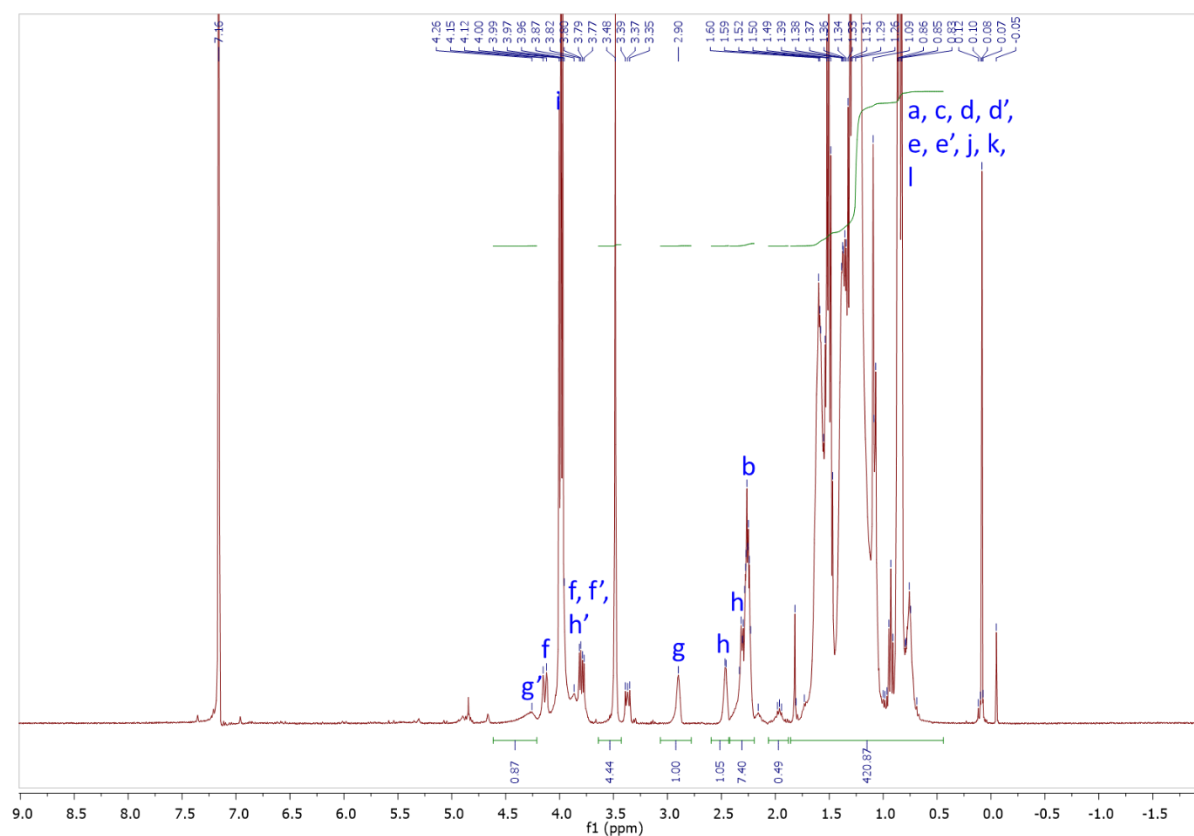
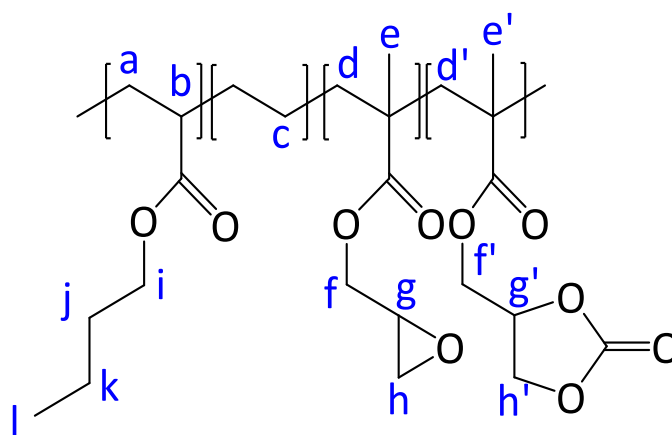


Figure S28.  $^1\text{H}$  NMR (TCE/ $\text{C}_6\text{D}_6$ , 400 MHz) spectrum of the modified E-GMA-BA with  $\text{CO}_2$  in extruder.



$^1\text{H}$  NMR (400 MHz, TCE/ $\text{C}_6\text{D}_6$ )  $\delta$ : 4.26 (m,  $g'$ ), 4.14 (dd,  $J = 11.4, 2.9$  Hz,  $f$ ), 4.09 – 3.69 (m,  $f, f', h', i$ ), 3.48 (methyl acrylate), 2.90 (m,  $g$ ), 2.53 – 2.21 (m,  $h, b$ ), 1.88 – 0.37 (m,  $a, c, d, d', e, e', j, k, l$ ).

$$\text{Yield of cyclic carbonate} = \frac{S_{g'}}{S_g + S_{g'}} = \frac{0.87}{0.87 + 1.00} = 47\%$$

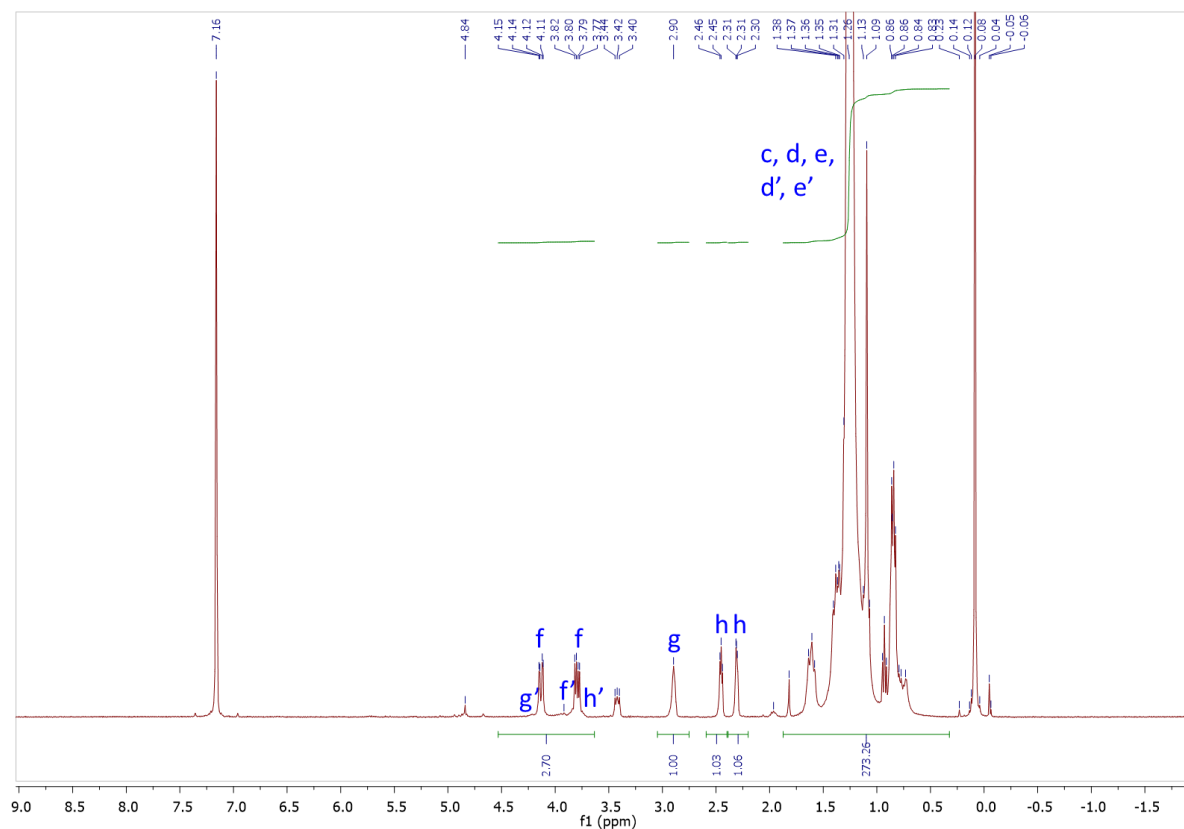
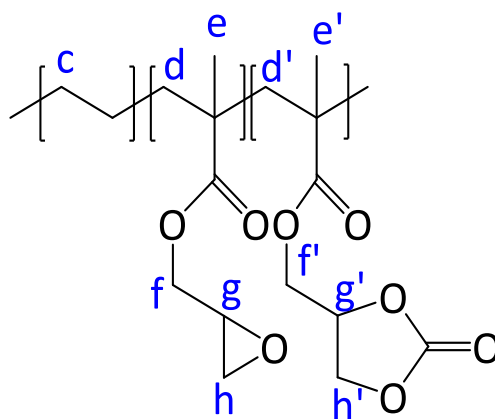


Figure S29.  $^1\text{H}$  NMR (TCE/ $\text{C}_6\text{D}_6$ , 400 MHz) spectrum of the modified E-GMA with  $\text{CO}_2$  in extruder.



$^1\text{H}$  NMR (400 MHz, TCE/ $\text{C}_6\text{D}_6$ )  $\delta$  : 4.38 – 3.61 (m, f, f', g', h'), 2.90 (m, g), 2.45 (dd, J = 5.1, 4.1 Hz, h), 2.30 (dd, J = 5.3, 2.4 Hz, h), 1.88 – 0.29 (m, c, d, d', e, e').

$$\text{Yield of cyclic carbonate} = \frac{S_{f'} + S_{g'} + S_{h'}}{S_f + S_g + S_h + S_{f'} + S_{g'} + S_{h'}} = \frac{2.70 - 2 \times 1.00}{2.70 + 1.00 + 2.09} = 12\%$$

I.4.c. DSC analyses

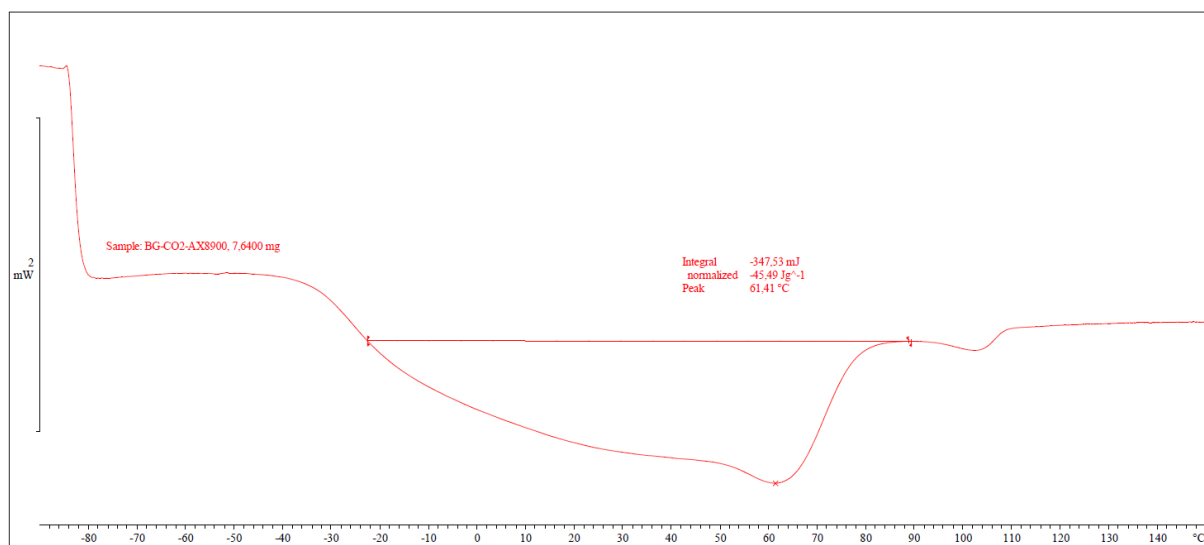


Figure S30. DSC analysis of the E-GMA-MA modified with CO<sub>2</sub> in extruder.

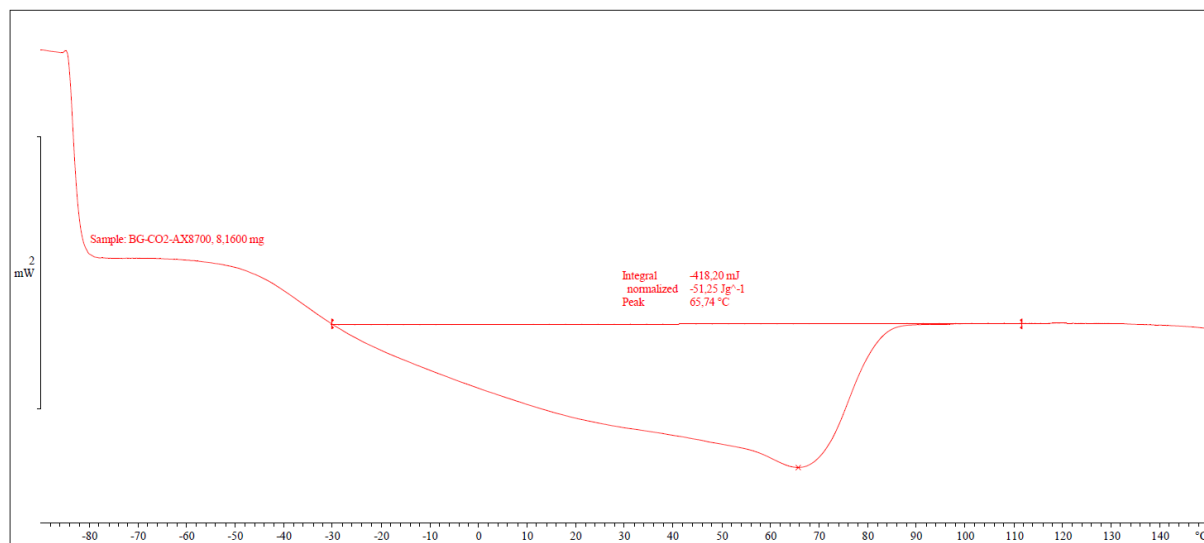


Figure S31. DSC analysis of the E-GMA-BA modified with CO<sub>2</sub> in extruder.



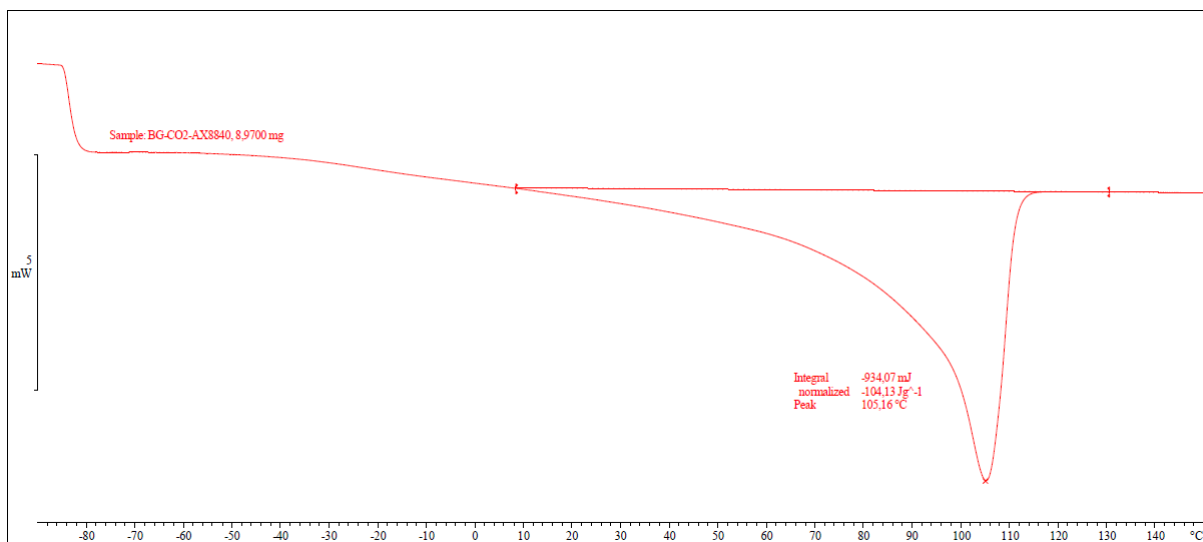


Figure S32. DSC analysis of the E-GMA modified with CO<sub>2</sub> in extruder.

### I.5. TGA

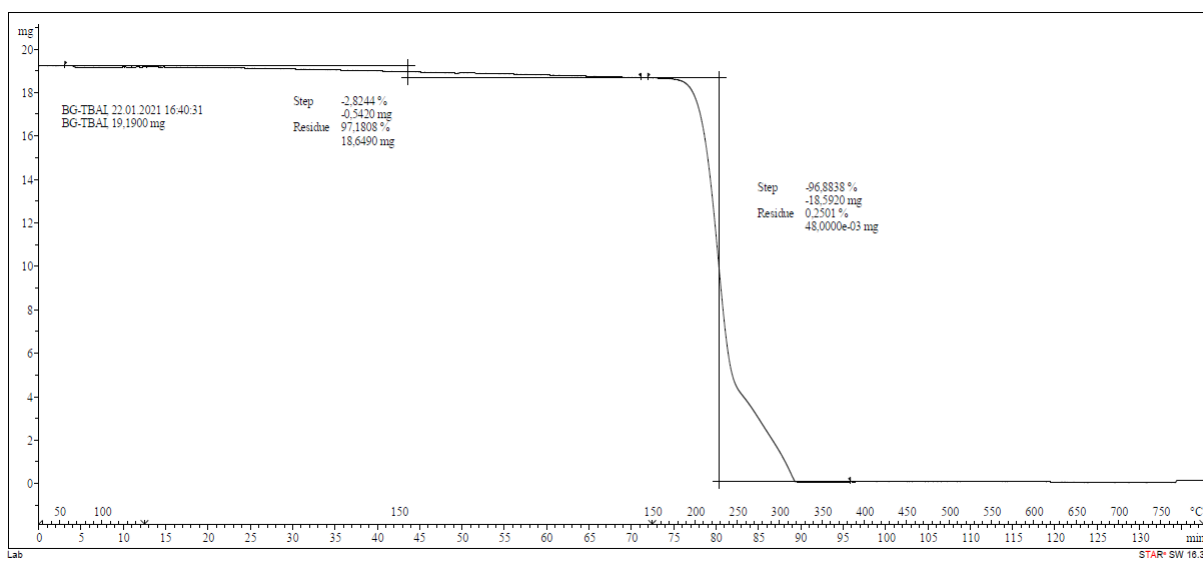


Figure S33. TGA of TBAI.

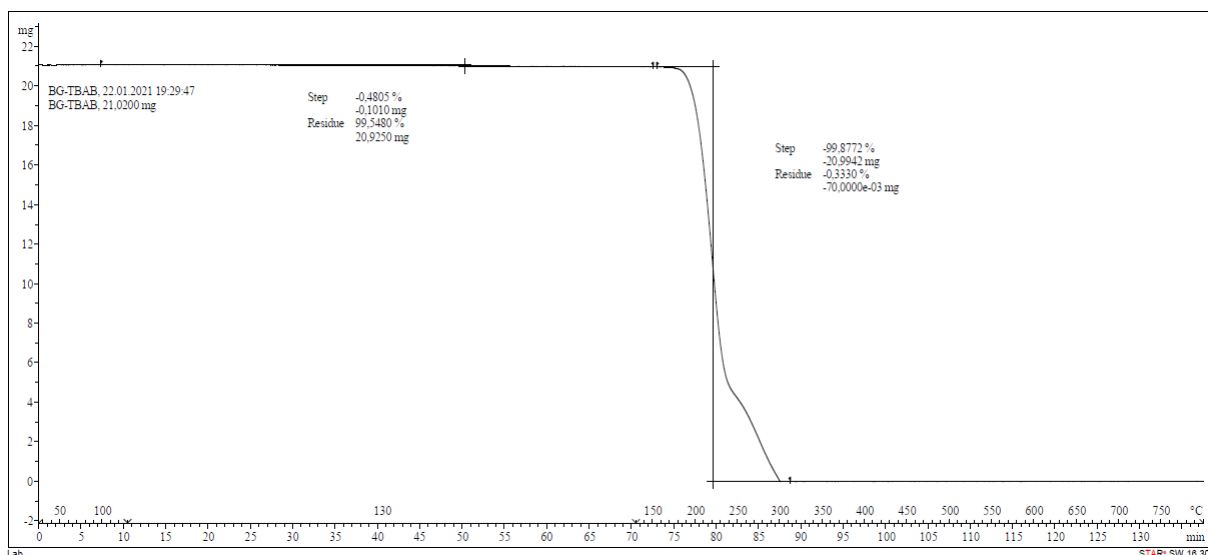


Figure S34. TGA of TBAB.

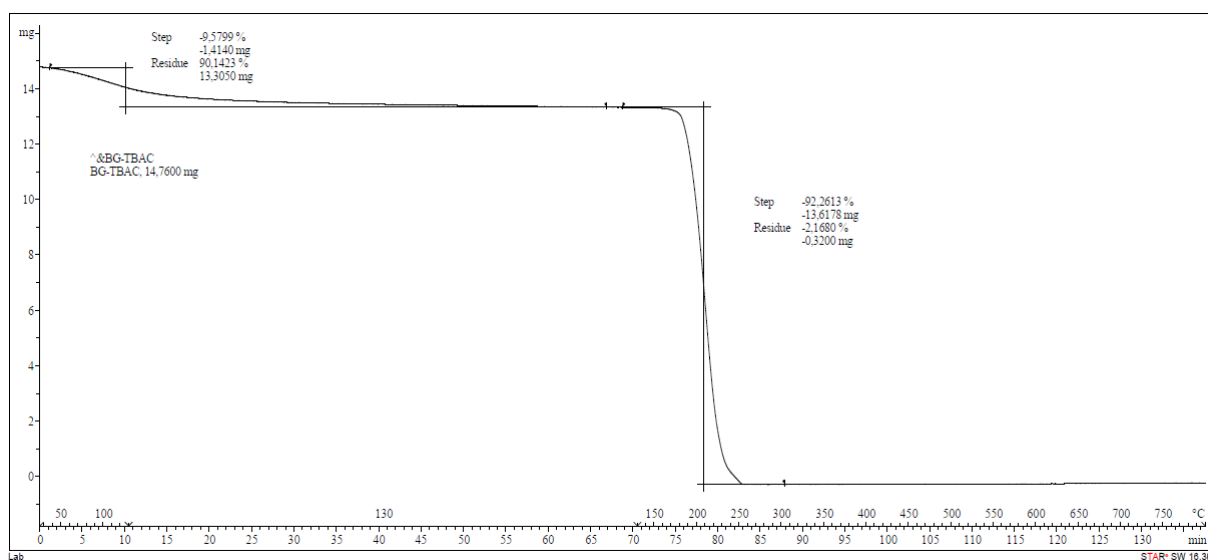


Figure S35. TGA of TBAC.

## I.6. High temperature SEC analyses in 1,2,4-TCB

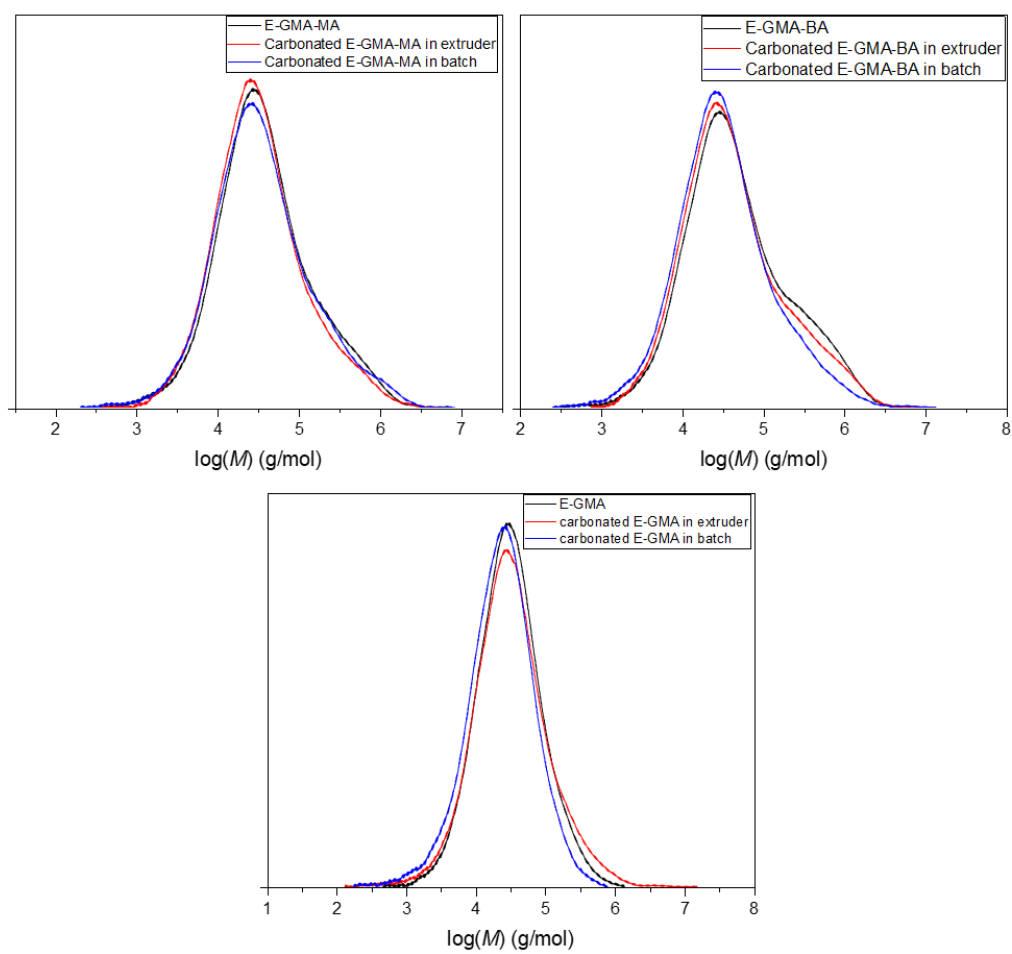


Figure S 36. DSC curves of the native and carbonated polymers.

I.7. Summary table of SEC and DSC analyses

Table S2. SEC and DSC analyses of the different polymers.

Entry	polymer	Sample	$M_n$ (g/mol)	$M_w$ (g/mol)	$\mathcal{D}$	$T_m$ (°C)
1	E-GMA-MA	1	16 600	101 300	6.1	62
2		2	16 900	84 500	5.0	
3	E-GMA-MA modified in batch	1	14 400	105 800	7.3	63
4		2	9 600	48 800	5.1	
5	E-GMA-MA modified in extruder	1	16 300	85 900	5.3	61
6		2	12 400	87 700	7.1	
7	E-GMA-BA	1	18 500	145 000	7.8	67
8		2	16 100	111 500	6.9	
9	E-GMA-BA modified in batch	1	14 300	101 500	7.1	66
10		2	10 100	54 800	5.4	
11	E-GMA-BA modified in extruder	1	18 800	133 700	7.1	66
12		2	11 700	113 600	9.7	
13	E-GMA	1	17 100	55 500	3.2	105
14		2	16 500	76 600	4.6	
15	E-GMA modified in batch	1	10 800	40 500	3.8	107
16		2	12 300	100 900	8.2	
17	E-GMA modified in extruder	1	13 500	81 200	6.0	105
18		2	15 300	106 400	7.0	

High values of dispersities  $\mathcal{D}$  are common for LDPE and LDPE-based copolymers synthesized using high temperatures (typically >200 °C) and high pressures (>1500 bar, up to 3000 bar): see for instance Ref [86].

## II. Chapter 3

### II.1. Solubility of the polymers and catalysts

*Table S3. Solubility of polymers and catalysts.*

Entry	Compound	Solubility in toluene	Solubility in MEK
1	TOAB	Soluble	Soluble
2	TBAC	Soluble	Soluble
3	PPNCl	Insoluble	Soluble
4	PBU-1	Soluble	Soluble
5	PBU-2	Soluble	Soluble
6	PBU-3	Soluble	Soluble
7	SBS	Soluble	Soluble
8	NR-1	Soluble	Soluble
9	SIS	Soluble	Soluble
10	DCPD-EPDM	Soluble	Insoluble
11	ENB-EPDM	Soluble	Insoluble
12	E-PBU-1	Soluble	Soluble
13	E-PBU-2	Soluble	Soluble
14	E-PBU-3	Soluble	Soluble
15	E-PBU-4	Soluble	Soluble
16	E-SBS	Soluble	Soluble
17	E-NR-1	Soluble	Soluble
18	E-NR-2	Soluble	Soluble
19	E-SIS	Soluble	Soluble
20	E-DCPD-EPDM	Soluble	Insoluble
21	E-ENB-EPDM	Soluble	Insoluble

## II.2. Characterization of the commercial polymers

### II.2.a. IR-ATR spectra

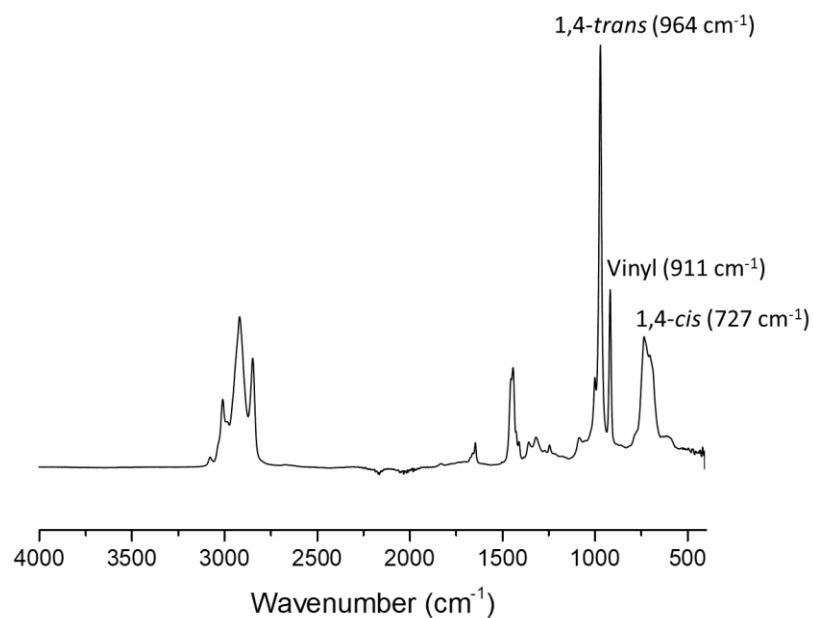


Figure S37. IR-ATR spectrum of PBU-1.

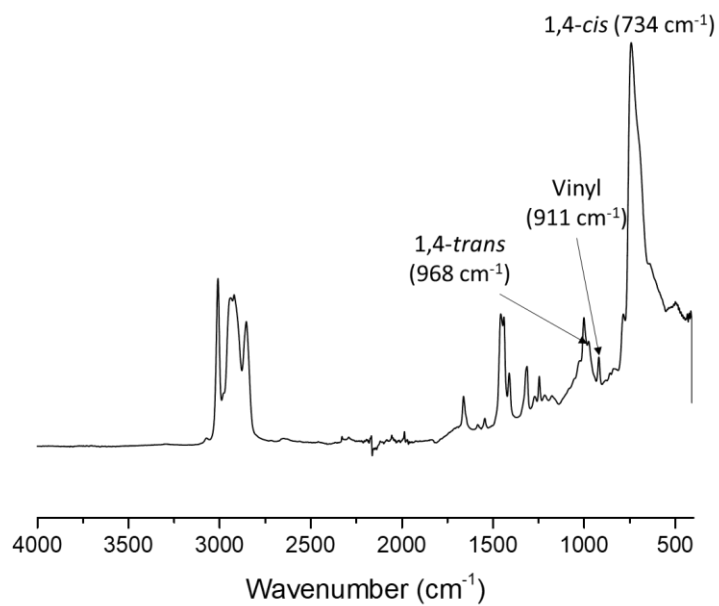


Figure S38. IR-ATR spectrum of PBU-2.

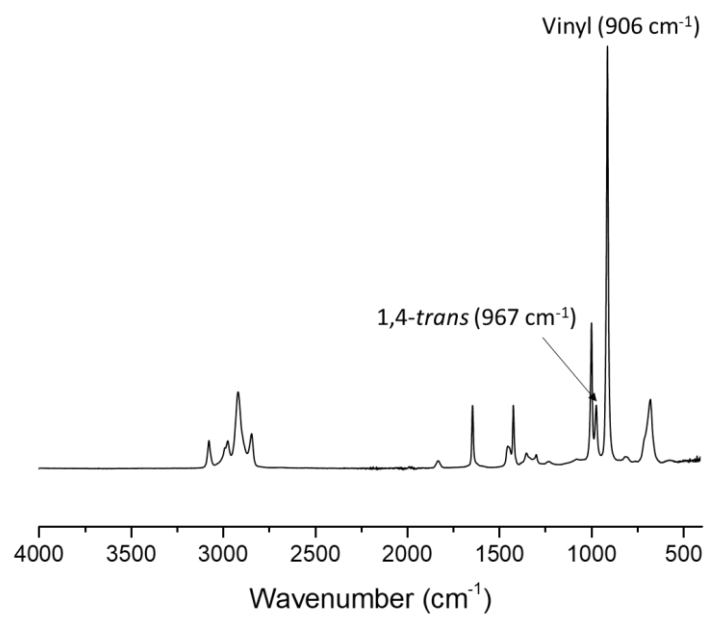


Figure S39. IR-ATR spectrum of PBU-3.

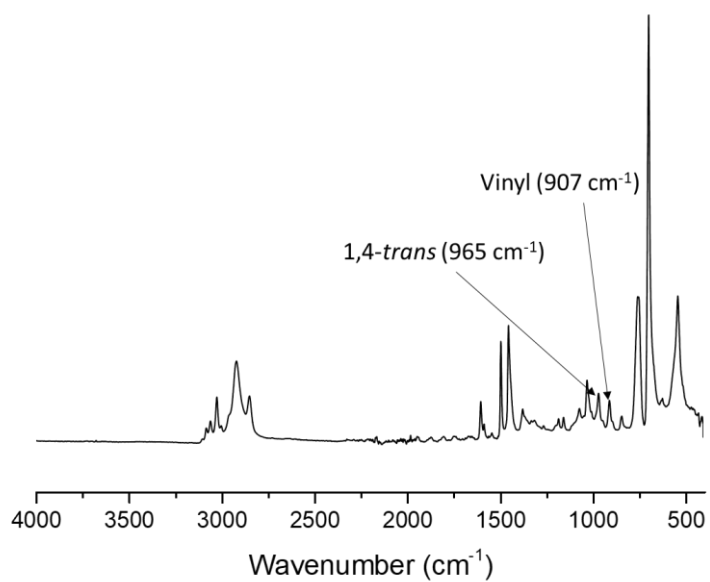


Figure S40. IR-ATR spectrum of SBS.

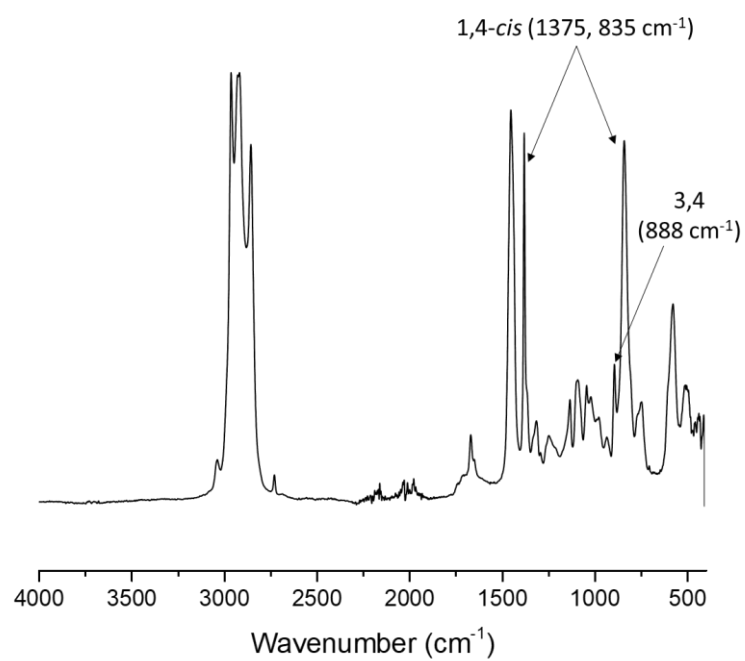


Figure S41. IR-ATR spectrum of NR-1.

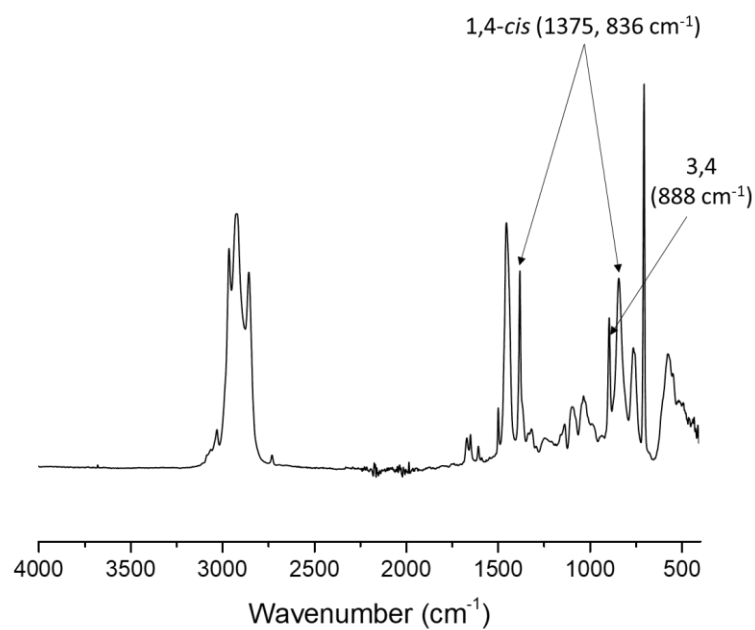


Figure S42. IR-ATR spectrum of SIS.



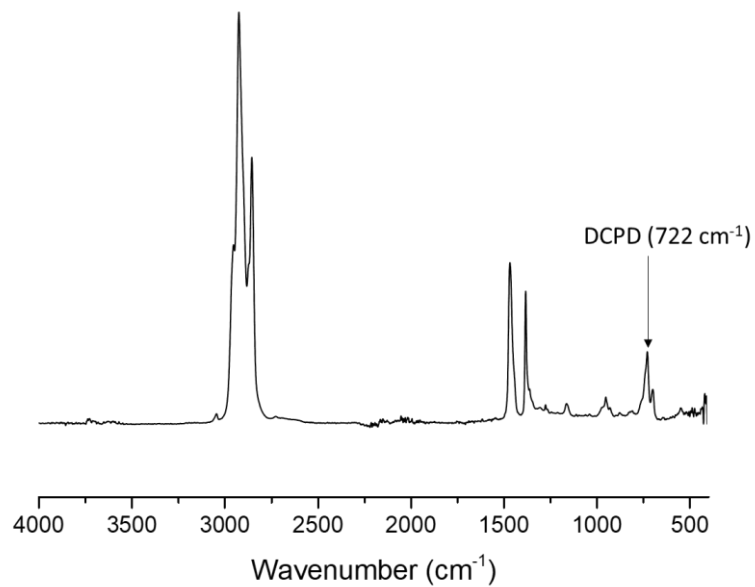


Figure S43. IR-ATR spectrum of EPDM-DCPD.

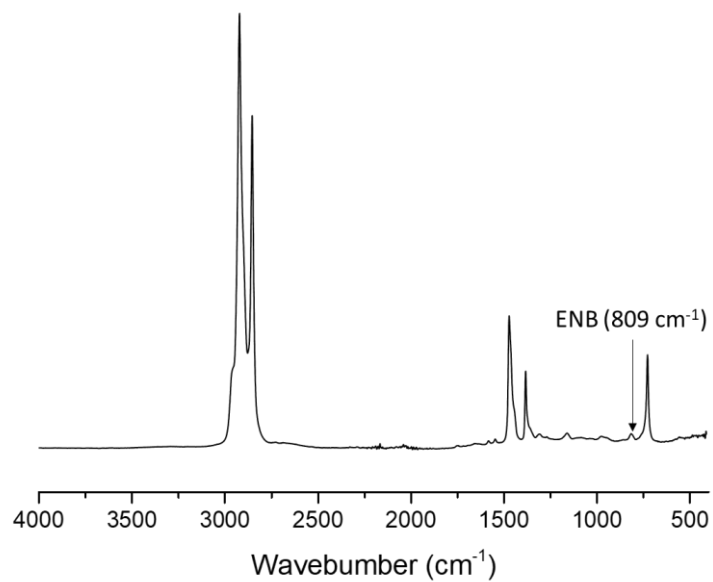


Figure S44. IR-ATR spectrum of EPDM-ENB.

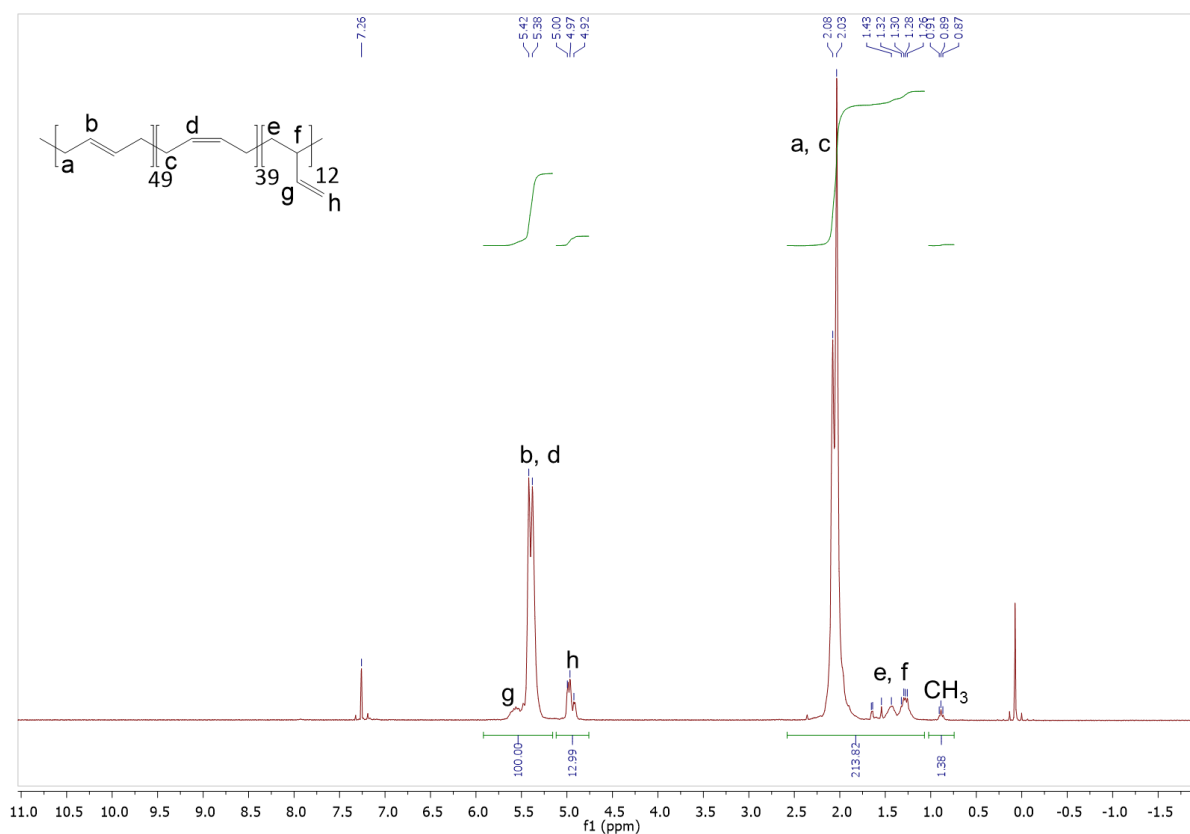
II.2.b.  $^1\text{H}$  NMR spectra


Figure S45.  $^1\text{H}$  NMR spectrum of PBU-1.

$^1\text{H}$  NMR (300 MHz,  $\text{CDCl}_3$ )  $\delta$ : 5.71-5.19 (m, b, d, g), 5.07-4.81 (m, h), 2.30-1.74 (m, a, c), 1.74-1.05 (m, e, f), 0.89 (t,  $J = 6.1$  Hz,  $\text{CH}_3$ ).

$$\text{Mol\% (1,4 units)} = \frac{S_b + S_d}{S_b + S_d + S_h} = \frac{100 - 12.99/2}{(100 - \frac{12.99}{2}) + 12.99} = 88 \text{ mol\%}$$

$$\text{Mol\% (1,2 units)} = 100 - \text{Mol\% (1,4 units)} = 12 \text{ mol\%}$$

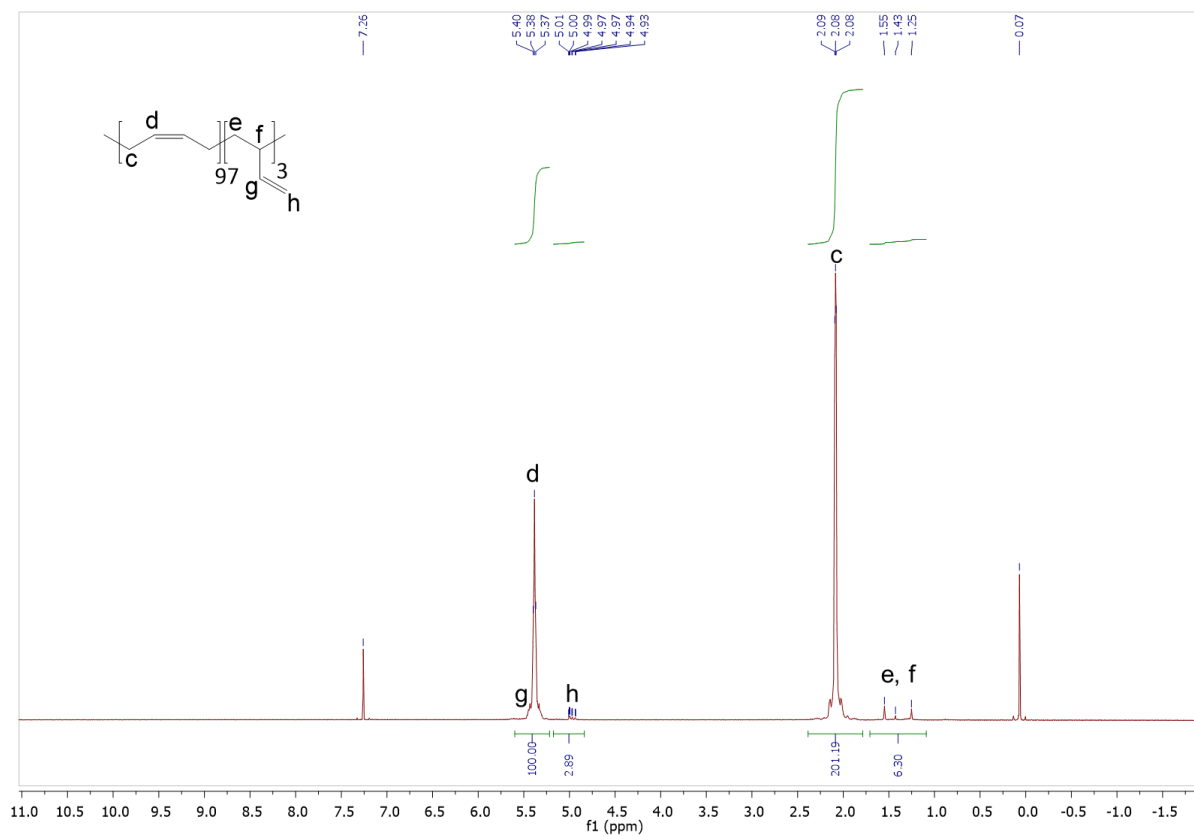


Figure S46.  $^1\text{H}$  NMR spectrum of PBU-2.

$^1\text{H}$  NMR (300 MHz,  $\text{CDCl}_3$ )  $\delta$ : 5.38 (m, d, g), 5.11 – 4.81 (m, h), 2.32 – 1.80 (m, c), 1.68 – 1.14 (m, e,f).

$$\text{Mol}\% (1,4 - \text{cis units}) = \frac{S_d}{S_d + S_h} = \frac{100 - 2.89/2}{(100 - \frac{2.89}{2}) + 2.89} = 97 \text{ mol}\%$$

$$\text{Mol}\% (1,2 \text{ units}) = 100 - \text{Mol}\% (1,4 \text{ units}) = 3 \text{ mol}\%$$

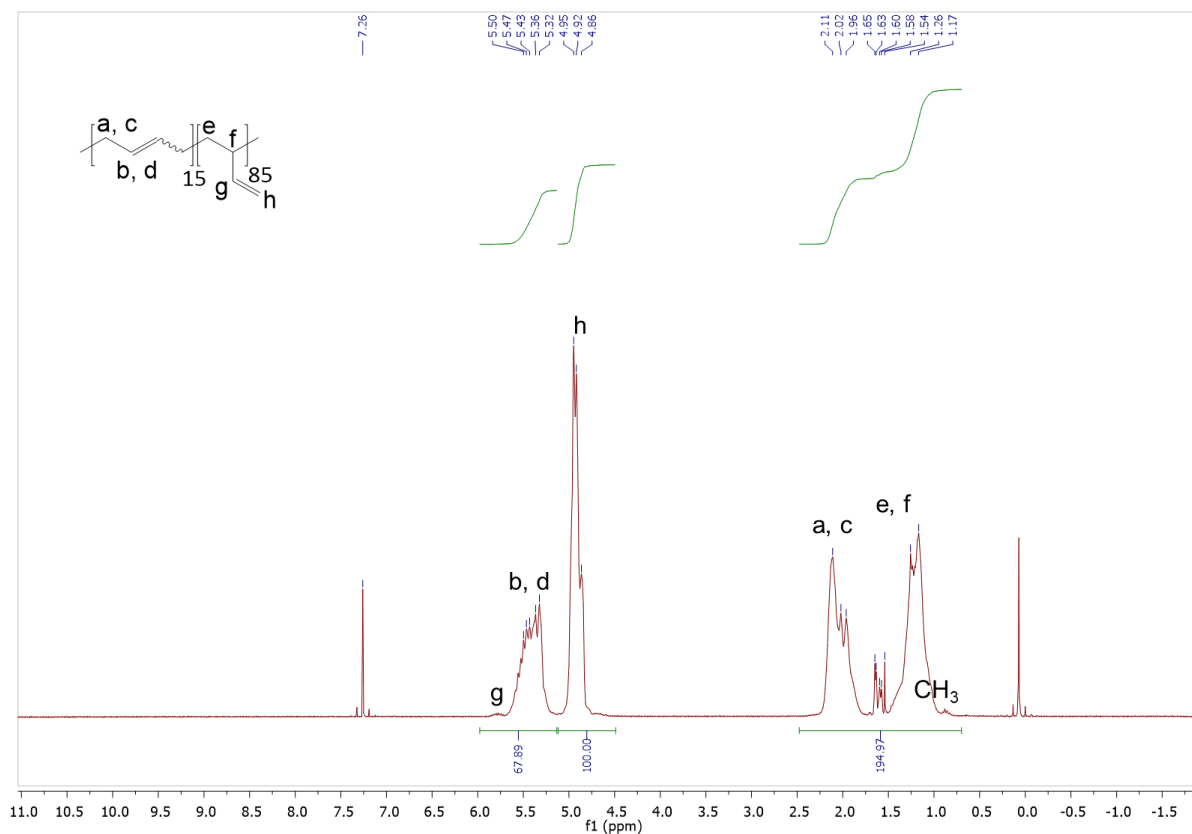


Figure S47.  $^1\text{H}$  NMR spectrum of PBU-3.

$^1\text{H}$  NMR (300 MHz,  $\text{CDCl}_3$ )  $\delta$ : 5.71-5.19 (m, b, d, g), 5.07-4.81 (m, h), 2.30-1.74 (m, a, c), 1.74-1.05 (m, e, f),

Calculation of the polymer compositions:

$$\text{Mol\% (1,4 units)} = \frac{S_b + S_d}{S_b + S_d + S_h} = \frac{67.89 - 100/2}{(67.89 - \frac{100}{2}) + 100} = 15 \text{ mol\%}$$

$$\text{Mol\% (1,2 units)} = 100 - \text{Mol\% (1,4 units)} = 85 \text{ mol\%}$$

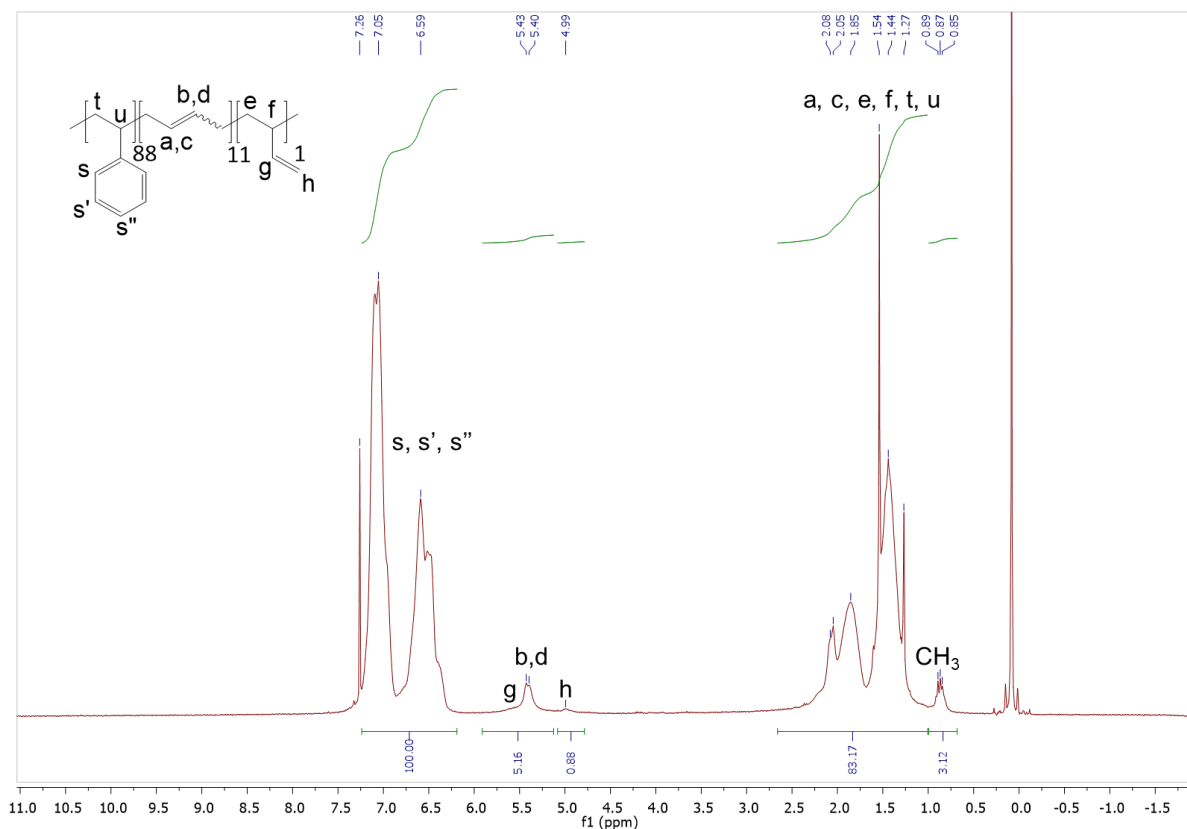


Figure S48. <sup>1</sup>H NMR spectrum of SBS.

<sup>1</sup>H NMR (300 MHz, CDCl<sub>3</sub>) δ 7.22 – 6.15 (m, s, s', s''), 5.96 – 5.14 (m, g, b, d), 5.16 – 4.74 (m, h), 2.67 – 1.04 (m, a, c, e, f, t, u), 1.07 – 0.60 (m, CH<sub>3</sub>).

Calculation of the polymer compositions:

$$\begin{aligned} \text{Mol\% (1,4 units)} &= \frac{S_b + S_d}{S_b + S_d + S_h + (S_s + S_{s'} + S_{s''})/3} = \frac{(5.16 - \frac{0.88}{2})/2}{(5.16 - \frac{0.88}{2})/2 + 0.88/2 + 100/5} \\ &= 10 \text{ mol\%} \end{aligned}$$

$$\begin{aligned} \text{Mol\% (1,2 units)} &= \frac{S_h}{S_b + S_d + S_h + (S_s + S_{s'} + S_{s''})/3} = \frac{0.88/2}{(5.16 - \frac{0.88}{2})/2 + 0.88/2 + 100/5} \\ &= 2 \text{ mol\%} \end{aligned}$$

$$\text{Mol\% (styrene)} = 100 - \text{Mol\% (1,2 units)} - \text{Mol\% (1,4 units)} = 88 \text{ mol\%}$$

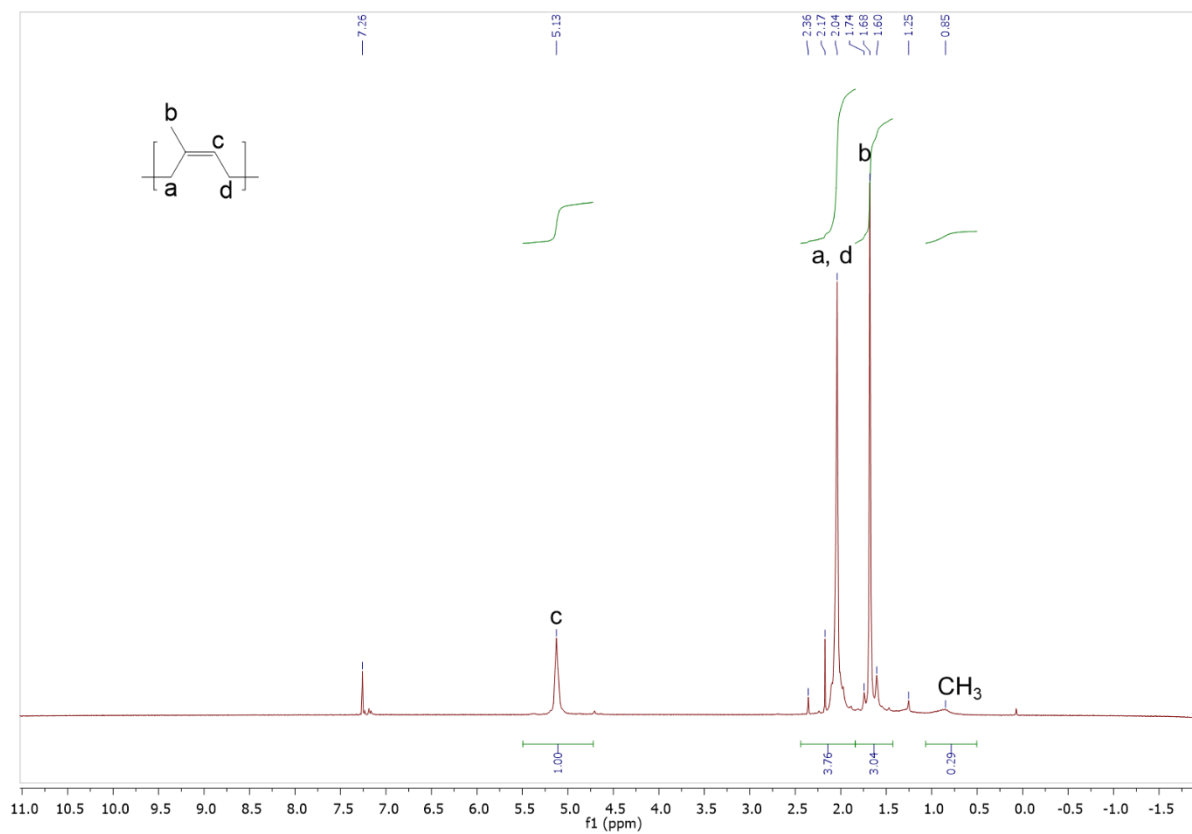


Figure S49.  $^1\text{H}$  NMR spectrum of NR-1.

$^1\text{H}$  NMR (300 MHz,  $\text{CDCl}_3$ )  $\delta$ : 5.13 (s, c), 2.55 – 1.84 (m, a, d), 1.83 – 1.48 (m, b), 0.85 (m,  $\text{CH}_3$ )

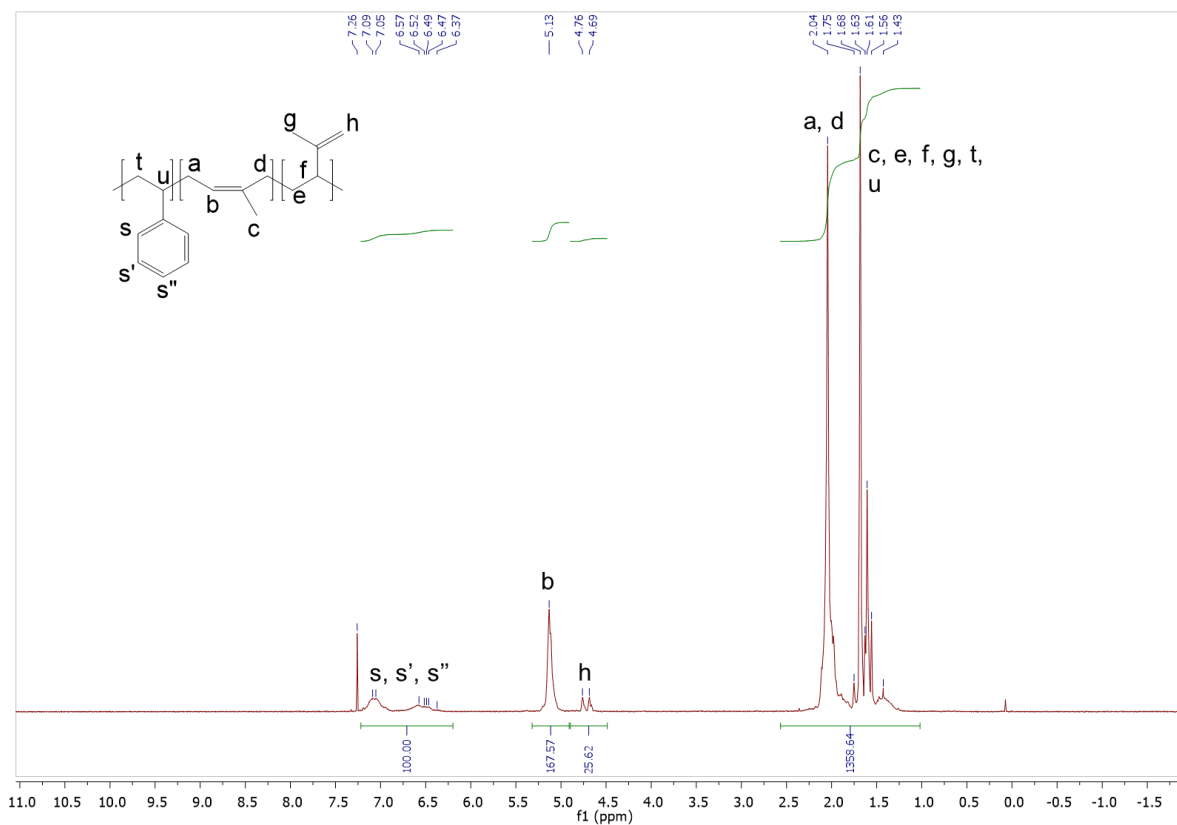


Figure S50. <sup>1</sup>H NMR spectrum of SIS.

<sup>1</sup>H NMR (300 MHz, CDCl<sub>3</sub>) δ: 7.21 – 6.25 (m, s, s', s''), 5.13 (s, b), 4.81 – 4.71 (m, h), 4.71 – 4.63 (m, h), 2.65 – 1.04 (m, a, d, c, e, g, t, u).

$$\text{Mol\% (1,4 - cis units)} = \frac{S_b}{S_b + S_h/2 + (S_s + S_{s'} + S_{s''})/6} = \frac{167.57}{167.57 + 25.62/2 + 100/5} = 84 \text{ mol\%}$$

$$\text{Mol\% (3,4 units)} = \frac{S_h/2}{S_b + S_h/2 + (S_s + S_{s'} + S_{s''})/6} = \frac{25.62/2}{167.57 + 25.62/2 + 100/5} = 6 \text{ mol\%}$$

$$\text{Mol\% (styrene)} = 100 - \text{Mol\% (1,2 units)} - \text{Mol\% (1,4 units)} = 10 \text{ mol\%}$$

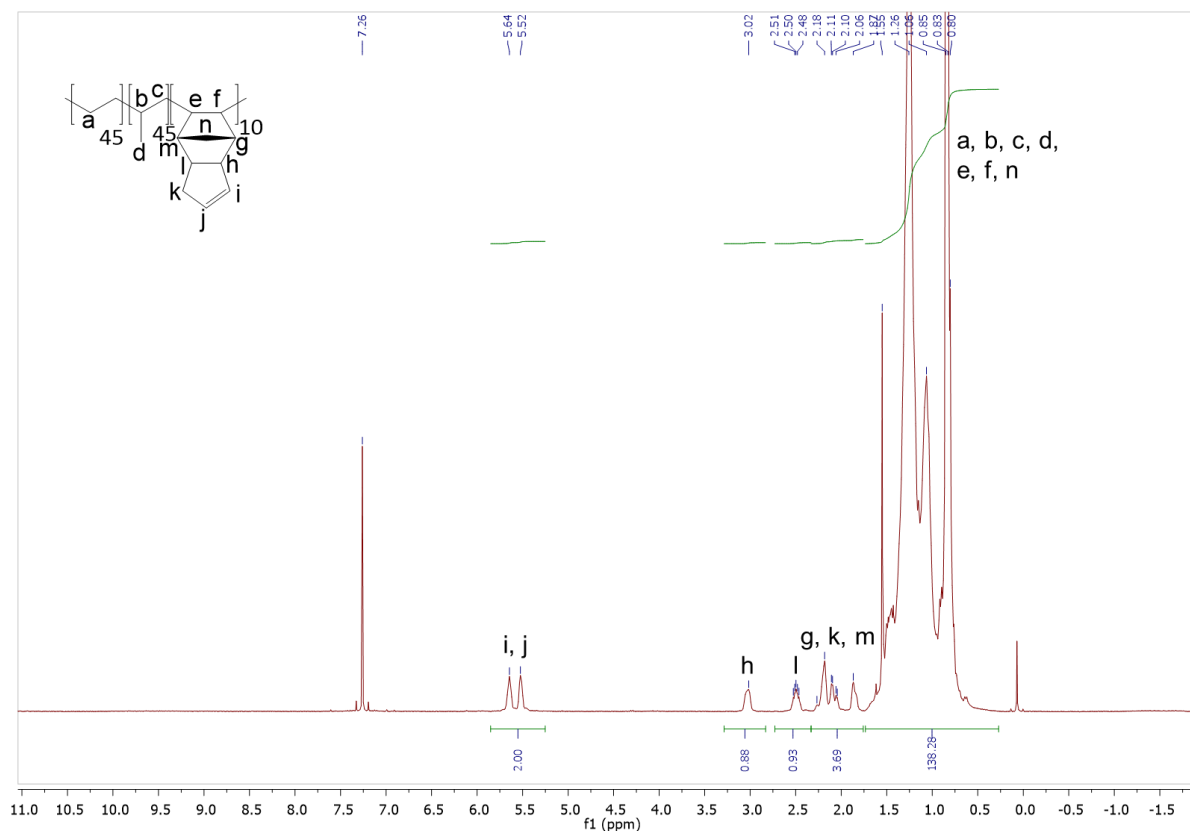


Figure S51.  $^1\text{H}$  NMR spectrum of EPDM-DCPD.

$^1\text{H}$  NMR (300 MHz,  $\text{CDCl}_3$ )  $\delta$  5.79 - 5.34 (m, i, j), 3.02 (m, h), 2.50 (m, l), 2.33 - 1.77 (m, g, k, m), 1.74 - 0.26 (m, a, b, c, d, e, f, n).

The molar composition of EPDM-DCPD (Trilene® 65) was calculated according to the weight composition reported by Lion Elastomers in technical data document (ethylene: 45 wt%, propylene: 45 wt%, dicyclopentadiene: 10 wt%).



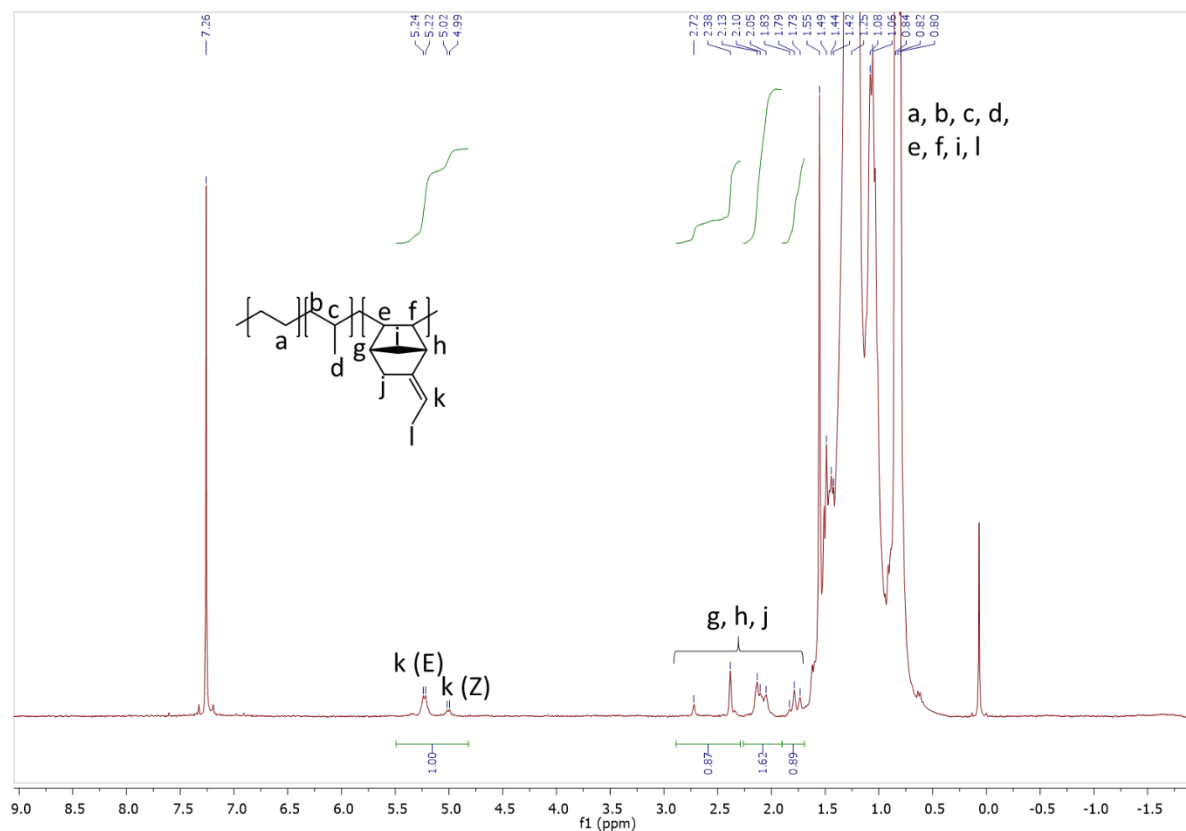


Figure S52.  $^1\text{H}$  NMR spectrum of EPDM-ENB.

$^1\text{H}$  NMR (300 MHz,  $\text{CDCl}_3$ )  $\delta$ : 5.32 – 5.15 (m,  $J = 6.7$  Hz,  $k$  (E)), 5.11 – 4.90 (m,  $J = 6.5$  Hz,  $k$  (Z)), 3.02 – 1.70 (m,  $g, h, j$ ), 1.67 – 0.33 (m,  $a, b, c, d, e, f, i, l$ ).

The molar composition of EPDM-ENB (MITSUI® EPT 3092PM) was calculated according to the weight composition reported by Mitsui Chemicals in technical data document (ethylene: 65wt%, propylene: 30.4 wt%, dicyclopentadiene: 4.6 wt%).

II.2.c. DSC analyses

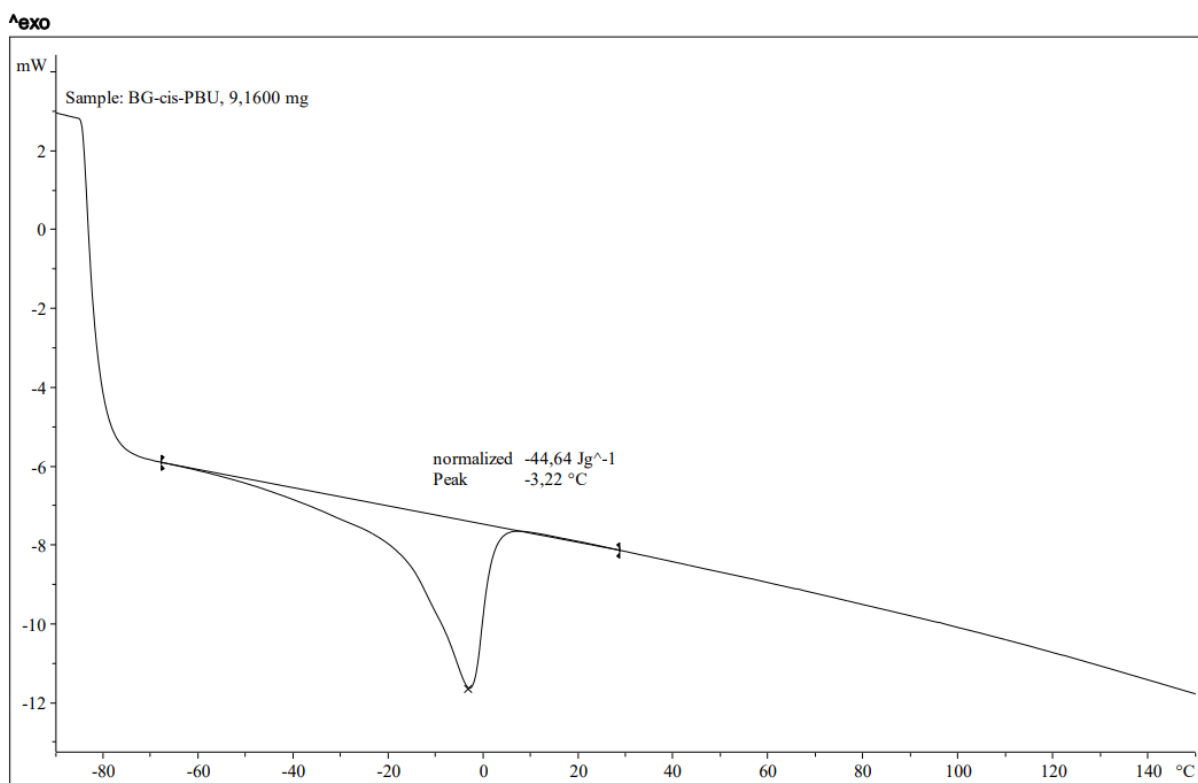


Figure S53. DSC of PBU-2.

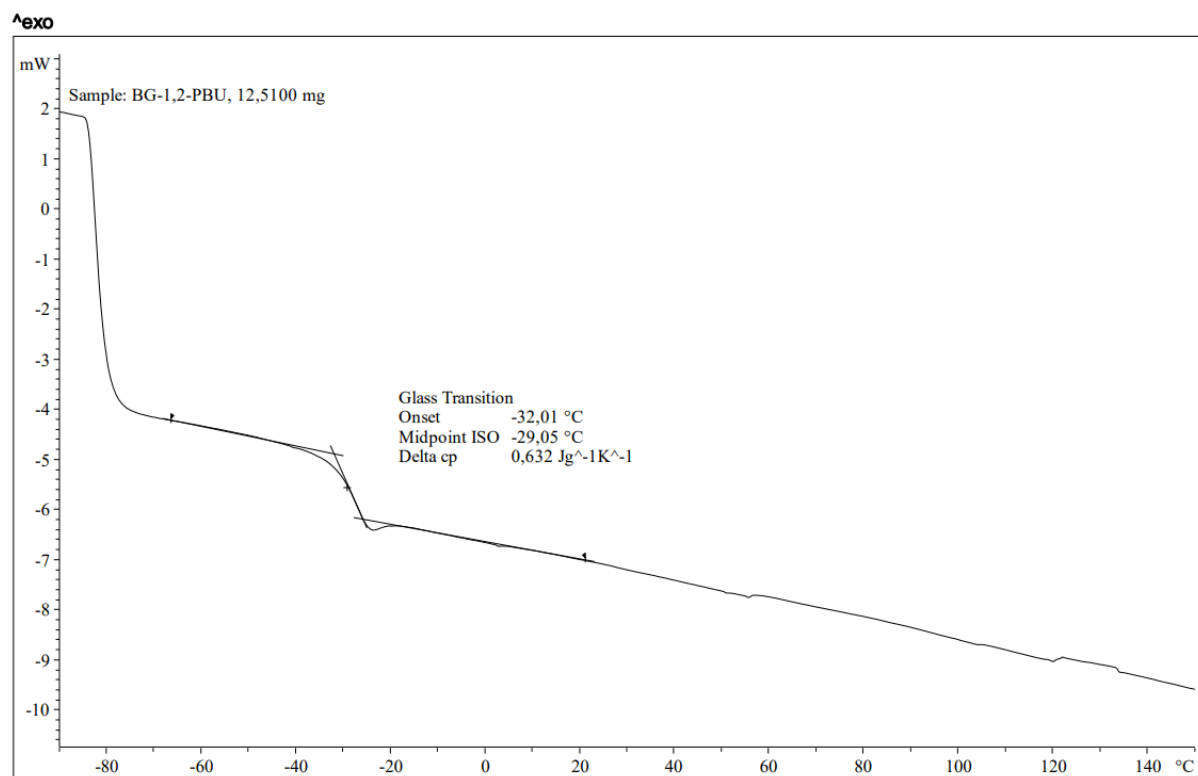


Figure S54. DSC of PBU-3.

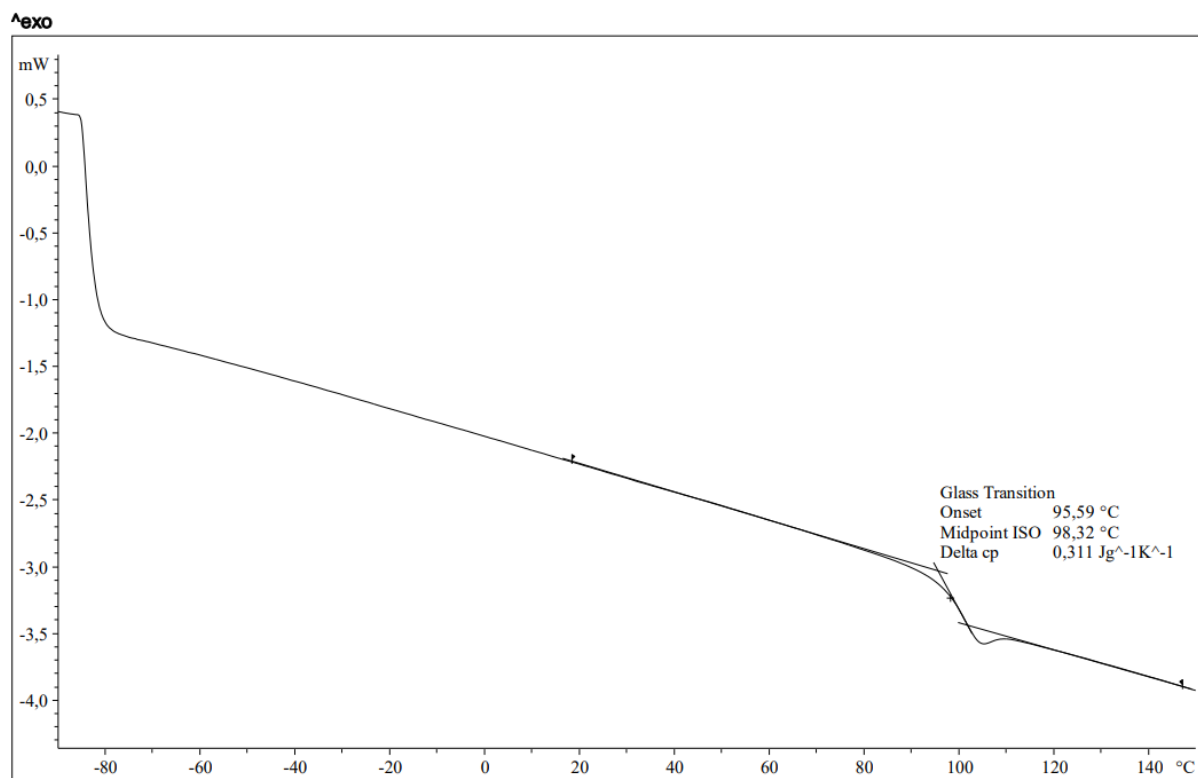


Figure S55. DSC of SBS.

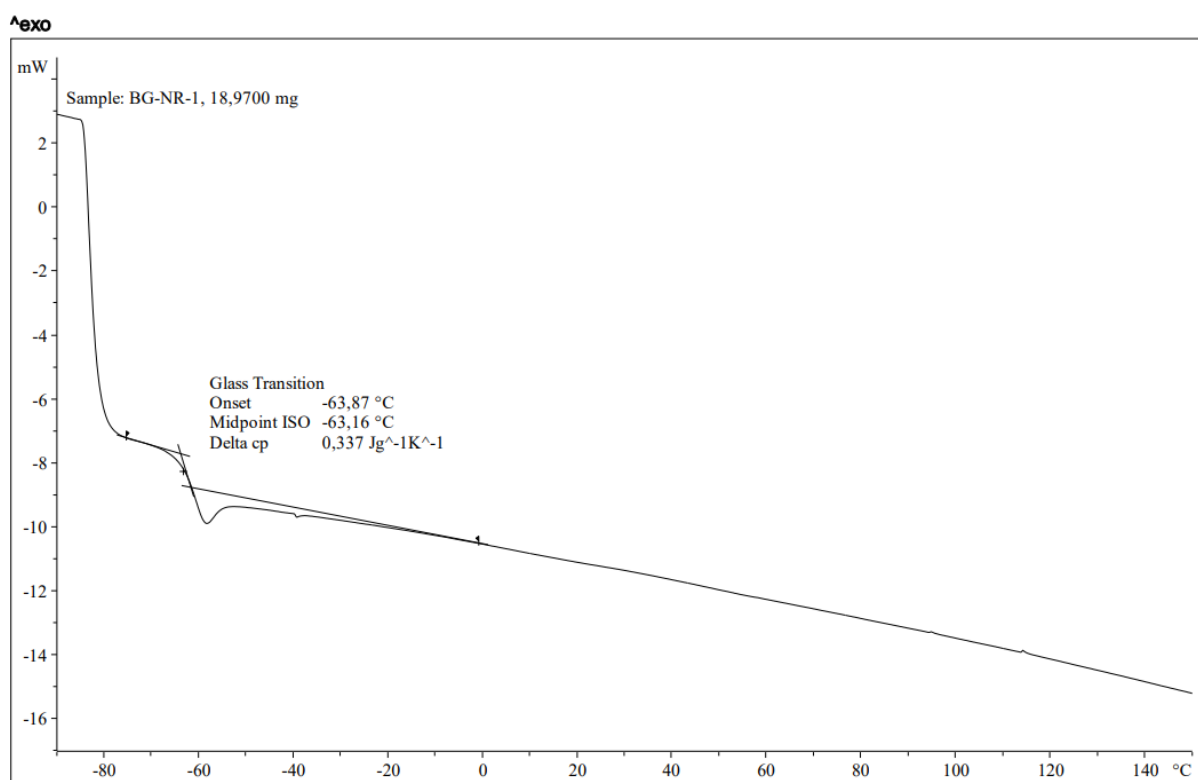


Figure S56. DSC of NR-1.

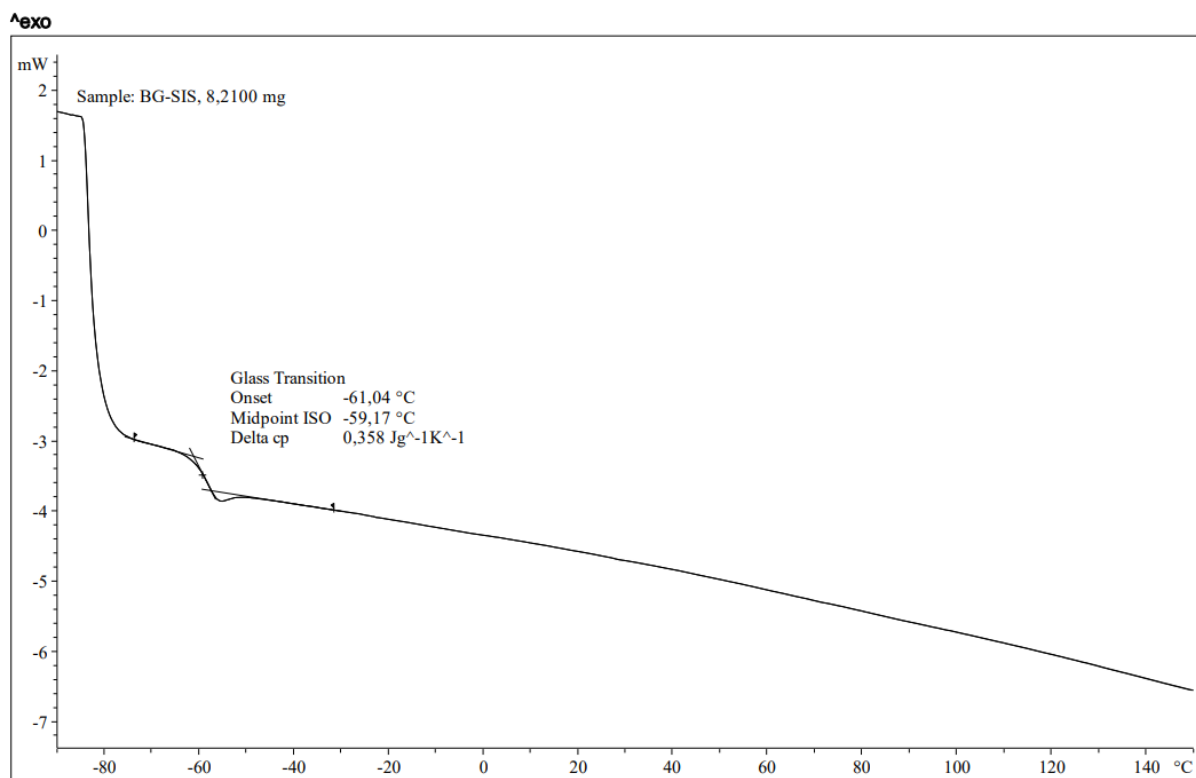


Figure S57. DSC of SIS.

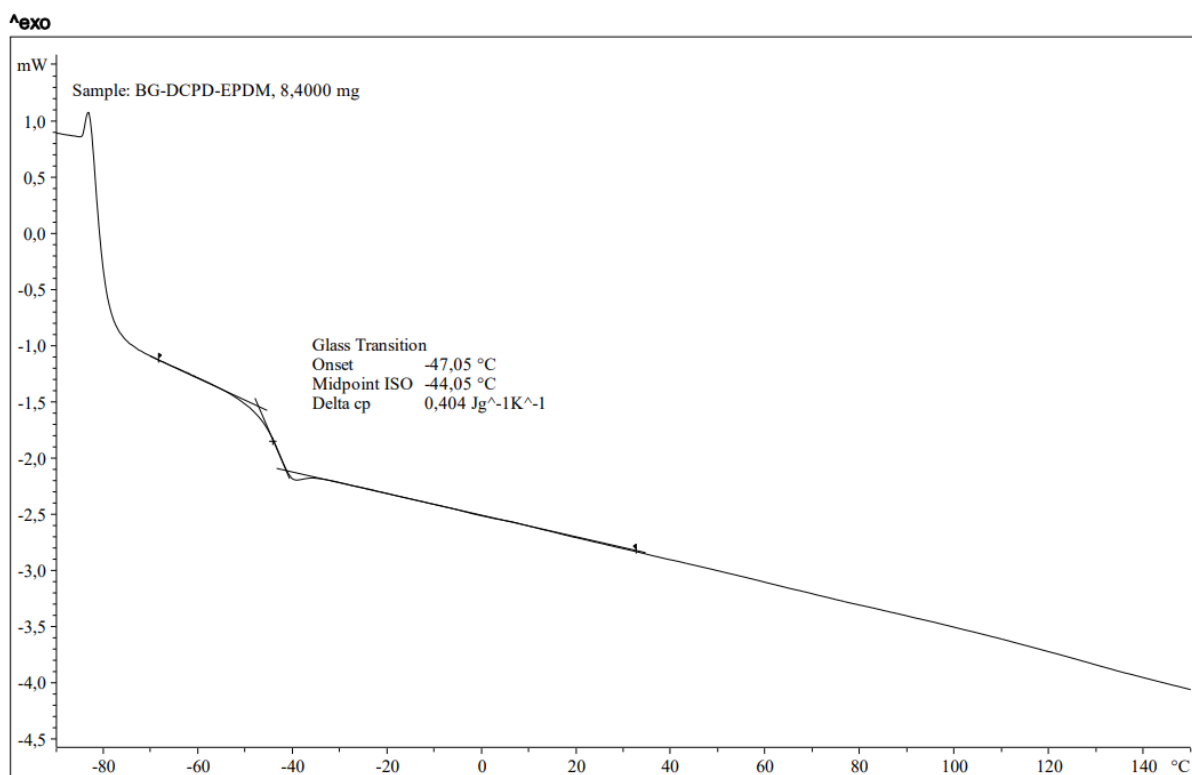


Figure S58. DSC of EPDM-DCPD.

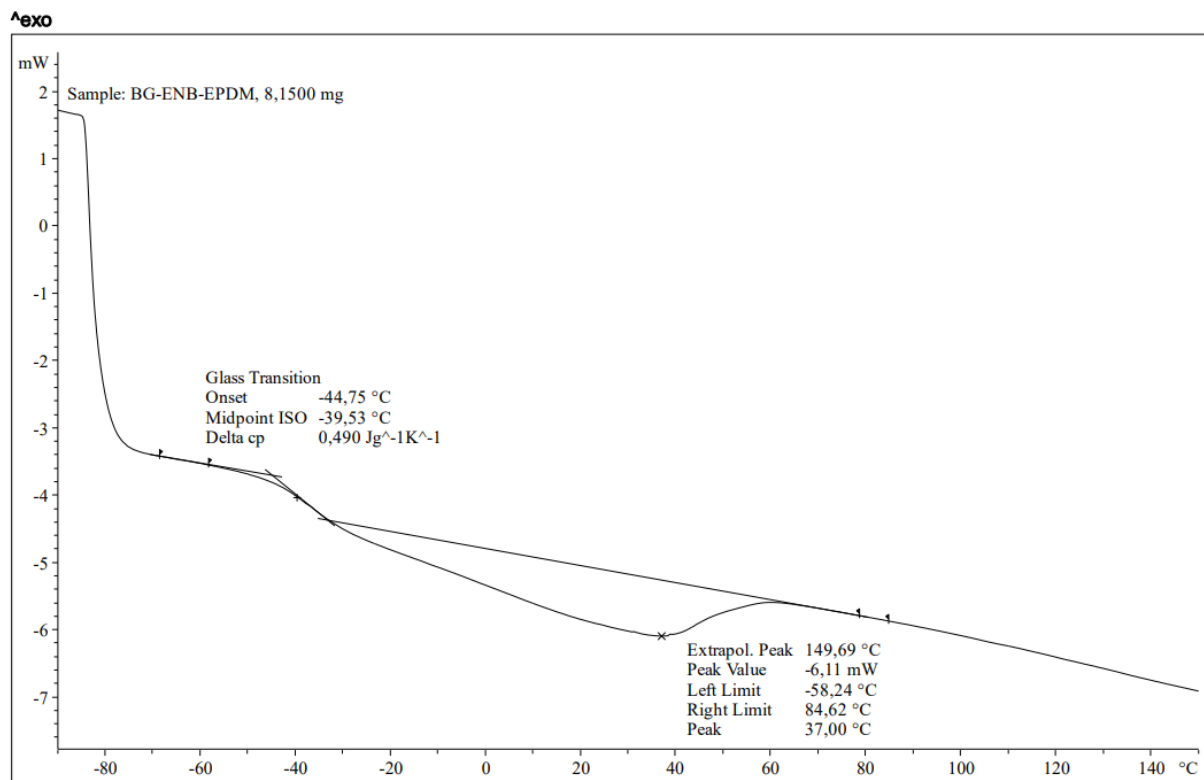


Figure S59. DSC of EPDM-ENB.

### II.3. Epoxidation of polydienes in batch

#### II.3.a. IR-ATR spectra

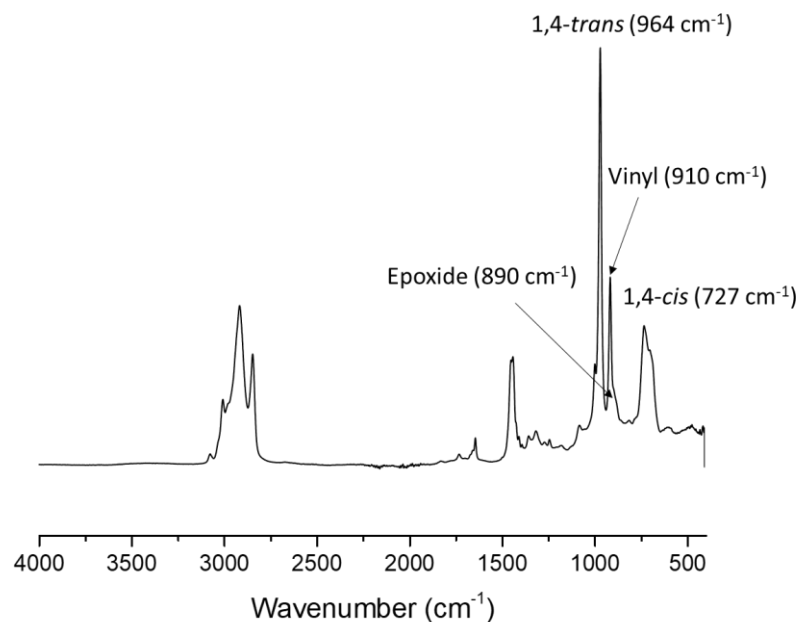


Figure S60. IR-ATR spectrum of E-PBU-1.

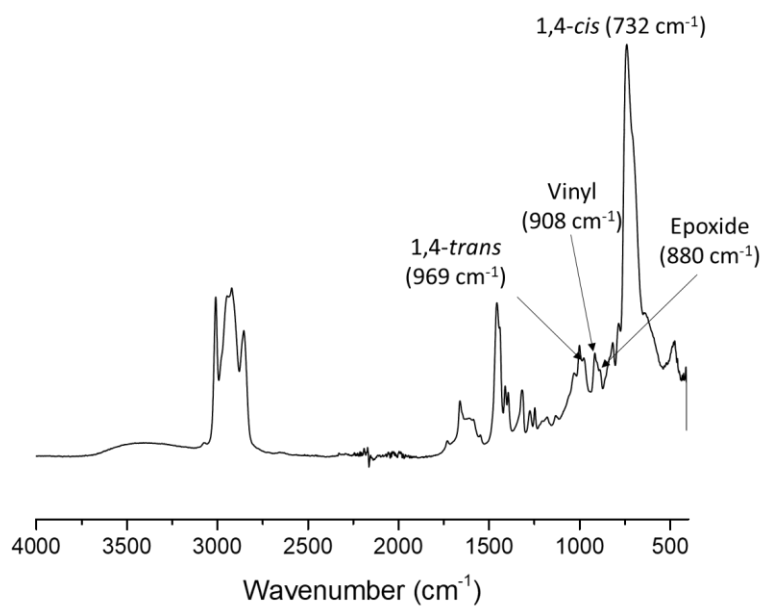


Figure S61. IR-ATR spectrum of E-PBU-2.

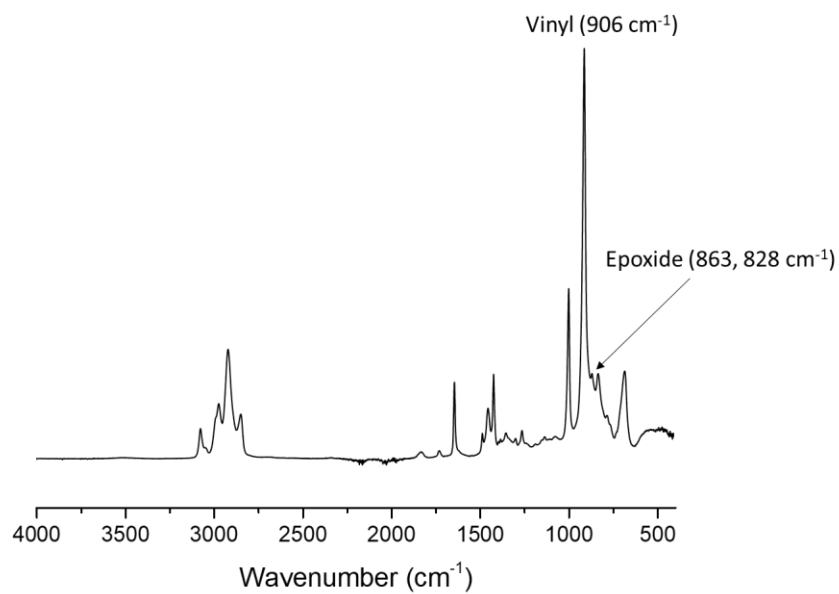


Figure S62. IR-ATR spectrum of E-PBU-3.

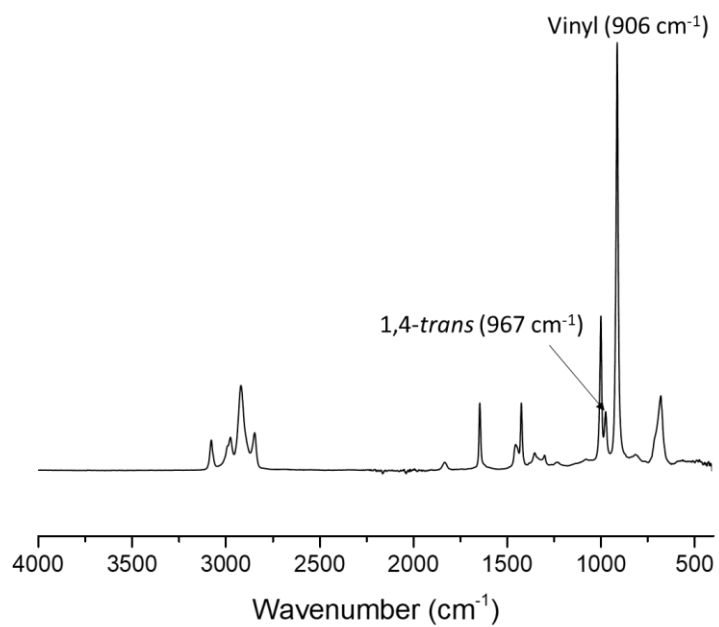


Figure S63. IR-ATR spectrum of E-PBU-4.

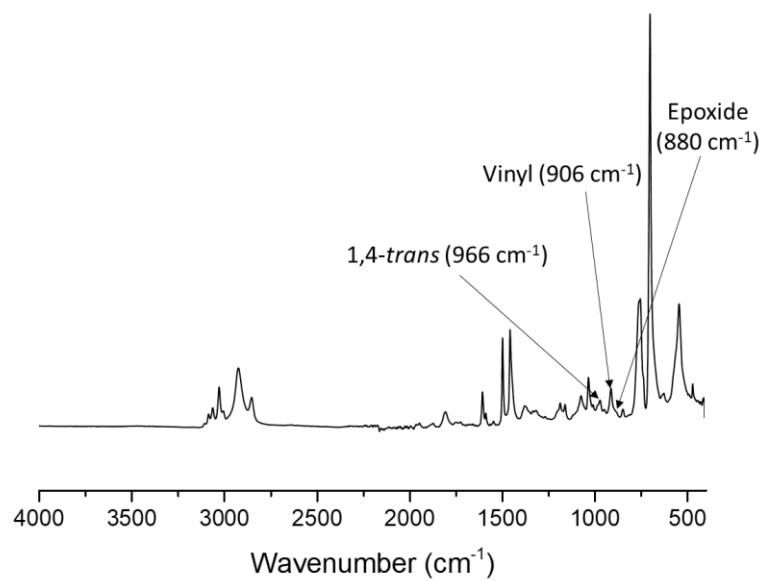


Figure S64. IR-ATR spectrum of E-SBS.

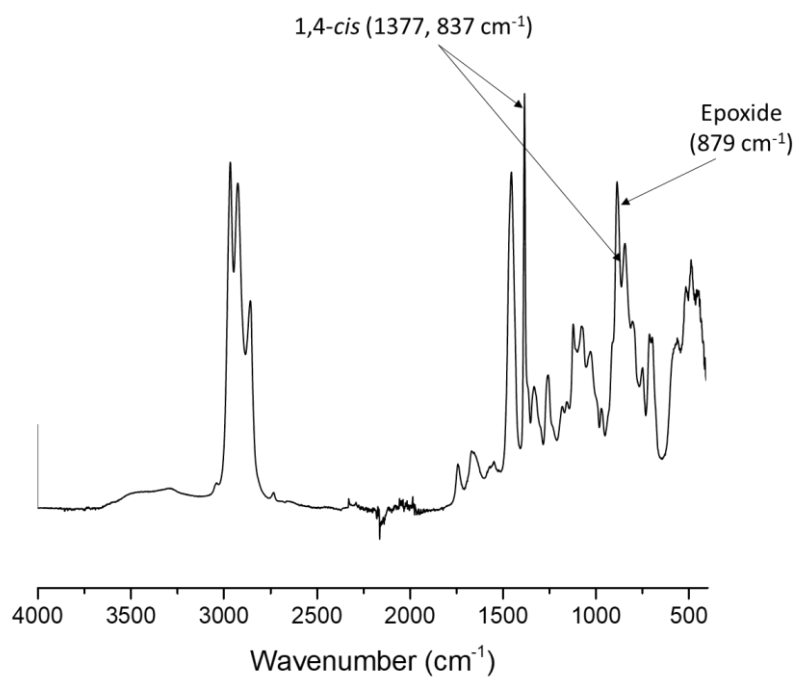


Figure S65. IR-ATR spectrum of E-NR-1.



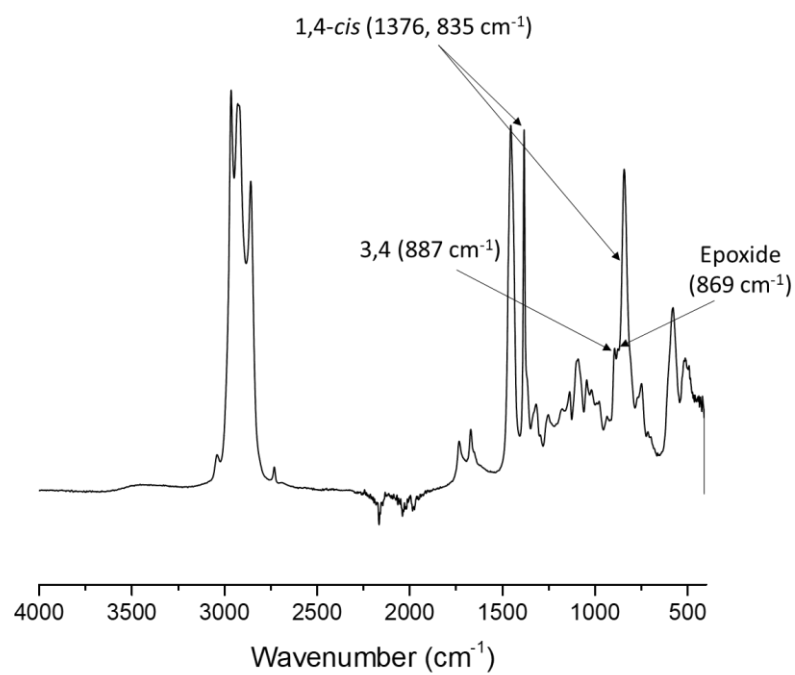


Figure S66. IR-ATR spectrum of E-NR-2.

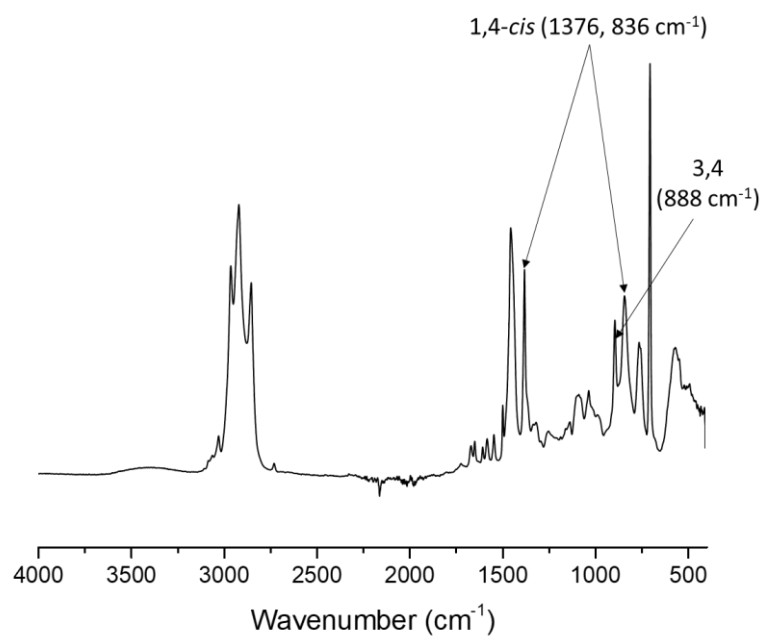


Figure S67. IR-ATR spectrum of E-SIS.

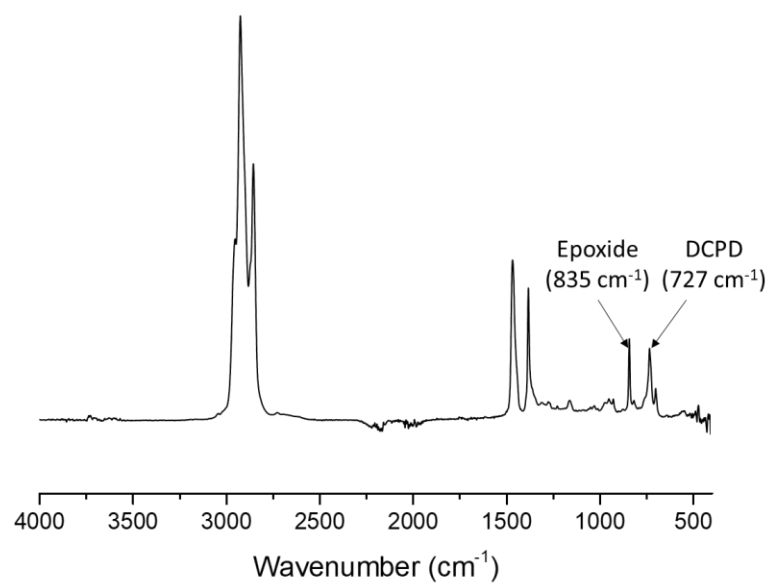


Figure S68. IR-ATR spectrum of E-EPDM-DCPD.

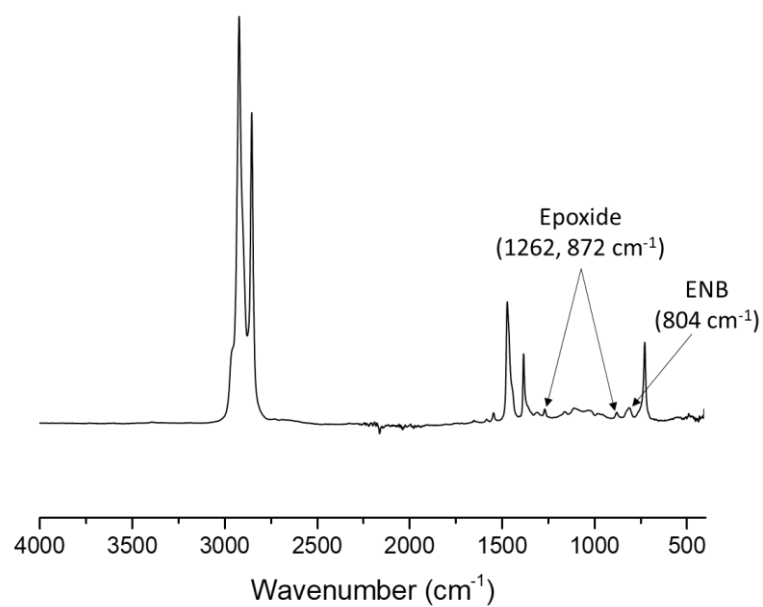


Figure S69. IR-ATR spectrum of E-EPDM-ENB.

### II.3.b. <sup>1</sup>H NMR spectra

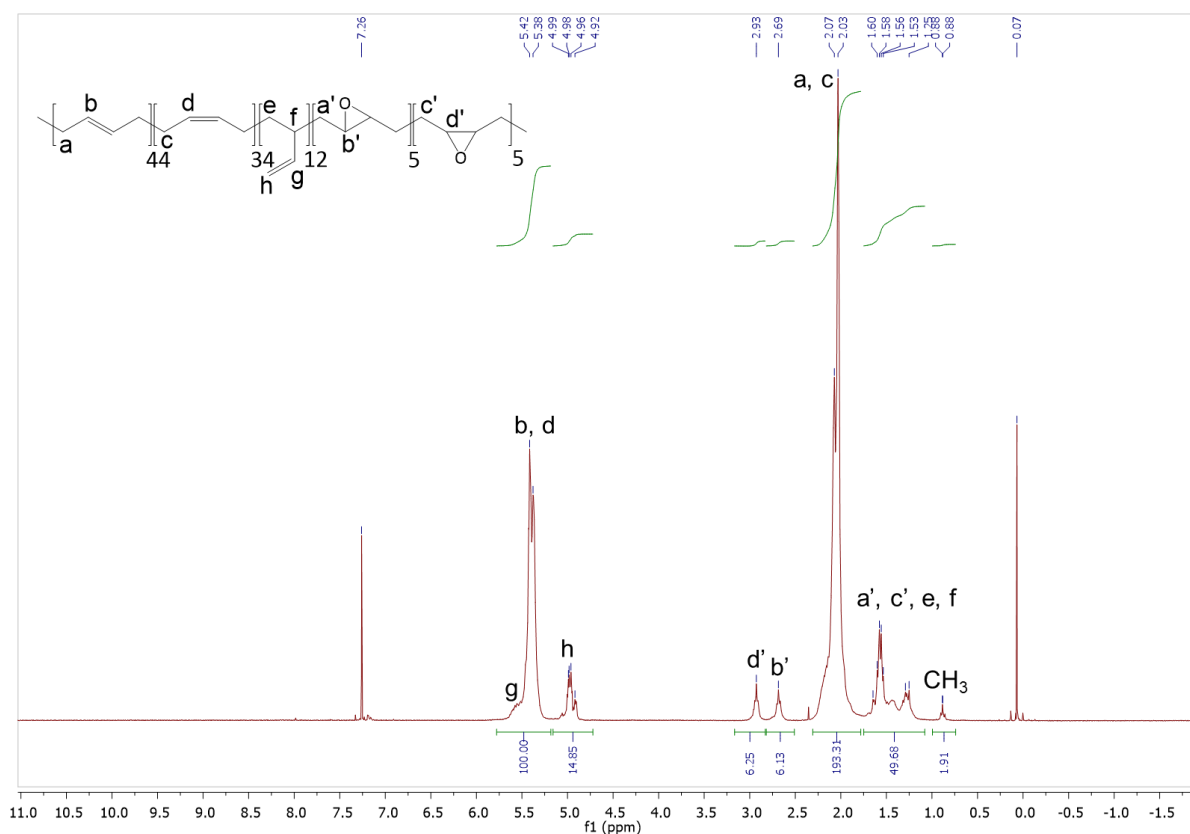


Figure S70. <sup>1</sup>H NMR spectrum of E-PBU-1.

<sup>1</sup>H NMR (300 MHz, CDCl<sub>3</sub>) δ 5.77 – 5.19 (m, b, d, g), 5.18 – 4.70 (m, h), 3.20 – 2.83 (m, d'), 2.82 – 2.53 (m, b'), 2.39 – 1.79 (m, a, c), 1.77 – 1.05 (m, a', c', e, f), 0.99 – 0.70 (m, CH<sub>3</sub>).

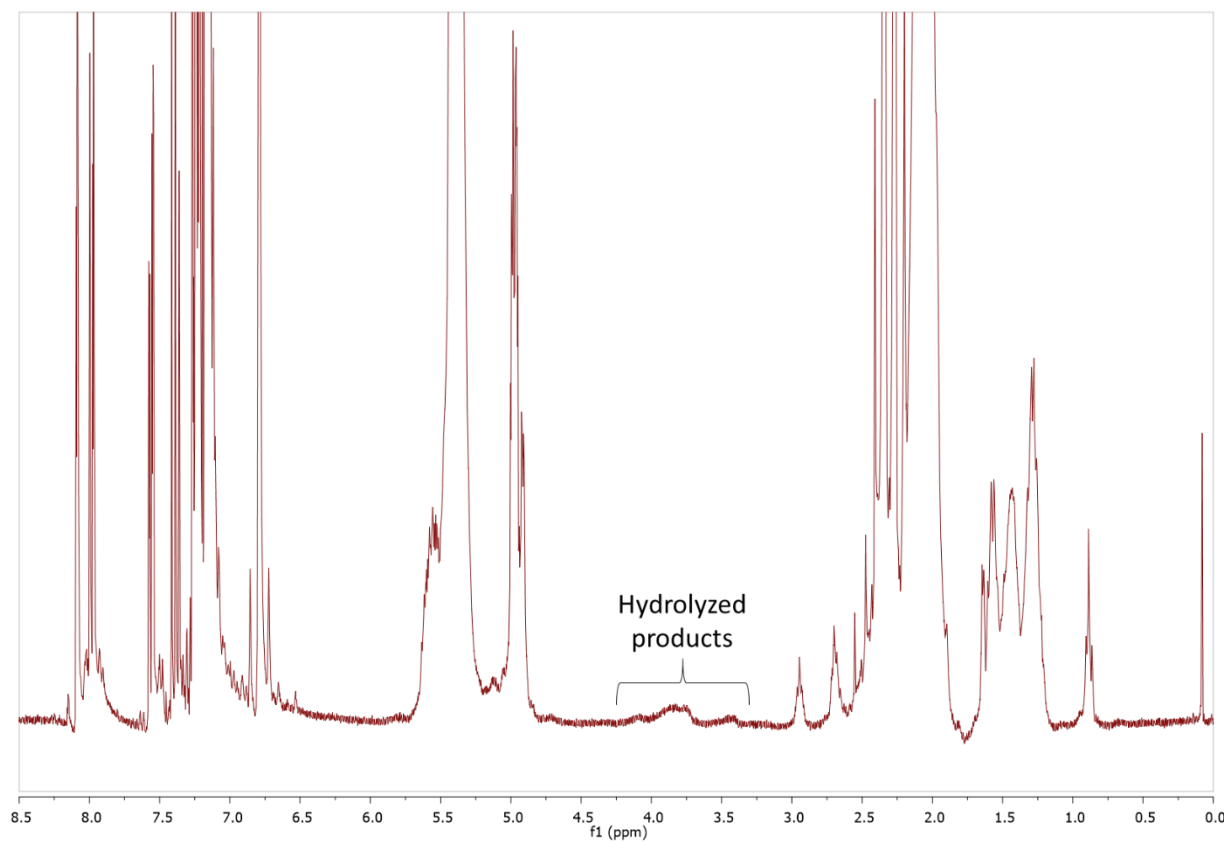
$$\text{Mol\% (cis epoxide units)} = \frac{S_{d'}}{S_b + S_d + S_h + S_{b'} + S_{d'}}$$

$$\text{Mol\% (cis epoxide units)} = \frac{6.25}{\left(100 - \frac{14.85}{2}\right) + 14.85 + 6.13 + 6.25} = 5 \text{ mol\%}$$

$$\text{Mol\% (trans epoxide units)} = \frac{6.13}{\left(100 - \frac{14.85}{2}\right) + 14.85 + 6.13 + 6.25} = 5 \text{ mol\%}$$

$$\text{Mol\% (1,4 units)} = \frac{\left(100 - \frac{14.85}{2}\right)}{\left(100 - \frac{14.85}{2}\right) + 14.85 + 6.13 + 6.25} = 77 \text{ mol\%}$$

$$\text{Mol\% (1,2 units)} = 100 - \text{Mol\% (1,4 units)} - \text{Mol\% (epoxide units)} = 13 \text{ mol\%}$$



*Figure S71.  $^1\text{H}$  NMR (300 MHz,  $\text{CDCl}_3$ ) spectrum of the crude mixture after epoxidation of PBU-1 with mCPBA at 110 °C (Figure 5).*

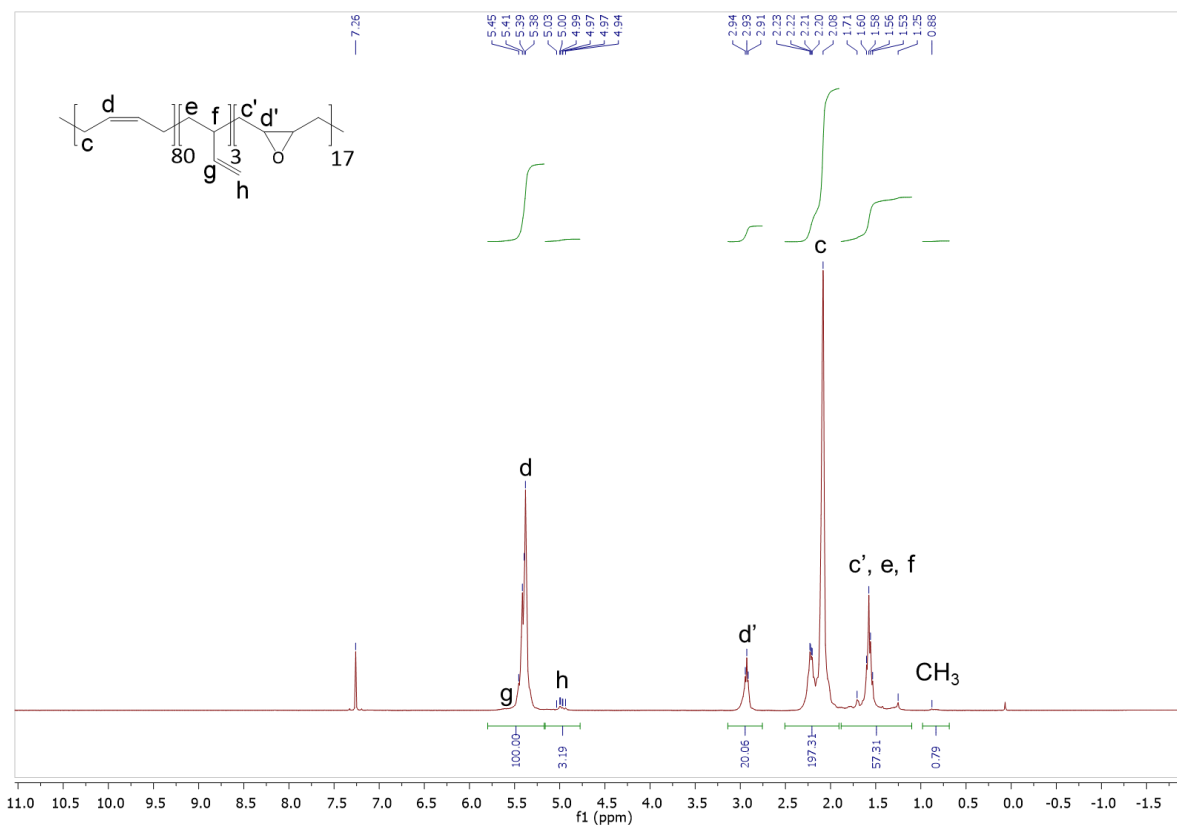


Figure S72.  $^1\text{H}$  NMR spectrum of E-PBU-2.

$^1\text{H}$  NMR (300 MHz,  $\text{CDCl}_3$ )  $\delta$ : 5.75 – 5.18 (m, d, h, g), 5.18 – 4.71 (m, h), 2.93 (t,  $J = 4.7$  Hz,  $d'$ ), 2.54 – 1.88 (m, c), 1.86 – 1.14 (m,  $c'$ , e, f), 1.00 – 0.70 (m,  $\text{CH}_3$ ).

$$\text{Mol\% (cis epoxide units)} = \frac{S_{d'}}{S_d + S_h + S_{d'}} = \frac{20.06}{\left(100 - \frac{3.19}{2}\right) + 3.19 + 20.06} = 16 \text{ mol\%}$$

$$\text{Mol\% (cis epoxide units)} = \frac{S_d}{S_d + S_h + S_{d'}} = \frac{100 - \frac{3.19}{2}}{\left(100 - \frac{3.19}{2}\right) + 3.19 + 20.06} = 81 \text{ mol\%}$$

$$\text{Mol\% (1,2 units)} = 100 - \text{Mol\% (1,4 units)} - \text{Mol\% (epoxide units)} = 3 \text{ mol\%}$$

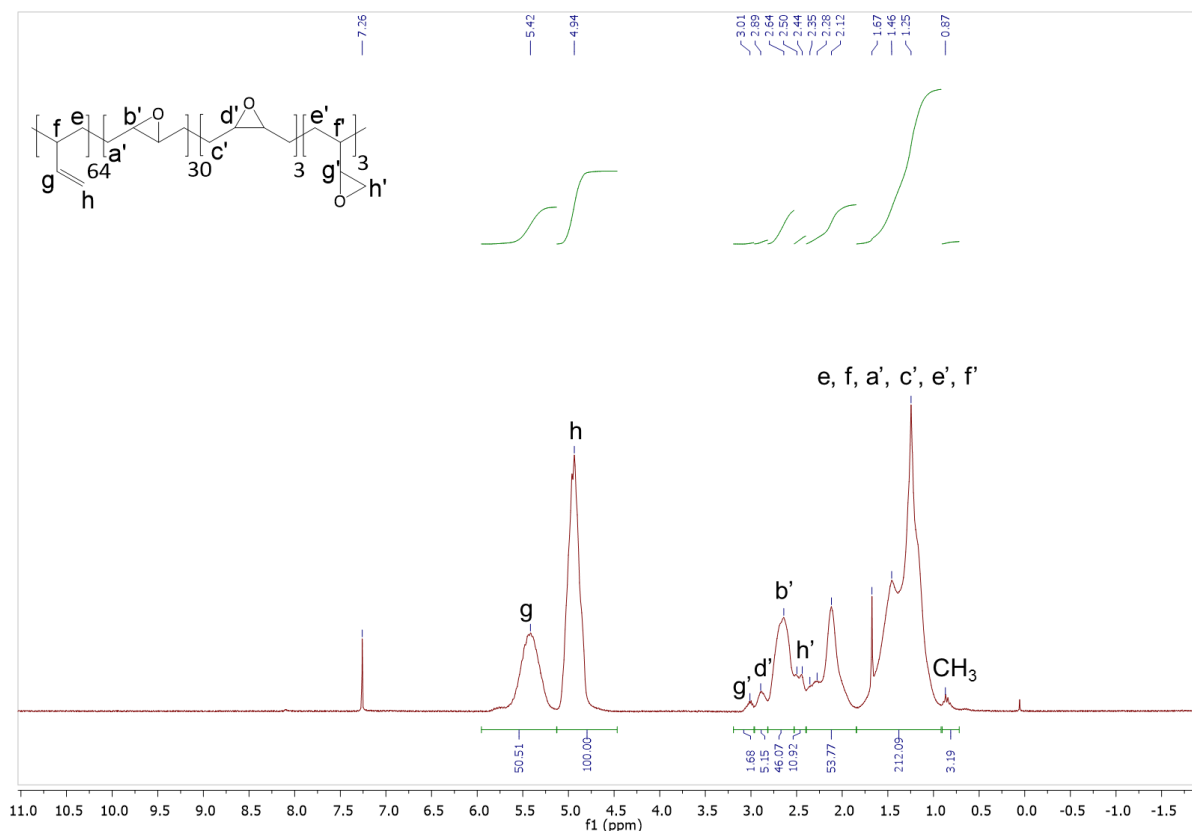


Figure S73.  $^1\text{H}$  NMR spectrum of E-PBU-3.

$^1\text{H}$  NMR (300 MHz,  $\text{CDCl}_3$ )  $\delta$ : 5.84 – 5.15 (m, g), 5.13 – 4.59 (m, h), 3.20 – 2.41 (m, g', d', b', h'), 2.37 – 1.79 (m, c', d'), 1.82 – 0.96 (m, e, e', f, f'), 0.91 – 0.68 (m,  $\text{CH}_3$ ).

**Calculation of the polymer compositions:**

$$\text{Mol\% (cis epoxide units)} = \frac{S_{a'}/2}{(S_h + S_{b'} + S_{a'})/2 + S_{g'}} = \frac{5.15/2}{(100 + 46.07 + 5.15)/2 + 1.68} = 3 \text{ mol\%}$$

$$\text{Mol\% (trans epoxide units)} = \frac{S_{b'}/2}{(S_h + S_{b'} + S_{a'})/2 + S_{g'}} = \frac{46.07/2}{(100 + 46.07 + 5.15)/2 + 1.68} = 30 \text{ mol\%}$$

$$\text{Mol\% (pendant epoxide units)} = \frac{46.07/2}{(100 + 46.07 + 5.15)/2 + 1.68} = 3 \text{ mol\%}$$

$$\text{Mol\% (1,2 units)} = 100 - \text{Mol\% (epoxide units)} = 64 \text{ mol\%}$$

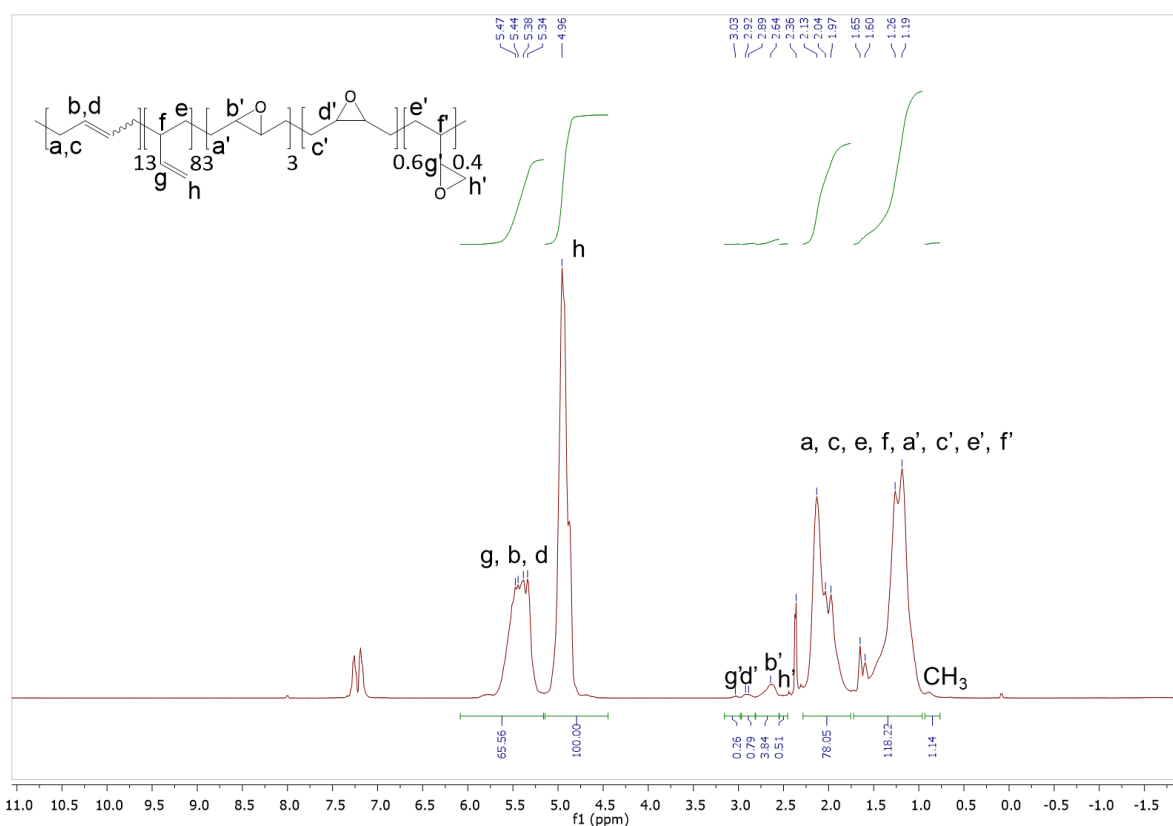


Figure S74.  $^1\text{H}$  NMR spectrum of E-PBU-4.

$^1\text{H}$  NMR (300 MHz,  $\text{CDCl}_3$ )  $\delta$  5.93 – 5.16 (m, g, b, d), 5.16 – 4.58 (m, h), 3.16 – 2.98 (m, g'), 2.98 – 2.81 (m, d'), 2.64 (s, b'), 2.53 – 2.46 (m, h'), 2.40 – 0.49 (m, a, c, e, f, a', c', e', f').

$$\text{Mol\% (cis epoxide units)} = \frac{\frac{S_{d'}}{2}}{\frac{S_b + S_d + S_h + S_{b'} + S_{d'}}{2} + S_{g'}}$$

$$\text{Mol\% (cis epoxide units)} = \frac{0.79/2}{\left(65.56 - \left(\frac{100}{2}\right) + 100 + 3.84 + 0.79\right)/2 + 0.26} = 0.6 \text{ mol\%}$$

$$\text{Mol\% (trans epoxide units)} = \frac{3.84/2}{\left(65.56 - \left(\frac{100}{2}\right) + 100 + 3.84 + 0.79\right)/2 + 0.26} = 3 \text{ mol\%}$$

$$\begin{aligned} \text{Mol\% (pendant epoxide units)} &= \frac{0.26}{\left(65.56 - \left(\frac{100}{2}\right) + 100 + 3.84 + 0.79\right)/2 + 0.26} \\ &= 0.4 \text{ mol\%} \end{aligned}$$

$$\text{Mol\% (1,4 units)} = \frac{\left(65.56 - \left(\frac{100}{2}\right)\right)/2}{\left(65.56 - \left(\frac{100}{2}\right) + 100 + 3.84 + 0.79\right)/2 + 0.26} = 13 \text{ mol\%}$$

$$\text{Mol\% (1,2 units)} = 100 - \text{Mol\% (1,4 units)} - \text{Mol\% (epoxide units)} = 83 \text{ mol\%}$$

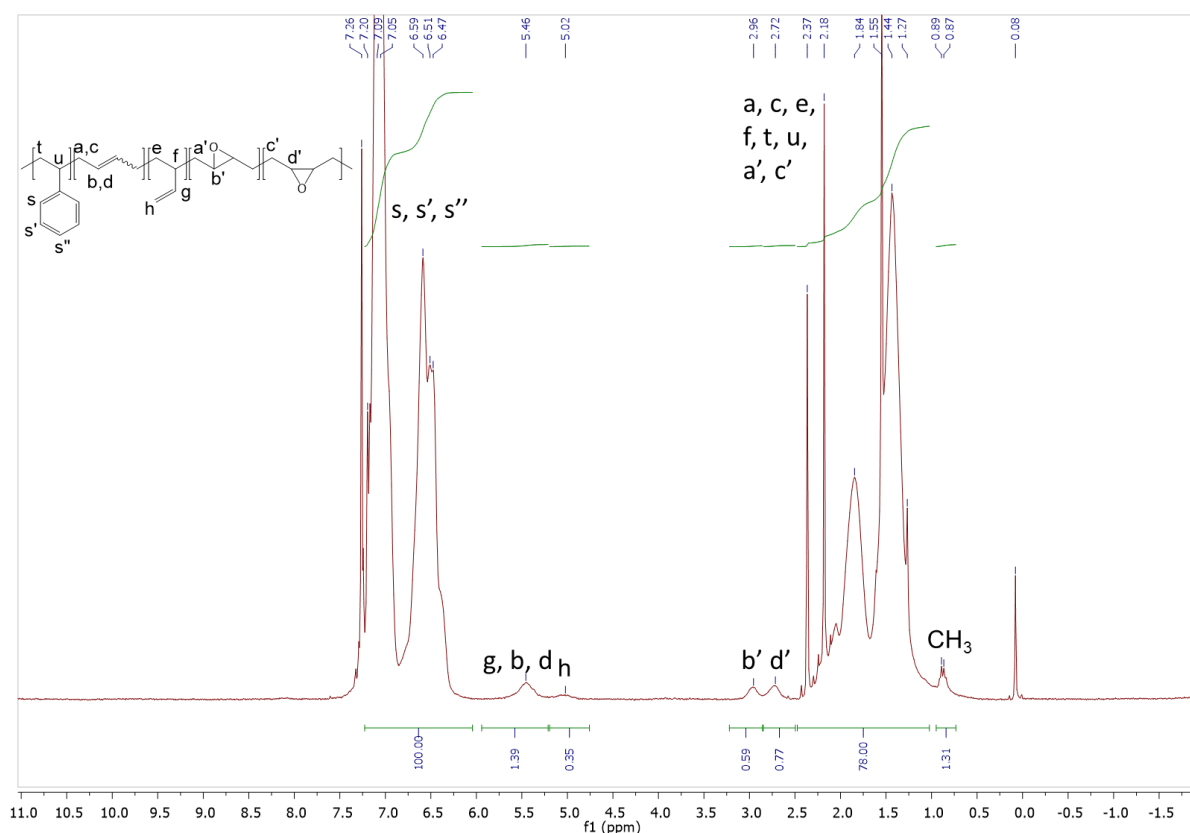


Figure S75.  $^1\text{H}$  NMR spectrum of E-SBS.

$^1\text{H}$  NMR (300 MHz,  $\text{CDCl}_3$ )  $\delta$  7.22 – 6.15 (m, s, s', s''), 5.96 – 5.14 (m, g, b, d), 5.16 – 4.74 (m, h), 2.96 (m, b'), 2.72 (m, d'), 2.67 – 1.04 (m, a, c, e, f, t, u, a', c'), 1.07 – 0.60 (m,  $\text{CH}_3$ ).

$$\begin{aligned} \text{Mol\% (cis epoxide)} &= \frac{S_{d'}/2}{(S_b + S_d + S_h + S_{b'} + S_{d'})/2 + (S_s + S_{s'} + S_{s''})/5} \\ &= \frac{0.59/2}{((1.39 - \frac{0.35}{2}) + 0.35 + 0.59 + 0.77)/2 + 100/5} = 1.4 \text{ mol\%} \end{aligned}$$

$$\text{Mol\% (trans epoxide)} = \frac{0.77/2}{((1.39 - \frac{0.35}{2}) + 0.35 + 0.59 + 0.77)/2 + 100/5} = 1.8 \text{ mol\%}$$

$$\text{Mol\% (1,4 units)} = \frac{(1.39 - \frac{0.35}{2})/2}{((1.39 - \frac{0.35}{2}) + 0.35 + 0.59 + 0.77)/2 + 100/3} = 2.8 \text{ mol\%}$$

$$\text{Mol\% (1,2 units)} = \frac{0.35/2}{((1.39 - \frac{0.35}{2}) + 0.35 + 0.59 + 0.77)/2 + 100/3} = 0.8 \text{ mol\%}$$



$$\begin{aligned} \text{Mol\% (styrene)} &= 100 - \text{Mol\% (1,2 units)} - \text{Mol\% (1,4 units)} - \text{Mol\% (epoxide)} \\ &= 93.2 \text{ mol\%} \end{aligned}$$

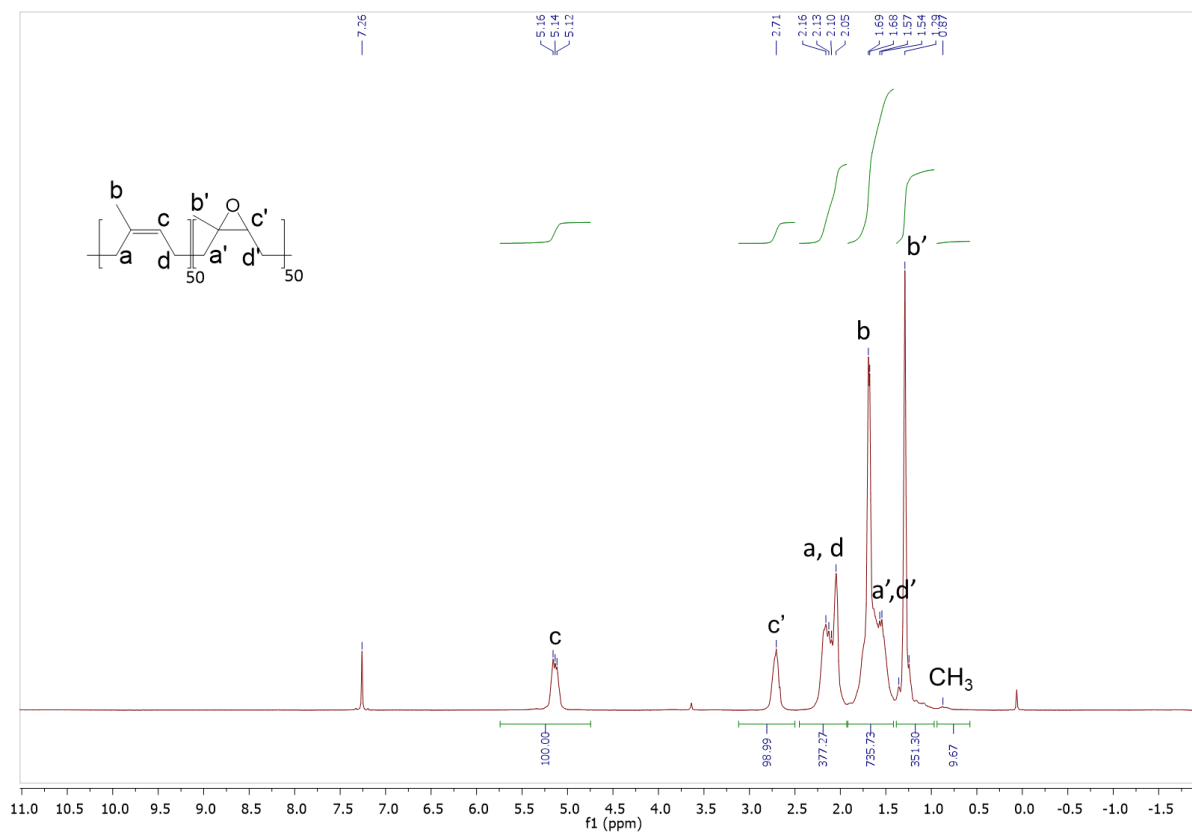


Figure S76.  $^1\text{H}$  NMR spectrum of E-NR-1.

$^1\text{H}$  NMR (300 MHz,  $\text{CDCl}_3$ )  $\delta$ : 5.13 (m, c), 2.71 (m, c'), 2.55 – 1.84 (m, a, d), 1.83 – 1.10 (m, b, a', b', d'), 0.87 (m,  $\text{CH}_3$ )

$$\text{Mol\% (1,4 units)} = \frac{S_c}{S_c + S_{c'}} = \frac{100}{100 + 98.99} = 50 \text{ mol\%}$$

$$\text{Mol\% (epoxide)} = 100 - \text{Mol\% (1,4 units)} = 50 \text{ mol\%}$$

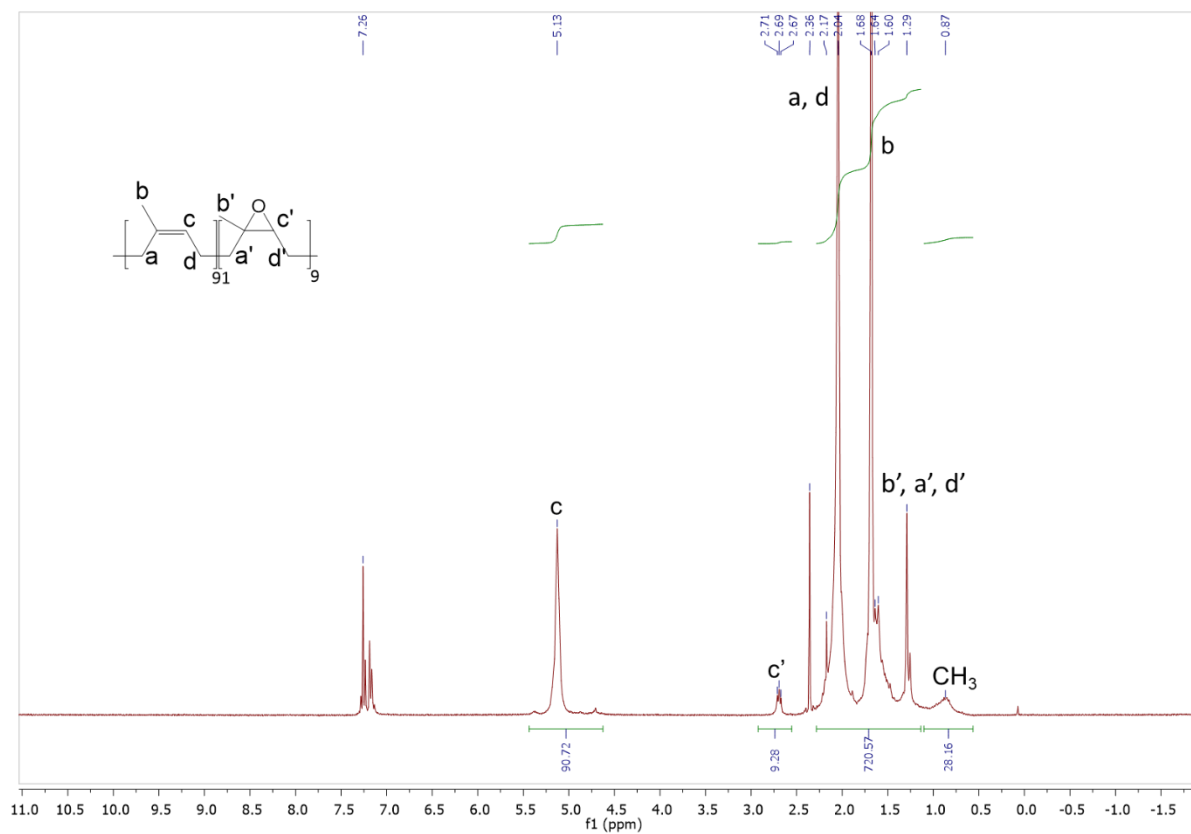


Figure S77. <sup>1</sup>H NMR spectrum of E-NR-2.

<sup>1</sup>H NMR (300 MHz, CDCl<sub>3</sub>) δ: 5.13 (m, c), 2.69 (m, c'), 2.55 – 1.10 (m, a, b, d, a', b', d'), 1.83 – 1.10 (m, b, a', b', d'), 0.87 (m, CH<sub>3</sub>)

$$\text{Mol\% (1,4 units)} = \frac{S_c}{S_c + S_{c'}} = \frac{90.72}{90.72 + 9.28} = 91 \text{ mol\%}$$

$$\text{Mol\% (epoxide)} = 100 - \text{Mol\% (1,4 units)} = 9 \text{ mol\%}$$

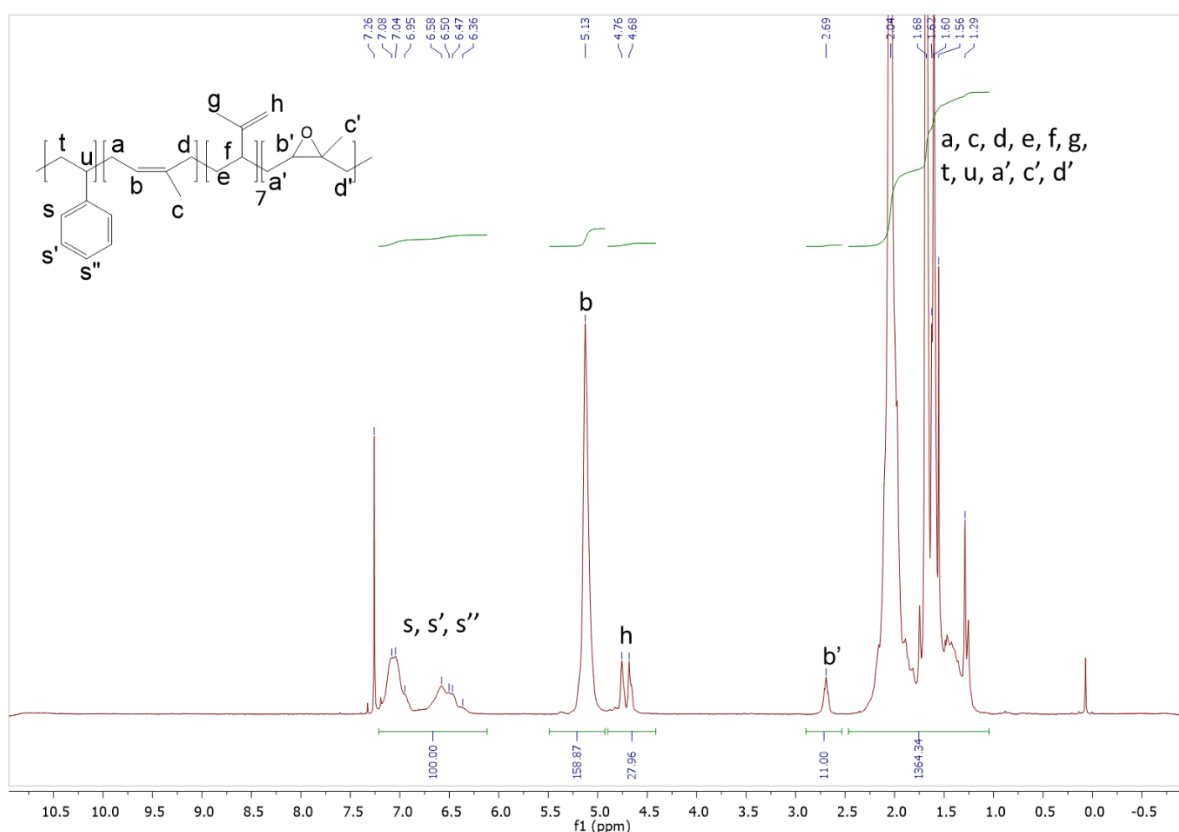


Figure S78.  $^1\text{H}$  NMR spectrum of E-SIS.

$^1\text{H}$  NMR (300 MHz,  $\text{CDCl}_3$ )  $\delta$ : 7.21 – 6.25 (m, s, s', s''), 5.13 (s, b), 4.81 – 4.71 (m, h), 4.71 – 4.63 (m, h), 2.69 (m, b'), 2.65 – 1.04 (m, a, d, c, e, f, g, t, u, a', c', d').

$$\begin{aligned} \text{Mol\% (epoxide)} &= \frac{S_{b'}}{S_b + S_h/2 + S_{b'} + (S_s + S_{s'} + S_{s''})/5} \\ &= \frac{11.00}{158.87 + \frac{27.96}{2} + 11.00 + 100/5} = 5 \text{ mol\%} \end{aligned}$$

$$\text{Mol\% (1,4 - units)} = \frac{158.87}{158.87 + \frac{27.96}{2} + 11.00 + 100/5} = 78 \text{ mol\%}$$

$$\text{Mol\% (3,4 - units)} = \frac{27.96/2}{158.87 + \frac{27.96}{2} + 11.00 + 100/5} = 7 \text{ mol\%}$$

$$\begin{aligned} \text{Mol\% (styrene)} &= 100 - \text{Mol\% (1,4 - units)} - \text{Mol\% (3,4 - units)} - \text{Mol\% (epoxide)} \\ &= 10 \text{ mol\%} \end{aligned}$$

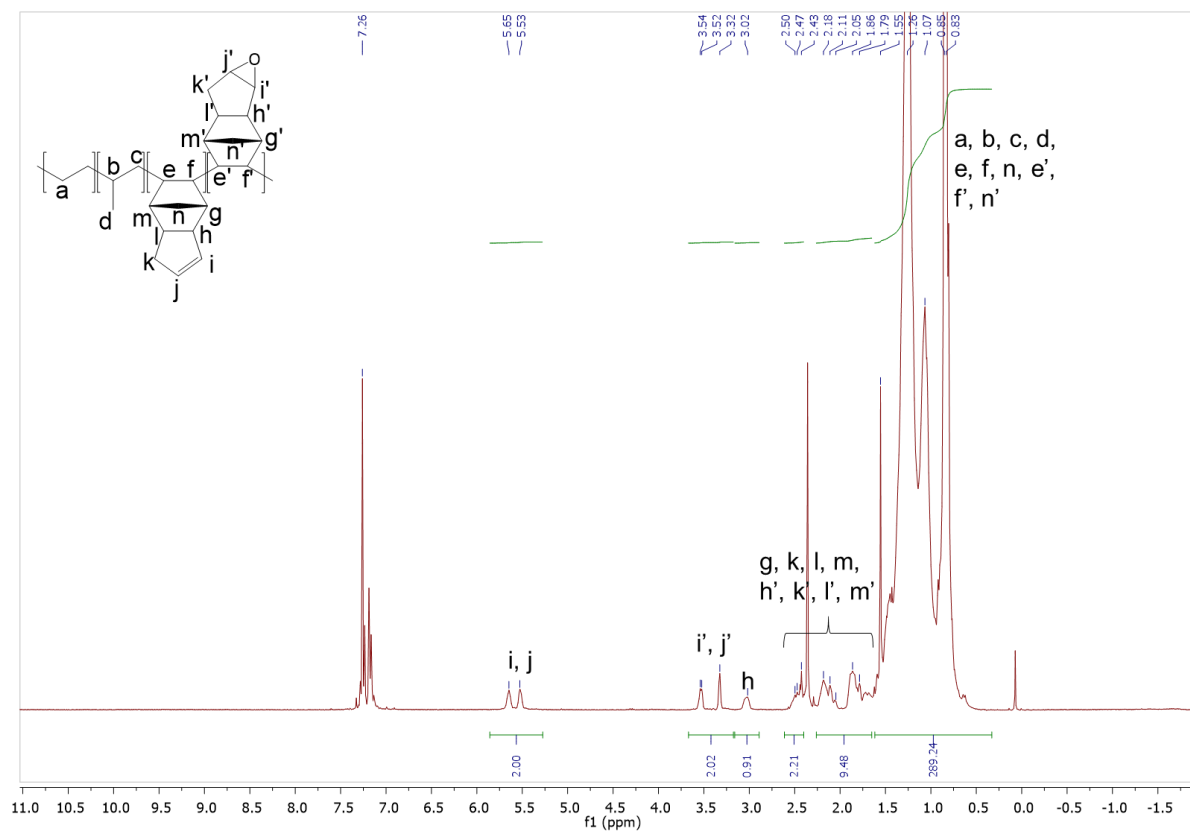


Figure S79.  $^1\text{H}$  NMR spectrum of E-EPDM-DCPD.

$^1\text{H}$  NMR (300 MHz,  $\text{CDCl}_3$ )  $\delta$  5.80 – 5.37 (m, I, j), 3.71 – 3.22 (m, i', j'), 3.19 – 2.86 (m, h), 2.66 – 1.68 (m, g, k, l, m, h', k', l', m'), 1.65 – 0.39 (m, a, b, c, d, e, f, n, e', f', n').

$$\text{Yield (epoxide)} = \frac{S_{i'} + S_{j'}}{S_i + S_j + S_{i'} + S_{j'}} = \frac{2.00}{2.00 + 2.02} = 50\%$$

$$\text{Mol\% (epoxide)} = \text{initial Mol\% (DCPD)} \times \text{Yield (epoxide)} = 1.5 \text{ mol\%}$$

$$\text{Mol\% (DCPD)} = \text{initial Mol\% (DCPD)} - \text{Mol\% (epoxide)} = 1.5 \text{ mol\%}$$

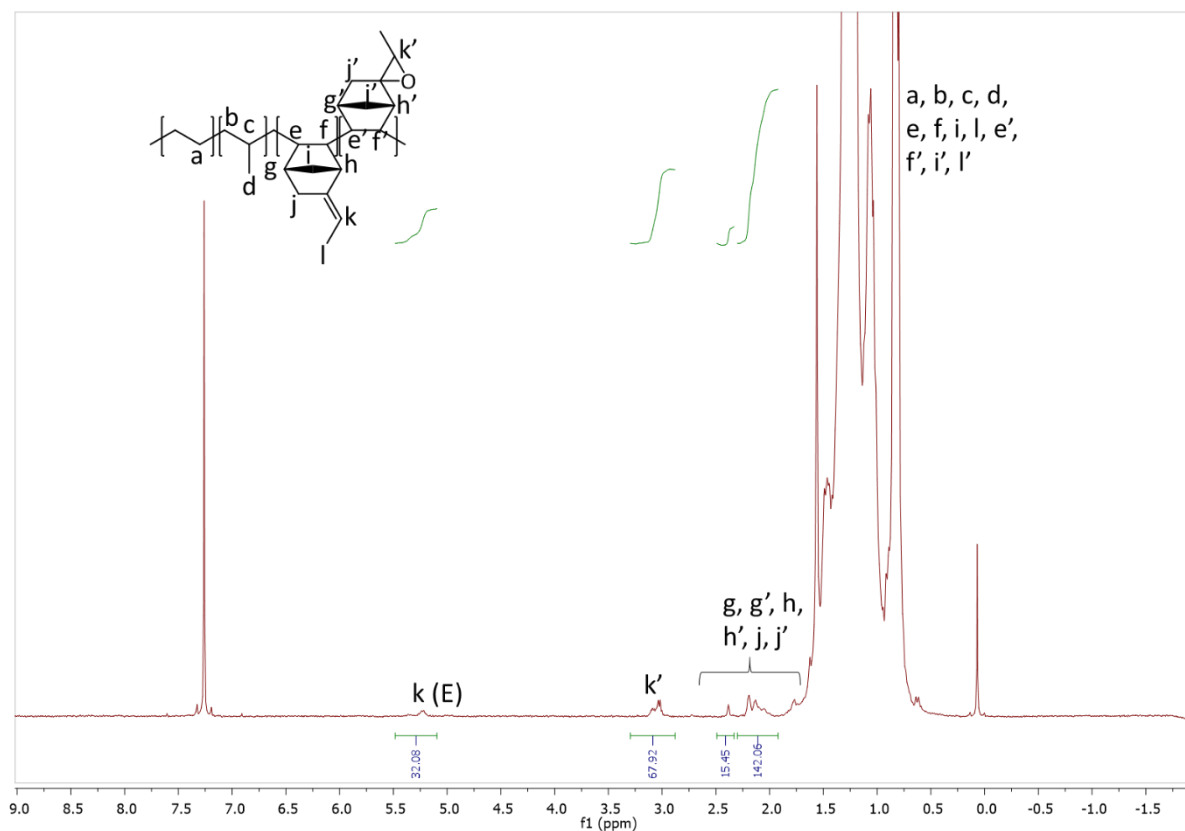


Figure S80. <sup>1</sup>H NMR spectrum of E-EPDM-ENB.

<sup>1</sup>H NMR (300 MHz, CDCl<sub>3</sub>) δ: 5.34 – 5.12 (m, k (E)), 3.25 – 2.93 (m, k'), 2.55 – 1.91 (m, g, g', h, h', j, j'), 1.94 – 0.28 (m, a, b, c, d, e, e', f, i, i', l, l').

$$\text{Yield (Epoxide)} = \frac{S_{k'}}{S_k + S_{k'}} = \frac{67.92}{32.08 + 67.92} = 68\%$$

$$\text{Mol\% (epoxide)} = \text{initial Mol\% (ENB)} \times \text{Yield (epoxide)} = 0.7 \text{ mol\%}$$

$$\text{Mol\% (ENB)} = \text{initial Mol\% (ENB)} - \text{Mol\% (epoxide)} = 0.3 \text{ mol\%}$$

II.3.c. DSC analyses

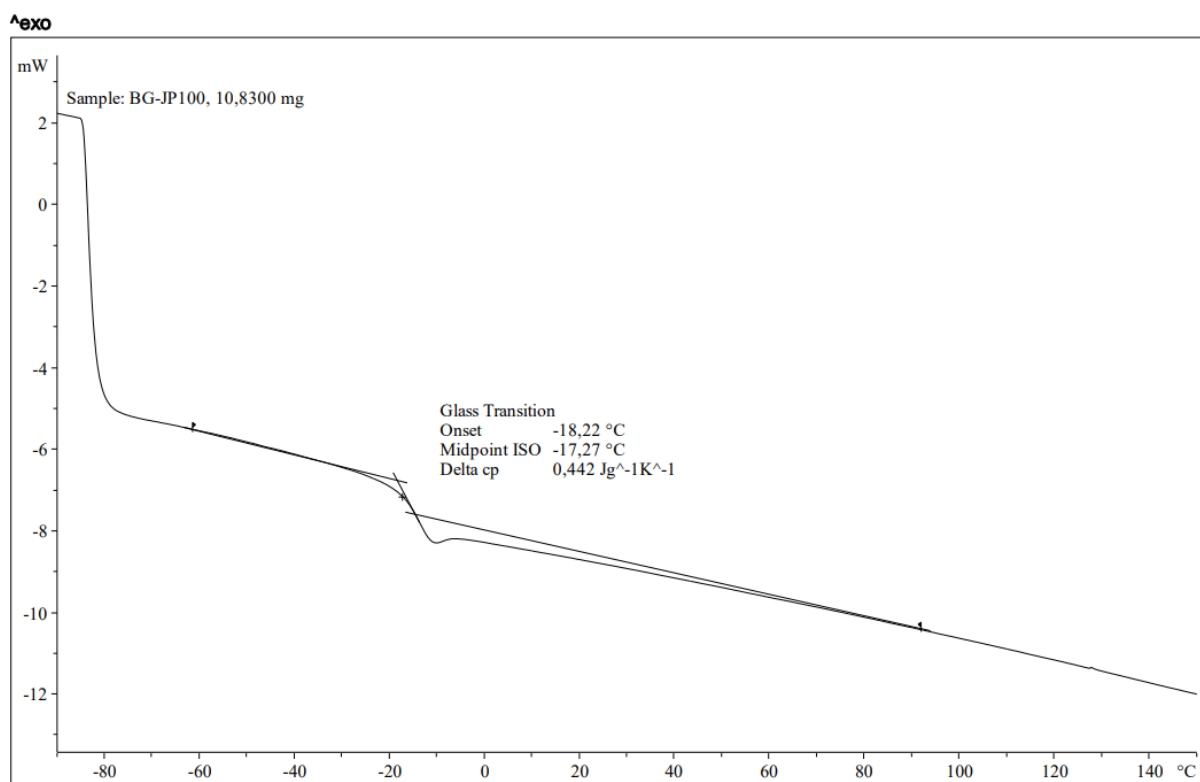


Figure S81. DSC of E-PBU-3.

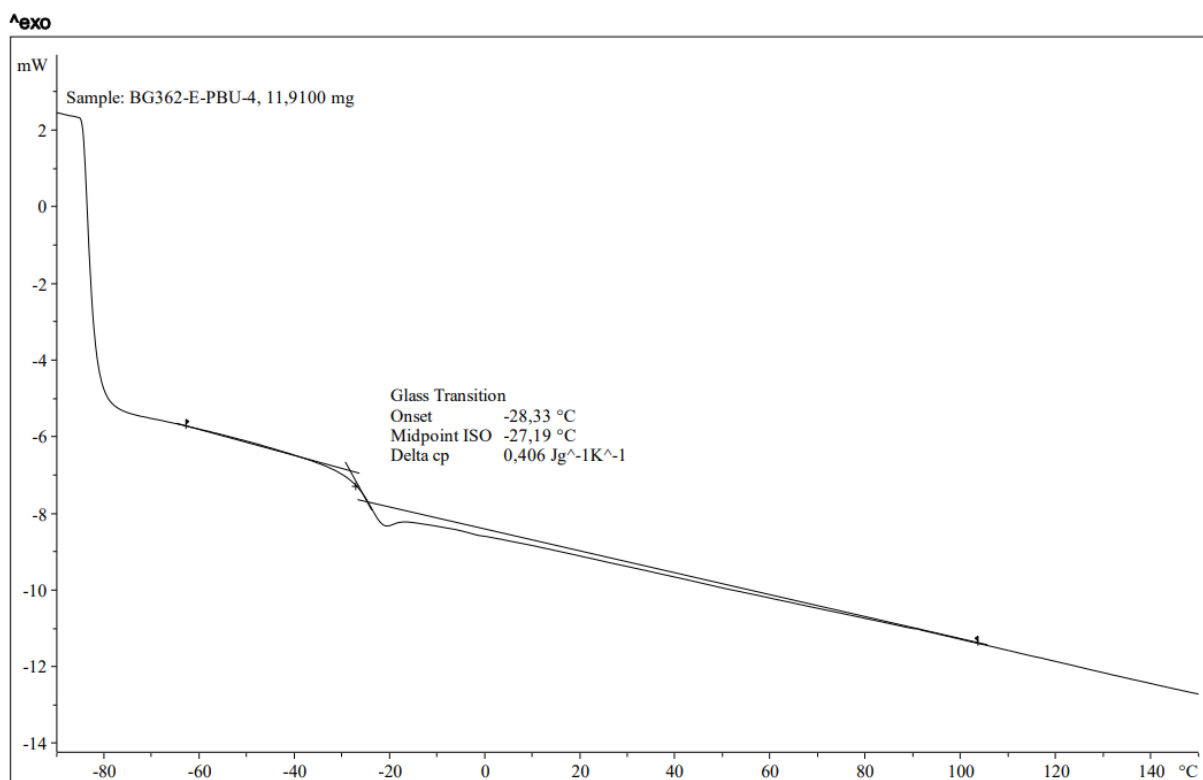


Figure S82. DSC of E-PBU-4.

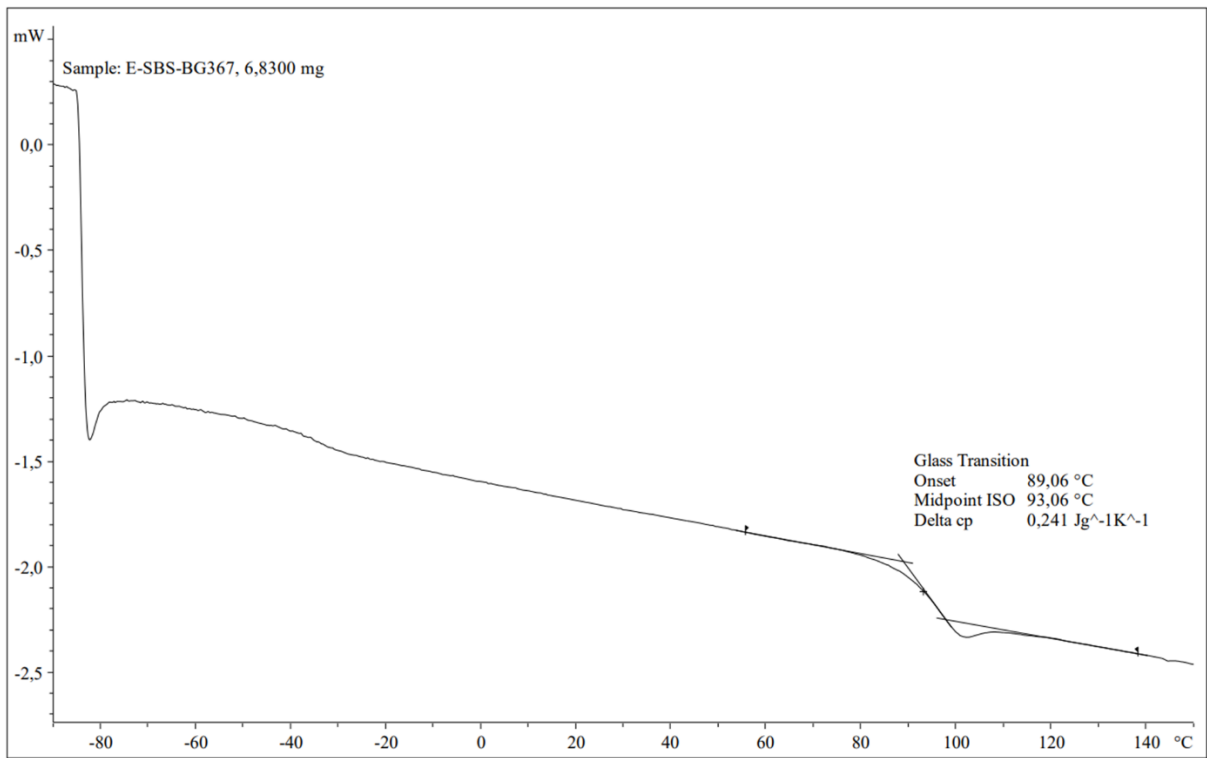


Figure S83. DSC of E-SBS.

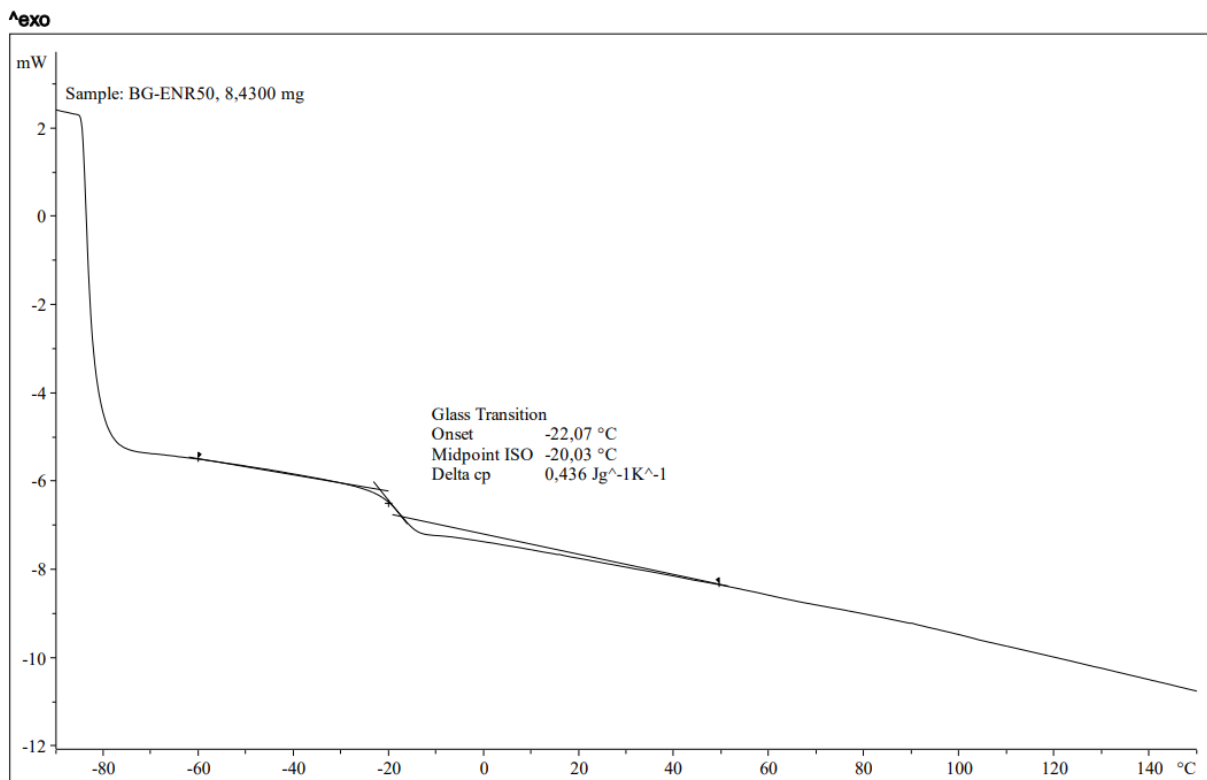


Figure S84. DSC of E-NR-1

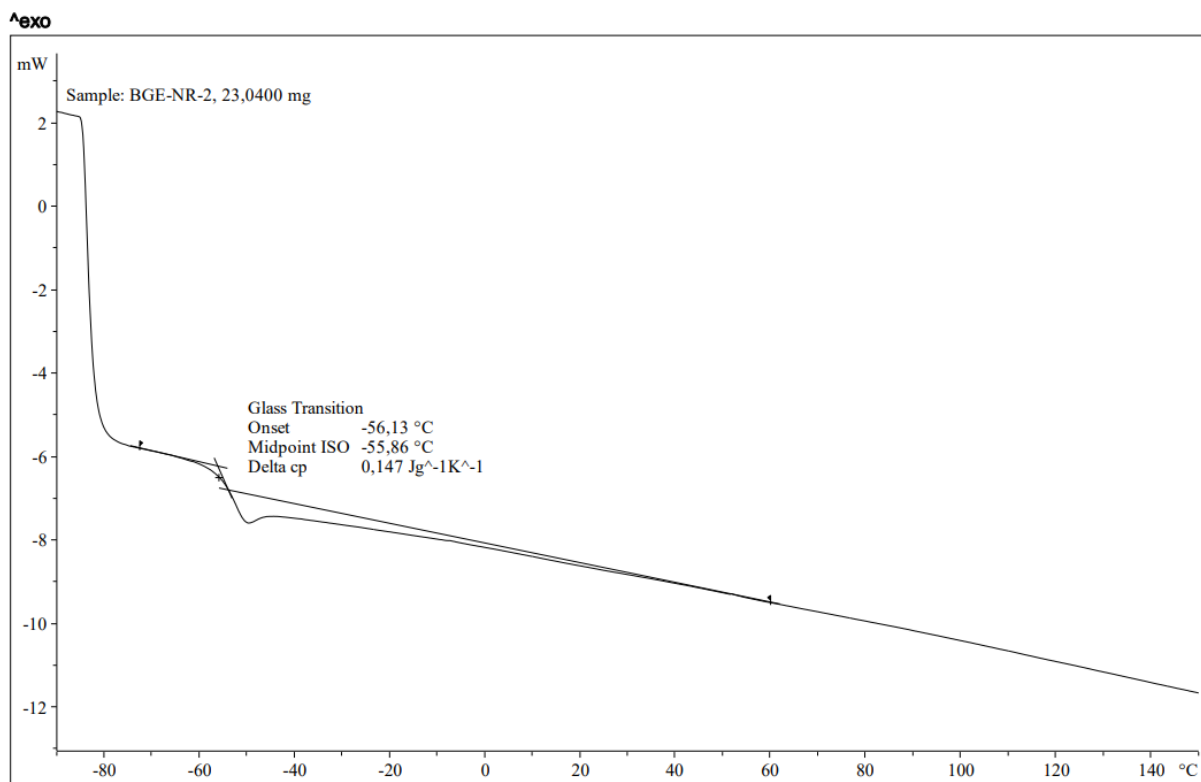


Figure S85. DSC of E-NR-2.

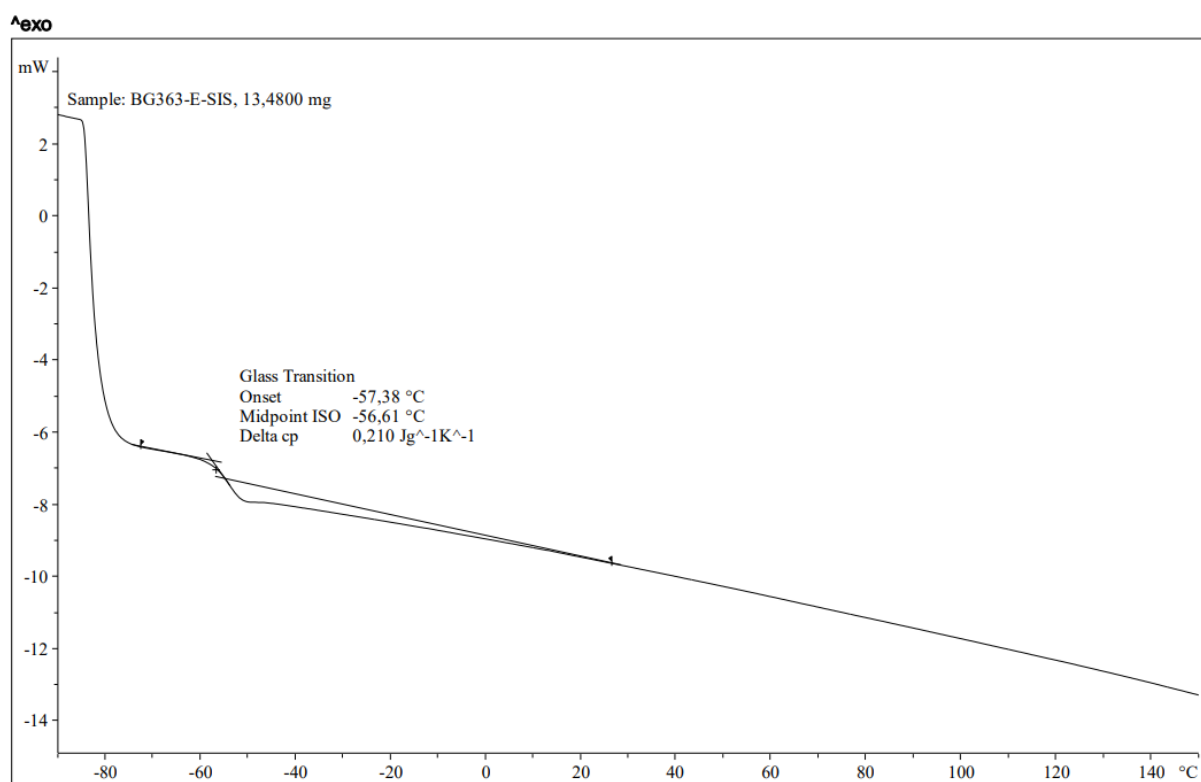


Figure S86. DSC of E-SIS.



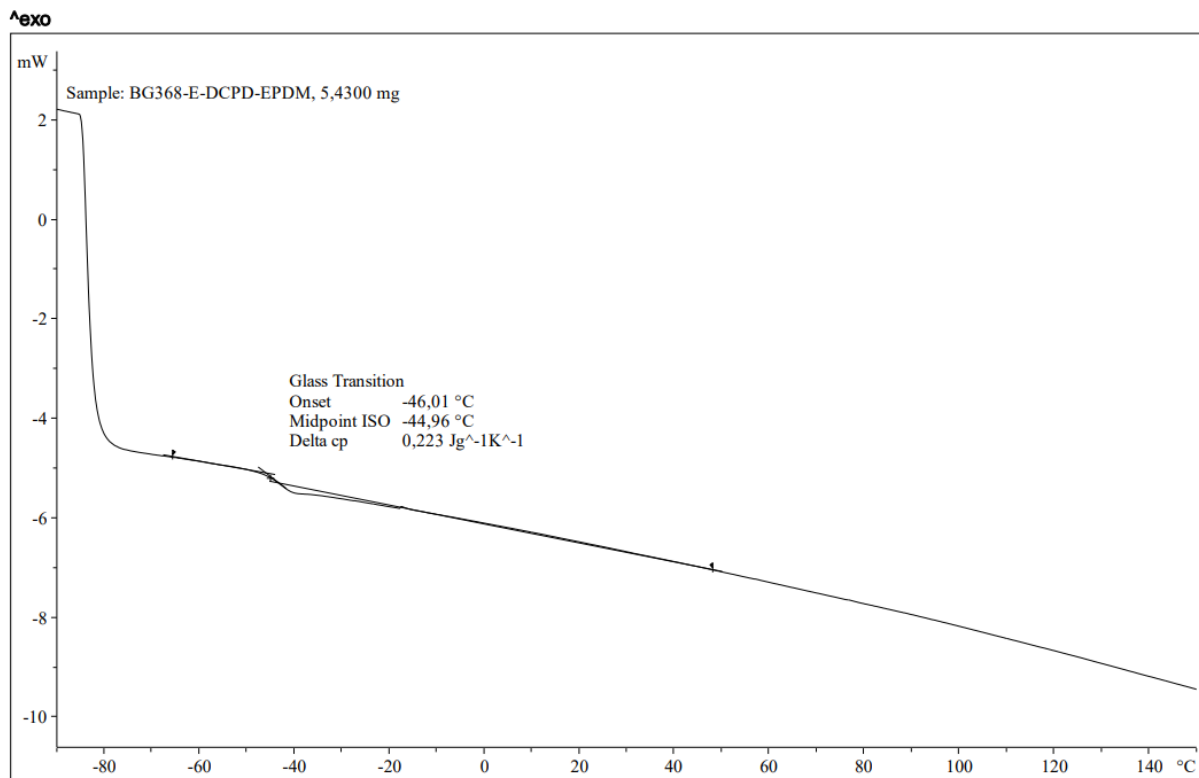


Figure S87. DSC of E-DCPD-EPDM.

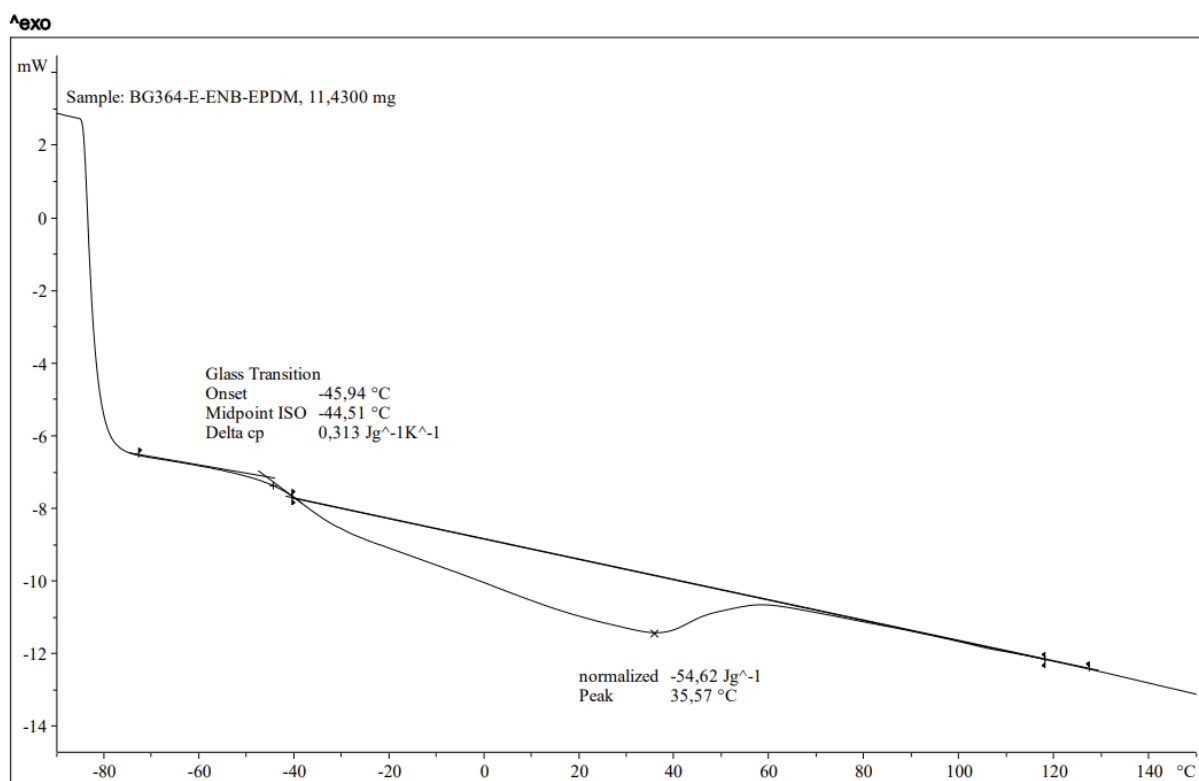


Figure S88. DSC of E-ENB-EPDM.

## II.4. Epoxidation of polybutadiene by reactive extrusion

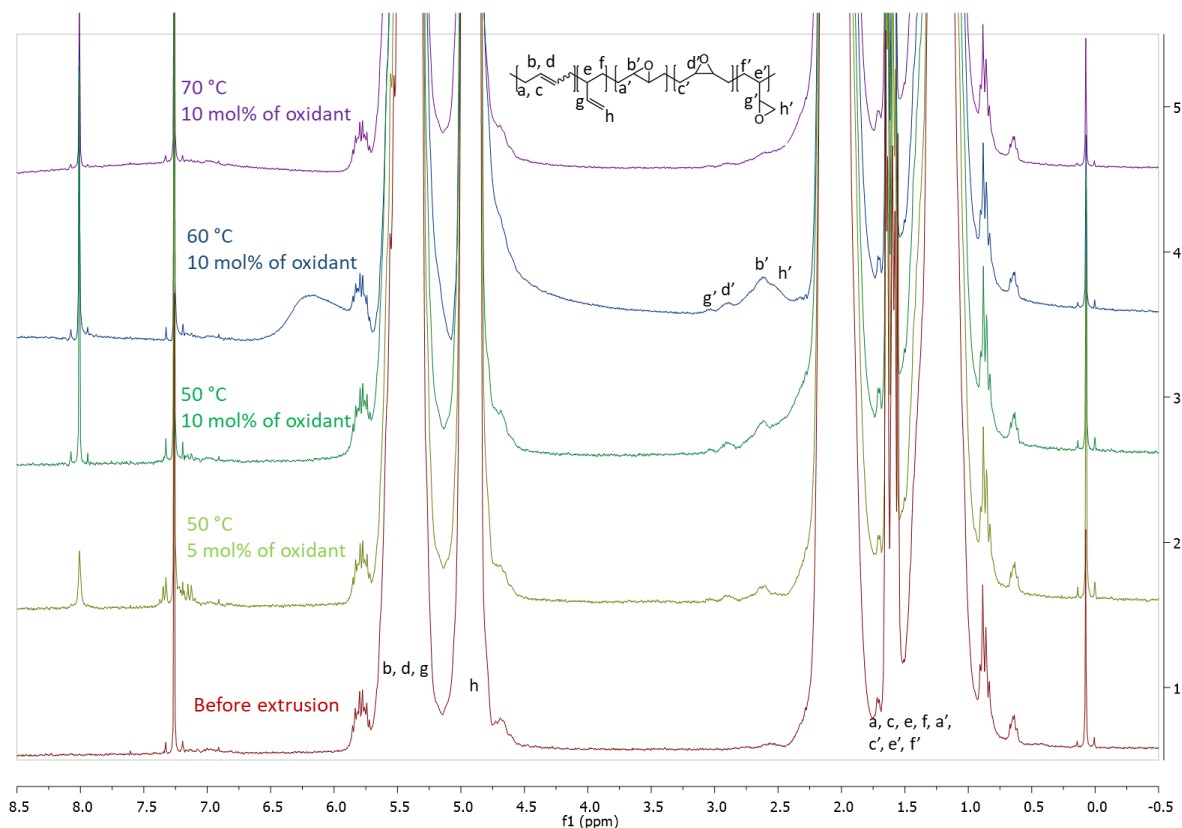
 II.4.a.  $^1\text{H}$  NMR spectra


Figure S89.  $^1\text{H}$  NMR spectra ( $\text{CDCl}_3$ , 300 MHz) of PBU-4 after epoxidation by reactive extrusion (350 g/h of PBU-4, 100 rpm).

$$\text{Mol\% (cis epoxide units)} = \frac{\frac{S_{d'}}{2}}{\frac{S_b + S_d + S_h + S_{b'} + S_{d'}}{2} + S_{g'}}$$

$$\text{Mol\% (trans epoxide units)} = \frac{\frac{S_{b'}}{2}}{\frac{S_b + S_d + S_h + S_{b'} + S_{d'}}{2} + S_{g'}}$$

$$\text{Mol\% (pendant epoxide units)} = \frac{S_{g'}}{\frac{S_b + S_d + S_h + S_{b'} + S_{d'}}{2} + S_{g'}}$$

## II.4.b. DSC analyses

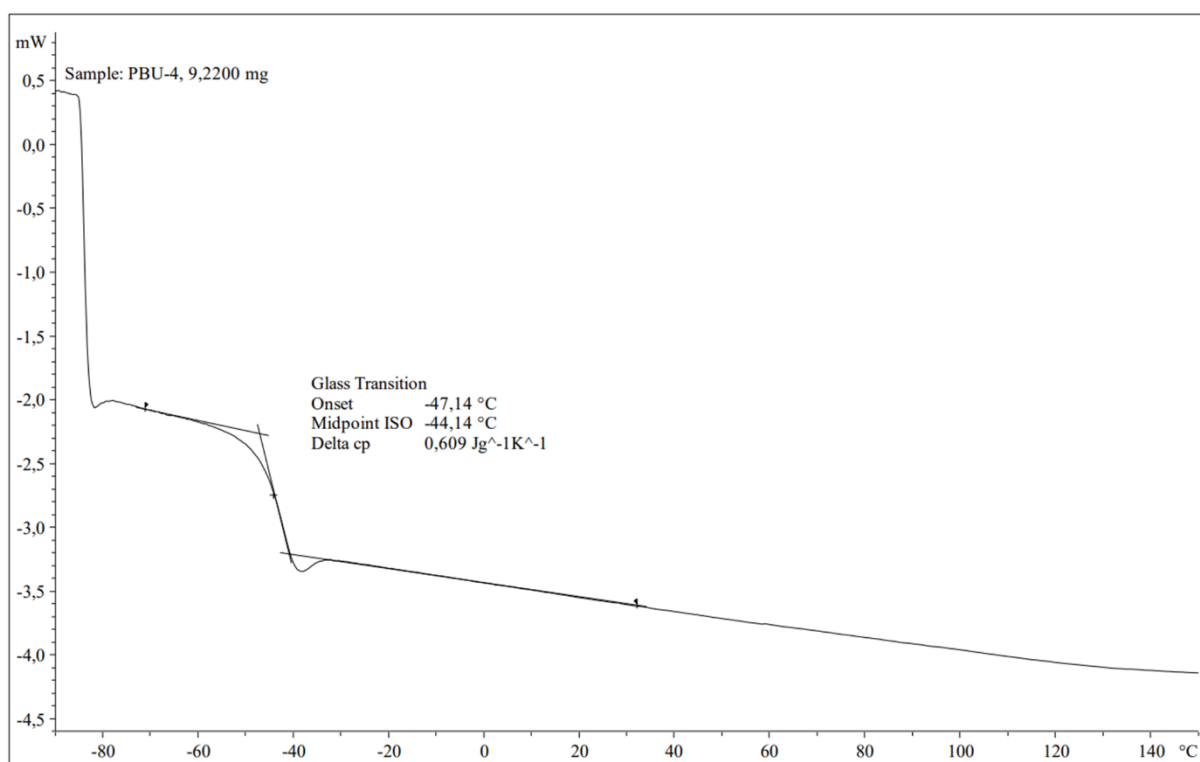


Figure S90. DSC of PBU-4.

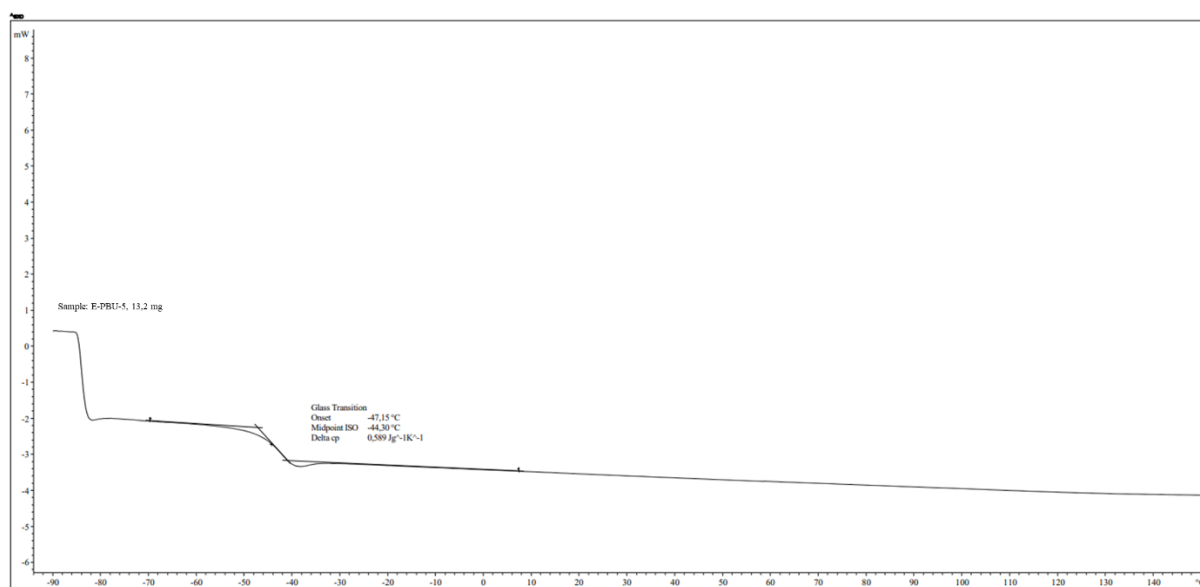


Figure S91. DSC of E-PBU-5.

## II.5. Carbonatation of partially epoxidized polydienes

### II.5.a. IR-ATR spectra

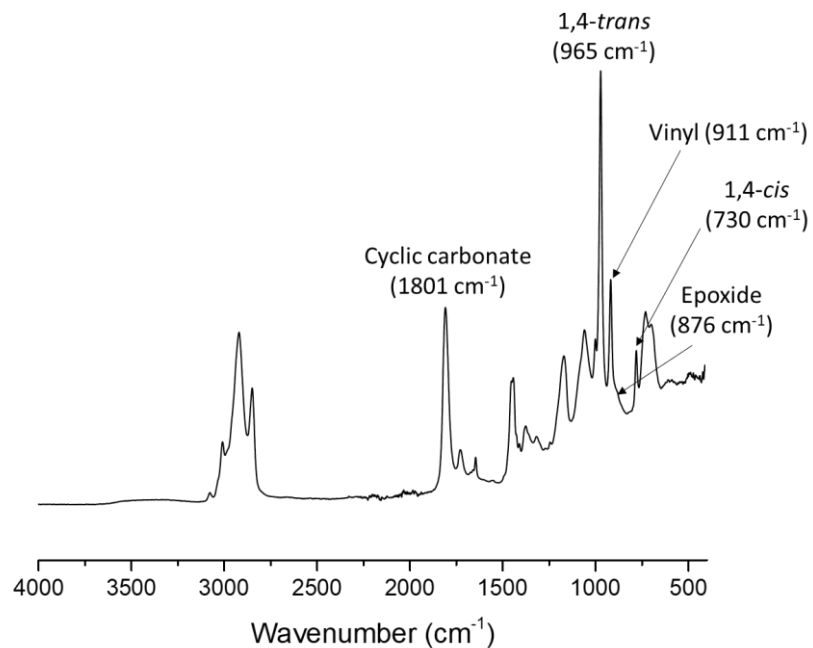


Figure S92. IR-ATR spectrum of C-PBU-1.

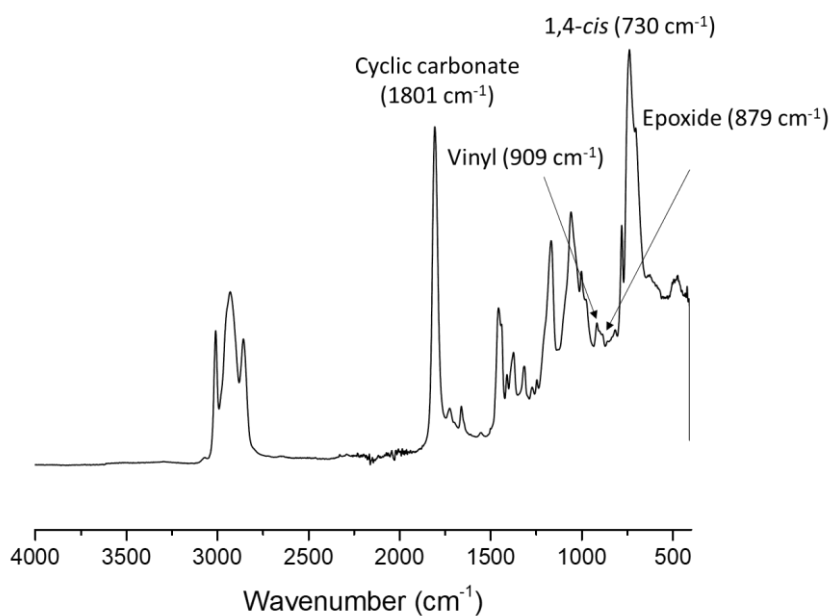


Figure S93. IR-ATR spectrum of C-PBU-2.

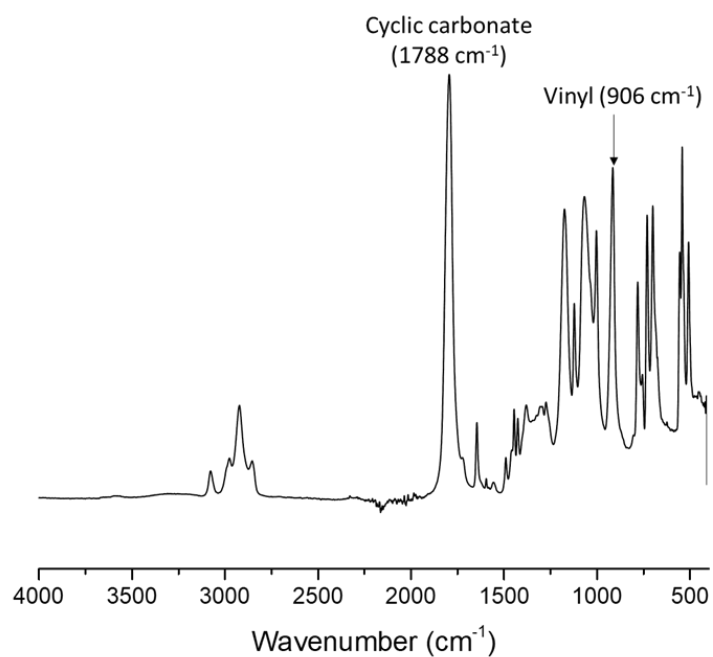


Figure S94. IR-ATR spectrum of C-PBU-3.

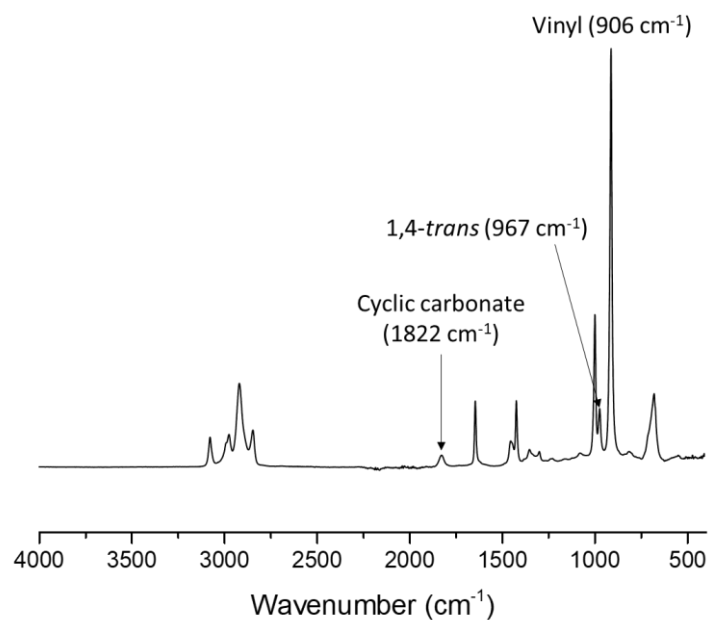


Figure S95. IR-ATR spectrum of C-PBU-4 (Table 4, entry 7).

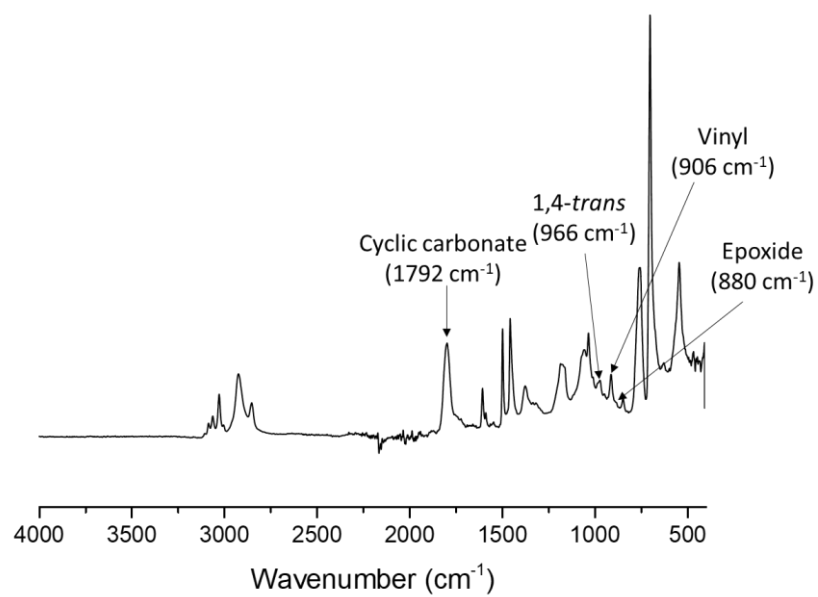


Figure S96. IR-ATR spectrum of C-SBS.

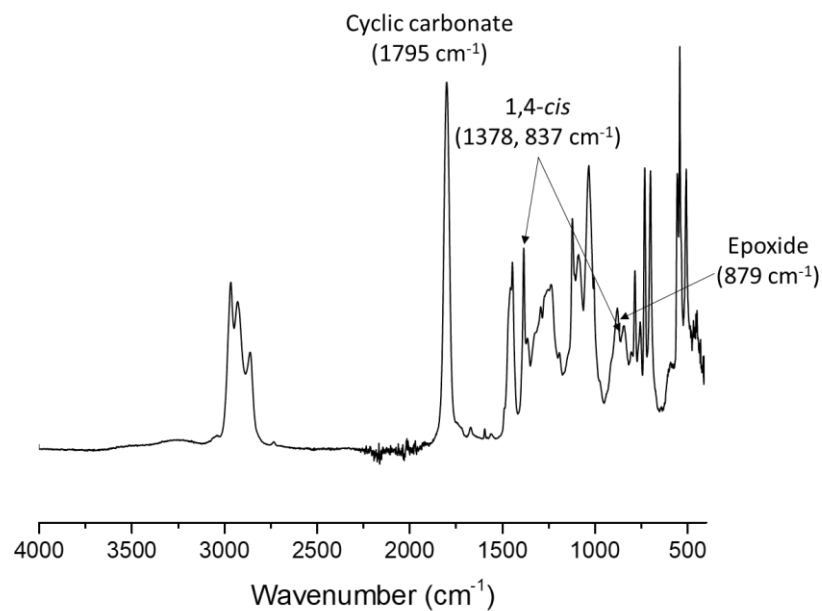


Figure S97. IR-ATR spectrum of C-NR-1.

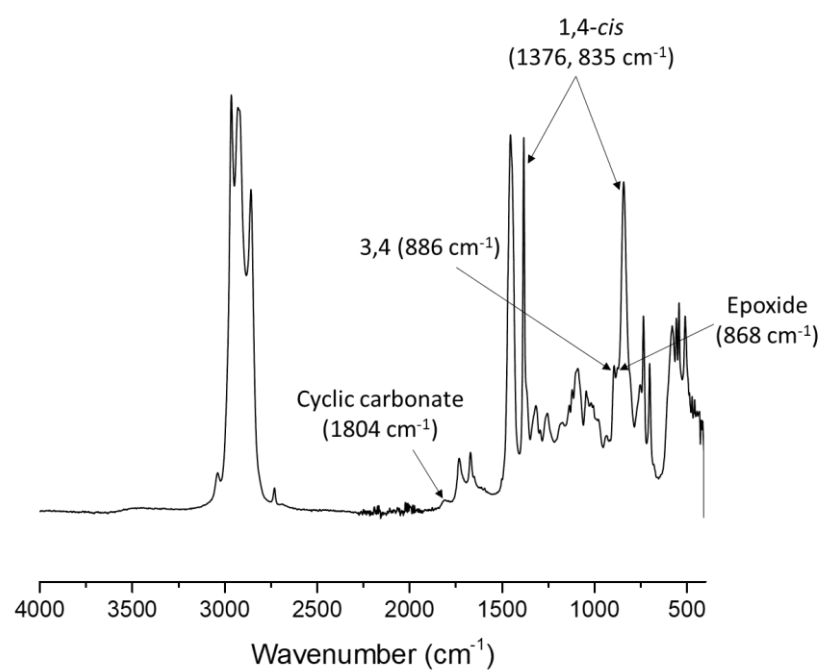
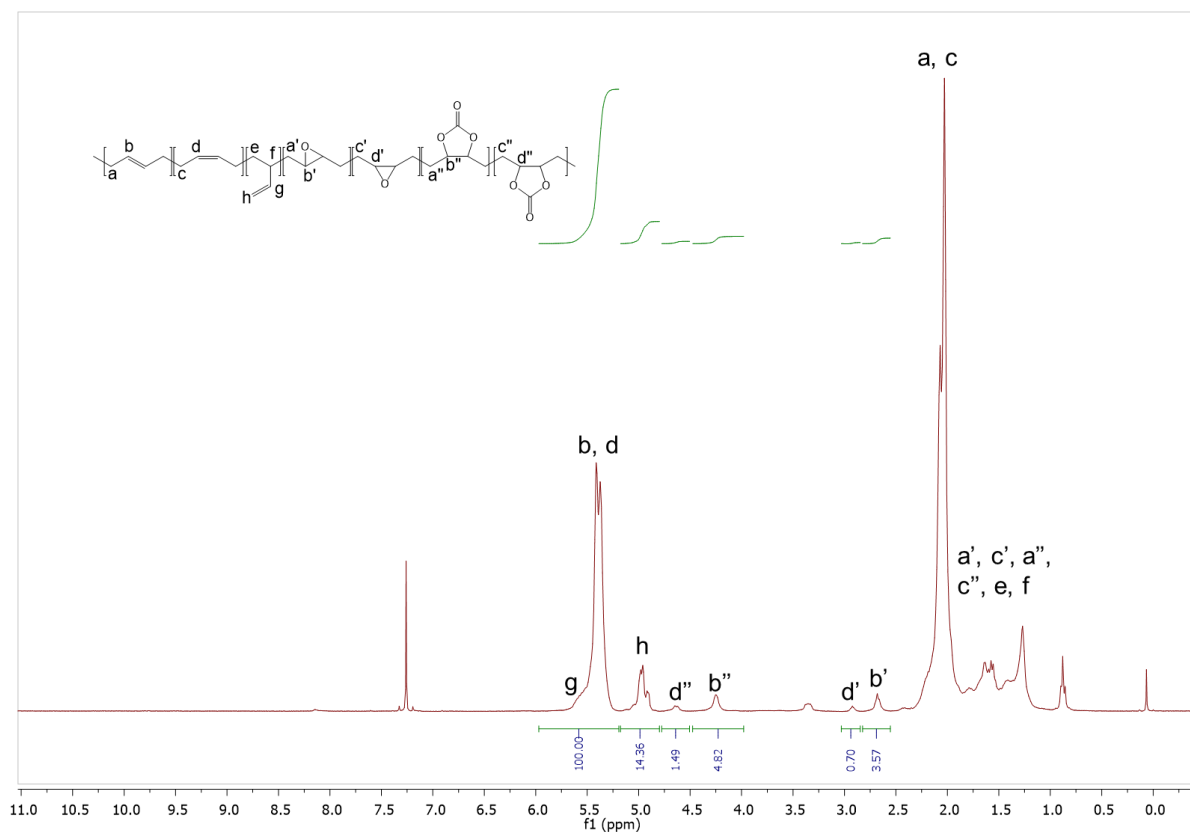


Figure S98. IR-ATR spectrum of C-NR-2 (Table 4, entry 15).

II.5.b.  $^1\text{H}$  NMR spectraFigure S99.  $^1\text{H}$  NMR spectrum of C-PBU-1.

$^1\text{H}$  NMR (300 MHz,  $\text{CDCl}_3$ )  $\delta$  5.77 – 5.19 (m, b, d, g), 5.18 – 4.70 (m, h), 4.65 (m, d''), 4.25 (m, b''), 3.20 – 2.83 (m, d'), 2.82 – 2.53 (m, b'), 2.39 – 1.79 (m, a, c), 1.77 – 1.05 (m, e, f, a', c', a'', c'')

$$\text{Mol\% (cis carbonate)} = \frac{S_{d''}}{S_b + S_d + S_h + S_{b'} + S_{d'} + S_{b''} + S_{d''}}$$

$$\text{Mol\% (cis carbonate)} = \frac{1.49}{\left(100 - \frac{14.36}{2}\right) + 14.36 + 3.57 + 0.70 + 4.82 + 1.49} = 1.3 \text{ mol\%}$$

$$\begin{aligned} \text{Mol\% (trans carbonate)} &= \frac{4.82}{\left(100 - \frac{14.36}{2}\right) + 14.36 + 3.57 + 0.70 + 4.82 + 1.49} \\ &= 4.1 \text{ mol\%} \end{aligned}$$

$$\text{Mol\% (cis epoxide)} = \frac{0.70}{\left(100 - \frac{14.36}{2}\right) + 14.36 + 3.57 + 0.70 + 4.82 + 1.49} = 0.6 \text{ mol\%}$$

$$\text{Mol\% (trans epoxide)} = \frac{3.57}{\left(100 - \frac{14.36}{2}\right) + 14.36 + 3.57 + 0.70 + 4.82 + 1.49} = 3.0 \text{ mol\%}$$



$$\text{Mol\% (1,4 units)} = \frac{\left(100 - \frac{14.36}{2}\right)}{\left(100 - \frac{14.36}{2}\right) + 14.36 + 3.57 + 0.70 + 4.82 + 1.49} = 73 \text{ mol\%}$$

$$\begin{aligned} \text{Mol\% (1,2 units)} &= 100 - \text{Mol\% (1,4 units)} - \text{Mol\% (epoxide units)} - \text{Mol\% (carbonate)} \\ &= 18 \text{ mol\%} \end{aligned}$$

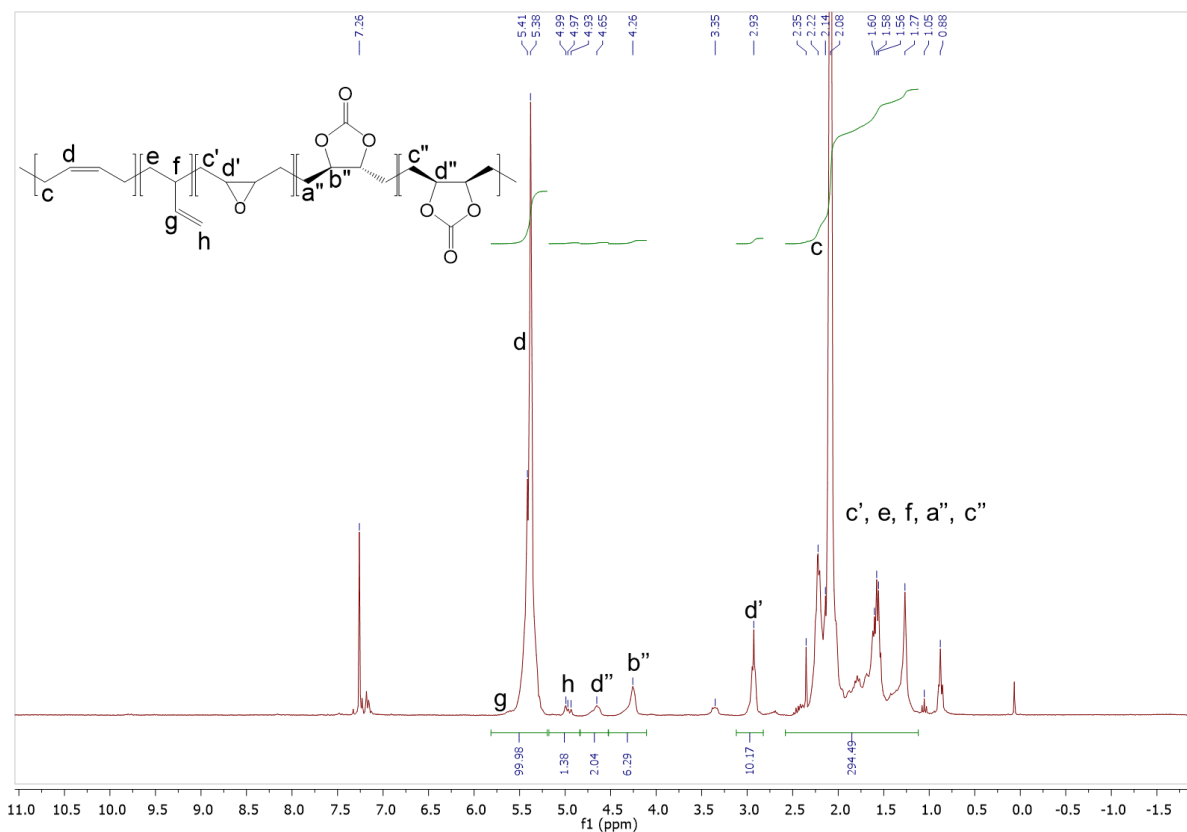


Figure S100.  $^1\text{H}$  NMR spectrum of C-PBU-2.

$^1\text{H}$  NMR (300 MHz,  $\text{CDCl}_3$ )  $\delta$ : 5.75 – 5.18 (m, d, h, g), 5.18 – 4.71 (m, h), 4.65 (m, d''), 4.26 (m, b''), 2.93 (t,  $J = 4.7$  Hz, d'), 2.54 – 1.88 (m, c), 1.86 – 1.14 (m, c', e, f), 1.00 – 0.70 (m,  $\text{CH}_3$ ).

$$\text{Mol\% (cis carbonate units)} = \frac{S_{d''}}{S_d + S_h + S_{d'} + S_{b''} + S_{d''}}$$

$$\text{Mol\% (cis carbonate)} = \frac{2.04}{\left(99.98 - \frac{1.38}{2}\right) + 1.38 + 10.17 + 6.29 + 2.04} = 2 \text{ mol\%}$$

$$\text{Mol\% (trans carbonate)} = \frac{6.29}{\left(99.98 - \frac{1.38}{2}\right) + 1.38 + 10.17 + 6.29 + 2.04} = 5 \text{ mol\%}$$

$$\text{Mol\% (cis epoxide)} = \frac{10.17}{\left(99.98 - \frac{1.38}{2}\right) + 1.38 + 10.17 + 6.29 + 2.04} = 8 \text{ mol\%}$$

$$\text{Mol\% (1,4 units)} = \frac{99.98 - \frac{1.38}{2}}{\left(99.98 - \frac{1.38}{2}\right) + 1.38 + 10.17 + 6.29 + 2.04} = 83 \text{ mol\%}$$

$$\begin{aligned} \text{Mol\% (1,2 units)} &= 100 - \text{Mol\% (1,4 units)} - \text{Mol\% (epoxide)} - \text{Mol\% (carbonate)} \\ &= 2 \text{ mol\%} \end{aligned}$$

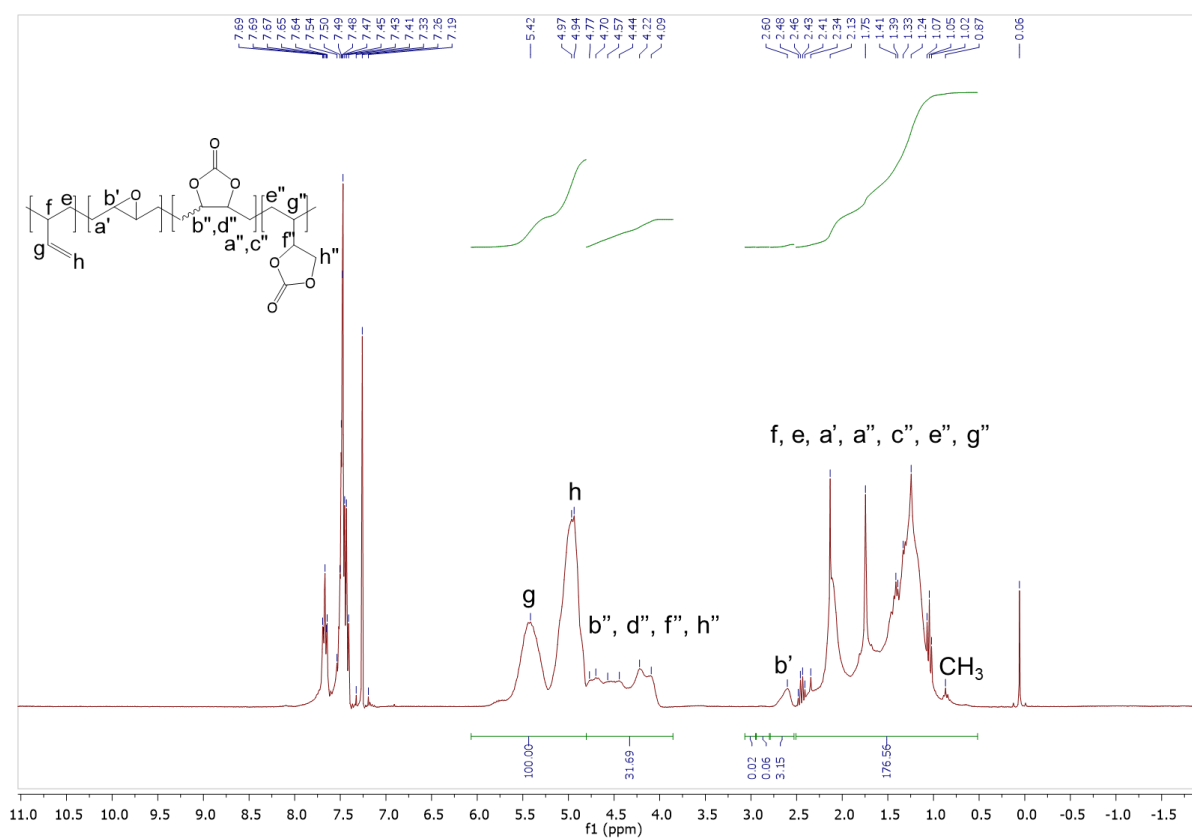


Figure S101. <sup>1</sup>H NMR spectrum of C-PBU-3.

<sup>1</sup>H NMR (300 MHz, CDCl<sub>3</sub>) δ: 5.84 – 5.15 (m, g), 5.13 – 4.77 (m, h), 4.77 – 4.00 (m, b'', d'', f'', h''), 2.60 (m, b'), 2.37 – 0.91 (m, e, f, a', a'', c'', e'', g''), 0.91 – 0.68 (m, CH<sub>3</sub>).

$$\text{Conversion (cis epoxide)} = 1 - \frac{S_{a'}}{S_{a',\text{initial}}} = 1 - \frac{0.06}{5.15} = 99 \%$$

$$\text{Conversion (trans epoxide)} = 1 - \frac{S_{b'}}{S_{b',\text{initial}}} = 1 - \frac{3.15}{46.07} = 93 \%$$

$$\text{Conversion (pendant epoxide)} = 1 - \frac{S_{g'}}{S_{g',\text{initial}}} = 1 - \frac{0.02}{1.68} = 99 \%$$

Mol% (pendant carbonate)

$$\begin{aligned} &= \text{initial Mol\% (pendant epoxide)} \times \text{Conversion (pendant epoxide)} \\ &= 3 \times 0.99 = 3 \text{ mol\%} \end{aligned}$$

Mol% (internal carbonate)

$$\begin{aligned} &= \text{initial Mol\% (cis epoxide)} \times \text{Conversion (cis epoxide)} \\ &+ \text{initial Mol\% (trans epoxide)} \times \text{Conversion (trans epoxide)} \\ &= 3 \times 0.99 + 30 \times 0.93 = 31 \text{ mol\%} \end{aligned}$$

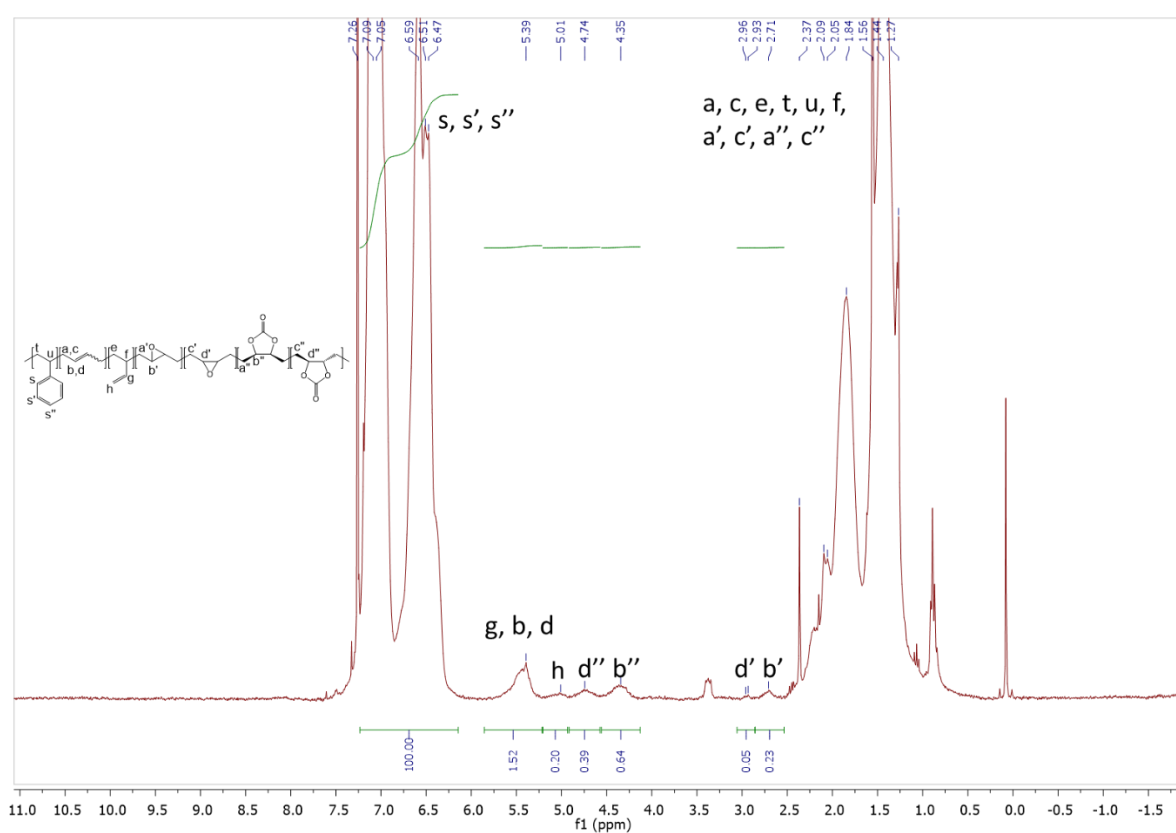


Figure S102.  $^1\text{H}$  NMR spectrum of C-SBS.

$^1\text{H}$  NMR (300 MHz,  $\text{CDCl}_3$ )  $\delta$  7.22 – 6.15 (m, s, s', s''), 5.96 – 5.14 (m, g, b, d), 5.16 – 4.80 (m, h), 4.74 (m, b''), 4.35 (m, d''), 2.96 (m, b'), 2.72 (m, d'), 2.67 – 1.04 (m, a, c, e, f, t, u, a', c', a'', c'').

$$\begin{aligned} \text{Mol\% (cis carbonate)} &= \frac{S_{d''}/2}{(S_b + S_d + S_h + S_{b'} + S_{d'} + S_{b''} + S_{d''})/2 + (S_s + S_{s'} + S_{s''})/5} \\ &= \frac{0.39/2}{((1.52 - \frac{0.20}{2}) + 0.20 + 0.23 + 0.05 + 0.64 + 0.39)/2 + 100/5} \\ &= 0.9 \text{ mol\%} \end{aligned}$$

$$\begin{aligned} \text{Mol\% (trans carbonate)} &= \frac{0.64/2}{\left(\left(1.52 - \frac{0.20}{2}\right) + 0.20 + 0.23 + 0.05 + 0.64 + 0.39\right)/2 + 100/5} \\ &= 1.5 \text{ mol\%} \end{aligned}$$

$$\begin{aligned} \text{Mol\% (cis epoxide)} &= \frac{0.05/2}{\left(\left(1.52 - \frac{0.20}{2}\right) + 0.20 + 0.23 + 0.05 + 0.64 + 0.39\right)/2 + 100/5} \\ &= 0.1 \text{ mol\%} \end{aligned}$$

$$\begin{aligned} \text{Mol\% (trans epoxide)} &= \frac{0.23/2}{\left(\left(1.52 - \frac{0.20}{2}\right) + 0.20 + 0.23 + 0.05 + 0.64 + 0.39\right)/2 + 100/5} \\ &= 0.5 \text{ mol\%} \end{aligned}$$

$$\begin{aligned} \text{Mol\% (1,4 units)} &= \frac{\left(1.52 - \frac{0.20}{2}\right)/2}{\left(\left(1.52 - \frac{0.20}{2}\right) + 0.20 + 0.23 + 0.05 + 0.64 + 0.39\right)/2 + 100/5} \\ &= 3 \text{ mol\%} \end{aligned}$$

$$\begin{aligned} \text{Mol\% (1,2 units)} &= \frac{0.20/2}{\left(\left(1.52 - \frac{0.20}{2}\right) + 0.20 + 0.23 + 0.05 + 0.64 + 0.39\right)/2 + 100/5} \\ &= 1 \text{ mol\%} \end{aligned}$$

*Mol% (styrene)*

$$\begin{aligned} &= 100 - \text{Mol\% (1,4 units)} - \text{Mol\% (1,2 units)} - \text{Mol\% (epoxide)} \\ &\quad - \text{Mol\% (carbonate)} = 93 \text{ mol\%} \end{aligned}$$

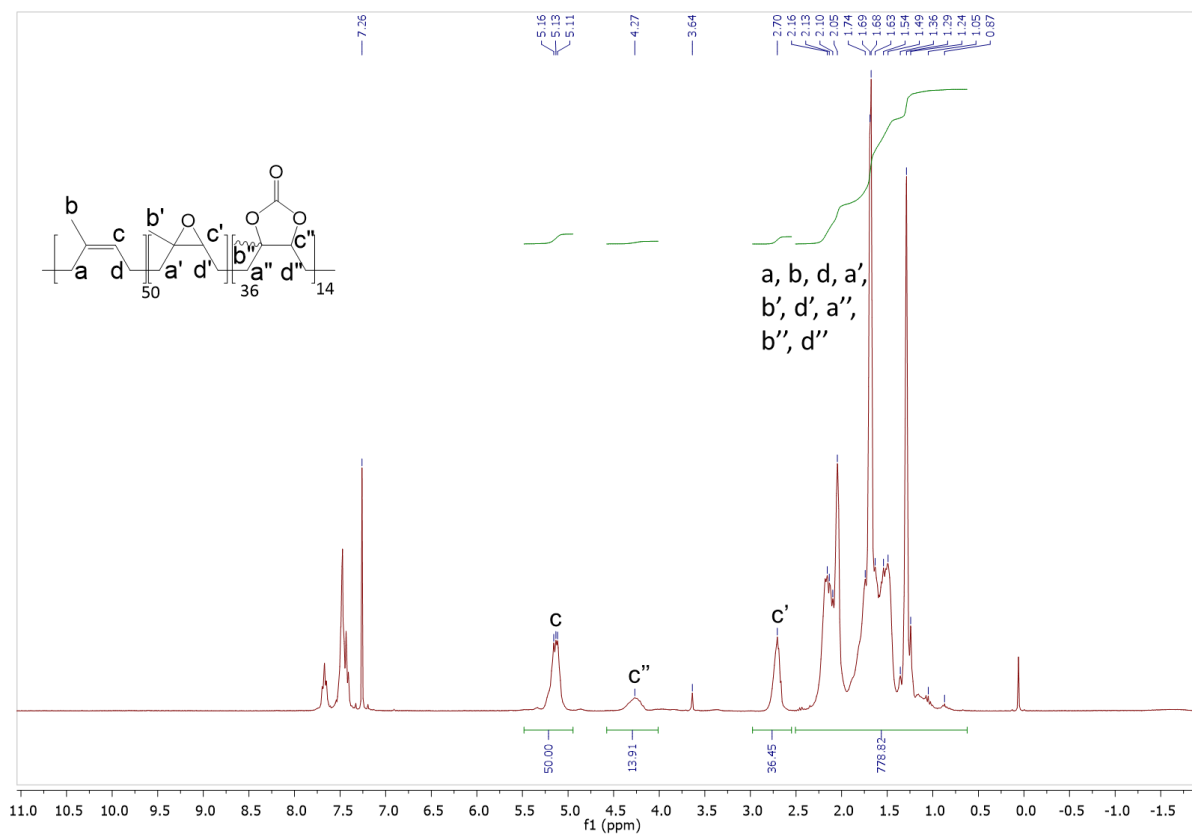


Figure S.103  $^1\text{H}$  NMR spectrum of C-NR-1.

$^1\text{H}$  NMR (300 MHz,  $\text{CDCl}_3$ )  $\delta$ : 5.13 (m, c), 4.27 (m, c''), 2.70 (m, c'), 2.55 – 1.84 (m, a, b, d, a', b', d', a'', b'', d''), 0.87 (m,  $\text{CH}_3$ )

$$\text{Mol\% (carbonate)} = \frac{S_c}{S_c + S_{c'} + S_{c''}} = \frac{13.91}{50 + 36.45 + 13.91} = 14 \text{ mol\%}$$

$$\text{Mol\% (epoxide)} = \frac{S_{c'}}{S_c + S_{c'} + S_{c''}} = \frac{36.45}{50 + 36.45 + 13.91} = 36 \text{ mol\%}$$

$$\text{Mol\% (1,4 units)} = 100 - \text{Mol\% (epoxide)} - \text{Mol\% (carbonate)} = 50 \text{ mol\%}$$

II.5.c. DSC analyses

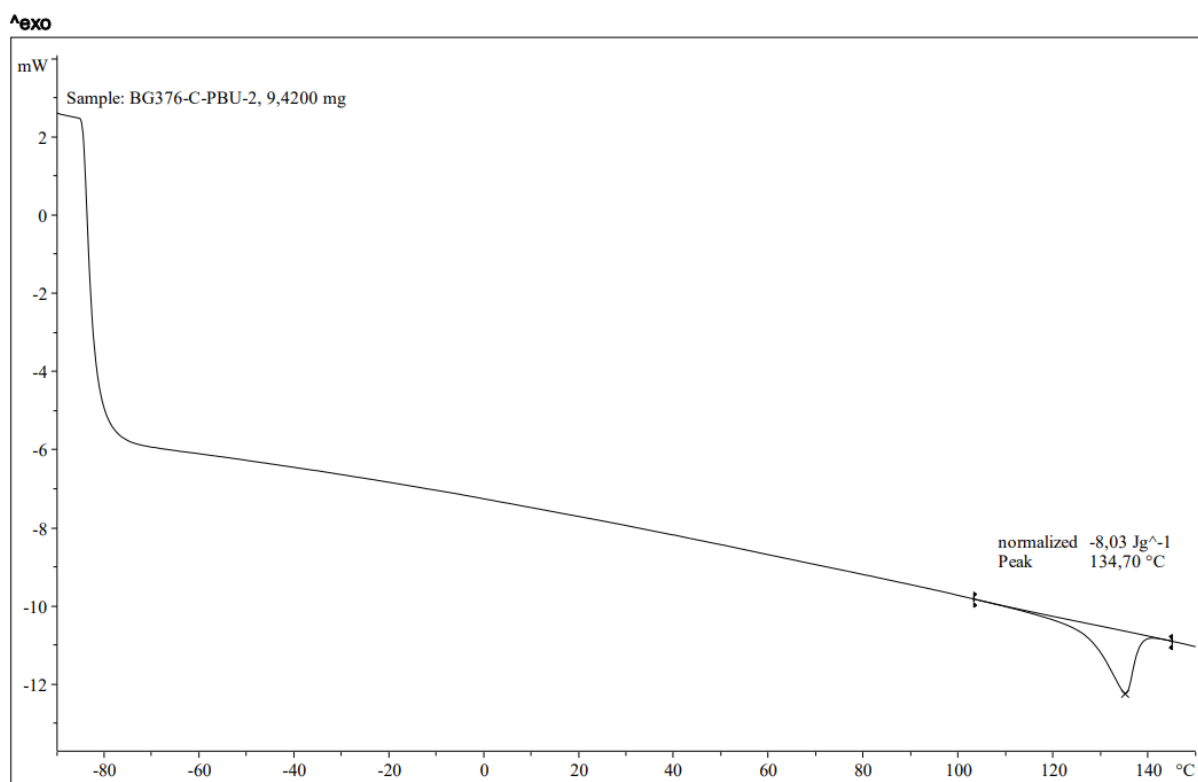


Figure S104. DSC of C-PBU-2.

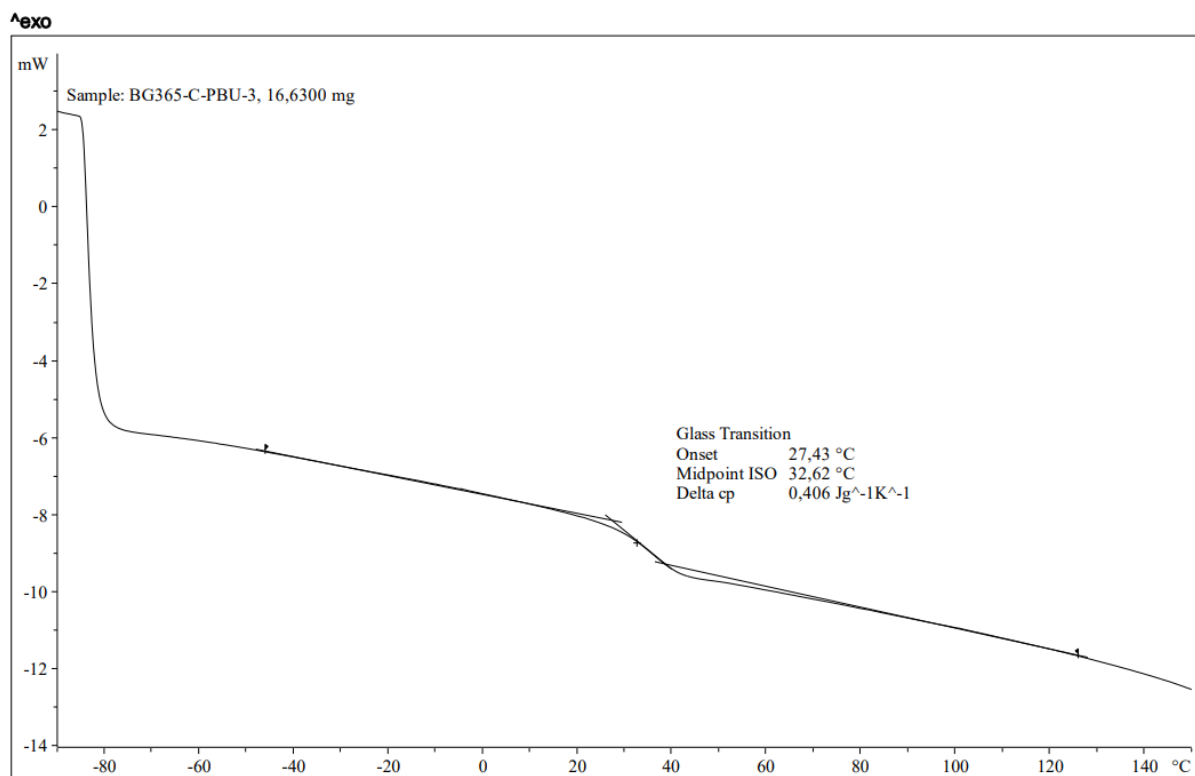


Figure S105. DSC of C-PBU-3.

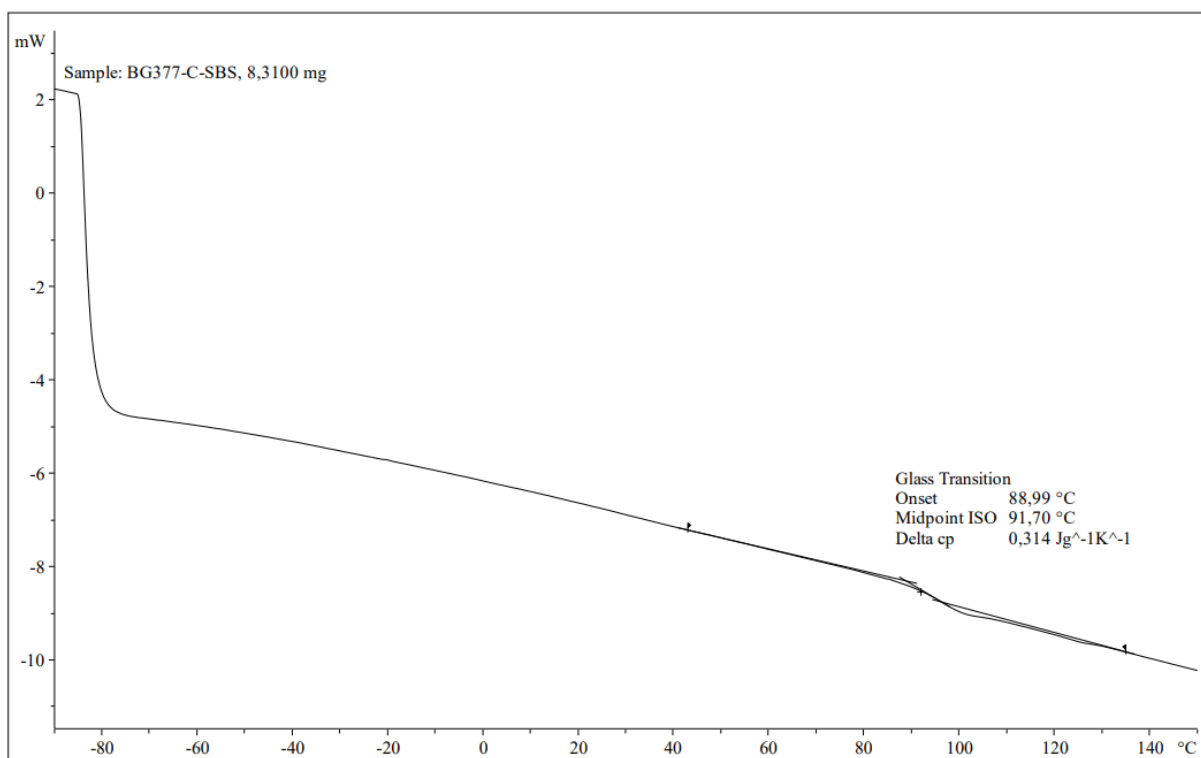


Figure S106. DSC of C-SBS.

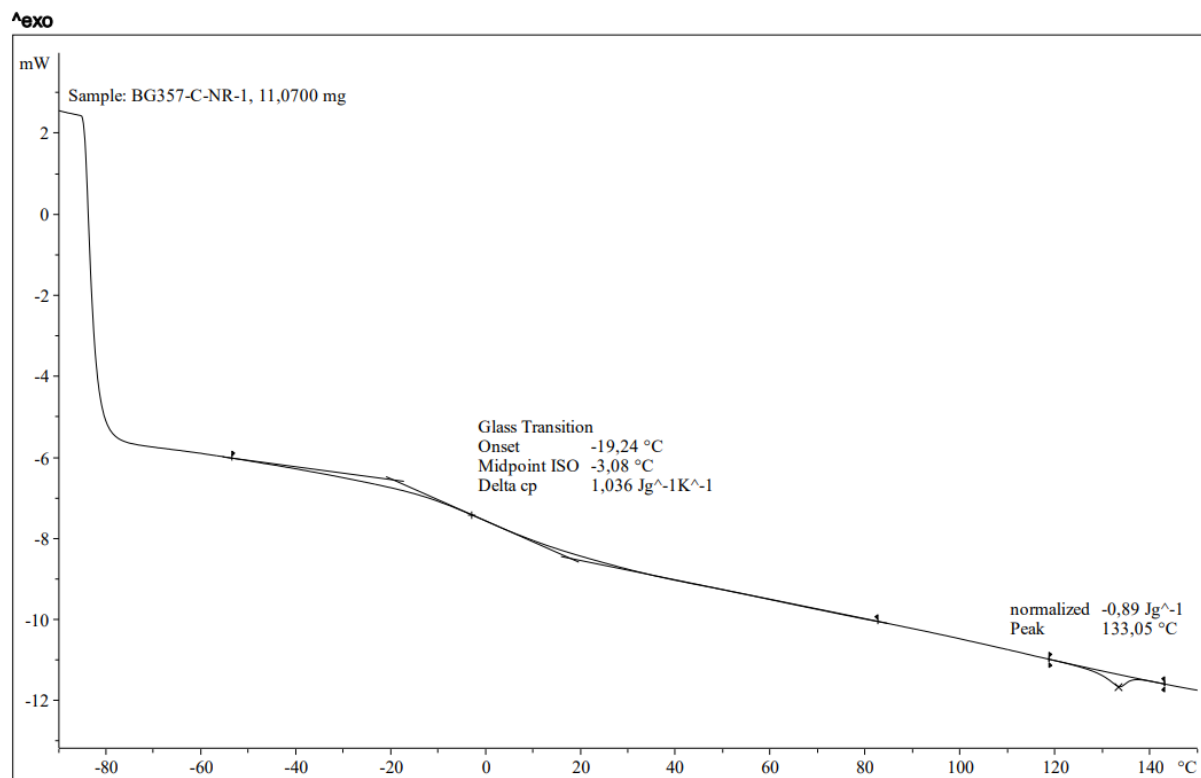


Figure S107. DSC of C-NR-1.

## III. Chapter 4

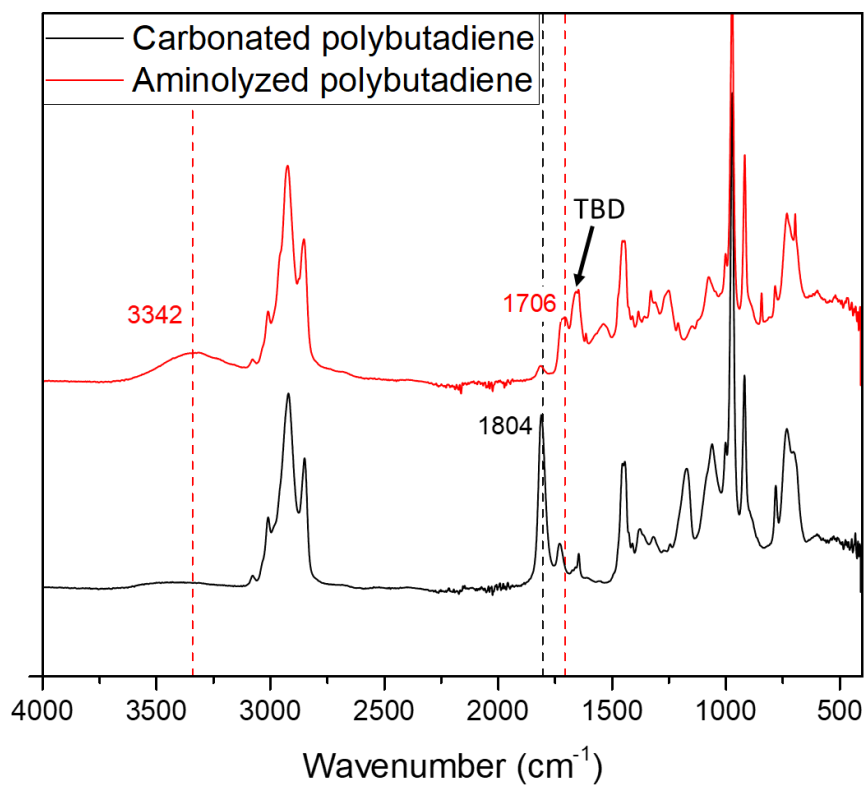


Figure S108. IR-ATR spectra before (black) and after (red) aminolysis of carbonated polybutadiene monitored by  $^1\text{H}$  NMR.



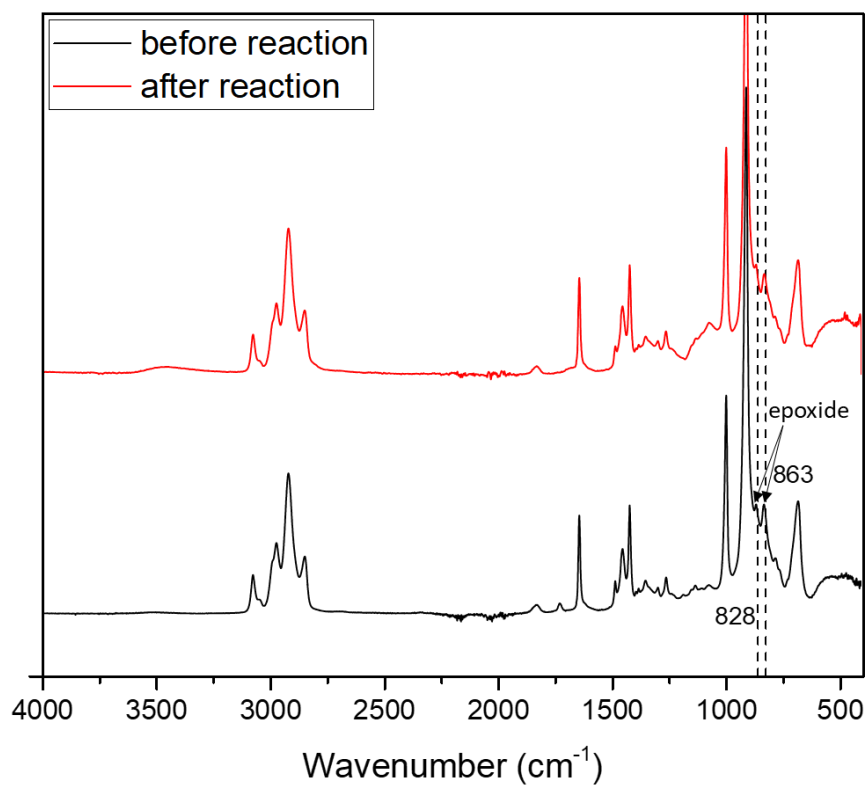
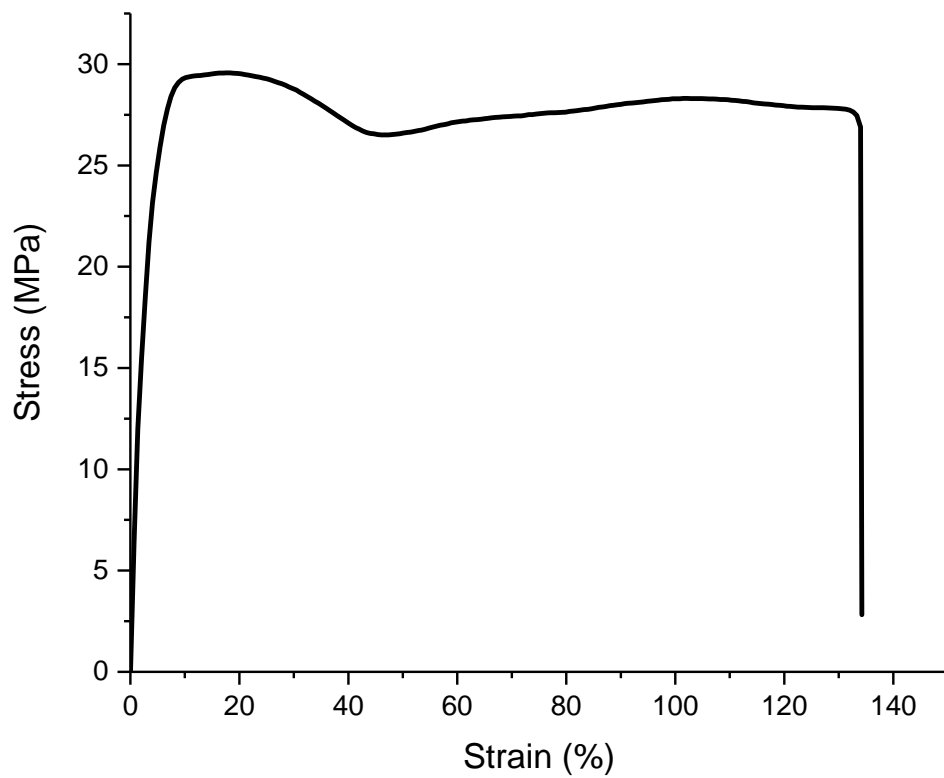


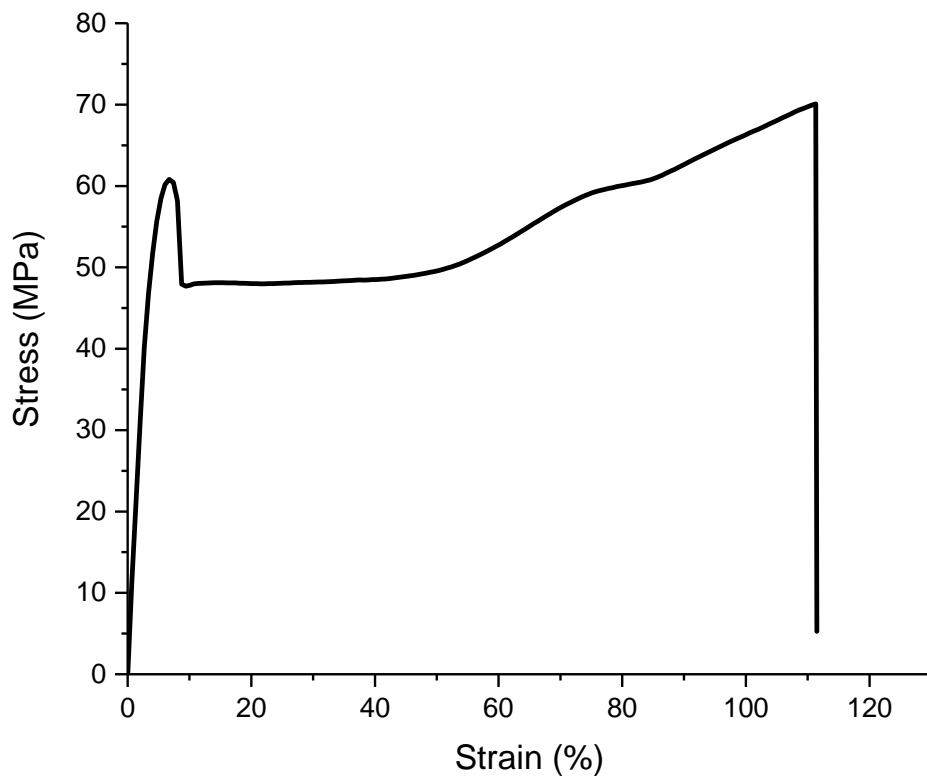
Figure S109. IR-ATR spectra before (black) and after (red) aminolysis of epoxidized polybutadiene (E-PBU-3).

## IV. Chapter 5

### IV.1. Tensile curves



*Figure S110. Tensile curve of HDPE.*



*Figure S111. Tensile curve of PC.*

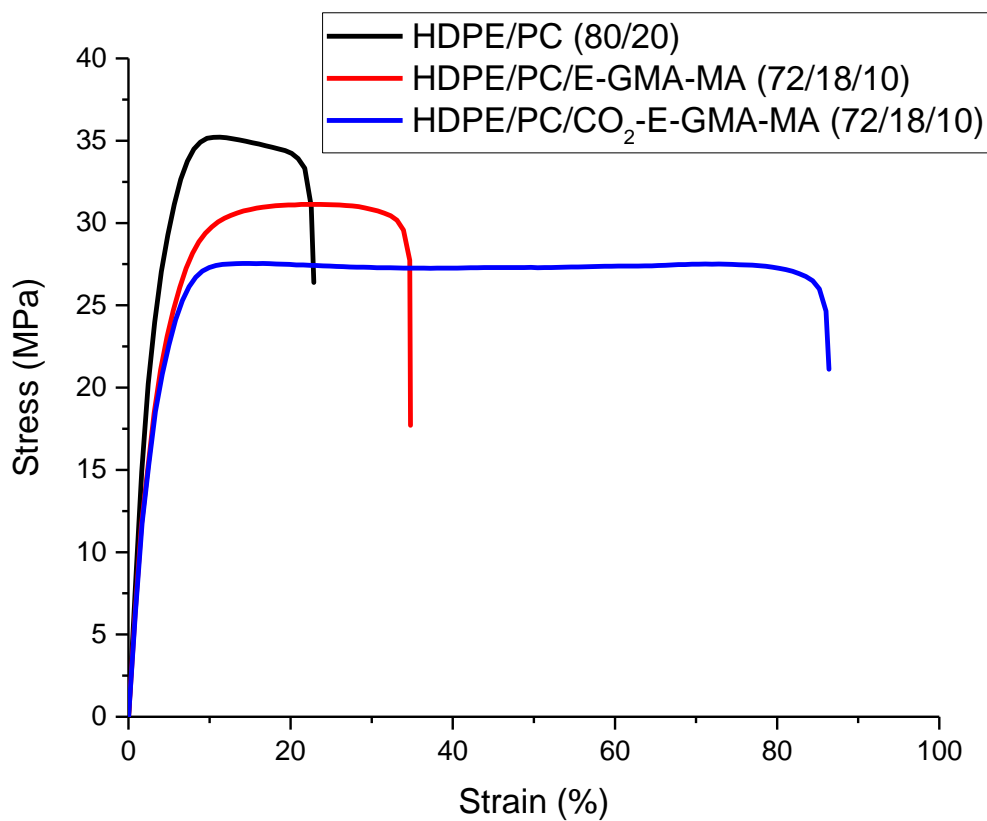
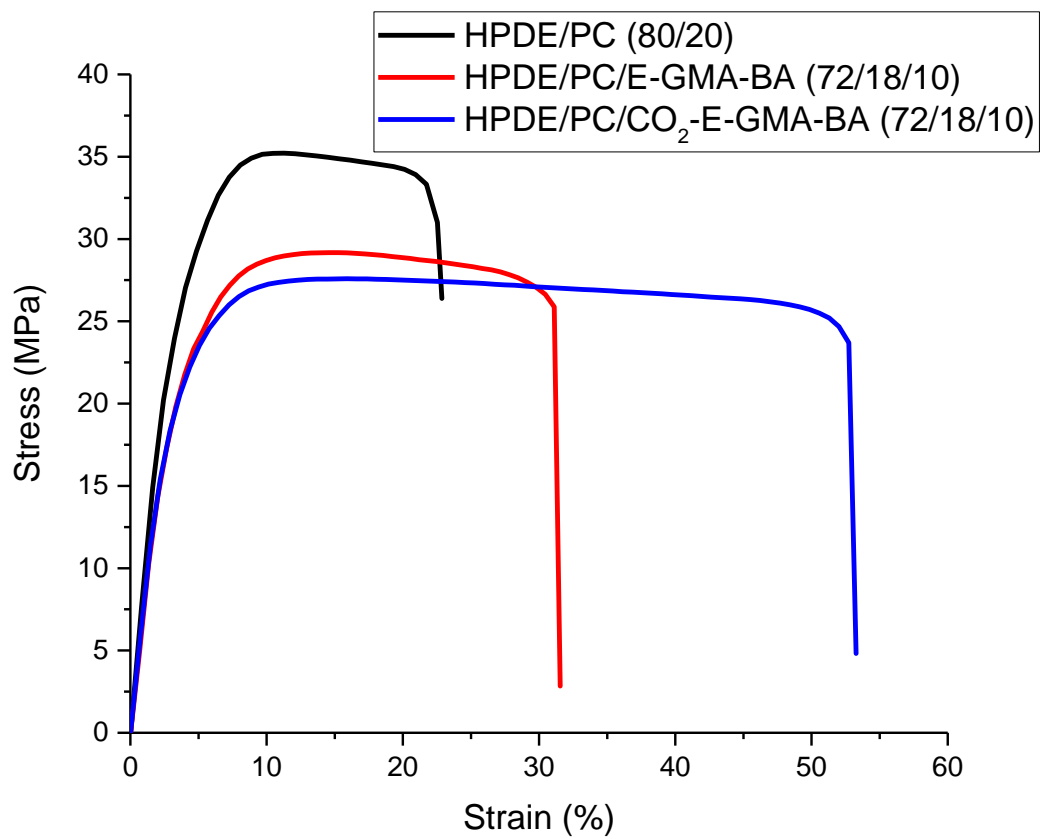


Figure S112. Tensile curve of HDPE/PC (80/20), HDPE/PC/E-GMA-MA (72/18/10) and HDPE/PC/CO<sub>2</sub>-E-GMA-MA (72/18/10) blends.



*Figure S113. Tensile curve of HDPE/PC (80/20), HDPE/PC/E-GMA-BA (72/18/10) and HDPE/PC/CO<sub>2</sub>-E-GMA-BA (72/18/10) blends.*

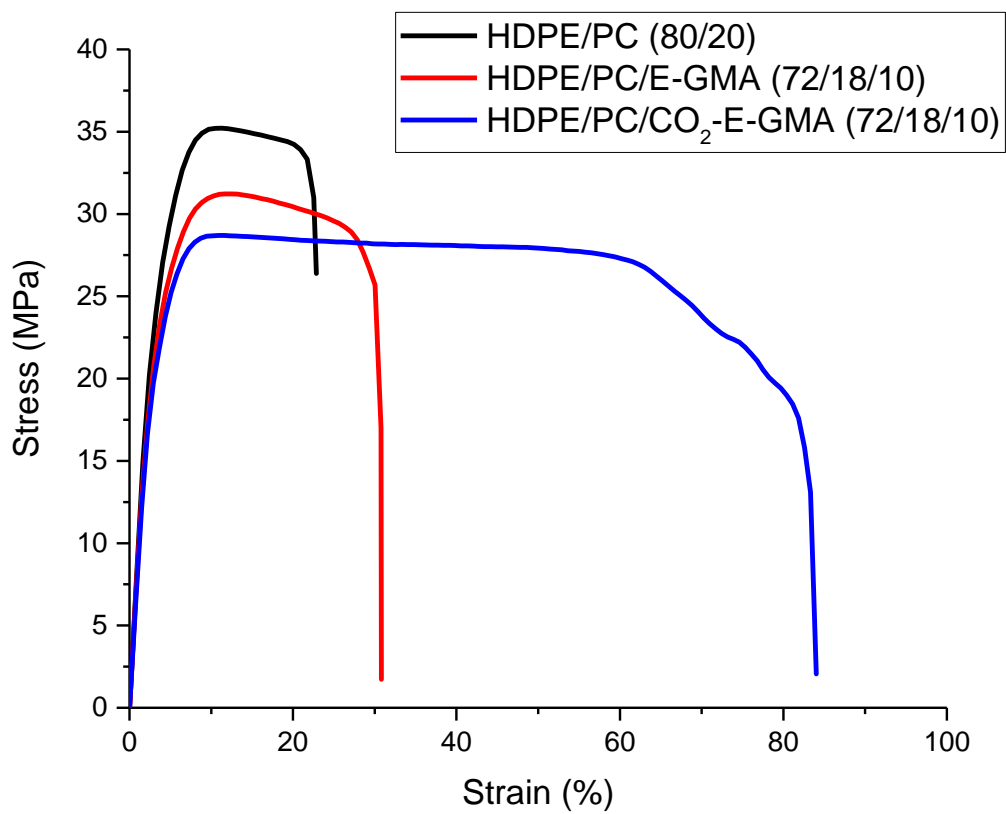


Figure S114. Tensile curve of HDPE/PC (80/20), HDPE/PC/E-GMA (72/18/10) and HDPE/PC/CO<sub>2</sub>-E-GMA (72/18/10) blends.

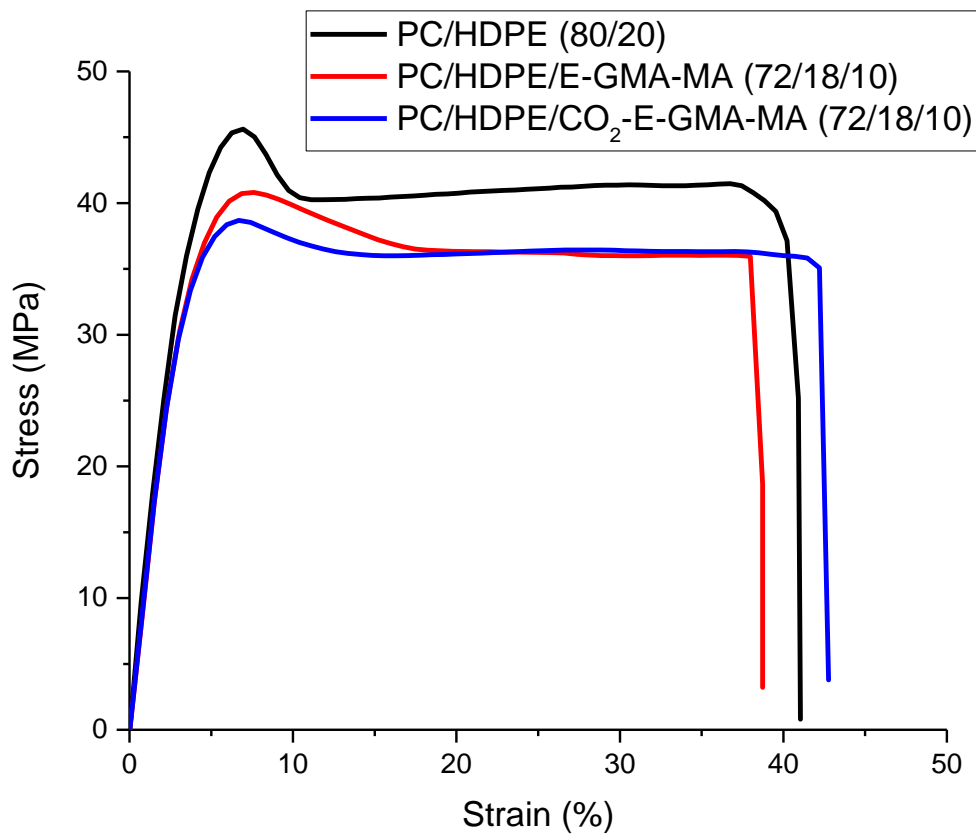


Figure S115. Tensile curve of PC/HDPE (80/20), PC/HDPE/E-GMA-MA (72/18/10) and PC/HDPE/CO<sub>2</sub>-E-GMA-MA (72/18/10) blends.

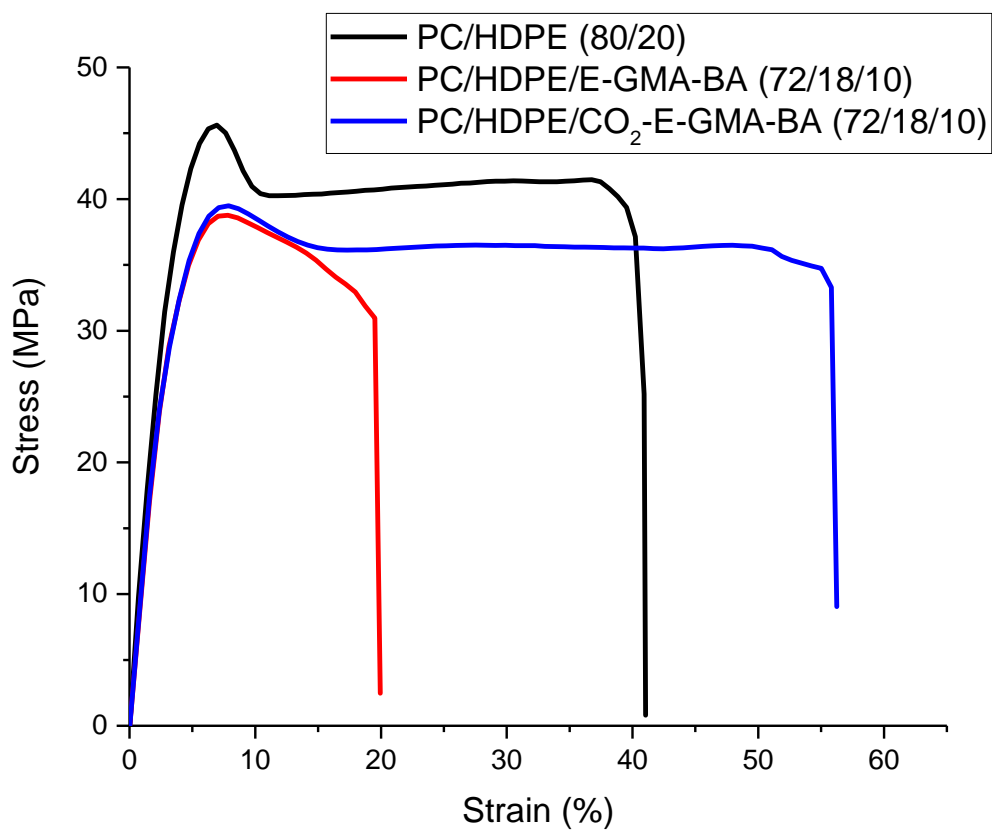


Figure S116. Tensile curve of PC/HDPE (80/20), PC/HDPE/E-GMA-BA (72/18/10) and PC/HDPE/CO<sub>2</sub>-E-GMA-BA (72/18/10) blends.



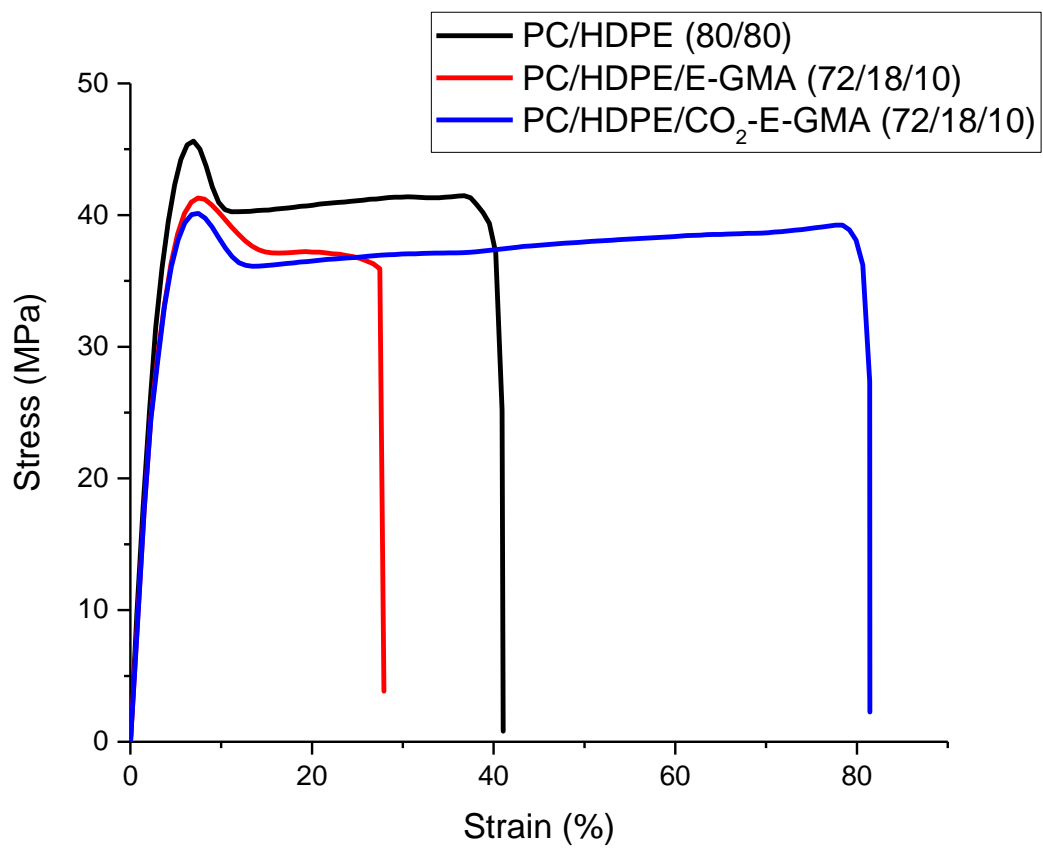


Figure S117. Tensile curve of PC/HDPE (80/20), PC/HDPE/E-GMA (72/18/10) and PC/HDPE/CO<sub>2</sub>-E-GMA (72/18/10) blends.

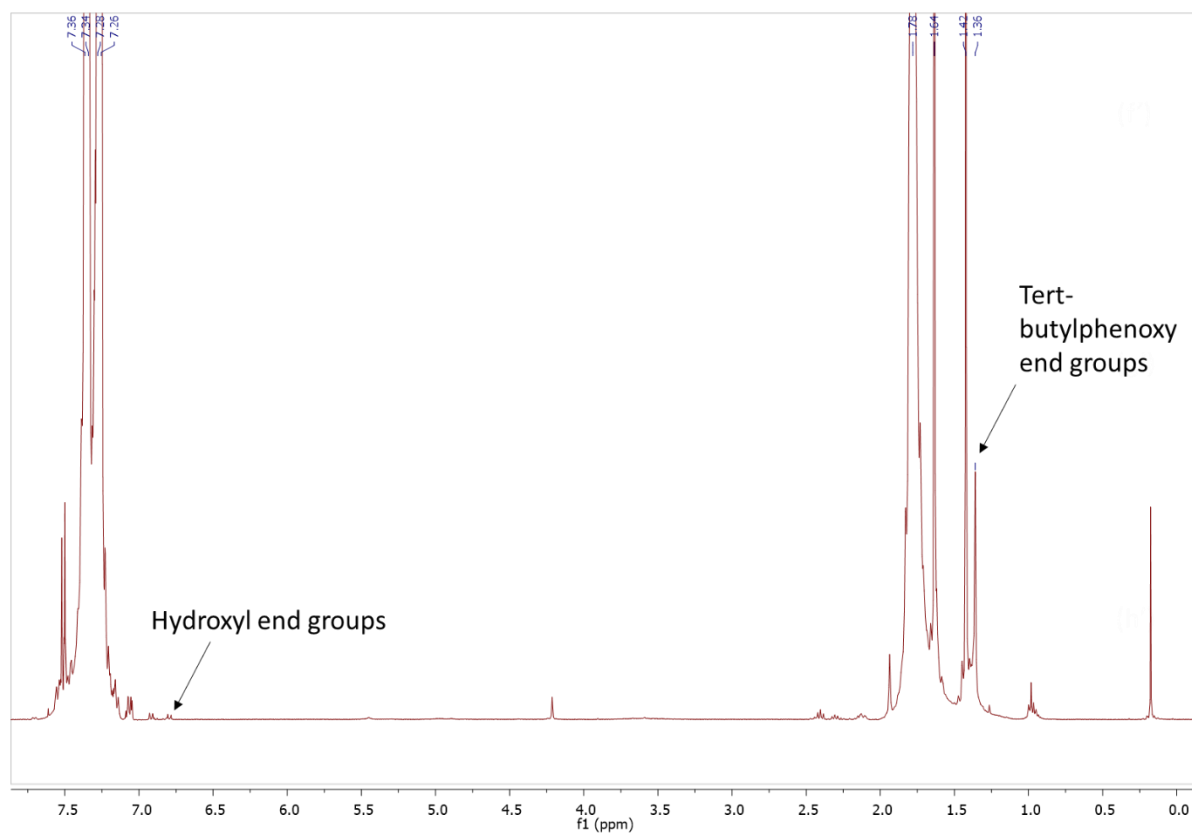
IV.2. NMR spectra of PC

Figure S118.  $^1\text{H}$  NMR spectrum (400 MHz,  $\text{CDCl}_3$ ) of PC.

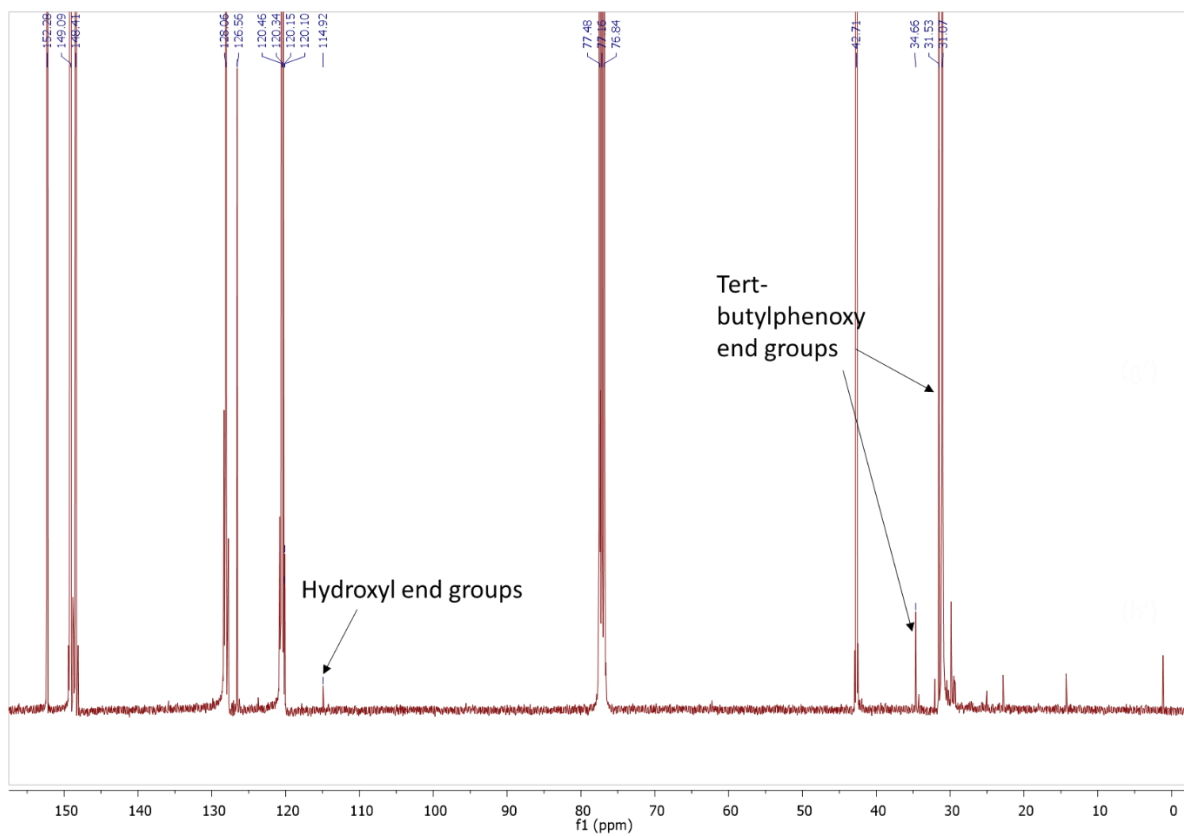


Figure S119.  $^{13}\text{C}$  NMR spectrum (100 MHz,  $\text{CDCl}_3$ ) of PC.



